"The Behaviour of Thin Spherical Shells under a Variety

of Load Actions"

Thesis presented for the Degree of

Doctor of Philosphy of the

University of Glasgow

by

A. S. Tooth, B.Sc. Tech. MSc. Tech.   A.M.C.S.T.

"Koinonia",
19 Myrtle Ave.
Lenzie
GLASGOW.   October 1963.

ProQuest Number: 10662294

ProQuest 10662294

I N D E X

C O N T E N T S

A B S T R A C T

The subject matter of the thesis concerns the analytical and experimental investigation of the elastic behaviour of shell structures, in particular that of spherical shells, under axi-symmetric, asymmetric and unsymmetric load systems.

Chapter I presents a critical survey of the relevant literature in the form of a dissertation. In view of the lack of a survey of this type it was felt desirable to present this in considerable detail so as to provide an up-to-date reference of the shell field. The survey clearly shows the need for an analytical procedure capable of handling all types of unsymmetrical load systems, and also establishes the lack of published experimental work. The paucity of the latter is most surprising in relation to the voluminous literature on the analysis of simple symmetrical load cases.

The plan of the research undertaken was, in consequence, designed to fill these gaps.

Chapter II presents a unified analytical approach based on the linear concepts of the shallow shell theory in which all load actions are considered as built up of the four basic actions of radial and tangential load, bending and twisting moments. Their evaluation is to the author's knowledge the first presentation of the unified approach to the analysis of such a complete range of load actions.

Further, analytical consideration is given to the correlation of this unified shallow shell approach with the general shell theory. It is shown that neglecting certain second order terms the general shell equations reduce to those of the shallow shell. The chapter culminates in the presentation of an Influence Line Method which, utilizing the permissibility of superposition in linear analysis, provides a ready approach to the solution of any type of unsymmetrical load action.

In Chapter III a number of load actions are analysed by means of the Influence Line Method. These examples, in the main, have been selected from a range for which conventional theoretical solutions are available. It is shown that good agreement is obtained in all cases between the Influence Line and conventional solutions.

The experimental investigations are described in Chapter IV covering the examination of the four basic load actions and certain selected composite actions. Some seventy tests were carried out covering a variety of radial and tangential area and ring loads, bending and twisting moments, and their combinations, applied directly to the continuous shell and to rigid inserts incorporated in the shell wall.

The experiments were carried out on shallow shell models of 60in radius, of $\frac{1}{4}$, $\frac{1}{2}$ and 1in thickness and on a complete spherical shell 13ft. 6in diam. which was a 1/10 scale model of the Dounreay Nuclear Reactor Containment Building.

The experimental and theoretical results are compared and fully discussed in Chapter V. It is generally shown that good agreement is obtained, fully substantiating the proposed analytical methods and their underlying concepts.

Chapter VI summarizes the main findings of the investigation regarding the basic aspects and their application to design analysis.

A Bibliography and Author's Index is provided in Chapter VII, followed in Chapter VIII by eight appendices giving the details of analyses considered in the thesis.

N O M E N C L A T U R E

The following presents an abbreviated list of typical symbols.

The complete list is shown in Appendix VIII.8

$\alpha, \beta, z \; ; x, y, z$	Orthogonal curvilinear and linear co-ordinates Fig. I.1
$\phi, \theta, R \; ; r, \theta$	Spherical Polar co-ordinates Fig. I.2
N_{xx}, N_{xy}, Q_{xz} --	Middle Plane, Normal Shear and Transverse Shear Forces. Suffixes consistent with all co-ordinate systems used.
$M_{xx}, M_{xy},$ ---	Bending and Twisting Moments. Suffixes consistent with all co-ordinate systems used
$X, Y, Z \; ; L, M.$	Components of External Load and Moment in x,y,z.
p_θ, p_r, p	Components of External Load in θ, ϕ , z co-ordinates.
P, M, T, H	External Radial Load, Bending Moment, Twisting Moment and Tangential Load
u, v, w	Components of Displacement of any point on the un-strained middle surface in the x,y and z directions.
$\sigma_x, \sigma_y, \sigma_z \; ;$ $\tau_{xy}, \tau_{xz}, \tau_{yz}.$	Normal and Shearing Components of Stress in rect-angular co-ordinates. Suffixes consistent with all co-ordinate systems used.
$\varepsilon_x, \varepsilon_y, \varepsilon_z \; ;$ $\gamma_{xy}, \gamma_{xz}, \gamma_{yz}.$	Normal and Shear Components of Strain in the x,y and z directions. Suffixes consistent with all co-ordinate systems used.
E, G	Modulii in Tension (or Compression) and Shear.
ν	Poisson's ratio.
D, C	Flexural and Extensional Rigidities of the Shell:- $D = Et^3/12(1-\nu^2) \; ; \quad C = Et/(1-\nu^2)$
t	Thickness of the Shell.
r_ρ	Radius of uniformly distributed load and radius of of Rigid Insert.
r_0	Radius of Loaded Ring.

INTRODUCTION

The study of thin shells has been the province of both the practicing engineer and the applied mathematician for over fifty years.

The theoretical aspects of shell design were pioneered by LOVE who formulated a general theory of thin shells. Owing to the complexity of the analysis approximations were introduced by later investigators to enable specific problems to be solved. In this theoretical work emphasis has been placed upon obtaining rigorous solutions to the shell problems. This has, in consequence, meant that solutions are available to only a limited number of cases which exhibit some form of symmetry or inverse-symmetry (asymmetry) of shell and/or loading. Further, the methods are invariably difficult in their application to particular design problems and are generally not substantiated by systematic experimental work.

The advent, in particular, of the large spherical containment vessel in the field of Nuclear Power Engineering has created an urgent need for a relatively flexible method of analysis, capable of wide application to the many unconventional stress and deformation problems which have arisen in this field.

With this background in mind the present programme of researc was initiated, sponsored by the Motherwell Bridge and Engineering Co., and directed towards the development of methods of analysis of the effects of load actions on shell forms.

CHAPTER I - REVIEW OF PUBLISHED LITERATURE.

Theoretical analyses and experimental investigations have been carried out in the subject of shell structures over a great many years.   The early work was directed toward improvements in the design of boilers and storage tanks and countless experimental tests were performed.   The theoretical aspects of shell design were pioneered by applied mathematicians such as ARON[1] and LOVE[2,3] who formulated a general theory of thin shells.   Owing to the complexity of the ensuing differential equations a number of approximations or assumptions have been made to enable specific problems to be solved. These are various and result in a large number of different theoretical treatments, which are discussed in this chapter.

The review is presented in two main sections dealing respectively with theoretical analyses and experimental investigations.

I.1   THEORETICAL ANALYSES

I.1.1   THE GENERAL EQUATIONS FOR SHELL FORMS

(a)   The Co-ordinate System.

(b)   The equations of Equilibrium.

(c)   The Strain Components.

(d)   The Resultant Force and Moment Actions.

(e)   The Stress-Strain Relations.

I.1.2   SIMPLIFICATION OF THE GENERAL EQUATIONS

(a)   Love's First Approximation.

(b)   Love's Second Approximation.

(c)   Approximation retaining the $(z/R)^m$ terms.

(d)   Approximation considering the transverse strains
and transverse normal stress.

(e)   General Comment.

I.1.3   THE SOLUTION OF THE SIMPLIFIED EQUATIONS WITH PARTICULAR REFERENCE TO SPHERICAL SHELLS

(a)   The 'General' Spherical Shell.

    (i)   The Symmetrically Loaded Shell.

    (ii)   The Asymmetrically Loaded Shell.

    (iii)   'Numerical Methods'.

(b)   Shallow Shells.
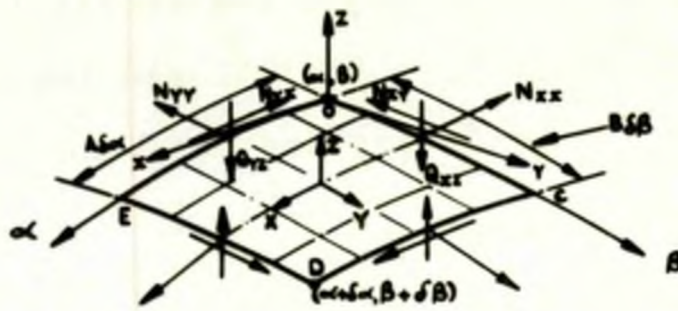
Fig. I.1a NORMAL AND SHEARING FORCE COMPONENTS
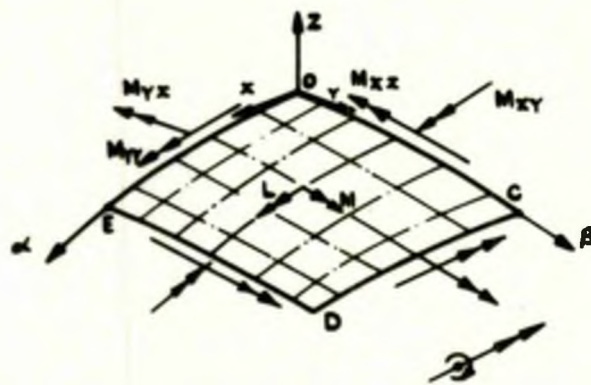
Fig. I.1b BENDING AND TWISTING MOMENT COMPONENTS
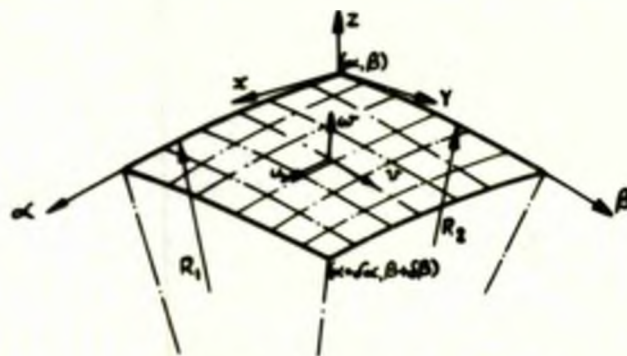
Fig. I.1c COMPONENTS OF DISPLACEMENT

Fig. I·1 NOMENCLATURE FOR GENERAL SHELL

I.1.1 THE GENERAL EQUATIONS FOR SHELL FORMS

The problem of curved plates and shells was first con-
sidered by ARON[1] in 1874.   He followed the procedure adopted
in the analysis of flat plates, and obtained an expression for
the potential energy of the strained shell which is of similar
form to that obtained by KIRCHHOFF for plates.   This work
was followed in 1888 and 1892-3 by that of LOVE[2,3] who
formulated a general theory of thin shells with reference to
orthogonal co-ordinates located on the middle surface.

The general equations obtained by LOVE have become the
classic basis of practically all theoretical analyses carried
out.

(a) The Co-ordinate System

The co-ordinate system to be considered throughout is that
of orthogonal curvilinear co-ordinates α, β, z which are capable
of defining the position of any point in the shell wall, as
shown in Fig. I.1.   The α and β curves are the lines of
principal curvature on the middle surface of the shell, $z = 0$.
The axes x and y are tangents to the curves α and β, respectively,
at their point of intersection O.

On the basis of the orthogonality of the curvilinear
co-ordinates one can state that a distance δs on the middle
surface, corresponding in magnitude and direction to the arc
distance from (α, β) to $(\alpha + \delta\alpha, \beta + \delta\beta)$ is:-

$$\delta s^2 = A^2 \delta\alpha^2 + B^2 \delta\beta^2$$

Thus when only one curvilinear co-ordinate is varied,

$$\delta s_1 = A\,\delta\alpha \; ; \qquad \delta s_2 = B\,\delta\beta \; ,$$

where δs_1, δs_2 are the increases in the arc length along the co-ordinate lines α, β corresponding to the increase of the curvilinear co-ordinates by $\delta\alpha, \delta\beta$ respectively. The quantities A and B are called the Lamé parameters and are in fact radii of curvature. They are functions of α and β and are characteristic of the shell form.

(b) The Equations of Equilibrium

The force and moment components per unit length acting on the middle surface of the shell element in the directions x, y, z are shown in Fig. I.1. For example, on the side OC of the element the normal and shearing forces are:-

$$-N_{xx}\,B\,\delta\beta \; ; \qquad -N_{xy}\,B\,\delta\beta \; ; \qquad -Q_{xz}\,B\,\delta\beta$$

while on the side OE these become:-

$-N_{yx}\,A\,\delta\alpha \; ; \quad -N_{yy}\,A\,\delta\alpha \; ; \quad -Q_{yz}\,A\,\delta\alpha$ in the x, y, z directions respectively.

Considering force equilibrium and allowing for the changes in shell geometry due to elastic deformation, the equations of equilibrium become:-

for normal and shearing forces,

$$\frac{\partial(N_{xx}B)}{\partial\alpha} + \frac{\partial(N_{yx}A)}{\partial\beta} - (r_1'N_{xy}B + r_2'N_{yy}A) + (q_1'Q_{xz}B + q_2'Q_{yz}A) + ABX\cdot = 0$$

$$\frac{\partial(N_{xy}B)}{\partial\alpha} + \frac{\partial(N_{yy}A)}{\partial\beta} - (p_1'Q_{xz}B + p_2'Q_{yz}A) + (r_1'N_{xx}B + r_2'N_{yx}A) + ABY = 0$$

$$\frac{\partial(Q_{xz}B)}{\partial\alpha} + \frac{\partial(Q_{yz}A)}{\partial\beta} - (q_1'N_{xx}B + q_2'N_{yx}A) + (p_1'N_{xy}B + p_2'N_{yy}A) + ABZ = 0$$

(I.1abc)

and bending and twisting moment actions,

$$-\frac{\partial(M_{xy}B)}{\partial\alpha} - \frac{\partial(M_{yy}A)}{\partial\beta} - (M_{xx}Br_1' + M_{yx}Ar_2') + (Q_{yz} + L)AB = 0$$

$$\frac{\partial(M_{xx}B)}{\partial\alpha} + \frac{\partial(M_{yx}A)}{\partial\beta} - (M_{xy}B r_1' + M_{yy}A r_2') - (Q_{xz} - M)AB = 0$$

$$M_{xx}B p_1' + M_{yy}A q_2' + (M_{xy}B q_1' + M_{yx}A p_2') + (N_{xy} - N_{yx})AB = 0$$

<div align="right">(I.2abc)</div>

In the above relationships p_1', q_1', r_1', p_2', q_2', r_2', are parameters arising from the elastic deformation of the middle surface, and corresponding to small rotations of the form, $p_1'\delta\alpha$, $q_1'\delta\alpha$ --- etc. They are defined as follows:-

$$p_1' = \frac{\partial}{\partial\alpha}\left(\frac{1}{B}\frac{\partial w}{\partial\beta} - \frac{v}{R_2}\right) - \frac{1}{B}\frac{\partial A}{\partial\beta}\left(\frac{1}{A}\frac{\partial w}{\partial\alpha} - \frac{u}{R_1}\right) + \frac{1}{R_1}\left(\frac{\partial v}{\partial\alpha} - \frac{u}{B}\frac{\partial A}{\partial\beta}\right)$$

$$q_1' = \frac{A}{R_1} - \frac{\partial}{\partial\alpha}\left(\frac{1}{A}\frac{\partial w}{\partial\alpha} - \frac{u}{R_1}\right) - \frac{1}{B}\frac{\partial A}{\partial\beta}\left(\frac{1}{B}\frac{\partial w}{\partial\beta} - \frac{v}{R_2}\right)$$

$$r_1' = -\frac{1}{B}\frac{\partial A}{\partial\beta} + \frac{\partial}{\partial\alpha}\left(\frac{1}{A}\frac{\partial v}{\partial\alpha} - \frac{u}{AB}\frac{\partial A}{\partial\beta}\right) - \frac{A}{R_1}\left(\frac{1}{B}\frac{\partial w}{\partial\beta} - \frac{v}{R_2}\right)$$

$$p_2' = -\frac{B}{R_2} + \frac{\partial}{\partial\beta}\left(\frac{1}{B}\frac{\partial w}{\partial\beta} - \frac{v}{R_2}\right) + \frac{1}{A}\frac{\partial B}{\partial\alpha}\left(\frac{1}{A}\frac{\partial w}{\partial\alpha} - \frac{u}{R_1}\right)$$

$$q_2' = -\frac{\partial}{\partial\beta}\left(\frac{1}{A}\frac{\partial w}{\partial\alpha} - \frac{u}{R_1}\right) + \frac{1}{A}\frac{\partial B}{\partial\alpha}\left(\frac{1}{B}\frac{\partial w}{\partial\beta} - \frac{v}{R_2}\right) + \frac{B}{AR_2}\left(\frac{\partial v}{\partial\alpha} - \frac{u}{B}\frac{\partial A}{\partial\beta}\right)$$

$$r_2' = \frac{1}{A}\frac{\partial B}{\partial\alpha} + \frac{\partial}{\partial\beta}\left(\frac{1}{A}\frac{\partial v}{\partial\alpha} - \frac{u}{AB}\frac{\partial A}{\partial\beta}\right) + \frac{B}{R_2}\left(\frac{1}{A}\frac{\partial w}{\partial\alpha} - \frac{u}{R_1}\right)$$

<div align="right">(I.3a-f)</div>

(c) The Strain Components

The extensional strains ε_1, ε_2 of the middle surface are defined as follows,

in the x direction, $\quad \varepsilon_1 = \dfrac{1}{A}\dfrac{\partial u}{\partial \alpha} + \dfrac{v}{AB}\dfrac{\partial A}{\partial \beta} + \dfrac{w}{R_1}$

and in the y direction, $\quad \varepsilon_2 = \dfrac{1}{B}\dfrac{\partial v}{\partial \beta} + \dfrac{u}{AB}\dfrac{\partial B}{\partial \alpha} + \dfrac{w}{R_2}$

The shear strain γ_{12} of the middle surface

$$= \dfrac{1}{A}\dfrac{\partial v}{\partial \alpha} + \dfrac{1}{B}\dfrac{\partial u}{\partial \beta} - \dfrac{u}{AB}\dfrac{\partial A}{\partial \beta} - \dfrac{v}{AB}\dfrac{\partial B}{\partial \alpha}$$

Due to the moment action on the element the middle surface will have curvature changes K_1 and K_2 in the direction x and y and also a change in twist K_3 defined as follows:-

$$K_1 = -\dfrac{1}{A}\dfrac{\partial}{\partial \alpha}\left(\dfrac{1}{A}\dfrac{\partial w}{\partial \alpha} - \dfrac{u}{R_1}\right) - \dfrac{1}{AB}\dfrac{\partial A}{\partial \beta}\left(\dfrac{1}{B}\dfrac{\partial w}{\partial \beta} - \dfrac{v}{R_2}\right)$$

$$K_2 = -\dfrac{1}{B}\dfrac{\partial}{\partial \beta}\left(\dfrac{1}{B}\dfrac{\partial w}{\partial \beta} - \dfrac{v}{R_2}\right) - \dfrac{1}{AB}\dfrac{\partial B}{\partial \alpha}\left(\dfrac{1}{A}\dfrac{\partial w}{\partial \alpha} - \dfrac{u}{R_1}\right)$$

$$K_3 = -\dfrac{1}{AB}\left(\dfrac{\partial^2 w}{\partial \alpha\, \partial \beta} - \dfrac{1}{A}\dfrac{\partial A}{\partial \beta}\dfrac{\partial w}{\partial \alpha} - \dfrac{1}{B}\dfrac{\partial B}{\partial \alpha}\dfrac{\partial w}{\partial \beta}\right) +$$

$$\dfrac{1}{R_1}\left(\dfrac{1}{B}\dfrac{\partial u}{\partial \beta} - \dfrac{1}{AB}\dfrac{\partial A}{\partial \beta}u\right) + \dfrac{1}{R_2}\left(\dfrac{1}{A}\dfrac{\partial v}{\partial \alpha} - \dfrac{1}{AB}\dfrac{\partial B}{\partial \alpha}v\right) \qquad \text{(I.4a-f)}$$

The corresponding values of the components of strain in the x, y, z directions for any general section of the shell situated a distance z from the middle surface become:-

$$\varepsilon_x = \dfrac{1}{1+z/R_1}\left[\varepsilon_1 + zK_1 + \dfrac{1}{A}\left(\dfrac{\partial \xi}{\partial \alpha} - r_1'\eta + q_1'\zeta\right)\right]$$

$$\varepsilon_Y = \dfrac{1}{1+z/R_2}\left[\varepsilon_2 + zK_2 + \dfrac{1}{B}\left(\dfrac{\partial \eta}{\partial \beta} - p_2'\zeta + r_2'\xi\right)\right]$$

$$\gamma_{xy} = \frac{\gamma_{12}}{1+z/R_2} + K_3 z \left(\frac{1}{1+z/R_1} + \frac{1}{1+z/R_2} \right) + \frac{z}{1+z/R_2} \left(\frac{q_2'}{B} + \frac{p_1'}{A} \right)$$

$$+ \frac{1}{(1+z/R_1)} \frac{1}{A} \left(\frac{\partial \eta}{\partial \alpha} - p_1' \zeta + r_1' \xi \right) + \frac{1}{1+z/R_2} \frac{1}{B} \left(\frac{\partial \xi}{\partial \beta} - r_2' \eta + q_2' \zeta \right)$$

$$\varepsilon_z = \frac{\partial \zeta}{\partial z}$$

$$\gamma_{zx} = \frac{\partial \xi}{\partial z} + \frac{1}{(1+z/R_1) A} \left(\frac{\partial \zeta}{\partial \alpha} - q_1' \xi + p_1' \eta \right)$$

$$\gamma_{yz} = \frac{\partial \eta}{\partial z} + \frac{1}{(1+z/R_2) B} \left(\frac{\partial \zeta}{\partial \beta} - q_2' \xi + p_2' \eta \right)$$

<div align="right">(I.5a-f)</div>

In the above expressions ξ, η, ζ are functions of α, β, z which have zero value when $z = 0$, i.e. on the middle surface. They may be considered as displacements in the x, y and z directions respectively, addition to those caused by the middle surface strains, allowing a point at a distance z from the middle surface to occupy any general position after straining.

(d)   The Resultant Force and Moment Actions

Denoting the internal stresses on the element as $\sigma_x, \sigma_y, \tau_{xy}$, τ_{yx}---etc. the resultant force and moment actions may be defined as follows:-

$$N_{xx} = \int_{-t/2}^{t/2} \sigma_x \left(1 + \frac{z}{R_2'} \right) dz \,, \qquad N_{xy} = \int_{-t/2}^{t/2} \tau_{xy} \left(1 + \frac{z}{R_2'} \right) dz$$

$$N_{yy} = \int_{-t/2}^{t/2} \sigma_y \left(1 + \frac{z}{R_1'} \right) dz \,, \qquad N_{yx} = \int_{-t/2}^{t/2} \tau_{yx} \left(1 + \frac{z}{R_1'} \right) dz$$

$$Q_{xz} = \int_{-t/2}^{t/2} \tau_{xz} \left(1 + \frac{z}{R_2'} \right) dz \qquad Q_{yz} = \int_{-t/2}^{t/2} \tau_{yz} \left(1 + \frac{z}{R_1'} \right) dz$$

$$M_{xx} = \int_{-t/2}^{t/2} \sigma_x \, z \left(1 + \frac{z}{R_2'}\right) dz \qquad M_{xy} = \int_{-t/2}^{t/2} \tau_{xy} \, z \left(1 + \frac{z}{R_2'}\right) dz$$

$$M_{yy} = \int_{-t/2}^{t/2} \sigma_y \, z \left(1 + \frac{z}{R_1'}\right) dz \qquad M_{yx} = \int_{-t/2}^{t/2} \tau_{yx} \, z \left(1 + \frac{z}{R_1'}\right) dz$$

(I.6a-j)

where R_1' and R_2' denote the radii of curvature of the normal section of the strained middle surface.

(e) The Stress-Strain Relations

Assuming the shell to be isotropic in all surfaces parallel to the middle but having different elastic constants normal to the middle surface, the stress-strain relations become:-

$$\sigma_x = \frac{E}{1-\nu^2}\left(\varepsilon_x + \nu\varepsilon_y\right) + \frac{\nu_z E}{(1-\nu)E_z}\,\sigma_z$$

$$\sigma_y = \frac{E}{1-\nu^2}\left(\varepsilon_y + \nu\varepsilon_x\right) + \frac{\nu_z E}{(1-\nu)E_z}\,\sigma_z$$

where,

$$\sigma_z = \frac{E_z}{1 - \frac{2(\nu_z)^2 E}{(1-\nu)E_z}}\left[\varepsilon_z + \frac{\nu_z E}{(1-\nu)E_z}\left(\varepsilon_x + \varepsilon_y\right)\right]$$

$$\tau_{xy} = G\,\gamma_{xy}, \qquad \tau_{xz} = G_z\,\gamma_{xz}, \qquad \tau_{yz} = G_z\,\gamma_{yz}$$

(I.7a-f)

For complete isotropy in the shell, $\left(\nu_z = \nu,\ E_z = E\right)$ eqts. I.7a-c become :-

$$\sigma_x = \frac{E}{1-\nu^2}\left(\varepsilon_x + \nu\varepsilon_y\right) + \frac{\nu\,\sigma_z}{1-\nu}$$

$$\sigma_y = \frac{E}{1-\nu^2}\left(\varepsilon_y + \nu\varepsilon_x\right) + \frac{\nu\,\sigma_z}{1-\nu}$$

$$\sigma_z = \frac{E}{1 - \frac{2\nu^2}{1-\nu}}\left[\varepsilon_z + \frac{\nu}{1-\nu}\left(\varepsilon_x + \varepsilon_y\right)\right]$$

(I.8a-c)

I.1.2 SIMPLIFICATION OF THE GENERAL EQUATIONS

The general equations I.1 to I.8 have been used as the basis of theoretical analyses of shell problems.   In order that a solution may be obtained a variety of approximations and assumptions are introduced, as the general equations have proved intractable.   Certain classical simplifications now to be considered were first introduced by LOVE, based undoubtedly upon those of KIRCHHOFF in his plate theory.   This is followed by an outline of more recent work in this field.

(a) LOVE'S First Approximation

This incorporated the following assumptions,

I   The thickness 't' of the shell is small compared with the least radius of curvature R of the middle surface.

II The strains and displacements are sufficiently small so that quantities of the second order and higher order magnitudes in the strain displacement relations may be neglected in comparison with the first order terms.   This assumption ensures the linearity of the resulting differential equations.

III The direct stress normal to the middle surface is small compared with other direct components of stress and may be neglected in the stress-strain relations.

IV The normals to the undeformed middle surface remain normal to the deformed middle surface and suffer no extension,   that is:- $\gamma_{xz} = \gamma_{yz} = \varepsilon_z = 0$ at all points.

In addition to the above, <u>LOVE</u> stipulated that the ratio of z/R is to be neglected in comparison with unity in the expressions of both the resultant force and moment actions and the strain component relations.

Using assumptions I and II and neglecting z/R the strain component equations I.5 may be written:-

$$\varepsilon_x = \varepsilon_1 + zK_1 \; ; \quad \varepsilon_y = \varepsilon_2 + zK_2 \; ; \quad \gamma_{xy} = \gamma_{12} + 2K_3 z$$

$$\gamma_{zx} = \frac{\partial \xi}{\partial z} \; ; \qquad \gamma_{yz} = \frac{\partial \eta}{\partial z} \; ; \qquad \varepsilon_z = \frac{\partial \xi}{\partial z} \qquad \text{(I.9a-f)}$$

Assumption III will modify the stress-strain equations 1.8 to:-

$$\sigma_x = \frac{E}{1-v^2}\left(\varepsilon_x + v\,\varepsilon_y\right)$$

$$\sigma_y = \frac{E}{1-v^2}\left(\varepsilon_y + v\varepsilon_x\right) \qquad \text{(I.10ab)}$$

Assumption IV which restricts the deformation of the normal so that $\varepsilon_z = \gamma_{xz} = \gamma_{yz} = 0$ will also imply that $\tau_{xz} = \tau_{yz} = 0$
Thus equations I.7 d, e, f reduce to:- $\quad \tau_{xy} = G\,\gamma_{xy} \qquad$ (I.11)

By substitution of eqts. I.9 in I.10 and I.11 expressions for σ_x, σ_y and τ_{xy} can be written:-

$$\sigma_x = \frac{E}{1-v^2}\left[\varepsilon_1 + v\varepsilon_2 + z(K_1 + vK_2)\right]$$

$$\sigma_y = \frac{E}{1-v^2}\left[\varepsilon_2 + v\varepsilon_1 + z(K_2 + vk_1)\right]$$

$$\tau_{xy} = G\left[\gamma_{12} + 2zK_3\right] \qquad \text{(I.12a-c)}$$

With these simplifications it is noted that Q_{xz} and Q_{yz} in equation I.6 are no longer retained. The other force and moment actions can now be written from eqt. I.6 using the above assumptions. To the first order in t, the force-strain equations are:-

$$N_{xx} = \frac{Et}{(1-v^2)}(\varepsilon_1 + v\varepsilon_2) \; , \qquad N_{yy} = \frac{Et}{(1-v^2)}(\varepsilon_2 + v\varepsilon_1)$$

$$N_{xy} = N_{yx} = \frac{Et}{2(1+v)}\gamma_{12} = Gt\,\gamma_{12} \qquad \text{(I.13a-d)}$$

and to the third order in t, the moment-strain equations are:-

$$M_{xx} = D\left[K_1 + \nu K_2 + \frac{1}{R_2'}(\varepsilon_1 + \nu\varepsilon_2)\right]$$

$$M_{yy} = D\left[K_2 + \nu K_1 + \frac{1}{R_1'}(\varepsilon_2 + \nu\varepsilon_1)\right]$$

$$M_{xy} = D(1-\nu)\left[K_3 + \frac{1}{2}\frac{\gamma_{12}}{R_2'}\right]$$

$$M_{yx} = D(1-\nu)\left[K_3 + \frac{1}{2}\frac{\gamma_{12}}{R_1'}\right]$$

(I.14a-d)

When the extensional strains are comparable with the flexural strains, then N_{xx}, N_{yy}, N_{yx}, N_{xy} are given by eqt. I.13a-d and M_{xx}, M_{yy} ---- by:-

$$M_{xx} = D\left[K_1 + \nu K_2\right]$$

$$M_{yy} = D\left[K_2 + \nu K_1\right]$$

$$M_{xy} = M_{yx} = D(1-\nu)K_3$$

(I.15a-d)

The equations of equilibrium I.1 and I.2 will also be modified by the foregoing assumptions relating to the omission of second order terms. It can be shown that the product of the force actions and p_1' and q_2' are of second order whereas certain parts of q_1', r_1', p_2', r_2', are of first order in the product relationships. These then lead to the equations of equilibrium in the following form:-

$$\frac{\partial(N_{xx}B)}{\partial\alpha} + \frac{\partial(N_{yx}A)}{\partial\beta} + N_{xy}\frac{\partial A}{\partial\beta} - N_{yy}\frac{\partial B}{\partial\alpha} + \frac{AB}{R_1}Q_{xz} + ABX = 0$$

$$\frac{\partial(N_{xy}B)}{\partial\alpha} + \frac{\partial(N_{yy}A)}{\partial\beta} + \frac{AB}{R_2}Q_{yz} - N_{xx}\frac{\partial A}{\partial\beta} + N_{yx}\frac{\partial B}{\partial\alpha} + ABY = 0$$

$$\frac{\partial(Q_{xz}B)}{\partial\alpha} + \frac{\partial(Q_{yz}A)}{\partial\beta} - \frac{AB}{R_1}N_{xx} - \frac{AB}{R_2}N_{yy} + ABZ = 0$$

$$\frac{\partial(M_{xy}B)}{\partial\alpha} + \frac{\partial(M_{yy}A)}{\partial\beta} - M_{xx}\frac{\partial A}{\partial\beta} + M_{yx}\frac{\partial B}{\partial\alpha} - (Q_{yz}+L)AB = 0$$

$$\frac{\partial(M_{xx}B)}{\partial\alpha} + \frac{\partial(M_{yx}A)}{\partial\beta} + M_{xy}\frac{\partial A}{\partial\beta} - M_{yy}\frac{\partial B}{\partial\alpha} + (-Q_{xz}+M)AB = 0$$

$$\frac{M_{xy}}{R_1} - \frac{M_{yx}}{R_2} + (N_{xy} - N_{yx}) = 0$$

(I.16a-f)

This formulation of the problem contains all the essential facts necessary for the treatment of thin shells as long as special conditions do not require inclusion of the effects of transverse shear and transverse normal stresses.

It is noted, however, that a theory which includes the two assumptions $\sigma_z = 0$ and $\varepsilon_z = 0$ would fail to lead to correct results in the special case of a flat plate subject to a state of homogeneous bending and stretching. This difficulty is usually avoided by neglecting σ_z in the stress-strain relation eqt. I.8c and by then determining from the resultant equation a value for the strain:-

$$\varepsilon_z = -\frac{\nu}{1-\nu}(\varepsilon_x + \varepsilon_y) \qquad (I.17)$$

and from eqts. I.9a,b:- $\varepsilon_z = -\frac{\nu}{1-\nu}\left[\varepsilon_1 + \varepsilon_2 + z(K_1 + K_2)\right]$ (I.18)

It is seen that the resulting equations for the force and moment actions, (eqts. I.13 and I.15) are extremely simple and are completely analogous with the corresponding formulae of the theory of flat plates. However, as NOVIZHILOV[4] points out in his recent book, certain contradictions or inconsistencies are present - these are considered to be of second order effect and to be no greater than the effects of the initial assumptions underlying the theory of thin shells. One point, however, will be mentioned at this stage owing to its use in a later section.

Following from assumption IV, the shear displacements γ_{xz}, γ_{yz} were neglected. The logical sequel to this is that the resultant transverse shear forces Q_{xz} and Q_{yz} are no longer retained. These forces, however, are present in the equilibrium equations I.16, and in a later section one such term is used as the dependent variable in the fundamental equation for the axi-symmetrically loaded spherical shell. NOVOZHILOV[4] indicates that the hypothesis which requires normals to remain normals is only applied to determine the law of deformation of a fibre of the shell, parallel to the middle surface, and is not used in the study of the equilibrium of forces. The resultant transverse shear forces - Q should thus be retained in the equilibrium equations. FLÜGGE[5] avoids this difficulty by envisaging that some of the elastic moduli have infinite value, so that $\varepsilon_z \equiv \gamma_{xz} \equiv \gamma_{yz} \equiv 0$ is satisfied and the required resultant force terms retained in the equilibrium equation.

(b) LOVE'S Second Approximation[3]

This approximation retained certain terms containing z/R and introduced terms in consequence of the partial inclusion of the effect of the transverse normal stress σ_z. Such an approximation LOVE deems unnecessary unless the extensional and shear strains of the mid-surface $\varepsilon_1, \varepsilon_2, \gamma_{12}$ are small compared with the flexural strains, zK_1, zK_2, zK_3

The basis of the approximation is to simplify the expressions for the components of strain - eqt. I.5. This is done in the following manner. The term $\varepsilon_1(1+z/R_1)^{-1}$ is replaced by ε_1

and the term $zK_1(1+z/R_1)^{-1}$ by $zK_1 - z^2\dfrac{K_1}{R_1}$. Values of ξ, η, ζ are substituted into eqt. I.5, those of ξ, η being zero as in the first approximation and $\zeta = -\dfrac{\nu}{1-\nu}\left[(\varepsilon_1 + \varepsilon_2)z + \tfrac{1}{2}(K_1 + K_2)z^2\right]$ (I.19) obtained by integrating eqt. I.18. Further the terms p_1', q_1', ----- that appear in eqt. I.5 may be replaced by the corresponding quantities relating to the unstrained shell, that is:- $p_1' = q_{12}' = 0$, $p_2' = -\dfrac{B}{R_2}$, $q_1 = \dfrac{A}{R_1}$ and finally rejecting terms of the type $\varepsilon_1 z/R_1$, $\varepsilon_1 K_1 z$, $K_1^2 z^2$ the modified strain component equations are obtained as follows:-

$$\varepsilon_x = \varepsilon_1 + zK_1 - z^2\frac{K_1}{R_1} - \frac{1}{2}\frac{\nu}{1-\nu}\frac{z^2(K_1 + K_2)}{R_1}$$

$$\varepsilon_y = \varepsilon_2 + zK_2 - z^2\frac{K_2}{R_2} - \frac{1}{2}\frac{\nu}{1-\nu}\frac{z^2(K_1 + K_2)}{R_2}$$

$$\gamma_{xy} = \gamma_{12} + 2K_3 z - K_3 z^2\left(\frac{1}{R_1} + \frac{1}{R_2}\right) \tag{I.20}$$

From the relationships given in eqts. I.6 and I.7d it is now possible to determine values for N_{xy} and N_{yx}, by using the value for γ_{xy} given above in eqt. I.20c and replacing the deformed curvature R_1' by R_1 and R_2' by R_2, fourth order terms in t being neglected. These are as follows:-

$$N_{xy} = \frac{E}{2(1+\nu)}\left[\gamma_{12}t + \frac{t^3}{6}\frac{K_3}{R_2} - \frac{t^3}{12}K_3\left(\frac{1}{R_1} + \frac{1}{R_2}\right)\right]$$

$$N_{yx} = \frac{E}{2(1+\nu)}\left[\gamma_{12}t + \frac{t^3}{6}\frac{K_3}{R_1} - \frac{t^3}{12}K_3\left(\frac{1}{R_1} + \frac{1}{R_2}\right)\right] \tag{I.21}$$

A further modification consists in determining a value for σ_z by substituting the values of σ_x and σ_y obtained in the first approximation in the equilibrium equation for stresses. The relevant equation, after neglecting z/R terms becomes:-

$$\frac{\partial \sigma_z}{\partial z} = \frac{\sigma_x}{R_1} + \frac{\sigma_y}{R_2}$$

This leads to $\dfrac{\partial \sigma_z}{\partial z} = \dfrac{E}{1-\nu^2} z\left(\dfrac{K_1 + \nu K_2}{R_1} + \dfrac{K_2 + \nu K_1}{R_2}\right)$ where σ_x and σ_y

are replaced by their first approximations and the extensional strains are neglected.   Since the value of σ_z must vanish at $z = \frac{t}{2}$ and $z = -\frac{t}{2}$,

$$\sigma_z = -\frac{1}{2}\frac{E}{1-\nu^2}\left(\frac{t^2}{4} - z^2\right)\left(\frac{K_1 + \nu K_2}{R_1} + \frac{K_2 + \nu K_1}{R_2}\right) \qquad (I.22)$$

From the stress-strain relations eqts. I.8a,b in conjunction with eqt. I.20 for ε_x and ε_y and eqt. I.22 for σ_z, it is possible using the resultant force and moment action expressions eqt. I.6 to write:-

$$N_{xx} = \frac{Et}{1-\nu^2}\left[(\varepsilon_1 + \nu\varepsilon_2) + \frac{t^2}{12}\left\{K_1\left(\frac{1}{R_2} - \frac{1}{R_1}\right) - \frac{1}{2}\frac{\nu}{1-\nu}(K_1 + K_2)\left(\frac{1}{R_1} + \frac{\nu}{R_2}\right)\right.\right.$$
$$\left.\left. - \frac{\nu}{1-\nu}\left(\frac{K_1 + \nu K_2}{R_1} + \frac{K_2 + \nu K_1}{R_2}\right)\right\}\right] \qquad (I.23)$$

together with the analogous expression for N_{yy}.   The resultant moment actions are not affected by the second approximation, provided that the terms of a higher order than DK_1 are not retained.

As in the first approximation of <u>LOVE</u>, τ_{xz} and τ_{yz} are not considered and the shear forces Q_{xz} and Q_{yz} are zero.

(c) <u>Approximation retaining the $(z/R)^m$ terms</u> (where $m = 1,2\text{---}$)

With a view to improving <u>LOVE</u>'s first approximation some investigators have sought new solutions of the classical theory by retaining the z/R terms in the strain component and the resultant force and moment action expressions, the other assumptions being retained as before.

<u>FLÜGGE</u>[5] modified the general expression for the force-strain and moment-strain equations for both cylindrical shells and shells of revolution, expressing them in terms of the displacements u, v, w and their differentials.   Those terms

which contained log f(t) were expanded in powers of t/R and fifth and higher powers were neglected.   The expressions for N_{xx}, N_{yy} --- M_{xx}, M_{yy} --- thus contain only the rigidity constants - the extensional rigidity, C and the flexural rigidity, D.

It is noted that in the resulting relationships the elastic change of curvature K_1, K_2, and K_3 influence the normal and shearing force actions and the strain in the middle surface ε_1, ε_2, γ_{12} influence the bending and twisting moment actions.   The moment expressions are of a similar type to eqt. I.14a-d, while additional terms involving t^3 (i.e. D) are considered in the normal and shearing force actions of LOVE's first approximation eqt. I.13a-d.   For the particular case of the spherical shell, first analysed by HAVERS[6], the log f(t) term does not appear, however, the term (1 + z/R) is retained in the resultant force and moment action expressions eqt. I.6.   The resulting expressions for the normal and shearing force action, however, are seen to correspond to eqt. I.13a-d and the moment actions to the corresponding eqt. I.15a-d. Thus it is seen that for the particular case of $R_1 = R_2$ the force-strain and moment-strain equations are those of LOVE's first approximation.

Similar work is presented by BIEZENO and GRAMMEL[7] for a cylindrical shell.   They expand the integrand of $\int \frac{dz}{R+z}$ in series, the terms of the third or lower powers of t being retained.   The results for the force and moment actions are presented in terms of u, v, w.   BYRNE[8] in a recent

publication followed a similar procedure which led to
expressions for N_{xx}, N_{yy}, etc. as below:—

$$N_{xx} = \frac{Et}{(1-v^2)} \left[\varepsilon_1 + v\varepsilon_2 - \frac{t^2}{12}\left(\frac{1}{R_1} - \frac{1}{R_2}\right)\left(K_1 - \frac{\varepsilon_1}{R_1}\right)\right]$$

$$N_{yy} = \frac{Et}{(1-v^2)} \left[\varepsilon_2 + v\varepsilon_1 - \frac{t^2}{12}\left(\frac{1}{R_2} - \frac{1}{R_1}\right)\left(K_2 - \frac{\varepsilon_2}{R_2}\right)\right] \qquad (I.24)$$

These equations differ from equations I.13 of LOVE's first
approximation in that certain terms of order t^3 are added to
the original expression.   Again it is noted that the
additional terms of eqt. I.24 disappear when the significant
radii of curvature of the middle surface are equal, that is,
in the cases of a flat plate and spherical shells.

A comparison of eqt. I.24 with that obtained by LOVE using
his second approximation (eqt. I.23) shows that eqt. I.23 includes
terms present in eqt. I.24 except for the terms $\frac{\varepsilon_1}{R_1}$ and $\frac{\varepsilon_2}{R_2}$.
Additional terms in the LOVE analysis, which are of the same
order as the correction terms present in BYRNE's eqt. I.24, are
introduced as a result of the inclusion of the effect of the
transverse normal stress σ_z.   The expressions of LOVE are
furthermore valid for $R_1 = R_2$

It was LOVE who pointed out that the values of N_{xy}, N_{yx},
N_{xx}, N_{yy}, obtained by his second approximation agree substan-
tially with those found by BASSET[9].   The method used in
BASSET's derivation is that of expanding the stress, strain and
displacement components in a shell in series of powers of z.
The order of each term, i.e. M_{xx}, M_{yy} --- γ_{xz}, γ_{yz} etc. is con-
sidered and those of fifth order or higher powers in t are

rejected.   This results in neglecting γ_{xz} and γ_{yz} .   The
expressions thus obtained contain the corrections introduced
by BYRNE[8] in eqt. I.24 as well as the additional terms
introduced by LOVE's second approximation equations I.21 and
I.23, together with further terms of third order value.

HILDEBRAND, REISSNER and THOMAS[10] commenting on the
procedure of BASSET in neglecting certain terms which involve
high powers of t, point out that such a procedure may not be
valid in those cases where an appreciable change in the magni-
tude of a moment occurs over a distance of the order of
magnitude of the thickness t or over a distance of $\sqrt{Rt}$ for
cylindrical and spherical shells, where 'R' is the radius of
the circles of curvature.   Such an appreciable change would
occur in the case of local surface loading causing high con-
centration of stress over a small area.   It is considered,
however, that the inclusion of the terms involving z/R and
the expansion of the various quantities in terms of powers of
the thickness co-ordinate does not add to the accuracy of the
result, since such terms are of the same order as the original
approximations made in the rest of the theory.

The work of KENNARD[11, 12] underlines the above.   This
work is based on that of EPSTEIN[13] who, starting from the
three-dimensional equations of elasticity, derived equations of
motion for the elastic vibrations in cylindrical shells.
KENNARD uses the resulting equations and obtains expressions
for the force-strain and moment-strain equations for circular
cylinders.   He justifies the neglect of terms which involve t^3.

Similar work carried out by VLASOV[14] must also be mentioned
in support of this argument.   He notes that in the force-
strain and moment-strain equations there exists certain terms
which are independent of the curvature of the shell and which
involve t^3.   After extensive theoretical analyses, supported
by experimental investigations, it is shown that these terms
are of second order and can be neglected without sensible
error, provided $t/R_{min} > 1/30$.   He quotes the work of
GALERKIN[15] on cylindrical shells and thin walled rods as
further evidence to substantiate this assumption.

(d) Approximation considering the transverse strains and the
     transverse normal stress -- i.e. ε_z, γ_{xz}, γ_{yz} and σ_z

     It has been previously mentioned that assumptions III and
IV of LOVE's first approximation (i.e. σ_z is small compared with
the other normal components of stress and $\gamma_{xz} = \gamma_{yz} = \varepsilon_z = 0$)
when taken together are not entirely satisfactory.   This has
lead certain authors to discard these two assumptions in order
to broaden the scope of the theory and enable it to embrace
the transverse strains and normal stress.   A method of
REISSNER[16] which is applied to the case of axi-symmetrical
deformation of a shell of revolution, consists of obtaining a
system of force-strain and moment-strain equations for a
co-ordinate system which has anisotropy in direction normal
to the shell (see eqts. I.7).   The method used incorporates
a variational principle previously used by REISSNER[17].
Assumed stresses and displacements are substituted into the
appropriate form of the variational equation, certain second

order terms are omitted, and a system of strain-force and moment equations developed. Those of $\mathcal{E}_1, \mathcal{E}_2, \gamma_z$ are shown below:-

$$\mathcal{E}_1 = \frac{1}{Et}\left\{N_{xx}\left[1 + \frac{1}{12}\left(\frac{t}{R_2} - \frac{t}{R_1}\right)\frac{t}{R_2}\right] - \nu N_{yy}\right\} - \frac{M_{xx}}{Et^2}\left(\frac{t}{R_2} - \frac{t}{R_1}\right) + \frac{\nu_z}{E_z t^2}\left(\frac{t}{R_1}M_{xx} + \frac{t}{R_2}M_{yy}\right)$$

$$\mathcal{E}_2 = \frac{1}{Et}\left\{N_{yy}\left[1 + \frac{1}{12}\left(\frac{t}{R_1} - \frac{t}{R_2}\right)\frac{t}{R_1}\right] - \nu N_{xx}\right\} - \frac{M_{yy}}{Et^2}\left(\frac{t}{R_1} - \frac{t}{R_2}\right) + \frac{\nu_z}{E_z t^2}\left(\frac{t}{R_1}M_{xx} + \frac{t}{R_2}M_{yy}\right)$$

$$\gamma_z = \frac{6}{5G_z t}Q_z$$

$$(I.25a\text{-}c)$$

REISSNER makes certain observations regarding these relations. Setting $\nu_z = 0$ and $G_z = \infty$ and expressing the N's and M's in terms of the $\mathcal{E}$'s and K's, BYRNE's[8] and FLÜGGE's[5] relations are obtained. He also notes that if the order of magnitude of the bending stresses is the same as that of the direct stresses, and if $t/R \ll 1$ and ν_z/E_z and $1/E_z$ are of the order of $1/E$ then all terms of eqt. I.25 which have t/R or $(t/R)^2$ as a factor are small compared with the terms that do not have this factor. When such a modification is carried out the force-strain and moment-strain equations that result are those of LOVE's first approximation, i.e. eqts. I.13 and I.15. REISSNER comments on this point, remarking - "Apart from the question of the transverse shear deformability, the force-strain and moment-strain equations of LOVE's first approximation are all that are needed for the application of the theory to specific problems."

Despite this comment, REISSNER seeks to improve these equations since they are deficient in certain terms which appear in LOVE's second approximation (eqts. I.21 and I.23).

The reason for this deficiency is that additional terms should have been included in the approximations for $\sigma_{\bar{z}}$ and 'w'. The terms $\sigma_{\bar{z}}$ and 'w' are thus defined in appropriately generalised form. The definition of 'w' includes a term of similar form to the relevant term of LOVE's second approximation, namely ζ , (eqt. I.19). The earlier method of analysis is repeated and force-strain and moment-strain equations are obtained which are both long and complex. They do, however, include the force-strain and moment-strain equations of LOVE's second approximations as a special case.

A recent paper by NAGHDI[18] follows similar lines to that of REISSNER[16] mentioned above. Like REISSNER he uses a variational principle in order to derive a system of force-strain and moment-strain equations. In defining the stresses and displacements NAGHDI adopts even more general forms than does REISSNER in obtaining his improved relationships. He presents the results for the force-strain and moment-strain equations in such a way that the influence of neglecting or including the transverse normal stress is clearly seen. For example, when $\sigma_{\bar{z}}$ is neglected and the transverse shear deformation is retained the equations for the force-strain and moment-strain equations simplify considerably. Neglecting the second order terms in t/R these become :-

$$N_{xx} = \frac{Et}{1-v^2}\left[\varepsilon_1 + v\varepsilon_2 - \frac{t^2}{12}\left(\frac{1}{R_1} - \frac{1}{R_2}\right)K_1\right] \qquad etc. \text{ for } N_{yy} --$$

$$M_{xx} = D\left[K_1 + vK_2 - \left(\frac{1}{R_1} - \frac{1}{R_2}\right)\varepsilon_1\right] \qquad etc. \text{ for } M_{yy} --$$

$$(I.26)$$

It is noted that in the case of a flat plate or a spherical shell these results simplify to those of LOVE's first approximation, except of course, that expressions are included for the resultant shear force Q_{xz} and Q_{yz}.

In the second place when the effect of the normal stress $\sigma_{\bar{z}}$ is considered the following expressions result:-

$$N_{xx} = \frac{Et}{1-v^2}\left[\varepsilon_1 + v\varepsilon_2 - \frac{t^2}{12}\left(\frac{1}{R_1} - \frac{1}{R_2}\right)K_1 - \frac{v}{1-v}\frac{t^2}{12}\left\{\frac{1}{2}\left(\frac{1}{R_1} + \frac{v}{R_2}\right)(K_1 + K_2) + \frac{K_1 + vK_2}{R_1} + \frac{K_2 + vK_1}{R_2}\right\}\right]$$

$$\text{etc.} \qquad + \frac{v}{1-v}\frac{t}{2}\left(\overset{+}{q} + \bar{q}\right)$$

$$M_{xx} = D\left[K_1 + vK_2 - \left(\frac{1}{R_1} - \frac{1}{R_2}\right)\varepsilon_1 - \frac{v}{1-v}\left\{\left(\frac{1}{R_1} + \frac{v}{R_2}\right)(\varepsilon_1 + \varepsilon_2) + \frac{1}{5}\left(\frac{\varepsilon_1 + v\varepsilon_2}{R_1} + \frac{\varepsilon_2 + v\varepsilon_1}{R_2}\right)\right\}\right]$$

$$\text{etc.} \qquad + \frac{6}{5}\frac{v}{1-v}\frac{t^2}{12}\left(\overset{+}{q} - \bar{q}\right) \qquad (I.27)$$

where $\overset{+}{q}$ and $\bar{q}$ are values of $\sigma_{\bar{z}}$ at $z = \pm t/2$.

Again comparison can be made with the work of LOVE. In this case it is noted that except for the shear resultants Q_{xz} and Q_{yz} and their effects on K_1 and K_2 the force-strain and moment-strain equations I.27 are similar in form to those of LOVE's second approximation.

(e)   General Comment

It would appear that the assumptions made by LOVE's 'first approximation' although not taking into account the transverse shear and normal stresses, form the basis of a simplified system of equations which are capable of solution. It was KOITER[19] who pointed out that it is meaningless, in general, to carry out refinement of LOVE's first approximation unless the effects of transverse shear and normal stresses are taken into account

at the same time.   Although such refinements have been carried
out, as referred to above in the papers of REISSNER and
NAGHDI[16,18] the present author doubts whether the complex
force-strain and moment-strain equations that ensue will enable
results to be obtained for practical loading problems.   It
would appear, therefore, that for the thin shell, the theory of
LOVE's 'first approximation' is sufficiently accurate and
further, is capable of providing a basis for the solution of a
wide range of shell problems.   The presence of the factor
$(1/R_1 - 1/R_2)$ in a number of the approximations is particularly
fortuitous in the analysis of the spherical shell.   This term,
which becomes zero for such shells, means that the majority of
the expressions discussed reduce to LOVE's 'first approximation.'

I.1.3   THE SOLUTION OF THE SIMPLIFIED EQUATIONS WITH PARTICULAR REFERENCE TO SPHERICAL SHELLS

The simplified differential equations in the form given in the preceeding section are not readily amenable to analytical solution. In fact throughout the history of shell analysis the solution of these equations in their various forms has involved the use of mathematical techniques not hitherto employed in such analyses.   In this section a review of these solutions is presented with particular reference to spherical shells, in both general form and as shallow shell structures.   Throughout, attention is confined to those differential equations which result from what is essentially LOVE's first approximation.

(a)   The 'General' Spherical Shell

The first successful application of the theory of thin shells was made by H. REISSNER[20] in 1912.   REISSNER suitably modified the equations of LOVE's first approximation to suit the spherical shell.   In this case the principal radii of curvature are the same and equal to the radius of the shell R.   The curvilinear co-ordinate system α, β used earlier in deriving the differential equations for the shell is modified to the system of ϕ and θ , where ϕ and θ are the co-latitudinal and co-longitudinal angles respectively.   The following equivalence between the quantities of Fig. I.1 and Fig. I.2 is noted:-

$$\alpha = \theta , \quad \beta = \phi , \quad Q_{xz} = Q_\theta , \quad Q_{yz} = Q_\phi .$$

$$N_{xx} = N_{\theta\theta} , \quad N_{yy} = N_{\phi\phi} , \quad N_{xy} = N_{\theta\phi} , \quad N_{yx} = N_{\phi\theta} .$$
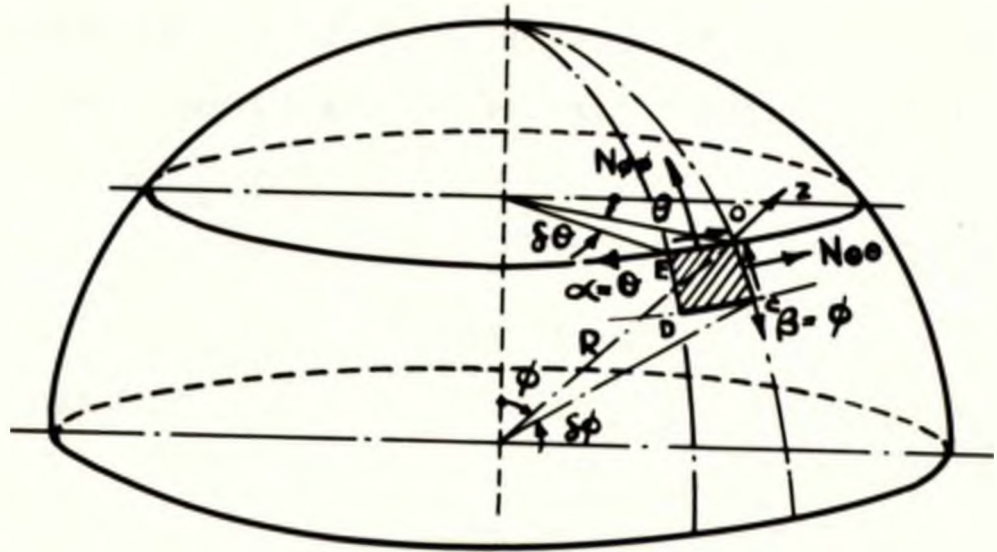
SPHERICAL SHELL SHOWING ELEMENT OCDE
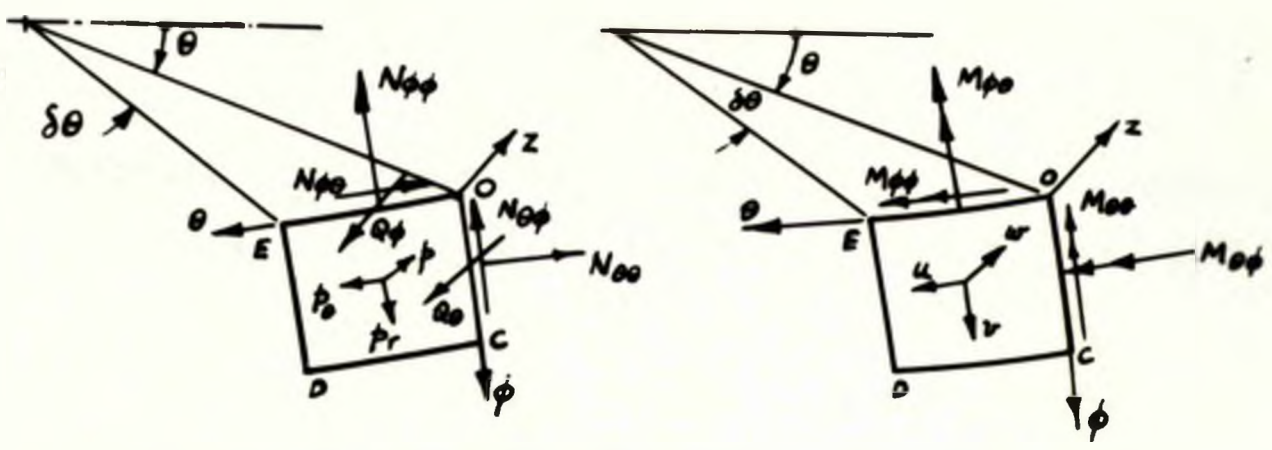
DETAILS OF FORCES AND MOMENTS ON ELEMENT OCDE.

FIG. I·2 NOMENCLATURE FOR THE 'GENERAL' SPHERICAL SHELL

and similarly for the moments. The externally applied forces
X, Y and Z become p_θ, p_r, and p respectively.

The arc of the parallel circle OE is given by $\delta s_1 = R \sin\phi . \delta\theta$
and the arc of the meridian OC by $\delta s_2 = R \delta\phi$. Thus the Lamé
parameters, A and B are:- $A = R \sin\phi$ and $B = R$

Using these values for A and B and the new nomenclature,
the equations of equilibrium corresponding to LOVE's first
approximation eqt. I.16a-f can be written, putting $M = L = 0$:-

$$R \frac{\partial N_{\theta\theta}}{\partial\theta} + \frac{\partial(rN_{\phi\theta})}{\partial\phi} + R N_{\theta\phi}\cos\phi - rQ_\theta + Rr p_\theta = 0$$

$$\frac{\partial(N_{\phi\phi}r)}{\partial\phi} + R\frac{\partial N_{\theta\phi}}{\partial\theta} - R N_{\theta\theta}\cos\phi + rQ_\phi + Rr p_r = 0$$

$$R\frac{\partial Q_\theta}{\partial\theta} + \frac{\partial(rQ_\phi)}{\partial\phi} - r(N_{\theta\theta} + N_{\phi\phi}) + Rr p = 0$$

$$R\frac{\partial M_{\theta\phi}}{\partial\theta} + \frac{\partial(rM_{\phi\phi})}{\partial\phi} - R M_{\theta\theta}\cos\phi - Rr Q_\phi = 0$$

$$R\frac{\partial M_{\theta\theta}}{\partial\theta} + \frac{\partial(rM_{\phi\theta})}{\partial\phi} + R M_{\theta\phi}\cos\phi - Rr Q_\theta = 0$$

$$M_{\theta\phi} - M_{\phi\theta} + R(N_{\theta\phi} - N_{\phi\theta}) = 0$$

where $r = R \sin\phi$ $\hspace{2cm}$ (I.28a-f)

In a similar manner the expressions for the middle surface
strains can also be modified. Those for ε_1, ε_2 & γ_{12} become:-

$$\varepsilon_\theta = \frac{1}{r}\frac{\partial u}{\partial\theta} + \frac{v}{r}\cos\phi + \frac{w}{R}$$

$$\varepsilon_\phi = \frac{1}{R}\frac{\partial v}{\partial\phi} + \frac{w}{R}$$

$$\gamma_{\theta\phi} = \frac{1}{r}\frac{\partial v}{\partial\theta} + \frac{1}{R}\frac{\partial u}{\partial\phi} - \frac{u}{r}\cos\phi \hspace{1cm} (I.29a-c)$$

and similarly for the changes in curvature.

When the shell is symmetrically loaded, all the derivatives
with respect to θ are dropped and many of the force and moment

components will vanish. The resulting equilibrium equations
can be written:-

$$\frac{d}{d\phi}(N_{\phi\phi}\sin\phi) - N_{\theta\theta}\cos\phi + Q_\phi\sin\phi + R\sin\phi.p_r = 0$$

$$\frac{d}{d\phi}(Q_\phi\sin\phi) - \sin\phi(N_{\theta\theta}+N_{\phi\phi}) + R\sin\phi.p = 0$$

$$\frac{d}{d\phi}(M_{\phi\phi}\sin\phi) - M_{\theta\theta}\cos\phi - R\sin\phi.Q_\phi = 0 \qquad \text{(I.30a-c)}$$

The middle surface strains become:-

$$\mathcal{E}_\theta = \frac{v}{R}\cot\phi + \frac{w}{R}, \qquad \mathcal{E}_\phi = \frac{1}{R}\frac{dv}{d\phi} + \frac{w}{R}, \qquad \gamma_{\theta\phi} = \frac{1}{R}\frac{du}{d\phi} - \frac{u}{R}\cot\phi$$

$$K_\theta = \frac{\cot\phi}{R^2}\left[v - \frac{dw}{d\phi}\right], \qquad K_\phi = \frac{1}{R^2}\left[\frac{dv}{d\phi} - \frac{d^2w}{d\phi^2}\right] \qquad \text{(I.31)}$$

and the force-strain and moment-strain equations may be
expressed:-

$$N_{\theta\theta} = \frac{Et}{1-v^2}\left[\mathcal{E}_\theta + v\mathcal{E}_\phi\right] = \frac{Et}{(1-v^2)R}\left[(v\cot\phi+w) + v\left(\frac{dv}{d\phi} + w\right)\right]$$

$$N_{\phi\phi} = \frac{Et}{1-v^2}\left[\mathcal{E}_\phi + v\mathcal{E}_\theta\right] = \frac{Et}{(1-v^2)R}\left[\left(\frac{dv}{d\phi} + w\right) + v(v\cot\phi+w)\right]$$

$$M_{\theta\theta} = D\left[K_\theta + vK_\phi\right] = -\frac{D}{R^2}\left[\left(\frac{dw}{d\phi} - v\right)\cot\phi + v\frac{d}{d\phi}\left(\frac{dw}{d\phi} - v\right)\right]$$

$$M_{\phi\phi} = D\left[K_\phi + vK_\theta\right] = -\frac{D}{R^2}\left[\frac{d}{d\phi}\left(\frac{dw}{d\phi} - v\right) + v\left(\frac{dw}{d\phi} - v\right)\cot\phi\right] \qquad \text{(I.32)}$$

In the first instance REISSNER gave the membrane solutions
for the state of stress and displacement in a shell under sym-
metrical and unsymmetrical loading. Neglecting the moment
effects and the difficulties associated with the boundary, the
cases dealt with are essentially statically determinate, since
a neglect of the moment terms leads to neglect of the normal
shearing forces Q_ϕ. Such analyses describe the stresses in a
shell satisfactorily if the boundary conditions are those which
can be fulfilled by the membrane forces. The membrane or
momentless shell must be free from external edge loading in the
form of transverse shearing stresses and bending moments and

thus w and $\frac{d\omega}{d\phi} \neq 0$ at the edge.   When the boundary conditions
are not those which the membrane forces can fulfil it becomes
necessary to apply to the edge of the shell additional forces
$N_{\phi\phi}$, Q_ϕ, and moments $M_{\phi\phi}$.   This 'mixed state' is invariably
confined to the edge regions of the shell, owing to its rapid
decay, and for that reason H. REISSNER called it the 'edge
effect.'   However, such a state of stress may occur within
the shell where there is an abrupt change of the curvature of
the shell or its thickness.

Thus REISSNER in tackling the general spherical shell
under the action of a symmetrical load, resolved the stress
problem into a membrane stress and displacement analysis, and
a bending theory analysis for the determination of the edge
forces required to satisfy the initial conditions of restraint
of the shell.   This is equivalent to stating that the non-
homogeneous solution of the differential equations (due to
surface loads) may be approximated by a corresponding membrane
solution.   This simplifies considerably the general problem
since it is reduced to a solution of the membrane case and a
consideration of the homogeneous equation - which essentially
represents the edge loaded shell.

In the following, solutions of the homogeneous equation
and the particular solutions of the general non-homogeneous
equation are discussed for both the axisymmetrically and
asymmetrically loaded shell.

(1)   The Axisymmetrically Loaded Shell - Homogeneous Solution

When the surface loads are removed the problem is esentially one of edge loading of a shell.   Credit again must go to H. REISSNER[20] who by a choice of the dependent variables expressed the behaviour of a spherical shell under axisymmetrical loading in terms of two ordinary second-order differential equations.   Utilising the equilibrium equations in the form eqt. I.30a-c with $p = p_r = 0$, and the middle surface strain values eqt. I.31 together with the force-strain and moment-strain equations I.32, he obtains the two governing equations:-

$$\Lambda^2 Q_\phi = \frac{d^2 K}{d\phi^2} + \frac{dK}{d\phi} \cot\phi - K(\cot^2\phi + \nu)$$

$$\Lambda^2 K = \frac{d^2 Q_\phi}{d\phi^2} + \frac{dQ_\phi}{d\phi} \cot\phi - Q_\phi(\cot^2\phi - \nu)$$

$$\text{(I.33a-b)}$$

where $\Lambda^4 = 12(1-\nu^2)\dfrac{R^2}{t^2}$ and $K = \dfrac{EtR}{\Lambda^2} K_\theta \tan\phi$

REISSNER suggested the possibility of an asymptotic method for their integration, based upon the work of BLUMENTHAL, and the introduction of new variables, namely $K\sqrt{\sin\phi}$ and $Q_\phi\sqrt{\sin\phi}$, which result in the disappearance of the first derivative. Expressions for K and Q_ϕ are given by REISSNER in terms of an exponential function of Λ, (which is related to the shell thickness) and a series in powers of the ratio of shell thickness to a representative dimension of the shell.   The method will be outlined in a later section.

The work of H. REISSNER was soon followed by that of . MEISSNER[21] who generalized REISSNER's result to accommodate symmetrical deformations of shells of revolution generated by

curves of constnat radii of curvature. Of particular interest
to this review is the reduction of the general fourth-order
differential equation, which results from REISSNER's equations
I.33a,b to a single second order differential equation.

MEISSNER used the more general forms of the equations of
equilibrium, etc. (eqts. I.30 to I.32), which involve the two
radii of curvature R_1 and R_2, and introduced two new variables:-

$$V = Q_\phi R_2 \qquad and \qquad U = R_2 K_\theta \tan\phi$$

By a method similar to REISSNER the two governing equations are
obtained for a shell of constant thickness t:-

$$L(V) + \nu V = Et\, UR.$$
$$L(U) - \nu U = -V\frac{R_1}{D} \qquad\qquad (I.34)$$

where $L(\ldots) = \dfrac{1}{\sin\phi} \cdot \dfrac{d}{d\phi}\left[\dfrac{R_2 \sin\phi}{R_1} \dfrac{d(\ldots)}{d\phi}\right] - \dfrac{R_1}{R_2}\cot^2\phi\,(\ldots)$

From these equations it is possible to obtain a fourth-
order differential equation for each of the two unknowns.
Thus for V:-

$$L\left[\frac{L(V)}{R_1}\right] + \nu L\left(\frac{V}{R_1}\right) - \frac{\nu}{R_1} L(V) - \nu^2\frac{V}{R_1} = -\frac{R_1 Et}{D} V \qquad (I.35)$$

Assuming that the radius of curvature R_1 is a constant, i.e.
the meridian is a circle (which is true for the sphere, the
torus and the cone) then:- $\quad L\left(\dfrac{V}{R_1}\right) = \dfrac{1}{R_1} L(V)$

Thus eqt. I.35 is simplified to:-

$$L.L(V) + 4\chi^4 V = 0 \qquad\qquad (I.36)$$

where $\quad \chi^4 = 3(1-\nu^2)\dfrac{R_1^2}{t^2} - \dfrac{\nu^2}{4}$

An analogous equation holds for U.

Eqt. I.36 separates into the conjugate second-order equations

$$L(V) + 2j\chi^2 V = 0$$
$$L(V) - 2j\chi^2 V = 0 \qquad\qquad (I.37a,b)$$

MEISSNER pointed out that the solutions of eqt.I.37b are complex conjugates of the solution of eqt.I.37a, so that one can essentially restrict oneself to the solution of eqt.I.37a. For the spherical shell eqt.I.37a further simplifies using $V = Q_\phi R_1$

to :-
$$L(Q_\phi) + 2j\chi^2 Q_\phi = 0$$

where $L(...) = \frac{d^2(...)}{d\phi^2} + \frac{d(...)}{d\phi}\cot\phi - (...)\cot^2\phi$

i.e. $\quad \frac{d^2 Q_\phi}{d\phi^2} + \frac{dQ_\phi}{d\phi}\cot\phi - Q_\phi\cot^2\phi + 2j\chi^2 Q_\phi = 0$ (I.38)

In a later paper by MEISSNER[22] this work is extended to cover shells with thickness which varies with ϕ.

The solution of eqt.I.38, which constitutes the solution of the homogeneous problem, has been tackled in a variety of ways;

-Hypergeometric Series. It was MEISSNER[21] in his earlier paper who demonstrated that eqt.I.38 could be solved exactly by a hypergeometric series. By introducing new variables,

$$x = \sin^2\phi \quad and \quad Q_\phi = z\sin\phi$$

equation I.38 becomes :-

$$x(x-1)\frac{d^2 z}{dx^2} + \left(\frac{5}{2}x - 2\right)\frac{dz}{dx} + \frac{1 \div 2j\chi^2}{4}z = 0 \qquad (I.39)$$

This is a hypergeometric equation with two solutions, one which

is regular :- $Z_a = 1 + \frac{3^2 - \delta^2}{16.1.2}x + \frac{(3^2 - \delta^2)(7^2 - \delta^2)}{16^2.1.2.2.3}x^2 + \cdots$ (I.40a)

where $\quad \delta^2 = 5 + 8j\chi^2$

and the other which has a singularity at $\phi = 0$:-

$$Z_b = Z_a \log x + \frac{1}{x}\varphi(x) \qquad\qquad (I.40b)$$

where $\varphi(x)$ is a power series that is convergent for $|x| < 1$.
The solution eqt.I.40b is not considered unless there is a hole at the top of the sphere. The real and imaginary parts of z_a (eqt.I.40a) are a set of two independent series solutions convergent for all values of x less than unity. Thus the

solution, for the closed shell, for Q_ϕ may be written:-

$$Q_\phi = z \sin \phi = (c_1 z_1 + c_2 z_2) \sin \phi$$

where C_1 and C_2 are arbitary constants.

A similar solution has been reached by FLÜGGE [5] using a slightly different transformation namely:-

$$x = \cos^2 \phi \qquad \text{and} \qquad Q_\phi = z \sin \phi$$

The resulting equation is a hypergeometric equation with two complex solutions whose real and imaginary parts are a set of four independent solutions. A linear combination of these i.e. z_1, z_2, z_3, z_4 having four arbitary constants C_1, C_2, C_3, C_4 is the general solution of the problem:-

$$Q_\phi = z \sin \phi = (c_1 z_1 + c_2 z_2 + c_3 z_3 + c_4 z_4) \sin \phi$$

The ease of application of this analysis depends on the rapidity of convergence of the series. This depends principally upon X. BOLLE [23] working under MEISSNER shows that for $X < 10$ the convergence of the series is satisfactory. The convergence of the series, however, becomes slower and more terms must be calculated as the ratio R/t increases- such a difficulty is a particular disadvantage for shallow shells. TIMOSHENKO [24] cites the calculation made by EKSTROM [25] who, for $R/t = 62.5$ ($X \approx 10.1$), finds it necessary to consider not less than 18 terms of the series.

FLÜGGE considers that it is practically impossible to apply his series to shells whose X is substantially greater than 5, and where the edge to be considered has a co-latitude angle ϕ of not less than $70°$. NOVOZHILOV [4] concludes that such efforts to obtain a mathematically exact solution are to a

great extent useless.   They are inconvenient to use in practice
and also inconsistent, since the basic assumptions of the
original equations involve errors of order t/R in comparison
with unity.   Hence there is little sence in retaining terms in
the solution of smaller order than t/R.

-Simplifications of the Homogeneous Differential Equation.   It
was BLUMENTHAL[26] in his classic paper on asymptotic integration
who examined the fundamental fourth-order differential equation
obtained from H.REISSNER's two simultaneous equations (I.33a,b).
In terms of Q_ϕ this equation can be written:-

$$\frac{d^4 Q_\phi}{d\phi^4} + \frac{2\cos\phi}{\sin\phi}\frac{d^3 Q_\phi}{d\phi^3} - \frac{3-\sin^2\phi}{\sin^2\phi}\frac{d^2 Q_\phi}{d\phi^2} + \frac{\cos\phi\,(3+2\sin^2\phi)}{\sin^3\phi}\frac{dQ_\phi}{d\phi} +$$

$$+ \left[(1-\upsilon^2)(1+12\frac{R^2}{t^2}) - \frac{3}{\sin^4\phi}\right]Q_\phi = 0 \qquad (I.41)$$

Introducing $\bar{z} = Q_\phi\sqrt{\sin\phi}$ eqt.I.41 becomes:-

$$\frac{d^4\bar{z}}{d\phi^4} + a_2\frac{d^2\bar{z}}{d\phi^2} + a_1\frac{d\bar{z}}{d\phi} + (b^4 + a_0)\bar{z} = 0 \qquad (I.42)$$

where $a_2 = -\dfrac{3}{2\sin^2\phi} + \dfrac{5}{2}$, $a_1 = \dfrac{3\cos\phi}{\sin^3\phi}$

$a_0 = -\dfrac{63}{16}\dfrac{1}{\sin^4\phi} + \dfrac{9}{8}\dfrac{1}{\sin^2\phi} + \dfrac{9}{16}$, $b^4 = (1-\upsilon^2)\left[1 + 12\dfrac{R^2}{t^2}\right]$

For thin shells R/t is a large number and b^4 is large in com-
parison with the other coefficients - provided of course that
the angle ϕ is not small.   Thus as an approximation eqt.I.42
can be written :- $\dfrac{d^4\bar{z}}{d\phi^4} + b^4\bar{z} = 0$ \qquad (I.43)
This equation is similar to that obtained in the investigation
of the symmetrical deformation of circular cylindrical shells.
A more usual form of eqt.I.43 is obtained when $b^4 = 4\rho^4$,

that is:- $\dfrac{d^4\bar{z}}{d\phi^4} + 4\rho^4\bar{z} = 0$ \qquad (I.44)

with a corresponding solution for Q_ϕ

$$Q_\phi = \frac{1}{\sqrt{\sin\phi}}\left[e^{\rho\phi}(C_1\cos\rho\phi + C_2\sin\rho\phi) + e^{-\rho\phi}(C_3\cos\rho\phi + C_4\sin\rho\phi)\right] \qquad (I.45)$$

For very thin shells, with large angle of opening a method

(I.1)

of GECKELER[27] is permissible.   This consists in modifying eqts.

I.34 as obtained by MEISSNER.   For the spherical shell these

may be written:-

$$\frac{d^2Q_\phi}{d\phi^2} + \frac{dQ_\phi}{d\phi} \cot\phi - Q_\phi(\cot^2\phi - v) = Et\, U$$

$$\frac{d^2U}{d\phi^2} + \frac{dU}{d\phi} \cot\phi - U(\cot^2\phi + v) = -Q_\phi \frac{R^2}{D} \qquad (I.46a,b)$$

For a thin shell Q_ϕ and U will be damped out rapidly, with the

same oscillatory character as eqt. I.45, as the distance from

the edge increases.   Thus since ρ of eqt. I.45 is large, the

first derivative of the function Q_ϕ is large compared with the

function itself, and the second derivative large in comparison

with the first.   Thus eqt. I.46a,b may be written:-

$$\frac{d^2Q_\phi}{d\phi^2} = Et\, U$$

$$\frac{d^2U}{d\phi^2} = -Q_\phi \frac{R^2}{D} \qquad (I.47a,b)$$

eliminating U from these:- $\dfrac{d^4Q_\phi}{d\phi^4} + 4\lambda^4 Q_\phi = 0$

where $\lambda^4 = 3(1-v^2)\left(\frac{R}{t}\right)^2$

The general solution for Q_ϕ is:-

$$Q_\phi = e^{\lambda\phi}\left[C_1 \cos\lambda\phi + C_2 \sin\lambda\phi\right] + e^{-\lambda\phi}\left[C_3 \cos\lambda\phi + C_4 \sin\lambda\phi\right] \qquad (I.48)$$

In an effort to improve GECKELER's work, HETÉNYI[28]

considered not only the second derivatives in eqts. 1.46a,b but

also the first derivatives.   He introduced the variables

$U = \dfrac{\bar{U}}{\sqrt{\sin\phi}}$ and $Q_\phi = \dfrac{\bar{Q}_\phi}{\sqrt{\sin\phi}}$ into eqt. I.46 resulting in the

disappearance of the first derivatives.   Neglecting $\bar{Q}_\phi$ and $\bar{U}$

in the left hand sides the equations have the simplified form:-

$$\frac{d^2\bar{Q}_\phi}{d\phi^2} = +Et\, \bar{U}$$

$$\frac{d^2\bar{U}}{d\phi^2} = -\frac{R^2}{D} \bar{Q}_\phi \qquad (I.49)$$

which are of similar form to those of eqts. I.47a,b.   Thus the

solution for Q_ϕ will be as follows:-

$$Q_\phi = \frac{1}{\sqrt{\sin\phi}}\left[e^{\lambda\phi}(C_1\cos\lambda\phi + C_2\sin\lambda\phi) + e^{-\lambda\phi}(C_3\cos\lambda\phi + C_4\sin\lambda\phi)\right] \qquad (I.50)$$

where $\qquad \lambda^4 = 3(1-v^2)\left(\frac{R}{t}\right)^2$

This equation (I.50) is identical to that obtained as BLUMENTHAL's

first approximation (eqt.I.45), since in practice $\rho \equiv \lambda$

The above approximate equation was also obtained by HETÉNYI

in a later publication[29]. He analysed the spherical shell

loaded symmetrically round the edge by reducing it to the

problem of flexure of elastically supported curved beams

consisting of meridional elements of the shell of variable width.

The governing differential equation is as follows:-

$$\frac{d^4Q_\phi}{d\phi^4} + \frac{2\cos\phi}{\sin\phi}\frac{d^3Q_\phi}{d\phi^3} - \frac{1+\sin^2\phi}{\sin^2\phi}\frac{d^2Q_\phi}{d\phi^2} + \frac{\cos\phi}{\sin\phi}\frac{dQ_\phi}{d\phi} + 12(1-v^2)\frac{R^2}{t^2}Q_\phi = 0 \qquad (I.51)$$

It is noted that the third and fourth derivatives of eqts. I.41

and I.51 are the same. Thus when making the substitution

$Q_\phi = \frac{\bar{Q}_\phi}{\sqrt{\sin\phi}}$, and neglecting the lower derivatives, first and second,

the following equation results:-

$$\frac{d^4\bar{Q}_\phi}{d\phi^4} + 4\lambda^4\bar{Q}_\phi = 0 \qquad (I.52)$$

where $\qquad \lambda^4 = 3(1-v^2)\left(\frac{R}{t}\right)^2$

The solution of this equation is eqt. I.50.

In ref.(28) HETÉNYI compares his own and GECKELER's

approximations with the hypergeometric series method of MEISSNER

for the case of a built in spherical cap loaded with uniformly

distributed radial pressure. Graphs of meridional bending

moment and circumferential force, with co-latitudinal angle ϕ,

are presented by HETÉNYI, and shown in Fig. I.3, showing that for

the particular case considered the approximation is completely

valid. HETÉNYI states that the ratio of computing work for
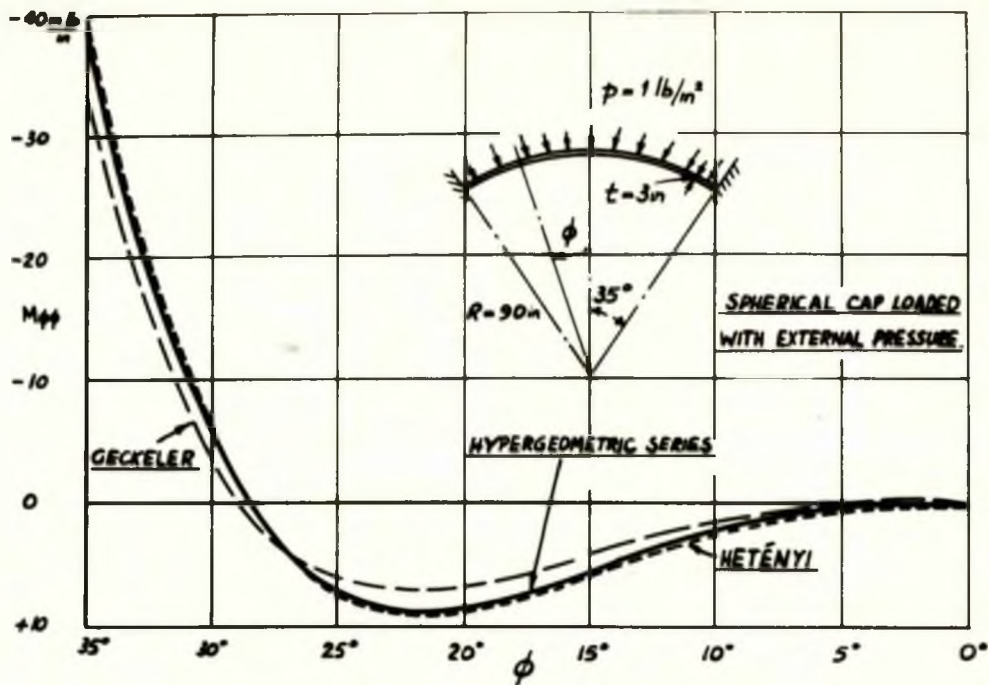
MERIDIONAL BENDING MOMENT ~ COLATITUDINAL ANGLE ϕ
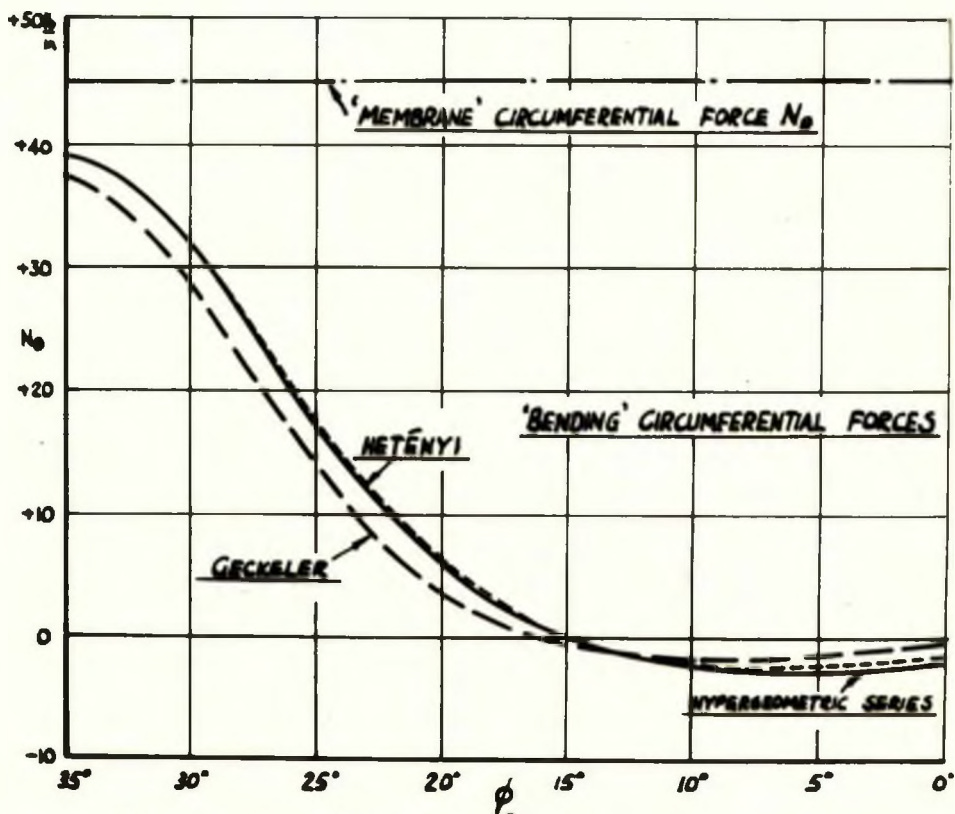
CIRCUMFERENTIAL DIRECT FORCES ~ COLATITUDINAL ANGLE ϕ.

FIG. I.3 COMPARISON BETWEEN HYPERGEOMETRIC SERIES, GECKELER, AND HETÉNYI SOLUTIONS.

GECKELER's, his own and the hypergeometric series was 1:2:20,
which is in line with the remark made earlier in connection
with the hypergeometric series.   Both the GECKELER and HETÉNYI
approximations fail to predict satisfactory results, however,
when the parameter $\frac{\cot\phi}{\lambda\sqrt{2}}$ is large.   Such occurs when ϕ is small
(i.e. at points close to the top of the shell) or when λ is
small, i.e. for thick shells.   It is also seen that the
parameter will be large for shallow shells, since the assumption
of shallowness is r/R small compared with unity.   Therefore,
the approximations are inapplicable to the case of the shallow
dome.

-Bessel Function Solution.   In 1930, GECKELER[30] developed a
Bessel function solution applicable to the shallow dome.   In
the vicinity of the pole $\phi = 0$, $\cot\phi$ may be expanded into:-

$$\cot\phi = \frac{1}{\phi} - \frac{\phi}{3} - \frac{\phi^3}{45} -$$

If ϕ is small enough $\cot\phi = \frac{1}{\phi}$.   Thus the governing equation
I.38 in Q_ϕ can be written:- $\dfrac{d^2 Q_\phi}{d\phi^2} + \dfrac{1}{\phi}\dfrac{dQ_\phi}{d\phi} - \dfrac{1}{\phi^2}Q_\phi + 2j\chi^2 Q_\phi = 0$ (I.53)
Introducing a new independent variable $\xi = \chi\sqrt{2j}\phi$ eqt. I.53 assumes
a standard Bessel form:- $\dfrac{d^2 Q_\phi}{d\xi^2} + \dfrac{1}{\xi}\dfrac{dQ_\phi}{d\xi} + (1 - \dfrac{1}{\xi^2})Q_\phi = 0$ (I.54)
The solution may be written in terms of the first derivatives
of the Kelvin function with a real variable - $\sqrt{2}\chi\phi$, yielding
a final solution for Q_ϕ as follows:-

$$Q_\phi = A_1\,\mathrm{ber}'\sqrt{2}\chi\phi + A_2\,\mathrm{bei}'\sqrt{2}\chi\phi + B_1\,\mathrm{ker}'\sqrt{2}\chi\phi + B_2\,\mathrm{kei}'\sqrt{2}\chi\phi \qquad (I.55)$$

the primes indicating the derivative with respect to ϕ.

A similar solution may be obtained by using functions
obtained by SCHLEICHER[31].   This is mentioned by TIMOSHENKO[24]
and has been used more recently in the examination of the

spherical shell by ESSLINGER[32] and PENNY[33]. The solution
may be written:- $Q_\phi = C_1\psi_1' + C_2\psi_2' + C_3\psi_3' + C_4\psi_4'$ (I.56)
where again the prime indicates the first derivative with
respect to ϕ .   These functions ψ_1 , ψ_2 -- are Schleicher functions
and are tabulated by TIMOSHENKO[24] and HETÉNYI[29]. They are
found to be proportional to the Kelvin functions:-

$$\psi_1(z) = ber\, z , \quad \psi_2(z) = -bei\, z, \quad \psi_3(z) = -\frac{2}{\pi}kei\, z \quad \& \quad \psi_4(z) = -\frac{2}{\pi}ker\, z \quad (I.57a\text{-}d)$$

Thus apart from the values of the constants, which are obtained
from the boundary conditions of the problem, eqts. I.55 and I.56
are identical.   These solutions are, of course, valid for small
openings and the shallow shell problem.   PENNY[33] considers
that the theory is applicable for opening diameters less than
about one-third of the vessel diameter.

-Asymptotic Integration.   The possibility of expressing the
localized bending effects in a shell in terms of asymptotic
developments, in powers of the ratio of the shell thickness to
a representative dimension of the shell, was first suggested by
H. REISSNER[20] on the advice of BLUMENTHAL.   BLUMENTHAL[26]
obtained such developments for the case of a spherical shell of
constant thickness.   More recently the method has received
attention by several authors.   A recent paper by LECKIE[34] is
particularly relevant in respect of this review.   LECKIE solves
the homogeneous equation for spherical shells - eqt. I.38 -
using two different methods of asymptotic integration, the
classical method as used by HILDEBRAND[35] and a method developed
by LANGER[36].

In the classical method the solution of eqt. I.38 is assumed

to be the product of a function describing oscillations, with
exponentially increasing or decreasing amplitude, and a series
of descending powers.   LECKIE takes this in the following form:-

$$Q_\phi = e^{x\delta} \sum_{n=0}^{\infty} Q_n x^{-n} \tag{I.58}$$

where δ, Q_o, Q_1 etc. are functions of ϕ.

The series eqt. I.58 is then substituted into the homogeneous
eqt. I.38 and by equating the co-efficients of x^2, x^1, x^o...
to zero, an infinite set of equations result.   Solving the
first three of these equations the following two-term series
solution is obtained for Q_ϕ :-

$$Q_\phi = \frac{e^{\pm(1-j)x\phi}}{\sqrt{\sin\phi}} \left[1 \pm \frac{1+j}{16x}(5\phi + 3\cot\phi) + \cdots \right] \tag{I.59}$$

When the R/t ratio is large and the shell edge is well
away from the pole, $\phi = 0$, then $(5\phi + 3\cot\phi)/16x \ll 1$ and only the
first term of the series need be used. Eqt I.59 may be written in
the now familiar form:-

$$Q_\phi = \frac{1}{\sqrt{\sin\phi}} \left[e^{x\phi}(C_1\cos x\phi + C_2\sin x\phi) + e^{-x\phi}(C_3\cos x\phi + C_4\sin x\phi) \right] \tag{I.60}$$

where $\qquad x^4 = 3(1-v^2)R^2/t^3 - v^2/4$

This is essentially that proposed as BLUMENTHAL's first approxi-
mation eqt. I.45 and HETÉNYI's eqt. I.48, since $\rho = \lambda = x$,
for large R/t ratios.   The expression, of course, suffers from
the restrictions imposed on these other solutions.

LANGER's asymptotic solution, however, does not suffer from
any of these difficulties, and is valid for all values of ϕ .
The differential equation I.38 is first transformed by means of
the substitution $\bar{\phi} = \sin\frac{\phi}{2}$ so that the co-efficients $\cot\phi$ and
$\cot^2\phi$ are expressed in polynomial form.   A further transformation

brings the equation into a form which may be compared with the <u>LANGER</u> equation, for which an asymptotic solution is available. For the shell problem this may be expressed in terms of Bessel functions of the first and second kinds, J_1 and Y_1 and of the first order. The final expression for Q_ϕ may be written:-

$$Q_\phi = \sqrt{\frac{\phi}{\sin\phi}} \left[A_1 ber'\sqrt{2}\chi\phi + A_2 bei'\sqrt{2}\chi\phi + B_1 ker'\sqrt{2}\chi\phi + B_2 kei'\sqrt{2}\chi\phi \right] \qquad (I.61)$$

This same result has also been obtained by <u>GALLETLY</u>[37] who normalized the homogeneous eqt. I.38 using the substitution $\bar{z} = Q_\phi \sqrt{\sin\phi}$, which of course is similar to that used by <u>H.REISSNER</u>. The resulting equation is:- $\frac{d^2\bar{z}}{d\phi^2} - \left(2j\chi^2 + \frac{3}{4}\cot^2\phi - \frac{1}{2}\right)\bar{z} = 0 \qquad (I.62)$ Two approximations are introduced into eqt.I.62, firstly the $\frac{1}{2}$ is neglected and also $1/\phi$ is substituted for $\cot\phi$. <u>GALLETLY</u> points out that the error in the approximation $\cot\phi \approx \frac{1}{\phi}$ will be small compared with the $2\chi^2$ term.

Thus:- $\frac{d^2\bar{z}}{d\phi^2} - \left(2j\chi^2 + \frac{3}{4\phi^2}\right)\bar{z} = 0 \qquad (I.63)$

The general solution of eqt. I.63 may be written:-

$$\bar{z} = \sqrt{\phi} \left[(C_1 + jD_1)(ber_1\sqrt{2}\chi\phi + jbei_1\sqrt{2}\chi\phi) + (C_2 + jD_2)(ker_1\sqrt{2}\chi\phi + jkei_1\sqrt{2}\chi\phi) \right] \qquad (I.64)$$

where C_1 , D_1 , C_2 , D_2 are arbitary constants.

Thus:- $Q_\phi = \sqrt{\frac{\phi}{\sin\phi}} \left[A bei_1\sqrt{2}\chi\phi + B ber_1\sqrt{2}\chi\phi + C kei_1\sqrt{2}\chi\phi + D ker_1\sqrt{2}\chi\phi \right]$

Expressing the first order Bessel and Kelvin functions in terms of the zero order functions, Q_ϕ can be further written:-

$$Q_\phi = \sqrt{\frac{\phi}{\sin\phi}} \left[A_1 ber'\sqrt{2}\chi\phi + A_2 bei'\sqrt{2}\chi\phi + B_1 ker'\sqrt{2}\chi\phi + B_2 kei'\sqrt{2}\chi\phi \right] \qquad (I.65)$$

which is identical to eqt. I.61.

It is of interest to note that when $\sqrt{\frac{\phi}{\sin\phi}} = 1$ i.e. for points near the pole eqts. I.61 or I.65 become:-

$$Q_\phi = A_1 ber'\sqrt{2}\chi\phi + A_2 bei'\sqrt{2}\chi\phi + B_1 ker'\sqrt{2}\chi\phi + B_2 kei'\sqrt{2}\chi\phi$$

which is the expression obtained by <u>GECKELER</u> by the assumption

$\cot \phi = \frac{1}{\phi}$ (eqt. I.55).

LECKIE[34] pointed out when discussing the two types of
asymptotic integration, that when $\sqrt{2}x\phi > 6$, ber$\sqrt{2}x\phi$, bei$\sqrt{2}x\phi$, etc
may be expressed by their asymptotic expressions.   If such
relationships are substituted into the LANGER - type form of
solution (eqt. I.61), the HETÉNYI type, or eqt. I.60, results.
Thus the HETÉNYI type may be considered satisfactory provided
$\phi > \frac{(3\sqrt{2})}{x}$ radians, i.e if R/t = 100, ϕ should be greater than 19°.
Actually McLACHLAN[38] and GALLETLY[37] state that when $\sqrt{2}x\phi > 10$,
the derivatives of ber, bei, etc. may be asymptotically expressed,
which gives $\phi > \frac{5\sqrt{2}}{x}$ radians for the minimum co-latitudinal angle.

-Discussion of the various types of solution.   In recent years
the asymptotic integration methods have been widely used in
preference to the more exact approaches of the Zurich school,
typified in the hypergeometric series, which is particularly
tedious for the shallow shell.   NOVOZHILOV[4] states in this
connection that the asymptotic solutions of shell theory are
accurate to within the same order of accuracy as the basic shell
equations.   It is thus pointless attempting to obtain more
accurate solutions.   The best asymptotic solutions are valid
over the entire shell and are applicable to the shallow shell.
They are obtained in closed form solution by the LANGER-type
technique, the papers of LECKIE[34,39] and GALLETLY[37] being
examples of the method.   However, for shells with a large opening,
the HETÉNYI solution, which is essentially the first term of the
asymptotic solution, is thought to be adequate, though as explained
earlier this solution is not valid for the shallow shell.

The Axi-symmetrically Loaded Shell- The Particular Integral.

It was H.REISSNER[20] who first suggested that the stress problem be resolved into the membrane and bending solutions, implying that the particular solution of the non-homogeneous equation be taken as the membrane solution. MEISSNER[21], however, presents certain particular solutions and where these are not availabe advocates a solution of the non-homogeneous system of equations. For the symmetrically loaded spherical shell this matter is discussed by FLÜGGE[5] in his recent book. He obtains the non-homogeneous equation in terms of Q_ϕ and its derivatives and the surface loadings p and p_r. Four possible loadings are then considered, internal pressure, self weight, hydrostatic pressure and centrifugal force. In all cases except the first where $Q_\phi \equiv 0$ there appears in the denominator of the expression for Q_ϕ, a term containing χ^4. For thin shells χ^4 is large, since it contains $(R/t)^2$, and thus the transverse resultant shear force Q_ϕ is very small compared with the normal forces $N_{\phi\phi}$ and $N_{\theta\theta}$. Thus, FLÜGGE concludes, the membrane solution, which assumes $Q_\phi \equiv 0$, is almost identical with a particular solution of the bending equation, justifying the general use, in spherical shells, of the membrane solutions in lieu of particular solutions of the complete bending theory or non-homogeneous equations.

HILDERBRAND[35] in his paper on asymptotic integration concludes that the approximation $Q_{\phi_P} = 0$ (where Q_{ϕ_P} is the value of Q_ϕ obtained from the particular solution) is acceptable if terms of order t^2/R^2 are to be neglected. A note of warning, however,

was given recently by GALLETLY and RADOK[40,41] who demonstrated the inadvisability of taking the membrane state as a particular solution for ellipsoidal and torispherical shells under the action of internal pressure.   Despite this, the approximation has been widely used[42, 32, 33, 43, 44].

NOVOZHILOV[4] comments that when the shell be of such a form, and with such surface loading that it is of a truly membrane type, i.e. a momentless shell, then the particular integral is exactly that of the membrane solution.   Thus the limitation imposed is that the state of stress caused by the surface loading should closely resemble that of the momentless shell.   In practice such is not realised and in the so called "membrane solution" there will exist membrane rotation and the corresponding "membrane moments."   HILDERBRAND[35] examines the order of these terms compared with the order of the terms obtained from the classical asymptotic integration of the homogeneous equation.   He concludes that as long as only the leading term is retained in the homogeneous developments (as in the HETÉNYI derivation) one should, for consistency, neglect the membrane rotation as well as the corresponding membrane moments, and when the loading intensity does not vary appreciably over a distance of the order $\sqrt{Rt}$.   When membrane rotation is important then at least the next term should be retained in the homogeneous development.   It should be noted that such a condition is automatically fulfilled in the closed form solution of the LANGER-type.

The relative importance of the membrane rotation and moment increases in the case of shallow shells, as is shown in the investigations to follow.

(ii) The Asymmetrically Loaded Shell

As mentioned earlier it was H. REISSNER[20] who examined the asymmetrically loaded shell, and solved the membrane problem. He introduced membrane resultant forces in the form of a Fourier series:-

$$N_{\phi\phi} = \Sigma N_{\phi\phi_n} \cos n\theta, \quad N_{\theta\theta} = \Sigma N_{\theta\theta_n} \cos n\theta, \quad N_{\phi\theta} = \Sigma N_{\phi\theta_n} \sin n\theta$$

and a similar series for the external loading, into the governing membrane equations selected from eqts. I.28a-f. This reduces the partial second order differential equation to that of an ordinary second order differential equation. As in the axisymmetrical case the problem is usually considered in two parts, the homogeneous equation and the non-homogeneous solution or particular integral.

The Asymmetrically Loaded Shell - Homogeneous Equation

It was HAVERS[6] in 1935 who solved the general problem of the asymmetrical shell obtaining expressions for the displacements and resultant forces arising from the edge loading of a spherical cap. Three partial differential equations for the displacements u, v and w were derived from the force and moment-strain equations. HAVERS then uses a transformation, employed by VAN DER NEUT[45] in the stability analysis of spherical shells, namely:-

$$u = \frac{\partial \Gamma}{\partial\theta \sin\phi} \quad , \qquad v = \frac{\partial \Theta}{\partial\phi}$$

$$(I.66a,b)$$

(I.1)

The differential operator H(y) was introduced:-

$$H(y) = \frac{\partial^2 y}{\partial \phi^2} + \frac{\partial y}{\partial \phi} \cot \phi + 2y + \frac{\partial^2 y}{\partial \theta^2 \sin^2 \phi} \tag{I.67a}$$

together with:-

$$\Pi = \Gamma - \Theta \qquad \text{and} \qquad \omega = \frac{\partial \Pi}{\partial \phi \sin \phi} \tag{I.67b,c}$$

By this means the problem of the edge loaded shell was reduced

to the solution of two basic equations:-

$$H(\omega) = 0$$

and $\quad H.H(T) - 2H(T) + (1-v^2)\frac{1+k}{k} T = 0 \tag{I.68a,b}$

where $\quad T = \Gamma - \omega + \frac{1}{2}\frac{\partial \omega}{\partial \phi} \sin \phi \tag{I.68c}$

and $\quad k = t^2/_{12R^2}$

Equation I.68b may be split into two equations:-

$$H(T) = S_1 T \qquad \text{and} \qquad H(T) = S_2 T \tag{I.69a,b}$$

inserting these into eqt. I.68b a quadratic equation with the

following roots:-

$$S_1 = 1 + \sqrt{1 - (1-v^2)\frac{1+k}{k}} \quad , \quad S_2 = 1 - \sqrt{1 - (1-v^2)\frac{1+k}{k}} \tag{I.70a,b}$$

is obtained.

Re-arranging eqt. I.70a,b and putting $\quad 4x^4 = 12(1-v^2)\frac{R^2}{t^2} - v^2$

$$S_1 = 1 + 2jx^2 \quad , \qquad S_2 = 1 - 2jx^2$$

Thus eqt. I.69a,b become:-

$$H(T) = (1+2jx^2)T \quad , \qquad H(T) = (1-2jx^2)T \tag{I.71a,b}$$

Let $R(\theta,\phi)$ be a solution of equation I.71a and $\bar{R}(\theta,\phi)$ a solution

of eqt. I.71b, so that R and $\bar{R}$ are conjugate complex numbers.

Thus from eqts. I.71a,b,

$$\frac{\partial^2 R}{\partial \phi^2} + \frac{\partial R}{\partial \phi} \cot \phi + (1-2jx^2)R + \frac{\partial^2 R}{\partial \theta^2 \sin^2 \phi} = 0$$

$$\& \quad \frac{\partial^2 \bar{R}}{\partial \phi^2} + \frac{\partial \bar{R}}{\partial \phi} \cot \phi + (1+2jx^2)\bar{R} + \frac{\partial^2 \bar{R}}{\partial \theta^2 \sin^2 \phi} = 0 \tag{I.72a,b}$$

The four solutions of equations I.72a,b are of an oscillatory nature decaying with increasing distance from the edge. HAVERS solved these equations by an asymptotic method similar in form to that of BLUMENTHAL[26]. The approach, however, is not valid for the case of the shallow dome. This difficulty has been overcome in the recent paper by LECKIE[39] who solves both the axisymmetrically and asymmetrically edge loaded spherical shell using the LANGER-type asymptotic technique, ref. 36.

In addition to the oscillatory solution obtained from eqt.I.69a,b the governing eqt. I.68b is also satisfied by the solution $T = 0$. This leads to $H(w) = 0$, i.e.

$$\frac{\partial^2 w}{\partial \phi^2} + \frac{\partial w}{\partial \phi} \cot \phi + 2w + \frac{\partial^2 w}{\partial \theta^2 \sin^2 \phi} = 0$$

Separating the variables by $w = w_n(\phi) \cos n\theta$

$$\frac{d^2 w_n}{d\phi^2} + \frac{dw_n}{d\phi} \cot \phi + w_n \left(2 - \frac{n^2}{\sin^2 \phi}\right) = 0 \qquad (I.73)$$

The resulting solutions of this equation are found to be exactly those of the membrane normal displacement w for the edge loaded shell, together with an inextensional deformation. Using this value of w_n the values of the other displacements can be determined. Here again these are found to consist of the corresponding membrane displacement for the edge loaded spherical shell together with an inextensional deformation. FLÜGGE comments on this point that it must not be concluded that the above is the case for any shell of revolution, but it may be expected that they will come very close to exact solutions if the middle surface is not too different from a sphere. A paper by FLÜGGE and LECKIE[46] on the shell of

(I.1)

revolution is interesting in this respect.

The general solution to the problem of the edge loaded spherical shell is, therefore, the sum of the following three effects:-

(1) <u>Membrane Displacement</u> - giving rise to membrane resultant forces, and to small 'membrane moments' of significance in the region of the pole (see p.43)

(2) <u>Inextensional Deformations</u> - these deformations occur when the strains ε_θ, ε_ϕ, $\gamma_{\phi\theta}$ and hence the membrane resultant forces are all zero. When the system is:-

(a) axisymmetrical (i.e. $n = 0$), these deformations can be conveniently taken as zero by a suitable choice of reference axis.

(b) asymmetrical of the first harmonic ($n = 1$), they represent two rigid body rotations and,

(c) asymmetrical and $n > 2$, they are true displacements yielding zero values of membrane resultant forces, and actual values of the resultant moments giving rise to inextensional bending stresses. It is noted that such deformations do not occur on a complete sphere.

(3) <u>Oscillatory Solutions</u> - which consist of four solutions which decay in an oscillatory manner with increasing distance from the edge.

<u>HAVERS</u> expressed the displacements u, v and w together with the membrane resultant forces and resultant moments in terms of

48.

these solutions which are valid for all values of ϕ. These general expressions were used by LECKIE[39] (in the paper already referred to on p.38) in dealing with two cases, namely the axisymmetric $n = 0$ and asymmetrical of $n = 1$ loading. In obtaining the oscillatory solutions the variables of eqts. I.72a,b are separated by taking R and $\bar{R}$ in the form:-

$$R = R_n(\phi)\cos n\theta \quad , \quad \bar{R} = \bar{R}_n(\phi)\cos n\theta$$

where R and $\bar{R}$ are complex conjugates.

Thus for $n = 0$ equation I.72a becomes:-

$$\frac{d^2R_0}{d\phi^2} + \frac{dR_0}{d\phi}\cot\phi + (1-2jx^2)R_0 = 0 \tag{I.74}$$

Differentiating with respect to ϕ eqt. I.74 can be written in the form of the basic equation for Q_ϕ used earlier (eqt. I.38) namely:-

$$\frac{d^3R_0}{d\phi^3} + \frac{d^2R_0}{d\phi^2}\cot\phi - \frac{dR_0}{d\phi}\cot^2\phi - 2jx^2\frac{dR_0}{d\phi} = 0 \tag{I.75}$$

where the first differential of R_0 is equivalent to Q_ϕ.

Thus using the LANGER technique

$$\frac{dR_0}{d\phi} = \sqrt{\frac{\phi}{\sin\phi}}\left[\bar{A}_1(ber'\sqrt{2}x\phi + jbei'\sqrt{2}x\phi) + \bar{B}_1(ker'\sqrt{2}x\phi + jkei'\sqrt{2}x\phi)\right]$$

similarly for $\bar{R}_0$:-

$$\frac{d\bar{R}_0}{d\phi} = \sqrt{\frac{\phi}{\sin\phi}}\left[\bar{A}_2(ber'\sqrt{2}x\phi - jbei'\sqrt{2}x\phi) + \bar{B}_2(ker'\sqrt{2}x\phi - jkei'\sqrt{2}x\phi)\right] \tag{I.76a,b}$$

From HAVERS' definition of the resultant shear Q_ϕ :-

$$\frac{Q_\phi R(1-v^2)}{Et} = \frac{dR}{d\phi} + \frac{d\bar{R}}{d\phi} \quad , \qquad Q_\phi \text{ can be written:-}$$

$$Q_\phi = \frac{Et}{R(1-v^2)}\left[\sqrt{\phi/\sin\phi}\left(A_1 ber\sqrt{2}x\phi + A_2 bei\sqrt{2}x\phi + B_1 ker\sqrt{2}x\phi + B_2 kei\sqrt{2}x\phi\right)\right] \tag{I.77}$$

It is seen that apart from the value of the constants A_1, A_2 -- this equation is the same as obtained by LECKIE earlier (eqt. I.61). Using eqt. I.76a,b the values of the resultant forces and moments can be obtained.

For $n = 1$ eqt. I.72a becomes:-

$$\frac{d^2R_1}{d\phi^2} + \frac{dR_1}{d\phi}\cot\phi - R_1\cot^2\phi - 2jx^2R_1 = 0 \tag{I.78}$$

(I.1)

Comparing this with eqt. I .75, <u>LECKIE</u> notes that $R_1 = \dfrac{dR_0}{d\phi}$

Hence $R_1 = \sqrt{\dfrac{\phi}{\sin\phi}}\left[\bar{A}_1(ber'\sqrt{2}\chi\phi + j\,bei'\sqrt{2}\chi\phi) + \bar{B}_1(ker'\sqrt{2}\chi\phi + j\,kei'\sqrt{2}\chi\phi)\right]$

and $\quad \bar{R}_1 = \sqrt{\phi/\sin\phi}\left[\bar{A}_2(ber'\sqrt{2}\chi\phi - j\,bei'\sqrt{2}\chi\phi) + \bar{B}_2(ker'\sqrt{2}\chi\phi - j\,kei'\sqrt{2}\chi\phi)\right]$ $\quad$ (I.79a,b)

By using the general expressions of <u>HAVERS</u> the oscillatory
edge values may be stated - these are given in Chapter II of the
thesis-and are valid for all values of ϕ . <u>LECKIE</u> shows that
these solutions may be simplified when ϕ is large, using the
asymptotic expansions of the Kelvin functions. For the axi-
symmetric case these reduce to the <u>HETÉNYI</u> form, a fact already
observed in his earlier paper (ref. 34). For the same range
of ϕ , <u>LECKIE</u> finds that the solutions for the asymmetric case
(n = 1) bear a striking resemblance to the <u>HETÉNYI</u> solution for
the axisymmetric case, namely:-

$$v_0 = v_1 \,, \quad w_0 = w_1, \quad N_{\phi\phi_0} = N_{\phi\phi_1}, N_{\theta\theta_0} = N_{\theta\theta_1}, \; M_{\phi\phi_0} = M_{\phi\phi_1} \text{ and } Q_{\phi_0} = Q_{\phi_1}$$

<u>LECKIE</u> further presents the membrane solutions -
displacements, membrane resultant forces and resultant moments -
for the case of the first harmonic (or moment and tangential
shear force loading).

A study of the <u>higher harmonics</u>, $n \geqslant 2$ has recently been
carried out by <u>LECKIE</u> and <u>PENNY</u>[47]. Three methods of
solutions of the homogeneous equations are discussed by these
authors and the results compared graphically.

In the first case a rigorous solution is obtained by use
of the <u>LANGER</u>-technique of asymptotic integration. The results
are expressed in terms of Kelvin functions of the n'th order
and requiring the use of a digital computer for their solution.

Secondly, a simplified asymptotic solution, suitable for small values of n is presented, which in fact is that given earlier for $n = 0$ and $n = 1$, and valid for all values of ϕ . For the higher harmonics these solutions are valid provided ϕ is small enough, but the range of ϕ decreases as n increases.

A third solution known as the 'Constant Edge Angle Solution' is also presented. This solution is of the <u>AAS JACOBSEN</u>[48] type, its essence being that the edge bending solutions die out very rapidly. Thus the value of the $\sin^2\phi$ may be replaced by $\sin^2\phi_0$ where ϕ_0 is the edge value of the co-latitudinal angle. From the results it is seen that these solutions give satisfactory results, when compared with the rigorous solutions, for all values of ϕ_0 provided $n \geqslant 5$. Even when $n = 0$, the results are satisfactory for the limits $10° < \phi_0 < 90°$.

<u>Singularity Conditions</u> - <u>HAVERS</u>[6] pointed out that the poles $\phi = 0$ and $\phi = \pi$ are singular points, i.e. points of infinite stress or displacement, of the governing differential equation. It is, therefore, possible by obtaining expressions for the total displacements in the vicinity of the pole $(\phi = 0)$ and applying continuity conditions at this point, to determine values of the constants inherent in the force and moment expressions. In this way <u>LECKIE</u> presents the solutions for the point radial load, the point tangential load and the point moment applied at the crown or pole, $\phi = 0$. Such loading cases on the closed shell can be dealt with by these essentially edge loading equations since $p = p_r = p_\theta = 0$ is always satisfied and the governing differential equations are always homogeneous.

(I.1)

The Asymmetrically Loaded Shell - The Particular Integral

Similar remarks can be made in regard to the particular integral of the asymmetrical case as was previously made for the axisymmetrical, namely, that for the spherical shell the membrane solution can be assumed to approximate to the particular integral of the non-homogeneous equation.

(iii) 'Numerical Methods' of Analysis of the General Shell

A very brief comment will be made on the 'numerical methods' aspect of solving the above shell equations.   It was PASTERNAK[49] in 1926 who applied the method of finite difference equations to the solutions of H. REISSNER's differential equations for the shell symmetrically loaded at the edge.   However, owing to the task of solving the large system of algebraic equations resulting from a finite-difference formulation of the problem, the method does not appear to have been widely used.   With the increasing availability of electronic computers, it is now possible to re-consider the matter.

In a recent paper PENNY[50] discusses this subject and indicates that the popularity of the method in shell design is increasing.   Undoubtedly, the method avoids many of the difficulties associated with analytical methods, in that variations in thickness, material properties, loading or temperature can be adequately handled.   Even the approximation referred to above, whereby the membrane solution is regarded as a particular solution of the governing differential equations, is no longer necessary.

Another numerical procedure has been used by GALLETLY in a number of papers[40,51] where the differential equations of equilibrium have been integrated numerically, by use of the Runge-Kutta techniques, on a high-speed digital computer. A similar procedure is advocated by M.Le COCQ[52]

(b)   Shallow Shells

A further modification may be introduced into the general theory of shells based upon the shallowness of the shell.   Such may be defined by considering the variation of the distance z, which is that perpendicular distance from a plane XX to a point on the middle surface of the shell, Fig. I.4. A shell (or segment of a shell) is said to be shallow whenever z/L (L being a reference length) and its first partial derivatives are small in comparison with unity.   In the case of a shallow spherical shell or spherical cap (Fig. I.5) L may be taken as the radius of curvature and $z = \sqrt{R^2 - r^2} - (R - h)$, where h is the rise from XX to $\phi = 0$.
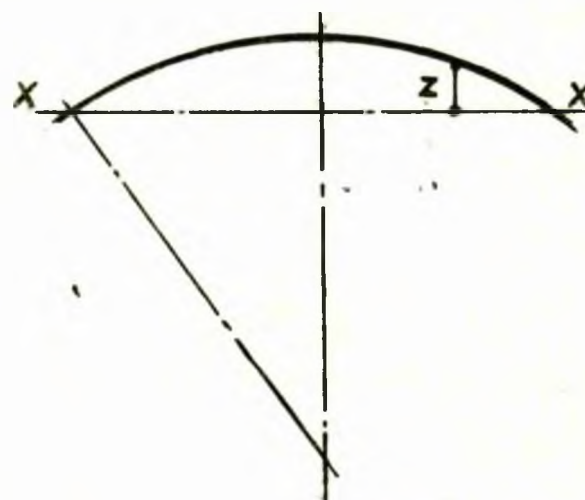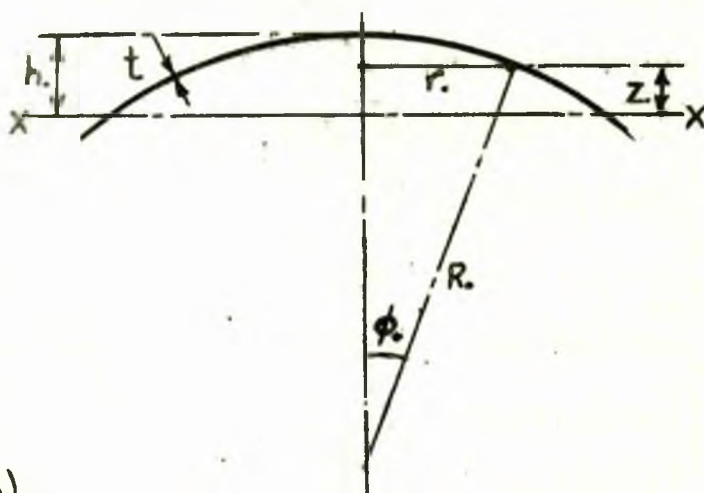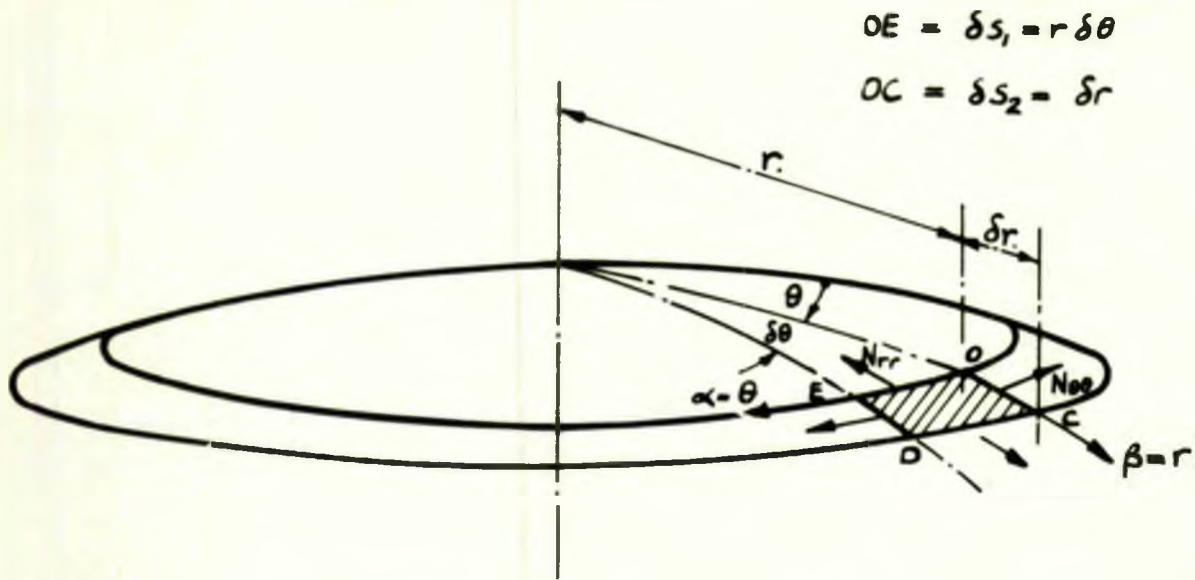
Fig. I.4 The Shallow Shell

Fig. I.5 The Shallow Spherical Shell

$$OE = \delta s_1 = r\,\delta\theta$$
$$OC = \delta s_2 = \delta r$$

SHALLOW SPHERICAL SHELL SHOWING ELEMENT OCDE
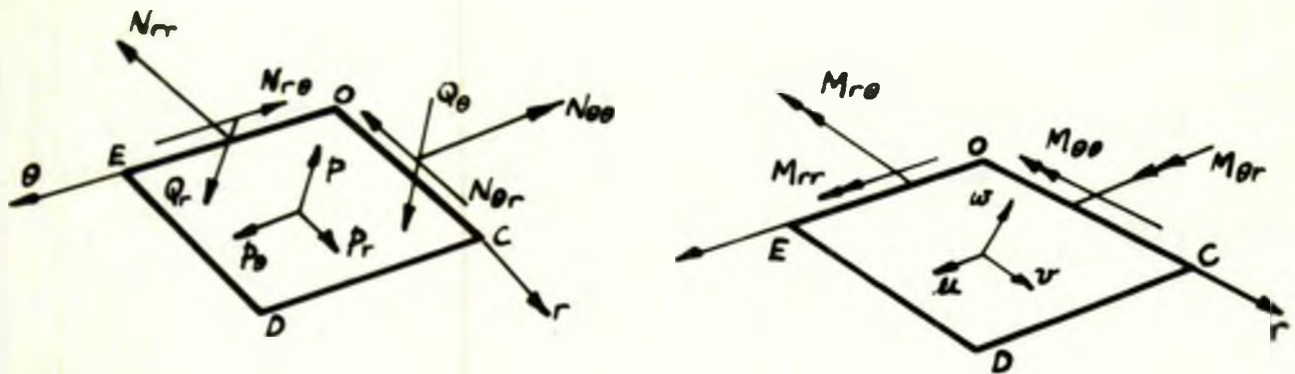
DETAILS OF FORCES AND MOMENTS ON ELEMENT OCDE

FIG I.6 NOMENCLATURE FOR THE SHALLOW SPHERICAL SHELL

(I.1)

The assumption of shallowness is expressed by the following order of magnitude relation, $\dfrac{dz}{dr} = -\dfrac{r}{\sqrt{R^2-r^2}} \approx -\dfrac{r}{R} = O(1)$ where $O(1)$ indicates for the significant values of r, that r/R is small compared with unity. In this connection, E. REISSNER[43] indicates that a segment will be called shallow if the ratio of its height to base diameter is less than say $\frac{1}{8}$. However, results obtained on the basis of this assumption will be applicable to shells which are not shallow, if the loads applied are such that the stresses are effectively restricted to shallow zones. As a consequence of the above approximation, the fundamental differential equations of LOVE's first approximation will simplify further. The curvilinear co-ordinate system α, β used by LOVE will now be modified to θ and r respectively where r is the distance from the apex of the shell measured in a plane parallel to the base plane (Fig. I.6). The resultant force terms are now written, $Q_{xz} = Q_\theta$, $Q_{yz} = Q_r$, $N_{xx} = N_{\theta\theta}$, $N_{yy} = N_{rr}$, $N_{xy} = N_{\theta r}$ and similarly for the moments. The external forces X, Y Z become p_θ, p_r and p respectively. The Láme parameters A and B are $A = r$ and $B = 1$.

Thus the equations of equilibrium, eqts. I.16a-f can be written:-

$$\frac{\partial(N_{\theta\theta})}{\partial\theta} + \frac{\partial(N_{r\theta}\cdot r)}{\partial r} + N_{\theta r} + \frac{r}{R}Q_\theta + r p_\theta = 0$$

$$\frac{\partial(N_{\theta r})}{\partial\theta} + \frac{\partial(N_{rr}\cdot r)}{\partial r} - N_{\theta\theta} + \frac{r}{R}Q_r + r p_r = 0$$

$$\frac{\partial(Q_\theta)}{\partial\theta} + \frac{\partial(Q_r\cdot r)}{\partial r} - \frac{r}{R}(N_{\theta\theta} + N_{rr}) + r p = 0$$

$$\frac{\partial(M_{\theta r})}{\partial\theta} + \frac{\partial(M_{rr}\cdot r)}{\partial r} - M_{\theta\theta} - r Q_r = 0$$

$$\frac{\partial(M_{\theta\theta})}{\partial\theta} + \frac{\partial(M_{r\theta}.r)}{\partial r} + M_{\theta r} - rQ_\theta = 0$$

$$M_{\theta r} - M_{r\theta} + (N_{\theta r} - N_{r\theta})R = 0$$

$$(I.80a-f)$$

The middle surface strain components eqts. I.4a-f may also be written in a simplified form:-

$$\varepsilon_\theta = \frac{1}{r}\frac{\partial u}{\partial\theta} + \frac{v}{r} + \frac{w}{R}$$

$$\varepsilon_r = \frac{\partial v}{\partial r} + \frac{w}{R}$$

$$\gamma_{r\theta} = \frac{1}{r}\frac{\partial v}{\partial\theta} + \frac{\partial u}{\partial r} - \frac{u}{r}$$

$$K_\theta = -\frac{1}{r}\frac{\partial}{\partial\theta}\left(\frac{1}{r}\frac{\partial w}{\partial\theta} - \frac{u}{R}\right) - \frac{1}{r}\left(\frac{\partial w}{\partial r} - \frac{v}{R}\right)$$

$$K_r = -\frac{\partial}{\partial r}\left(\frac{\partial w}{\partial r} - \frac{v}{R}\right)$$

$$K_{r\theta} = -\frac{1}{r}\left(\frac{\partial^2 w}{\partial\theta.\partial r} - \frac{1}{r}\frac{\partial w}{\partial\theta}\right) + \frac{1}{R}\left(\frac{\partial u}{\partial r} - \frac{u}{r}\right) + \frac{1}{R}\left(\frac{1}{r}\frac{\partial v}{\partial\theta}\right) \qquad (I.81a-f)$$

The force-strain and moment-strain equations are those of LOVE's first approximation, eqts. I.13a-d, I.15a-d, which may be written:-

$$N_{\theta\theta} = \frac{Et}{(1-\nu^2)}\left[\varepsilon_\theta + \nu\varepsilon_r\right] , \qquad N_{rr} = \frac{Et}{(1-\nu^2)}\left[\varepsilon_r + \nu\varepsilon_\theta\right]$$

$$N_{r\theta} = Gt\,\gamma_{r\theta}$$

$$M_{\theta\theta} = D\left[K_\theta + \nu K_r\right] , \qquad M_{rr} = D\left[K_r + \nu K_\theta\right]$$

$$M_{r\theta} = (1-\nu)D\,K_{r\theta} \qquad\qquad (I.82a-f)$$

E. REISSNER[43] has indicated that the equations for K_θ, K_r and $K_{r\theta}$ (eqts. I.81d-f) may be further modified since the normal deflection w when it occurs at all, will be large

compared with u and v.   Thus K_θ, K_r and $K_{r\theta}$ may be written:-

$$K_\theta = -\frac{1}{r}\frac{\partial w}{\partial r} - \frac{1}{r^2}\frac{\partial^2 w}{\partial \theta^2}$$

$$K_r = -\frac{\partial^2 w}{\partial r^2}$$

$$K_{r\theta} = -\frac{1}{r}\left(\frac{\partial^2 w}{\partial \theta \partial r} - \frac{1}{r}\frac{\partial w}{\partial \theta}\right) = -\frac{\partial}{\partial r}\left(\frac{1}{r}\frac{\partial w}{\partial \theta}\right) \qquad (I.83a-c)$$

These equations are the same expressions as those in the theory

of bending of plates.   The use of such expressions, <u>REISSNER</u>

adds, is supported by known results for the buckling of

circular cylindrical shells where the buckling modes sub-

divide the shell into independent shallow panels.   The above

approximation would appear to be justified even when u and v

have similar values to w, since the neglected terms are all

divided by the radius of curvature.

REISSNER then reduces the above system of equations to

two simultaneous differential equations involving a stress

function F and the normal displacement w.   Their use is

suggested by the theory of plane stress and the theory of plate

bending to which the present equations reduce when $R = \infty$

When the transverse shear forces Q_r and Q_θ are neglected in

eqt. I.80a,b, these equations reduce to the equilibrium

equations of plane stress, and may be satisfied by use of the

Airy membrane stress function F.

Limiting attention to the case where the external load

terms p_r and p_θ are derivable from a load potential Ω

$$p_r = -\frac{\partial \Omega}{\partial r} \quad , \qquad p_\theta = -\frac{1}{r}\frac{\partial \Omega}{\partial \theta} \qquad (I.84a,b)$$

The simplified equations I.80a,b are satisfied by setting,

$$N_{\theta\theta} = \frac{\partial^2 F}{\partial r^2} + \Omega$$

56.

$$N_{rr} = \frac{1}{r}\frac{\partial F}{\partial r} + \frac{1}{r^2}\frac{\partial^2 F}{\partial \theta^2} + \Omega$$

$$N_{r\theta} = -\frac{\partial}{\partial r}\left(\frac{1}{r}\frac{\partial F}{\partial \theta}\right) \tag{I.85a-c}$$

A differential equation for F is obtained from the relevant equations of compatibility, by using eqts. I.81a-c and I.85:-

$$\nabla^2\nabla^2 F - \frac{tE}{R}\nabla^2 w = -(1-\nu)\nabla^2\Omega \tag{I.86}$$

where $\nabla^2 \equiv \frac{\partial^2}{\partial r^2} + \frac{1}{r}\frac{\partial}{\partial r} + \frac{1}{r^2}\frac{\partial^2}{\partial \theta^2}$ is the Laplacian operator.

The second fundamental equation in F and w is obtained by introducing the equilibrium equations I.80d and e into I.80c, thus eliminating the transverse shear terms Q_θ, Q_r. Expressing the resultant moments Mrr, M$\theta\theta$, Mrθ in terms of w, and its differentials from equations I.82d-f and I.83, and introducing these into the equations derived by eliminating Q_θ and Q_r the following is obtained:-

$$D.\ \nabla^2\nabla^2 w + \frac{1}{R}\nabla^2 F = p - \frac{2\Omega}{R} \tag{I.87}$$

Equations I.86 and I.87 are considered to be the two governing simultaneous differential equations of the shallow shell problem. In reference 43 E. REISSNER shows that eqts. I.86 and I.87 with the loading terms zero, i.e. the homogeneous equations, may be reduced to two independent second order equations. Equation I.87 is multiplied by $\frac{1}{D}$ and I.86 by a factor $\bar{\lambda}$. Adding these the result is:-

$$\nabla^2\nabla^2(w + \bar{\lambda}F) - \bar{\lambda}(tE/R)\nabla^2(w - F/\bar{\lambda}tED) = 0 \tag{I.88}$$

Putting $\bar{\lambda} = -1/\bar{\lambda}tED$ or $\bar{\lambda} = j\sqrt{12(1-\nu^2)}/Et^2$, and defining a quantity ℓ by the relation $\bar{\lambda}tE/R = j/\ell^2$ so that $\ell = \dfrac{\sqrt{Rt}}{\sqrt[4]{12(1-\nu^2)}}$;

equation I.88 can be written:-

$$\nabla^2\nabla^2(w + \bar{\lambda}F) - (j/\ell^2)\nabla^2(w + \bar{\lambda}F) = 0 \tag{I.89}$$

Next setting $w + \bar{\lambda}F = \Phi + \Psi$ \hfill (I.90)

where Φ and Ψ are the general solutions of

$$\nabla^2\Phi = 0 , \qquad \nabla^2\Psi - (j/\ell^2)\Psi = 0 \qquad\qquad (I.91a,b)$$

Thus the two homogeneous simultaneous equations of the fourth

order are reduced to the solution of two independent equations

of the second order.   E. REISSNER[43] then solves eqts. I.91a,b

for rotationally symmetric case giving :-

$$\Phi = A_1 + A_2 \ln r$$

$$\Psi = A_3 I_0(\sqrt{j}\, r/\ell) + A_4 K_0(\sqrt{j}\, r/\ell) \qquad\qquad (I.92a,b)$$

where A_1, A_2 ... are arbitrary complex constants and Io and Ko

are modified Bessel functions of the zero'th order.

Further $\qquad\quad I_0(\sqrt{j}\, x) = ber\, x + j\, bei\, x$

and $\qquad\qquad K_0(\sqrt{j}\, x) = ker\, x + j\, kei\, x \qquad\qquad (I.93a,b)$

    Substituting eqts. I.93 and I.92 into I.90 separating real

and imaginary parts, the following expressions are obtained for

w and F

$$w = C_1 ber\, r/\ell + C_2 bei\, r/\ell + C_3 ker\, r/\ell + C_4 kei\, r/\ell + C_5 + C_7 \ln r/\ell$$

$$F = Et^2/\sqrt{12(1-\nu^2)}\left[C_1 bei\, r/\ell - C_2 ber\, r/\ell + C_3 kei\, r/\ell - C_4 ker\, r/\ell + C_6 \ln r/\ell + C_8\right] \qquad (I.94)$$

where C_1, C_2 ... are real constants.

    In discussing the particular integrals of eqts. I.86 and I.87

for various types of loading such as uniform normal load, para-

bolic normal load, inertia load of a rotating shell, two methods

are mentioned, the one being that of assuming power series for

F and w, the other being the previously discussed membrane

solution.

    E. REISSNER then obtained explicit solutions for the

following three problems, (1) a shell with no edge restraint

carrying a radial point load at the crown, (2) a shell with no

edge restraint carrying a radial load uniformly distributed over a small circular area with centre at the crown, (3) a shell with edge restraint carrying a point load at the apex. Further axisymmetric spherical shell problems using the same fundamental equations are dealt with by BERMAN[53]. These include uniformly distributed vertical loading over the shell, uniform radial edge moment and uniform horizontal force loadings on either the inner or outer edge of the shell; hydrostatic loading, varying from zero to a maximum intensity.

When the shell is only loaded with a distributed normal load p then the general equations I.86 and I.87 simplify to:-

$$\nabla^4 F - (tE/R)\nabla^2 \omega = 0$$

$$\nabla^4 \omega + (1/RD)\nabla^2 F = P/D \qquad (I.95a,b)$$

From these may be obtained two sixth order differential equations for w and F. That for w may be written as:-

$$\nabla^4 \omega + (1/\ell^4)\omega = P/D$$

$$\nabla^2 \omega = 0 \qquad (I.96a,b)$$

BIJLAARD[54] points out that from eqt. I.96a, a shallow spherical shell acts as a flat plate on an elastic foundation whose general equation is:- $\nabla^4 \omega + \dfrac{k}{D}\omega = \dfrac{P}{D}$ where kw is the reaction of the elastic foundation to the given distributed load p per unit area - Ref. 24.

The equivalent foundation modulus for the shallow shell is thus:-

$$k = \frac{D}{\ell^4} = \frac{tE}{R^2} \qquad (I.97)$$

BIJLAARD[54] indicates that the above result was found earlier by VLASOV[55].

(I.1)

A further point noted by BIJLAARD is that the elastic restraints kw of the equivalent flat plate are related to the membrane forces Nrr and $N_{\theta\theta}$. So that from a consideration of membrane equilibrium, i.e. neglecting Q's in eqt. I.80c:-

$(N_{rr} + N_{\theta\theta})/R = \flat$ where $\flat$ is the normal load per unit area, and thus equivalent to kw.

$$\therefore \quad (N_{rr} + N_{\theta\theta})/R = k\omega \qquad (I.98)$$

Substituting for Nrr and $N_{\theta\theta}$ in terms of F from eqts. I.85 and k from I.97, BIJLAARD obtained the following equation:-

$$\nabla^2 F = (tE/R)\,\omega \qquad (I.99)$$

Applying the operation ∇^2 to eqt. I.99, equation I.95 results, thus confirming the use of the plate on elastic foundation analogy.

BIJLAARD then proceeds to obtain general expressions for w and F, from eqts. I.96, I.95 and I.99, for the rotational symmetrical case, which are identical to those of E. REISSNER[43] using the above analogy. These general expressions for w and F serve as the basis for a solution of the problem of a radial load acting upon a rigid cylindrical insert at the crown of a shallow shell.

In dealing with cases without axial symmetry, BIJLAARD shows that for $p = 0$ eqt. I.96a is satisfied if:-

$$\frac{\partial^2 \omega}{\partial r^2} + \frac{1}{r}\frac{\partial \omega}{\partial r} + \frac{1}{r^2}\frac{\partial^2 \omega}{\partial \theta^2} \pm \frac{j}{\ell^2}\,\omega = 0 \qquad (I.100)$$

putting $w = \Sigma \omega_n \cos.n\theta$ equation I.100 can be written:-

$$\frac{d^2 \omega_n}{dr^2} + \frac{1}{r}\frac{d\omega_n}{dr} + \left(\pm\frac{j}{\ell^2} - \frac{n^2}{r^2}\right)\omega_n = 0 \qquad (I.101)$$

This is a Bessel type equation, the solution of which may be written in the following form:-

$$\omega_n = C_{1n}\, ber_n\, \gamma_\ell + C_{2n}\, bei_n\, \gamma_\ell + C_{3n}\, ker_n\, \gamma_\ell + C_{4n}\, kei_n\, \gamma_\ell \qquad (I.102)$$

To this must be added the solution of eqt. I.96b.

So that :-

$$\omega_n = C_{1n}\, ber_n\, \gamma_\ell + C_{2n}\, bei_n\, \gamma_\ell + C_{3n}\, ker_n\, \gamma_\ell + C_{4n}\, kei_n\, \gamma_\ell + C_5 (\gamma_\ell)^n + C_6 (\gamma_\ell)^{-n} \qquad (I.103)$$

As an example of such a case, BIJLAARD gives the solution of the external moment acting on a rigid insert, i.e. n = 1.

Two further cases have been solved by CHINN[56]. In the first case a radial line load was applied to the shell over the circumference of a circle. The same basic solutions for w and F were used as in REISSNER and BIJLAARD's work. The stresses inside and outside the loaded circle were determined by a consideration of the various boundary conditions. The second case was that of external moment loading of the circle and here the corresponding unsymmetrical forms were used for w and F. These loadings correspond to radial load and moment loading on the sphere applied by means of an infinitely flexible pipe of zero width. The moment loading may be considered as a radial load of varying magnitude applied round the circumference of the loading circle.

In a further paper REISSNER[57] tackles the asymmetric bending of the shallow spherical shell for the harmonic order n = 1. A shallow cap with a rigid concentric insert is sub-jected to a side force and bending moment, and six simultaneous differential equations are obtained to formulate the problem. Certain second order terms are neglected, in these equations, and solutions with severe limitations are obtained. These limitations restrict the shell and insert dimensions to such

(I.1)

an extent that they are not applicable to the solution of practical shell problems, other than those where the insert dimensions are very large, or the shell extremely thin.

A method of particular application in the complex loading of shells has been presented by the author and KENEDI[58-61]. This introduces the Influence Line Concept to shell analysis and provides a generally applicable and flexible technique capable of yielding solutions to a variety of complex design problems. The influence lines are derived from the effects of 'basic' actions such as radial, tangential, and moment (bending or twisting) loading. In the range considered the basic actions are of an essentially local character using the assumption of shallowness and the corresponding governing equations relating to the shallow shell. Highly unsymmetrical loading is analysed using these relatively simple 'basic' actions. The method and its extension to shells other than shallow is discussed in greater detail in Chapters II and III.

The work of CHINN[56] is also of interest in connection with the influence line approach. He obtains influence surfaces for the various internal actions (resultant membrane forces and moment actions) when a spherical shell is under the action of rotationally symmetrical radial load.

The Influence Line technique is gaining increasing acceptance as is indicated, for example, by its use in the analysis of a gusset load on a spherical vessel (BAILEY and HICKS[62]), and most recently by the recommendation of LECKIE and PENNY[47] for use in cases where the loading does not lend itself to the appropriate Fourier representation.

I.2   EXPERIMENTAL INVESTIGATIONS

I.2.1   GENERAL EXPERIMENTAL WORK ON SHELLS

I.2.2   LOCAL LOADING OF SHELLS

I.2.1   GENERAL EXPERIMENTAL WORK ON SHELLS

Experimental investigations relating to the general testing of pressure vessels have been the concern of Engineers for over fifty years. The main object of their early work was to provide suitable empirical relationships capable of application in the design of cylindrical shells with a variety of different drum-heads under internal pressure.   Ellipsoidal, torispherical and spherical, plain and pierced heads were investigated.   This work was undertaken mainly by experimenters on the Continent - BACH, DIEGEL, SIEBEL, KORBER and others [63-70]. Considerable difficulty was experienced by these early workers in that they were not able to measure the values of the strain on the inside surface and thus were not able to compute with certainty the stresses on this surface.   Estimated values were obtained from measurements of external changes in curvature, such as was used by SIEBEL [66].

This work was extended to cover;   a wide range of nozzle attachments with different types of reinforcements by TAYLOR and WATERS [71];   to investigate manholes in various types of heads by SIEBEL and SCHWAIGERER [72];   and concentrated loading in cylinders by ROARK [73].   Once again the experimental work was hampered by the difficulties of instrumentation and again had a bias toward the derivation of empirical relationships.

The advent of the electrical resistance strain gauge enabled strain gauge work to be directed toward the measurement of strains within the vessel during the application of internal pressure.   Such an advance stimulated further investigations

on cylindrical vessels with many forms of drumhead, with and without manholes and nozzles. Various types of nozzles with and without reinforcement and having proportions in relation to drum diameter and thickness were investigated; also nozzle arrangements with unequal and staggered pitching together with investigations on the reduction of stress concentration due to changes in section were carried out. The types of drumhead included - spherical, ellipsoidal, torispherical, conical and toriconical. The workers of particular note in this field are COOPER and SMITH, CARLSON and McKEAN, LANE and WELLS and THE BRITISH WELDING RESEARCH ASSOCIATION (B.W.R.A.).[74-77].

More recent work on the above subject on radial and oblique nozzles with types of reinforcement is given in the following references, (78-82). A photoelastic approach is given by TAYLOR and SCHWEIKER[82].

It was realised that in many vessels, particularly those used in the Nuclear Reactor Field, the nozzles and their reinforcement would be loaded with a variety of load actions in addition to the internal pressure effects. Several investigators have studied this field experimentally and tests on both cylindrical and spherical vessels have been carried out. The work of SCHOESSOW and KOOISTRA, MEHRINGER and COOPER, CRANCH and DALLY is of interest in this field[83-86].

Numerous tests have been undertaken to check experimentally particular designs or arrangements. Various experimental methods have been employed - photoelastic, electrical resistance strain gauges or brittle coating. Some of this work has been carried
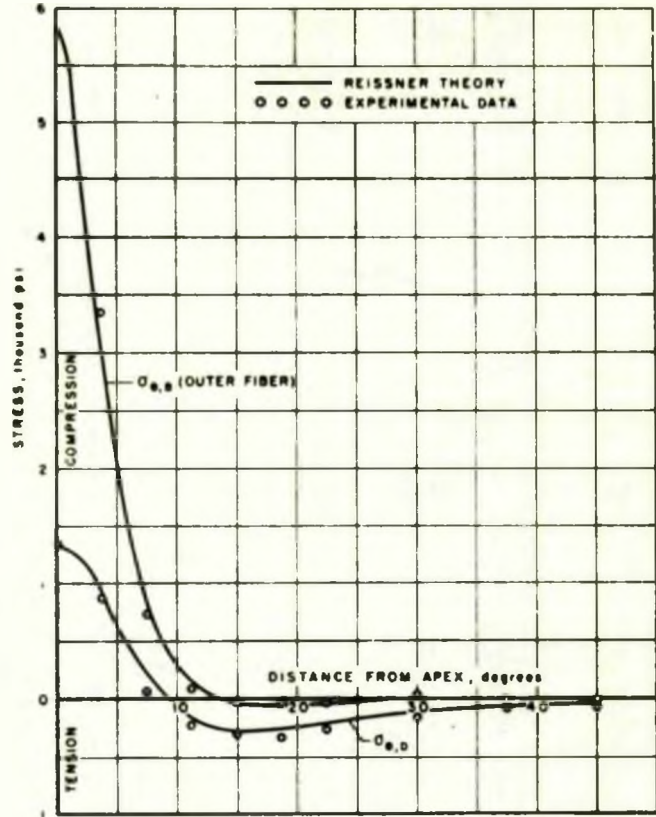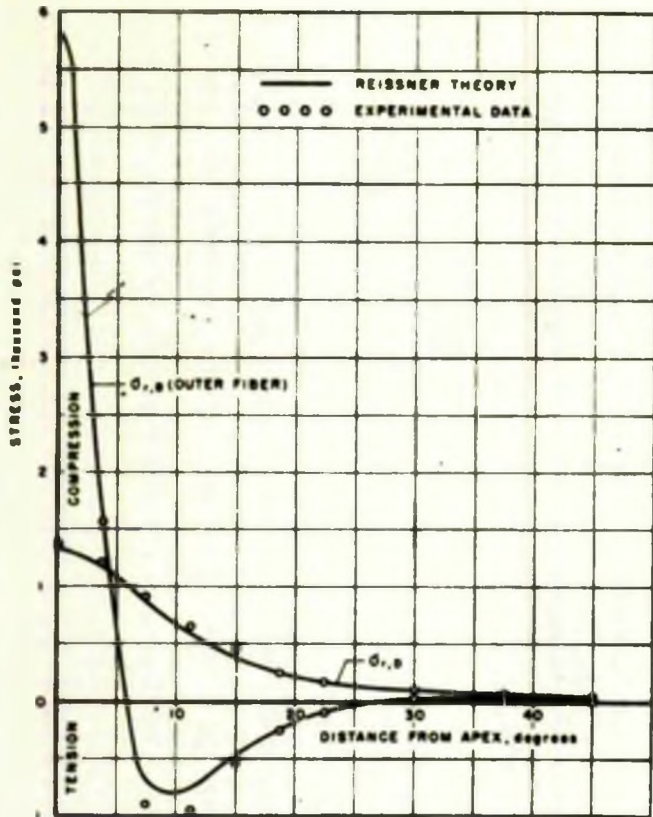
Fig.I.7   Stresses Produced by 100lb. Load Distribution Over
½in Diameter Area at the Apex of the Hemispherical
Shell having a 6in Radius and 0.110in Wall Thickness
by CARR ref. (99)

out on full size vessels, in addition to work on models.   A
wide variety of loading has been applied - bolting up loading,
pressure and dead weight loading and thermal cycling - to
assimilate actual working conditions.   Some vessels have been
taken to the point of actual collapse in an effort to examine
buckling effects and plastic deformation.   The following
references give   an indication of the range of such work(87-98).

I.2.2   THE LOCAL LOADING OF SHELLS

In this section it is proposed to discuss in detail two
papers dealing with the fundamental problem of local radial
loading of spherical shells.   The work of J. H. CARR(99) will
be mentioned first.   This paper reports tests carried out on
three hemispherical steel shells of different thicknesses -
0.095, 0.110 and 0.150 inches and each of 12 in diameter.

The shells were mounted onto a special fixture which
permitted the specimen to be tipped so that the radial load
could be applied at the apex of the hemisphere or at 30, 45 or
60 deg. from the apex.   Radial loads were applied as 'concentrated'
and distributed loads.   The distributed loads being applied to
the shell surface over three diameters $\frac{1}{4}$, $\frac{1}{2}$ and $\frac{3}{4}$ in. by means
of cylindrical loading noses and $\frac{1}{8}$ in. thick neoprene pads.
Electrical resistance strain gauges of $\frac{1}{8}$ in. and $\frac{1}{4}$ in. gauge
lengths were fixed to the inner and outer surfaces in the cir-
cumferential and meridional directions.   For the case of the
$\frac{1}{2}$ in. diameter area loading applied at the apex, CARR compared
the experimentally computed stresses with REISSNER's theory,
ref. 43.   These are shown in Fig. I.7 of the thesis.

It will be noted that the theoretical values show good
agreement with the experimental results. From the results of
the tests of the concentrated loading at 30, 45 and 60 deg.
from the apex, the influence of the welded boundary on the
distribution of the strain is examined. These results are
shown in Fig. I.8. It was concluded that the strain dis-
tribution curve shows very little distortion even when the
load centre is only 30 deg. from the fixed boundary.

The second paper is by a group of authors, VOSS and
others[100] and is the results of a test on a thin-shelled
model dome of plaster of Paris. The model was $\frac{1}{4}$ in. thick
and of $8\frac{1}{2}$ ft. radius. The base diameter was 8 ft. with a
rise of 1 ft. and a 2 in. diameter hole at the crown. The
initial tests were carried out in 1940 and, therefore, the
choice of a suitable strain gauge for measuring the surface
strains was somewhat restricted. They used in fact an
electrical resistance wire gauge composed either of a straight
wire of 3 in. in length or 'hairpin' of 1.5 in. length, placed
in the circumferential and meridional directions on the 0°,
90°, 135°, 180°, 270° and 315° meridian lines. These were,
however, restricted to the upper surface of the model. The
model was loaded with a 'concentrated' load - which was actually
assumed distributed over 6.25 sq. in. - at several points on the
0° meridian between the springing and the crown, and also at
other points between the 45° and 315° meridians.

Sand loads were distributed uniformly over an eighth and a
quarter segment to study the transition from a concentrated load
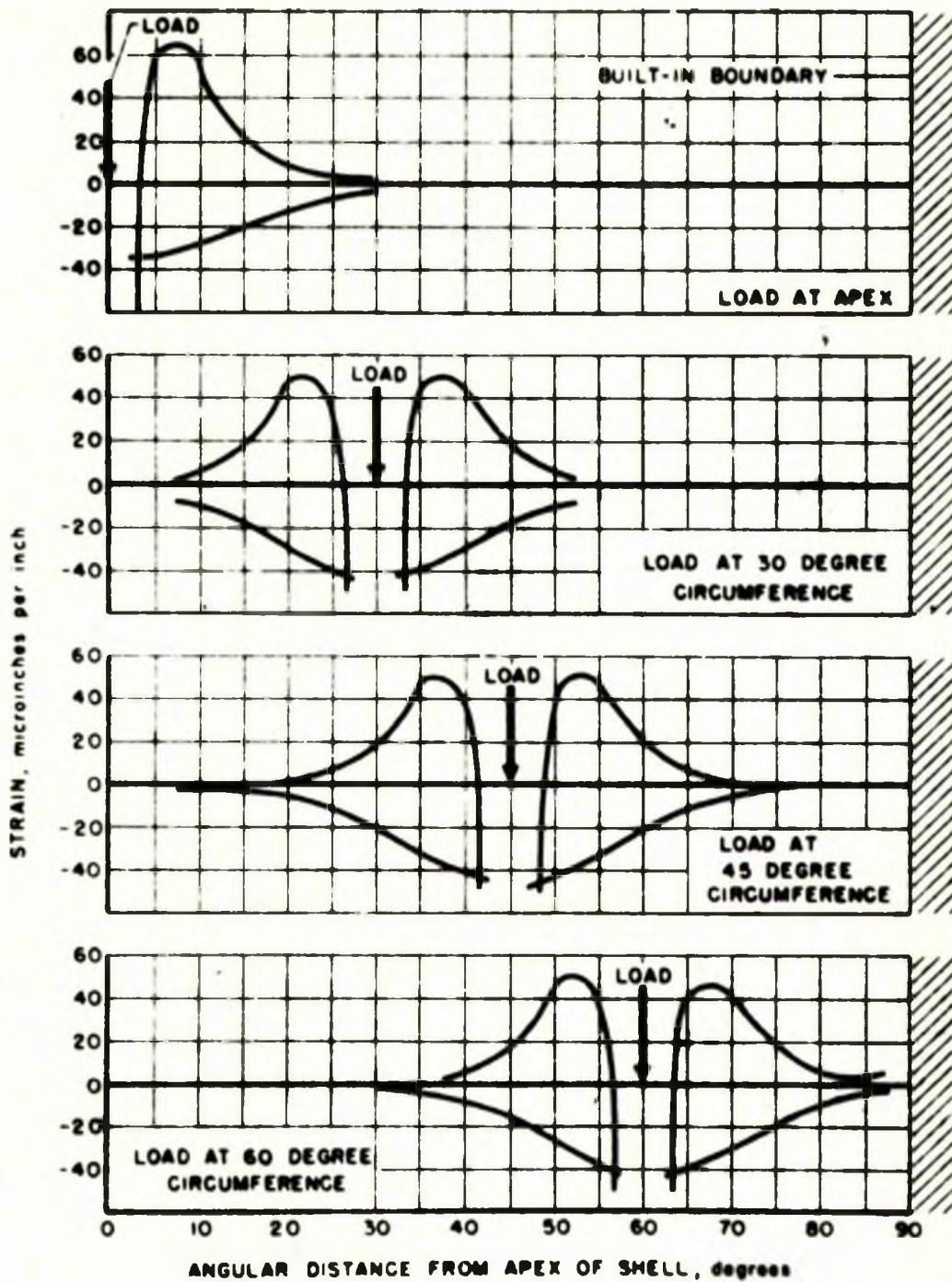
Fig.I.8   Effect of Built-In Boundary on Meridional Strain
Distribution for Concentrated Load of 100 lb on
Hemispherical Shell Having a 6-in. Radius and
0.095-in. Wall Thickness by CARR ref.(99)
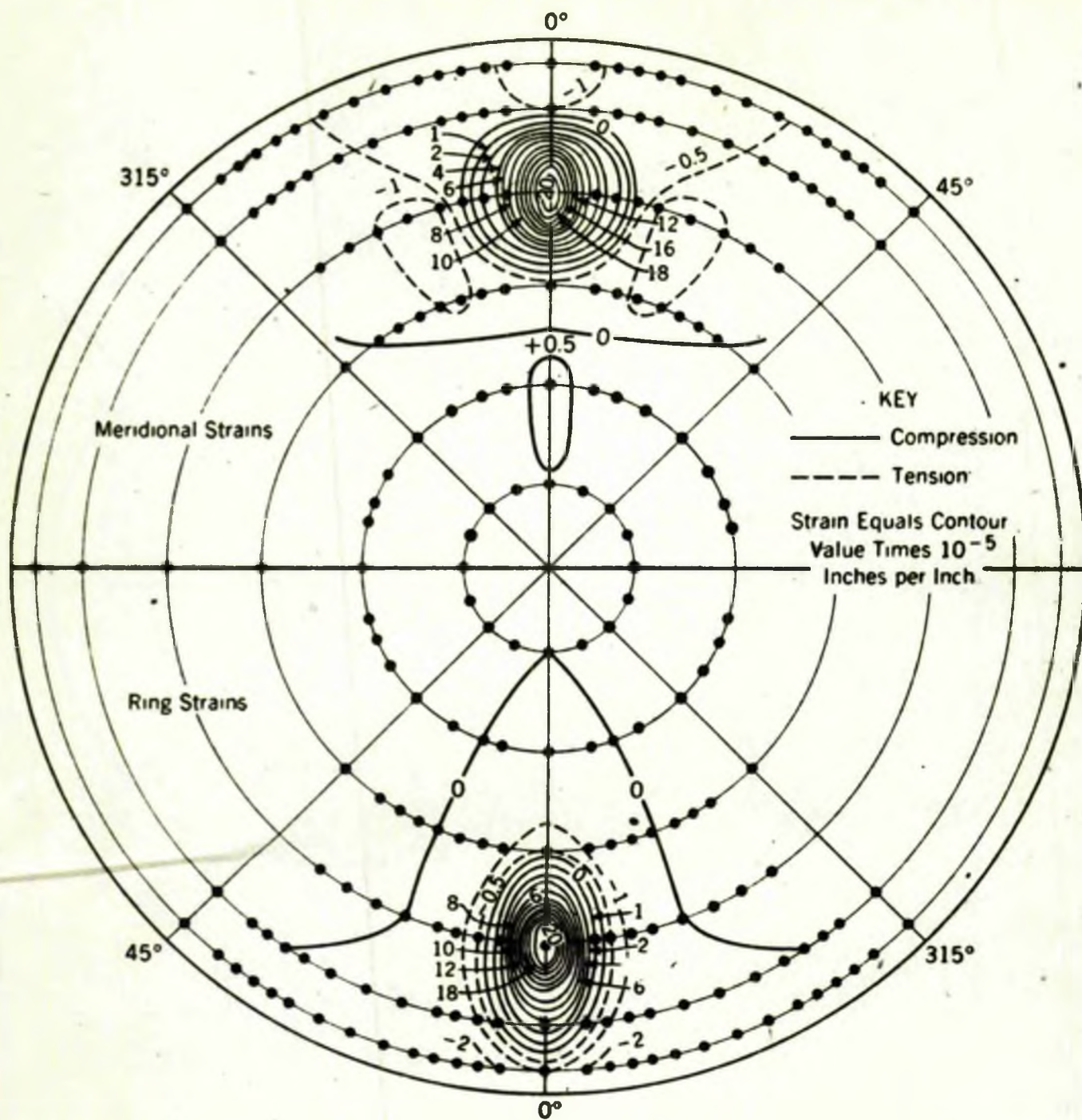
Fig.I.9.—Strain Contours for a Concentrated Load of 40 Lb at Station 5,6 for Plaster of Paris Model ref.(100)

to a uniformly distributed load over the entire surface. A
'concentrated' load test to failure completed the series.

An example of the strain contours on the upper surface, for
a concentrated load between the springing and the crown, is shown
on Fig. I.9. On this diagram the contour lines connect points
of the same strain value. The upper part of the diagram shows
the meridional strains and the lower part the 'ring' or circum-
ferential strains. These contours have been obtained by
applying the load at measured distances along the circumference
line through the gauge point - in this case 5, 6 i.e. at $34\frac{1}{2}$ in
from the crown.

It is pointed out that immediately under the loaded area
in both the meridional and circumferential directions large
compressive strains occur; these decrease rapidly outside
the loaded area and further away small tensile strains occur,
often followed by equally small compressive strains. Near the
loaded area, the meridional contours are approximately circular
whereas the circumferential contours are elliptical. Fig. I.10
shows the actual distributions of strain for a concentrated load
at the same point as the contours - 5,6. Fig. I.10a gives the
meridional and circumferential strain distribution along the 0°
meridian, and Fig. I.10b the strains along six circumferential
lines. It is noted that the numerical values of the maximum
strains in the meridional and circumferential directions at the
same station are approximately equal.

Further test results indicated that as the position of
application of the load was moved up the meridian toward the

crown of the dome, the strains increased to a maximum at the
station nearest the hole - some $7\frac{1}{2}$ in. from the crown. Values
of the maximum compressive stresses for the various stations
were computed from the strain values on the surface. In order
to do this the material constants for the plaster of Paris were
determined. These stresses are, of course, combined stresses,
i.e. bending and direct. The following are their results for
a 40 lb. load.

TABLE I.1

Station	Distance from Crown	Meridional Stress, σ_r	Circumferential Stress, σ_θ
1,2	44.5 in.	164 lb/in^2	167 lb/in^2
3,4	42.0	437	436
5,6	34.5	462	476
7,8	25.5	471	453
9,10	16.5	545	545
21,22	7.5	596	631

The figures in Table I.1 were compared with the maximum
value obtained by the REISSNER theory[43] for a similar shell
under similar loading conditions. The maximum stresses on
the upper surface according to REISSNER are $\sigma_r = \sigma_\theta = 603\,lb/in^2$
(compressive). The results approximate closely to the
maximum stresses given by the 21,22 station even though this
station is near the hole.

In the author's opinion, the station 1,2 at the springer
and 21,22 nearest the 2 in. diameter hole are not sufficiently
remote from these discontinuities to allow comparison with the
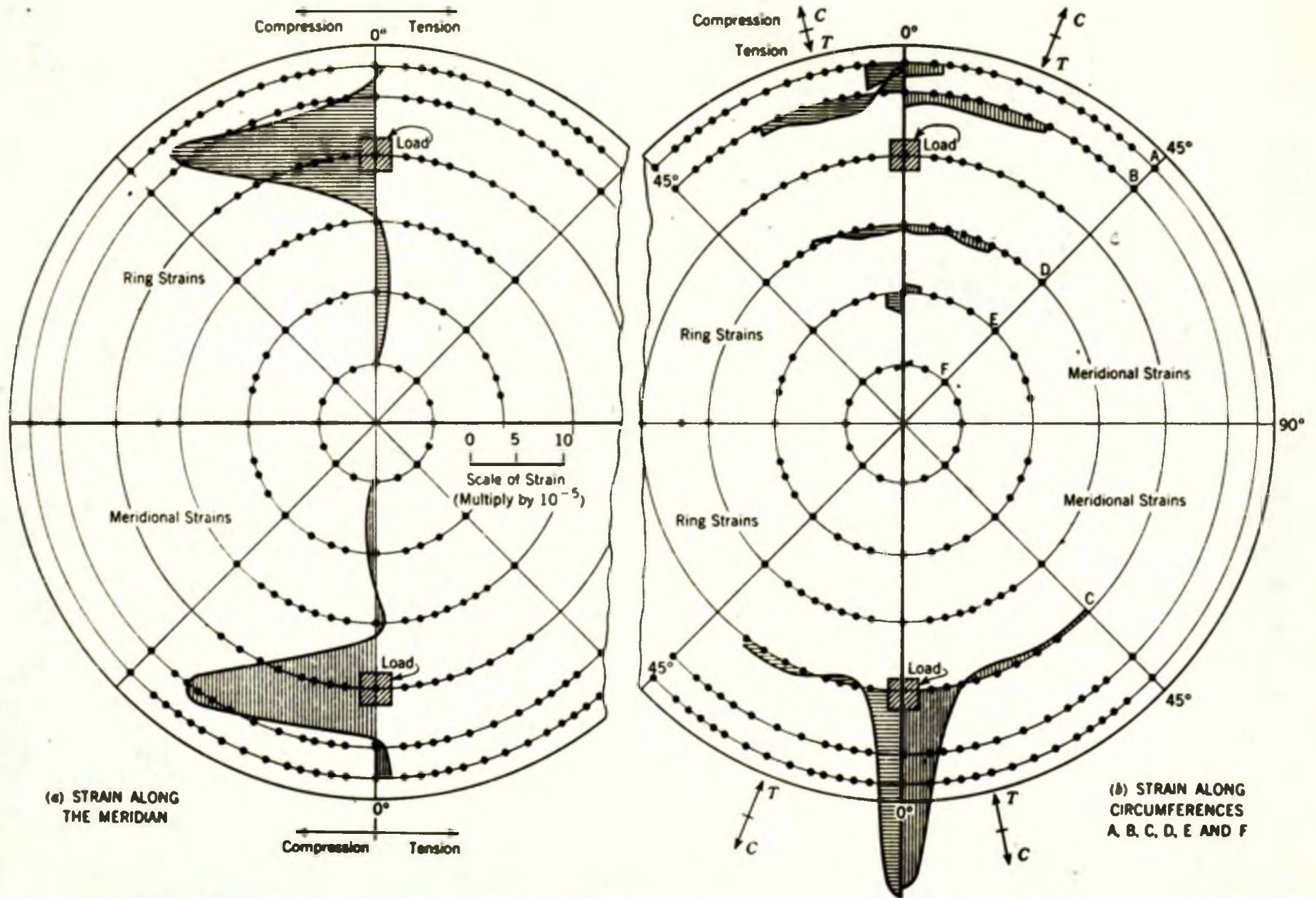
Fig.I.10 —Analysis of Strain Variation for a Concentrated Load of 40 Lb at Station 5,6 for Plaster of Paris Model ref.(100)
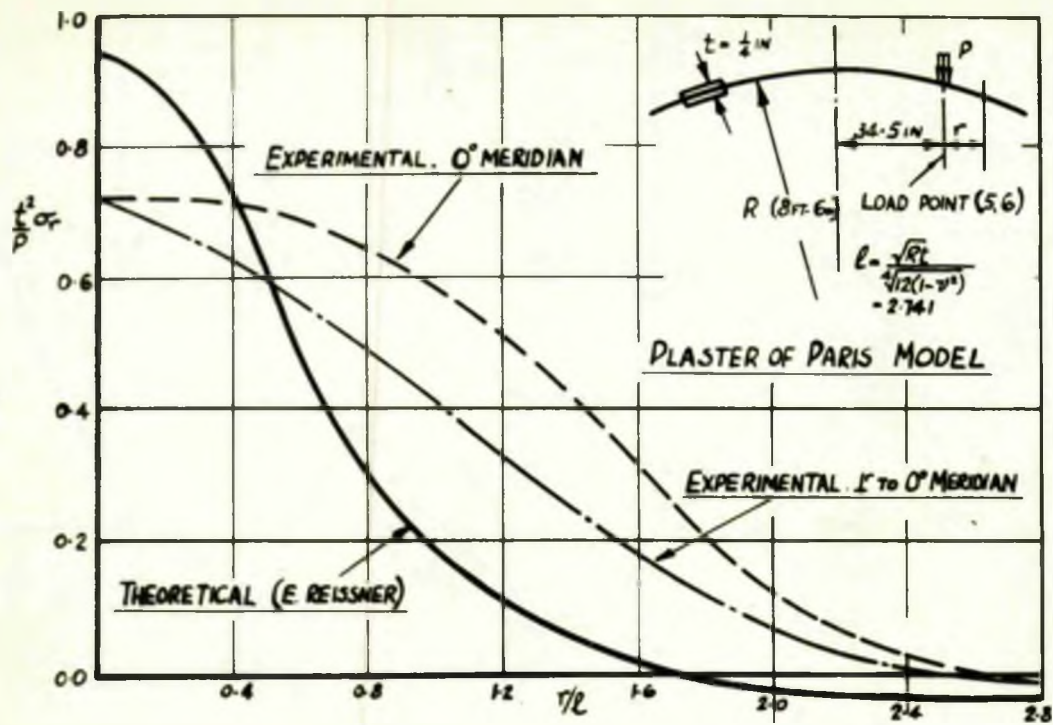
FIG. I.11a   TOTAL MERIDIONAL STRESS (ie DIRECT & BENDING)
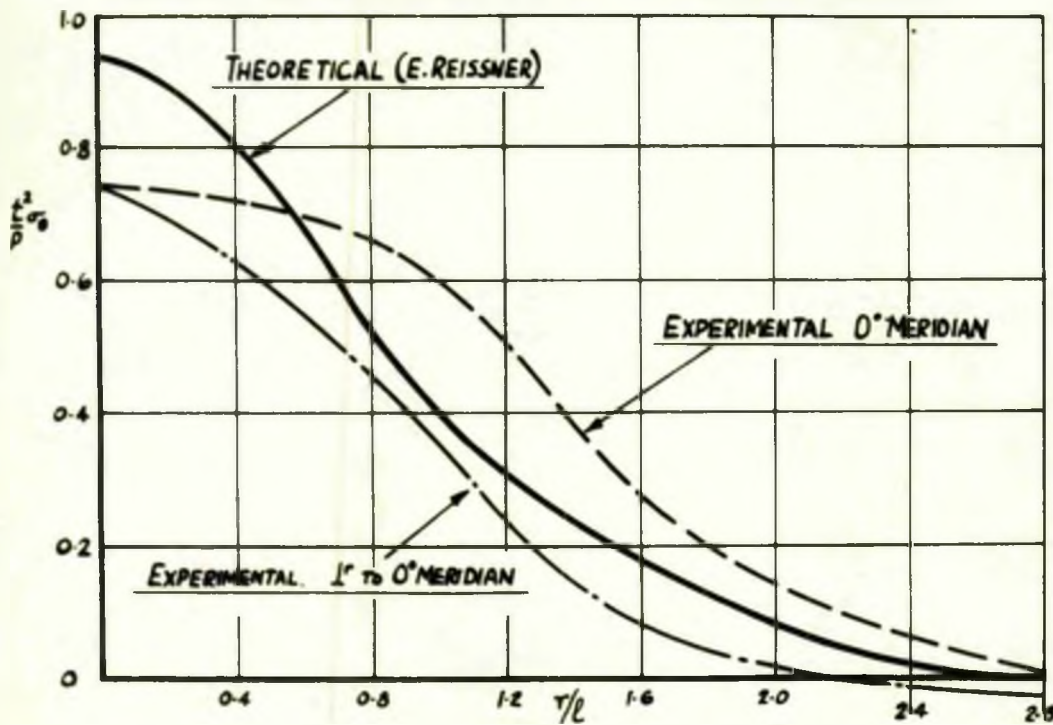
FIG. I.11b   TOTAL CIRCUMFERENTIAL STRESS (ie DIRECT & BENDING)

FIG I.11   THE TOTAL MERIDIONAL AND CIRCUMFERENTIAL STRESSES ALONG TWO DIRECTIONS RADIATING FROM THE LOAD POINT 5.6 DUE TO A LOAD P, ON A PLASTER OF PARIS MODEL BY VOSS etc[100] COMPARED WITH THE THEORY OF E REISSNER[43].

REISSNER theory.   The presence of the hole at the centre would
increase the maximum stress and the presence of the boundary
would reduce the value - as indicated by Table I.1.   The maximum
values within these two extremes are more nearly equal, though it
is evident in this model, that even these values are influenced
to some extent by the boundaries.

VOSS and his colleagues comment on the similarity of their
curves with those of REISSNER - but unfortunately no graphical
comparison is made.   The author has endeavoured to make this com-
parison, using the contour plots of Fig. I.9 and a table presented
in the paper, for the load point 5,6, i.e. $34\frac{1}{2}$ in. from the crown.
The meridional and circumferential strains were obtained in the
direction of the 0° meridian and also perpendicular to this line.
The computed meridional stresses (Fig. I.11a) do not exhibit the
same rapid die out as does the REISSNER curve, although the
position of zero stress is approximately the same.   In the case
of the circumferentially computed stresses (Fig. I.11b) the two
sets of curves lie one on either side of the theoretical.   VOSS
and his colleagues conclude this section by noting that the
results from one series of tests are not conclusive.

The distributed loads were applied over two different areas -
eighth and quarter segments - centred at the 0° meridian.   As
in the earlier work the meridional and circumferential strains
were measured along the meridian lines.   In both cases the
loading intensity was the same, however, the computed stress
values are much lower for the quarter segment loading, illus-
trating the tendency for the stresses to decrease as a larger

area is loaded.   A study of the plastic behaviour in the plaster was carried out, by leaving the dome loaded for periods up to 4-8 days.   At regular intervals of time the strains were recorded.   It was found that re-adjustments took place in the strain values, which tended to reduce the strains in the upper surface of the loaded area.

More recent work by the author and KENEDI[58-61] and by the author[101-103] has endeavoured to substantiate experimentally the whole range of local loading - radial, tangential and moment (twisting and bending) actions.   The work has been carried out on:-   (1) steel spherical domes of 60 in. radius and base diameter of approximately 3 ft. 9 in. and of thicknesses 1 in. and $\frac{1}{4}$ in., and (ii) a complete sphere 13 ft. 6 in. diameter which in overall dimensions is one tenth of the Dounreay Containment Building.   The experimental programme has also sought to substantiate the influence line approach referred to earlier on p. 61.   All this work is presented in Chapter IV of the thesis.

1.3   CRITICAL SUMMARY

I.3   CRITICAL SUMMARY

The load actions and their resulting effects on a shell may
be classified under the following three headings:-

(1)   Axisymmetric - where the load is applied to the
       shell so as to produce a rotationally symmetric
       stress system.

(2)   Asymmetric - where the resulting effects are con-
       sidered to be of an inverse-symmetrical type, the
       moment and tangential load being examples of this
       type.

(3)   Unsymmetric - where no symmetry of the loading or
       its resulting effects exists.

In the published analytical investigations of these effects
emphasis has been placed upon obtaining rigorous solutions to the
shell equations.   This, however, has proved virtually impossible
in the general unsymmetrical case and in consequence has resulted
in a restriction of load cases that have been considered. Until
recently, only solutions of the axisymmetric cases were available.
Even these latter cases have proved intractable from a rigorous
point of view and innumerable approximations have been introduced
into the differential equations to permit the derivation of
solutions.   The most widely accepted approximation is that known
as LOVE's first approximation, introduced primarily, one suspects,
due to its simplicity and to the correspondence of the resulting
equations to the flat plate relations.

These simplified equations, however, are still not readily

amenable to solution and necessitated both the introduction of further simplifications and the use of mathematical techniques not hitherto employed in shell analysis.

It is significant that the tendency in published work has been to assess the value of a solution by comparison with the rigorous analytical solution of the problem, leading to further and further simplification of the load system considered.

Recently cases of loading have been examined containing various degrees of asymmetry; in 1961 LECKIE[39] considered the first harmonic and more recently LECKIE and PENNY[47] the higher harmonics.

A general procedure for the analysis of all types of un-symmetrical load systems (inclusive of axisymmetric and asymmetric) has been outlined by the author and KENEDI[58-61] under the title - 'The Influence Line Technique.' This method utilizes the 'basic' actions into which any loading at a point may be resolved. The analytical solutions for the necessary range of these 'basic' actions were not available in the published literature, nor in fact have those available been substantiated experimentally. Further, the validity of the approximations inherent in the solutions available were not tested in relation to load cases likely to be encountered in practice.

In consequence, the analytical research efforts presented in Chapters II and III of the thesis were directed towards:-

(a) Unification of the available solutions for the 'basic' actions together with those derived by the author for

(I.3)

        hitherto unsolved cases of twisting moment and
        tangential load

(b)   Evolution of a technique, which by utilizing these
      'basic' actions provides complete flexibility of
      analysis suitable for the symmetric and unsymmetric
      cases.   Such a technique would translate the problem
      into a form readily amenable to solution by a semi-
      graphical method, by a desk calculator or by a
      digital computer.

On the experimental side, the gaps are so obvious that they
need not be emphasised.   The experimental results that were
available to the author from the published literature are either
inapplicable due to inappropriate material (plaster of Paris)
and inadequate gauging, etc., or are of no value because the
experimental work, lacking in direction, was not carried out in
association with analytical development.

The paucity of such results required the initiation, planning
and execution of a complete experimental programme designed to
test the accuracy and range of applicability of:-

(a)   the analytical solutions of the 'basic' actions -
      radial, tangential and moment loadings,

(b)   the proposed technique for the analysis of complex
      load systems.

The complete experimental programme carried out by the
author, briefly mentioned in the preceeding review (p.70), is
presented in Chapter IV.

CHAPTER II   THEORETICAL ANALYSIS OF FORCE ACTIONS ON
                        A SPHERICAL SHELL

Any load action at a point on a shell can be broken down
into the basic components of radial and tangential loads,
'bending' and 'twisting' moments. Analyses which are capable
of predicting the stress and displacement distribution under such
load actions will now be presented.

In the first instance, the analyses are directed toward
the solution of shallow spherical shells under various local
load actions.   The radial and bending moment loadings at the
crown have been dealt with by E.REISSNER[43] and BIJLAARD[54].
These authors both start from the governing shallow shell equation
I.86 and I.87 obtaining results for the cases tackled by diff-
erent methods - as indicated in Chapter I.

In the present work, relationships for the normal displace-
ment w and the membrane stress function F are derived in general
terms capable of application to any value of n.   Thus a more
unified analysis is presented for these 'basic' actions.

In the second part of the chapter the 'basic' actions are
further examined utilizing the general shell equations; the
solutions for the oscillatory terms being those obtained by
asymptotic integration and given by LECKIE[39]. A comparison
between the shallow shell approach and the general shell approach
is made for each basic load case.

The final part of the chapter deals with a simplified
analysis, referred to in the review, which, using the 'basic'
actions, enables a complex loading problem to be solved.

II.1   SHALLOW SPHERICAL SHELL THEORY

II.1.1   GENERAL SOLUTION FOR w AND F.

     (a)   The Basic Differential Equations.

     (b)   Integration of the Differential Equations.

     (c)   Generalized Form of w and F.

II.1.2   RADIAL LOAD

     (a)   Uniformly Distributed Loading at the Crown.

     (b)   Concentrated Load at the Crown.

     (c)   Uniform Loading of a Rigid Cylindrical Insert built into the Discontinuous Shell.

II.1.3   'BENDING' MOMENT

II.1.4   'TWISTING' MOMENT

II.1.5   'TANGENTIAL' LOAD

II.1   SHALLOW SPHERICAL SHELL THEORY

II.1.1   GENERAL SOLUTION FOR w AND F.

(a)   The Basic Differential Equations

Consider a shallow shell subjected to load components in the radial, meridional and circumferential directions, of intensity p, p_r, p_θ.   The two governing simultaneous differential equation: for shallow shells are eqts. I.86 and I.87, given in Chapter I as follows:-

$$\nabla^2 \nabla^2 F - \frac{tE}{R} \nabla^2 \omega = - (1-\upsilon) \nabla^2 \Omega \qquad \text{(II.1)}$$

$$D \nabla^2 \nabla^2 \omega + \frac{1}{R} \nabla^2 F = p - \frac{2\Omega}{R} \qquad \text{(II.2)}$$

where Ω is a load function obtained from eqt. I.84a,b namely :-

$$p_r = -\frac{\partial \Omega}{\partial r} \qquad \text{and} \qquad p_\theta = -\frac{1}{r}\frac{\partial \Omega}{\partial \theta} \qquad \text{(II.3a,b)}$$

The force resultants are those defined in eqt. I.85a-c :-

$$N_{rr} = \frac{1}{r}\frac{\partial F}{\partial r} + \frac{1}{r^2}\frac{\partial^2 F}{\partial \theta^2} + \Omega$$

$$N_{\theta\theta} = \frac{\partial^2 F}{\partial r^2} + \Omega$$

$$N_{r\theta} = - \frac{\partial}{\partial r}\left(\frac{1}{r}\frac{\partial F}{\partial \theta}\right)$$

and the moment actions from eqts. I.82d-f and I.83a-c

$$M_{rr} = - D\left[\frac{\partial^2 \omega}{\partial r^2} + \upsilon\left(\frac{1}{r}\frac{\partial \omega}{\partial r} + \frac{1}{r^2}\frac{\partial^2 \omega}{\partial \theta^2}\right)\right]$$

$$M_{\theta\theta} = - D\left[\frac{1}{r}\frac{\partial \omega}{\partial r} + \frac{1}{r^2}\frac{\partial^2 \omega}{\partial \theta^2} + \upsilon\frac{\partial^2 \omega}{\partial r^2}\right]$$

$$M_{r\theta} = - (1-\upsilon)D \frac{\partial}{\partial r}\left(\frac{1}{r}\frac{\partial \omega}{\partial \theta}\right) \qquad \text{(II.4a-f)}$$

From the equilibrium equations I.80 and eqts. II.4, the transverse shear forces are :-

$$Q_r = - D\frac{\partial \nabla^2 \omega}{\partial r} , \qquad Q_\theta = - D\frac{1}{r}\frac{\partial \nabla^2 \omega}{\partial \theta} \qquad \text{(II.5a,b)}$$

(b) Integration of the Differential Equations

From eqt.II.1 $\nabla^2 F - \dfrac{tE}{R}\omega \;=\; \dfrac{tE}{R}\omega_{\phi} - (1-v)\Omega$ (II.6)

where w_{ϕ} is a solution of $\nabla^2 \omega_{\phi} = 0$, so that :-

$$\omega_{\phi} = A_0 + B_0 \ln r + \sum_{n=1}^{n=\infty}(A_n r^n + B_n r^{-n})\cos n\theta \qquad (II.7)$$

Thus from eqt. II.6 $\nabla^2 F = \dfrac{tE}{R}(\omega_{\phi} + \omega) - (1-v)\Omega$ (II.8)

Substituting eqt.II.8 into eqt.II.2 the following is obtained:-

$$D\nabla^2\omega + \frac{1}{R}\left[\frac{tE}{R}(\omega_{\phi}+\omega) - (1-v)\Omega\right] = p - \frac{2\Omega}{R}$$

which after simplification becomes:-

$$\nabla^4\omega + \frac{\omega}{\ell^4} = \frac{1}{D}\left[p - \frac{(1+v)\Omega}{R}\right] - \frac{\omega_{\phi}}{\ell^4} \qquad (II.9)$$

where $\ell = \dfrac{\sqrt{Rt}}{\sqrt[4]{12(1-v^2)}}$

The solution of eqt. II.9 may be expressed in three parts,

i.e $\omega = \omega_h + \omega_p - \omega_{\phi}$ (II.10)

where w_h is the solution of $\nabla^2\nabla^2\omega_h + \dfrac{\omega_h}{\ell^4} = 0$ (II.11)

and w_p is the particular integral of the equation:-

$$\nabla^2\nabla^2\omega_p + \frac{\omega_p}{\ell^4} = \frac{1}{D}\left[P - \frac{(1+v)\Omega}{R}\right] \qquad (II.12)$$

By substituting $w_h = w_n(r)\cos n\theta$ into eqt.II.11 and then

factorizing , the following two equations result:-

$$\left[\nabla^2 + \left(\frac{j}{\ell^2} - \frac{n^2}{r^2}\right)\right]\omega_n(r) = 0$$

$$\left[\nabla^2 - \left(\frac{j}{\ell^2} + \frac{n^2}{r^2}\right)\right]\omega_n(r) = 0 \qquad (II.13a,b)$$

where $j = \sqrt{-1}$

These equations have solutions which are complex, those of eqt. II.13b being the conjugate of those of eqt.II.13a.   The two pairs of solutions are therefore linearly independent and constitute together a set of four solutions of eqt. II.11.   It is therefore only necessary to solve one second order differential equation, either II.13a or b.   As eqt. II.13b has solutions which can be expressed as Kelvin functions, this is selected.

(II.1)

It can be written in the form:-

$$\frac{d^2 w_n}{dr^2} + \frac{1}{r}\frac{d w_n}{dr} - \left(\frac{j}{\ell^2} + \frac{n^2}{r^2}\right) w_n = 0 \tag{II.14}$$

This equation is the modified Bessel equation and has a solution:-

$$w_n = C_{1\alpha} I_n(\sqrt{j}\, r/\ell) + C_{2\alpha} K_n(\sqrt{j}\, r/\ell) \tag{II.15}$$

where I_n is a modified Bessel function of the first kind-n'th order
and K_n is a modified Bessel function of the second kind-n'th order
and defined:-

$$I_n(\sqrt{j}\, r/\ell) = j^{-n}\left[ber_n\, r/\ell + j\, bei_n\, r/\ell\right]$$

$$K_n(\sqrt{j}\, r/\ell) = j^{n}\left[ker_n\, r/\ell + j\, kei_n\, r/\ell\right] \tag{II.16a,b}$$

Introducing eqts.II.16a,b into eqt.II.15 gives:-

$$w_n = C_{1\alpha} j^{-n}\left[ber_n\, r/\ell + j\, bei_n\, r/\ell\right] + C_{2\alpha} j^{n}\left[ker_n\, r/\ell + j\, kei_n\, r/\ell\right] \tag{II.17}$$

After separating the real and imaginary parts of this equation
and noting that $w_h = w_n(r)\cos n\theta$; substituting for w_n from eqt.II.17
gives:- $w_h = (C_{1n}\, ber_n\, r/\ell + C_{2n}\, bei_n\, r/\ell + C_{3n}\, ker_n\, r/\ell + C_{4n}\, kei_n\, r/\ell)\cos n\theta$ (II.18)
for all values of n.

A verification of eqt.II.18 is given in Appendix VIII.1

To solve for the stress function F, eqts. II.10 and II.18
are substituted into eqt.II.6 giving:-

$$\nabla^2 F = \frac{tE}{R}\left(C_{1n}\, ber_n\, r/\ell + C_{2n}\, bei_n\, r/\ell + C_{3n}\, ker_n\, r/\ell + C_{4n}\, kei_n\, r/\ell\right)\cos n\theta + w_p - (1-v)\Omega \tag{II.19}$$

F may be written as:- $F = F_h + F_P + F_{\phi}$ (II.20)

where F_{ϕ} is the solution of $\nabla^2 F_{\phi} = 0$ and has the same form as that
of w_{ϕ} given in eqt.II.7 that is:-

$$F_{\phi} = a_o + b_o \ln r/\ell + \sum_{n=1}^{n=\infty}\left[a_n (r/\ell)^n + b_n (r/\ell)^{-n}\right]\cos n\theta \tag{II.21}$$

F_h is the solution of:-

$$\nabla^2 F_h = \frac{tE}{R}\left[C_{1n}\, ber_n\, r/\ell + C_{2n}\, bei_n\, r/\ell + C_{3n}\, ker_n\, r/\ell + C_{4n}\, kei_n\, r/\ell\right]\cos n\theta \tag{II.22}$$

and finally, $\nabla^2 F_P = \frac{tE}{R} w_p - (1-v)\Omega$ (II.23)

81.

Taking the form of solution of eqt.II.22 as:-

$$F_h = (P_n \, ber_n \, {}^r\!/_\ell + Q_n \, bei_n \, {}^r\!/_\ell + R_n \, ker_n \, {}^r\!/_\ell + S_n \, kei_n \, {}^r\!/_\ell) \cos n\theta \qquad (II.24)$$

and using eqts.VIII.2 of Appendix VIII.1 an expression for $\nabla^2 F_h$ can be written:-

$$\nabla^2 F_h = \frac{1}{\ell^2} (-P_n \, bei_n \, {}^r\!/_\ell + Q_n \, ber_n \, {}^r\!/_\ell - R_n \, kei_n \, {}^r\!/_\ell + S_n \, ker_n \, {}^r\!/_\ell) \cos n\theta \qquad (II.25)$$

Comparing eqt.II.25 with eqt.II.22

$$P_n = -\frac{\ell^2 t E}{R} C_{2n} \qquad , \qquad Q_n = -\frac{\ell^2 t E}{R} C_{1n}$$

$$R_n = -\frac{\ell^2 t E}{R} C_{4n} \qquad , \qquad S_n = -\frac{\ell^2 t E}{R} C_{3n}$$

Thus:-

$$F_h = -\frac{\ell^2 t E}{R} (C_{2n} \, ber_n \, {}^r\!/_\ell - C_{1n} \, bei_n \, {}^r\!/_\ell + C_{4n} \, ker_n \, {}^r\!/_\ell - C_{3n} \, kei_n \, {}^r\!/_\ell) \cos n\theta \qquad (II.26)$$

(c) Generalized Form of w and F.

It is now possible to write the general forms for w and F. For w; eqts.II.18 and the appropriate form of II.7 are substituted into eqt.II.10 giving:-

$$\omega = \sum_{n=0}^{n=\infty} (C_{1n} \, ber_n \, {}^r\!/_\ell + C_{2n} \, bei_n \, {}^r\!/_\ell + C_{3n} \, ker_n \, {}^r\!/_\ell + C_{4n} \, kei_n \, {}^r\!/_\ell) \cos n\theta$$
$$- A_0 - B_0 \ln {}^r\!/_\ell - \sum_{n=1}^{n=\infty} \left[A_n \left(\frac{r}{\ell}\right)^n + B_n \left(\frac{r}{\ell}\right)^{-n} \right] \cos n\theta + \omega_p \qquad (II.27)$$

For F; eqts.II.26 and II.21 are substituted into eqt.II.20 giving:

$$F = \sum_{n=0}^{n=\infty} \frac{\ell^2 t E}{R} (-C_{2n} \, ber_n \, {}^r\!/_\ell + C_{1n} \, bei_n \, {}^r\!/_\ell - C_{4n} \, ker_n \, {}^r\!/_\ell + C_{3n} \, kei_n \, {}^r\!/_\ell) \cos n\theta$$
$$+ a_0 + b_0 \ln {}^r\!/_\ell + \sum_{n=1}^{n=\infty} \left[a_n \left({}^r\!/_\ell\right)^n + b_n \left({}^r\!/_\ell\right)^{-n} \right] \cos n\theta + F_p \qquad (II.28)$$

These equations (II.27 and 28), first presented by BERMAN [53], will be used to derive the displacement and stress distributions for the 'basic' load actions of radial and tangential loads, 'bending' and 'twisting' moments.

These generalized forms for w and F are also usable for the study of the higher harmonics.

II.1.2. RADIAL LOAD

In this section the behaviour of the continuous shallow spherical shell under the action of a radial load at the crown, uniformly distributed over a circular area of radius r_p , is examined.   Two additional cases are also considered, namely :- a concentrated load at the crown and a uniform load on a rigid cylindrical insert built into the discontinuous shell.   These latter two are essentially particular examples of the uniformly distributed area load, and are deduced directly from this case.

The equations II.27 and II.28 which express w and F in genera terms form the basis of the analyses.   The particular integrals w_p and F_p for the various sections of the loaded shell are deter- mined for each case of loading.   The other constants in the expressions are determined from the boundary conditions of the shell in question.

(a)   Uniformly Distributed Radial Area Load at the Crown - FigII.1

From rotational symmetry it follows from eqts. II.27 and II.28 that:-

$$w = C_1 \, ber \, r/\ell + C_2 \, bei \, r/\ell + C_3 ker \, r/\ell + C_4 kei \, r/\ell$$

$$- A_o - B_o \ln r/\ell + w_P \qquad (II.29)$$
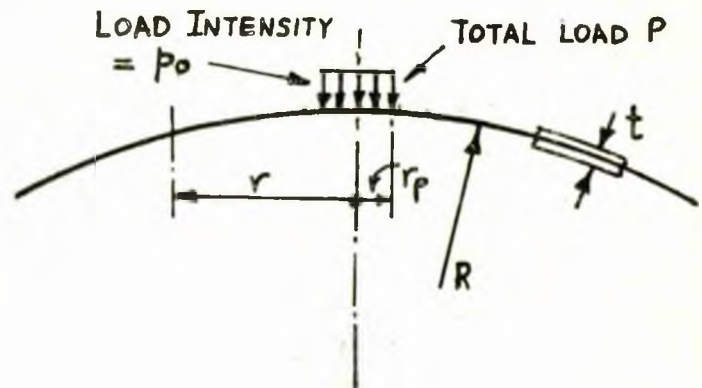
Fig.II.1   Radial Load at the Crown

$$F = \frac{\ell^2 t E}{R}\left[- C_2 \, ber \, r/\ell + C_1 bei \, r/\ell - C_4 ker \, r/\ell + C_3 kei \, r/\ell \right] + a_o + b_o \ln r/\ell + F_P \quad (II.30)$$

Derivation of constants a_o and B_o

1.   Since only derivatives of F appear in the force equations II.4a-c the constant a_o is immaterial.

2. The constant B_o is shown to be equal to zero by the following analysis:-

The values of the meridional and circumferential strains for $n = 0$ are as follows :-

$$\varepsilon_r = \frac{dv}{dr} + \frac{w}{R} = \frac{1}{tE}\left[N_{rr} - \upsilon N_{\theta\theta}\right]$$

$$\varepsilon_\theta = \frac{v}{r} + \frac{w}{R} = \frac{1}{tE}\left[N_{\theta\theta} - \upsilon N_{rr}\right] \qquad (II.31a,b)$$

Substituting for w from eqt.II.6 and for N_{rr} and $N_{\theta\theta}$ from eqts.II.4a-c, eqts.II.31a,b become:-

$$\frac{dv}{dr} - \frac{w\delta}{R} = -\frac{(1+\upsilon)}{tE}\frac{d^2F}{dr^2}$$

$$\frac{v}{r} - \frac{w\phi}{R} = -\frac{(1+\upsilon)}{tE}\frac{1}{r}\frac{dF}{dr} \qquad (II.32a,b)$$

Multiplying II.32b by r and differentiating with respect to r gives :- $\frac{dv}{dr} - \frac{1}{R}\frac{d}{dr}(r.w_\phi) = -\frac{(1+\upsilon)}{tE}\frac{d^2F}{dr^2}$ (II.33)

From eqts.II.33 and II.32a, $w_\phi = \frac{d}{dr}(r w_\delta)$ This is only possible when $B_o = 0$ (Eqt.II.7)

The solution to the distributed load problem is considered in two parts, (i) the part of the shell inside the loaded area,

(ii) the part of the shell outside the loaded area.

(i) Inside the Loaded Area i.e. $0 < r < r_p$

The subscript 'i' will be used for this region. Thus from eqts.II.29 and II.30:-

$w_i = C_1 ber \frac{r}{l} + C_2 bei \frac{r}{l} + C_3 ker \frac{r}{l} + C_4 kei \frac{r}{l} - A_o + w_p$

$F_i = \frac{l^2 tE}{R}\left(-C_2 ber \frac{r}{l} + C_1 bei \frac{r}{l} - C_4 ker \frac{r}{l} + C_3 kei \frac{r}{l}\right) + b_o \ln \frac{r}{l} + F_p$ (II.34a,b)

Particular Integrals:- The loading is radial i.e. $p = -p_o = -\frac{P}{\pi r_p^2}$ and $p_\theta = p_r = 0$, therefore $\Omega = 0$

The value w_p is the P.I. of $\nabla^2\nabla^2 w_p + \frac{w_p}{l^4} = \frac{1}{D}\left[p - \frac{(1+\upsilon)\Omega}{R}\right]$ (II.12)

For this case eqt.II.12 simplifies to $\nabla^2\nabla^2 w_p + \frac{w_p}{l^4} = -\frac{p_o}{D}$

Thus $\quad \omega_P \quad = \quad -\dfrac{p_o R^2}{Et}$ $\hspace{3cm}$ (II.35)

The value F_P is the P.I. of $\quad \nabla^2 F_P = \dfrac{tE}{R}\omega_P - (1-v)\Omega$ $\hspace{1cm}$ (II.23)

For this case eqt.II.23 simplifies to $\quad \nabla^2 F_P = -p_o R$

Thus $\quad\quad F_P = -\dfrac{p_o R r^2}{4}$ $\hspace{3cm}$ (II.36)

Derivation of constants C_3, C_4 and b_o

At $r = 0$ $\quad$ $\begin{cases} \text{w to be finite} \\[4pt] \underset{lim}{\mathcal{L}}(2\pi r\, Q_r) \to 0 \\[4pt] N_{rr} \text{ to be finite} \end{cases}$ $\quad$ Yielding $\quad$ $\begin{cases} C_3 = 0 \\[4pt] C_4 = 0 \\[4pt] b_o = 0 \end{cases}$

$\hspace{10cm}$ (II.37a-c)

Details of the derivation of these constants are given in
Appendix VIII.2.1 p. 257

Substituting eqts.II.35,36 and 37 into II.34a,b, w_i and F_i may be
written:-

$$\omega_i = C_1 ber\, {}^r\!/\!\ell + C_2 bei\, {}^r\!/\!\ell + C_5$$

$$F_i = \dfrac{\ell^2 tE}{R}\left[C_1 bei\, {}^r\!/\!\ell - C_2 ber\, {}^r\!/\!\ell \right] - \dfrac{p_o R r^2}{4} \hspace{1.5cm} (\text{II.38a,b})$$

where $\quad C_5 = -A_o - \dfrac{p_o R^2}{Et}$

(ii) $\quad$ Outside the Loaded Area i.e. $\quad r_p \leqslant r \leqslant \infty$

The subscript 'o' will be used for this region. Thus from eqts.
II.29 and II.30, introducing other constants and noting that,
as before, $B_o = 0$ and a_o is immaterial, the following is obtained:-

$$\omega_o = C_6 ber\, {}^r\!/\!\ell + C_7 bei\, {}^r\!/\!\ell + C_8 ker\, {}^r\!/\!\ell + C_9 kei\, {}^r\!/\!\ell - A_1 + \omega_P$$

$$F_o = \dfrac{\ell^2 tE}{R}\left(C_6 bei\, {}^r\!/\!\ell - C_7 ber\, {}^r\!/\!\ell - C_9 ker\, {}^r\!/\!\ell + C_8 kei\, {}^r\!/\!\ell \right) + b_1 \ell n\, {}^r\!/\!\ell + F_P \hspace{0.5cm} (\text{II.39a,b})$$

Particular Integrals

$p = p_\theta = p_r = 0$, thus $\Omega = 0$ and eqt.II.12 is satisfied when

$$w_P = 0 \hspace{5cm} (\text{II.40})$$

Therefore from eqt.II.23 $\quad \nabla^2 F_P = 0 \quad$ and $\quad F_P = A + B\ln {}^r\!/\!\ell \quad$ (II.41)

The constant A, however, is immaterial, since only derivatives
of F appear in the force equations II.4a-c, and the constant B

is combined with b_1 such that $C_{10} = (B+b_1)\dfrac{\sqrt{12(1-v^2)}}{Et^2}$ (II.42)

Derivation of constants C_6 , C_7 and A_1

As $r \rightarrow \infty$
$$\begin{cases} M_{\theta\theta} \rightarrow 0 \\ M_{rr} \rightarrow 0 \\ w \rightarrow 0 \end{cases} \text{yielding} \begin{cases} C_6 = C_7 = 0 \\ \\ A_1 = 0 \end{cases} \quad \text{(II.43a-c)}$$

Details of the derivation of these constants are given in

Appendix VIII.2.1b, p. 257

Derivation of constant C_{10} defined as eqt.II.42

The summation of vertical forces acting on any parallel circle

must be zero.   Thus from Fig.II.2 the sum of the vertical com-

ponents of N_{rr} and Q_r is

$Q_r - \dfrac{r}{R} N_{rr} = \dfrac{P}{2\pi r}$ (II.44)

From eqts.II.5 and II.4a,

eqt.II.44 becomes:-

$-D\dfrac{d}{dr}(\nabla^2 w) - \dfrac{dF}{Rdr} = \dfrac{P}{2\pi r}$

Substituting for w and F

Fig.II.2

from eqts.II.39a,b utilizing

eqts.II.42 and II.43a-c, $C_{10} = -\dfrac{PR\sqrt{12(1-v^2)}}{2\pi Et^2}$ (II.45)

Derivation of constants C_1 , C_2 , C_3 , C_8 and C_9

There remain thus <u>FIVE</u> constants which are determined from

the conditions at $r = r_p$.   It is convenient to define a para-

meter μ by $\mu = r_p/\ell$, and express the constants C_n in terms of a

new series of non-dimensional constants c_n , given by the

relationship:- $C_n = \dfrac{c_n PR \sqrt{12(1-v^2)}}{\pi Et^2 \mu^2}$

The expressions for w and F can thus be written from eqts. II.38,

II.39a,b utilizing eqts.II.43a-c and II.45:-
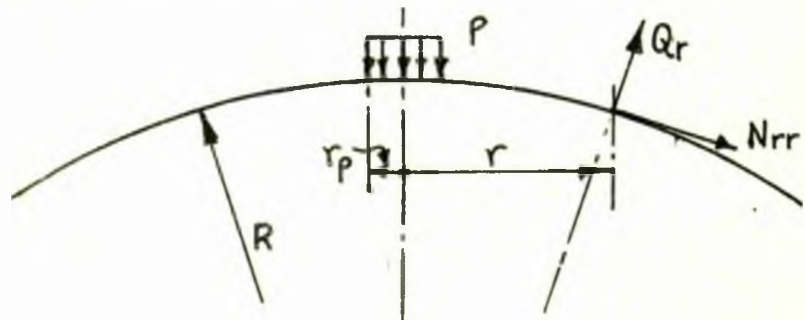
$$\omega_i = \frac{PR\sqrt{12(1-\upsilon^2)}}{Et^2\pi\mu^2}\left[c_1 ber\,^r\!/_\ell + c_2 bei\,^r\!/_\ell + c_5\right]$$

$$\omega_o = \frac{PR\sqrt{12(1-\upsilon^2)}}{Et^2\pi\mu^2}\left[c_8 ker\,^r\!/_\ell + c_9 kei\,^r\!/_\ell\right]$$

$$F_i = \frac{PR}{\pi\mu^2}\left[c_1 bei\,^r\!/_\ell - c_2 ber\,^r\!/_\ell - \frac{1}{4}\left(^r\!/_\ell\right)^2\right]$$

$$F_o = \frac{PR}{\pi\mu^2}\left[c_8 kei\,^r\!/_\ell - c_9 ker\,^r\!/_\ell - \frac{\mu^2}{2}\ell n\,^r\!/_\ell\right] \qquad\qquad (II.46a\text{-}d)$$

<u>At $r = r_p$</u>
$$\begin{cases}\omega_i = \omega_o \\[4pt] \dfrac{d\omega_i}{dr} = \dfrac{d\omega_o}{dr} \\[4pt] \nabla^2\omega_i = \nabla^2\omega_o \\[4pt] \dfrac{dF_i}{dr} = \dfrac{dF_o}{dr} \\[4pt] \nabla^2 F_i = \nabla^2 F_o\end{cases}$$

yielding, after
solving five
simultaneous
linear equations

$$\begin{cases}c_1 = -\mu\,ker'\mu \\[4pt] c_2 = \mu\,kei'\mu \\[4pt] c_5 = -1 \\[4pt] c_8 = -\mu\,ber'\mu \\[4pt] c_9 = \mu\,bei'\mu\end{cases}$$
$(II.47a\text{-}e)$

Full details of the derivation of these constants are given

in Appendix VIII.2.1c   p. *258*

Substituting eqts. II.46a-d into eqts. II.4 it is possible to

express the forces and moments in terms of the constants c_1,

c_2, c_5, c_8, c_9 which are known for a particular μ from eqt. II.47a-e.

The following relationships:-

$$N_{rr} = \sigma_{rD}t \quad , \qquad N_{\theta\theta} = \sigma_{\theta D}t$$

$$M_{rr} = \frac{\sigma_{rB}t^2}{6} \quad , \qquad M_{\theta\theta} = \frac{\sigma_{\theta B}t^2}{6} \qquad\qquad (II.48a\text{-}d)$$

enable a further modification to be made and the direct and

bending stress to be written in the following form:-

<u>Inside the Loaded Area   i.e. $0 \leqslant r \leqslant r_p$</u>

$$\sigma_{r,D} = \frac{P\sqrt{12(1-\upsilon^2)}}{\pi\mu^2 t^2}\left[c_1\frac{bei'\,^r\!/_\ell}{^r\!/_\ell} - c_2\frac{ber'\,^r\!/_\ell}{^r\!/_\ell} - \frac{1}{2}\right]$$

$$\sigma_{\theta,D} = \frac{P\sqrt{12(1-\upsilon^2)}}{\pi\mu^2 t^2}\left[c_1 bei''\,^r\!/_\ell - c_2 ber''\,^r\!/_\ell - \frac{1}{2}\right]$$

$$\sigma_{rB} = \pm\frac{6P}{\pi t^2\mu^2}\left\{-c_1\left[bei\,^r\!/_\ell + \frac{(1-\upsilon)ber'\,^r\!/_\ell}{^r\!/_\ell}\right] + c_2\left[ber\,^r\!/_\ell - \frac{(1-\upsilon)bei'\,^r\!/_\ell}{^r\!/_\ell}\right]\right\}$$

$$\sigma_{\theta B} = \pm \frac{6P}{\pi t^2 \mu^2}\left\{ c_1\left[\frac{(1-\upsilon)\,ber'\,r/\ell}{r/\ell} - \upsilon\,bei\,r/\ell\right] + c_2\left[\frac{(1-\upsilon)\,bei'\,r/\ell}{r/\ell} + \upsilon\,ber\,r/\ell\right]\right\}$$

$$\omega = \frac{PR\sqrt{12(1-\upsilon^2)}}{\pi E t^2 \mu^2}\left[c_1\,ber\,r/\ell + c_2\,bei\,r/\ell + c_5\right] \qquad\text{(II.49a-e)}$$

In particular at $r = 0$, using the appropriate series expansion

given in the Appendix VIII.8

$$\sigma_{rD}(0) = \sigma_{\theta D}(0) = \frac{P\sqrt{12(1-\upsilon^2)}}{2\pi\mu^2 t^2}(c_1 + c_5)$$

$$\sigma_{rB}(0) = \sigma_{\theta B}(0) = \pm\frac{3P(1+\upsilon)}{\pi\mu^2 t^2}\,c_2$$

$$\omega(0) = \frac{PR\sqrt{12(1-\upsilon^2)}}{\pi E t^2 \mu^2}(c_1 + c_5) \qquad\text{(II.50a-c)}$$

where $c_1 = -\mu\,ker'\mu$, $c_2 = \mu\,kei'\mu$ and $c_5 = -1$

Outside the Loaded Area $\quad r \geqslant r_p$

$$\sigma_{r,D} = \frac{P\sqrt{12(1-\upsilon^2)}}{\pi\mu^2 t^2}\left[c_8\frac{kei'\,r/\ell}{r/\ell} - c_9\frac{ker'\,r/\ell}{r/\ell} - \frac{1}{2}\left(\frac{\mu}{r/\ell}\right)^2\right]$$

$$\sigma_{\theta,D} = \frac{P\sqrt{12(1-\upsilon^2)}}{\pi\mu^2 t^2}\left[c_8\,kei''r/\ell - c_9\,ker''r/\ell + \frac{1}{2}\left(\frac{\mu}{r/\ell}\right)^2\right]$$

$$\sigma_{r,B} = \pm\frac{6P}{\pi\mu^2 t^2}\left\{-c_8\left[kei\,r/\ell + \frac{(1-\upsilon)ker'\,r/\ell}{r/\ell}\right] + c_9\left[ker\,r/\ell - \frac{(1-\upsilon)kei'\,r/\ell}{r/\ell}\right]\right\}$$

$$\sigma_{\theta,B} = \pm\frac{6P}{\pi\mu^2 t^2}\left\{-c_8\left[\upsilon\,kei\,r/\ell - \frac{(1-\upsilon)ker'\,r/\ell}{r/\ell}\right] + c_9\left[\upsilon\,ker\,r/\ell + \frac{(1-\upsilon)kei'\,r/\ell}{r/\ell}\right]\right\}$$

$$\omega = \frac{PR\sqrt{12(1-\upsilon^2)}}{\pi E t^2 \mu^2}\left[c_8\,ker\,r/\ell + c_9\,kei\,r/\ell\right] \qquad\text{(II.51a-e)}$$

where $c_8 = -\mu\,ber'\mu$ and $c_9 = \mu\,bei'\mu$

From equations II.49 and II.51 it is possible to derive values

of stress for particular values of μ i.e. r_p/ℓ . Figs. II.3 →

II.5 present the equations graphically for various values of μ.

The relationships for ber'', bei'', ker'', kei'' used in this

derivation, are given in Appendix VIII.8

(b) The Concentrated Load at the Crown. Fig.II.6

The concentrated load is essentially a particular example of

the uniformily distributed load case, where r_p i.e. $\mu = 0$.
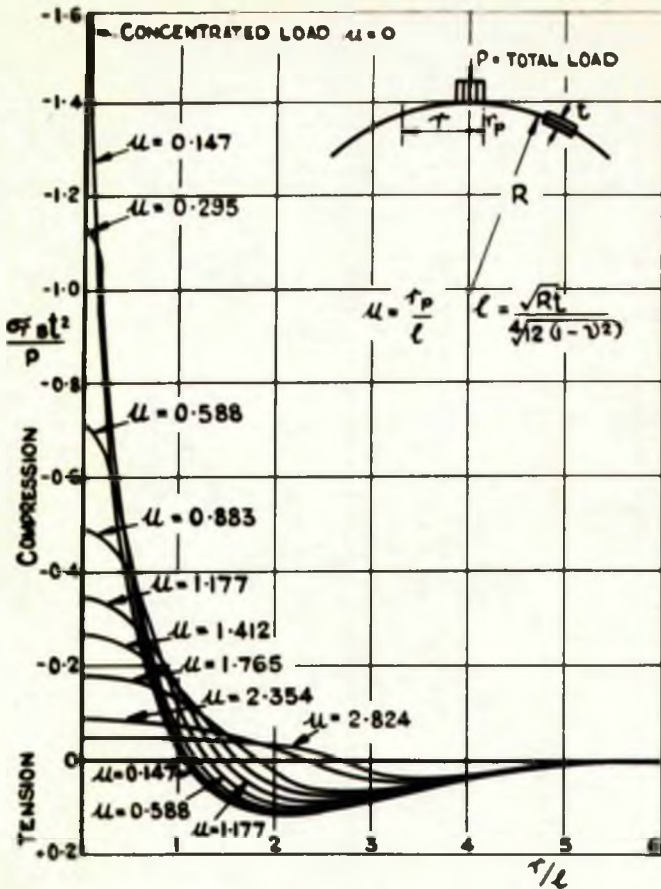
FIG II 3a THE DISTRIBUTION OF MERIDIONAL BENDING STRESS ON THE OUTSIDE SURFACE
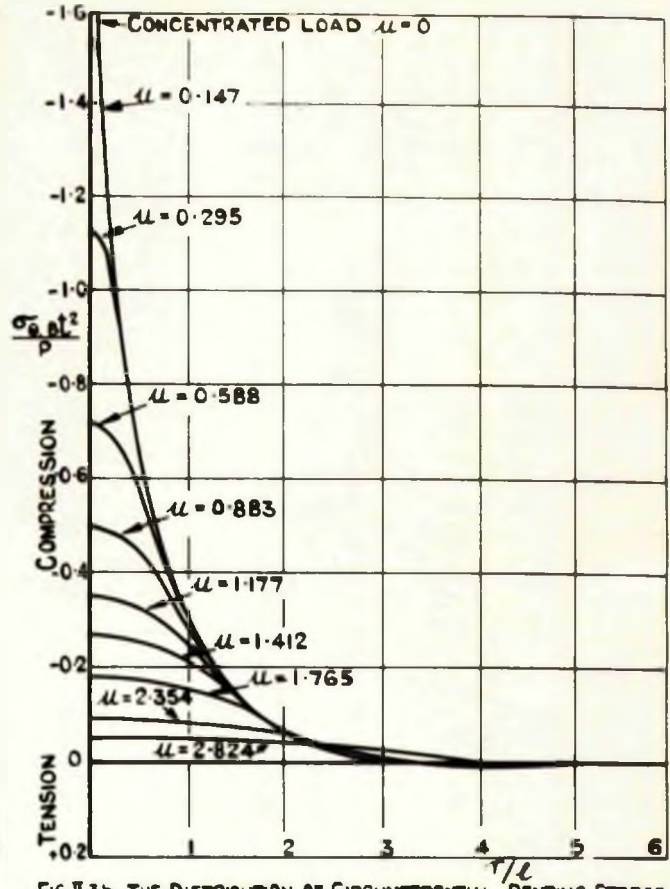
FIG II 3b THE DISTRIBUTION OF CIRCUMFERENTIAL BENDING STRESS ON THE OUTSIDE SURFACE
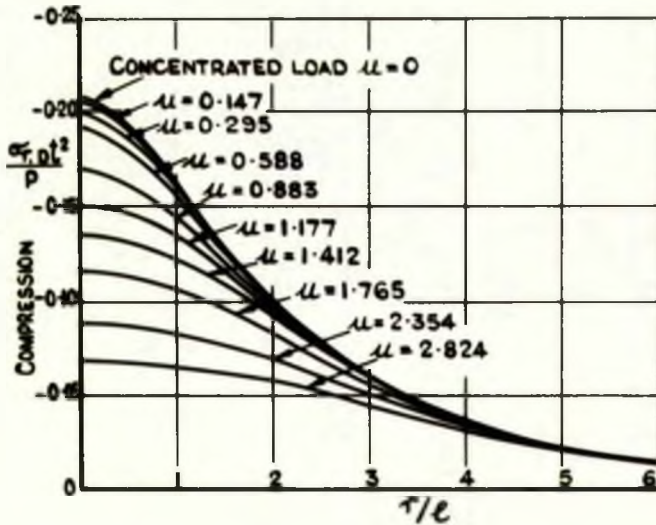
FIG II 3c THE DISTRIBUTION OF MERIDIONAL DIRECT STRESS
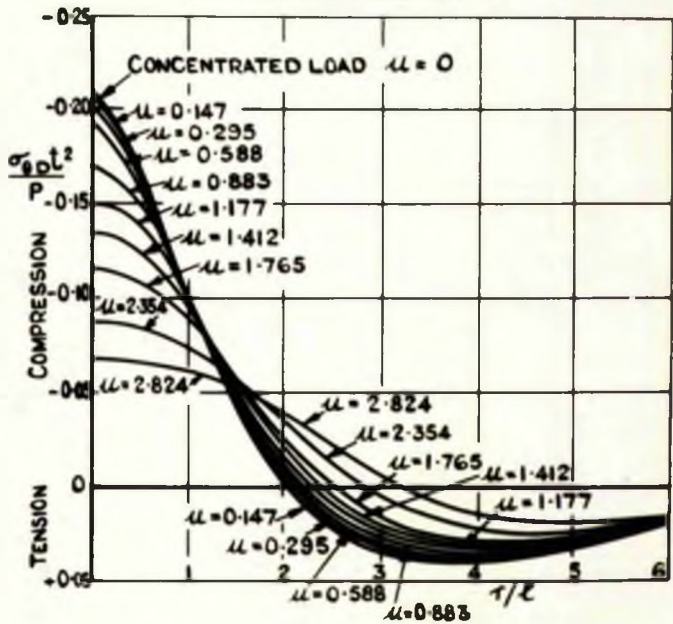
FIG II 3d THE DISTRIBUTION OF CIRCUMFERENTIAL DIRECT STRESS

FIG II 3 THE DISTRIBUTION OF BENDING AND DIRECT STRESS IN A SHALLOW SPHERICAL SHELL DUE TO A CONCENTRATED AND UNIFORMLY DISTRIBUTED LOAD AT THE CROWN, FOR VARIOUS μ VALUES
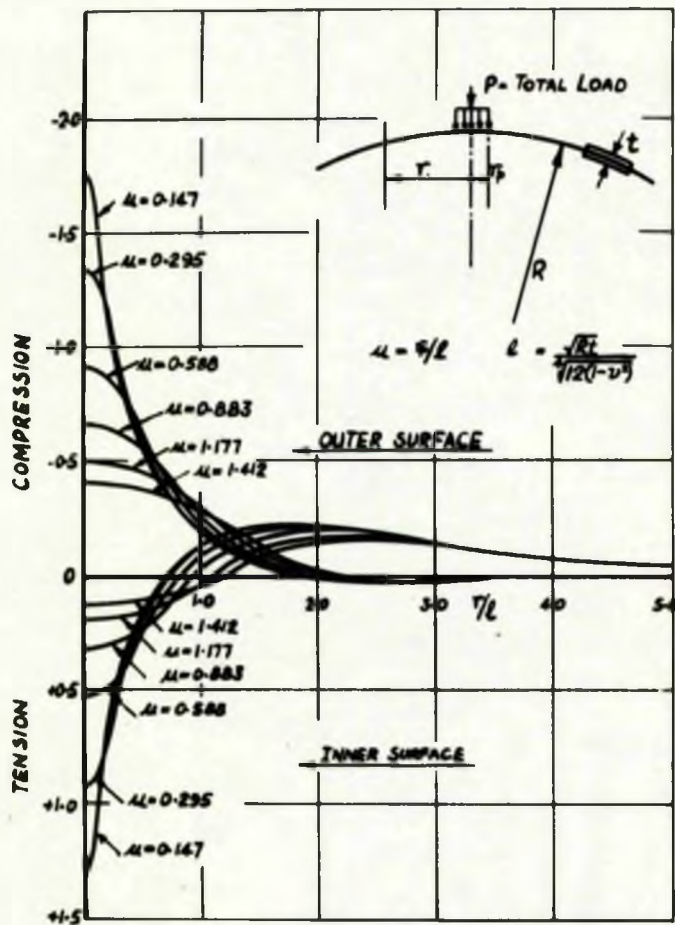
Fig.Ⅱ·4a. THE DISTRIBUTION OF TOTAL MERIDIONAL STRESS ON THE OUTER AND INNER SURFACES
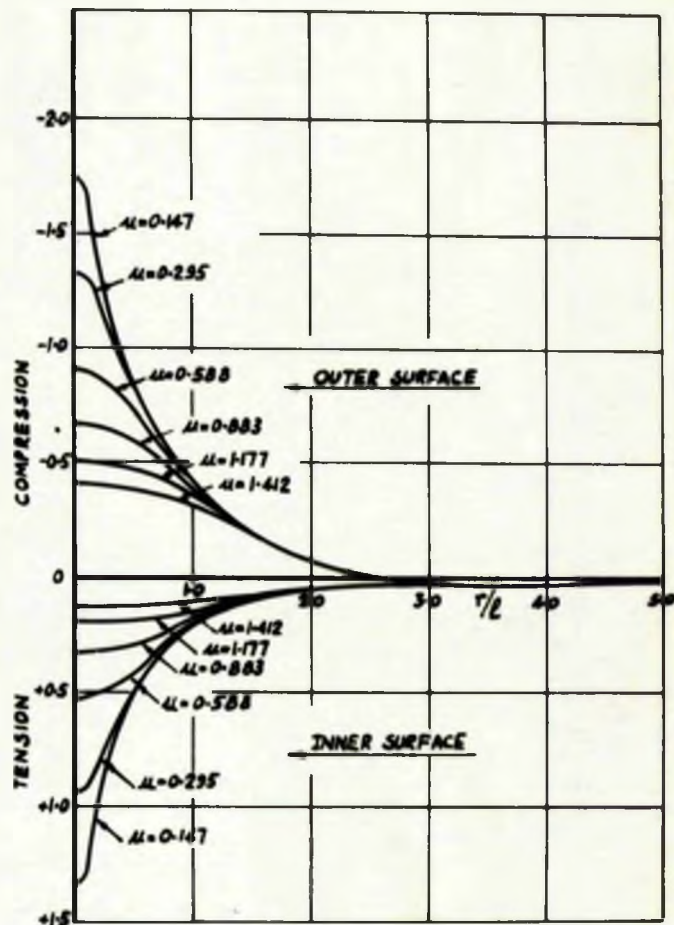
Fig.Ⅱ·4b. THE DISTRIBUTION OF TOTAL CIRCUMFERENTIAL STRESS ON THE OUTER AND INNER SURFACES

Fig.Ⅱ·4   THE DISTRIBUTION OF TOTAL STRESSES (ie DIRECT & BENDING) IN A SHALLOW SPHERICAL SHELL DUE TO A U.D. LOAD AT THE CROWN, FOR VARIOUS μ VALUES.
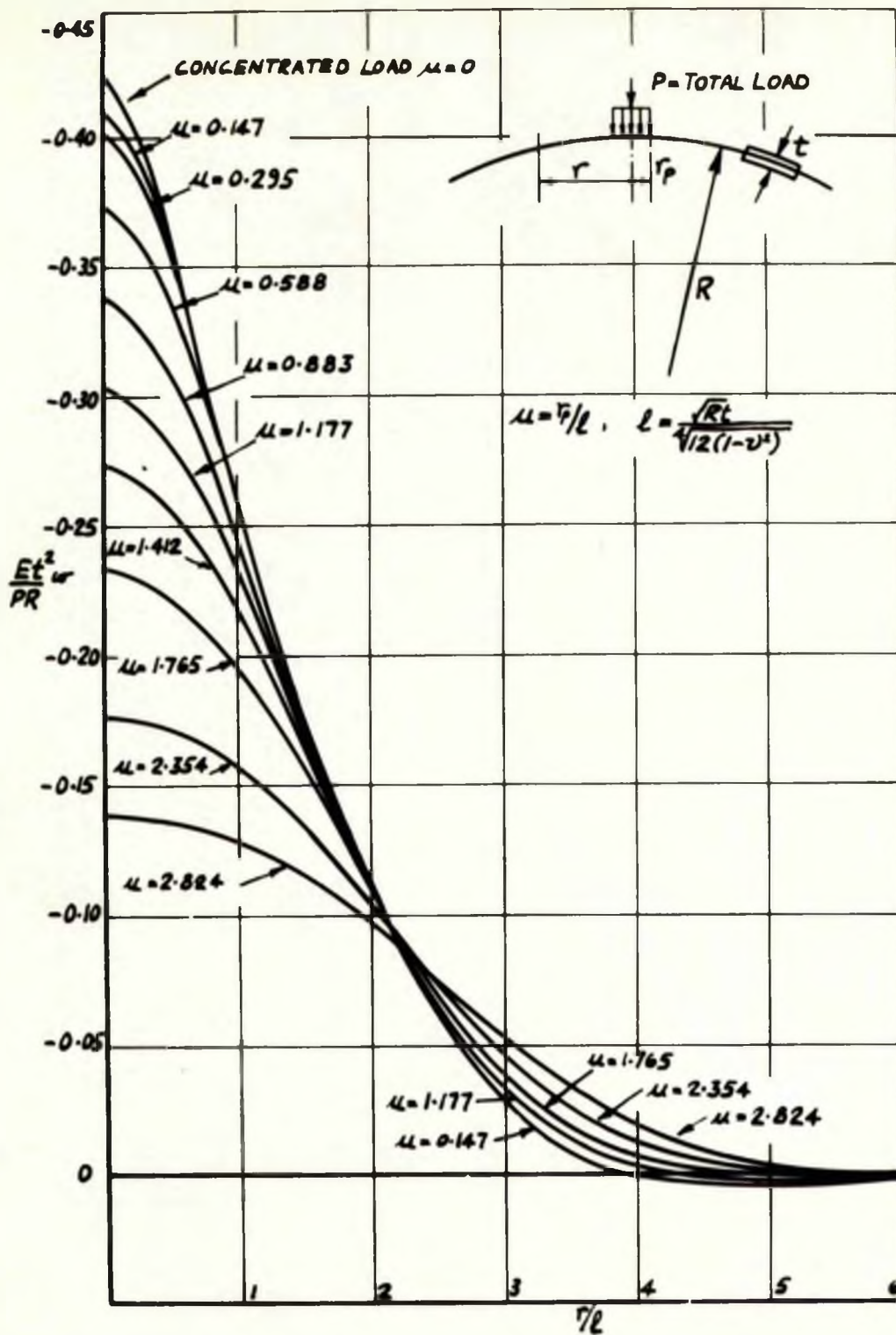
FIG. II·5 THE DISTRIBUTION OF RADIAL DEFLECTION OF A SHALLOW SPHERICAL SHELL DUE TO A UNIFORMLY DISTRIBUTED RADIAL LOAD AT THE CROWN, FOR VARIOUS μ VALUES.

Thus considering the equations relevant
to outside the loaded area, eqts. II.51a-e,
and substituting for c_θ and ρ_q from eqt.
II.47d,e, the eqt. for $\sigma_{r.D}$ may be written:-
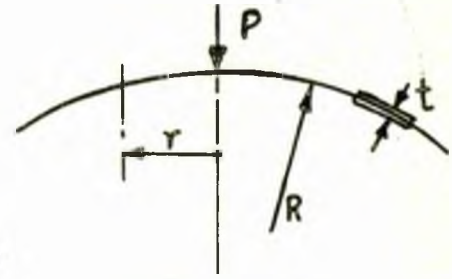
$$\sigma_{r.D} = \frac{P\sqrt{12(1-v^2)}}{\pi t^2}\left[-\frac{ber'\mu}{\mu}.\frac{kei'r/\ell}{r/\ell} - \frac{bei'\mu}{\mu}\frac{ker'r/\ell}{r/\ell} - \frac{1}{2}\left(\frac{1}{r/\ell}\right)^2\right]$$ (II.52)

From the definitions of $\dfrac{ber'\mu}{\mu}$ and $\dfrac{bei'\mu}{\mu}$ given in Appendix VIIL.8:

$\underline{\text{for } \mu=0}$; $\dfrac{ber'\mu}{\mu} = 0$ and $\dfrac{bei'\mu}{\mu} = \dfrac{1}{2}$ (II.53a,b)

Thus II.52 can be written,

$$\sigma_{r.D} = -\frac{P\sqrt{12(1-v^2)}}{2\pi t^2}\left[\frac{ker'r/\ell}{r/\ell} + \left(\frac{1}{r/\ell}\right)^2\right]$$ (II.54a)

In a similar way the relationships for $\sigma_{\theta.D}$, σ_{rB}, $\sigma_{\theta B}$ and w can be
written:-

$$\sigma_{\theta.D} = +\frac{P\sqrt{12(1-v^2)}}{2\pi t^2}\left[\frac{ker'r/\ell}{r/\ell} + kei\,r/\ell + \left(\frac{1}{r/\ell}\right)^2\right]$$

$$\sigma_{rB} = \pm\frac{3P}{\pi t^2}\left[ker\,r/\ell - \frac{(1-v)\,kei'r/\ell}{r/\ell}\right]$$

$$\sigma_{\theta B} = \pm\frac{3P}{\pi t^2}\left[\frac{(1-v)\,kei'r/\ell}{r/\ell} + v\,ker\,r/\ell\right]$$

$$w = \frac{PR\sqrt{12(1-v^2)}}{2\pi E t^2}\,kei\,r/\ell$$ (II.54b-e)

When the radius $r = 0$, it is possible to obtain finite expres-
sions for w, σ_{rD} and $\sigma_{\theta D}$, using the definitions of $kei\,z$, $\dfrac{ker'z}{z}$,

$ker\,z$ and $\dfrac{kei'z}{z}$ given in Appendix VIII.8. These are as

follows:- $w(0) = -\dfrac{1}{4}\sqrt{3(1-v^2)}\,\dfrac{PR}{Et^2}$

$$\sigma_{rD}(0) = -\frac{1}{8}\sqrt{3(1-v^2)}\,\frac{P}{t^2}$$

$$\sigma_{\theta D}(0) = -\frac{1}{8}\sqrt{3(1-v^2)}\,\frac{P}{t^2}$$

Approximate values of σ_{rB} and $\sigma_{\theta B}$ for small values of r/ℓ are

also obtained $\sigma_{rB} \approx \pm\dfrac{3P}{\pi t^2}\dfrac{(1+v)}{2}\ln r/\ell$

$$\sigma_{\theta B} \approx \pm\frac{3P}{\pi t^2}\frac{(1+v)}{2}\ln r/\ell$$ (II.55a-e)

Equation II.54a-e are shown graphically on Figs. II.3 and 5.

(c) The Loading of a rigid cylindrical insert built into the discontinuous shell (Fig.II.7)

The relevant equations for w and F governing this problem are those of the shell with a uniformly distributed load in the region outside the loaded area, i.e. II.46b,d namely:-

Fig.II.7

$$\omega = \frac{PR\sqrt{12(1-\upsilon^2)}}{Et^2\pi\mu^2}\left[C_8 \ker \frac{r}{\ell} + C_9 \kei \frac{r}{\ell}\right]$$

$$F = \frac{PR}{\pi\mu^2}\left[c_8 \kei \frac{r}{\ell} - c_9 \ker \frac{r}{\ell} - \frac{\mu^2}{2}\ln \frac{r}{\ell}\right]$$
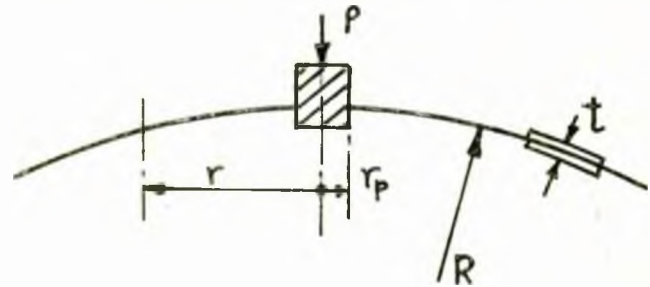
Giving the following equations:-

$$\sigma_{rD} = \frac{P\sqrt{12(1-\upsilon^2)}}{\pi\mu^2 t^2}\left[c_8 \frac{\kei'\frac{r}{\ell}}{\frac{r}{\ell}} - c_9 \frac{\ker'\frac{r}{\ell}}{\frac{r}{\ell}} - \frac{1}{2}\left(\frac{\mu}{\frac{r}{\ell}}\right)^2\right]$$

$$\sigma_{\partial D} = \frac{P\sqrt{12(1-\upsilon^2)}}{\pi\mu^2 t^2}\left[c_8 \kei'\frac{r}{\ell} - c_9 \ker''\frac{r}{\ell} + \frac{1}{2}\left(\frac{\mu}{\frac{r}{\ell}}\right)^2\right]$$

$$\sigma_{rB} = \pm \frac{6P}{\pi\mu^2 t^2}\left\{-c_8\left[\kei\frac{r}{\ell} + \frac{(1-\upsilon)\ker'\frac{r}{\ell}}{\frac{r}{\ell}}\right] + c_9\left[\ker\frac{r}{\ell} - \frac{(1-\upsilon)\kei'\frac{r}{\ell}}{\frac{r}{\ell}}\right]\right\}$$

$$\sigma_{\partial B} = \pm \frac{6P}{\pi\mu^2 t^2}\left\{-c_8\left[\upsilon\kei\frac{r}{\ell} - \frac{(1-\upsilon)\ker'\frac{r}{\ell}}{\frac{r}{\ell}}\right] + c_9\left[\upsilon\ker\frac{r}{\ell} + \frac{(1-\upsilon)\kei'\frac{r}{\ell}}{\frac{r}{\ell}}\right]\right\}$$

$$\omega = \frac{PR\sqrt{12(1-\upsilon^2)}}{\pi Et^2\mu^2}\left[c_8 \ker\frac{r}{\ell} + c_9 \kei\frac{r}{\ell}\right]$$

(II.56a-e)

Derivation of the constants c_8 and c_9

In this case the two constants c_8 and c_9 are obtained by considering the boundary $r = r_p$

at $r = r_p$ $\begin{cases} \dfrac{d\omega}{dr} = 0 \\ \\ \varepsilon_\theta = \dfrac{(N_{\theta\theta} - \upsilon N_{rr})}{Et} = 0 \end{cases}$ yielding:- $\begin{cases} c_8 = -\dfrac{(1+\upsilon)\mu \kei'\mu}{2[V]} \\ \\ c_9 = -c_8 \dfrac{\ker'\mu}{\kei'\mu} \end{cases}$ (II.57a,b)

where $[V] = [\mu(\kei'\mu \ker\mu - \ker'\mu \kei\mu) - (1+\upsilon)(\kei'^2\mu + \ker'^2\mu)]$

The derivation of the above constants is given in Appendix VIII VIII.2.2a p. 260.
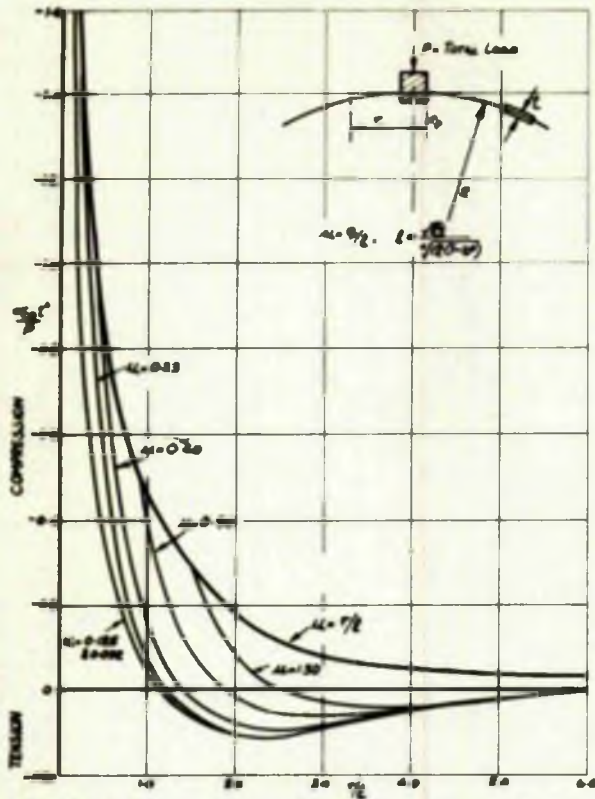
Fig II-8a. The Distribution of Meridional Bending Stress on outer surface.
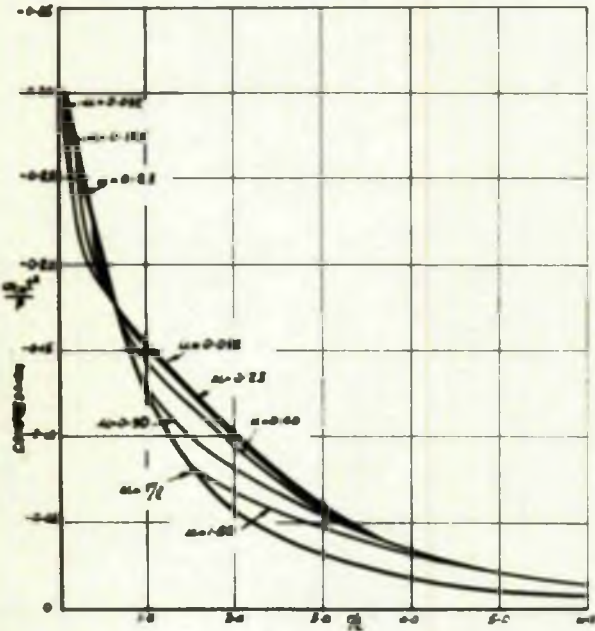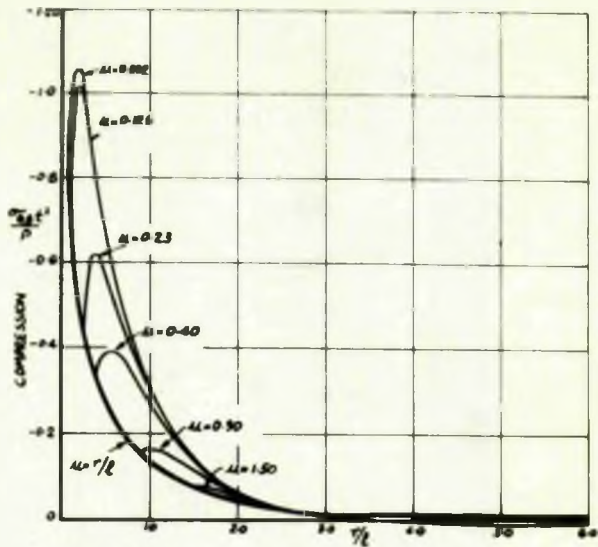
Fig II-8b. The Distribution of Circumferential Bending Stress on the outer surface.
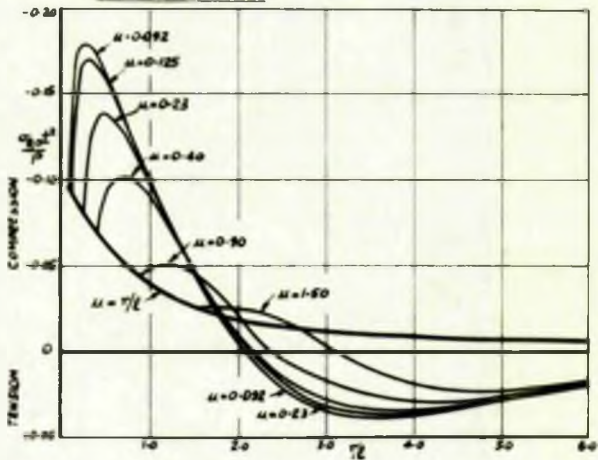
Fig. II-8d. The Distribution of Circumferential Direct Stress.

Fig II-8c. The Distribution of Meridional Direct Stress.
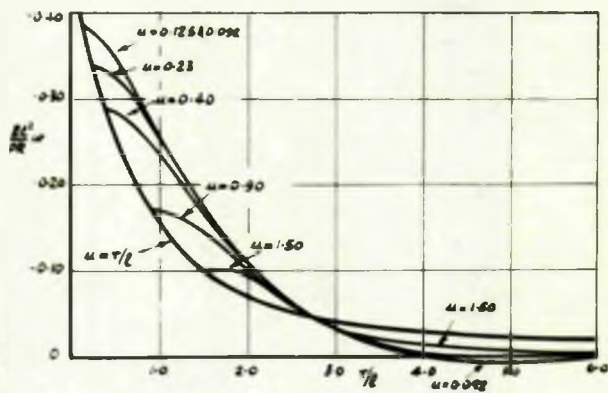
Fig II-8e. The Distribution of Radial Deflection.

Fig. II·8 The Distribution of Direct Stress & Bending Stress on the outer surface & Radial Deflection, due to Radial Loading applied to a Shallow Spherical Shell by means of a Rigid Insert at the crown. For various μ values.
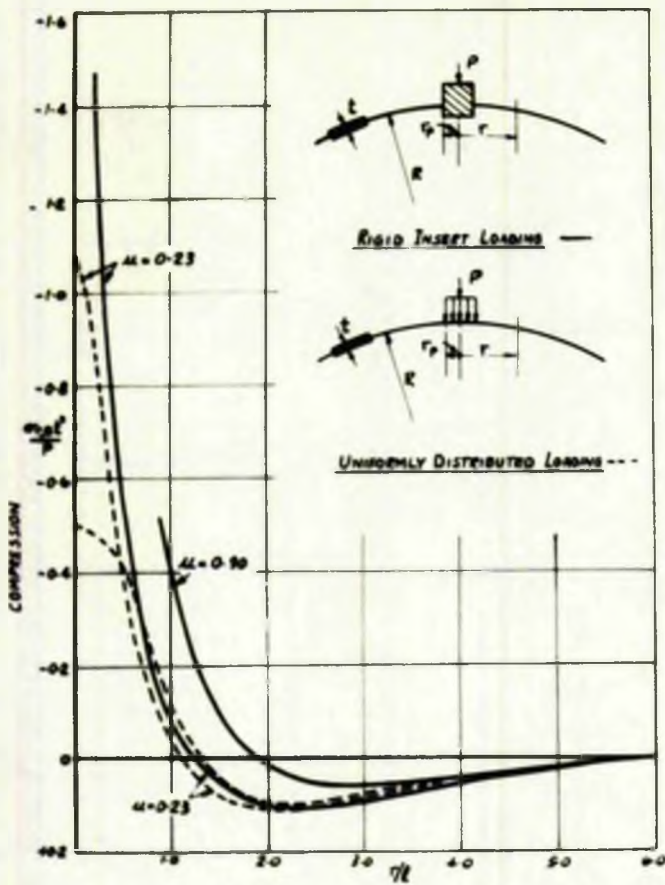
FIG. II·9a THE DISTRIBUTION OF MERIDIONAL BENDING STRESS

FIG. II·9b THE DISTRIBUTION OF CIRCUMFERENTIAL BENDING STRESS
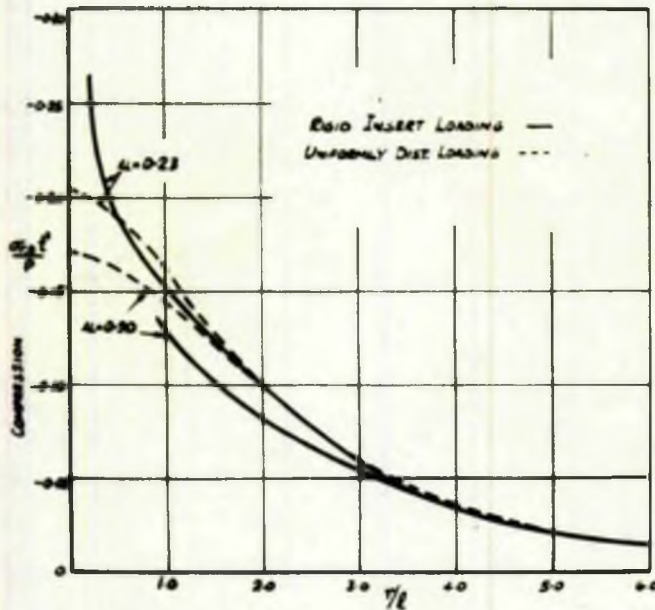
FIG. II·9c THE DISTRIBUTION OF MERIDIONAL DIRECT STRESS
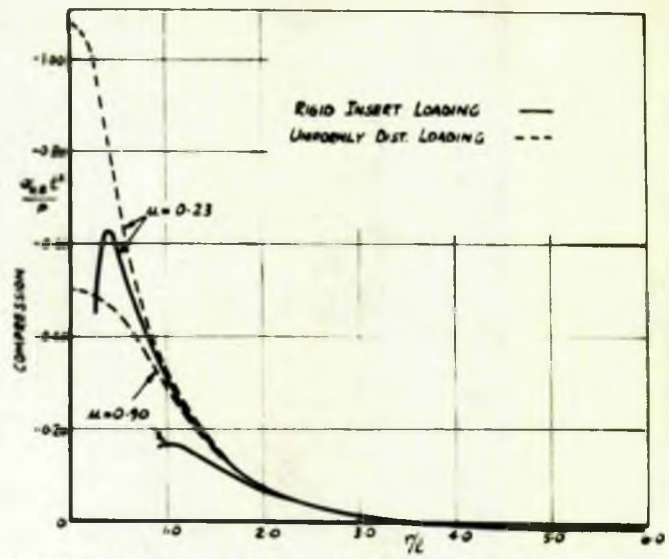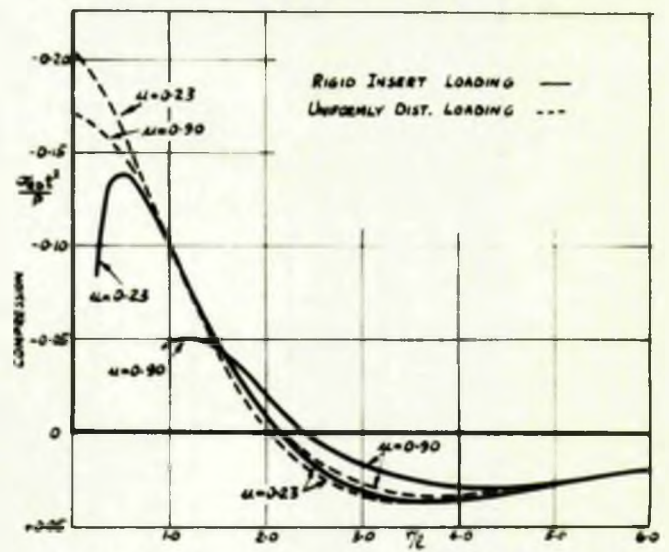
FIG. II·9d THE DISTRIBUTION OF CIRCUMFERENTIAL DIRECT STRESS
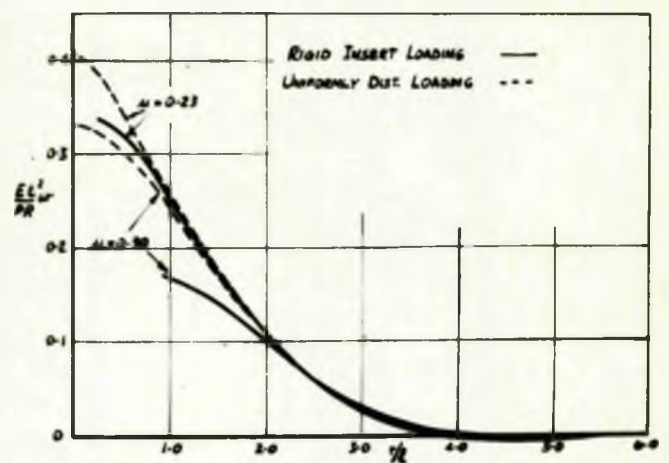
FIG. II·9e THE DISTRIBUTION OF RADIAL DEFLECTION

FIG. II·9 A COMPARISON BETWEEN THE STRESSES AND RADIAL DEFLECTIONS FOR RIGID INSERT AND UNIFORMLY
DIST. RADIAL LOADING FOR μ = 0·23 AND 0·90.

Equations II.56 and .57 have been presented graphically in
Fig .II.8 for different values of μ.

A comparison between the stresses and radial deflection
predicted for the uniformly distributed and rigid insert radial
loadings is shown graphically for two μ values on Fig.II.9. It
is noted that the main differences occur in the case of the
circumferential stresses in the region of the insert.

II.1.3 'BENDING' MOMENT - Fig.II.10

This section is concerned with the
moment loading of a shallow shell
through a rigid cylindrical insert
at the crown.   The moment M is
acting in a plane which contains
the normals drawn from a meridional
line, and will be designated a
'bending' moment.   The procedure
is as previously outlined.   The
general expressions for w and F,
eqts. II.27 and II.28 are considered.
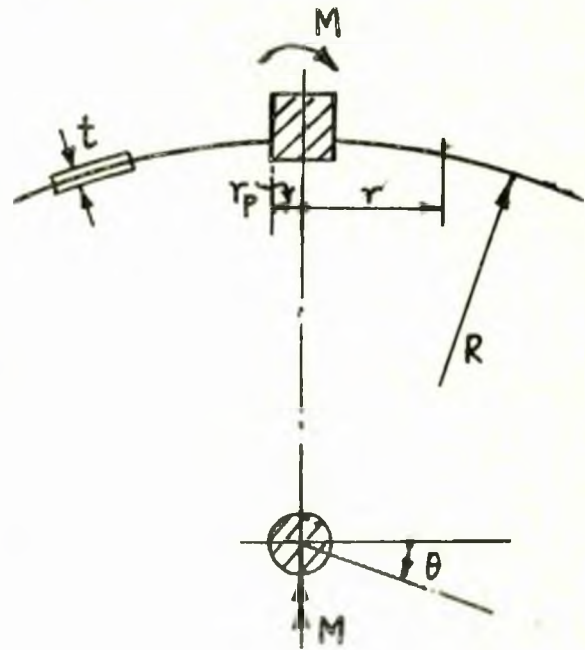
Fig.II.10

For this case the harmonic order n is equal to <u>one</u>.   Thus the
equations for w and F may be written :-

$$w = \left[C_{11} ber_1 \, r/\ell + C_{21} bei_1 \, r/\ell + C_{31} ker_1 \, r/\ell + C_{41} kei_1 \, r/\ell \right] \cos\theta$$

$$- \left[A_1 \, r/\ell + B_1 (r/\ell)^{-1} \right] \cos\theta + w_p$$

$$F = \frac{\ell^2 tE}{R} \left[-C_{21} ber_1 \, r/\ell + C_{11} bei_1 \, r/\ell - C_{41} ker_1 \, r/\ell + C_{31} kei_1 \, r/\ell \right] \cos\theta$$

$$+ \left[a_1 r/\ell + b_1 (r/\ell)^{-1} \right] \cos\theta + F_p \qquad (II.58a,b)$$

Eqts. II.58a and b contain the Bessel and Kelvin functions of
the first order.   These may be modified to those of zero
order using the following relationships (McLACHLAN (38)):-

$$ber_1 \, r/\ell = \frac{1}{\sqrt{2}} (ber' r/\ell - bei' r/\ell)$$

$$bei_1 \, r/\ell = \frac{1}{\sqrt{2}} (ber' r/\ell + bei' r/\ell)$$

$$ker_1 \, r/\ell = \frac{1}{\sqrt{2}} (ker' r/\ell - kei' r/\ell)$$

$$kei_1 \, r/\ell = \frac{1}{\sqrt{2}} (ker' r/\ell + kei' r/\ell) \qquad (II.59a-d)$$

Substituting these into equations II.58a,b, and introducing a
new set of constants w and F may be written:-

$$\omega = \left[C_1 ber' r/\ell + C_2 bei' r/\ell + C_3 ker' r/\ell + C_4 kei' r/\ell - A_1 r/\ell - B_1 \ell/r \right] \cos\theta + \omega_p$$

$$F = \left\{ \frac{\ell^2 tE}{R} \left[-C_2 ber' r/\ell + C_1 bei' r/\ell - C_4 ker' r/\ell + C_3 kei' r/\ell \right] \right.$$
$$\left. + \left[a_1 r/\ell + b_1 \ell/r \right] \right\} \cos\theta + F_p \qquad (II.60a,b)$$

Particular Integrals

The shell surface is free from loading, thus $w_p = 0$ and it
follows using the general relationship for F_p in eqt. II.23
that:-

$$F_p = \left(A \, r/\ell + B \, \ell/r \right) \cos\theta \qquad (II.61a,b)$$

Derivation of constants a_1, A and B_1

As in the case of $n = 0$, it is possible to determine certain
constants before considering the boundary conditions.

1.   It can be shown that the constants a_1 and A are immaterial
      in the membrane force expressions, for details see Appendix
      VIII.2.3a, p. 260

2.   Further it follows that $B_1 = 0$.   This can be verified in a
      manner similar to that used to prove $B_0 = 0$.   It is shown
      in Appendix VIII.2.3b. p. 261

Derivation of constants C_1, C_2 and A_1

$$r \to \infty \quad \begin{cases} M_{\theta\theta} \to 0 \\ M_{rr} \to 0 \\ \omega \to 0 \end{cases} \quad \text{yielding:-} \quad \begin{cases} C_1 = C_2 = A_1 = 0 \\ \\ (II.62a-c) \end{cases}$$

Full details of the derivation of these constants are given in
Appendix VIII.2.3c. p. 262

The equations for w and F (II.60a,b) may, therefore, be written,
utilizing eqts. II.61a,b and 11.62:-

$$w = (C_3 \, ker' \, r/\ell + C_4 \, kei' \, r/\ell) \cos \theta$$

$$F = \frac{Et^2}{\sqrt{12(1-\upsilon^2)}} \left[C_3 \, kei' \, r/\ell - C_4 \, ker' \, r/\ell + C_5 (r/\ell)^{-1} \right] \cos \theta \qquad \text{(II.63a,b)}$$

$$\text{where } C_5 = (\beta + b.) \frac{\sqrt{12(1-\upsilon^2)}}{Et^2}$$

Derivation of constant C_5

For large values of r, the applied moment M is taken by the membrane force Nrr – Fig. II.11.

The total moment M can be equated to these forces, thus

$$M = -2 \int_0^{\pi} N_{rr} \, \frac{r^3}{R} \cos \theta \cdot d\theta$$

$$= - \frac{\pi r^3}{R} N_{rr}^{*}$$

$$\text{Thus } Nrr = - \frac{MR \cos \theta}{\pi r^3} \qquad \text{(II.64)}$$

This force, Nrr, can also be expressed in terms of C_3, C_4 and C_5, using eqt. II.63b for F and II.4a for Nrr. For large values of r, this simplifies to $Nrr = -\frac{Et^2}{\sqrt{12(1-\upsilon^2)}} \left(2 C_5 \frac{\ell}{r^3} \right) \cos \theta$ (II.65)

Comparing eqts. II.64 and II.65, $C_5 = \frac{RM \cdot \sqrt{3(1-\upsilon^2)}}{\pi E t^2 \ell}$ (II.66)

Derivation of C_3 and C_4

$$r = r_p \quad \begin{cases} \dfrac{dw}{dr} = \dfrac{w}{r} \\[2mm] \mathcal{E}_\theta = \dfrac{(N_{\theta\theta} - \upsilon N_{rr})}{Et} = 0 \end{cases} \text{yielding} \begin{cases} C_3 = \dfrac{-(1+\upsilon)[12(1-\upsilon^2)]^{\frac{1}{2}}(2 \, kei'\mu - \mu \, ker\mu) MR}{\pi \mu [X]} \dfrac{MR}{Et^2 \ell} \\[3mm] C_4 = -\dfrac{C_3 (2 \, ker'\mu + \mu \, kei\mu)}{2 \, kei'\mu - \mu \, ker\mu} \end{cases} \text{(II.67a,b)}$$

where

$$[X] = (1+\upsilon)[\mu^2(ker^2\mu + kei^2\mu) + 4(kei'^2\mu + ker'^2\mu)$$
$$+ 4\mu(ker'\mu \, kei\mu - ker\mu \, kei'\mu)] - [\mu^3(ker'\mu \, ker\mu + kei'\mu \, kei\mu)]$$

The derivation of the above constants is given in Appendix VIII.2.3d, p. 263

It will be noted that the constants C_3, C_4 and C_5 are not non-dimensional. In this instance their use in this form is just as convenient as in a converted non-dimensional form.

As in earlier cases it is possible to express the stresses in terms of the constants C_3, C_4 and C_5 using the equations for
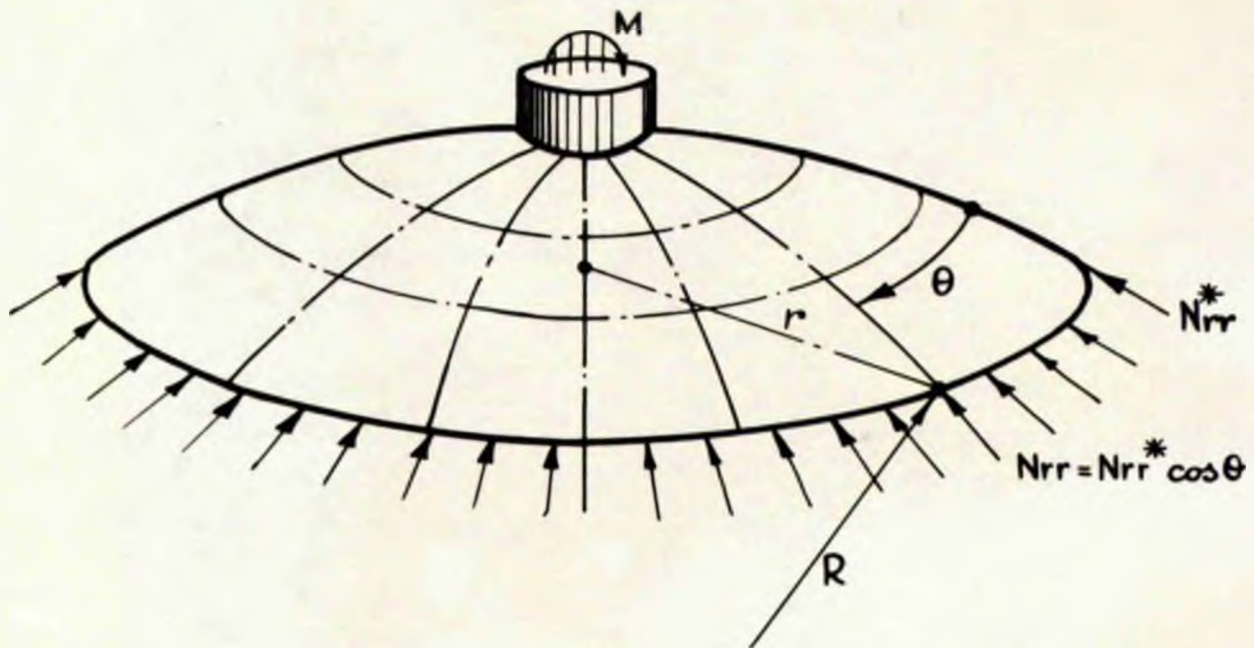
FIG. II·11 THE MERIDIONAL NORMAL FORCE (N_{rr}) ON THE SHELL
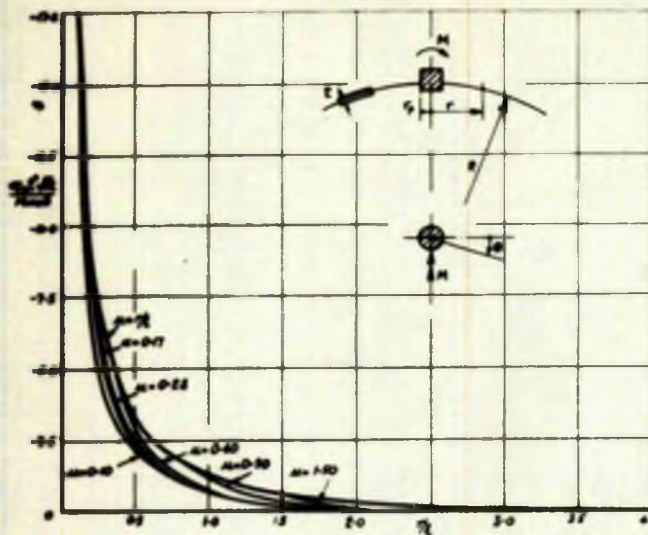
FIG. II-12a THE DISTRIBUTION OF MERIDIONAL BENDING STRESS ON THE OUTER SURFACE
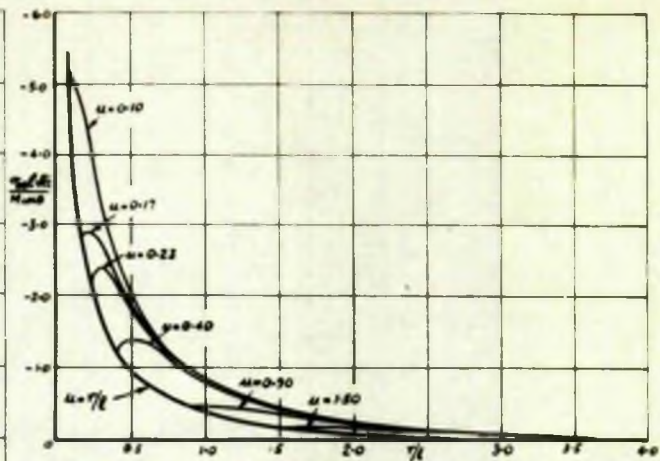
FIG. II-12b THE DISTRIBUTION OF CIRCUMFERENTIAL BENDING STRESS ON THE OUTER SURFACE
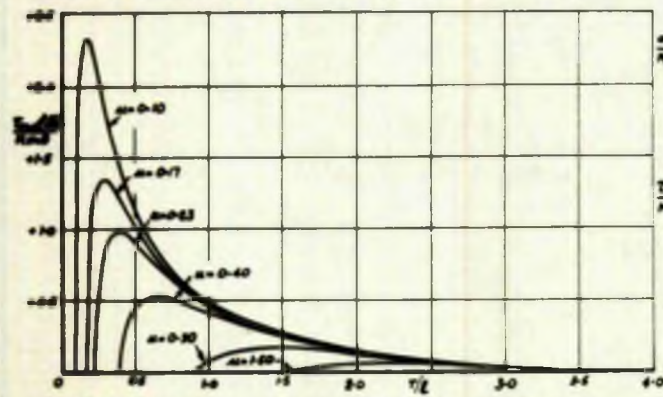
FIG. II-12c THE DISTRIBUTION OF "BENDING" SHEAR STRESS ON OUTER SURFACE
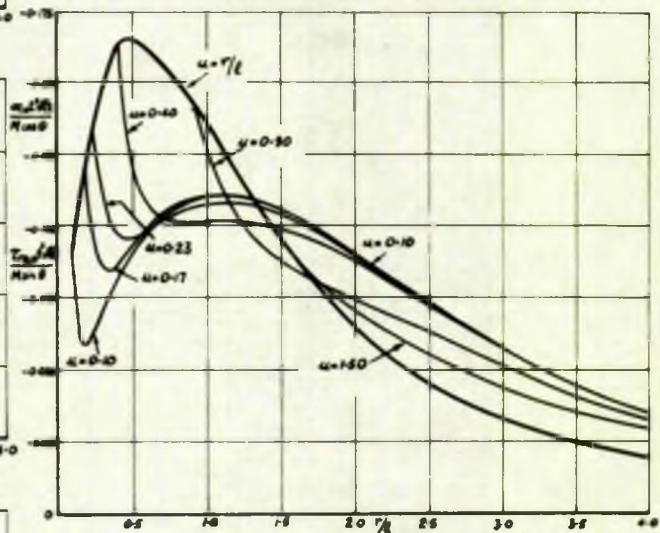
FIG. II-12d THE DISTRIBUTION OF MERIDIONAL DIRECT STRESS AND "MID-SURFACE" SHEAR STRESS
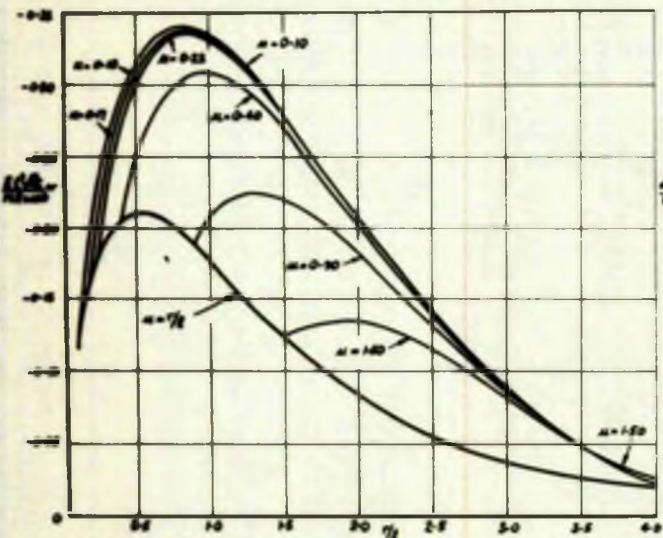
FIG. II-12e THE DISTRIBUTION OF RADIAL DEFLECTION
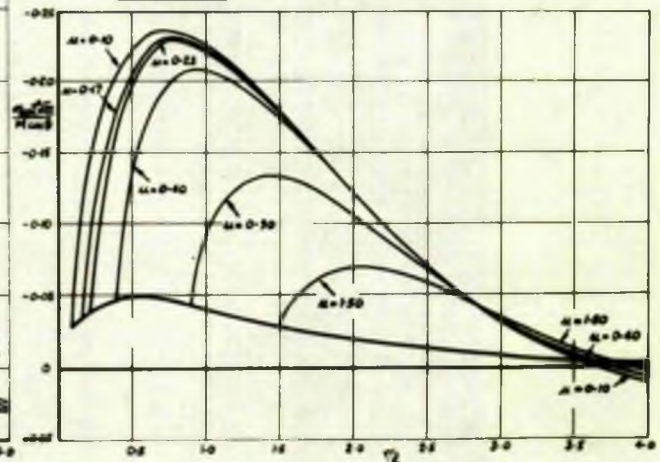
FIG. II-12f THE DISTRIBUTION OF CIRCUMFERENTIAL DIRECT STRESS

FIG. II-12 THE DISTRIBUTION OF BENDING AND DIRECT STRESSES AND RADIAL DEFLECTION DUE TO THE APPLICATION OF A BENDING MOMENT TO A SHALLOW SPHERICAL SHELL BY MEANS OF A RIGID INSERT AT THE CROWN. FOR VARIOUS μ VALUES

w and F (eqts. II.63a,b) in eqt. II.4 with the aid of II.48 and
the equations for kei* and ker* as given in Appendix VIII.8.

$$\sigma_{rD} = \frac{N_r}{t} = \frac{E}{R(r/\ell)}\left[C_3\left(\ker r/\ell - \frac{2\ker' r/\ell}{r/\ell}\right) + C_4\left(\kei r/\ell + \frac{2\ker' r/\ell}{r/\ell}\right) - 2C_5\left(\frac{r}{\ell}\right)^{-2}\right]\cos\theta$$

$$\sigma_{\theta D} = \frac{N_{\theta\theta}}{t} = \frac{E}{R}\left[C_3\left(\ker' r/\ell - \frac{\ker r/\ell}{r/\ell} + \frac{2\kei' r/\ell}{(r/\ell)^2}\right) + C_4\left(\kei' r/\ell - \frac{\kei r/\ell}{r/\ell} - \frac{2\ker' r/\ell}{(r/\ell)^2}\right)\right.$$
$$\left. + 2C_5\left(\frac{r}{\ell}\right)^{-3}\right]\cos\theta$$

$$\tau_{r\theta,D} = \frac{N_{r\theta}}{t} = \frac{E}{R(r/\ell)}\left[C_3\left(\ker r/\ell - \frac{2\kei' r/\ell}{r/\ell}\right) + C_4\left(\kei r/\ell + \frac{2\ker' r/\ell}{r/\ell}\right) - 2C_5\left(\frac{r}{\ell}\right)^{-2}\right]\sin\theta$$

$$\sigma_{rB} = \pm\frac{M_{rr}6}{t^2} = \mp\frac{6E}{R\sqrt{12(1-\nu^2)}}\left\{+C_3\left[\frac{(1-\nu)\kei r/\ell}{r/\ell} + \frac{2(1-\nu)\ker' r/\ell}{(r/\ell)^2} - \kei' r/\ell\right]\right.$$
$$\left. + C_4\left[\frac{-(1-\nu)\ker r/\ell}{r/\ell} + \frac{2(1-\nu)\kei' r/\ell}{(r/\ell)^2} + \ker' r/\ell\right]\right\}\cos\theta$$

$$\sigma_{\theta B} = \pm\frac{M_{\theta\theta}6}{t^2} = \mp\frac{6E}{R\sqrt{12(1-\nu^2)}}\left\{-C_3\left[\frac{(1-\nu)\kei r/\ell}{r/\ell} + \frac{2(1-\nu)\ker' r/\ell}{(r/\ell)^2} + \nu\kei' r/\ell\right]\right.$$
$$\left. + C_4\left[\frac{(1-\nu)\ker r/\ell}{r/\ell} - \frac{2(1-\nu)\kei' r/\ell}{(r/\ell)^2} + \nu\ker' r/\ell\right]\right\}\cos\theta$$

$$\tau_{r\theta,B} = \pm\frac{M_{r\theta}6}{t^2} = \pm\frac{6E}{R\sqrt{12(1-\nu^2)}}\left\{-C_3\left[\frac{\kei r/\ell}{r/\ell} + \frac{2\ker' r/\ell}{(r/\ell)^3}\right]\right.$$
$$\left. + C_4\left[\frac{\ker r/\ell}{r/\ell} - \frac{2\kei' r/\ell}{(r/\ell)^2}\right]\right\}\sin\theta$$

(II.68a-f)

Using eqts. II.68a-f in conjunction with the equations for C_3, C_4 and C_5 (eqt. II.67a,b and eqt. II.66) the distribution of the stresses can be determined for any μ value. These are shown graphically in Fig. II.12 for various values of μ.

II.1.4   'TWISTING' MOMENT

The shell is here loaded by a moment T in the tangent
plane of the shell at its crown.   The moment is transmitted
to the shell by means of a rigid
cylindrical insert as in Fig.II.13
and is designated a 'twisting'
moment.
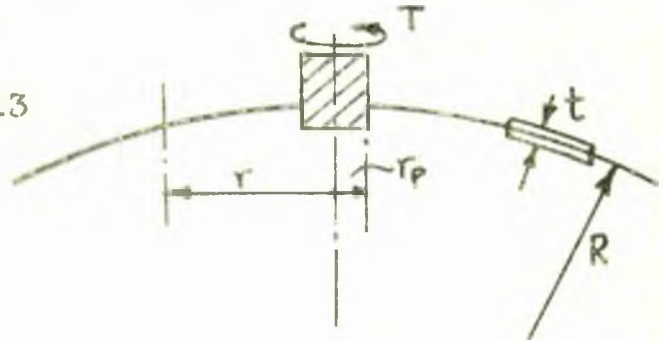
This problem is similar in
certain respects to the case of

Fig.II.13

rotational symmetry $(n=0)$ in that the multivalued functions of
$\sin \theta$ and $\cos \theta$ can not be present in the stress function, also
the displacement and stress resultants must be independent of θ.
The relations of w and F may be written as follows from eqts.
II.27 and II.28:-

$$w = C_1 \, ber \, r/\ell + C_2 \, bei \, r/\ell + C_3 \, ker \, r/\ell + C_4 \, kei \, r/\ell - A_0 + w_P$$

$$F = \frac{\ell^2 t E}{R}\left[-C_2 \, ber \, r/\ell + C_1 \, bei \, r/\ell - C_4 \, ker \, r/\ell + C_3 \, kei \, r/\ell\right] + b_0 \, \ln r/\ell + F_P \qquad (II.69a,$$

Particular Integrals

For this case $w_P = 0$ (as for the radial loads and bending
                              moment)   (II.70a)

F_P must therefore satisfy:- $\nabla^2 F_P = 0$ and meet the restric-
tions of the torsion problem.   Such a value is given by:-

$$F_P = A + B \, \ln r/\ell + C_5 \theta \qquad (II.70b)$$

Derivation of Constant A

Since only derivatives of F appear in the force equations
II.4a-c, A is immaterial.

Derivation of Constants C_1, C_2 and A_0

$r \to \infty$ $\begin{cases} M_{rr} \to 0 \\ M_{\theta\theta} \to 0 \\ w \to 0 \end{cases}$ yielding:- $\begin{cases} C_1 = C_2 = A_0 = 0 \end{cases}$

                                                                       (II.71a,b)
This derivation is similar to that of eqts. II.43a-c.

Derivation of B and b_o

At any radius r, the sum of vertical forces acting on any parallel circle must be zero. In this case the applied twisting moment T is assumed to be taken by the shear forces $N_{r\theta}$ in the plane of the shell. Thus eqt. II.44 will become :-

$$Q_r - \frac{r}{R} N_{rr} = 0 \qquad\qquad (II.72)$$

using eqt. II.5 and II.4a eqt. II.72 becomes :-

$$-D \frac{d}{dr}(\nabla^2 \omega) - \frac{dF}{R dr} = 0 \qquad\qquad (II.73)$$

Substituting eqts. II.69a,b and II.70a,b with II.71a,b into II.73 yields :-

$$B + b_o = b_2 = 0 \qquad\qquad (II.74)$$

Derivation of C_3 and C_4

At $r = r_f$ $\begin{cases} \dfrac{d\omega}{dr} = 0 \\ \mathcal{E}_\theta = 0 \end{cases}$ yielding :- $\begin{cases} C_3 = C_4 = 0 \end{cases}$ (II.75)

The derivation of these constants is given in Appendix VIII.24, p.263 Thus w and F may now be written

$$w = 0, \qquad F = C_5 \theta \qquad\qquad (II.76a,b)$$

Derivation of Constant C_5

From rotational equilibrium it is assumed that :-

$$N_{r\theta} 2\pi r^2 = T \qquad\qquad (II.77)$$

Also from eqt. II.4c and II.70b, $N_{r\theta} = C_5/r^2$ (II.78)

From eqts. II.77 and 78, $C_5 = T/2\pi$ (II.79)

Thus eqts. II.76 a,b become :- $w = 0$; $F = \frac{T}{2\pi}\theta$ (II.80)

The Tangential Displacement u

This can be obtained from the shear strain $\gamma_{r\theta}$, defined as eqt. I.81c in conjunction with the force - strain relation eqt. I.82c.

Thus from eqts. I.81c and I.82c :-

$$\gamma_{r\theta} = \frac{\partial v}{r \partial \theta} + \frac{\partial u}{\partial r} - \frac{u}{r} = \frac{N_{r\theta}}{tG} \qquad\qquad (II.81)$$

since $\frac{\partial v}{\partial \theta} = 0$, eqt. II.81 may be expressed,

$$\gamma_{r\theta} = r\frac{\partial}{\partial r}\left(\frac{u}{r}\right) = \frac{N_{r\theta}}{tG} = \frac{T}{2\pi tGr^2} \qquad \text{from eqt. II.77}$$

i.e $\frac{u}{r} = -\frac{T}{4\pi tGr^2} + \bar{K}$.

$\therefore u = -\frac{T}{4\pi tGr} + \bar{K}r$

when $r \to \infty$, $u \to 0$ $\therefore \bar{K} = 0$

and $u = -\frac{T}{4\pi tGr}$ (II.82)

Meridional Displacement v

This is obtained from the meridional strain $\mathcal{E}_r$ (eqt.I.81b) and the force-strain relations of eqt. I.82a,b. Thus

$$\mathcal{E}_r = \frac{\partial v}{\partial r} + \frac{w}{R} = \frac{1}{tE}[N_{rr} - \upsilon N_{\theta\theta}] \qquad (II.83)$$

Substituting for w from eqt. II.6 and Nrr and Nθθ from eqt. II.4a-c, eqt. II.83 may be written :-

$$\frac{\partial v}{\partial r} - \frac{w\phi}{R} = -\frac{(1+\upsilon)}{tE}\frac{\partial^2 F}{\partial r^2}$$

Thus $v = -\frac{(1+\upsilon)}{tE}\frac{\partial F}{\partial r} + \int \frac{w\phi}{R}.dr + f(\theta)$ (II.84), where $f(\theta)$ is a function of θ.

The function of θ, $f(\theta)$, must be zero, together with the first differential of F. Thus eqt. II.84 can be written :-

$v = \int \frac{w\phi}{R}.dr$ It is noted from II.7 that for this case $w_{\phi} = A_0 + B_0 \ell_n r = 0$.

Thus $v = 0$ (II.85)

The results may be summarised:-

$w = N_{rr} = N_{\theta\theta} = M_{rr} = M_{\theta\theta} = M_{r\theta} = v = 0$

$$\mathcal{T}_{r\theta} = \frac{N_{r\theta}}{t} = \frac{T}{2\pi r^2 t} \; , \quad u = -\frac{T}{4\pi Gt\,r} \qquad (II.86a-1)$$

It is seen that these equations are similar to eqts. VIII.73a-d and eqt. VIII.74 of Appendix VIII.3. 'A Twisting Moment applied to a Flat Plate.'

A graphical representation of equation II.86 is shown on Fig. II.14 and is common for all radii of insert r_ρ , with a suitable 'cut-off' at $r = r_\rho$.
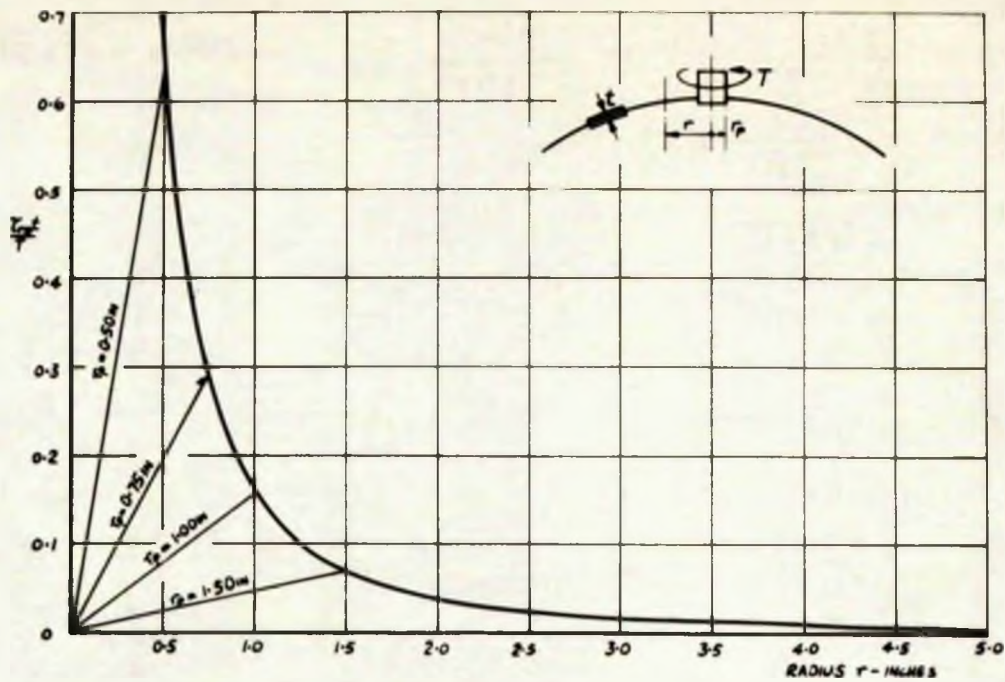
FIG. II.14a   THE DISTRIBUTION OF SHEAR STRESS
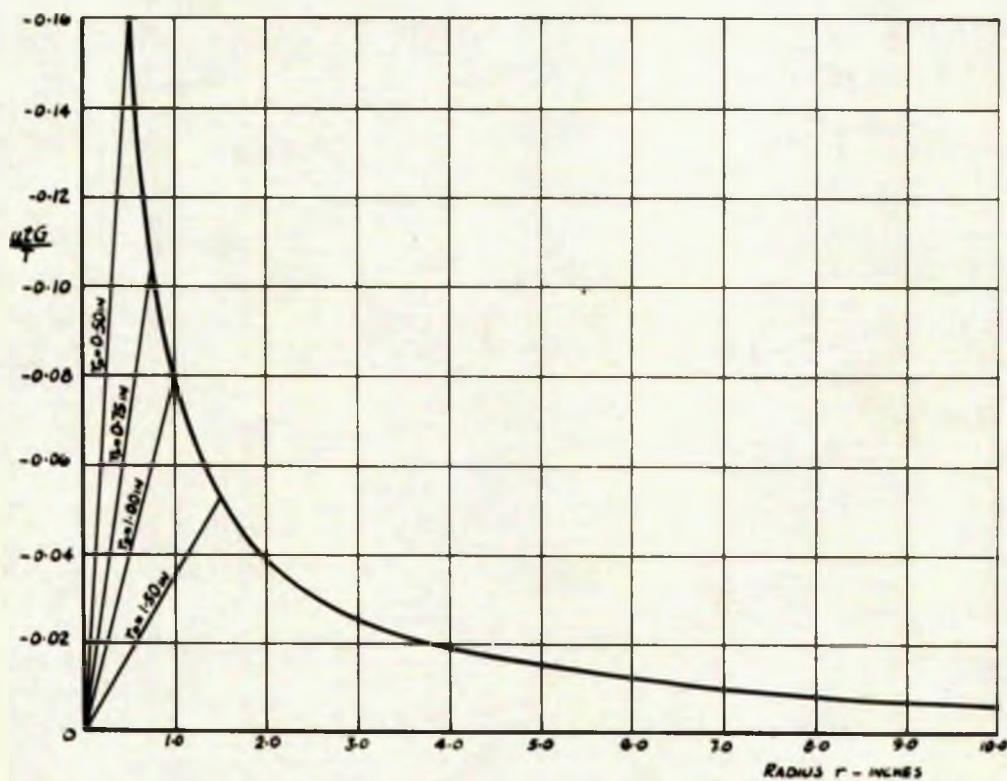
FIG. II.14b   THE DISTRIBUTION OF TANGENTIAL DISPLACEMENT

FIG. II.14   THE DISTRIBUTION OF SHEAR STRESS AND TANGENTIAL DISPLACEMENT DUE TO THE APPLICATION OF A 'TWISTING' MOMENT TO A SHALLOW SPHERICAL SHELL BY MEANS OF A RIGID INSERT AT THE CROWN. FOR VARIOUS r_0 VALUES (INCH UNITS)

II.1.5   'TANGENTIAL' LOADING ON THE SHALLOW SHELL

A shell is loaded by a load H in the tangent plane to
the shell at its crown.   The force is transmitted to the
shell by means of a rigid cylindrical insert at the crown as
in Fig. II.15.   Following out the
procedure, as in the other cases and
considering the general expressions
for w and F (eqts. II.27 and II.28),
noting that this case can be represen-
ted by $n = 1$, the basic equations are
seen to be similar in form to the
bending moment loading, i.e. eqts.
II.60a,b.   The values of the
particular integrals II.61a,b and of
the constants a_1, A and B_1 are also
similar.   The equations can thus be
written:-

Fig. II.15

$$w = (C_1 ber'r/\ell + C_2 bei'r/\ell + C_3 ker'r/\ell + C_4 kei'r/\ell - A_1 r/\ell) \cos\theta$$

$$F = \left[\frac{\ell^2 t E}{R}(-C_2 ber'r/\ell + C_1 bei'r/\ell - C_4 ker'r/\ell + C_3 kei'r/\ell) + (b_1 + B)\frac{\ell}{r}\right]\cos\theta \quad (II.87a,b)$$

Derivation of constants C_1, C_2 and A_1

When the outside radius r_2 of the shallow shell is large
compared with the insert radius r_p , the stresses on the boun-
dary will be very small.   This is particularly the case for
the bending stresses which, for a shallow shell subject to a
tangential load, will be small, compared with the direct stresses
for all positions of r.
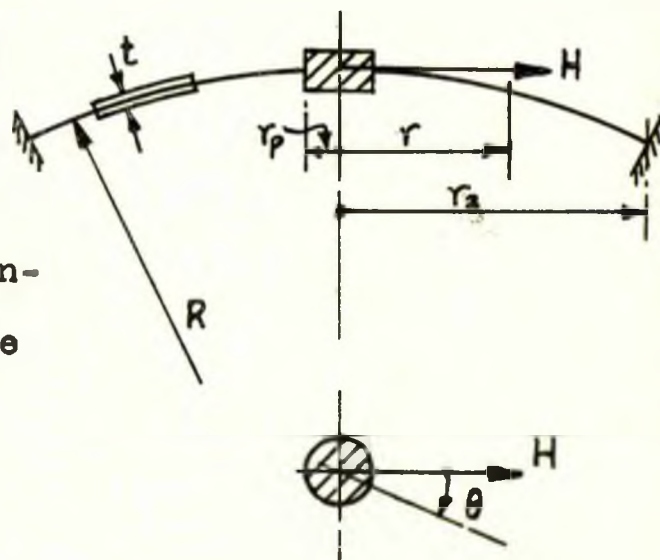
Thus at $r = r_2$ $\begin{cases} M_{\theta\theta} \to 0 \\ M_{rr} \to 0 \\ \omega = 0 \end{cases}$ yielding:- $\begin{cases} C_1 = C_2 = 0 \\ A_1 = 0 \end{cases}$ (II.88a-c)

The derivation of these constants is similar to those of eqts. II.62a-c and are shown in Appendix VIII.2.3c, p. 262.

The expressions for w and F can therefore be written:-

$$w = (C_3 \ker' r/\ell + C_4 \kei' r/\ell) \cos\theta$$

$$F = \left[\frac{Et^2}{\sqrt{12(1-\nu^2)}}(C_3 \kei' r/\ell - C_4 \ker' r/\ell) + C_5\left(\frac{r}{\ell}\right)^{-1}\right]\cos\theta \qquad \text{(II.89a,b)}$$

where $C_5 = (B + b_1)$

The corresponding expressions for Nrr and Nrθ using II.4a,c

$$N_{rr} = \left\{\frac{Et}{R(r/\ell)}\left[C_3\left(\ker r/\ell - \frac{2\kei' r/\ell}{r/\ell}\right) + C_4\left(\kei r/\ell + \frac{2\ker' r/\ell}{r/\ell}\right)\right] - 2C_5\frac{\ell}{r^3}\right\}\cos\theta$$

$$N_{r\theta} = \left\{\frac{Et}{R(r/\ell)}\left[C_3\left(\ker r/\ell - \frac{2\kei' r/\ell}{r/\ell}\right) + C_4\left(\kei r/\ell + \frac{2\ker' r/\ell}{r/\ell}\right)\right] - 2C_5\frac{\ell}{r^3}\right\}\cos\theta \qquad \text{(II.90a,b)}$$

The solutions for Nrr and Nrθ are however deficient inasmuch as they do not represent the resultant tangential force H defined by $H = -2\int_0^\pi (N_{rr}\cos\theta - N_{r\theta}\sin\theta)\, r\, d\theta$ (II.91)

Substituting eqt. II.90a,b into eqt. II.91 and integrating, the right hand side is found to be zero. It is, therefore, necessary to modify the stress function in a suitable manner in order to incorporate terms in the forces and displacements capable of representing the tangential force H. The following form is found suitable for this additional stress function:-

$$F'' = \frac{C_6}{2}r\theta\sin\theta + (C_7 r^3 + C_8 r^{-1} + C_9 r\log r)\cos\theta \qquad \text{(II.92)}$$

with corresponding additional values for Nrr, $N_{\theta\theta}$ and Nrθ from eqt. II.4.

The form of w given in eqt. II.89a is assumed to remain unchanged

Derivation of C_3 and C_4

Before setting down all the equations for the forces and displacements the constants C_3 and C_4 may be found from

considering the shell at $r = r_p$

$$r = r_p \begin{cases} \dfrac{\partial w}{\partial r} = 0 \\[2mm] Q_r = D\dfrac{\partial \nabla^2 w}{\partial r} = 0 \end{cases} \quad \text{yielding:-} \begin{cases} C_3 = C_4 = 0 \end{cases} \tag{II.93}$$

Details of this derivation are found in Appendix VIII.2.5, p.264

The Stress function may thus be written from eqts. II.89b and II.92

$$F = \frac{C_6}{2}\, r.\theta.\sin\theta + \left[C_7 r^3 + C_8 r^{-1} + C_9 r\, \ell n\, r + C_5 \left(\tfrac{r}{\ell} \right)^{-1} \right] \cos\theta$$

$$F = \frac{C_6}{2}\, r.\theta.\sin\theta + \left[C_7 r^3 + C_{10} r^{-1} + C_9 r\, \ell n\, r \right] \cos\theta \tag{II.94}$$

$$\text{where } C_{10} = C_8 + \ell C_5$$

The force components from eqts. II.4 are:-

$$N_{rr} = \frac{C_6}{r}\cos\theta + \left(2C_7 r - \frac{2C_{10}}{r^3} + \frac{C_9}{r} \right) \cos\theta$$

$$N_{\theta\theta} = \left(6 C_7 r + 2\frac{C_{10}}{r^3} + \frac{C_9}{r} \right) \cos\theta$$

$$N_{r\theta} = \left(2C_7 r - 2\frac{C_{10}}{r^3} + \frac{C_9}{r} \right) \sin\theta \tag{II.95a-c}$$

The strain, displacement, force relations obtained from eqts. I.81 and I.82 with $w = 0$ (since $C_3 = C_4 = 0$) may be written,

$$\varepsilon_r = \frac{\partial v}{\partial r} = \frac{1}{tE}(N_{rr} - \upsilon N_{\theta\theta})$$

$$\varepsilon_\theta = \frac{v}{r} + \frac{1}{r}\frac{\partial u}{\partial \theta} = \frac{1}{tE}(N_{\theta\theta} - \upsilon N_{rr})$$

$$\gamma_{r\theta} = \frac{\partial v}{r\,\partial \theta} + \frac{\partial u}{\partial r} - \frac{u}{r} = \frac{N_{r\theta}}{tG} \tag{II.96a-c}$$

Substituting for N_{rr}, $N_{\theta\theta}$ and $N_{r\theta}$ in eqts. II.96a-c and integrating:-

$$v = \frac{1}{tE}\left[C_6\, \ell n\, r + C_7 r^2 (1-3\upsilon) + \frac{C_{10}}{r^2}(1+\upsilon) + (1-\upsilon) C_9\, \ell n\, r \right] \cos\theta + f(\theta) \tag{II.97}$$

$$\text{where } f(\theta) \text{ is a function of } \theta.$$

Using eqt. II.97:-

$$u = \frac{1}{tE}\left[-C_6 (\upsilon + \ell n\, r) + C_7 r^2 (5+\upsilon) + \frac{C_{10}(1+\upsilon)}{r^2} + C_9(1-\upsilon)(1-\ell n\, r) \right]\sin\theta - \int f(\theta)d\theta + F(r) \tag{II.98}$$

$$\text{where } F(r) \text{ is a function of } r.$$

Further, using eqts. II.97 and 98:-

$$\gamma_{r\theta} = \frac{1}{tE}\left[\frac{C_6}{r}(\upsilon-1) + 4C_7 r(1+\upsilon) - \frac{4C_{10}(1+\upsilon)}{r^3} + 2\frac{C_9}{r}(\upsilon-1) \right]\sin\theta$$

$$+ F'(r) - \frac{F(r)}{r} + \frac{\int f(\theta)}{r} + \frac{f'(\theta)}{r} \tag{II.99}$$

The value of $\gamma_{r\theta}$ is obtained from eqts. II.95c and 96c.

$$\gamma_{r\theta} = \frac{2\sin\theta\,(1+\upsilon)}{tE}\left[2C_7 r - \frac{2C_{10}}{r^3} + \frac{C_9}{r}\right] \qquad (II.100)$$

Equating II.99 and II.100

$$r\,F'(r) - F(r) + \int f(\theta) + f'(\theta) = \frac{\sin\theta}{tE}\left[-C_6(\upsilon-1) + 4C_9\right]$$

equating the r's :- $r\,F'(r) - F(r) = -C_{11}$

$$\therefore \quad F(r) = C_{12}r + C_{11} \qquad (II.101)$$

where C_{11} and C_{12} are constants of integration.

equating the θ's :- $\int f(\theta) + f'(\theta) = C_{11} + \frac{\sin\theta}{tE}\left[-C_6(\upsilon-1) + 4C_9\right]$

Thus $f(\theta) + f''(\theta) = \frac{\cos\theta}{tE}\left[-C_6(\upsilon-1) + 4C_9\right]$

$$\therefore f(\theta) = C_{13}\sin\theta + C_{14}\cos\theta + \left[4C_9 - C_6(\upsilon-1)\right]\frac{\theta\sin\theta}{2Et} \qquad (II.102)$$

where C_{13} and C_{14} are constants of integration.

In eqts. II.99 $\rightarrow$ 102. $F(r)$ indicates the first differential w.r.t, r

$f'(\theta)$ "   "   "   "   " θ

$f''(\theta)$ "   " second differential   " θ

The eqts. II.97 and 98 for υ and u can thus be written, sub-stituting for $f(\theta)$ and $F(r)$ from eqts. II.101 and 102:-

$$\upsilon = \frac{1}{tE}\left[C_6 \ln r + C_7 r^2(1-3\upsilon) + \frac{C_{10}}{r^2}(1+\upsilon) + C_9(1-\upsilon)\ln r\right]\cos\theta$$

$$+ C_{13}\sin\theta + C_{14}\cos\theta + \left[4C_9 - C_6(\upsilon-1)\right]\frac{\theta\sin\theta}{2Et}$$

$$u = \frac{1}{tE}\left[-C_6(\upsilon+\ln r) + C_7 r^2(5+\upsilon) + \frac{C_{10}}{r^2}(1+\upsilon) + C_9(1-\upsilon)(1-\ln r)\right]\sin\theta$$

$$+ C_{13}\cos\theta - C_{14}\sin\theta - \frac{\left[4C_9 - C_6(\upsilon-1)\right](\sin\theta - \theta\cos\theta)}{2Et} + C_{12}r \qquad (II.103a,b)$$

The equations II.95a-c and II.103a,b contain in all __seven__ con-stants:-

C_6, C_7, C_9, C_{10}, C_{12}, C_{13}, and C_{14}, which are determined from the boundary conditions.

Derivation of constant C_6

The resultant tangential force H is defined by eqt. II.91. Substituting values for N_{rr} and $N_{r\theta}$ from II.95 into eqt. II.91

gives $C_6 = -\dfrac{H}{\pi}$ (II.104)

Derivation of constants C_{12} and C_{13}

Points on the meridional line $\theta = 0^\circ$ have no circumferential displacement, i.e. $u = 0$ for all values of r. Such is only satisfied when

$$C_{12} = 0 \text{ and } C_{13} = 0 \qquad\qquad \text{(II.105a,b)}$$

Derivation of C_7, C_9, C_{10} and C_{14}

At $r = r_2$, $\qquad \theta = \dfrac{\pi}{2} \qquad \begin{cases} v = 0 \\[2mm] u = 0 \qquad \text{yielding the following} \\ \qquad\qquad \text{values for the four} \\ v = 0 \qquad \text{constants:--} \\[2mm] \mathcal{E}_\theta = \dfrac{(N_{\theta\theta} - \upsilon N_{rr})}{Et} = 0 \end{cases}$

$\theta = 0^\circ$

$r = r_p$

$$C_7 = -\frac{C_6(1+\upsilon)^2}{8(\upsilon-3)(r_2^2+r_p^2)} \quad , \qquad C_9 = \frac{C_6(\upsilon-1)}{4} \quad , \qquad C_{10} = \frac{C_6(1+\upsilon)r_p^2}{8} \cdot \frac{r_2^2}{r_2^2+r_p^2}$$

$$C_{14} = -\frac{C_6}{Et}\left[\frac{(1+\upsilon)(3-\upsilon)}{4}\ln r_2 + \frac{r_p^2(1+\upsilon)^2}{8(r_2^2+r_p^3)} - \frac{r_2^2(1-3\upsilon)(1+\upsilon)^2}{8(\upsilon-3)(r_2^2+r_p^2)} \right] \qquad \text{(II.106a-d)}$$

Using the values of the constants contained in eqts. II.104 →
II.106 the stresses, resultant forces and displacements can be
written:--

$$\sigma_{rD} = \frac{N_{rr}}{t} = -\frac{H}{4\pi rt}\left\{ 3+\upsilon - \frac{(1+\upsilon)^2 r^2}{(\upsilon-3)[r_2^2+r_p^2]} - \frac{(1+\upsilon)r_p^2}{\left[1 + r_p^2/r_2^2\right]r^2} \right\}\cos\theta$$

$$\sigma_{\theta D} = \frac{N_{\theta\theta}}{t} = \frac{H}{4\pi rt}\left\{ \frac{3r^2(1+\upsilon)^2}{(\upsilon-3)[r_2^2+r_p^2]} - \frac{r_p^2(1+\upsilon)}{\left[1 + r_p^2/r_2^2\right]r^2} + (1-\upsilon) \right\}\cos\theta$$

$$\tau_{r\theta,D} = \frac{N_{r\theta}}{t} = \frac{H}{4\pi rt}\left\{ \frac{r^2(1+\upsilon)^2}{(\upsilon-3)[r_2^2+r_p^3]} + \frac{r_p^2(1+\upsilon)}{\left[1 + r_p^2/r_2^2\right]r^2} + (1-\upsilon) \right\}\sin\theta$$

$$v = \frac{-H}{8t\pi G}\left\{ (3-\upsilon)\ln \frac{r}{r_2} - \left[\frac{r^2/r_2^2 - 1}{r_p^2/r_2^2 + 1}\right]\frac{\upsilon+1}{2}\left[\frac{r_p^2}{r^2} + \frac{1-3\upsilon}{\upsilon-3}\right] \right\}\cos\theta$$

$$u = \frac{+H}{8t\pi G}\left\{ (3-\upsilon)\ln\frac{r}{r_2} + \frac{(1+\upsilon)}{\left[1 + r_p^2/r_2^2\right]}\frac{(5+\upsilon)r/r_2^2 + (1-3\upsilon)}{2(\upsilon-3)} \right.$$

$$\left. - \frac{(1+\upsilon)r_p^2}{2 \; r^2}\left[\frac{r^2/r_2^2 + 1}{r_p^2/r_2^2 + 1}\right] + (1+\upsilon) \right\}\sin\theta$$

$$\text{(II.107a-e)}$$

When the outer radius $r_2 \rightarrow \infty$ the equations for the stresses modify to the following:-

$$\sigma_{ro} = -\frac{H}{4\pi t}\left[\frac{3+\upsilon}{r} - \frac{(1+\upsilon)\, r_p^2}{r^3}\right]\cos\theta$$

$$\sigma_{\theta o} = \frac{H}{4\pi t}\left[\frac{1-\upsilon}{r} - \frac{(1+\upsilon)\, r_p^2}{r^3}\right]\cos\theta$$

$$\tau_{r\theta, o} = \frac{H}{4\pi t}\left[\frac{1-\upsilon}{r} + \frac{(1+\upsilon)\, r_p^2}{r^3}\right]\sin\theta \qquad\text{(II.108a-c)}$$

When $r_p \rightarrow 0$ equations II.108a-c simplify to those presented by TIMOSHENKO [104] for the flat plate:-

$$\sigma_{ro} = -\frac{(3+\upsilon)\,H}{4\pi r t}\cos\theta$$

$$\sigma_{\theta, o} = \frac{(1-\upsilon)\,H}{4\pi r t}\cos\theta$$

$$\tau_{r\theta, o} = \frac{(1-\upsilon)\,H}{4\pi r t}\sin\theta \qquad\text{(II.109a-c)}$$

The expressions of equations II.107a-e are plotted in Figs. II.16 and 17 for values of $r_p = 0.00$, 0.50, 0.75, 1.00 and 1.50 inches.
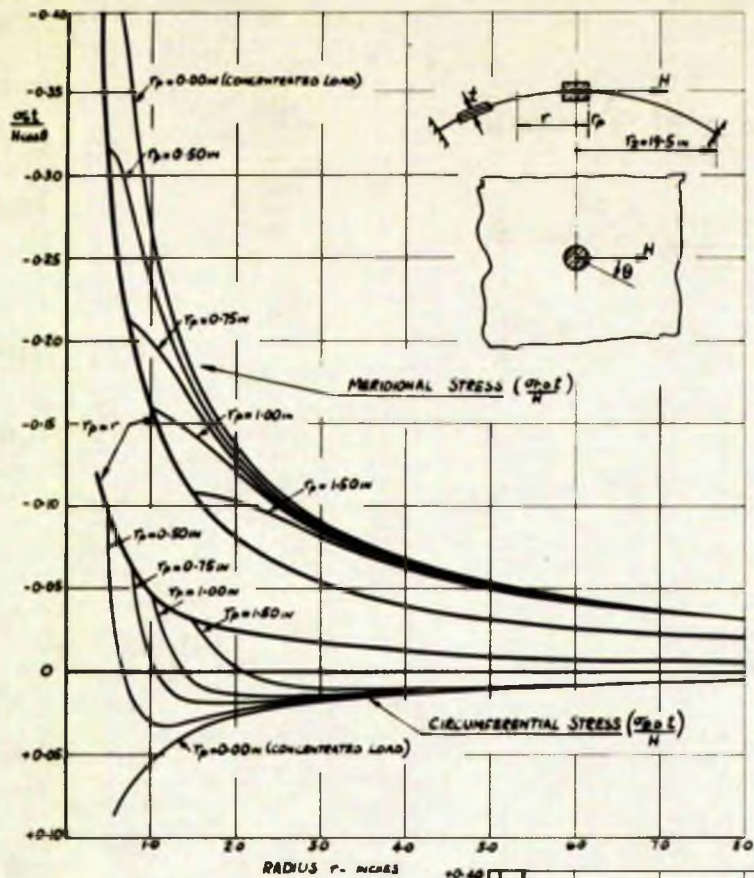
Fig. II·16a The Distribution of Meridional and Circumferential Direct Stresses

Fig. II·16b The Distribution of Shearing Stress
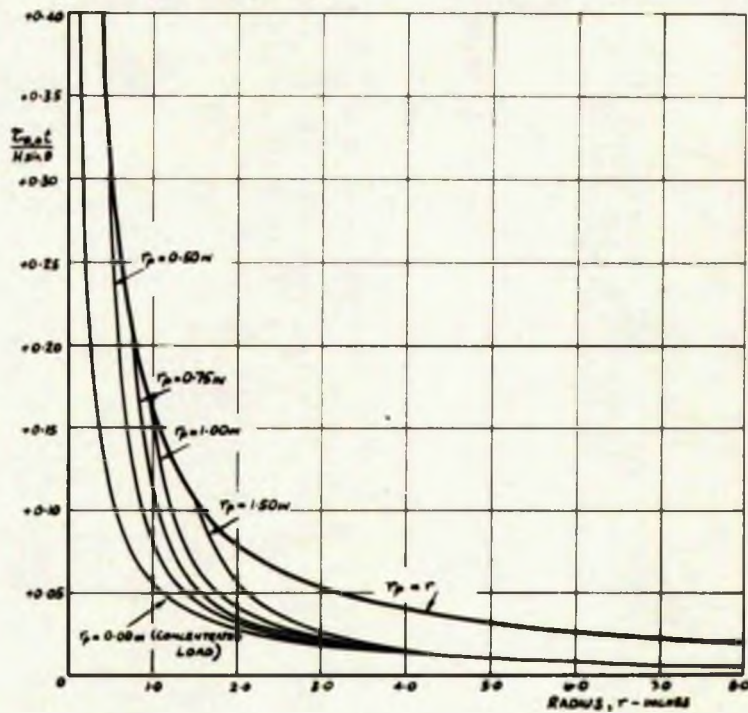
Fig. II·16 The Distribution of Normal and Shearing Stress in a Shallow Spherical Shell due to the Application of a Tangential Load applied by means of a Rigid Insert at the crown for various r_p values (inch units) — SHALLOW SHELL TREATMENT
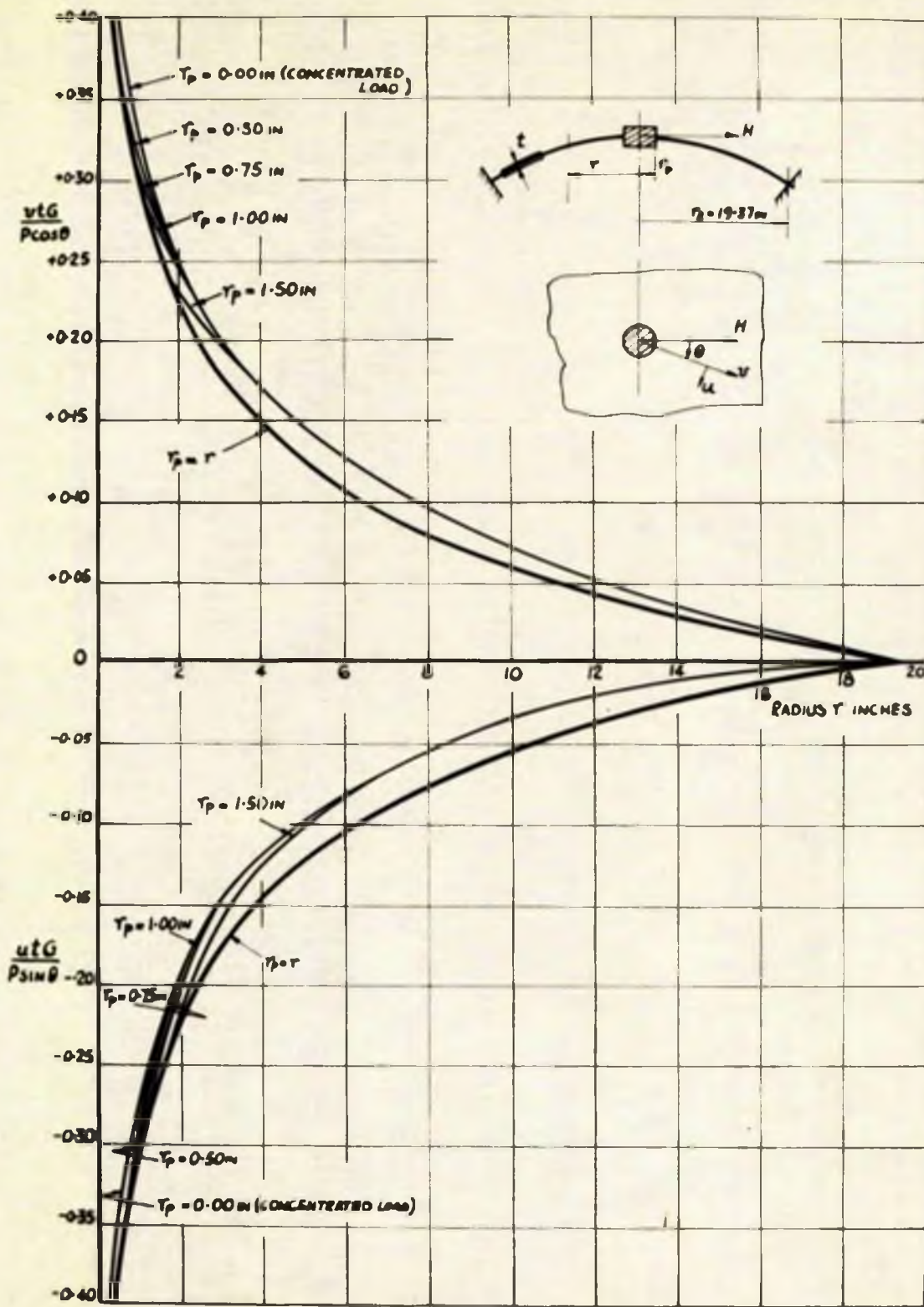
FIG. II.17 THE DISTRIBUTION OF DISPLACEMENTS IN A SHALLOW SPHERICAL SHELL DUE TO THE APPLICATION OF A TANGENTIAL LOAD APPLIED BY MEANS OF A RIGID INSERT AT THE CROWN, FOR VARIOUS r_p VALUES (INCH UNITS)

II.2   THE GENERAL SPHERICAL SHELL THEORY

II.2.1   RADIAL LOAD

(a) The Loading of a Rigid Cylindrical Insert built into the discontinuous shell.

(b) The concentrated Load at the crown.

II.2.2   'BENDING' MOMENT.

II.2.3   'TWISTING' MOMENT.

II.2.4   TANGENTIAL LOAD.

II.2   THE GENERAL SPHERICAL SHELL THEORY

In the analysis developed by the author and presented in this section, extensions of the solutions for the general equations are considered applied to the case of a spherical shell with a radially cylindrical insert at the crown, and subjected to radial and tangential loads and moment actions.

The essentially local nature of the stress dealt with is recognised in the analysis by assuming the co-latitude angle ϕ to be small throughout.   It is then shown that the solutions tend to assume forms similar to that obtained for the shallow shell.

II.2.1   RADIAL LOAD

For the axisymmetrical case ($n = 0$) only the membrane and oscillatory terms need to be considered (see Chapter I, p.47)

Membrane Solutions

From a consideration of the equilibrium of the shell:-
$$N_{\phi\phi_o} = -\frac{P}{2\pi R \sin^2\phi} \quad , \qquad N_{\theta\theta_o} = \frac{P}{2\pi R \sin^2\phi} \qquad \text{(II.110 a,b)}$$
where $N_{\phi\phi_o}$ and $N_{\theta\theta_o}$ are the meridional and circumferential membrane force actions respectively for $n = 0$.   The strain, displacement – resultant force equations are
$$\mathcal{E}_\theta = \frac{1}{Et}(N_{\theta\theta_o} - \upsilon N_{\phi\phi_o}) = \frac{\upsilon_o}{R}\cot\phi + \frac{w_o}{R}$$

$$\mathcal{E}_\phi = \frac{1}{Et}(N_{\phi\phi_o} - \upsilon N_{\theta\theta_o}) = \frac{1}{R}\frac{d\upsilon_o}{d\phi} + \frac{w_o}{R} \qquad \text{(II.111a,b)}$$

Subtracting:- $\dfrac{d\upsilon_o}{d\phi} - \upsilon_o\cot\phi = -\dfrac{R}{Et}[N_{\theta\theta_o} - N_{\phi\phi_o}](1+\upsilon)$ $\qquad$ (II.112)

substituting for $N_{\theta\theta_o}$ and $N_{\phi\phi_o}$ from eqt. II.110a,b., eqt.
II.112 may be written:- $\dfrac{d\upsilon_o}{d\phi} - \upsilon_o\cot\phi = -\dfrac{P(1+\upsilon)}{Et\pi\sin^2\phi} = f(\phi)$

Thus $\quad v_0 = \left[\int \dfrac{f(\phi)}{\sin \phi} + C \right] \sin \phi$ $\qquad$ (II.113)

and $\quad w_0 = \dfrac{P(1+v)}{2\pi E t \sin^2 \phi} - \left[\int \dfrac{f(\phi)}{\sin \phi} + C \right] \cos \phi$ $\qquad$ (II.114)

and $\quad \dfrac{dw_0}{d\phi} = \left[\int \dfrac{f(\phi)}{\sin \phi} + C \right] \sin \phi$ $\qquad$ (II.115)

The tangent rotation $\quad X_0 = \dfrac{1}{R}\left(\dfrac{dw_0}{d\phi} - \dot{v}_0 \right)$ $\qquad$ (II.116)

From eqts. II.113 and II.115 $\qquad X_0 = 0$

Eqt. II.114 reduces to $\quad w_0 = \dfrac{P(1+v)}{2\pi E t}\left[1 + \cos\phi \, \ln \tan \dfrac{\phi}{2} \right]$

$$= \dfrac{P(1+v)}{\pi E t}\left[2 + \cos\phi \, \ln \dfrac{1 - \cos\phi}{1 + \cos\phi} \right] \quad (II.117)$$

Oscillatory Solutions

These are presented below:—

$$N_{\phi\phi_0} = - \dfrac{Et \cot\phi}{(1-v^2)R}\left(A_1 T_1 + A_2 T_2 + B_1 T_3 + B_2 T_4 \right)$$

$$N_{\theta\theta_0} = - \dfrac{Et}{(1-v^2)R}\left(A_1 \dot{T}_1 + A_2 \dot{T}_2 + B_1 \dot{T}_3 + B_2 \dot{T}_4 \right)$$

$$X_0 = \dfrac{2\chi^2}{R(1-v^2)}\left[A_1\left(T_2 - \dfrac{v}{2\chi^2}T_1\right) - A_2\left(T_1 + \dfrac{v}{2\chi^2}T_2\right) + B_1\left(T_4 - \dfrac{v}{2\chi^2}T_3\right) - B_2\left(T_3 + \dfrac{v}{2\chi^2}T_4\right) \right]$$

$$\dfrac{dw_0}{d\phi} = \dfrac{1}{(1-v^2)}\left[A_1\left(T_1 + 2\chi^2 T_2\right) + A_2\left(T_2 - 2\chi^2 T_1\right) + B_1\left(T_3 + 2\chi^2 T_4\right) + B_2\left(T_4 - 2\chi^2 T_3\right) \right]$$

$$M_{\phi\phi_0} = \dfrac{2Et^3\chi^2}{12(1-v^2)^2 R^2}\left[A_1\left\{ \dot{T}_2 + v\cot\phi \, T_2 - \dfrac{v}{2\chi^2}\left(\dot{T}_1 + v\cot\phi \, T_1\right) \right\} \right.$$

$$- A_2\left\{ \dot{T}_1 + v\cot\phi \, T_1 + \dfrac{v}{2\chi^2}\left(\dot{T}_2 + v\cot\phi \, T_2\right) \right\}$$

$$+ B_1\left\{ \dot{T}_4 + v\cot\phi \, T_4 - \dfrac{v}{2\chi^2}\left(\dot{T}_3 + v\cot\phi \, T_3\right) \right\}$$

$$\left. - B_2\left\{ \dot{T}_3 + v\cot\phi \, T_3 + \dfrac{v}{2\chi^2}\left(\dot{T}_4 + v\cot\phi \, T_4\right) \right\} \right]$$

$$M_{\theta\theta_0} = \dfrac{2Et^3\chi^2}{12(1-v^2)^2 R^2}\left[A_1\left\{ v\dot{T}_2 + \cot\phi \, T_2 - \dfrac{v}{2\chi^2}\left(v\dot{T}_1 + \cot\phi \, T_1\right) \right\} \right.$$

$$- A_2\left\{ v\dot{T}_1 + \cot\phi \, T_1 + \dfrac{v}{2\chi^2}\left(v\dot{T}_2 + \cot\phi \, T_2\right) \right\}$$

$$+ B_1\left\{ v\dot{T}_4 + \cot\phi \, T_4 - \dfrac{v}{2\chi^2}\left(v\dot{T}_3 + \cot\phi \, T_3\right) \right\}$$

$$\left. - B_2\left\{ v\dot{T}_3 + \cot\phi \, T_3 + \dfrac{v}{2\chi^2}\left(v\dot{T}_4 + \cot\phi \, T_4\right) \right\} \right]$$

$\qquad$ (II.118a)

In the above equations:-

$$4\chi^4 = \frac{12(1-\upsilon^2)R^2}{t^2} - \upsilon^2 \qquad (II.119)$$

$$T_1 = \sqrt{\frac{\phi}{\sin\phi}}\, ber'z \quad , \qquad T_2 = \sqrt{\frac{\phi}{\sin\phi}}\, bei'z$$

$$T_3 = \sqrt{\frac{\phi}{\sin\phi}}\, ker'z \qquad T_4 = \sqrt{\frac{\phi}{\sin\phi}}\, kei'z \qquad (II.120a\text{-}d)$$

$$\text{where} \quad z = \sqrt{2}\,\chi\phi$$

and the derivatives of $T_1 \ldots T_4$ w.r.t. ϕ are

$$\dot{T}_1 = -\sqrt{2}\,\chi\sqrt{\frac{\phi}{\sin\phi}}\left[bei\, z + \frac{1}{2\sqrt{2}\,\chi}\left(\frac{1}{\phi} + \cot\phi\right)ber'z\right]$$

$$\dot{T}_2 = \sqrt{2}\,\chi\sqrt{\frac{\phi}{\sin\phi}}\left[ber\, z - \frac{1}{2\sqrt{2}\,\chi}\left(\frac{1}{\phi} + \cot\phi\right)bei'z\right]$$

$$\dot{T}_3 = -\sqrt{2}\,\chi\sqrt{\frac{\phi}{\sin\phi}}\left[kei\, z + \frac{1}{2\sqrt{2}\,\chi}\left(\frac{1}{\phi} + \cot\phi\right)ker'z\right]$$

$$\dot{T}_4 = \sqrt{2}\,\chi\sqrt{\frac{\phi}{\sin\phi}}\left[ker\, z - \frac{1}{2\sqrt{2}\,\chi}\left(\frac{1}{\phi} + \cot\phi\right)kei'z\right] \qquad (II.121a\text{-}d)$$

In the equations II.118a-f the terms associated with A_1 and A_2 are functions of ϕ which increase as ϕ increases, consequently, they are associated with the lower, or outer edge of the shell. The terms associated with B_1 and B_2 decrease with damped oscillations as ϕ increases, and describe the stresses caused by loads acting at the edges of a hole at the top or by forces applied at the crown of the shell. In the work which follows it is assumed that the outer edge of the shell is sufficiently remote that the stresses associated with these boundaries, i.e. 'A_1 and A_2 stresses' do not influence those associated with the 'crown' loading.

Assumption of Localized Effect of Load

The expressions stated above may be simplified considerably by assuming that the co-latitude angle ϕ representing the extent of load effect on the shell, is small. This results in the

following:- $\phi \approx r/R$ and $\cot \phi \approx 1/\phi$ and $\sqrt{R^2 - r^2} \approx R$ (II.122a-c)

Further restricting consideration to thin shells $\frac{\upsilon^2}{4}$ may be considered small compared with $\left(\frac{R}{t}\right)^2$. Thus eqt. II.119 for χ may be written:-

$$\chi = \frac{R}{\sqrt{2}\,\ell} \qquad\qquad (II.123)$$

where, $\ell = \dfrac{\sqrt{Rt}}{\sqrt[4]{12(1-\upsilon^2)}}$

In the following two examples of the radial load are considered, namely:- (a) The loading of a rigid cylindrical insert built into the discontinuous shell, and (b) The concentrated load at the crown.

(a) The Loading of a Rigid Cylindrical Insert built into the discontinuous shell - Fig. II.7.

The expressions giving the force and moment resultants, are given in eqts. II.118a-f. These may be simplified using the assumptions of eqts. II.122a-c and II.123 and may be written:-
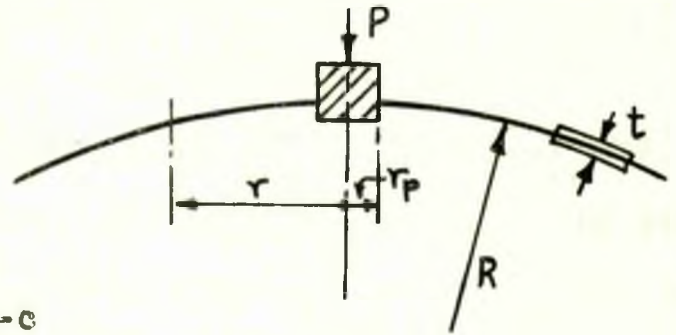
Fig. II.7

$$N_{\phi\phi_0} = -\frac{Et}{(1-\upsilon^2)r}\left[B_1\,ker'\,r/\ell + B_2\,kei'\,r/\ell\right] - \frac{PR}{2\pi r^2}$$

$$N_{\theta\theta_0} = -\frac{Et}{(1-\upsilon^2)\ell}\left[-B_1\left(kei\,r/\ell + \frac{ker'\,r/\ell}{r/\ell}\right) + B_2\left(ker\,r/\ell - \frac{kei'\,r/\ell}{r/\ell}\right)\right] + \frac{PR}{2\pi r^2}$$

$$M_{\phi\phi_0} = \frac{Et^3}{12(1-\upsilon^2)\ell^2}\left[B_1\left\{\frac{R}{\ell}\left(ker\,r/\ell - \frac{kei'\,r/\ell}{r/\ell}\right) + \upsilon\frac{R}{r}\,kei'\,r/\ell \right.\right.$$

$$\left.- \upsilon\frac{\ell^2}{R^2}\left(-\frac{R}{\ell}\left[kei\,r/\ell + \frac{ker'\,r/\ell}{r/\ell}\right] + \upsilon\frac{R}{r}\,ker'\,r/\ell\right)\right\}$$

$$-B_2\left\{-\frac{R}{\ell}\left(kei\,r/\ell + \frac{ker'\,r/\ell}{r/\ell}\right) + \upsilon\frac{R}{r}\,ker'\,r/\ell \right.$$

$$\left.\left.+ \upsilon\frac{\ell^2}{R^2}\left(\frac{R}{\ell}\left[ker\,r/\ell - \frac{kei'\,r/\ell}{r/\ell}\right] + \upsilon\frac{R}{r}\,kei'\,r/\ell\right)\right\}\right]$$

$$M_{\theta\theta_0} = \frac{Et^3}{12(1-\nu^2)^2\,\ell^2}\left[B_1\left\{ \frac{\nu R}{\ell}\left(\ker{}'\tfrac{r}{\ell} - \frac{\kei{}'\tfrac{r}{\ell}}{r/\ell}\right) + \frac{R}{r}\kei{}'\tfrac{r}{\ell} - \right. \right.$$

$$\left. -\nu\frac{\ell^2}{R^2}\left(-\frac{\nu R}{\ell}\left[\kei\tfrac{r}{\ell} + \frac{\ker{}'\tfrac{r}{\ell}}{r/\ell}\right] + \frac{R}{r}\ker{}'\tfrac{r}{\ell}\right)\right\}$$

$$-B_2\left\{ -\nu\frac{R}{\ell}\left(\kei\tfrac{r}{\ell} + \frac{\ker{}'\tfrac{r}{\ell}}{r/\ell}\right) + \frac{R}{r}\ker{}'\tfrac{r}{\ell} + \right.$$

$$\left.\left. + \nu\frac{\ell^2}{R^2}\left(\nu\frac{R}{\ell}\left[\ker\tfrac{r}{\ell} - \frac{\kei{}'\tfrac{r}{\ell}}{r/\ell}\right] + \frac{R}{r}\kei{}'\tfrac{r}{\ell}\right)\right\}\right] \qquad \text{(II.124a-d)}$$

The simplified radial deflection expression is obtained by integrating eqt. II.118d and adding eqt. II.117 and utilizing the assumptions of eqts. II.122 and II.123 :-

$$\omega_0 = \frac{\ell}{R(1-\nu^2)}\left[B_1\left(\ker\tfrac{r}{\ell} + \frac{R^2}{\ell^2}\kei\tfrac{r}{\ell}\right) + B_2\left(\kei\tfrac{r}{\ell} - \frac{R^2}{\ell^2}\ker\tfrac{r}{\ell}\right)\right] + \frac{P(1+\nu)}{2Et\,\pi}\left[1 + \ell n\frac{r}{2R}\right] \qquad \text{(II.125)}$$

These equations contain two constants B_1 and B_2 which are determined from the boundary conditions at the insert.

Determination of the constants

The boundary conditions at the insert $r = r_p$, $\frac{r}{\ell} = \mu$ are

$$\frac{d\omega_0}{dr} = 0 \quad \text{and} \quad \mathcal{E}_\theta = (N_{\theta\theta} - \nu N_{\phi\phi})/Et = 0 \qquad \text{(II.126a,b)}$$

From which the values of the constants B_1 and B_2 are as follows :-

$$B_1 = -\frac{PR(1+\nu)(1-\nu^2)}{2\pi r_p Et\left(\ker{}'\mu + \frac{R^2}{\ell^2}\kei{}'\mu\right)}\left[1 + \frac{(\kei{}'\mu - \frac{R^2}{\ell^2}\ker{}'\mu)(-\ker{}'\mu - \frac{R^2}{\ell^2}\kei{}'\mu + \mu\kei\mu + (1+\nu)\ker{}'\mu)}{\left[-\mu\kei{}'\mu\kei\mu - \mu\ker\mu\ker{}'\mu + \frac{R^2}{\ell^2}(\mu\kei\mu\ker{}'\mu) + (1+\nu)\ker{}'^2\mu - \mu\kei{}'\mu\ker\mu + (1+\nu)\kei{}'^2\mu\right]}\right]$$

$$B_2 = \frac{PR(1+\nu)(1-\nu^2)}{2\pi r_p Et}\left[\frac{(-\ker{}'\mu - \frac{R^2}{\rho^2}\kei{}'\mu + \mu\kei\mu + (1+\nu)\ker{}'\mu)}{\left[-\mu\kei{}'\mu\kei\mu - \mu\ker\mu\ker{}'\mu + \frac{R^2}{\rho^2}(\mu\kei\mu\ker{}'\mu) + (1+\nu)\ker{}'^2\mu - \mu\kei{}'\mu\ker\mu + (1+\nu)\kei{}'^2\mu)\right]}\right] \qquad \text{(II.127a,b)}$$

The derivation of these constants is shown in Appendix VIII.2.6, p. 265.

The magnitude of B_1 and B_2 is thus dependent upon the size of the insert and the particular R/t ratio. From the magnitudes of B_1 and B_2 the values of resultant force and moments, (eqts. II.124a-d) are obtained.

For small values of μ, where the dominant terms are ker$'\mu$ and those involving $\frac{R^2}{\ell^2}$ (or $\frac{R}{t}$), the expressions for B_1 and B_2 (eqts. II.127a,b) can be simplified considerably to:-

$$B_1 = -\frac{PR(1+\upsilon)(1-\upsilon^2)}{2\pi r_p Et}\left[\frac{1}{(1+\upsilon)ker'\mu}\right]$$

$$B_2 = \frac{PR(1+\upsilon)(1-\upsilon^2)}{2\pi r_p Et}\left[-\frac{R^2}{\ell^2}kei'\mu +\upsilon ker'\mu\right]\frac{\ell^2}{R^2(1+\upsilon)ker'^2\mu} \qquad \text{(II.128a,b)}$$

These simplified expressions for B_1 and B_2 can be substituted in the resultant force and moment equations (II.124a-d). As an example the meridional direct force is selected, i.e. eqt. II.124a.

$$\sigma_{rD} = \frac{N_{\phi\phi_0}}{t} = -\frac{Et}{(1-\upsilon^2)rt}\left(B_1 ker'\frac{r}{\ell} + B_2 kei'\frac{r}{\ell}\right) - \frac{PR}{2\pi r^2 t}$$

i.e. $\sigma_{rD} = +\frac{\sqrt{12(1-\upsilon^2)}}{2\pi\mu}\frac{P}{t^2}\left[\left(\frac{1}{ker'\mu}\right)\frac{ker'\frac{r}{\ell}}{\frac{r}{\ell}} - \left(\frac{\upsilon ker'\mu - \frac{R^2}{\ell^2}kei'\mu}{\frac{R^2}{\ell^2}ker'^2\mu}\right)\frac{kei'\frac{r}{\ell}}{\frac{r}{\ell}} - \frac{\mu}{(\frac{r}{\ell})^2}\right]$ (II.1

The constants previously obtained by the shallow shell treatment can also be simplified when μ is small. Hence C_8 and C_q of eqt. II.57a,b become:-

$$C_8 = \frac{\mu kei'\mu}{2 ker'^2\mu} \quad , \qquad C_q = -\frac{\mu}{2 ker'\mu} \qquad \text{(II.130)}$$

The meridional direct stress from eqt. II.56a can be written:-

$$\sigma_{rD} = \frac{P\sqrt{12(1-\upsilon^2)}}{2\pi\mu t^2}\left[\left(\frac{kei'\mu}{ker'^2\mu}\right)\frac{kei'\frac{r}{\ell}}{\frac{r}{\ell}} + \left(\frac{1}{ker'\mu}\right)\frac{ker'\frac{r}{\ell}}{\frac{r}{\ell}} - \frac{\mu}{(\frac{r}{\ell})^2}\right] \qquad \text{(II.131)}$$

The difference in eqts. II.129 and II.131 lies in the constant associated with $\frac{kei'\frac{r}{\ell}}{\frac{r}{\ell}}$, its actual value being smaller in the case of the shallow shell relationship. (eqt. II.131). The percentage difference between the constants is shown in Fig. II.18, for various values of R/t and μ. Although this is large it has negligible effect on the final stress, owing to the very small value of the constant compared with the other constant :- $\left(\frac{1}{ker'\mu}\right)$, and the association of the former constant
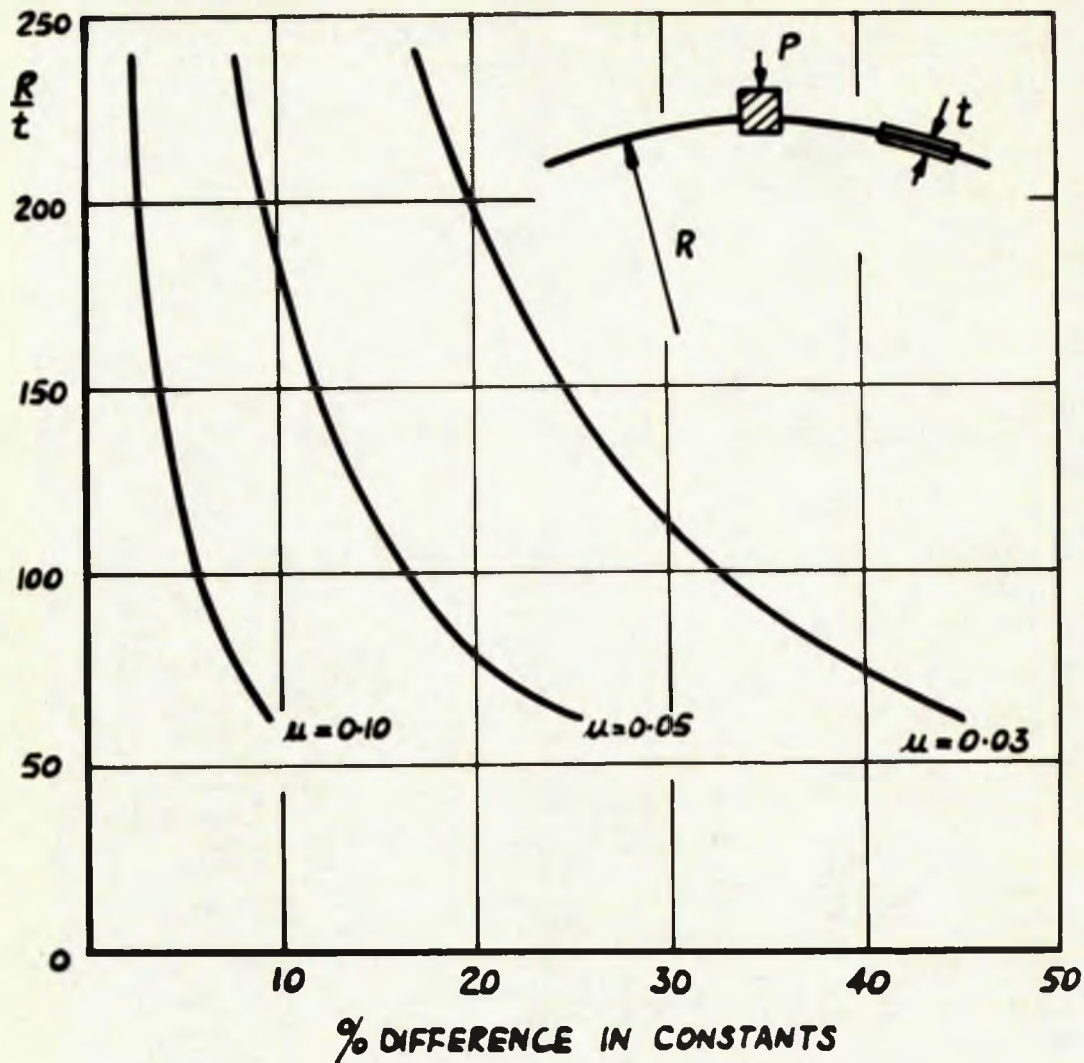
FIG. II.18 THE PERCENTAGE DIFFERENCE BETWEEN THE CONSTANT TERMS ASSOCIATED WITH $\frac{kei'r/l}{r/l}$ IN EQTS. II.129 & II.131 (GENERAL & SHALLOW SHELLS RESPECTIVELY) FOR VARIOUS R/t RATIOS AND μ VALUES, WHEN A RIGID INSERT IS RADIALLY LOADED

with the less dominant term in the expression.

For larger values of μ, the dominant terms in the constants B_1 and B_2 eqts. II.127a,b are always those involving R/t (or R^2/ℓ^2), all other terms are insignificant.   In this case the constants B_1 and B_2 reduce to a similar form as C_8 and C_9 (eqt. II.57a,b) and the stresses predicted are, therefore, identical.

In a similar manner, the resultant moments and normal displacements have been examined and compared with the shallow shell expressions.   As a result of this it is concluded that in the region of the 'die out' distance, the 'shallow shell' theory predicts results in agreement with the 'general shell' approach for all values of μ.

(b) The Concentrated Load at the Crown.   Fig. II.6

The expressions for the resultant force and moment actions and for the radial deflections are those quoted above for the rigid insert eqts. II.124a-d and II.125. The values of the two constants B_1 and B_2 can be found in two ways.
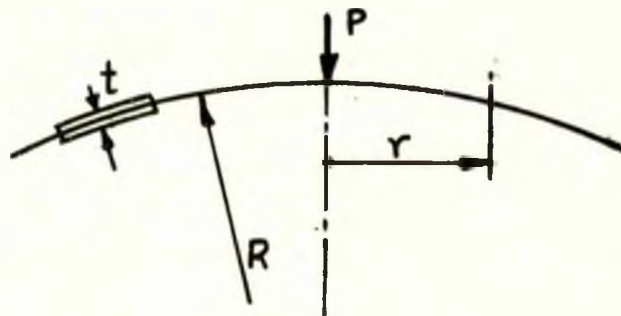
Fig. II.6

Firstly by allowing the radius of the rigid insert, r_p to tend to zero, and secondly by examining the singularity at the crown.

Using the first approach, the values of B_1 and B_2 are those of eqts. II.128a,b.

$$B_1 = -\frac{PR(1+\upsilon)(1-\upsilon^2)}{2\pi r_p E t}\left[\frac{1}{(1+\upsilon)\,\mathrm{ker}'\mu}\right]$$

$$B_2 = \frac{PR(1+\upsilon)(1-\upsilon^2)}{2\pi r_p E t}\left[-\frac{R^2}{\ell^2}\mathrm{kei}'\mu + \upsilon\,\mathrm{ker}'\mu\right]\frac{\ell^2}{R^2(1+\upsilon)\,\mathrm{ker}'^2\mu} \qquad (\text{II.128a,b})$$

Utilizing the relationships for ker' and kei' given in
App. VIII.8 , it is noted that for small values of μ;

$$\text{ker}'\mu \rightarrow -\frac{1}{\mu} \quad \text{and} \quad \text{kei}'\mu \rightarrow -\frac{\mu \, lu \, \mu}{2} \qquad \text{(II.132a,b)}$$

Eqts. II.128a,b thus modify to:-

$$B_1 = + \frac{PR(1-v^2)}{2\pi Et\,\ell}$$

$$B_2 = \frac{PR(1-v^2)}{2\pi Et\,\ell}\left[-\mu^2 lu\,\mu - v\frac{\ell^2}{R^2}\right]$$

where $r_p \rightarrow 0$, $\mu \rightarrow 0$ and

$$B_1 = \frac{PR(1-v^2)}{2\pi Et\,\ell} \qquad \text{as before}$$

$$B_2 \rightarrow -\frac{P(1-v^2)v\ell}{2\pi EtR} \qquad \text{(II.133a,b)}$$

In the second approach to determine B_1 and B_2, the expressions
for Nrr_0 and $N_{\theta\theta_0}$ from eqt. II.124a,b are considered in the
vicinity of the crown.

For small values of r/ℓ ;

$$\text{ker}\,r/\ell \rightarrow -lu\,r/\ell\,,\,\text{kei}\,r/\ell \rightarrow -\frac{\pi}{4}\,,\,\text{ker}'r/\ell \rightarrow -\frac{1}{r/\ell}\,,\,\text{kei}'r/\ell \rightarrow -r/\ell\,\frac{lu\,r/\ell}{2}\;\text{(II.134a-d)}$$

Thus:- $N_{\phi\phi_0} = \frac{Et}{(1-v^2)\ell}\left[B_1 - \frac{PR(1-v^2)}{Et\,\ell\cdot 2\pi}\right]\frac{1}{(r/\ell)^2} + B_2\frac{Et\,lu\,r/\ell}{2\ell(1-v^2)}$

$N_{\theta\theta_0} = -\frac{Et}{(1-v^2)\ell}\left[B_1 - \frac{PR(1-v^2)}{Et\,\ell\cdot 2\pi}\right]\frac{1}{(r/\ell)^2} - \frac{Et}{(1-v^2)\ell}\frac{\pi}{4}B_1 + B_2\frac{Et\,lu\,r/\ell}{2\ell(1-v^2)}$ (II.135a,b)

Similarly an expression for X_0 can be written from eqt. II.118c
using the assumptions of eqts. II.122a-c and II.123 and the
relationships of eqts. II.134a-d.

$$X_0 = \frac{R}{\ell^2(1-v^2)}\left[(B_1v\frac{\ell^2}{R^2}+B_2)\frac{1}{r/\ell} + B_1\left(\frac{r}{\ell}\cdot\frac{lu\,r/\ell}{2}\right) - B_2\left(v\frac{\ell^2}{R^2}\frac{r}{\ell}\cdot\frac{lu\,r/\ell}{2}\right)\right] \qquad \text{(II.135c)}$$

The horizontal deflection of the shell is given by the

expression: $\Delta = \frac{R\sin\phi}{Et}(N_{\theta\theta_0} - vN_{\phi\phi_0})$

Utilizing the assumption of eqts. II.122 $\Delta = \frac{r}{Et}(N_{\theta\theta_0} - vN_{\phi\phi_0})$

which from eqts. II.135a,b is shown to approach the singular

value at the origin:- $\frac{1}{(1-v^2)}\left[\frac{PR(1-v^2)}{Et\,\ell\,2\pi} - B_1\right]\frac{1}{r/\ell}$ (II.136)

For continuity, $\Delta = 0$ at the origin. Thus from eqt. II.136

$$B_1 = \frac{PR(1-\upsilon^2)}{Et\,\ell\,2\pi} \qquad (II.137)$$

Similarly at the origin X_o approaches the singular value,

obtained from eqt. II.135c, of :- $\dfrac{R}{\ell^2(1-\upsilon^2)}\left[B_1\upsilon\dfrac{\ell^2}{R^2} + B_2\right]\dfrac{1}{r/\ell}$ (II.138)

For continuity at the origin $X_o = 0$, thus :-

$$B_2 = -\frac{\upsilon\ell^2}{R^2}B_1 = -\frac{P\upsilon\ell(1-\upsilon^2)}{Et\,2\pi R} \qquad (II.139)$$

It is seen that the two methods yield identical results for B_1 & B_2.

Using these constants the force and moments, and from these

the direct and bending stresses, may be written from eqts. II.124 :-

$$N_{\phi\phi_o} = -\frac{PR}{2\pi\ell r}\left[ker'\,r/\ell - \upsilon\frac{\ell^2}{R^2}kei'\,r/\ell\right] - \frac{PR}{2\pi r^2}$$

which reduces to :- $\sigma_{r_D} = -\dfrac{P\sqrt{12(1-\upsilon^2)}}{2\pi t^2}\left[\dfrac{ker'\,r/\ell}{r/\ell} - \dfrac{\upsilon\ell^2}{R^2}\dfrac{kei'\,r/\ell}{r/\ell} + \dfrac{1}{(r/\ell)^2}\right]$ (II.140a)

$$N_{\theta\theta_o} = \frac{PR}{2\pi\ell^2}\left[kei\,r/\ell + \frac{ker'\,r/\ell}{r/\ell} + \frac{\upsilon\ell^2}{R^2}\left(ker\,r/\ell - \frac{kei'\,r/\ell}{r/\ell}\right) + \frac{1}{(r/\ell)^2}\right]$$

giving :- $\sigma_{\theta,D} = \dfrac{P\sqrt{12(1-\upsilon^2)}}{2\pi t^2}\left[kei\,r/\ell + \dfrac{ker'\,r/\ell}{r/\ell} + \dfrac{\upsilon\ell^2}{R^2}\left(ker\,r/\ell - \dfrac{kei'\,r/\ell}{r/\ell}\right) + \dfrac{1}{(r/\ell)^2}\right]$ (II.140b)

$$M_{\phi\phi_o} = \frac{P}{2\pi}\left[ker\,r/\ell - \frac{kei'\,r/\ell}{r/\ell} + \upsilon\frac{kei'\,r/\ell}{r/\ell}\right]\left(1 + \upsilon^2\frac{\ell^4}{R^4}\right)$$

Thus $\sigma_{r,B} = \pm\dfrac{3P}{\pi t^2}\left[ker\,r/\ell - (1-\upsilon)\dfrac{kei'\,r/\ell}{r/\ell}\right]\left(1 + \upsilon^2\dfrac{\ell^4}{R^4}\right)$ (II.140c)

$$M_{\theta\theta_o} = \frac{P}{2\pi}\left[\upsilon ker\,r/\ell - \frac{\upsilon kei'\,r/\ell}{r/\ell} + \frac{kei'\,r/\ell}{r/\ell}\right]\left(1 + \upsilon^2\frac{\ell^4}{R^4}\right)$$

Thus $\sigma_{\theta,B} = \pm\dfrac{3P}{\pi t^2}\left[\dfrac{(1-\upsilon)kei'\,r/\ell}{r/\ell} + \upsilon ker\,r/\ell\right]\left(1 + \upsilon^2\dfrac{\ell^4}{R^4}\right)$ (II.140d)

From eqt. II.125, $w_o = \dfrac{P}{2\pi Et}\left[(1+\upsilon)(ker\,r/\ell + 1 + \ell n\,r/2R) + \dfrac{R^2}{\ell^2}kei\,r/\ell\left(1-\upsilon\dfrac{\ell^4}{R^4}\right)\right]$

$$w_o = \frac{PR\sqrt{12(1-\upsilon^2)}}{2\pi Et^2}\left[kei\,r/\ell + \frac{(1+\upsilon)(ker\,r/\ell + 1 + \ell n\,r/2R)}{(R/\ell)^2(1-\upsilon\ell^4/R^4)}\right] \qquad (II.140e)$$

It is noted that using the assumption of localized load

effect, ϕ being small, the expressions for resultant force and

moment derived by LECKIE[39] reduce to those quoted above in

eqts. II.140 (neglecting $\dfrac{\upsilon\ell^4}{R^4}$ as small compared with unity).

Comparing these equations (II.140) with the shallow shell
expressions eqts. II.54a-e, it should be noted that terms con-
taining t/R (or ℓ^2/R^2) are not present in the latter. For thin
shells, the terms containing t/R may be considered negligible
and for such shells the general shell equations solved for small
co-latitude angles reduce to the shallow shell expressions for
all values of r, excepting those extremely close to the crown
r = 0. At the crown the 'general shell' approach and also the
'shallow shell' theory, allowing the rigid insert radius r_p to
approach zero, predict infinite values for the direct stress
terms, σ_{r_0} and σ_{θ_0}. However, using the 'shallow shell' theory
again but in this case allowing the uniformly distributed area
loads of radius r_p to approach zero, it is noted that the values
of σ_{r_0} and σ_{θ_0} are forced to remain finite, due to the boundary
conditions at r = 0.

II.2.2   'BENDING' MOMENT - FIG.II.19

The insert is fixed to the shell
at the crown, and loaded with a
moment M acting in the plane con-
taining the normals drawn from a meridional
line.   The approach to this problem is
the same as for the axisymmetrical case,
in that membrane, inextensional and
oscillatory solutions must be con-
sidered.   For the moment loading,   **Fig. II.19**
the first harmonic is of relevance, i.e. $n = 1$.
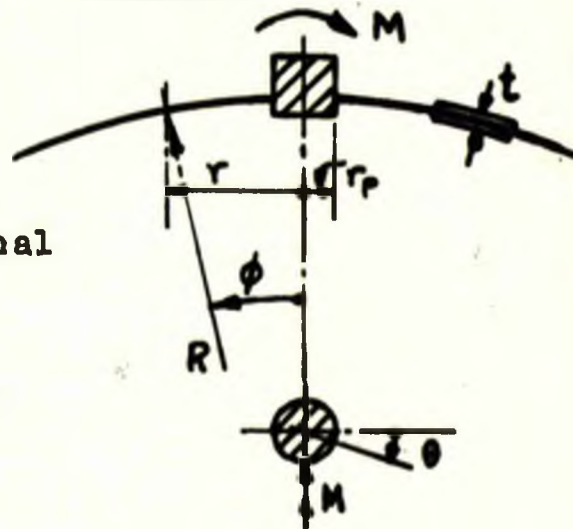
Membrane and Inextensional Solutions

Reference has been made to these solutions in Chapter I,
p.47 and 48 . An outline of the relevant material is given in
Appendix VIII.5 from whence the following solutions are quoted,
relevant for this type of loading.

Membrane Displacements for $n = 1$

From eqts. VIII.109, 110 and 111

$$v_1 = -\frac{M(1+v)}{4\pi REt}\left[\ell u \frac{1-\cos\phi}{1+\cos\phi} - \frac{2\cos\phi}{\sin^2\phi}\right]$$

$$w_1 = 0$$

$$u_1 = +\frac{M(1+v)}{4\pi REt}\left[\frac{2}{\sin^2\phi} + 2 + \cos\phi \, \ell u \frac{1-\cos\phi}{1+\cos\phi}\right] \qquad (II.141a-c)$$

Inextensional Displacements

For $n = 1$, these correspond to body movements

$$v_1 = D_2 - D_1 \cos\phi$$

$$w_1 = -D_1 \sin\phi$$

$$u_1 = D_1 - D_2 \cos\phi \qquad (II.142a-c)$$

where D_1 corresponds to a lateral displacement and D_2 a rotation.

Resultant Force and Moments

These are obtained from eqts. VIII.101 and VIII.114 of App. VIII.5

$$N_{\phi\phi_1} = -N_{\theta\theta_1} = -\frac{M}{\pi R^2 \sin^3\phi} \quad , \quad N_{\phi\theta_1} = -\frac{M\cos\phi}{\pi R^2 \sin^3\phi}$$

$$M_{\phi\phi_1} = -M_{\theta\theta_1} = \frac{Mk}{\pi R \sin^3\phi} \quad , \quad M_{\phi\theta_1} = \frac{Mk\cos\phi}{\pi R\sin^3\phi} \qquad \text{(II.143a-1}$$

$$\text{where} \quad k = t^2/12R^2$$

Oscillatory Solutions

These are presented below:-

$$(1-\upsilon)u_1 = -\frac{1}{\sin\phi}(A_1 T_1 + A_2 T_2 + B_1 T_3 + B_2 T_4)$$

$$(1-\upsilon)\upsilon_1 = A_1\dot{T}_1 + A_2\dot{T}_2 + B_1\dot{T}_3 + B_2\dot{T}_4$$

$$(1-\upsilon^2)\omega_1 = A_1(T_1 + 2\chi^2 T_2) + A_2(T_2 - 2\chi^2 T_1) + B_1(T_3 + 2\chi^2 T_4) + B_2(T_4 - 2\chi^2 T_3)$$

$$N_{\phi\phi_1} = \frac{Et}{(1-\upsilon^2)R}\left[-A_1\left(\dot{T}_1\cot\phi - \frac{T_1}{\sin^2\phi}\right) - A_2\left(\dot{T}_2\cot\phi - \frac{T_2}{\sin^2\phi}\right)\right.$$
$$\left. - B_1\left(\dot{T}_3\cot\phi - \frac{T_3}{\sin^2\phi}\right) - B_2\left(\dot{T}_4\cot\phi - \frac{T_4}{\sin^2\phi}\right)\right]$$

$$N_{\theta\theta_1} = \frac{Et}{(1-\upsilon^2)R}\left[A_1(2\chi^2 T_2 + \dot{T}_1\cot\phi - T_1\cot^2\phi) - A_2(2\chi^2 T_1 - \dot{T}_2\cot\phi + T_2\cot^2\phi)\right.$$
$$\left. + B_1(2\chi^2 T_4 + \dot{T}_3\cot\phi - T_3\cot^2\phi) - B_2(2\chi^2 T_3 - \dot{T}_4\cot\phi + T_4\cot^2\phi)\right]$$

$$N_{\phi\theta_1} = N_{\theta\theta_1} = \frac{Et}{(1-\upsilon^2)R}\left[A_1\left(\frac{T_1\cos\phi}{\sin^2\phi} - \frac{\dot{T}_1}{\sin\phi}\right) + A_2\left(\frac{T_2\cos\phi}{\sin^2\phi} - \frac{\dot{T}_2}{\sin\phi}\right)\right.$$
$$\left. + B_1\left(\frac{T_3\cos\phi}{\sin^2\phi} - \frac{\dot{T}_3}{\sin\phi}\right) + B_2\left(\frac{T_4\cos\phi}{\sin^2\phi} - \frac{\dot{T}_4}{\sin\phi}\right)\right]$$

$$M_{\theta\theta_1} = \frac{Et^3}{12(1-\upsilon^2)R^2(1+\upsilon)}\left\{A_1\left[2\chi^2\left(\dot{T}_2\cot\phi - \frac{T_2}{\sin^2\phi}\right) + \upsilon\left(-2\chi^2 T_2 - \dot{T}_1\cot\phi + T_1\left[\frac{1}{\sin^2\phi} + \frac{1+\upsilon}{k}\right]\right)\right]\right.$$
$$+ A_2\left[-2\chi^2\left(\dot{T}_1\cot\phi - \frac{T_1}{\sin^2\phi}\right) + \upsilon\left(2\chi^2 T_1 - \dot{T}_2\cot\phi + T_2\left[\frac{1}{\sin^2\phi} + \frac{1+\upsilon}{k}\right]\right)\right]$$
$$+ B_1\left[2\chi^2\left(\dot{T}_4\cot\phi - \frac{T_4}{\sin^2\phi}\right) + \upsilon\left(-2\chi^2 T_4 - \dot{T}_3\cot\phi + T_3\left[\frac{1}{\sin^2\phi} + \frac{1+\upsilon}{k}\right]\right)\right]$$
$$\left. + B_2\left[-2\chi^2\left(\dot{T}_3\cot\phi - \frac{T_3}{\sin^2\phi}\right) + \upsilon\left(2\chi^2 T_3 - \dot{T}_4\cot\phi + T_4\left[\frac{1}{\sin^2\phi} + \frac{1+\upsilon}{k}\right]\right)\right]\right.$$

$$M_{\phi\phi_1} = \frac{Et^3}{12(1-\upsilon^2)R^2(1+\upsilon)}\left[A_1\left[\frac{(1+\upsilon)T_1}{k} - 2\chi^2\cot\phi(\dot{T}_2 - T_2\cot\phi) + \upsilon\cot\phi(\dot{T}_1 - T_1\cot\phi)\right]\right.$$

$$+ A_2\left[\frac{(1+\upsilon)T_2}{k} + 2\chi^2\cot\phi(\dot{T}_1 - T_1\cot\phi) + \upsilon\cot\phi(\dot{T}_2 - T_2\cot\phi)\right]$$

$$+ B_1\left[\frac{(1+\upsilon)T_3}{k} - 2\chi^2\cot\phi(\dot{T}_4 - T_4\cot\phi) + \upsilon\cot\phi(\dot{T}_3 - T_3\cot\phi)\right]$$

$$+ \left. B_2\left[\frac{(1+\upsilon)T_4}{k} + 2\chi^2\cot\phi(\dot{T}_3 - T_3\cot\phi) + \upsilon\cot\phi(\dot{T}_4 - T_4\cot\phi)\right]\right]$$

$$M_{\theta\phi_1} = M_{\phi\theta_1} = \frac{Et^3}{12(1-\upsilon^2)R^2(1+\upsilon)}\left[\frac{A_1}{\sin\phi}\left[-2\chi^2(\dot{T}_2 - T_2\cot\phi) + \upsilon(\dot{T}_1 - T_1\cot\phi)\right]\right.$$

$$+ \frac{A_2}{\sin\phi}\left[2\chi^2(\dot{T}_1 - T_1\cot\phi) + \upsilon(\dot{T}_2 - T_2\cot\phi)\right]$$

$$+ \frac{B_1}{\sin\phi}\left[-2\chi^2(\dot{T}_4 - T_4\cot\phi) + \upsilon(\dot{T}_3 - T_3\cot\phi)\right]$$

$$+ \left. \frac{B_2}{\sin\phi}\left[2\chi^2(\dot{T}_3 - T_3\cot\phi) + \upsilon(\dot{T}_4 - T_4\cot\phi)\right]\right]$$

(II.144a-i)

where $T_1 \rightarrow T_4$ and $\dot{T}_1 \rightarrow \dot{T}_4$ are given by eqts. II.120 and II.121 and $k - t^2/12R^2$

The above expressions containing four constants give the resultant force and moments in general form. As previously the terms associated with A_1 and A_2 describe the stresses caused by loading of the lower or outer edge, and those with B_1 and B_2 the top or crown of the shell. In the work that follows it is assumed that the outer edge of the shell is sufficiently remote that the stresses associated with these boundaries do not influence those associated with the 'crown' loading.

Utilizing the assumptions of the localized effect of the load contained in eqts. II.122a-c and of thin shells, eqt. II.123, the resultant forces and moments may be written from eqts. II.143 and II.144, and the normal deflection w, from eqts. II.141b and

II.144c, as follows:-

$$N_{\phi\phi_1} = \frac{Et}{(1-\upsilon^2)}\frac{R}{\ell^2}\left[B_1\left(\frac{kei'r/\ell}{r/\ell} + \frac{2ker'r/\ell}{(r/\ell)^2}\right) - B_2\left(\frac{ker\,r/\ell}{r/\ell} - \frac{2kei'r/\ell}{(r/\ell)^2}\right)\right] - \frac{MR}{\pi r^3}$$

$$N_{\theta\theta_1} = \frac{Et}{(1-\upsilon^2)}\frac{R}{\ell^2}\left[B_1\left(kei'r/\ell - \frac{kei\,r/\ell}{r/\ell} - \frac{2ker'r/\ell}{(r/\ell)^2}\right) - B_2\left(ker'r/\ell - \frac{ker\,r/\ell}{r/\ell} + \frac{2kei'r/\ell}{(r/\ell)^2}\right)\right] + \frac{MR}{\pi r^3}$$

$$N_{\phi\theta_1} = \frac{Et}{(1-\upsilon^2)}\frac{R}{\ell^2}\left[B_1\left(\frac{kei\,r/\ell}{r/\ell} + \frac{2ker'r/\ell}{(r/\ell)^2}\right) - B_2\left(\frac{ker\,r/\ell}{r/\ell} - \frac{2kei'r/\ell}{(r/\ell)^2}\right)\right] - \frac{MR}{\pi r^3}$$

$$M_{\phi\phi_1} = \frac{Et^3}{12(1-\upsilon^2)R^2(1+\upsilon)}\left\{B_1\left[\frac{(1+\upsilon)12R^2\,ker'r/\ell}{t^2} - \frac{R^4}{\ell^4}\left(\frac{ker\,r/\ell}{r/\ell} - \frac{2kei'r/\ell}{(r/\ell)^2}\right)\right.\right.$$
$$\left.- \upsilon\frac{R^2}{\ell^2}\left(\frac{kei\,r/\ell}{r/\ell} + \frac{2ker'r/\ell}{(r/\ell)^2}\right)\right]$$
$$+ B_2\left[\frac{(1+\upsilon)12R^2\,kei'r/\ell}{t^2} - \frac{R^4}{\ell^4}\left(\frac{kei\,r/\ell}{r/\ell} + \frac{2ker'r/\ell}{(r/\ell)^2}\right)\right.$$
$$\left.\left.+ \upsilon\frac{R^2}{\ell^2}\left(\frac{ker\,r/\ell}{r/\ell} - \frac{2kei'r/\ell}{(r/\ell)^2}\right)\right]\right\} + \frac{Mt^2}{12\pi r^3}$$

$$M_{\theta\theta_1} = \frac{Et^3}{12(1-\upsilon^2)R^2(1+\upsilon)}\left\{B_1\left[\frac{\upsilon(1+\upsilon)12R^2\,ker'r/\ell}{t^2} + \frac{R^4}{\ell^4}\left(\frac{ker\,r/\ell}{r/\ell} - \frac{2kei'r/\ell}{(r/\ell)^2}\right)\right.\right.$$
$$\left.+ \upsilon\frac{R^2}{\ell^2}\left(-kei'r/\ell + \frac{kei\,r/\ell}{r/\ell} + \frac{2ker'r/\ell}{(r/\ell)^2}\right)\right]$$
$$+ B_2\left[\frac{\upsilon(1+\upsilon)12R^2\,kei'r/\ell}{t^2} + \frac{R^4}{\ell^4}\left(\frac{kei\,r/\ell}{r/\ell} + \frac{2ker'r/\ell}{(r/\ell)^2}\right)\right.$$
$$\left.\left.+ \upsilon\frac{R^2}{\ell^2}\left(ker'r/\ell - \frac{ker\,r/\ell}{r/\ell} + \frac{2kei'r/\ell}{(r/\ell)^2}\right)\right]\right\} - \frac{Mt^2}{12\pi r^3}$$

$$M_{\theta\phi_1} = \frac{Et^3}{12(1-\upsilon^2)R^2(1+\upsilon)}\left\{B_1\left[-\frac{R^4}{\ell^4}\left(\frac{ker\,r/\ell}{r/\ell} - \frac{2kei'r/\ell}{(r/\ell)^2}\right) + \upsilon\frac{R^2}{\ell^2}\left(-\frac{kei\,r/\ell}{r/\ell} - \frac{2ker'r/\ell}{(r/\ell)^2}\right)\right]\right.$$
$$\left.+ B_2\left[\frac{R^4}{\ell^4}\left(-\frac{kei\,r/\ell}{r/\ell} - \frac{2ker'r/\ell}{(r/\ell)^2}\right) + \upsilon\frac{R^2}{\ell^2}\left(\frac{ker\,r/\ell}{r/\ell} - \frac{2kei'r/\ell}{(r/\ell)^2}\right)\right]\right\} + \frac{Mt^2}{12\pi r^3}$$

$$\omega_1 = \frac{1}{(1-\upsilon^2)}\left[B_1\left(ker'r/\ell + \frac{R^2}{\ell^2}kei'r/\ell\right) + B_2\left(kei'r/\ell - \frac{R^2}{\ell^2}ker'r/\ell\right)\right]$$

(II.145a-

These equations contain two constants B_1 and B_2 which are determined from the boundary conditions at the insert.

Determination of the Constants

The boundary conditions at the insert, $r = r_p$, $\frac{r}{\ell} = \mu$ are:-

$$\frac{d\omega}{dr} = \frac{\omega}{r} \quad , \quad \mathcal{E}_\theta = (N_{\theta\theta} - \upsilon N_{rr})/Et = 0 \qquad (II.146a,b)$$

From which the values of the constants B_1 and B_2 are as follows:-

$$B_1 = -\frac{M(1+\upsilon)(1-\upsilon^2)\left[\mu\,ker\,\mu - 2kei'\mu + \frac{R^2}{\ell^2}(2ker'\mu + \mu kei\mu)\right]}{\pi Et\mu\ell\left\{\frac{R^2}{\ell^2}\left[\mu^3(kei'\mu\,kei\mu + ker'\mu\,ker\mu) - (1+\upsilon)\left\{\mu^2(kei^2\mu + ker^2\mu) + 4(kei'^2\mu + ker'^2\mu) + 4\mu(ker'\mu\,kei\mu - kei'\mu\,ker\mu)\right\}\right] + \mu^3(kei'\mu\,ker\mu - ker'\mu\,kei\mu) - 2\mu^2(kei'^2\mu + ker'^2\mu)\right\}}$$

$$B_2 = -\frac{M(1+\upsilon)(1-\upsilon^2)\left[\mu\,kei\,\mu + 2ker'\mu + \frac{R^2}{\ell^2}(2kei'\mu - \mu ker\,\mu)\right]}{\pi Et\mu\ell\left\{\frac{R^2}{\ell^2}\left[\mu^3(kei'\mu\,kei\mu + ker'\mu\,ker\mu) - (1+\upsilon)\left\{\mu^2(kei^2\mu + ker^2\mu) + 4(kei'^2\mu + ker'^2\mu) + 4\mu(ker'\mu\,kei\mu - kei'\mu\,ker\mu)\right\}\right] + \mu^3(kei'\mu\,ker\mu - ker'\mu\,kei\mu) - 2\mu^2(kei'^2\mu + ker'^2\mu)\right\}}$$

$$(II.147a,b)$$

The derivation of these constants is shown in Appendix.VIII.2.7 (p265)

The magnitudes of B_1 and B_2, which are dependent upon the size of the insert and the particular R/t ratio, enable the values of the resultant force and moments (eqts. II.145a-g) to be obtained.

As in the case of the radial loading, comparison is to be made between the expressions for resultant force and moment obtained by the shallow shell theory and those obtained in this section.

Considering firstly the resultant force expressions for different μ values:-

For small values of μ, where the dominant terms are $ker'\mu$ and those involving R/t (or R^2/ℓ^2), the expressions for B_1 and B_2 (eqts. II.147a,b) can be simplified considerably:-

Thus :- $B_1 = \dfrac{M(1+\nu)(1-\nu^2)}{\pi E t \mu \ell} \dfrac{(2ker'\mu + \mu kei\,\mu)}{[X]}$

$B_2 = \dfrac{M(1+\nu)(1-\nu^2)}{\pi E t \mu \ell} \dfrac{\left[2ker'\mu + \frac{R^2}{\ell^2}(2kei'\mu - \mu ker\mu)\right]}{\frac{R^2}{\ell^2}[X]}$ (II.148a,b)

where $[X] = (1+\nu)\left[\mu^2(kei^2\mu + ker^2\mu) + 4(kei'^2\mu + ker'^2\mu)\right.$

$\left. + 4\mu(ker'\mu\,kei\,\mu - kei'\mu\,ker\mu)\right] - \mu^3(ker'\mu\,ker\mu + kei'\mu\,kei\,\mu)$

These simplified expressions for B_1 and B_2 when substituted in eqts. II.145 yield values for the resultant forces and moments.   As an example of the resultant force, the meridional direct stress is as follows:-

$\sigma_{rD} = \dfrac{N\phi\phi}{t} = \dfrac{N\phi\phi}{t}\cos\theta = \dfrac{ER}{(1-\nu^2)\ell^2}\left[B_1\left(\dfrac{kei\frac{r}{\ell}}{\frac{r}{\ell}} + \dfrac{2ker'\frac{r}{\ell}}{(r/\ell)^2}\right) + B_2\left(\dfrac{ker\frac{r}{\ell}}{\frac{r}{\ell}} - \dfrac{2kei'\frac{r}{\ell}}{(r/\ell)^2}\right)\right]\cos\theta$

$- \dfrac{MR\cos\theta}{\pi r^3 t}$

$\sigma_{rD} = \dfrac{M\sqrt{12(1-\nu^2)}\,(1+\nu)}{t^2\pi\mu\ell[X]}\left\{(2ker'\mu + \mu kei\,\mu)\left[\dfrac{kei\frac{r}{\ell}}{\frac{r}{\ell}} + \dfrac{2ker'\frac{r}{\ell}}{(r/\ell)^2}\right]\right.$

$\left. -\dfrac{(2ker'\mu + \frac{R^2}{\ell^2}(2kei'\mu) - \frac{R^2}{\ell^2}\mu ker\mu)}{(\frac{R}{\ell})^2}\left[\dfrac{ker\frac{r}{\ell}}{\frac{r}{\ell}} - \dfrac{2kei'\frac{r}{\ell}}{(r/\ell)^2}\right]\right\}\cos\theta$

$- \dfrac{MR\cos\theta}{\pi r^3 t}$ (II.149)

The equation for σ_{rD} obtained by the shallow shell treatment is presented in eqt. II.68a and by substituting for the constants C_3, C_4 and C_5 from eqts. II.66 and II.67a,b, may be written as follows:-

$\sigma_{rD} = \dfrac{M(1+\nu)\sqrt{12(1-\nu^2)}}{t^2\pi\mu\ell[X]}\left\{(2ker'\mu + \mu kei\,\mu)\left[\dfrac{kei\frac{r}{\ell}}{\frac{r}{\ell}} + \dfrac{2ker'\frac{r}{\ell}}{(\frac{r}{\ell})^2}\right]\right.$

$\left. - (2kei'\mu - \mu ker\mu)\left[\dfrac{ker\frac{r}{\ell}}{\frac{r}{\ell}} - \dfrac{2kei'\frac{r}{\ell}}{(\frac{r}{\ell})^2}\right]\right\}\cos\theta - \dfrac{MR\cos\theta}{\pi r^3 t}$

(II.150)

As in the radial loading a difference occurs in the values
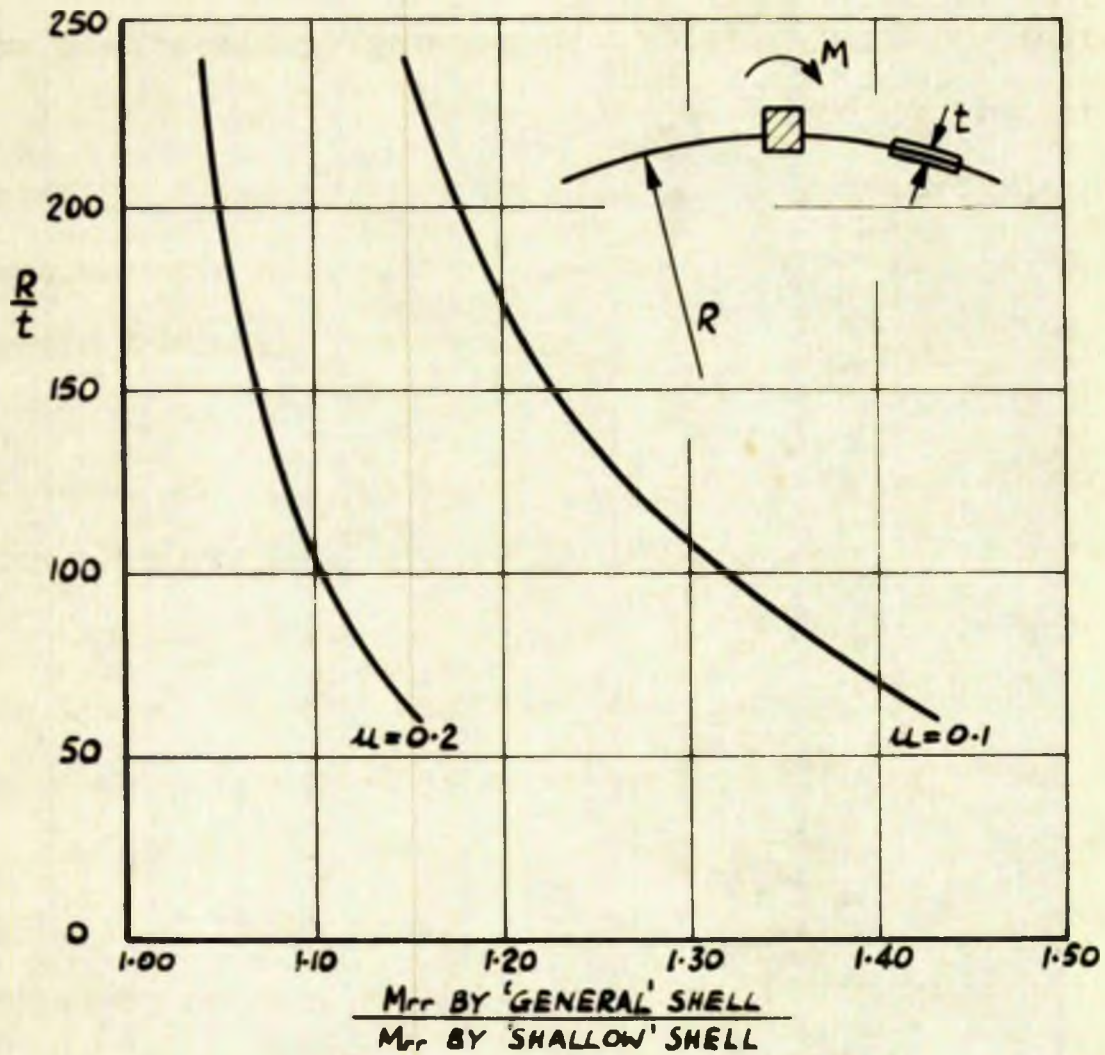
FIG. II·20 The Ratio of the Maximum Meridional Moment, M_{rr} (at $r = r_p$) Predicted by the General and Shallow Shell Treatments for Various R/t ratios and μ values, when a Rigid Insert is Loaded with a Bending Moment

of the smaller of the two constants obtained by the two methods
of approach.   The magnitude of this difference depends upon the
particular R/t ratio and the μ value.   Although the percentage
difference is large, greater in magnitude though similar in form
to the radial case, Fig. II.18, it has negligible effect on the
final stress owing to the small magnitude of the constant, com-
pared with the other larger constant, and the association of
the constant with the less dominant term in the expression.

Similar remarks may also be made about the other direct
stresses.

For the larger values of μ, the dominant terms in B_1 and
B_2 are always those involving R/t, and the constants B_1 and B_2
reduce to the same form as C_3 and C_4 of eqts. II.67a,b.

It may, therefore, be concluded that for all values of μ
the direct stresses obtained from the shallow shell theory are
in agreement with those predicted by the general shell approach.

Regarding the resultant moments, it is noted that in the
immediate vicinity of the insert considerable divergence occurs
between the shallow shell and the general shell treatments.
This is mainly influenced by the term $\frac{Mt^2}{12\pi r^3}$ which is present in
the expressions for Mrr_1, $M_{\theta\theta_1}$ and $M_{\theta r_1}$, eqts. II.145d-f.   This
term is the moment arising from the membrane or mid-surface dis-
placements.   The difference in the results obtained by two
methods depends upon μ and the R/t ratio, and is shown in Fig.
II.20, for the maximum meridional moment Mrr_1 (at $r = r_1$).   In
this case the general shell treatment predicts values which are
higher than the shallow shell.   This difference, however, is

a purely local effect in the immediate vicinity of the insert, as indicated by Fig. II.21.

A comparison between the two treatments for the other moment actions yields a similar type of result to that presented for $M_{\phi\phi}$. As pointed out above, and shown in Fig. II.21, these effects are only of significance in the region of the insert, and then only of importance when μ is small.

as indicated by Fig. II.21.
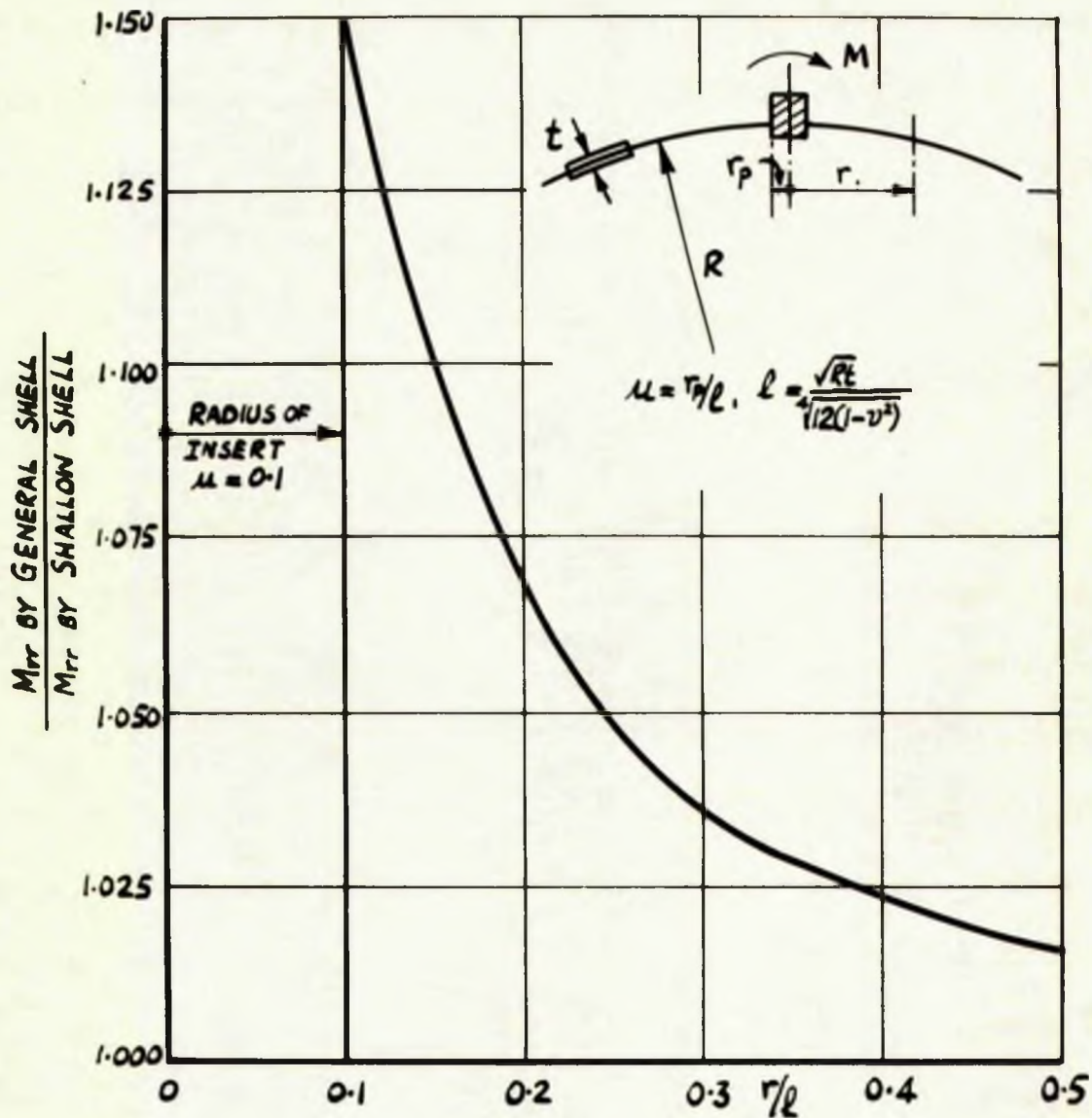
FIG. II·21   THE VARIATION OF THE RATIO OF M_{rr} VALUES PREDICTED BY THE
GENERAL & SHALLOW SHELL TREATMENTS FOR $R/t = 240$ AND
$\mu = 0·1$, AS r/ℓ INCREASES.

II.2.3 'TWISTING' MOMENT - Fig.II.22

The shell is loaded by a moment T
in the plane of the shell and
acting at its crown, and trans-
mitted to the shell by a rigid
insert, as indicated in Fig.II.22.
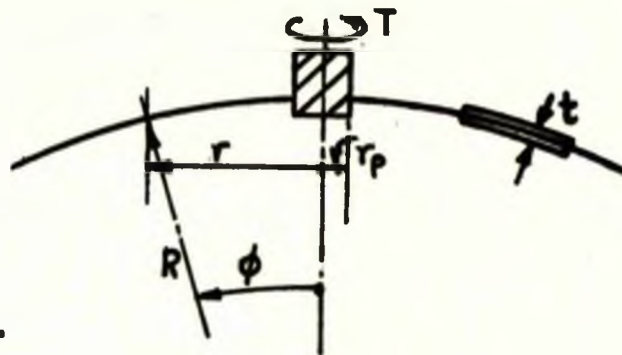
Fig.II.22

Membrane Solutions

Resultant Forces $\quad N_{\phi\phi} = N_{\theta\theta} = 0$, $N_{\phi\theta} = \dfrac{T}{2\pi r^2}$ $\qquad$ (II.151a-c)

Displacements

The relevant deformation-strain relationship is given in
Appendix VIII.5:-

$$\frac{\partial u}{\partial \phi} \sin\phi \quad - u\cos\phi \quad + \frac{\partial v}{\partial \theta} = R\gamma_{\phi\theta} \sin\phi \qquad \text{(VIII.102c)}$$

which in this case simplifies to:- $\dfrac{du}{d\phi} - u\cot\phi = R\gamma_{\phi\theta}$ $\quad$ (II.152)

Using the appropriate strain relationship:- $\gamma_{\phi\theta} = \dfrac{N_{\phi\theta}}{Gt}$ $\quad$ (II.153)

and substituting eqts. II.151c into eqt. II.152, the following
is obtained:-

$$\frac{du}{d\phi} - u\cot\phi = \frac{RT}{2\pi r^2 Gt}$$

Thus $\quad u = \dfrac{T}{8\pi RGt}\left[-2\cot\phi + \sin\phi . \ln\dfrac{1-\cos\phi}{1+\cos\phi}\right] + C_1\sin\phi$ $\qquad$ (II.154)

where $C_1\sin\phi$ may be considered as an inextensional displacement.

Since $N_{\theta\theta} = N_{\phi\phi} = 0$, it follows that $\varepsilon_\theta = \varepsilon_\phi = 0$. Thus the

strain-displacement equations, eqts. VIII.102, (Appendix VIII.5)

become:- $\quad \dfrac{dv}{d\phi} + w = 0 \; ; \quad v\cos\phi + w\sin\phi = 0$ $\qquad$ (II.155a,b)

From eqts. II.155a,b, $\qquad \dfrac{dv}{d\phi} - v\cot\phi = 0$

and, therefore, $v = C_2 \sin\phi$ $\quad$ and thus $w = -C_2\cos\phi$ $\quad$ (II.156a,b)

Eqt. II.156a can only satisfy the physical aspects of the problem

when $C_2 = 0$. $\quad$ Thus $v = w = 0$. $\qquad$ (II.157)

Resultant Moments

As in the case of the earlier types of loading, the displacement u will produce moment actions $M_{\phi\theta}$. These relationships are given in full in Appendix VIII.5 eqts. VIII.112; for this case they simplify to:-

$$M_{\theta\theta} = M_{\phi\phi} = 0$$

$$M_{\phi\theta} = \frac{Et^3}{12(1-v^2)R^2} \frac{1-v}{2} \left[u\cot\phi - \frac{\partial u}{\partial\phi} \right] \qquad (II.158a-c)$$

Substituting eqt. II.154 in eqt. II.158c:-

$$M_{\phi\theta} = \frac{Tt^2}{24\pi R^3 \sin^2\phi} \qquad (II.159)$$

Outer Boundary

If the shell is fixed at the outer boundary $r = r_2$, or $\phi = \phi_2$. Then $u = 0$. Thus from eqt. II.154, $C_1 = \frac{T}{8\pi RGt}\left[2\cot\phi_2 - \sin\phi_2 \, \ell u \frac{1-\cos\phi_2}{1+\cos\phi_2}\right]\frac{1}{\sin}$ and in eqt. II.154:-

$$u = \frac{T}{8\pi RGt}\left[-2\cot\phi + \sin\phi \, \ell u \frac{1-\cos\phi}{1+\cos\phi} + 2\cot\phi_2 \frac{\sin\phi}{\sin\phi_2} - \sin\phi \, \ell u \frac{1-\cos\phi_2}{1+\cos\phi_2}\right] \quad (II.160)$$

Using r and r_2 , $\quad \sin\phi = r/R$, $\quad \cot\phi = \frac{\sqrt{R^2-r^2}}{r}$

$$u = \frac{T}{4\pi tG}\left[\frac{\sqrt{R^2-r_2^2}}{Rr_2^2} - \frac{\sqrt{R^2-r^2}}{Rr^2} + \frac{1}{R^2} \ell u \left(\frac{r}{r_2}\right)\left(\frac{R+\sqrt{R^2-r_2^2}}{R+\sqrt{R^2-r^2}}\right)\right] r \qquad (II.161)$$

when $R = \infty$, i.e. for the flat plate

$$u = \frac{T}{4\pi tG}\left[\frac{1}{r_2^2} - \frac{1}{r^2}\right] r , \qquad\qquad \text{which is identical to eqt.}$$

VIII.73e of Appendix VIII.3. 'A Twisting Moment applied to a Flat Plate.'

Oscillatory Solutions

In the case of the torsion problem equations, II.151a-c, 158a,b, 159 and II.161, represent the complete solution. HAVERS[6] and LECKIE[39] point out that the form of R in the oscillatory solution would be $\theta R(\phi)$. (For the other cases,

$R = R_n (\phi) \cos n\theta$ was adequate).   However, when this is sub-stituted in the oscillatory forms of u, v and w which are

$$(1-v)u = \left[\frac{\partial R}{\partial \theta} + \frac{\partial \bar{R}}{\partial \theta} \right] \frac{1}{\sin \phi} \, , \quad (1-v)v = \frac{\partial R}{\partial \phi} + \frac{\partial \bar{R}}{\partial \phi} \qquad \text{and}$$

$$(1-v)w = F_1 R + F_2 \bar{R} \, , \text{ where } \quad F_1 = \frac{1 - 2i\chi^2}{1+v} \qquad \text{and } F_2 = \frac{1 + 2i\chi^2}{1+v} \, ,$$

it is noted that while u is independent of θ, and dependent only upon ϕ, the values of v and w are not independent of θ. Thus the oscillatory solutions cannot exist.

The relationships for $N_{\phi\theta}$ and for u have also been obtained by an alternative method, given in Appendix VIII.4.   The expressions are seen to be identical.

A comparison of the relationships for the resultant forces obtained by this and by the shallow-shell approach eqts. II.86 indicate that the two are identical.   The values of u predicted by equations II.861 (shallow shell) and II.161 (general shell), do not differ by more than 0.2% for the range of thin shell used in this investigation.   The term $M_{\phi\theta}$ is of very small magnitude compared to $N_{\phi\theta}$.   For the shells used in this investigation $\frac{N_{\phi\theta}}{M_{\phi\theta}}$ varies from 720 to 11500 and is thus neglected.

II.2.4 TANGENTIAL LOAD - Fig.II.23

A spherical shell is loaded by a
tangential load H in the plane of
the shell and acting at its crown.
The force is transmitted to the
shell by means of a rigid cylindri-
cal insert.   This case is similar
to the moment loading and can be
represented by the first harmonic, n = 1.
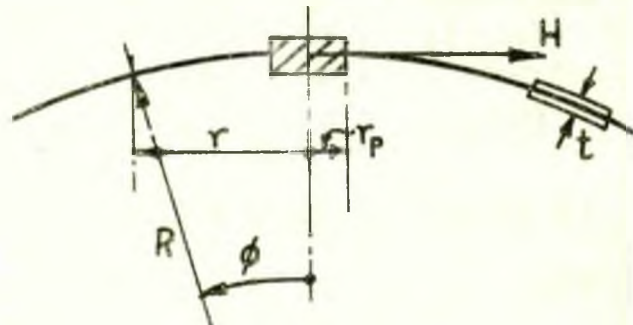
Fig. II.23

Three solutions
exist as before - membrane, inextensional and oscillatory.

Membrane and Inextensional Solutions

An outline of these solutions is given in Appendix VIII.5
from whence the following solutions are quoted, relevant to this
type of loading.

Membrane Displacements

From eqts. VIII.109, 110 and 111

$$v_1 = -\frac{H(1+v)}{4\pi Et}\left[\frac{2(1-\cos\phi)}{\sin^2\phi} + 2 + (1+\cos\phi)\ln\frac{1-\cos\phi}{1+\cos\phi}\right]$$

$$w_1 = -\frac{H(1+v)}{4\pi Et}\left[\sin\phi\,\ln\frac{1-\cos\phi}{1+\cos\phi} - 2\frac{\cos\phi}{\sin\phi}\right]$$

$$u_1 = +\frac{H(1+v)}{4\pi Et}\left[\frac{2(1-\cos\phi)}{\sin^2\phi} + 2 + (1+\cos\phi)\ln\frac{1-\cos\phi}{1+\cos\phi}\right]$$

(II.162a-c)

Inextensional Displacements (for n = 1. These are body movement

$$v_1 = D_2 - D_1\cos\phi$$

$$w_1 = -D_1\sin\phi$$

$$u_1 = D_1 - D_2\cos\phi$$

(II.163a

Resultant Force and Moments

These are obtained from eqts. VIII.101 and VIII.114 of
Appendix VIII.5.

$$-N_{\phi\phi_1} = N_{\theta\theta_1} = N_{\phi\theta_1} = \frac{H(1-\cos\phi)}{\pi R \sin^3\phi}$$

$$M_{\phi\phi_1} = -M_{\theta\theta_1} = \frac{Hk}{\pi \sin^3\phi}, \quad M_{\phi\theta_1} = \frac{Hk\cos\phi}{\pi \sin^3\phi} \qquad (II.164a\text{-}f)$$

where $k = t^2/12R^2$

Oscillatory Solutions

These are exactly those of eqts. II.144a-i which are
valid for values of ϕ in the region $\pi > \phi > 0$. The complexity
of these expressions can be reduced when $\sqrt{2}\chi\phi > 6$ by using the
asymptotic expansions of the Bessel and Kelvin functions. Such
simplified expressions relevant to this analysis are given below:-

$$U_1 = -\frac{R(1+v)}{\sqrt{2}\chi E t \sin^{3/2}\phi}\left\{e^{\chi\phi}\left[C_1\sin\left(\chi\phi+\frac{\pi}{4}\right) - C_2\cos\left(\chi\phi+\frac{\pi}{4}\right)\right]\right.$$
$$\left. - e^{-\chi\phi}\left[E_1\cos\left(\chi\phi+\frac{\pi}{4}\right) + E_2\sin\left(\chi\phi+\frac{\pi}{4}\right)\right]\right\}$$

$$V_1 = \frac{R(1+v)}{E t \sqrt{\sin\phi}}\left\{e^{\chi\phi}\left[C_1\cos\chi\phi + C_2\sin\chi\phi\right]\right.$$
$$\left. + e^{-\chi\phi}\left[E_1\cos\chi\phi + E_2\sin\chi\phi\right]\right\}$$

$$\omega_1 = \frac{\sqrt{2}\chi R}{E t \sqrt{\sin\phi}}\left\{- e^{\chi\phi}\left[C_1\cos\left(\chi\phi+\frac{\pi}{4}\right) + C_2\sin\left(\chi\phi+\frac{\pi}{4}\right)\right]\right.$$
$$\left. + e^{-\chi\phi}\left[E_1\sin\left(\chi\phi+\frac{\pi}{4}\right) - E_2\cos\left(\chi\phi+\frac{\pi}{4}\right)\right]\right\}$$

$$(II.165a\text{-}c)$$

In this particular case the effect of the outer edge is
examined, which in the earlier cases has been assumed remote.
The boundary conditions at this outer edge are used to determine

the values of the inextensional displacements and also the result
ant forces at the edge.

As will be appreciated from the foregoing, the analytical
solutions are exceedingly complex.   In this instance the exam-
ination of the outer-edge conditions introduces additional
complications which makes the presentation of a wholly symbolic
solution exceedingly clumsy.   In consequence and also as a matt
of variety, in this instance, a numerical solution is presented
for a specific case which has been examined by the author
experimentally.

The Analysis of a $\frac{1}{4}$in Shell of 60in radius Fixed at the Outer
Edge, and Loaded with a Tangential Load H. - Fig.II.24

Taking Young's modulus for steel $= 13400T/in^2$
and Poisson's ratio $\upsilon = 0.3$
the constant $\chi = \sqrt[4]{\frac{3(1-\upsilon^2)R^2}{t} - \frac{\upsilon^2}{4}}$

$= 19.913$
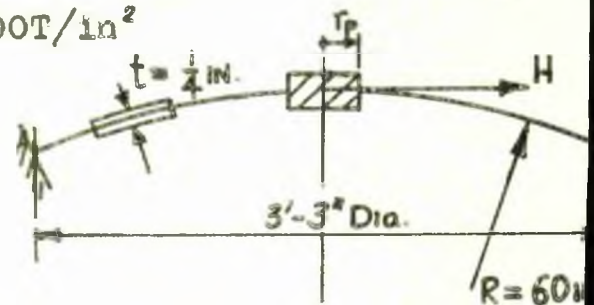
Fig.II.24

Outer Edge Connection $\phi = 0.325\text{rad} = 18°\text{-}58'$
Membrane Displacements

Substituting the relevant dimensions in eqts. II.162a-c:-
$$U_1 = +1.2467 \times 10^{-4} H$$
$$w_1 = +2.1616 \times 10^{-4} H$$
$$u_1 = -1.2467 \times 10^{-4} H \qquad (II.166a\text{-}c)$$

The expression for the tangent rotation X_1 is obtained from:-
$$X_1 = \frac{1}{R}\left(\frac{du_1}{d\phi} - \upsilon_1\right) \qquad \text{and from eqts. II.162a,b:-}$$
$$X_1 = -\frac{H(1+\upsilon)}{4\pi E t R}\left[\frac{2\cos\phi}{\sin^2\phi} - \ln\frac{1-\cos\phi}{1+\cos\phi}\right] \qquad (II.167)$$
Thus at the outer edge $\quad X_1 = -0.1108 \times 10^{-4} H \qquad (II.166d)$

Inextensional Displacements from eqt.II.163a-c

$$v_1 = D_2 - D_1 \times 0.94571$$

$$w_1 = -D_1 \times 0.32500$$

$$u_1 = D_1 - D_2 \times 0.94571 \qquad \text{(II.168a-c)}$$

The corresponding value of X_1 is obtained from $X_1 = \frac{1}{R}\left(\frac{dw_1}{d\phi} - v_1\right)$

i.e. $X_1 = -D_2/60$ \qquad (II.168d)

Oscillatory Displacements

When considering the outer edge it is possible to use the simplified relations, eqts.II.165a-c, since $\sqrt{2}\chi\phi\,(=9.16) > 6$. The relevant part of the equations II.165a-c are those involving $e^{\chi\phi}$, it being assumed that the edge-bending effects die out so that they do not affect the other edge.

Thus
$$u_1 = -\frac{R(1+v)}{\sqrt{2}\,\chi\,Et\sin^{3/2}\phi}\left[\bar{C}_1\sin\left(\chi\phi+\frac{\pi}{4}\right) - \bar{C}_2\cos\left(\chi\phi+\frac{\pi}{4}\right)\right]$$

$$v_1 = \frac{R(1+v)}{Et\sqrt{\sin\phi}}\left[\bar{C}_1\cos\chi\phi + \bar{C}_2\sin\chi\phi\right]$$

$$w_1 = \frac{\sqrt{2}\,\chi R}{Et\sqrt{\sin\phi}}\left[-\bar{C}_1\cos\left(\chi\phi+\frac{\pi}{4}\right) - \bar{C}_2\sin\left(\chi\phi+\frac{\pi}{4}\right)\right] \qquad \text{(II.169a-c)}$$

where $\bar{C}_1 = e^{\chi\phi}c_1$ \qquad and \qquad $\bar{C}_2 = e^{\chi\phi}C_2$ \qquad (II.170a,b)

Thus at the outer edge the oscillatory displacement terms are:-

$$u_1 = -0.00397\bar{C}_1 + 0.00207\bar{C}_2$$

$$v_1 = 0.0389\bar{C}_1 + 0.0125\bar{C}_2$$

$$w_1 = -0.4080\bar{C}_1 - 0.7846\bar{C}_2$$

$$RX_1 = 8.103\bar{C}_1 - 22.572\bar{C}_2 \qquad \text{(II.171a-d)}$$

Boundary Condition at the Outer Edge

$$u_1 = v_1 = w_1 = X_1 = 0 \qquad \text{(II.172a-d)}$$

These relationships give rise to four simultaneous equations, obtained by combining the membrane, inextensional and oscillatory displacements, from which the four constants can be determined.

Using in addition eqt.II.170a,b , these are found to be:-

$C_1 = +0.500 \times 10^{-6} H,$ $C_2 = +0.151 \times 10^{-6} H,$ $D_1 = -0.671 \times 10^{-4} H,$ $D_2 = -2.05 \times 10^{-4}$

(II.173a-d

Details of the derivation of these constants is given in Append

VIII.2.8 p.266

It is thus possible to determine the stress distribution at the

outer edge from the resultant force and moment expressions,

suitably simplified, since $\sqrt{2} \times \phi > 6$. The resultant force express

are as follows:- $N_{\phi\phi_1} = -\frac{\cot\phi}{\sqrt{\sin\phi}}\left[e^{\chi\phi}(C_1\cos\chi\phi + C_2\sin\chi\phi)\right] - \frac{H(1-\cos\phi)}{\pi R \sin^3\phi}$

$$N_{\theta\theta_1} = \frac{\sqrt{2}\,\chi}{\sqrt{\sin\phi}}\left[-e^{\chi\phi}\left\{C_1\cos\left(\chi\phi + \frac{\pi}{4}\right) + C_2\sin\left(\chi\phi + \frac{\pi}{4}\right)\right\}\right] + \frac{H(1-\cos\phi)}{\pi R \sin^3\phi}$$

$$N_{\phi\theta_1} = -\frac{1}{\sqrt{\sin\phi}}\left[e^{\chi\phi}(C_1\cos\chi\phi + C_2\sin\chi\phi)\right] + \frac{H(1-\cos\phi)}{\pi R \sin^3\phi} \quad (II.174$$

These results are presented for the particular shell, using

the values obtained for C_1 and C_2, in Fig. II.25.   As expected

the values of the above resultant forces are relatively small

compared with those at the insert.

In a similar manner the resultant moments can be determine

These have small magnitude, though give rise to approximately t

same value of stress on the surface as do the corresponding dir

stresses.

Rigid Insert Connection

Various sizes of insert have been considered in the invest

gation.   By way of example $r_p = 0.50$ in is selected.

In determining the stresses in the shell it is necessary

to consider both the membrane and oscillatory solutions, i.e.

eqts. II.162, II.164 and II.144.   In the case of the oscil-

latory solutions, only those terms associated with B_1 and B_2 ar

considered since the edge-bending effects die out quickly.   Thu
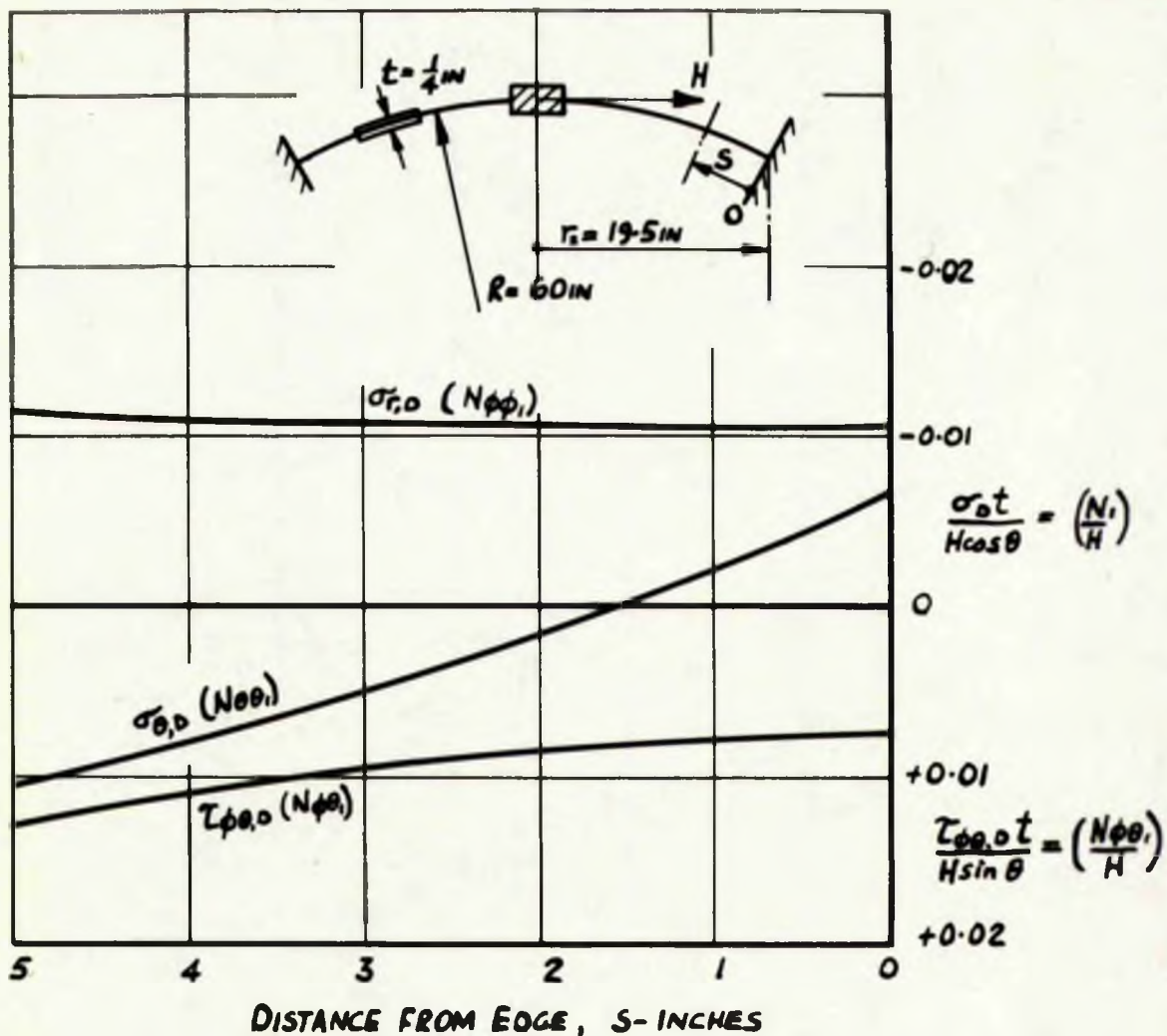
FIG.II.25 THE DISTRIBUTION OF THE NORMAL & SHEARING STRESSES AT THE FIXED
OUTER BOUNDARY ($r_2=$ 19·5IN) OF THE SHELL SUBJECTED TO A TANGEN-
TIAL FORCE H
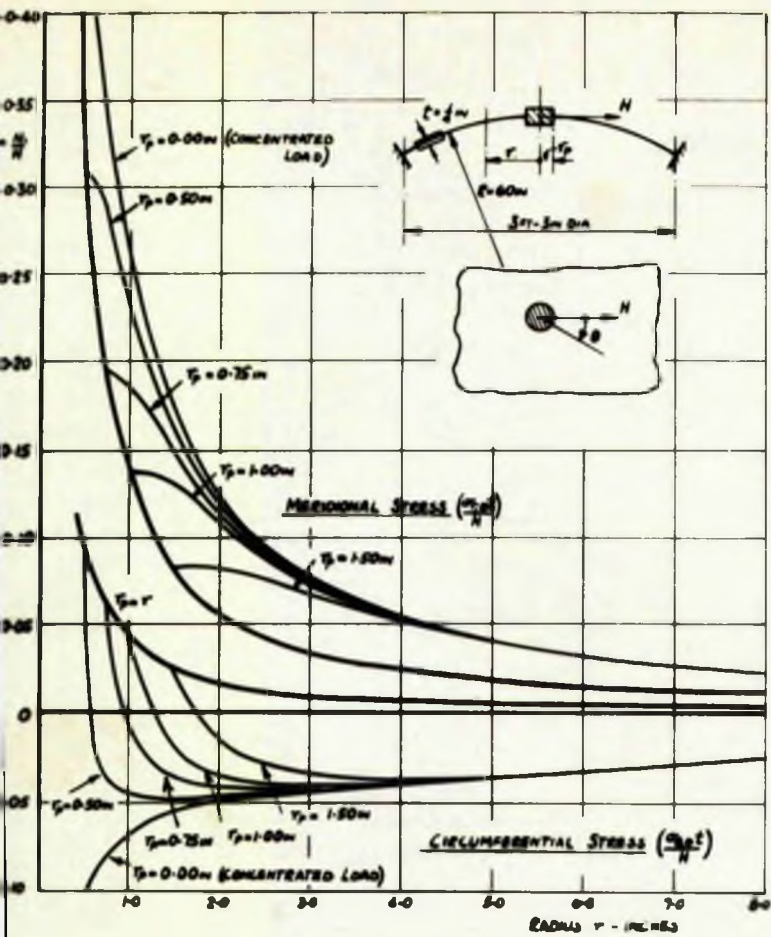
Fig. II.26a The Distribution of Meridional and Circumferential Direct Stress
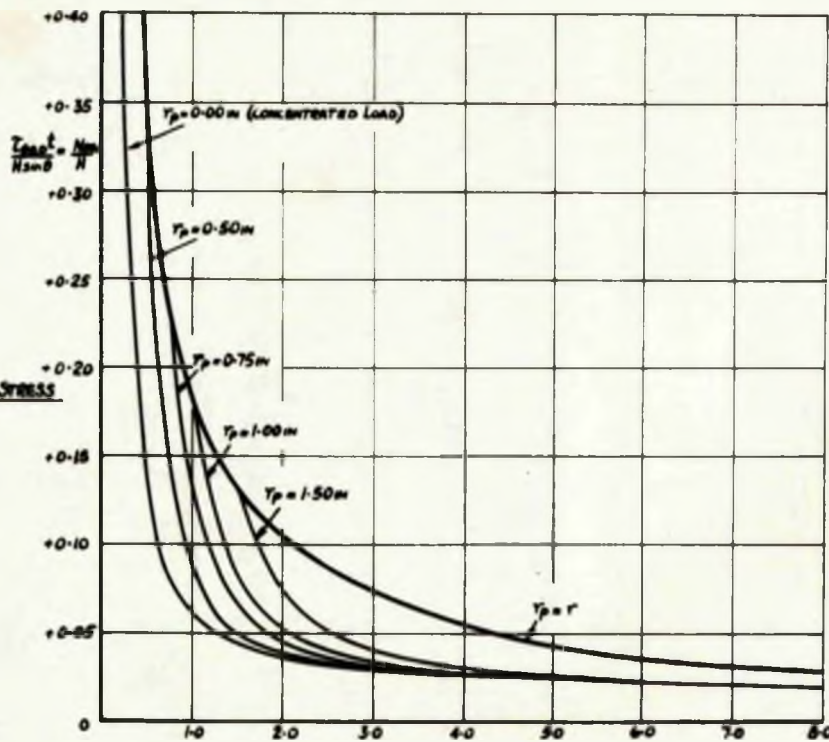
26b The Distribution Shearing Stress

26 THE DISTRIBUTION OF NORMAL & SHEARING STRESSES IN A ½IN THICK SPHERICAL SHELL, R=60IN DUE TO THE APPLICATION OF A TANGENTIAL LOAD BY MEANS OF A RIGID INSERT AT THE CROWN FOR VARIOUS G VALUES — GENERAL SHELL TREATMENT

two constants B_1 and B_2 must be determined for solution.   These

are obtained by considering the boundary conditions at $r = r_p$

<u>Boundary Conditions</u>   at $r = r_p = 0.50$ in , $\phi = 0.0083$ radian

$$\frac{d\omega}{d\phi} = 0 \qquad \text{and} \qquad \varepsilon_\theta = (N_{\theta\theta} - \upsilon N_{rr})/Et = 0 \qquad\qquad (\text{II.175a,b})$$

By combining membrane, inextensional and oscillatory solutions,

two simultaneous equations in B_1 and B_2 are obtained by consider-

ing eqts. II.175a,b.   The resulting values for B_1 and B_2 are

as follows:- $B_1 = -2.622 \times 10^{-8} H$, $B_2 = -1.920 \times 10^{-6} H$ (II.176a,b)

It is of interest to point out that for the point or concen-

trated horizontal force $B_1 = 0$, and $B_2 = -2.000 \ H \times 10^{-6}$.

The values of B_1 and B_2 obtained in eqt. II.176a,b provide the

basis of computation for determining the resultant forces at any

particular ϕ value (or r value), using the oscillatory expressions

eqts. II.144a-i and the corresponding membrane expressions II.164.

In this investigation a range of values of r_p have been

examined namely $r_p = 0.00$, 0.50, 0.75, 1.00 and 1.50 in.   The pro-

cedure for solution is as above, in that the constants B_1 and B_2

are found for the particular insert.   These values then serve

as the basis of further computations for finding the resultant

forces or direct stresses for any ϕ or r value.   The complete

family of curves is presented in Figs. II.26.

It is noted that these curves are similar in form to those

obtained for the shallow shell analysis (Fig.II.16) but with

light differences particularly noticeable in the circumferential

stresses.   Graphs are plotted in Fig.II.27 showing this

comparison for $r_p = 0.50$ in and 1.50 in.

The Resultant Moments which have been considered negligible in the shallow shell treatment can also be calculated from the oscillatory and membrane solutions of the general theory. These are of small magnitude compared with the resultant forces and are therefore not shown.

The derivation of the constants given in eqt.II.176a,b is given in detail in Appendix VIII.2.8b p.267.
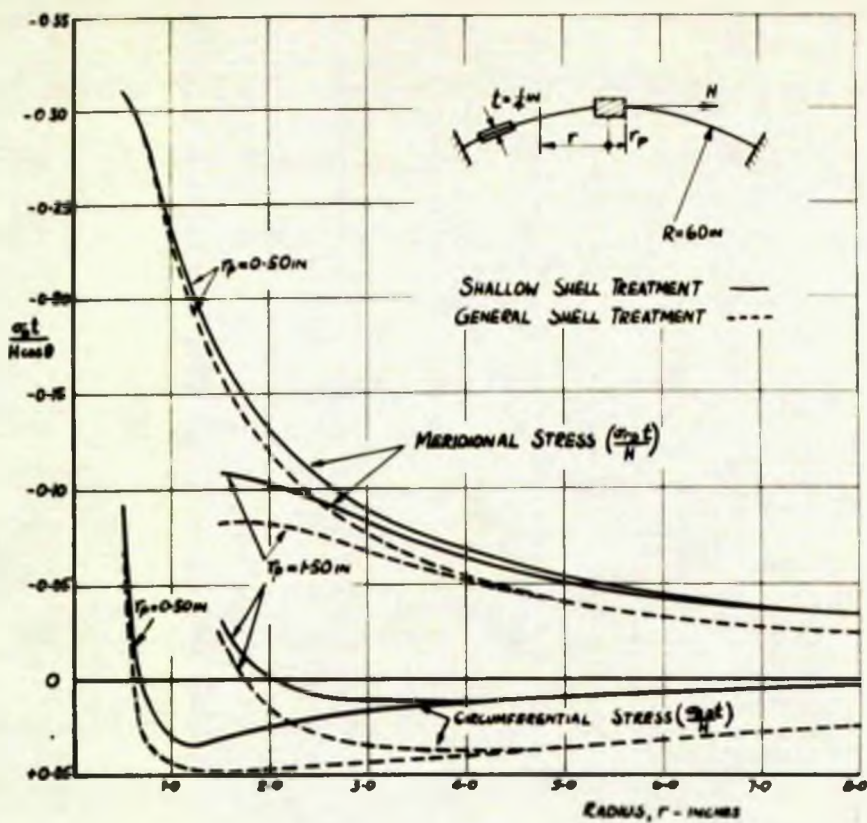
Fig. II.27a The Distribution of Meridional and Circumferential Direct Stress
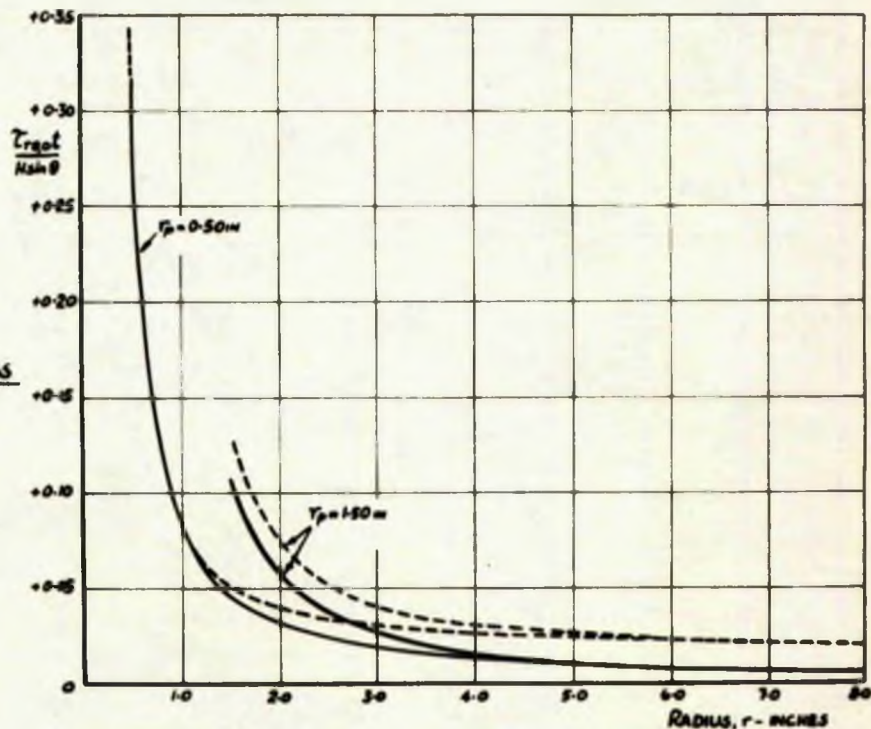
Fig. II.27b The Distribution of Shearing Stress

Fig. II.27 A Comparison between the Stresses predicted by the Shallow and General Shell Treatments for a Spherical Shell subjected to a Tangential Load, for $r_p = 0.50$ in. and 1.50 in.

II.3   THE INFLUENCE LINE APPROACH

II.3.1   'BASIC' OR UNIT ACTIONS

II.3.2   INFLUENCE LINES

II.3.3   THE SHALLOW CAP

II.3   INFLUENCE LINE APPROACH

In the field of shell analysis there is a need for a generally applicable and flexible method capable of yielding solutions to a wide variety of complex design problems.   The principle of superposition lends itself to the development of such a method utilizing an influence line concept derived from the effects of 'basic' unit actions.   This method is well known in other fields of structural analysis, and its application to shell problems is a restatement rather than a rediscovery of its basic ideas.

The resultant force, moment and displacement relations presented in this thesis have been obtained from fundamental differential equations which have been simplified and linearized to enable them to be solved.   This implies that within the approximations stipulated the principle of superposition is applicable to both the stresses and displacements.

II.3.1   'BASIC' or UNIT ACTIONS

Any load action at a point on a shell can be broken down into basic components of radial and tangential loads, 'bending' and 'twisting' moments.   If the principle of superposition is assumed to apply, the stresses and displacements due to the original load action may be obtained by combining appropriately those corresponding to the individual basic actions.   These individual basic actions have been fully analysed in Chapter II.1 and 2 of the thesis and the solutions obtained will now be utilised in connection with the method presented.

The main feature common to both stresses and deformations arising from these basic actions is their localized nature, in that their magnitudes reduce to practically negligible values within a relatively short distance from the point of application of the load action.   Such a distance is referred to as the 'die out' distance.

II.3.2   INFLUENCE LINES

The basic concept can best be outlined in a qualitative manner with reference, for example, to the determination of deformations such as normal deflections of a shell.   The method is naturally of general application for the analysis of both deformations and stress actions.

Consider two points C and D on the surface of a shell shown in Fig. II.28.   If the principle of superposition applies, Maxwell's reciprocal theorem for deflections is also operative. In simple terms this reduces to a statement of 'reciprocal symmetry', $w_{CD} = w_{DC}$ where w_{CD} is, say, the normal deflection at C due to a radial unit load at D, while w_{DC} is the normal deflection at D due to a unit normal load at C.   In consequence, the variation of the normal deflection at C, as a unit load travels along the load path AB, may be obtained rapidly by evaluating the normal deflections at every point along AB due to a unit normal load applied at C only to the otherwise unloaded shell. The curve so obtained is the influence line for the normal deflection at C, and may be derived for spherical shells for the 'basic' action presented earlier.

To show the use of the method, consider a radial line load
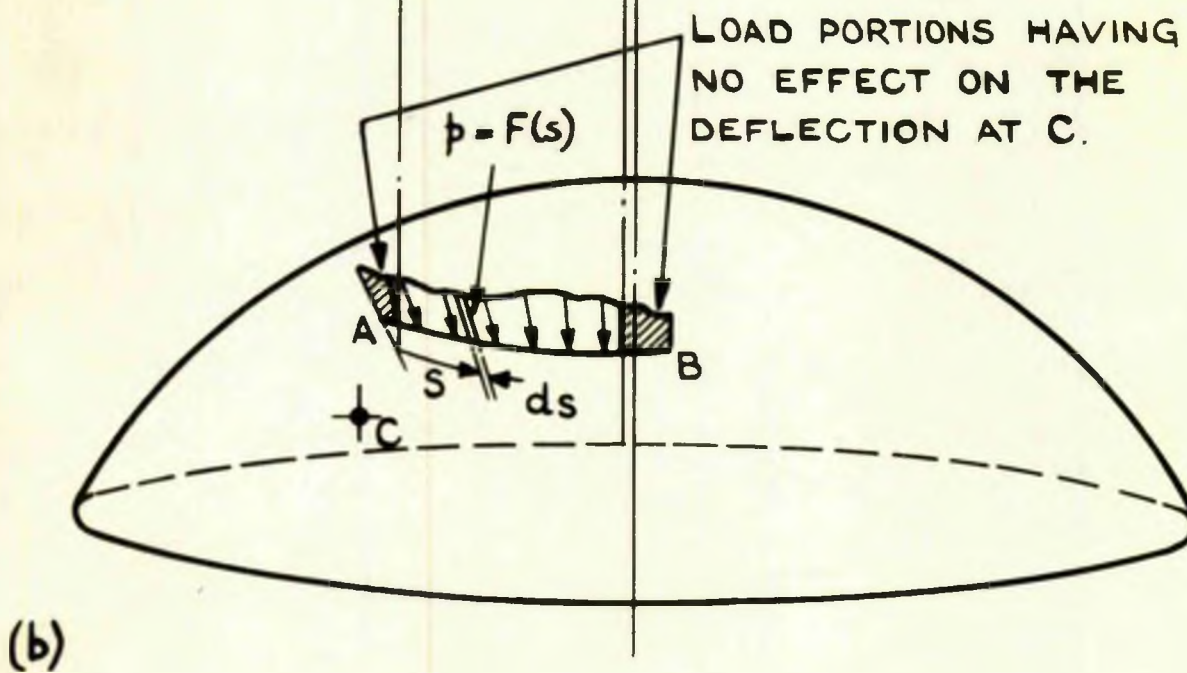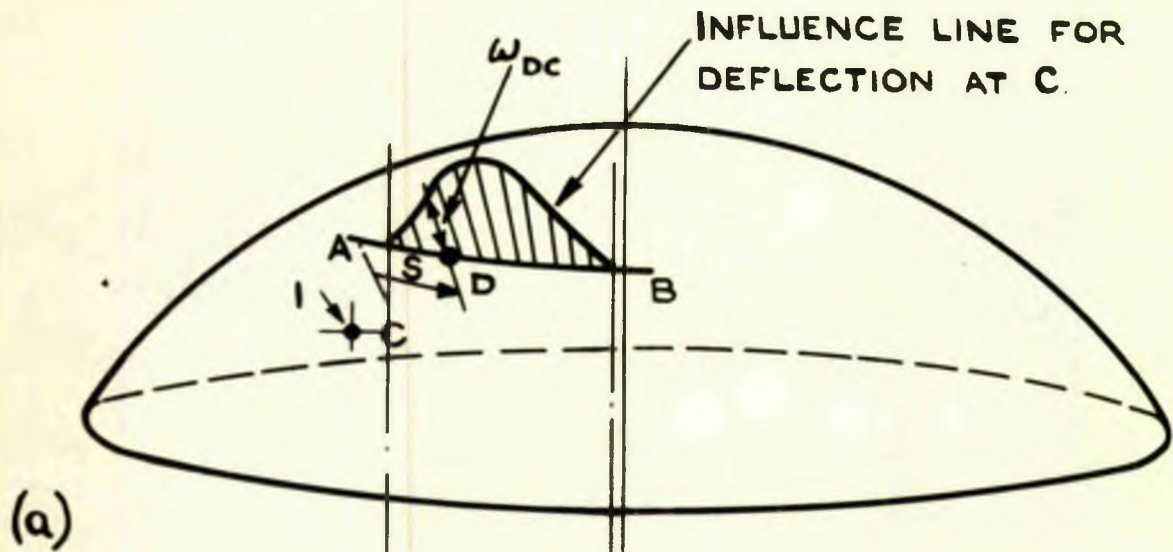
FIG. II·28 THE INFLUENCE LINE CONCEPT

of varying distribution $p = F(s)$, acting on the surface of a shell along the path AB as shown in Fig. II.28. It is required to obtain the normal deflection at a point C on the surface of the shell.

Assume that the load p is removed and a unit concentrated normal load is applied at C and that the normal deflections along the path AB, due to this unit load are known from the influence line as given in Fig. II.28. The deflection at C due to the loading p becomes:-

$$\Delta_s \; = \; \int_A^B p \, w \, ds \; = \; \int_A^B F(s) w \, ds.$$

The integral represents the area from A to B under a curve obtained by multiplying each ordinate of the load distribution with the corresponding ordinate of the influence line. This can be evaluated by direct integration or in cases of irregular loading by graphical, semi graphical or numerical means.

If the load p is not a 'concentrated' line load but acts over a finite width d, this can be catered for sufficiently accurately in design analysis, by applying the unit load at C not as a concentrated load but distributed over a circular area of diameter d.

Where the load p acts over an area rather than a line path, a series of similar influence lines covering the load area and providing an influence surface can be derived. The integral effect at C is then obtained as the volume between the shell and a surface derived by multiplying each load ordinate by its appropriate influence ordinate, the evaluation again being carried out by any convenient means.

II.3.3   THE SHALLOW CAP

The basic advantage of the method is that the primary analysis necessary is always that of a unit radial or tangential load, moment or torque, as the case may be, concentrated or distributed over a small area.   These analyses are presented earlier in this section.   The unit action may then be considere to act at the centre or crown of a shallow cap the extent of which corresponds to the 'die out' distance for the particular action in question.   In this way the analysis of essentially unsymmetrical problems may be tackled and a solution obtained, reference being made only to the corresponding unit actions.

There is a further point of interest which permits the application of the method outlined as an approximation to shells of varying form.   The effects of a load acting at a point or small area on a plate-structure die out fairly rapidly with distance from the point of action.   This implies that the analysis of the effect of the unit action is influenced primarily by the shape of the shell at, and in the near vicinity of, the point where the unit action is applied.   Generally the shape of any shell, provided it is of relatively large radius of curvature, can be approximated to that of a spherical or cylindrical segment, in the localized region where the effect of the load is considered, i.e. within the 'die out' distance. For th region, in consequence, the available relevant unit action soluti may be utilised. If the shell is of such a form that this appro mation is not permissible and no analysis of the unit action is possible, recourse may be had to model experiments from which t appropriate influence lines can be obtained empirically.

The next section of the thesis presents the solution of a series of problems, using the method outlined.

CHAPTER III.   APPLICATIONS OF THE INFLUENCE
                        LINE METHOD TO SPHERICAL SHELLS.

The Influence Line Method outlined in Chapter II.3 is capable of wide application to cases of complex loading, without any restriction as to uniformity and symmetry of load distribution and loading path.

Although the method is applicable to complex loading, certain applications are presented in this chapter, which are also capable of solution by conventional methods.   These relatively simple applications have been intentionally included so as to serve to establish the validity of the Influence Line Meth through comparisions of solutions obtained by the method with those derived by conventional means.

The applications presented illustrate the use of the method for each of the basic actions given earlier, in Chapter II, namely: radial and tangential loading, bending and twisting moments.   A final application is included which illustrates the method applied to the solution of interaction problems.
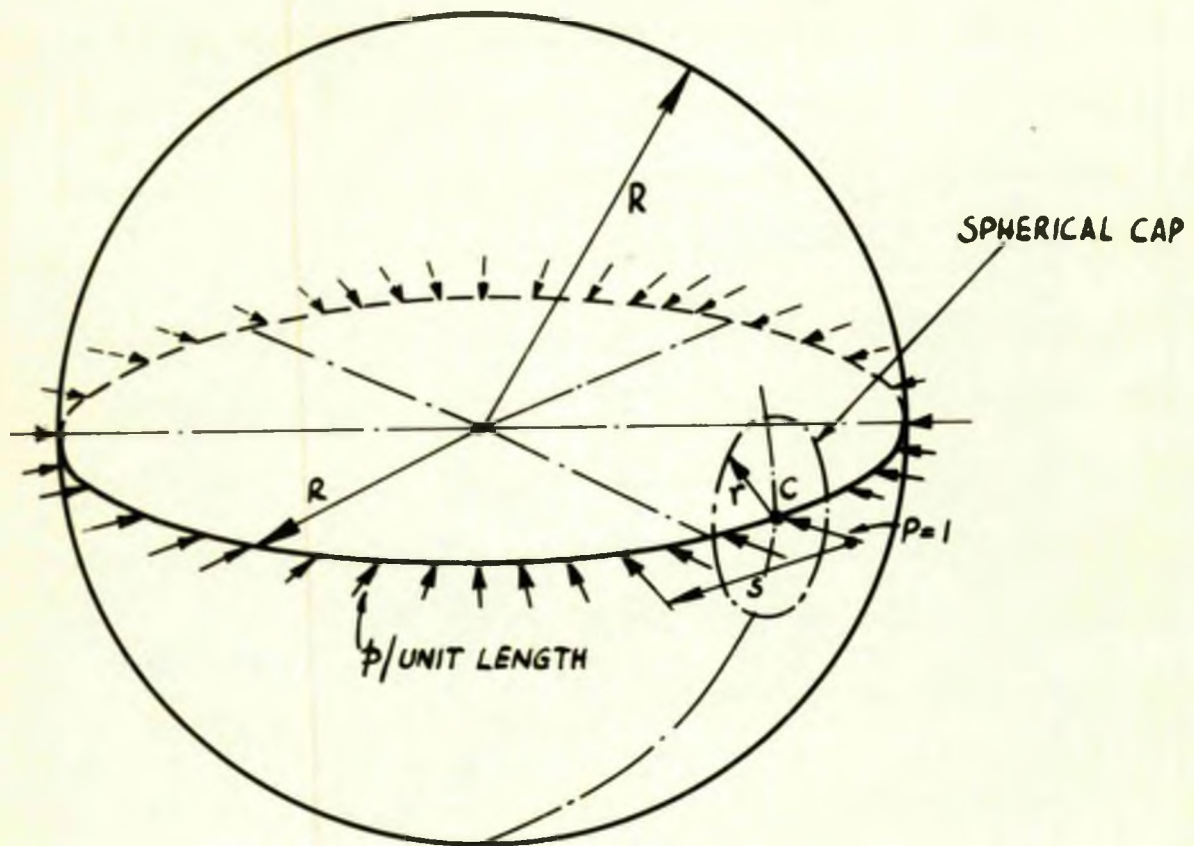
FIG. III·1   A RADIAL LINE LOAD ON THE EQUATOR OF A
SPHERICAL SHELL.

III.1   A UNIFORMLY DISTRIBUTED RADIAL LOAD
ON A SPHERICAL VESSEL

III.1.1   UNIFORMLY DISTRIBUTED ON A COMPLETE GREAT CIRCLE

The first example is that of a radial line load (i.e. zero wide) $p/$ unit length, uniformly distributed on a complete great circle of the spherical shell, Fig.III.1.   Both the radial deflection and resultant moments will be determined at any point C, on the loaded great circle.

Derivation of Radial Deflection at C   (see Fig.III.1)

The applied load, $p/$ unit length, is removed and a unit concentrated radial load is applied at C.   The radial deflections along the great circle due to this unit load are given by eqt. II.54e :-
$$\omega = \frac{PR\sqrt{12(1-\upsilon^2)}}{2\pi E t^2} \, kei\,r/\ell$$

Putting $P = 1$ and re-arranging,
$$\omega = \frac{R\left[3(1-\upsilon^2)\right]^{\frac{1}{2}} kei\,r/\ell}{\pi E t^2} \tag{III.1}$$

where r is the polar radius within the spherical cap. (Fig.II.1)
The total deflection due to the loading over the whole great circle is thus :-
$$\Delta_c = \int_A^B p\,\omega\,ds \tag{III.2}$$

where A and B are the limits of the integration.

Owing to the rapid die out of the Kelvin functions, it may be assumed that the arc distance $s = r$.
Thus eqt. III.2 becomes :-
$$\Delta_c = \int_A^B p\,\omega\,dr$$
From eqt. III.1,
$$\Delta_c = \int_A^B p \cdot \frac{R}{\pi E t^2}\left[3(1-\upsilon^2)\right]^{\frac{1}{2}} kei\,r/\ell\,dr$$
when the equator loading $p/$ unit length is constant :-
$$\Delta_c = \frac{pR}{\pi E t^2}\left[3(1-\upsilon^2)\right]^{\frac{1}{2}} \int_A^B kei\,r/\ell\,dr \tag{III.3}$$

Since the function $kei\,r/\ell$ rapidly becomes negligible, the limits A and B of eqt. III.3 may be taken to infinity, i.e.

$$\Delta_c = \frac{PR}{\pi E t^2}\left[3(1-v^2)\right]^{\frac{1}{2}}\int_{-\infty}^{\infty} kei \, \frac{r}{\ell} \, dr \qquad\qquad (III.4)$$

$$\Delta_c = \frac{PR \, 2\ell}{\pi E t^2}\left[3(1-v^2)\right]^{\frac{1}{2}}\int_{0}^{\infty} kei \, q \cdot dq \qquad (III.5) \text{ where } q = \frac{r}{\ell}$$

A closed form of $\int_{0}^{\infty} kei \, q \cdot dq$ was not readily available. How-
ever, owing to the rapid die out of the function, the integration
was evaluated from the tabulated values (38, 106, 107) giving
$\int_{0}^{\infty} kei \, q \cdot dq = 1.1105$. Hence the radial deflection at C by eqt. III.5
may be simplified to:-

$$\Delta_c = \frac{PR}{2Et}\left[3(1-v^2)\left(\frac{R}{t}\right)^2\right]^{\frac{1}{4}} \qquad\qquad (III.6)$$

Derivation of Resultant Moments at C

The method may be applied to the computation of the resul-
tant moments in precisely the same fashion. Considering the
shallow spherical cap, loaded with a radial load P= 1, the
meridional and circumferential resultant moments, specified as
M_{rr}^c and $M_{\theta\theta}^c$ respectively are obtained from eqts. II.54c,d.

$$M_{rr}^c = -\frac{1}{2\pi}\left[ker \, \frac{r}{\ell} - \frac{(1-v)}{\frac{r}{\ell}} kei'\frac{r}{\ell}\right]$$

$$M_{\theta\theta}^c = -\frac{1}{2\pi}\left[v \, ker \, \frac{r}{\ell} + \frac{(1-v)}{\frac{r}{\ell}} kei'\frac{r}{\ell}\right] \qquad (III.7a,)$$

The planes in which these moments act are shown in Fig.III.
Thus for a uniformly distributed load round the equator, the mer
dional moment for the spherical shell $M_{rr} = P\int_{-\infty}^{\infty} M_{\theta\theta}^c \, dr$

Thus from eqt. III.7b; $Mrr = \frac{P}{\pi}\int_{0}^{\infty}\left(v \, ker \, \frac{r}{\ell} + \frac{(1-v)}{\frac{r}{\ell}} kei'\frac{r}{\ell}\right)dr$

$$= \frac{P\ell}{\pi}\int_{0}^{\infty}\left(v \, ker \, q + (1-v)\frac{kei' \, q}{q}\right)dq$$

(III

The integrals contained in eqt. III.8 are dealt with as
before. However, in the case of $\int kerq \cdot dq$ owing to the singul
ity condition of the function at q = 0, the integral is dealt wi

SPHERICAL CAP

$M_{\theta\theta}^c$ = CIRCUMFERENTIAL MOMENT ON CAP

M_{rr}^c = MERIDIONAL MOMENT ON CAP

$P=1$
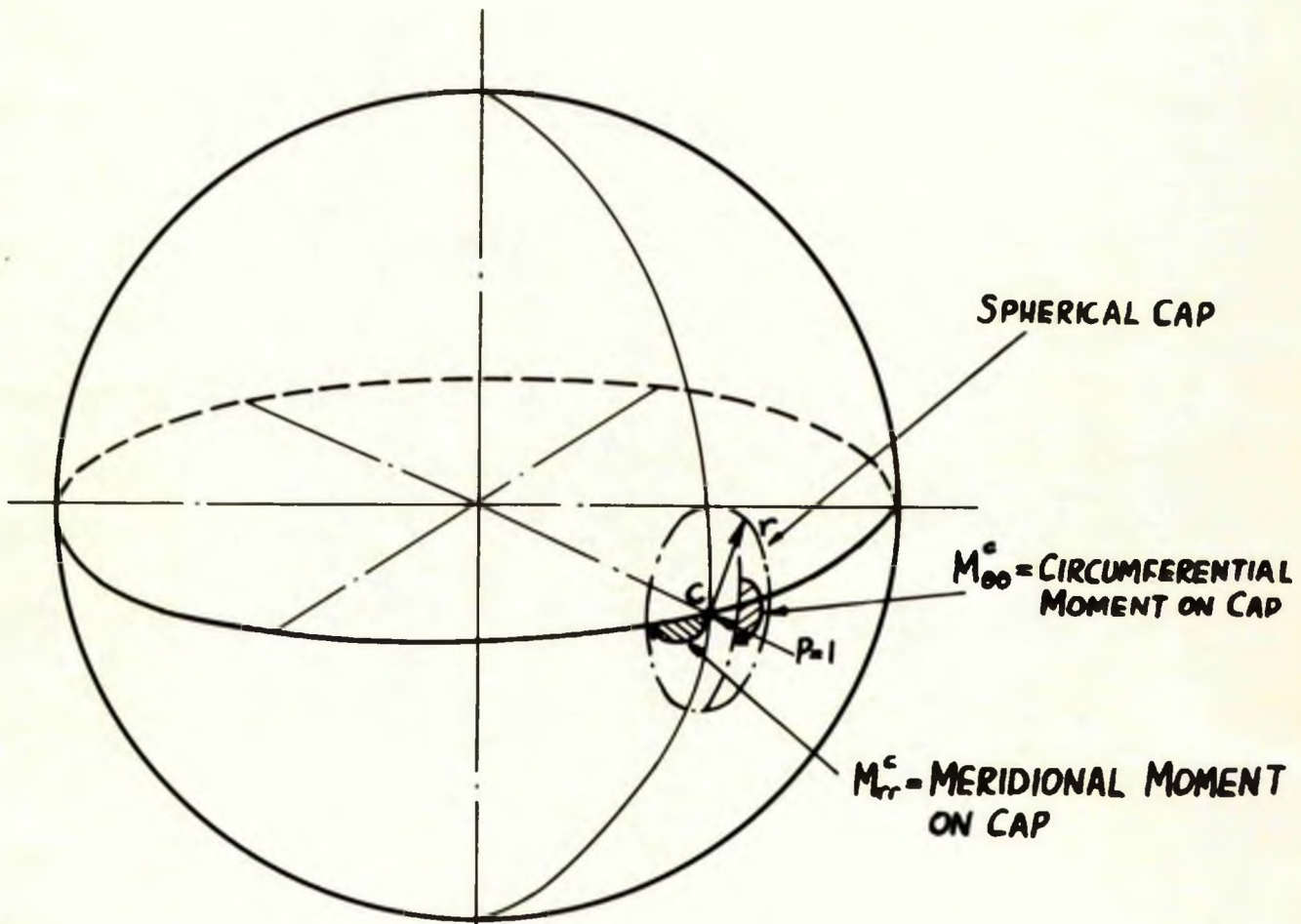
FIG. III·2   MOMENTS ON THE SHALLOW SPHERICAL CAP DUE
TO A LOAD P

in two parts, i.e. $\int_0^\infty \text{ker}q \cdot dq = \int_0^1 \text{ker}q \, dq + \int_1^\infty \text{ker}q \cdot dq$.

The integral $\int_0^1 \text{ker}q \cdot dq$ is obtained by integrating $\text{ker}q$.

$$\text{ker}q = (0.11593 - \log_e q) + \frac{1}{4} \cdot \pi \cdot \frac{1}{4} q^2 - \frac{1}{4}(0.11593 - \log_e q + 1.5)\frac{q^4}{16} - \frac{\pi}{144} \cdot \frac{q^6}{64}$$

$$\int \text{ker}q \cdot dq = 0.11593q - q(\log q - 1) + \frac{\pi}{16 \times 3}q^3 - \frac{1.61593}{5 \times 64}q^5 + \frac{1}{64}\left[\frac{q^5 \log q}{5} - \frac{q^5}{25}\right] - \frac{\pi}{144 \times 64 \cdot 7} \cdot \frac{q^7}{}$$

Thus $\int_0^1 \text{ker}q \cdot dq = 1.17571$.

The integral $\int_1^\infty \text{ker}q \cdot dq$ being obtained in the manner as outlined earlier.

The total integral is evaluated to give:-

$$\text{Mrr} = \frac{PR}{4}\left[3(1-v^2)\left(\frac{R}{t}\right)^2\right]^{-\frac{1}{4}} \tag{III.9}$$

and by a similar method:-

$$\text{Mee} = v\frac{PR}{4}\left[3(1-v^2)\left(\frac{R}{t}\right)^2\right]^{-\frac{1}{4}} \tag{III.10}$$

An alternative solution of this problem is obtained by utilizing the expressions obtained by HETÉNYI[29] for a shallow spherical cap. The edge is loaded by a uniformly distributed horizontal force $\bar{p}$ per unit length and moments Mrr per unit length. (Fig. III.3).

The horizontal displacement due to $\bar{p}$ is $\dfrac{2\lambda R \sin^2\phi}{Et}\bar{p}$ and due to Mrr is $\dfrac{2\lambda^2 \sin\phi}{Et} \cdot \text{Mrr}$

Fig.III.3.

The angular rotation of the edge of the shell,

due to $\bar{p}$ is $\dfrac{2\lambda^2 \sin\phi}{Et}\bar{p}$

due to Mrr is $\dfrac{4\lambda^3}{ERt}\text{Mrr}$ (III.11a-d)

where $\lambda^4 = 3(1-v^2)\left(\dfrac{R}{t}\right)^2$

In the present case a complete sphere is loaded round a
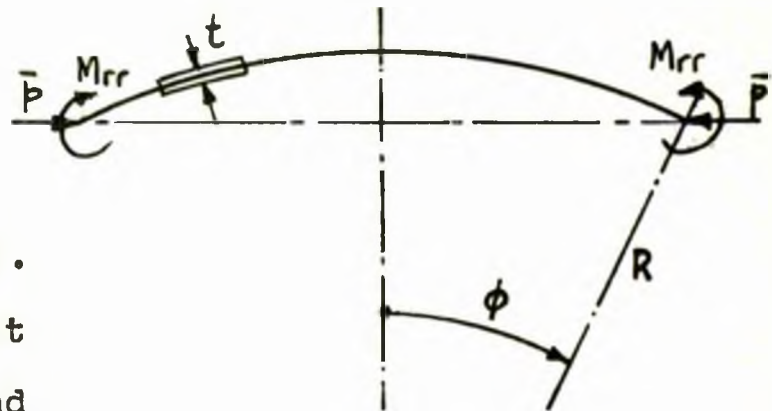
great circle with a radial line load.   The problem, however,
may be considered as that of two hemispheres externally loaded
with a horizontal (i.e. radial) uniformly distributed load $P/2$
per unit length, and by the internal moment Mrr per unit length
acting as an external moment at the edge.

Utilizing equations III.11a-d, the horizontal displacement :-
due to $P/2$ is $\dfrac{\lambda R P}{Et}$ and due to Mrr is $\dfrac{2\lambda^2 M_{rr}}{Et}$
and the rotation of the edge:-

due to $P/2$ is $\dfrac{\lambda^2 P}{Et}$ and due to Mrr is $\dfrac{4\lambda^3 M_{rr}}{ERt}$ (III.12a-d)

At the edge the change in slope is zero .   Thus equating
eqts. III.12c and d, $M_{rr} = \dfrac{R}{4\lambda} p = \dfrac{Rp}{4}\left[3(1-\upsilon^2)\left(\dfrac{R}{t}\right)^2\right]^{-\frac{1}{4}}$ (III.13)

The total radial deflection of the edge from eqts. III.12a,b and
III.13 :-

$$\Delta = \frac{\lambda R p}{Et} - \frac{2\lambda^2 M_{rr}}{Et}$$

$$\Delta = \frac{Rp}{2Et}\left[3(1-\upsilon^2)\left(\frac{R}{t}\right)^2\right]^{\frac{1}{4}}$$ (III.14)

It is noted that the values for Mrr and Δ obtained by this
analysis are exactly those of eqts. III.9 and III.6 obtained by
the Influence Line method.

UNIFORMLY DISTRIBUTED RADIAL RING LOAD
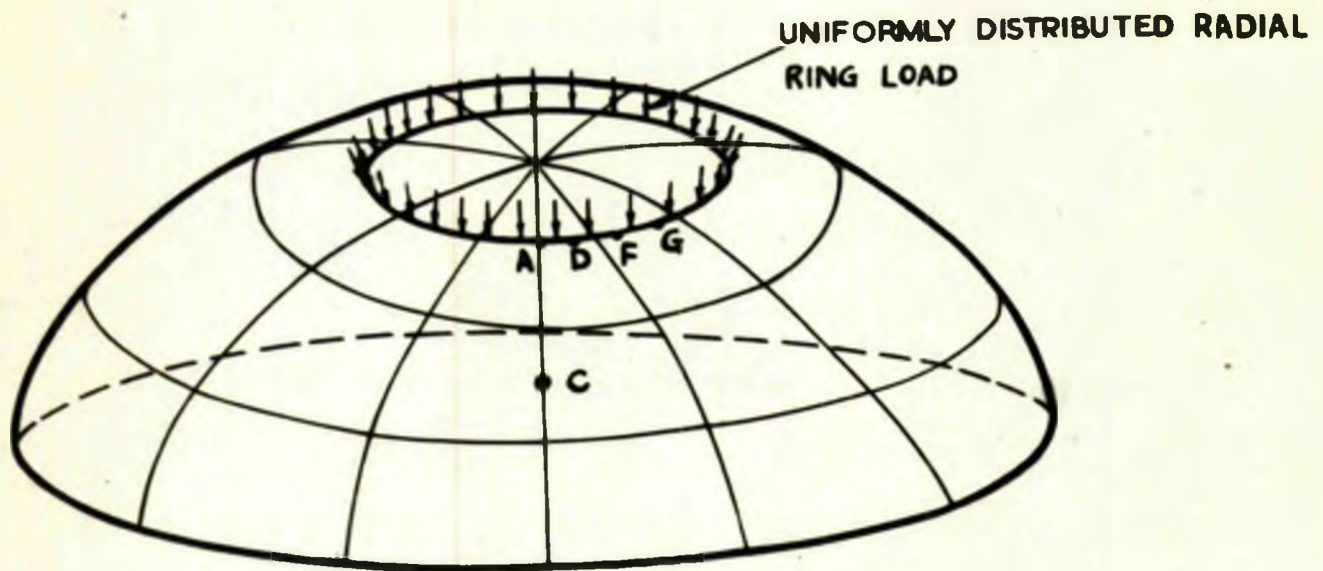
FIG. III. 4   THE SPHERICAL SHELL, SUBJECTED TO A RADIAL RING LOAD

III.1.2   UNIFORMLY DISTRIBUTED RADIAL LOAD ON A SPHERICAL
           VESSEL ROUND THE CIRCUMFERENCE OF A CIRCULAR RING -
           NOT A GREAT CIRCLE

In the second case of uniformly distributed radial loading,
the load is of a given width and distributed round the circum-
ference of a circular ring - not a great circle - as in Fig.III.4.
In this case an alternative approach by CHINN [56] is available for
comparison with the Influence Line Method.

It should be noted that while in the previous example
stresses and deformations have been evaluated for a point on
the load path, the wide applicability of the Influence Line
Method is illustrated in this case by considering the stress and
deformation conditions at points out with the load path.

The two cases analysed are as follows:-

(1) No restriction on change of slope of the shell, due to the
     loading, across and along the load path.

(2) Complete fixity of the shell, across and along the load
     path completely preventing a change of slope in the loaded
     region.

These cases incidentally correspond in practical terms to
the load being transferred to the shell by an infinitely flexible
and infinitely stiff tube respectively.   In consequence the
unit actions for the first case are those corresponding to uni-
formly distributed radial load (eqts. II.49 and II.51) while in
the second case those given by the rigid insert loading (eqts.II.56).

In order to illustrate the analysis only the case of radial
ring loading, with no restriction on change of slope will be
presented in detail, that obtaining in the case of complete fixity.

being identical in approach.

It is further proposed to solve this case by means of a graphical approach, illustrating the method by considering a particular size of ring - $5\frac{1}{2}$ inch mean dia. and of $\frac{1}{4}$ inch width acting on a 10 ft. diameter steel spherical shell of $\frac{1}{4}$ inch wall thickness and subjected to a radial ring load of 1.60 ton uniform distributed over the circular path.

For this type of loading, the distance r_o for the ring is taken as the mean radius of the load, i.e. $5.50/2 = 2.75$ in. Since $\ell = \dfrac{\sqrt{Rt}}{\sqrt[4]{12(1-\upsilon^2)}} = 2.125$ for this case, the value of μ for this ring $= 2 \cdot 75/2 \cdot 125 = 1.29$.

Determination of Radial Deflection.   Consider any point C, (Fig. III.4), at which the radial deflection is required.   The ring load is removed and a unit radial load applied at C which is uniformly distributed over a circular area of diameter equal to the ring load path width, in this case $\frac{1}{4}$ inch.   The shell under the action of this unit load only, may be regarded as rotationally symmetrical about C.   The point C corresponds to the crown of a 'shallow cap' loaded with a radial load at C. It is observed from the graphical representation of the equation for the radial deflection in Fig. II.5, that the influence of the factor 'μ' is primarily manifested at small r/l values, the curve at higher values of r/l practically coinciding.   From Fig.III. it is seen, that for the range of μ, from 0.03 to 0.10 the value of deflection, for all practical purposes coincide.   The curve may be used, therefore, to give the value of radial deflection of any point, radius r from C, (Fig. III.4) since for this
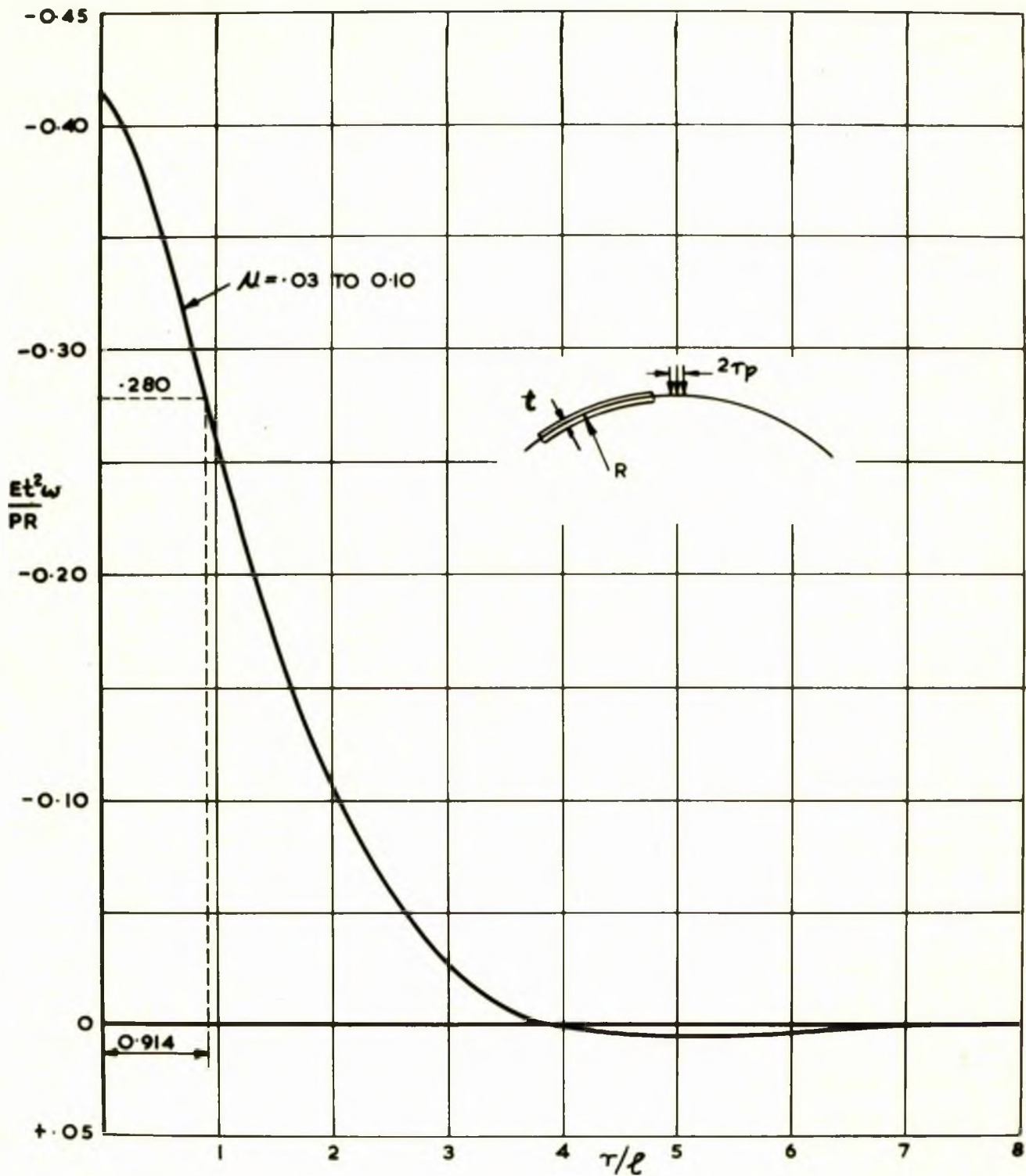
FIG. III.5 THE DISTRIBUTION OF RADIAL DEFLECTION DUE TO A UNIFORMLY DISTRIBUTED RADIAL LOAD ON A SHALLOW SPHERICAL SHELL FOR μ VALUES 0.03 TO 0.10
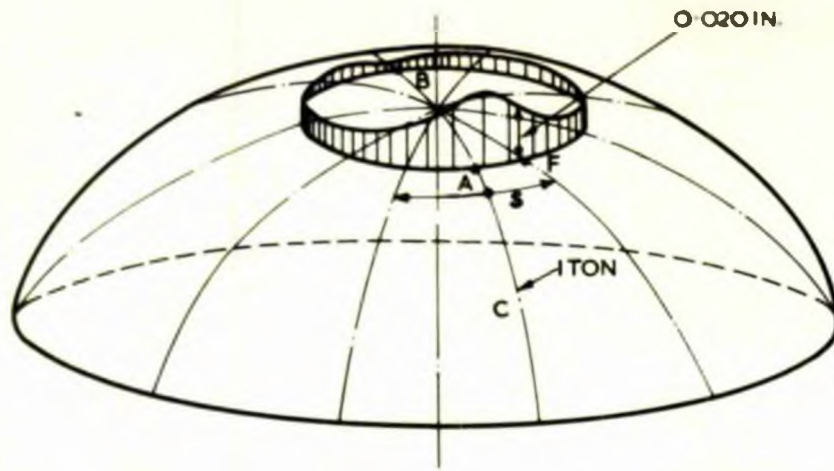
Fig III.6a DISTRIBUTION OF RADIAL DEFLECTION ROUND LOADING
PATH AB. SHOWN PICTORIALLY
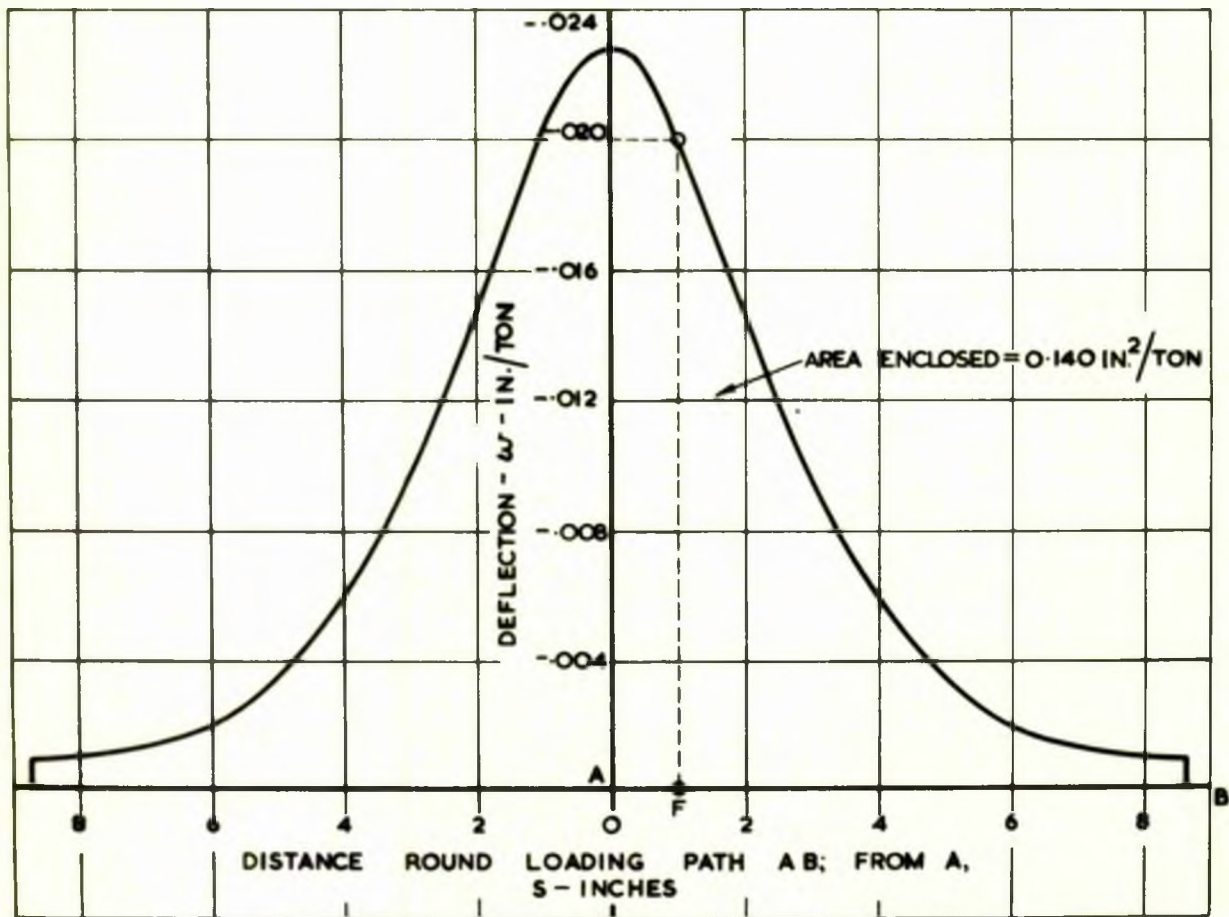
FIG. III.6b RADIAL DEFLECTIONS ROUND THE DEVELOPED LENGTH OF THE LOADING PATH AB

FIG III.6   THE DISTRIBUTION OF RADIAL DEFLECTION ROUND THE LOADING PATH A,B
DUE TO A UNIT LOAD AT C

particular case $l = 2.125$ and μ for the loading $= r/l - \dfrac{0.25}{2 \times 2.125} = 0.0568$.

Consider by way of example one point on the loading path - point F - a distance $r_3 = 1.94$ in. from C (see Fig.III.4 and III.9) that is having a value of $r/l = 1.94/2.125 = 0.914$. From Fig.III.5 this corresponds to a value of $\dfrac{Et^3}{PR} w = 0.280$. Using the given shell dimensions, $E = 13400$ Ton/in^2 and $P = 1$; $w = 0.020$ in.

Radial deflections at other points of the load path such as A, D, G etc. (Figs. III.4 and III.6a) are obtained in exactly the same way. The distribution of these deflections along the ring load path are shown pictorially (for easier visualization) in Fig. III.6a and are replotted on the base of the developed length of the ring load path in Fig. III.6b. This distribution is in fact the influence line for radial deflection at C, corresponding to a unit load traversing along the load path AB. The total radial deflection at C, due to the ring load along AB is, therefore, given by the summation of the products; load x appropriate ordinate of the influence line.

In the given case the ring load intensity is a constant equal to $1.60/\pi$ x $5.5 = 0.0927$ ton per in. Thus the total deflection at C becomes:- 0.0927 x Area enclosed by the influence line of Fig. III.6b. This area may be evaluated numerically or graphically and is found to be 0.140 in^2 per ton. Hence the deflection at C $= 0.0927$ x $0.140 = 0.013$ in. This is shown non-dimensionally as $\dfrac{Et^3}{PR} w$ on Fig. III.7. The ordinate for the point C being $\dfrac{13400 \times (\frac{1}{4})^2}{1.60 \times 60}$ x $0.013 = 0.113$ and the abscissa $\dfrac{r}{l} = \dfrac{4.250}{2.125} = 2$, where r is the radial distance of C measured from the crown of the actual shell, i.e. the centre of the ring load.

The complete distribution of radial deflection along a grea
circle is derived by taking a number of points, such as C along
the selected great circle and computing the deflection for each
as outlined above, this is shown on Fig. III.7.   This distri-
bution is also compared with that obtained using the line load
analysis (i.e. zero width) proposed by CHINN[56].   Any slight
deviation that occurs takes place in the region of the load and
is due to the fact that an allowance is made for the load path
width in the influence line method, as opposed to the analysis
developed by CHINN which deals with a line load of zero width.
Bending and Direct Stresses.   The basic procedure is exactly
the same as for the radial deflections, although in the stress
case, four quantities have to be considered.   These are the
circumferential and meridional bending and direct stress actions.

Considering, as previously, a point such as C (Fig. III.6a)
on the surface of the shell, the ring load is removed and a unit
radial load is applied at C as before.   As in the case of the
radial deflection, it is seen from the graphical representation
of the bending and direct stresses, in Fig. II.3,4 that the
influence of the factor 'μ' is primarily manifested at small
r/ℓ values.   It is seen in Fig. III.8 that for the range of μ
from 0.03 to 0.10 only the bending stress curves show any notic-
able variation as different 'μ' values are considered. Therefo
envelope curves are used for this range of 'u' values in relati
to the direct and bending stresses.

In the case of the bending stress curves, the maximum heig
of the curve is more sensitive to the changes in 'μ' value.   Th
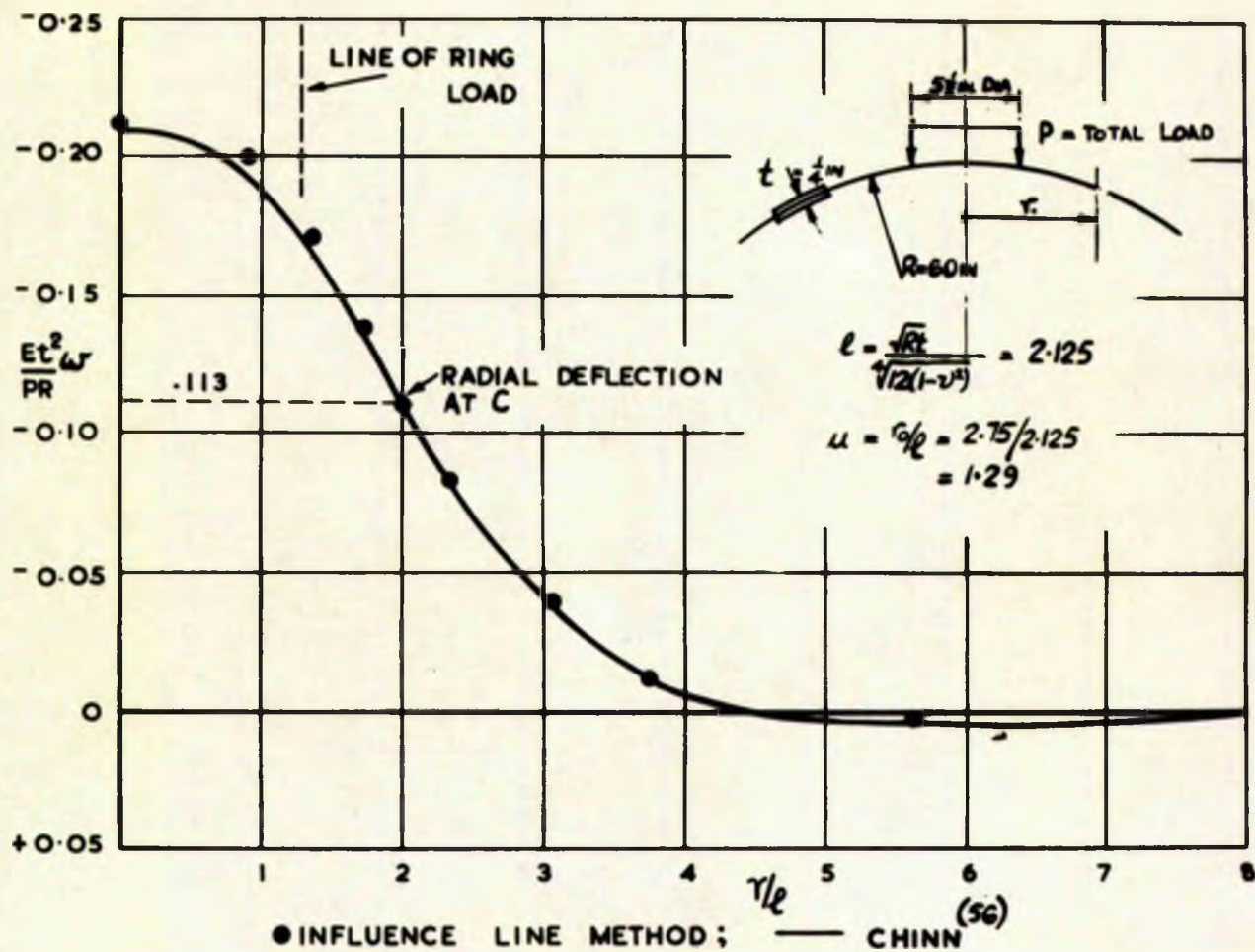
FIG. II.7 THE DISTRIBUTION OF RADIAL DEFLECTION ON A SHALLOW SHELL SUBJECT TO A RADIAL RING LOAD P, APPLIED WITH NO RESTRICTION OF THE SLOPE AT THE LOAD, $\mu = 1.29$ — A COMPARISON BETWEEN THE INFLUENCE LINE AND CHINN[56] ANALYSES
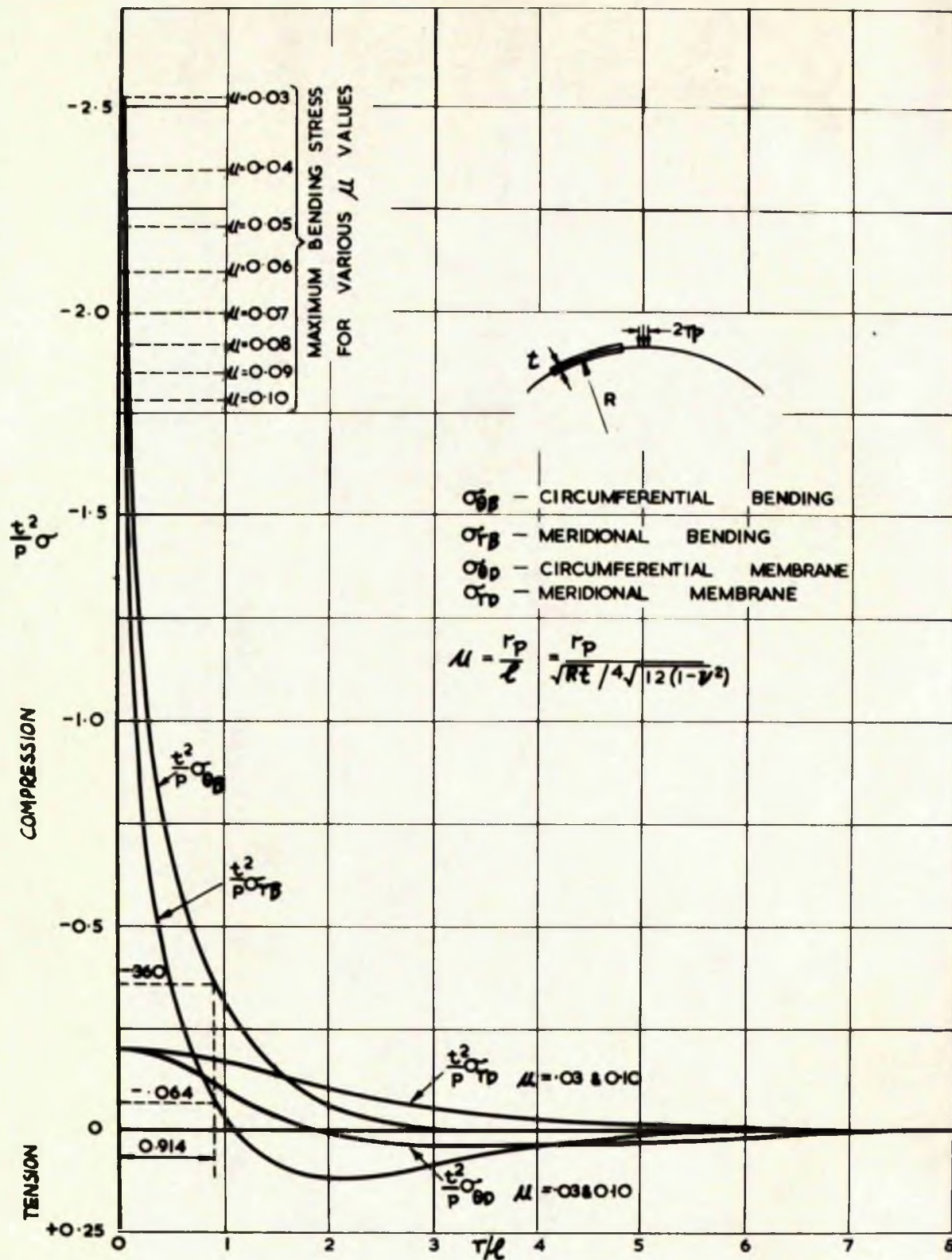
FIG. III.8 THE DISTRIBUTION OF BENDING STRESS, ON THE OUTER SURFACE, AND DIRECT STRESS ON A SHALLOW SPHERICAL SHELL DUE TO A UNIFORMLY DISTRIBUTED LOAD, FOR VARIOUS u VALUES VARYING FROM 0.03 TO 0.10
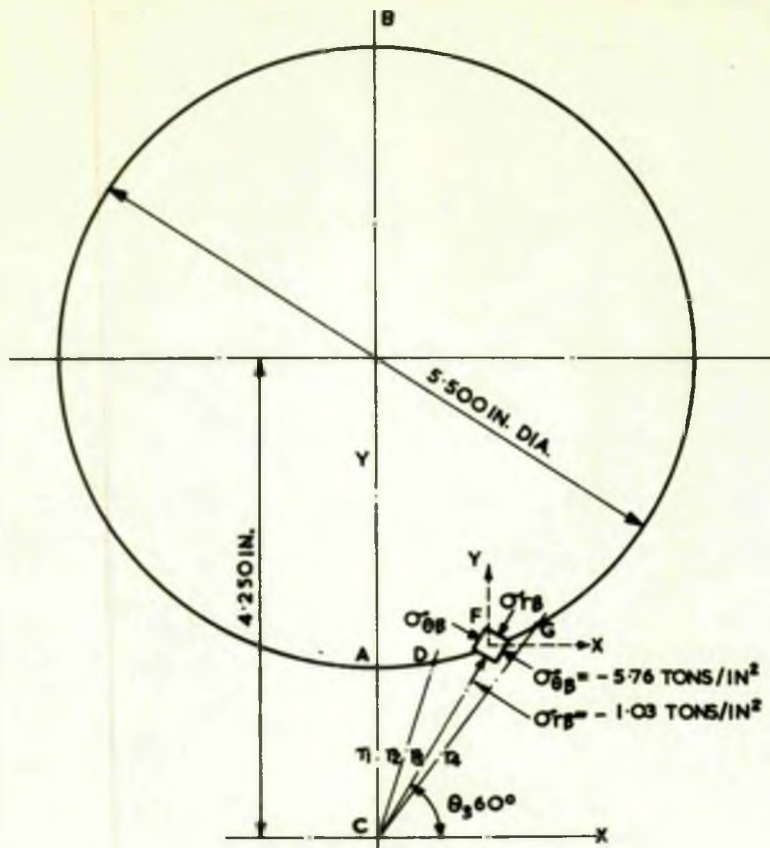
FIG. III.9. PLAN VIEW ON THE LOADING PATH A B. SHOWING THE BENDING STRESSES AT F DUE TO A UNIT LOAD AT C
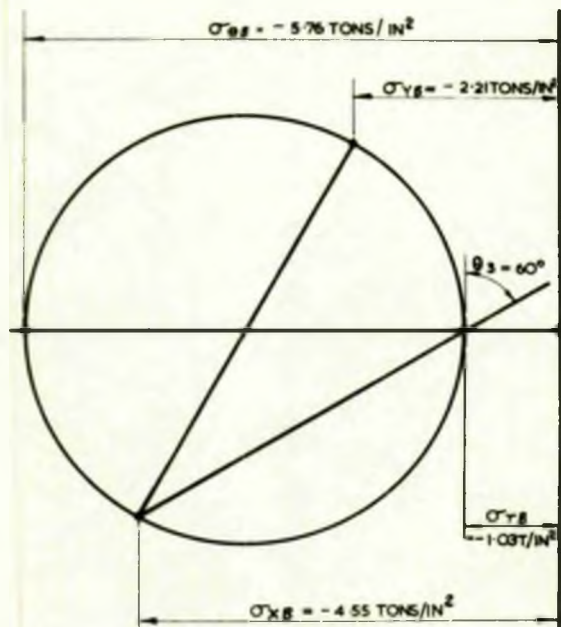
FIG. III.10 MOHR CIRCLE RESOLUTION FOR THE BENDING STRESSES AT F

maximum bending stresses for a range of 'μ' values from 0.03 in
increments of 0.01 to 0.10 are shown in Fig. III.8.   The complete
bending stress curve for any 'μ' value within the above range is
then obtained by using the envelope curve up to the relevant maxi-
mum.   Utilising Fig. III.8 and considering as before the point F
(Fig.III.9) on the load path, as an example (the relevant $^{r}/_{l}$ = 0.914)
the corresponding non-dimensional values of the bending stresses on
the outer loaded surface are $\frac{\sigma_{\theta B} t^2}{P} = -0.360$ (compression) and
$\sigma_{rB} \frac{t^2}{P} = -0.064$ (compression).

Substituting $t = \frac{1}{4}$ in and $P = 1$ ton, the actual 'unit load'
bending stress values acting at F in Fig. III.9 are obtained as
$\sigma_{\theta B} = -5.76$ ton/in^2 and $\sigma_{rB} = -1.03$ ton/in^2 .   These stresses are
the circumferential and meridional actions at F with respect to
C as the crown of the shell.   Their lines of actions in plan are
perpendicular and parallel to the line CF as shown in Fig. III.9.

The ultimate aim of the analysis is to deduce the circum-
ferential and meridional stresses at C due to the ring load.   The
lines of action of these stresses, from symmetry, are in the X and
Y directions at C and consequently only stress components in these
directions are relevant.   Thus the component actions in the X
and Y directions of the stresses shown at F in Fig. III.9 have to
be determined.

A convenient graphical method is the Mohr circle diagram
shown in Fig. III.10 giving the stress components at F in the X
and Y directions respectively as $\sigma_{xB} = -4.55$ tons/in^2 and
$\sigma_{YB} = -2.21$ tons/in^2 .   The effect of shell curvature has been
disregarded in the stress resolutions as it is generally negligible

in comparison with the effects of orientation.

Deriving the X and Y components of the bending stresses due to the unit load at C for other points of the load path A, D, G etc. leads, as in the case of deflections, to the appropriate influence lines for stress at C corresponding to a unit load traverse along the load path AB. These influence lines for the circumferential and meridional bending stresses at C, σ_{XB} and σ_{YB} respectively are shown plotted on the base of the developed length of the load path AB in Fig. III.11. The influence lines for the direct stress are obtained in an exactly similar way.

As in the case of deflections the appropriate total values at C due to the ring load are given by: ring load intensity x area enclosed by the relevant influence line. Hence the circumferential bending stress $\sigma_{\theta B}$ at C = 0.0927 x (area enclosed by σ_{X0} influence line = -17.70) = -1.64 $tons/in^2$, i.e. compressive on the outer surface. The meridional bending stress σ_{YB} at C = 0.0927 x (area enclosed by σ_{YB} influence line = +3.99) = +0.37 ton/in i.e. tensile on the outer surface.

The complete distribution of all stresses along a great circle perpendicular to the ring load path is shown plotted in non-dimensional form in Fig. III.12. These are derived, as in the case of the deflections, by repeating the above procedure for other points such as C along the selected great circle. The co ordinate values in Fig. III.12 relevant to point C, with r now referred to the centre of the ring load circle became $\frac{r}{\ell} = \frac{4.250}{2.125} = 2,$

$$(t^2/\rho)\sigma_{\theta B} = \frac{(\frac{1}{4})^2 \times (-1.64)}{1.60} = -0.0640, \quad \text{and}$$

$$(t^2/\rho)\sigma_{rB} = \frac{(\frac{1}{4})^2 \times (0.37)}{1.60} = +0.0145 \text{ and are as shown on the graphs.}$$
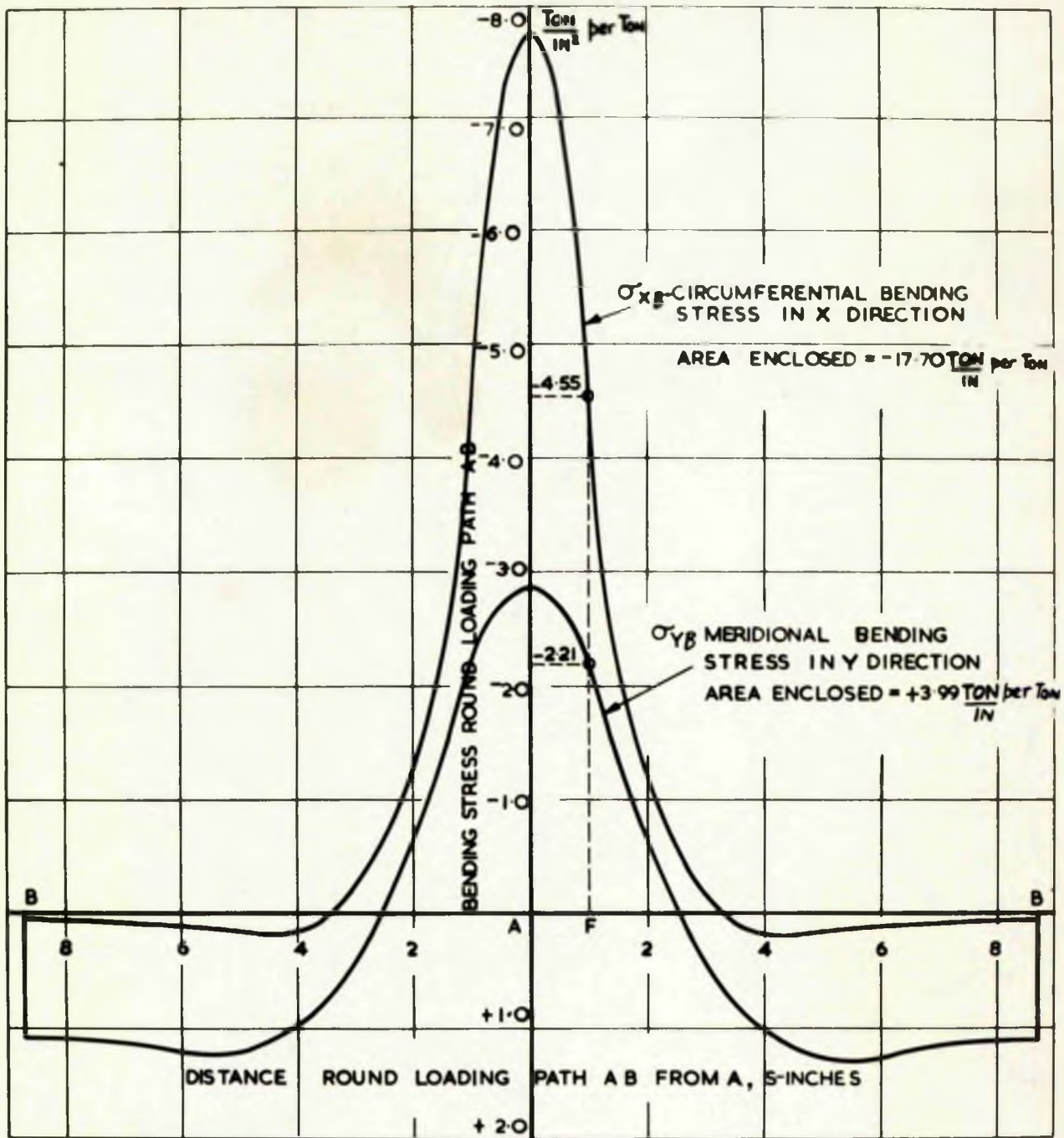
FIG. III.11 THE DISTRIBUTION OF BENDING STRESSES ROUND THE LOADING PATH A B
DUE TO A UNIT LOAD AT C.
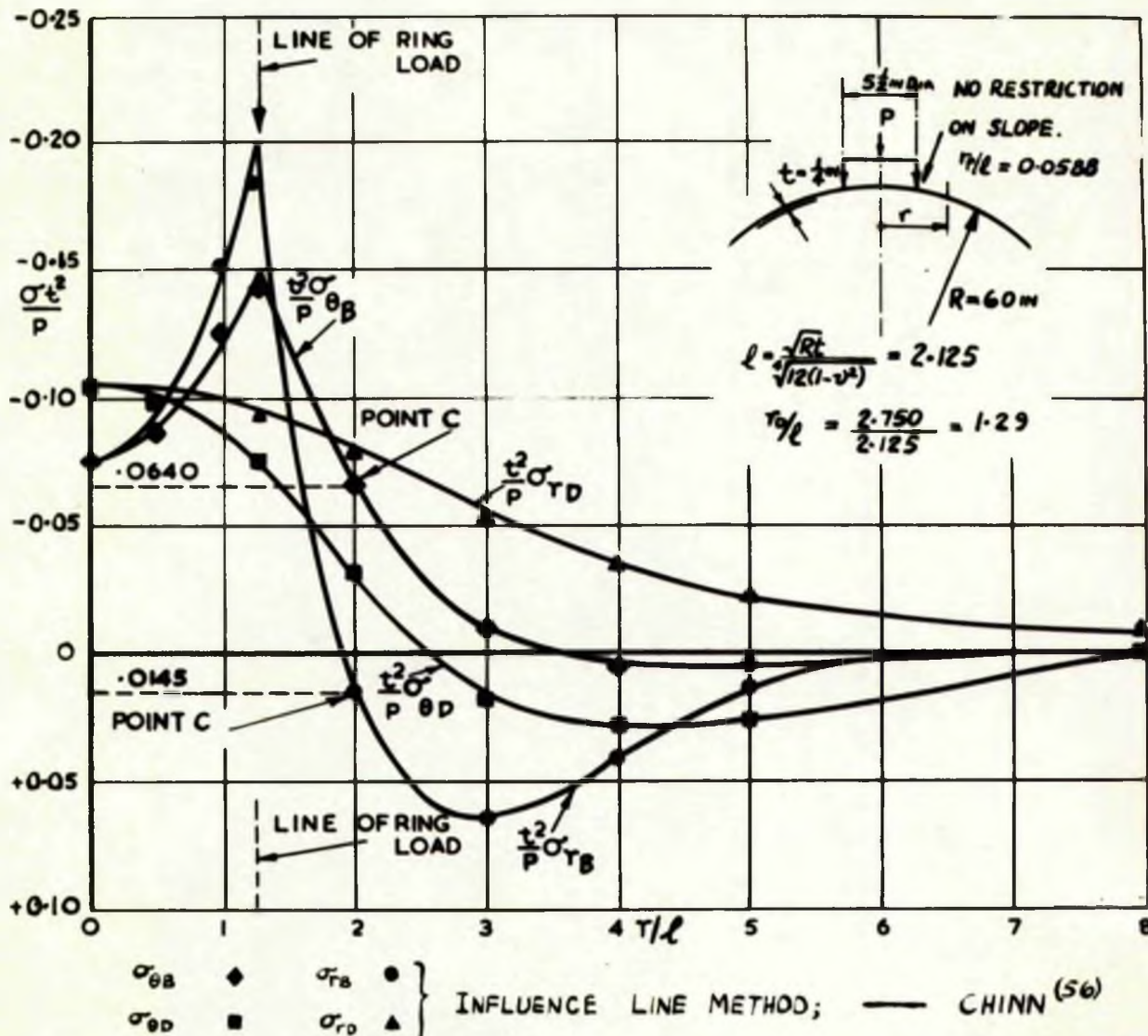
FIG. III.12 THE DISTRIBUTION OF DIRECT STRESSES AND BENDING STRESSES ON THE OUTER SURFACE OF A SHALLOW SHELL SUBJECT TO A RADIAL RING LOAD P, APPLIED WITH NO RESTRICTION OF SLOPE AT THE LOAD. $\mu = 1.29$ — A COMPARISON BETWEEN THE INFLUENCE LINE (LOAD PATH WIDTH $r_0/\ell = 0.0588$) AND CHINN[56] ANALYSES
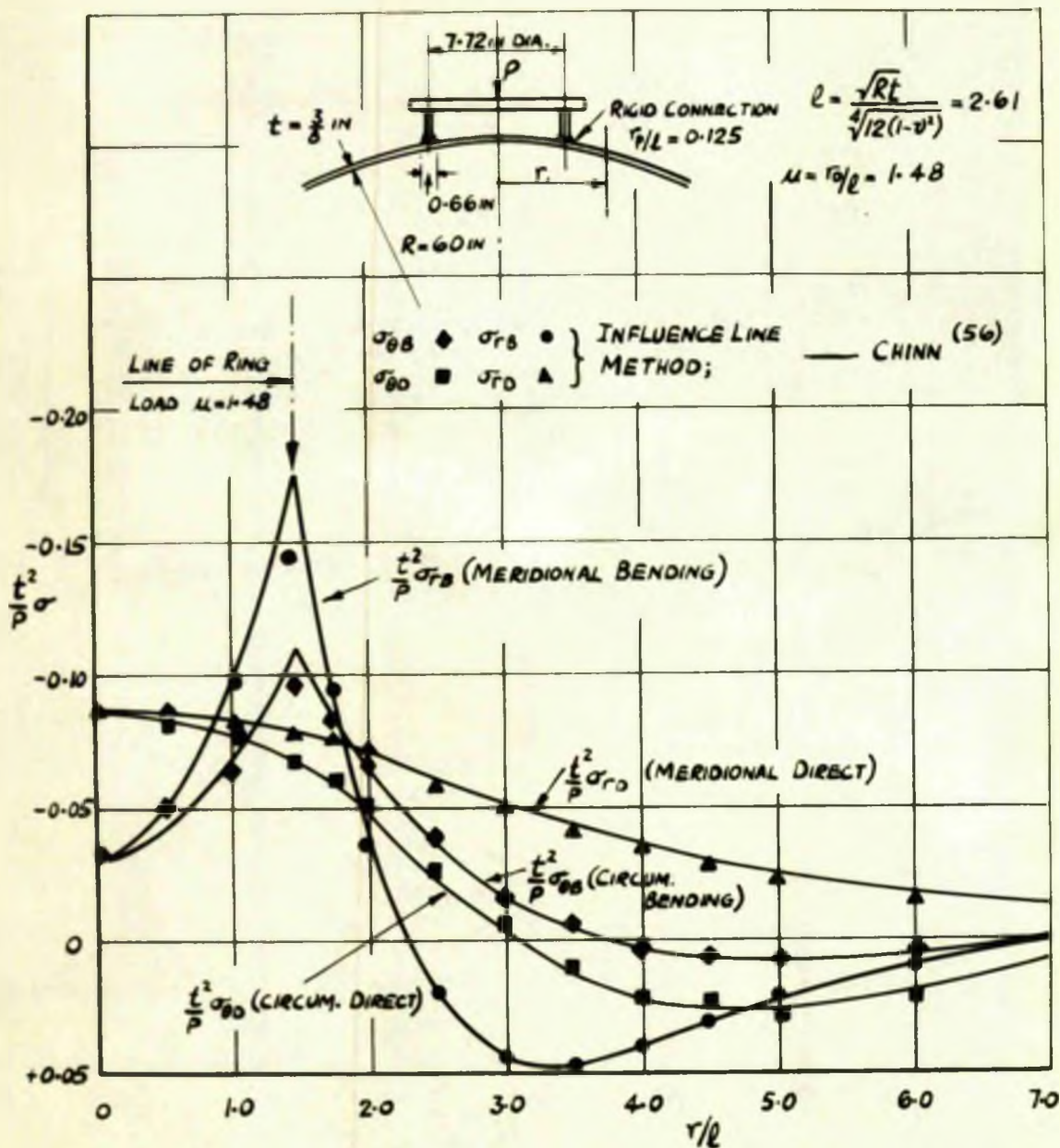
FIG. III.13   THE DISTRIBUTION OF DIRECT STRESSES AND BENDING STRESSES ON THE OUTER SURFACE OF A SHALLOW SHELL SUBJECT TO A RADIAL RING LOAD P, APPLIED BY A RIGID CONNECTION, $\mu = 1.48$ — A COMPARISON BETWEEN THE INFLUENCE LINE (LOAD PATH WIDTH $r_P/\ell = 0.125$) AND CHINN [56] ANALYSES

As in the case of the deflections, these distributions are compared with those obtained using the analysis proposed by CHINN [56]. A slight deviation occurs in the region of the load, and as expected the Influence Line approach predicts values of bending stress slightly lower than the Chinn analysis.

The same procedure has been repeated for the case where the loading is applied by complete fixity of the shell across and along the load path. In this case the equations for the rigid insert loading serve as the basis for the unit actions, i.e. Eqts. II.56. A ring of 7.72 in mean diameter is welded to a spherical shell of $\frac{3}{8}$ in thickness and 60 in radius. This corresponds to a value of μ for the ring of 1.48. The width of the load path is 0.66 in, which leads to a μ for the load of 0.125. The unit actions are obtained from Fig. II.8 utilising the curves for $\mu = 0.125$.

The Influence Line approach is compared, as previously, with the CHINN analysis on Fig. III.13, and is seen to predict results which are in agreement for all values of r, other than in the immediate vicinity of the load.

Using the Influence Line approach a family of curves for different ring μ values can be obtained. It is, however, noted that comparing these values with those obtained by considering a line load (i.e. zero width) the variations only take place in the immediate vicinity of the load, for both cases. When the width of the line load is small compared with the diameter of the ring itself, it is seen that the distribution of radial deflection and direct stresses approximate closely to those of the line load. In

consequence the bending stress distribution may be obtained for
design purposes from the zero width line load distribution by
'cutting-off' the peak of these stresses, over a width equal to t
width of the load.   These are shown on Fig. III.14 for a range
of ring μ values indicating a suitable 'cut-off' for a particular
width of load.

III.2   A VARYING RADIAL LOAD DISTRIBUTED ROUND THE CIRCUM-
FERENCE OF A CIRCULAR RING

A varying radial load of the form p.cosθ, where p is the
load intensity at θ = 0, is distributed around the circumference
of the load path (which may be defined by the tube-spherical she
junction), as indicated in Fig. III.15.

It is required to determine the distribution of radial de-
flections and stresses in the shell due to the above loading.
An alternative solution for a load path of zero width is present
by CHINN [56], and this enables the accuracy of the results from
the Influence Line Method to be assessed.

In order to illustrate the method a specific case will be
dealt with, namely, a spherical shell of $\frac{1}{2}$ in wall thickness and
60 in radius.   The circular ring is 5 in mean diameter and of
1 in width.   From the shell dimensions $\ell = \frac{\sqrt{Rt}}{\sqrt[4]{12(1-v^2)}} = 3.006$ in. Thus
μ for the ring is $2.500/3.006 = 0.832$

The approach to this problem is as in previous examples,
except that since the radial loading is not uniformly distribut
round the load path, its variation (p.cosθ) must be considered.
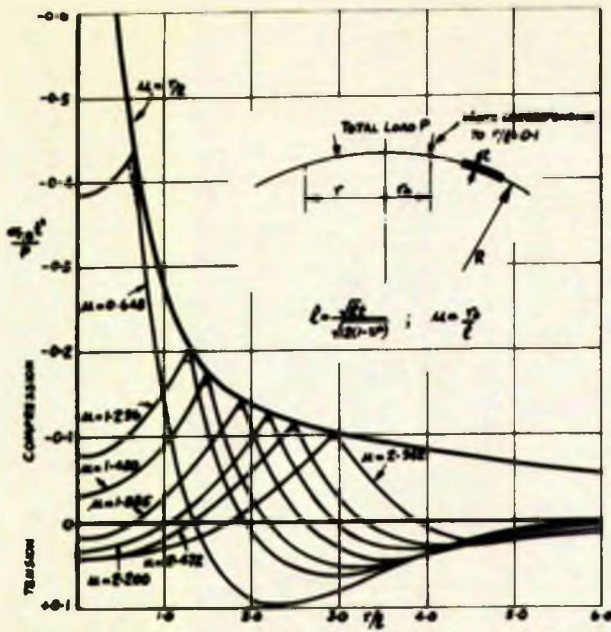
Fig. III. 14a. The Distribution of Meridional Bending Stress on the Outer Surface
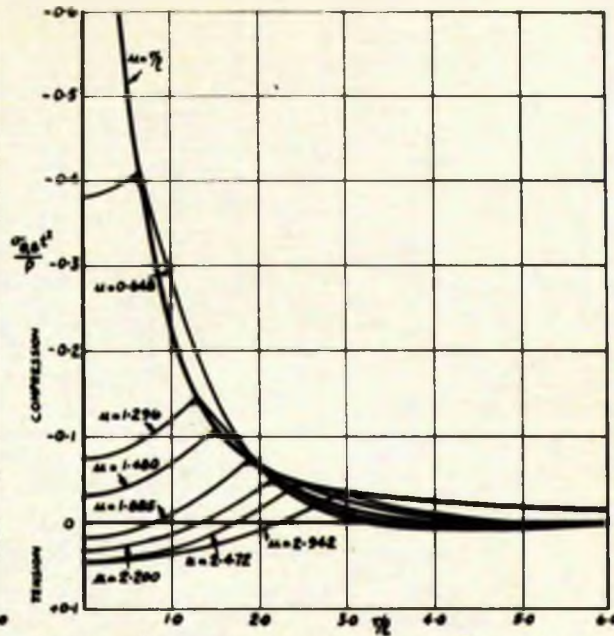
Fig. III. 14b. The Distribution of Circumferential Bending Stress on the Outer Surface
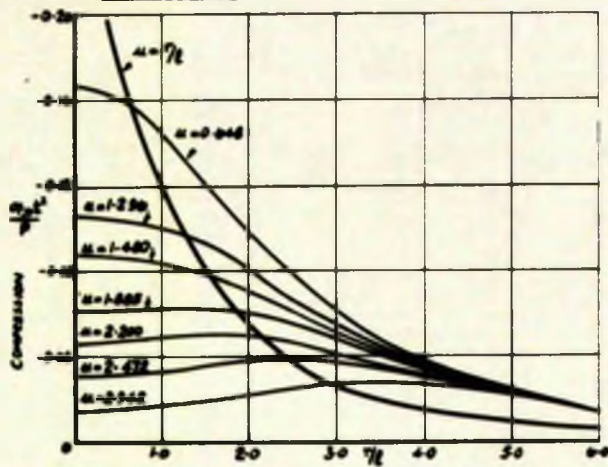
Fig. III. 14c. The Distribution of Meridional Direct Stress
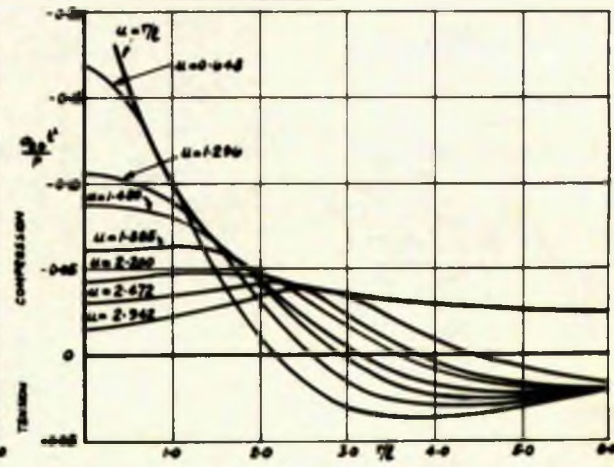
Fig. III. 14d. The Distribution of Circumferential Direct Stress
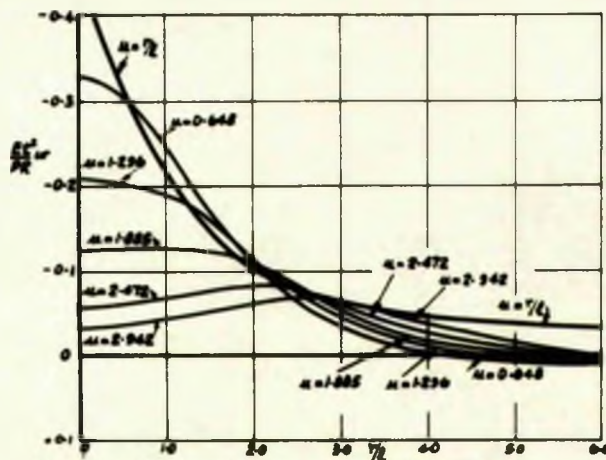
Fig. III. 14e. The Distribution of Radial Deflection

Fig. III. 14. The Distribution of Direct Stresses and Bending Stresses on the outer surface of a Shallow Spherical Shell subject to a Radial Ring Load P for various μ values, with a load path width corresponding to $r/\ell = 0.1$
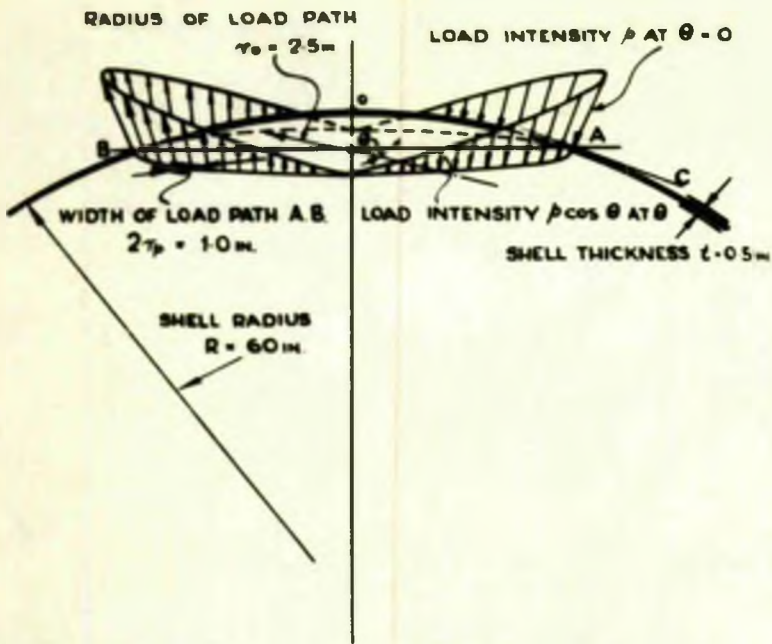
FIG. II-15 VARYING RADIAL LOAD ON SPHERICAL SHELL

Labels in figure:
RADIUS OF LOAD PATH $r_0 = 2.5$ in
LOAD INTENSITY p AT $\theta = 0$
WIDTH OF LOAD PATH A.B. $2r_p = 1.0$ in
LOAD INTENSITY $p \cos \theta$ AT θ
SHELL THICKNESS $t = 0.5$ in
SHELL RADIUS $R = 60$ in

AREA BETWEEN GRAPH AND BASE LINE =

$$2\int_0^3 \left(\frac{\delta^3}{p}\right) ds = 1.80 \times 10^3 \text{ in}^2/\text{unit of load}$$

$t = 0.5$ in
$R = 60$ in
$S = 2.5$ in
1.75 in
23°
3.75 in
LOAD PATH IN PLAN
RADIAL LOAD PER UNIT LENGTH AT $F = p \cos 23°$

DISTANCE ROUND LOAD PATH
S - IN
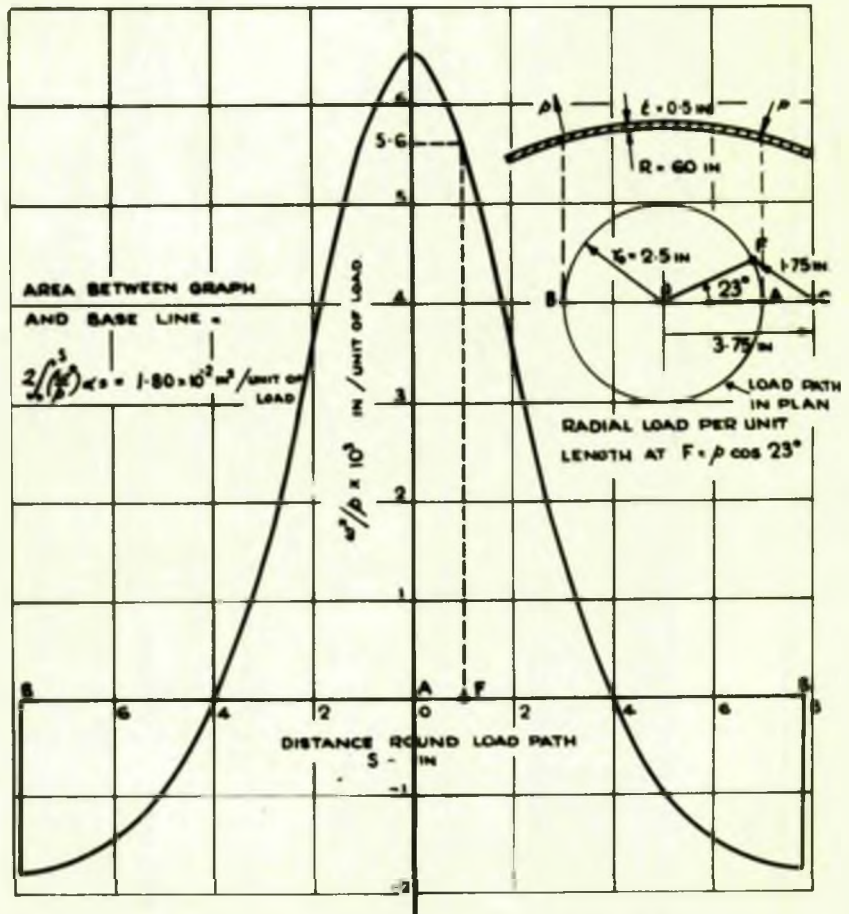
FIG. III-16 INFLUENCE LINE DIAGRAM FOR RADIAL DEFLECTION AT C FOR THE LOADING AS SHOWN IN FIG II 15

In order to illustrate the approach the radial deflection will
be determined.

Considering a point C (Fig. III.16) on the surface of the
shell at a distance 3.75 in ($r/\ell = 1.25$) measured in plan from the
load path centre at O.   The ring load is removed and a unit load
(P = 1) is applied at C uniformly distributed over a circular
area of radius r_ρ equal to the half width of the load path, in
this case 0.50 in.   The corresponding value of r_ρ/ℓ for the
load is 0.17.

Considering further a point F (Fig. III.16) on the load
path of radial distance $r = 1.75$ in ($r/\ell = 0.583$) and using
Fig. II.5 for $\mu = 0.17$ (by interpolation for very small
values) it is possible to obtain a value for $Et^2 w/PR$ at $r/\ell = 0.583$
namely $Et^2 w/PR = 0.339$. Thus for $P = 1$, $w = 6.06 \times 10^{-3}$ in.
The load intensity per unit load path length at F ($\theta = 23°$) is
$p \cos23°$, giving the contribution of the load per unit length
at F to the deflection at C, as $w^* = 6.06 \times 10^{-3} p \cos23°$ or $w^*/p = 5.6 \times 10^{-3}$.   Repeating the procedure for successive points such
as F on the load path the influence line diagram for the radial
deflection at C, for the loading shown in Fig. III.15 is obtained.
It is shown in Fig. III.16.

The area under the influence line gives the total radial
deflections at C due to the imposed loading,

i.e. $w/p = 1.80 \times 10^{-2}$ in^2 per unit of load   (III.15)

It is noted that the distribution of radial loading, $p \cos\theta$,
on the spherical shell would be produced by the application of a
bending moment M to a tube of mean diameter equal to that of the

load path, and in the plane $\theta = 0$.   It being assumed that the tube is only capable of applying radial loading to the shell.

The magnitude of the applied moment M is obtained from Fig. III.15:- $M = 4 \int_{0}^{\frac{\pi}{2}} p\cos\theta \cdot r_0 \cdot r_0 \cos\theta \cdot d\theta = \pi r_0^2 p$ (III.16)

where r_0 is the mean radius of the load path, in this case 2.5 in

Thus from eqt. III.15 and 16 $\dfrac{\omega}{M} = \dfrac{1 \cdot 80 \times 10^{-2}}{\pi r_0^2} = 0 \cdot 917 \times 10^{-3}$

Plotting this as a non-dimensional parameter, $\dfrac{Et^3}{\sqrt{Rt}\cos\theta} \dfrac{\omega}{M} = 0 \cdot 280$

against the r/ℓ value for the point C ($r/\ell = 1.25$) a point on the distribution curve for radial deflection is obtained.

Repeating the whole procedure outlined above, for successive points such as C along the great OC, the distribution of radial deflection is obtained, as in Fig. III.17.   This is compared wi the analysis obtained using the line load analysis (i.e. zero width) proposed by CHINN [56] - again the agreement is excellent.

In obtaining the distributions of bending and direct stress along a great circle, the procedure for analysis of the stresses is the same as in the case of the uniformly distributed load in section III.1.2.   The method of dealing with the varying radial load is the same as in the above derivation of the radial deflec tions.   Following this procedure the complete results for this size of ring ($\mu = 0.832$) with a 1 in path width are presented in Fig.III.18.

Any variation between these results and those obtained by the CHINN analysis occurs in the region of the loaded ring.
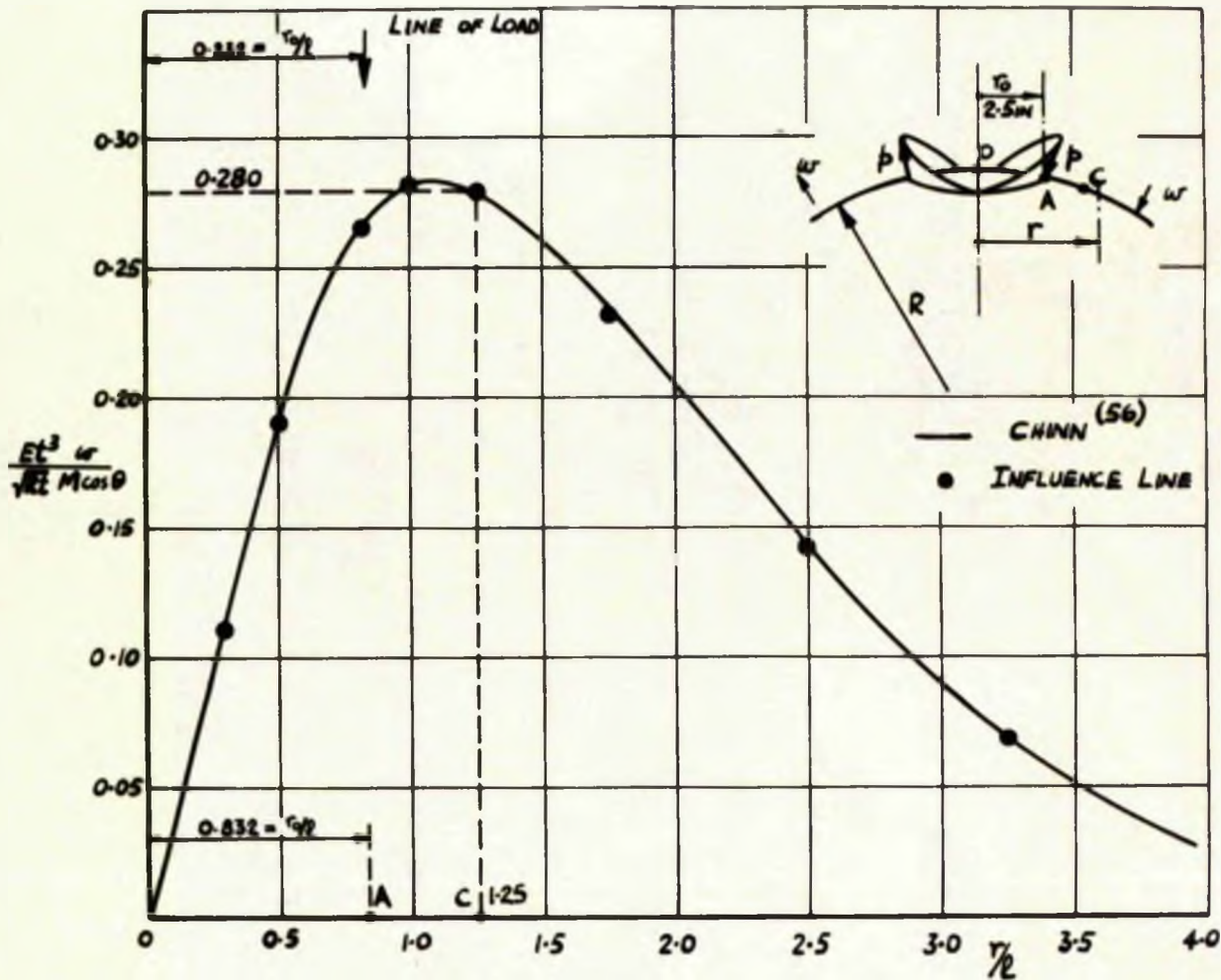
FIG. III.17 THE DISTRIBUTION OF RADIAL DEFLECTION DUE TO A BENDING MOMENT APPLIED AS A VARYING RADIAL LOAD - A COMPARISON BETWEEN THE INFLUENCE LINE METHOD AND CHINN[56]
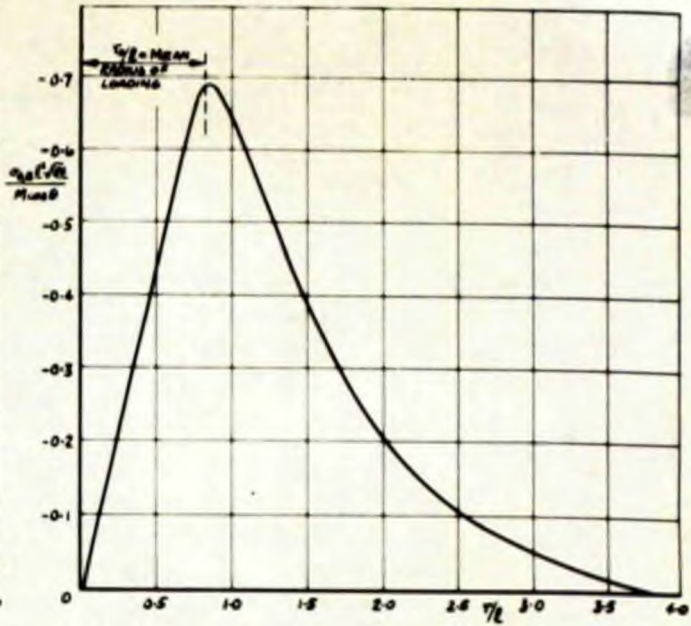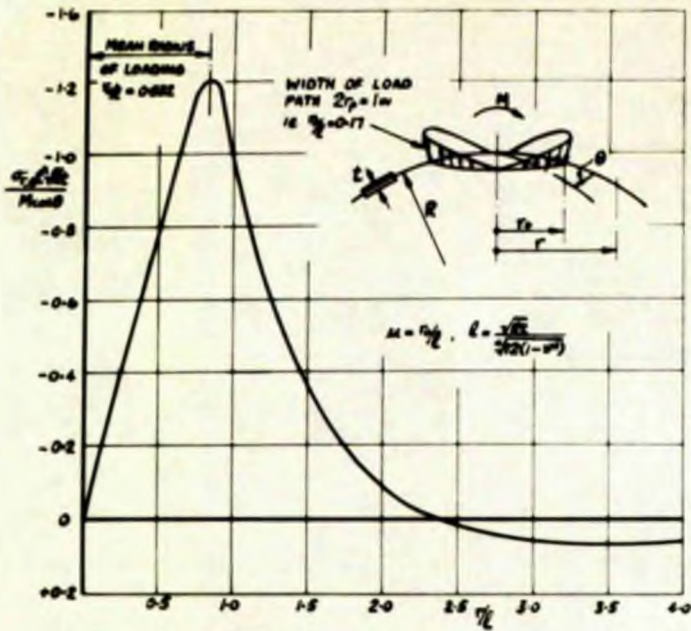
Fig. III.18a The Distribution of Meridional Bending Stress on the Outer Surface

Fig. III.18b The Distribution of Circumferential Bending Stress on the Outer Surface
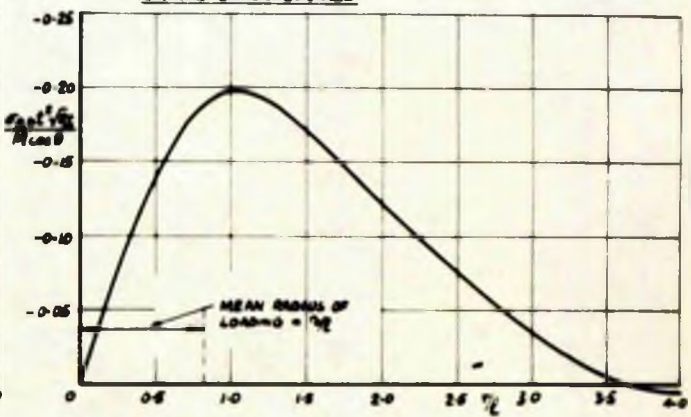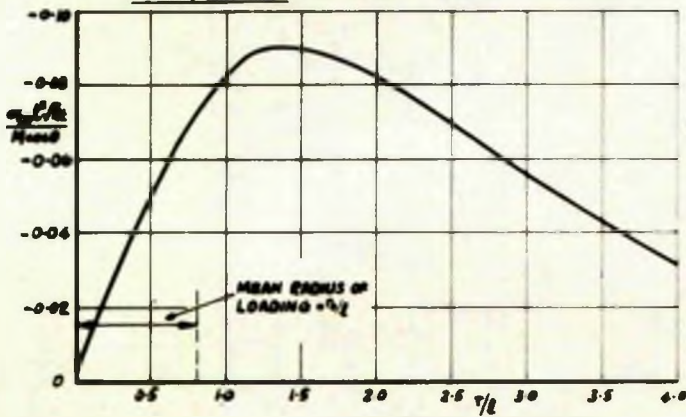
Fig. III.18c The Distribution of Meridional Direct Stress

Fig III.18d The Distribution of Circumferential Direct Stress
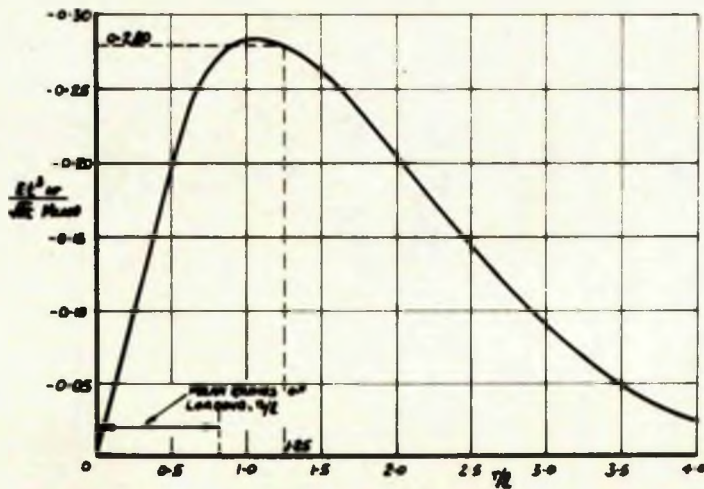
Fig. III.18e The Distribution of Radial Deflection

Fig. III.18 The Distribution of Direct and Bending Stress and Radial Deflection of a Shallow Shell Subject to a Varying Radial Load Distributed Round the Circumference of a Circular Ring, $\mu = r_0/\ell = 0.832$ and of Path Width 1 in ($r_p/\ell = 0.17$)

APPLIED MOMENT ON LOAD PATH : m AT $\theta = 0$ AND

$m \cos \theta$ AT θ

SHELL THICKNESS
$t = 0.5$ IN

LOAD PATH RADIUS $\tau_0 = 2.5$ IN

B

A

C

θ

O

SHELL RADIUS R
$= 60$ IN

LOAD PATH WIDTH $2\tau_p = 1.0$ IN

TWISTING MOMENT $M\tau\theta$

SHELL ELEMENT

CIRCUMFERENTIAL BENDING
MOMENT $M\theta\theta$

MERIDIONAL BENDING
MOMENT

$M\tau\tau$
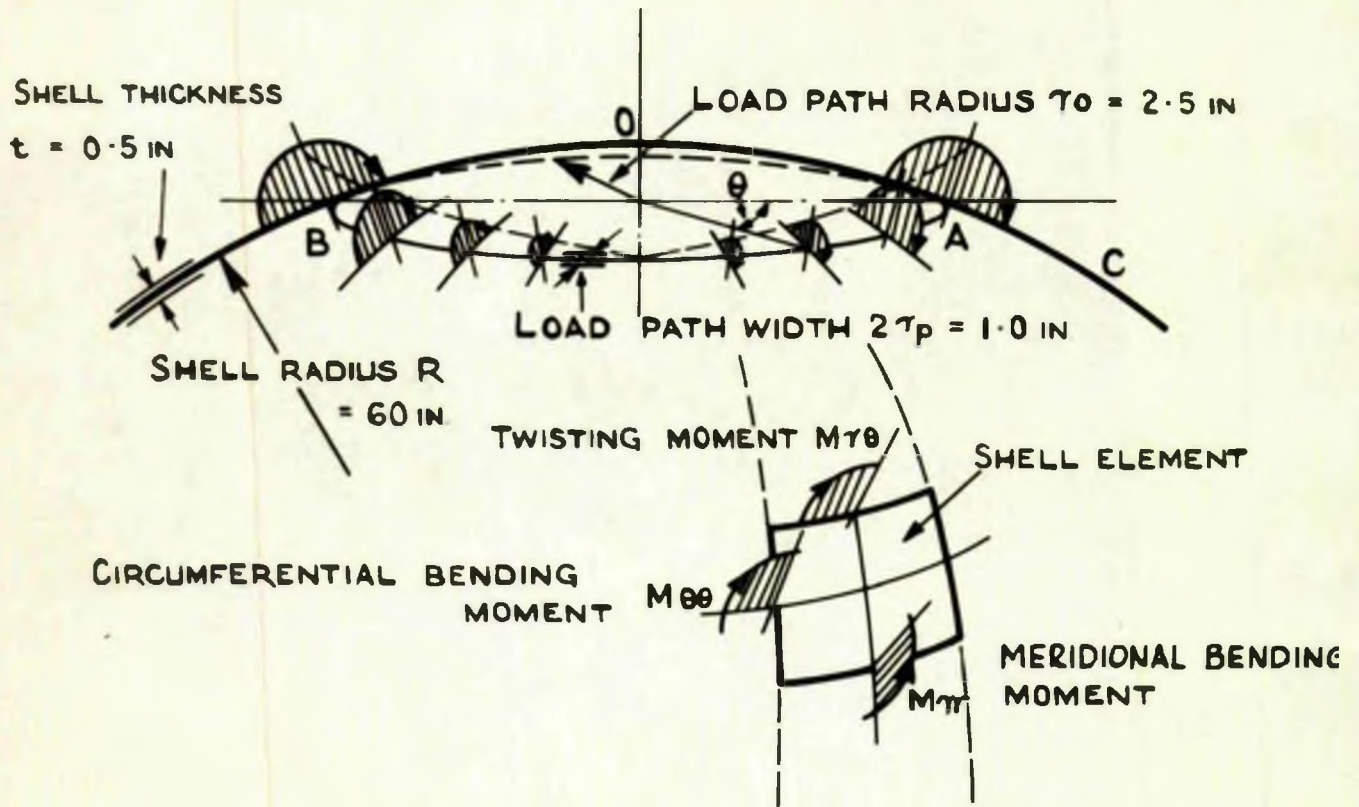
FIG. III·19 VARYING BENDING MOMENTS ON A SPHERICAL SHELL

III.3   A VARYING 'BENDING' MOMENT DISTRIBUTED ROUND THE
        CIRCUMFERENCE OF A CIRCULAR RING

A varying meridional moment of the form $m \cos\theta$, where m is the moment intensity at $\theta = 0$, is applied to the shell and distributed around the circumference of the load path (which may be defined by the tube-spherical shell junction) as in Fig. III.19.

As in earlier examples it is required to determine the distribution of radial deflections and stresses in the shell due to the above loading.

The same shell and tube dimensions used in section III.2 again serve to illustrate the approach, i.e. $t = \frac{1}{2}$ in, $R = 60$ in, $r_0 = 2\frac{1}{2}$ in and 1 in load path width, yielding:- $\ell = 3.006$, μ for the ring = 0.832 and μ for the load = 0.17.

Considering again point C $\left(\frac{r}{\ell} = 1.25\right)$ on the great circle and F $\left(\frac{r}{\ell} = 0.583 \text{ with respect to C}\right)$ on the load path - Fig. III.20. To satisfy the 'reciprocal symmetry' conditions necessary for the derivation of the influence line, the unit moment vector applied at C must be parallel in line of action, but opposite in direction to the specified moment vector on the load path acting at the point considered.   Thus to obtain the ordinate at F of the influence line for the appropriate bending moment at C the unit moment vector is applied at C as shown in Fig.III.20a.

The effect of this unit moment, at any radius r, measured in plan from C on the otherwise unloaded shell is given in non-dimensional form by Fig. II.12.   The load path width is allowed for as in the earlier cases, by a rigid circular insert of radius

$r_\rho = 0.50$ in $(^r\!\rho/\ell = 0.17)$. The resulting values of the bending stresses are obtained from Figs. II.12a-c for $r = 1.75$ $(^r/\ell = 0.583)$ as $\dfrac{\sigma_{r\theta}\,\ell^2\sqrt{Rt}}{M\cos\theta} = -1.80$, $\dfrac{\sigma_{\theta\theta}\,t^2\sqrt{Rt}}{M\cos\theta} = -1.62$, $\dfrac{\tau_{r\theta,\theta}\,t^2\sqrt{Rt}}{M\sin\theta} = +0.87$

The angle θ in the above is that of the unit actions, and is noted as θ^υ on Fig. III.20a, in this case (Point F) $\theta^\upsilon = 58°$. Thus when $M = 1$ ton in and R and t as above (60 in and $\frac{1}{2}$ in respectively); $\sigma_{r,\theta} = -0.696$ t/in^2, $\sigma_{\theta\theta} = -0.626\,t/in^2$, $\tau_{r\theta,\theta} = +0.540\,t/in^2$

Resolving these stress actions in the X and Y directions by means of the Mohr circle diagram Fig. III.20b gives $\sigma_{\widetilde{x}} = -1.185\,t/in^2$ which is the ordinate at F of the influence line for the meriodional bending stress at C. The specified moment intensity per unit load path length at F $(\theta = 23°)$ is m cos 23° giving the contribution of the moment per unit length at F to th meriodional bending stress at C as $\sigma_{\widetilde{x}}^{\bullet} = -1.185$ m cos 23°, i.e. $\dfrac{\sigma^{\bullet}}{m} = -1.082$.

Repeating this procedure for successive points such as F on the load path, the influence line diagram for the meridional bending stress at C, for the moment loading shown in Fig.III.19 is obtained. It is shown in Fig. III.21.

The area between the graph and the base line gives the tot meridional bending stress at C due to the imposed loading, for this case equal to -4.82 in^{-1}. That is:-

$$\sigma_{r\theta}/m \quad = \quad -4.82 \left(\tfrac{ton}{in}\right) \text{ per ton in.} \qquad (III.17)$$

It is noted that the distribution of moment, m cosθ, on th spherical shell would arise due to the application of a bending moment M to a tube of mean diameter equal to that of the load path, and in the plane $\theta = 0$. The tube being of such a form
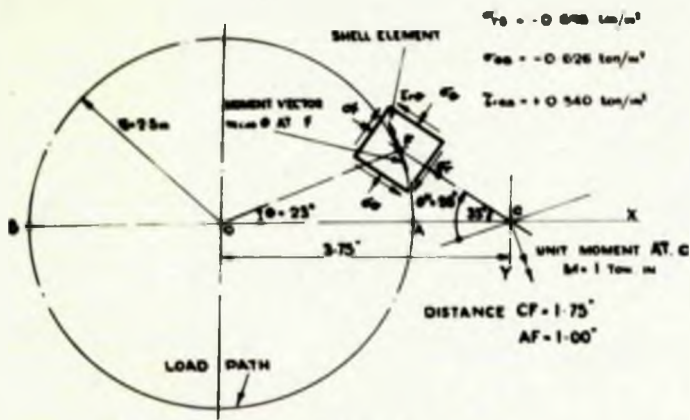
(a) APPLICATION OF UNIT MOMENT
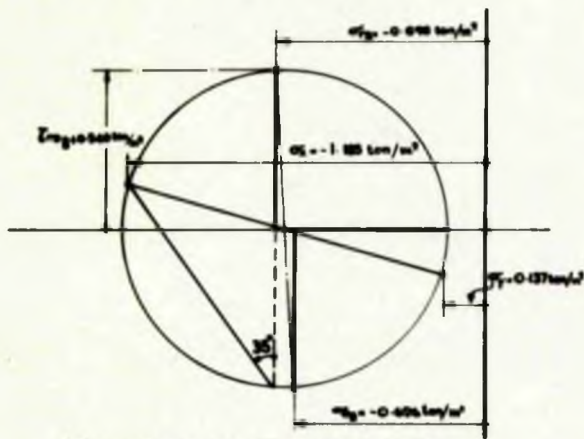
(b) MOHR'S CIRCLE FOR BENDING STRESS

FIG. III 20 PLAN VIEW OF THE LOADING PATH, SHOWING THE BENDING STRESSES DUE TO THE UNIT MOMENT AT C
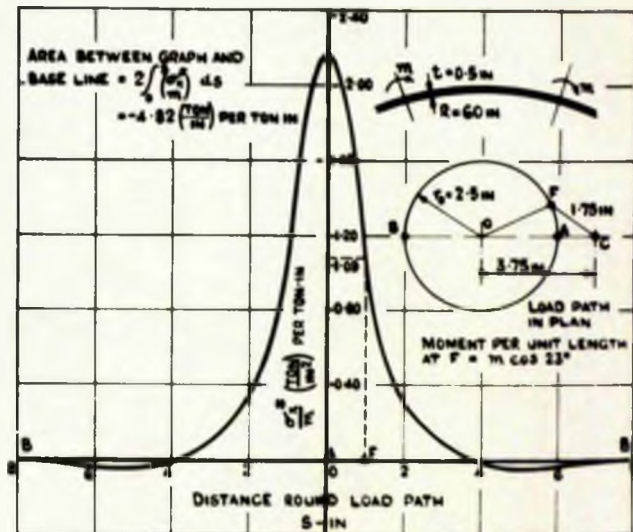
FIG. III 21 INFLUENCE LINE FOR MERIDIONAL BENDING STRESS AT C FOR THE LOADING SHOWN IN FIG III 19
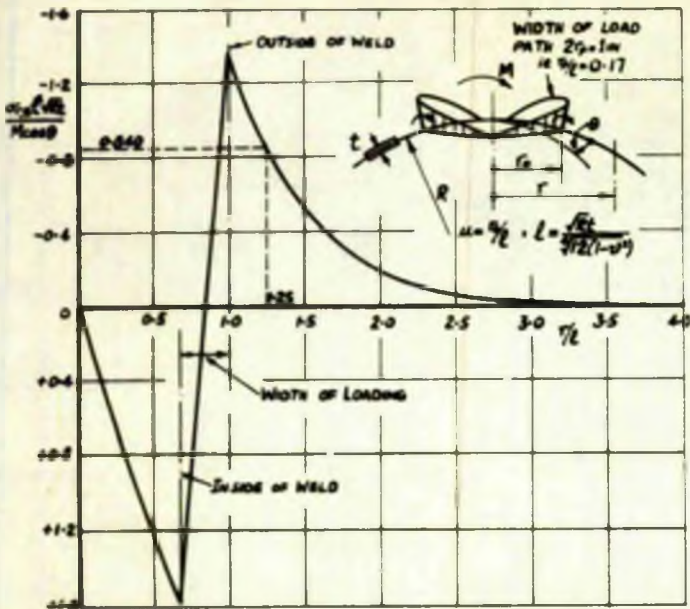
Fig. II·22a The Distribution of Meridional Bending Stress on the Outer Surface
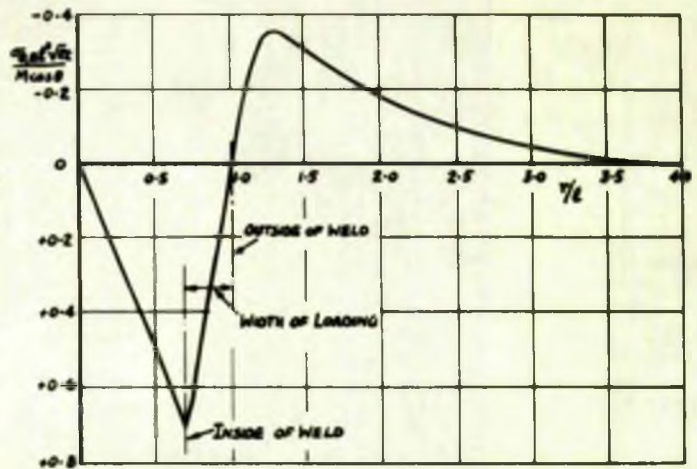
Fig. II·22b The Distribution of Circumferential Bending Stress on the Outer Surface
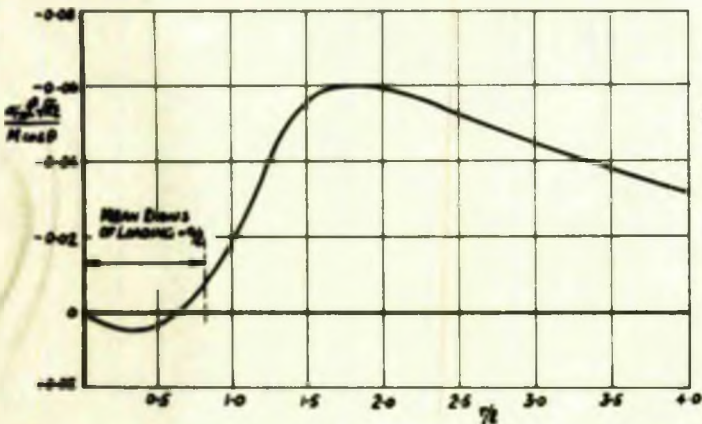
Fig. II·22c The Distribution of Meridional Direct Stress
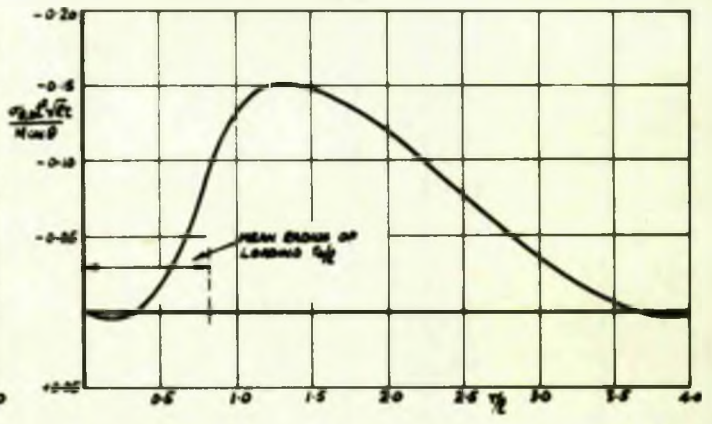
Fig. II·22d The Distribution of Circumferential Direct Stress
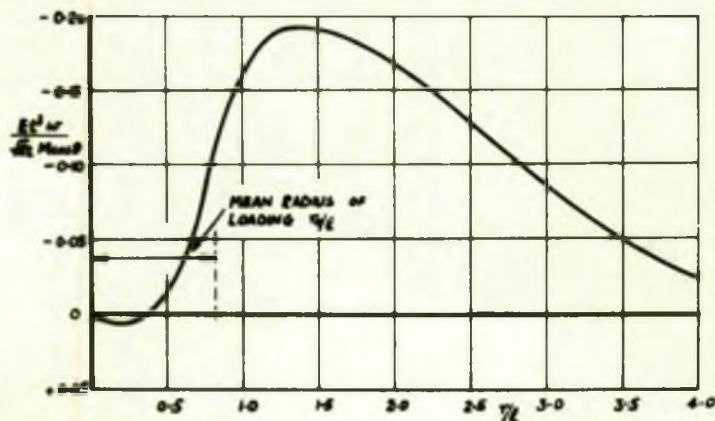
Fig. II·22e The Distribution of Radial Deflection

Fig. II·22 The Distribution of Direct and Bending Stress and Radial Deflection of a Shallow Shell Subject to a Varying Bending Moment Distributed Round the Circumference of a Circular Ring, $\mu = r/l = 0.85$ and Path Width 1 in $(r_0/l = 0.17)$

that it is capable only of applying meridional moment to the shell.

The magnitude of the applied moment M is obtained from Fig. III.19

$$M = 4 \int_0^{\frac{\pi}{2}} m \cos\theta . \cos\theta . r_o \, d\theta = \pi \, r_o \, m \qquad (III.18)$$

where r_o is the mean radius of the load path $= 2.5$in in this case.

Thus from eqts. III.17 and 18; $\sigma_{r\theta}/M = - 4.82/\pi_{,2.5} = - 0.614 \, in^{-3}$

Plotting this as a non-dimensional parameter, $\frac{\sigma_{r\theta} t^2 \sqrt{Rt}}{M \cos\theta} = - 0.840$

against the r/ℓ value for point C ($r/\ell = 1.25$) a point on the distribution curve for meridional bending stress is obtained.

Repeating the whole procedure outlined for successive points such as C along the great circle OC, the complete distribution of meridional bending stress is obtained, as in Fig. III.22a.   The load path width effect is clearly seen in this case, the rigid insert concept leading to the linear transition of bending moment across the load path width.

The distribution of the circumferential bending stress is obtained using the σ_γ value obtained in Fig. III.20b, together with other similar values.   This is plotted also on Fig. III.22b.

The direct stress and radial deflection distributions are obtained by a similar procedure, and are shown on Fig. III.22

III.4   A 'TWISTING' MOMENT UNIFORMLY DISTRIBUTED ROUND THE CIRCUMFERENCE OF A CIRCULAR RING

A twisting moment T' is uniformly distributed round the load path, defined by the tube-spherical shell junction as in Fig. III.23.

It is required to determine the distribution of shear stres

and tangential displacement along a great circle due to the abov

loading.

An alternative approach has been derived by the author and

is presented in Appendix VIII.6.   In this analysis the basic

shallow shell equations are utilized directly and using the

boundary values the distributions of shear stress and circum-

ferential displacement are obtained for a twisting moment appli

over a path of zero width.   This approach is hereafter referred

to as the 'Rigorous' Method.

As in the earlier case the Influence Line Method is compar

with the alternative method in order to substantiate and assess

the accuracy of the Influence Line Method.

The approach is illustrated using a spherical shell (Young

modulus $E = 13,400$ ton/in^2 and Poisson's ratio $\nu = 0.28$) of 60

radius, and $\frac{1}{2}$ in thickness.   The load path radius r_0 is 2.5 i

and the width 1 in. Fig. III.23.

Derivation of Shear Stress Distribution.   Consider a point C

(Fig. III.24a) on the surface of the shell at a distance of $r = 4$

measured in plan from the load path centre O, and a point F on

the load path at a distance of 1.98 in from C.

The applied twisting moments T' are removed and a unit twis

ing moment $(T = 1)$ is imposed at C acting in the direction show

This direction is such as to satisfy the condition of reciproca

symmetry between C and the point F on the load path.   The allo

ance for the load path width is again effected by applying the

unit action at C via a rigid insert of diameter equal to the

5 in MEAN DIA. = 2G

$t = \frac{1}{2}$ in

1 in

R = GO in

TWISTING MOMENT
PER UNIT LENGTH

$T' = \frac{T}{2\pi r_G}$

PLAN VIEW ON THE LOAD PATH
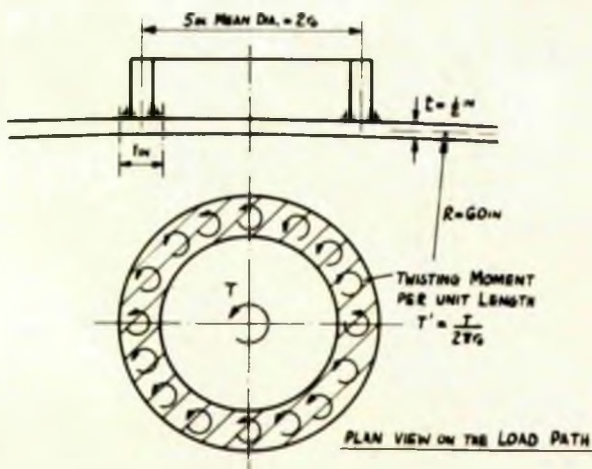
FIG III.23   THE APPLICATION OF A 'TWISTING' MOMENT UNIFORMLY
DISTRIBUTED ROUND THE CIRCUMFERENCE OF A CIRCULAR RING

LOAD PATH
WIDTH 1 in

5·0 IN MEAN DIA

SHELL ELEMENT

X

AF = 1·00 IN
CF = 1·98 IN
∝ = 30°

$r_G = 2.5$ IN   Y

$\tau_{r\theta} t$

T = 1 TON IN

B   O   A   C

$\frac{\tau_{r\theta} t}{T} = 0.040$ in^{-2}

4·00 IN

(a)   APPLICATION OF UNIT TWISTING MOMENT

$\frac{\tau_{r x} t}{T} = -.020$ in^{-2}

$\frac{\tau_{r\theta} t}{T} = 0.040$ in^{-2}

σ

∝ = 30°

τ

(b)   MOHR CIRCLE FOR TWISTING MOMENTS ACTIONS
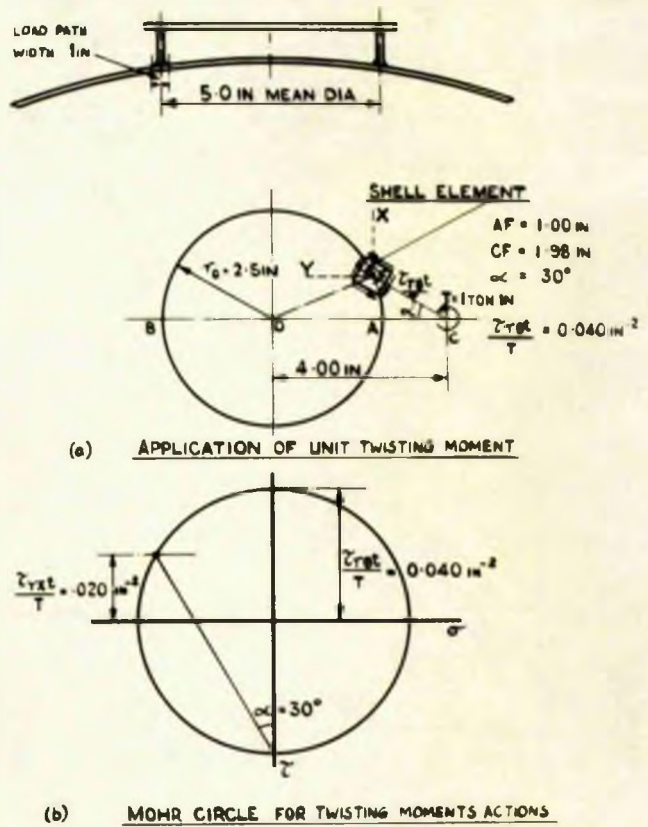
FIG III.24   PLAN VIEW OF LOADING PATH AB SHOWING THE STRESSES AT
F DUE TO A UNIT TWISTING MOMENT AT C
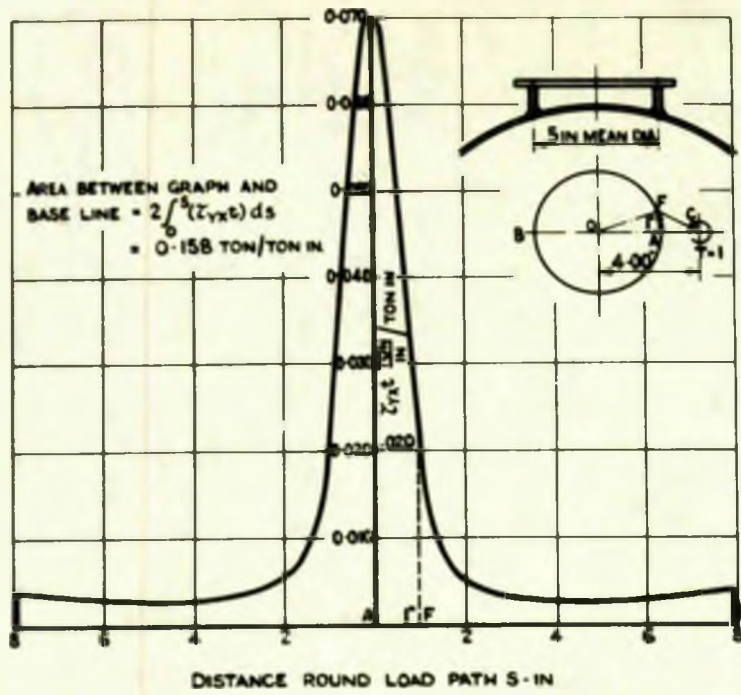
FIG. III.25 THE INFLUENCE LINE FOR SHEAR STRESS AT C BY TWISTING MOMENTS (INCH UNITS)
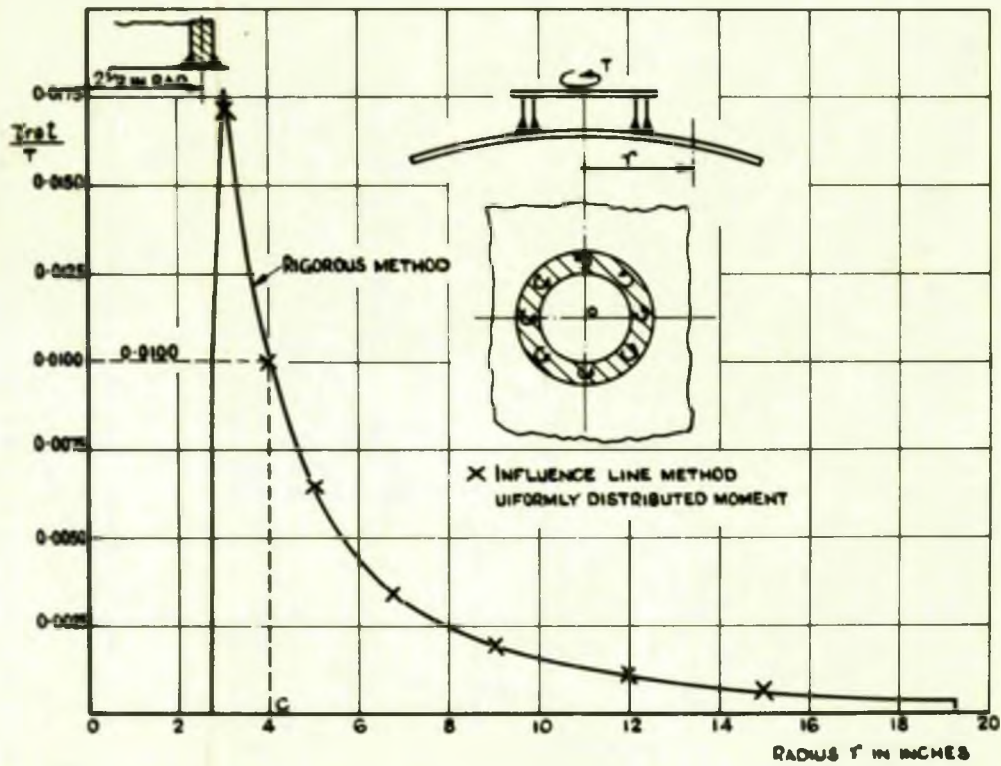
FIG III 26 THE DISTRIBUTION OF SHEAR STRESS ON A SHALLOW SHELL DUE TO A UNIFORMLY DISTRIBUTED TWISTING MOMENT ROUND THE CIRCUMFERENCE OF A CIRCULAR RING A COMPARISON BETWEEN THE INFLUENCE LINE METHOD AND THE RIGOROUS METHOD (INCH UNITS)

load path width, i.e. $r_p = 0.50$ in.

Consider, as before, the stresses at F due to the unit twisting moment at C, that is distance $r = 1.98$ in. From Fig. II.14a, $\tau_{r\theta}t/T = +0.040 \text{in}^{-2}$. This is resolved, using the Mohr circle, to enable the stresses on the X, Y planes to be determined, see Fig. III. 24b. Only the Shear stresses τ_{yx} are relevant, since the resultant normal stresses are zero - obtained by summing over the whole load path. In this case $\tau_{yx}t/T = 0.020 \text{ in}^{-2}$. Thus the ordinate value at F of the influence line for shear stress at C due to the unit moment traverse of the load path is $\tau_{yx}t/T = 0.020$ (ton/in) per ton in. The complete distribution is obtained by considering other points on the load path - Fig. III.25. This is the influence line for Shear stress at C.

The resultant Shear stress = Load Intensity x Area under Influence Line

$$\therefore \quad \tau_{r\theta}t \quad = \quad T' \text{ x } 0.158 \qquad (III.19)$$

The uniformly distributed twisting moment T' round the load path is equivalent to a total twisting moment T, where

$$T = T' \text{ x } 2\pi r_o \qquad\qquad (III.20).$$

Thus from eqts. III.19 and 20; $\tau_{r\theta}t/T = 0.0100 \text{in}^{-2}$ This is plotted on Fig. III.26 with other values obtained in a similar manner and a comparison is made with the 'Rigorous' method.

Derivation of Circumferential Displacement Distribution. The circumferential displacement u at F due to the unit moment action at C is obtained from Fig. II.14b corresponding to $r = 1.98$ in. Thus $\frac{utG}{T} = 0.0395 \text{in}^{-1}$ giving the displacement at F in the X direction (Fig. III.27b) as $u_x tG/T = 0.0346 \text{in}^{-1}$. Plotting such values in

Fig. III.28 the appropriate influence line for displacement at

C is obtained.   Thus the value of utG at C =   Load Intensity

Area under influence line

$$= \quad T' \quad x \; 0.303$$

and from eqt. III.20, $utG/_T$ = 0.0193 ton per ton-in

This value is shown on Fig. III.29 with other values

obtained in a similar manner, and further compared with the

Rigorous Method.

It is seen that for both the shear stress and tangential

displacement distributions along a great circle, excellent

agreement is obtained between the Rigorous Method and the

Influence Line Method.

III.5   A TANGENTIAL SHEAR LOAD UNIFORMLY DISTRIBUTED ROUND THE CIRCUMFERENCE OF A CIRCULAR RING

A tangential shear load, p_θ, is uniformly distributed round

the load path, defined by the tube-spherical shell junction as

in Fig. III.30.   It is required to determine the distribution

of shear stress and tangential displacement along a great circl

due to the above loading.

The alternative approach derived by the author, given in

Appendix VIII.6 is used to compare the results of the Influence

Line Method and thus assess its accuracy.   This approach is

referred to as the 'Rigorous' Method.

The method is again illustrated by a numerical example,

the relevant shell dimensions being as in Section III.4 and

shown on Fig. III.30.

LOAD PATH
WIDTH 1 IN.

5 IN MEAN DIA.

ELEVATION OF SHELL

PLAN OF
LOAD PATH

$r_0 = 2.5$ IN.

AF = 1·00 IN.
CF = 1·98 IN.
$\alpha = 30°$

$\dfrac{UtG}{T} = ·0395$ IN.$^{-1}$

$T = 1$ TON IN.

4·00 IN.

(a)   APPLICATION OF UNIT MOMENT AT C

$\dfrac{UntG}{T} = ·0346$

$\dfrac{UtG}{T} = ·0395$ IN.$^{-1}$

$\alpha = 30°$
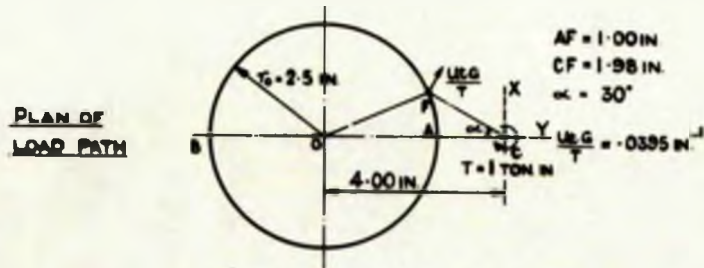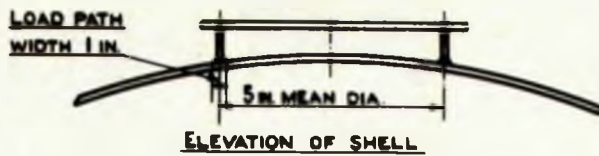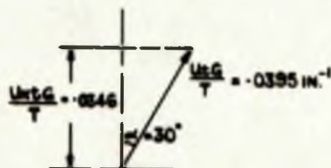
(b) DERIVATION OF DISPLACEMENT IN X - DIRECTION

FIG III.27 PLAN VIEW OF THE LOADING PATH AB SHOWING THE DISPLACEMENTS
AT F DUE TO THE UNIT MOMENT AT C

·060

AREA BETWEEN GRAPH AND
BASE LINE $= 2\displaystyle\int_0^S (V_x t G)\, ds$

$= 0·303$ TON IN./TON IN.

·050

·040

·0346

0·030

$V_x t G.$ TON/TON IN.

0·020

0·010

5 IN MEAN DIA.

$T = 1$

B   4·00 IN.

LOAD PATH
IN PLAN

A   1″ F   B

DISTANCE ROUND LOAD PATH S - IN.

8   6   4   2   2   4   6   8
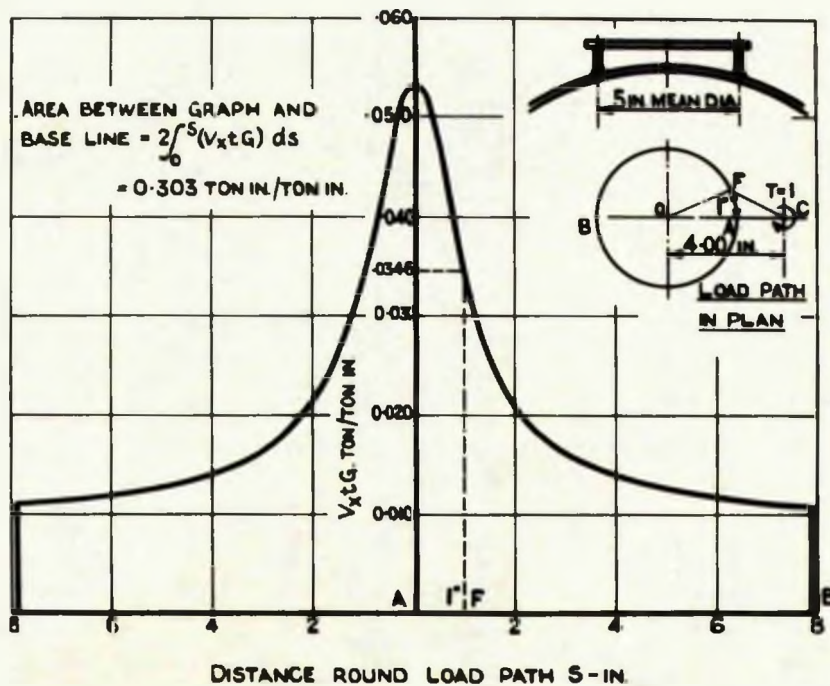
FIG III.28 INFLUENCE LINE FOR DISPLACEMENT AT C BY TWISTING MOMENTS (INCH UNITS)
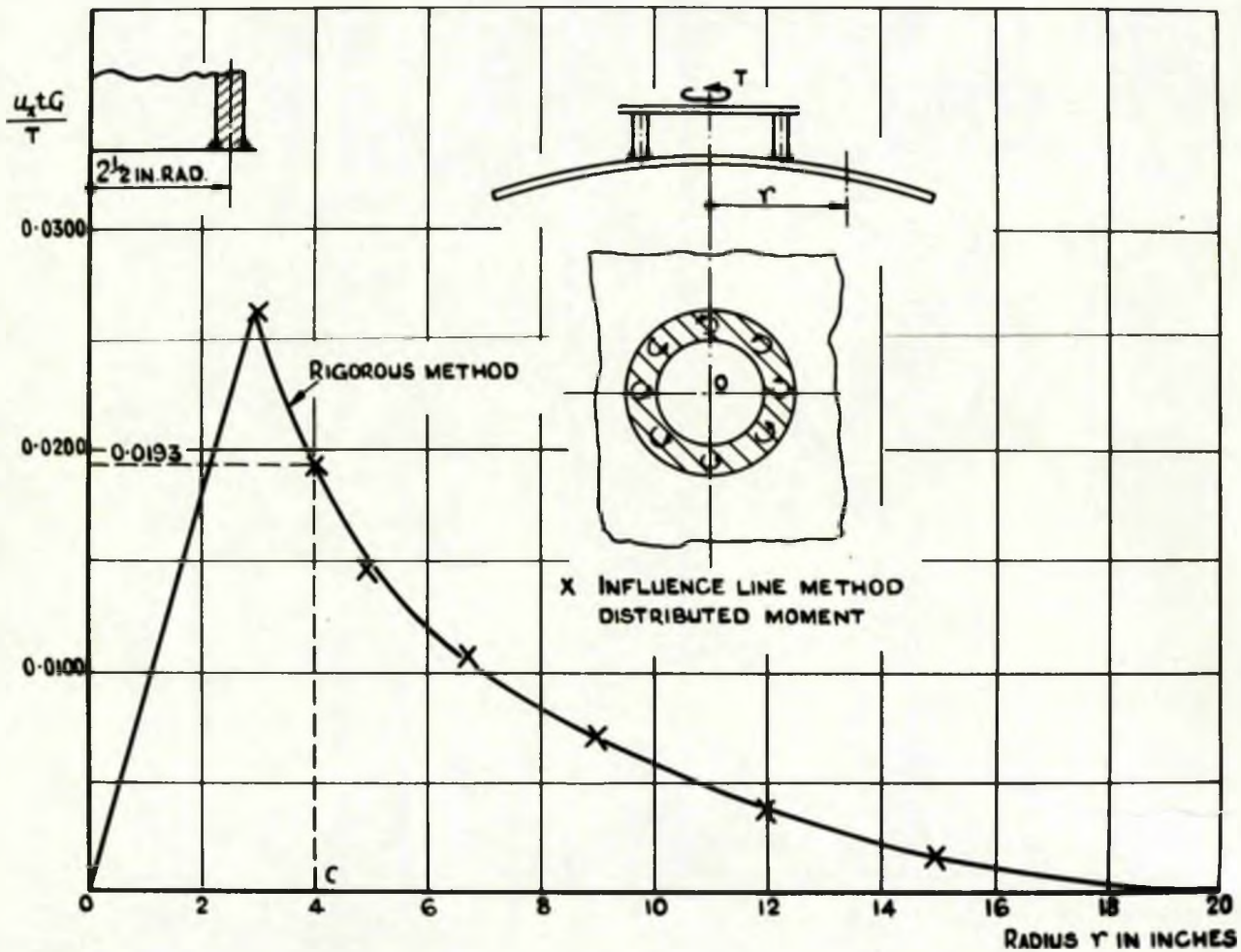
FIG. III 29 THE DISTRIBUTION OF CIRCUMFERENTIAL DISPLACEMENT ON A SHALLOW SHELL DUE TO A UNIFORMLY DISTRIBUTED TWISTING MOMENT ROUND THE CIRCUMFERENCE OF A CIRCULAR RING. A COMPARISON BETWEEN THE INFLUENCE LINE METHOD AND THE RIGOROUS METHOD (INCH UNITS).
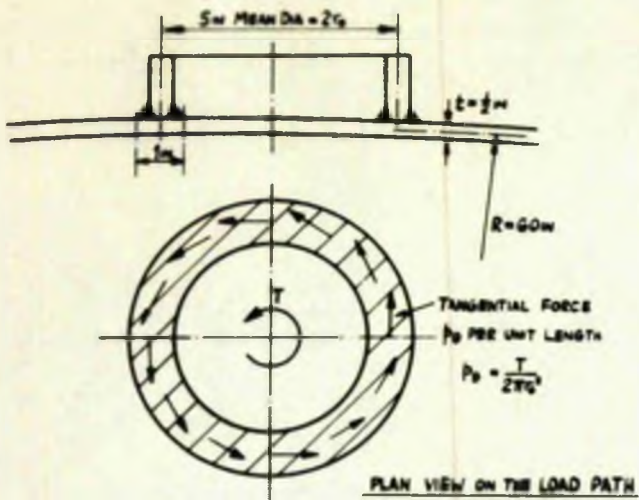
Fig II.30 The Application of a Tangential Shear Force Uniformly
Distributed Round the Circumference of a Circular Ring
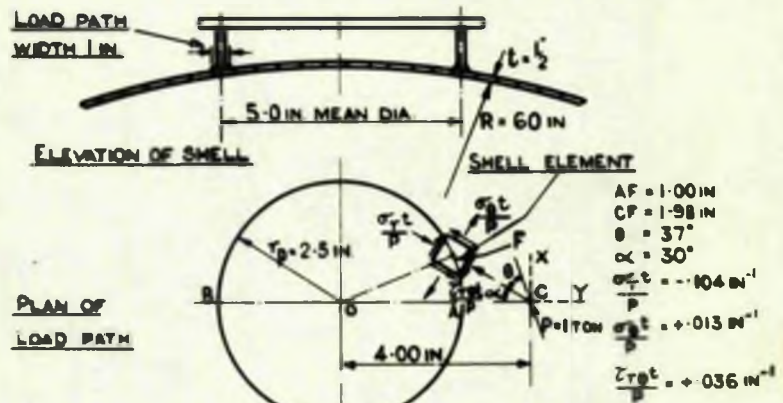
(a) APPLICATION OF UNIT SHEAR LOAD AT C
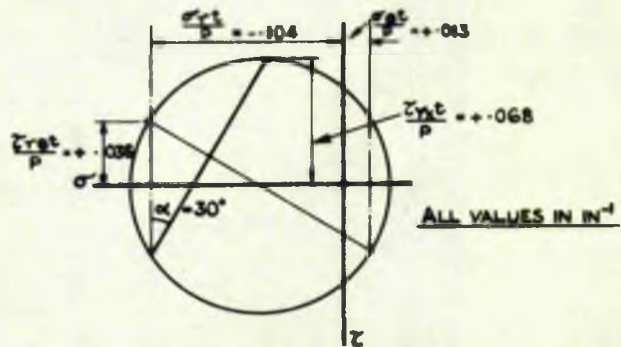
(b) MOHR CIRCLE FOR SHEAR LOAD ACTIONS

Fig II.31 PLAN VIEW OF THE LOADING PATH AB SHOWING THE STRESSES AT F
DUE TO THE UNIT TANGENTIAL SHEAR FORCE AT C

Derivation of Shear Stress Distribution.   Consider a point
C (Fig. III.31) on the surface of the shell at a distance of
r = 4 in measured in plan from the load path centre O, and a
point F on the load path at a distance of 1.98 in from C. The
applied load, p_θ, is removed and a unit tangential load (P = 1)
is imposed at C acting through a rigid circular insert of radius
r_ρ equal to half the width of the load path, in this case 0.5 in.
The line of action of this unit load at C is parallel to the line
of the applied shear at F (tangential to the load path circle at
F).   In the direction it is oriented as shown in Fig. III.31a so
as to satisfy the condition of reciprocal symmetry $\tau_{cf} = \tau_{fc}$ where
τ is the shear stress in the shell due to the appropriate unit
actions.

        The circumferential and meridional normal and shear stresses
due to the unit action at C are obtained from Figs. II.16a,b,
using the curve $r_\rho = 0.50$ in for distance r = 1.98 in which is
the distance of F from C.   These are:-

$$\sigma_{ro} t / p_{\cos\theta} = -0.130, \quad \sigma_{\theta D} t / p_{\cos\theta} = +0.025, \quad \tau_{r\theta} t / p_{\sin\theta} = +0.032$$

Noting that θ for F measured at C is 37°, giving:- $\sigma_{ro} t / p = -0.104$ in^{-1}
$\sigma_{\theta D} t / p = +0.013$ in^{-1} and $\tau_{r\theta D} t / p = +0.036$ in^{-1} .   Resolving these
actions in the X and Y directions by means of a Mohr circle
diagram, Fig. III.31b, it is seen that the shear stress τ_{yx} is
the only action which will have a value at C due to the imposed
loading.   The resultant values of σ_x and σ_y become zero at
C when the imposed load effect is obtained by summation over the
whole load path.   In consequence, the ordinate value at F of the
influence line for shear stress at C due to a unit load traverse

of the load path is $\tau_{yx}t/P = +0.068$ ton/in per ton.   This value,
together with similar values obtained in the same way for other
points on the load path, is plotted on a basis of developed lengt
of load path in Fig.III.32 forming the influence line for shear
stress at C.   The shear stress at C $\tau_{n}t$ due to the imposed
load is thus = Load Intensity x Area under the influence line

$$= p_\theta \times 0.397 \text{ ton/in} \qquad\qquad\qquad \text{(III.21)}$$

The uniformly distributed tangential shear p_θ, round the load
path is equivalent to a total twisting moment T about the
rotational axis, where $T = p_\theta \times 2\pi\, r_o^2$ $\qquad\qquad$ (III.22)
Hence from eqts.III.21 and 22, $\tau_{r\theta}t/T = 0.0255 \times 0.397 = 0.0102\left(\frac{ton}{in}\right) per\, ton\cdot in$
This value is shown plotted, in Fig.III.33, against the radial
distance of 4in, relevant to the point C.

Repeating the above procedure for other locations on the
great circle, the complete distribution is obtained- Fig.III.33
This is compared with the Rigorous Method given in Appendix VII
Derivation of Circumferential Displacement Distribution.   As in
the case of the derivation of shear stress, the behaviour of th
shell at F is examined due to the tangential shear force at C.
From Fig.II.17, for the curve $r_\rho = 0.50$in at the point r = 1.98in,
$\frac{vtG}{P\cos\theta} = +0.247$ and $\frac{utG}{P\sin\theta} = -0.200$.   Using the appropriate values
for $\cos\theta$ and $\sin\theta$, vtG/P = 0.197 and   utG/P = -0.120 -Fig.III.34a
Combining vtG/P and utG/P as in Fig.III.34b the resultant value
in the X direction is, $u_x tG/P = -0.205$.   The resultant values
in the Y direction becomes zero at C when the imposed load effe
is evaluated by summation over the whole load path.   The ordin-
ate value at F of the influence line for circumferential disp-
lacement is thus $u_x tG/P = -0.205$ ton/ton   (Fig.III.35)
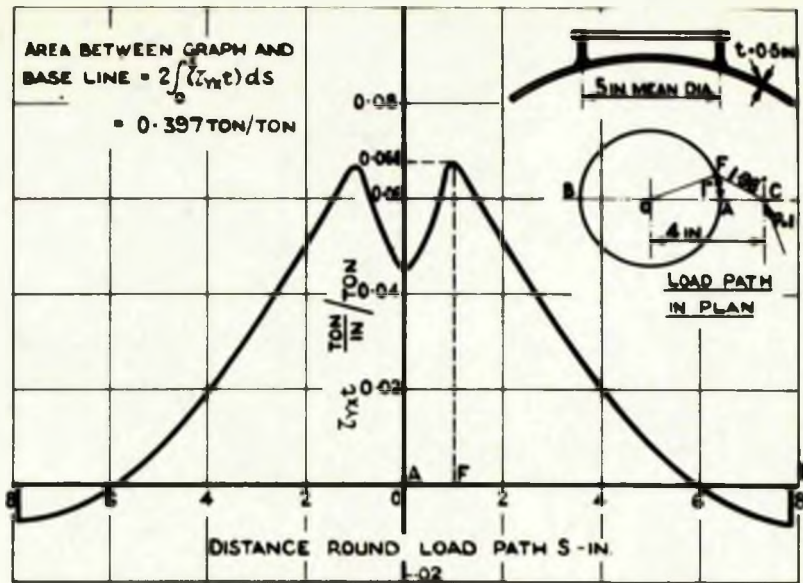
FIG. III.32   INFLUENCE LINE FOR SHEAR STRESS AT C BY TANGENTIAL SHEAR FORCE (INCH UNITS)
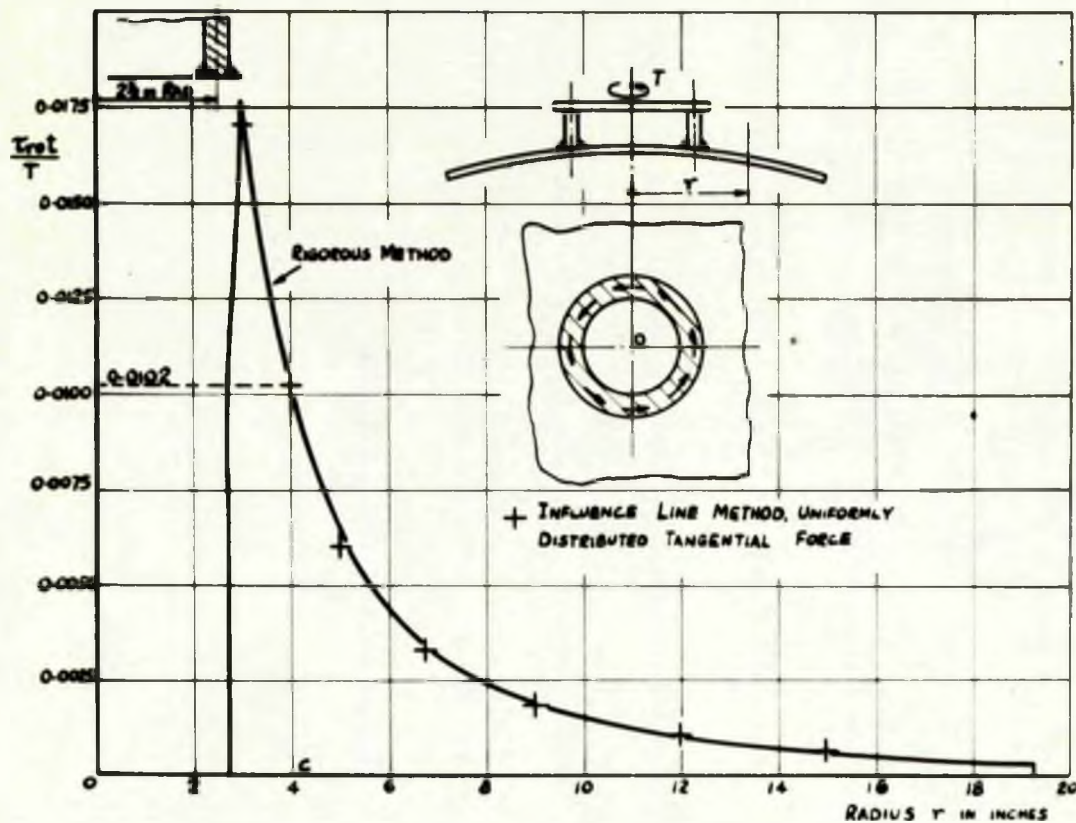
FIG. III.33   THE DISTRIBUTION OF SHEAR STRESS ON A SHALLOW SHELL DUE TO A UNIFORMLY DISTRIBUTED TANGENTIAL SHEAR FORCE ROUND THE CIRCUMFERENCE OF A CIRCULAR RING - A COMPARISON BETWEEN THE INFLUENCE LINE METHOD AND THE RIGOROUS METHOD (INCH UNITS)

APPLICATION OF UNIT SHEAR LOAD (a)
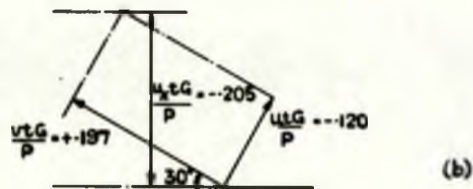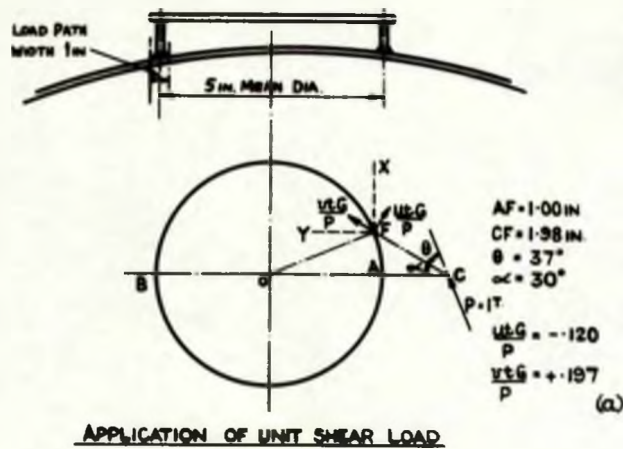
DERIVATION OF DISPLACEMENT IN X - DIRECTION (b)

FIG. III.34 PLAN VIEW SHOWING THE DISPLACEMENTS AT F DUE TO THE UNIT TANGENTIAL SHEAR FORCE AT C
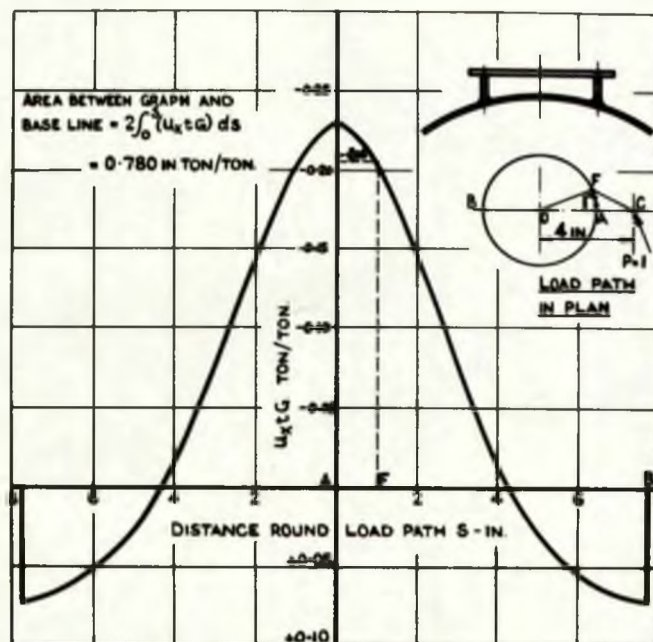
FIG. III.35 INFLUENCE LINE FOR CIRCUMFERENTIAL DISPLACEMENT AT C BY TANGENTIAL SHEAR FORCE (INCH UNITS)
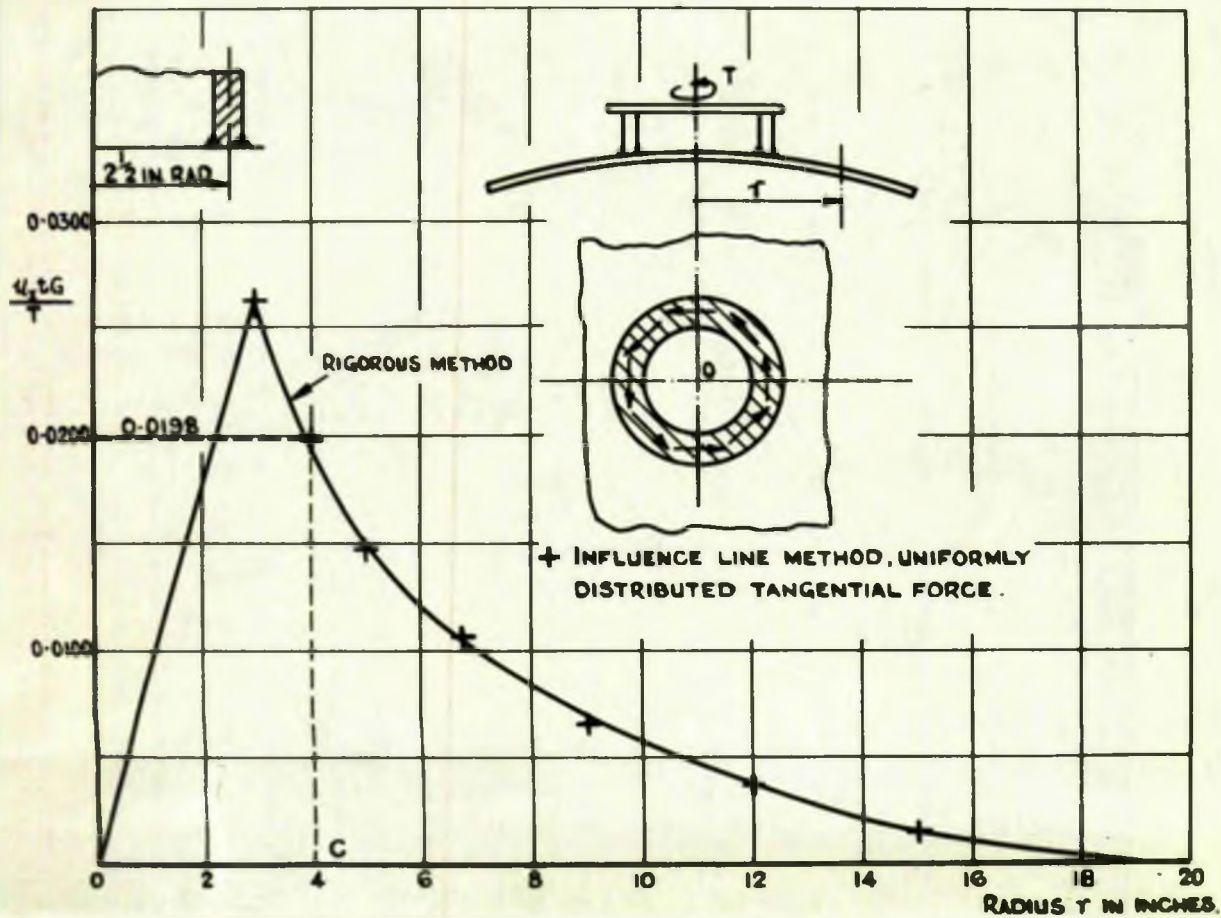
FIG. III 38 THE DISTRIBUTION OF CIRCUMFERENTIAL DISPLACEMENT ON A SHALLOW SHELL DUE TO A UNIFORMITY DISTRIBUTED TANGENTIAL SHEAR FORCE ROUND THE CIRCUMFERENCE OF A CIRCULAR RING - A COMPARISON BETWEEN THE INFLUENCE LINE METHOD AND THE RIGOROUS METHOD (INCH UNITS)

The complete influence line is obtained by considering other points on the load path.   The resultant circumferential displacement at C due to the imposed loading is thus :-

utG = (Load Intensity) x Area under Influence Line

utG = p_θ x 0.780

From eqt. III.22 $utG/T = 0.0198 \, in^{-1}$

This value is plotted on Fig. III.36 against the radial distance of 4 in relevant to the point C.

Repeating the above procedure for other locations on the great circle, the complete distribution is obtained.   This is compared with the Rigorous Method (given in Appendix VIII.6) on Fig. III.36.

It is seen that for both the shear stress and tangential displacement distributions along the great circle, excellent agreement is obtained between the Rigorous Method and the Influence Line Method.

III.6   THE INTERACTION EFFECTS BETWEEN A SPHERICAL SHELL AND A CYLINDRICAL SKIRT

In order to obtain the induced stresses in any vessel, due to the constraining effects of the supports or the flexibility of the loading attachment, it is first necessary to determine the redundant forces present at the point, or surface, of attachment. The approach in such a case is to equate the displacements and rotations of the various elements, and from these relationships compute the redundant actions - forces and moments. In obtaining the displacements and rotations, the influence line analysis is

particularly valuable - since it enables complex forms to be
readily dealt with.

In order to illustrate the method the following example is
presented.

A complete spherical steel shell, subjected to an internal
pressure p, is rigidly connected to a cylindrical steel skirt
support as shown in Fig. III.37a.   It is required to evaluate
the redundant actions q and m as indicated in Fig. III.37b.
In the particular example chosen, the sphere has a constant
thickness t_s = 1.75 in and diameter 135 ft ⌐ 0 in and the skirt
thickness t_c = 1.312 in.

Considering in the first place the deflections of the shell

The force q - which is the redundant force in the horizonta
direction - is uniformly distributed round the intersection and
can be considered as consisting of two components, namely - radi
and tangential at the surface.   The radial deflection caused b
the radial component of q is obtained by considering the influer
line for radial deflections for any point such as 0 on the load
path.

In this case the load path width is taken as the thickness
of the skirt at its intersection with the sphere, measured tan-
gential to the sphere, and is equal to 1.454 in.   Thus the
value of r_p is 0.727 in. From the sphere dimensions
$\ell = \sqrt{Rt}/\sqrt{12(1-v^2)}$ = 20.71 in   and $\mu = r_p/\ell$ =   0.035

Utilising the basic curve for radial deflection given from
Fig. III.5, it being noted that for this small value of μ the
uniformly distributed and rigid insert graphs are identical for
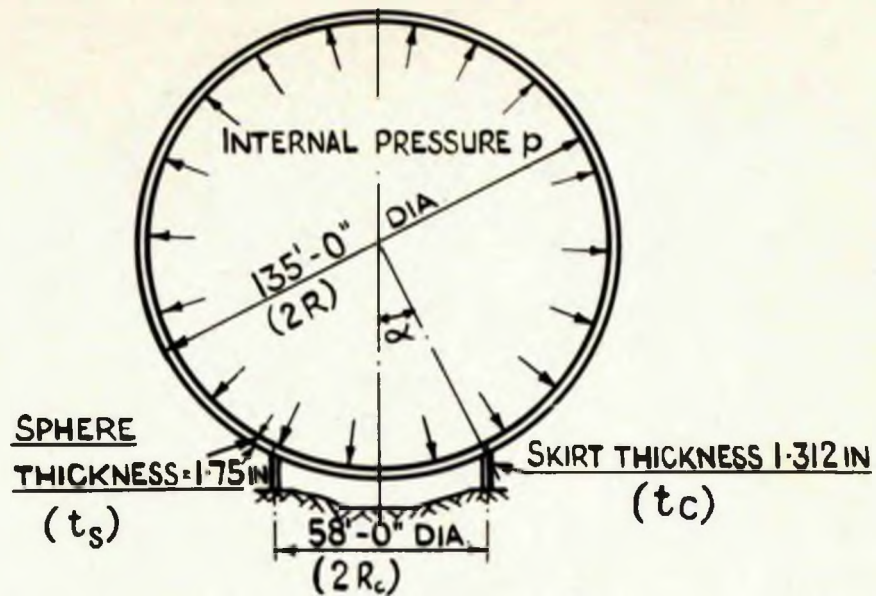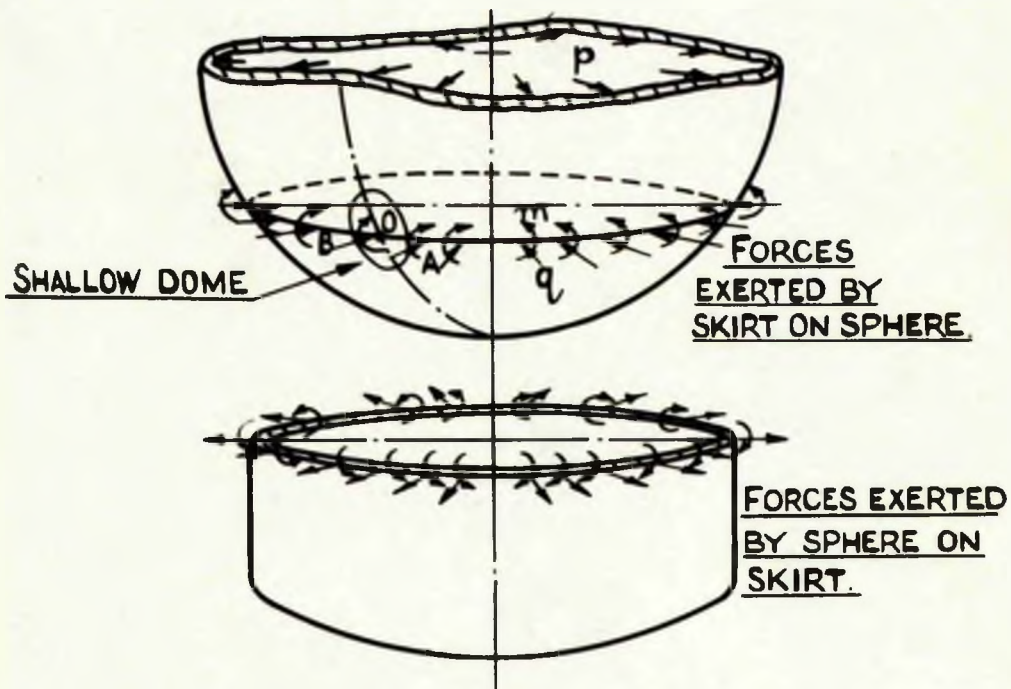
FIG. III·37 THE INTERACTION EFFECTS BETWEEN A SPHERICAL SHELL AND A CYLINDRICAL SKIRT

The plot shows:
- Vertical axis: RADIAL DEFLECTION INCHES/TON, peaking at 0.90×10^{-2} IN/TON
- Horizontal axis: DISTANCE ROUND LOAD PATH S IN.

AREA UNDER CURVE
$= 46.6 \times 10^{-2}$ IN^2/TON

$r_p = 0.727$ IN $\quad t = 1.75$ IN $\quad$ A

$R = 67.5$ FT.

$$\ell = \frac{\sqrt{Rt}}{\sqrt[4]{12(1-\upsilon^2)}} = 20.71 \text{ IN}$$

$$\mu L = \frac{r_p}{\ell} = \frac{0.727}{20.71} = 0.035$$

$$E = 13400 \text{ TON/IN}^2$$

$$\upsilon = 0.28$$
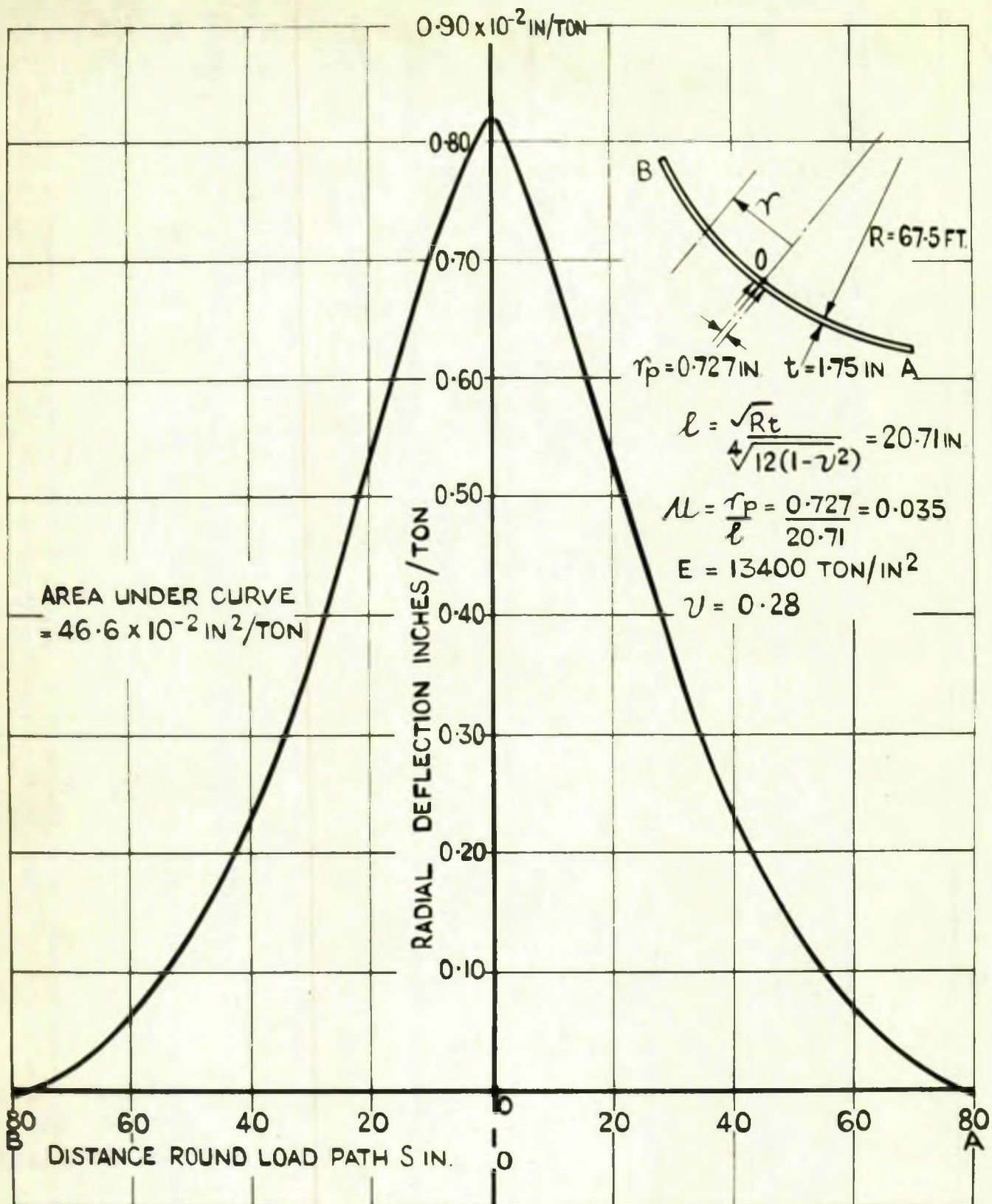
FIG. III 38   THE INFLUENCE LINE FOR RADIAL DEFLECTION AT O

all relevant points of r/ℓ , the influence line for deflection

at O can be constructed.   This is shown in Fig. III.38.

Thus the radial deflection of the sphere due to the __horizontal__

load q per unit length $=$ q sinα x area under influence line

$$= q \times \frac{58}{135} \quad \times 46.6 \times 10^{-2}$$
$$= 20.0 \times 10^{-2} q \quad \text{radially inwards.}$$

Due to the internal pressure p the change in radius of

the sphere (free membrane action only) $= \frac{pR^2}{2Et_s}(1-\upsilon)$

where $t_s = 1.75$ in and corresponds to the thickness of

the sphere.

The change in radius due to p $= \dfrac{p(135 \times 12/2)^2(1-0.28)}{2 \times 13400 \times 1.75} = 9.79p$ radially outwards

Thus the radial deflection $=$ $9.79p - 20.0 \times 10^{-2} q$

The horizontal deflection $=$ $(9.79p - 20.0 \times 10^{-2} q)$ sinα (III.23)

It will be noted that the influence of the tangential com-

ponent of q, acting on the sphere can be evaluated in a manner

similar to that of the radial component, but using the tangential

load data as in Section III.5.   However, it can be shown that

its effect is of negligible order and in consequence it has been

disregarded in eqt. III.23.

The horizontal deflection of the cylindrical skirt due to

a uniformly distributed force q and moment m (the standard case

of an edge loaded cylinder, ref. (24)) is given by:-

$\dfrac{1}{2\beta^3 D}(m+q)$ where in this case $D = \dfrac{Et_c^3}{12(1-\upsilon^2)}$ and $\beta^4 = \dfrac{3(1-\upsilon^2)}{R_c^2 t_c^2}$

Also in this case the radius of the cylindrical skirt, $R_c = 29$ ft

and the wall thickness of skirt, $t_c = 1.312$ in.

Thus horizontal deflection of the skirt $=$ $0.0496m + 0.828q$ (III.24)

Equating horizontal deflection of sphere and skirt, from eqts.III.23

and 24:- $9.73p = 0.115m + 2.125q$ (III.25)

In the second place, by considering the rotation of the sphere and cylinder another equation involving m and q can be found.

The change of slope of the sphere in the plane of moment m at any point, O, on the attachment line due to the moment m per unit length, is obtained from the influence line for the change of slope at the point O.

In order to derive this influence line the relationship between the slope change and the radius must be obtained.

It is seen from eqt. II.63a that:- $w = (C_3 \ker' r_1/_\ell + C_4 \kei' r_1/_\ell)\cos\theta$
This relationship predicts the radial deflection, w, at a point r, θ on the shell, where the constants C_3 and C_4 are obtained from eqts. II.67a,b.

Since the change of slope in the plane of the moment m is required, it is necessary to obtain the change of slope at various distances from O along the intersection circle OA and in planes containing the lines of the great circles (Fig. III.39a),

i.e. $\dfrac{dw}{dr_2}$ at $\theta = \pi/2$.

From eqt. II.63a:- $\dfrac{dw}{dr_2} = \left[C_3 \ker'' r_1/_\ell + C_4 \kei'' r_1/_\ell\right]\dfrac{d\,r_1/_\ell}{dr_2}\cos\theta + \left[C_3 \ker' r_1/_\ell + C_4 \kei' r_1/_\ell\right](-\sin\theta)\dfrac{d\theta}{dr_2}$

At $\theta = \pi/2$ $\dfrac{dw}{dr_2} = \left[C_3 \ker' r_1/_\ell + C_4 \kei' r_1/_\ell\right](-1)\dfrac{d\theta}{dr_2}$

Since $\cos\theta = r_2/r$ and $r = \sqrt{r_1{}^2 + r_2{}^2}$, $\dfrac{d\theta}{dr_2} = -\dfrac{r_1{}^2}{r^3 \sin\theta}$

and when $\theta = \dfrac{\pi}{2}, \dfrac{d\theta}{dr_2} = -\dfrac{1}{r_1}$ i.e. $\dfrac{dw}{dr_2} = (C_3 \ker' \dfrac{r_1}{\ell} + C_4 \kei' \dfrac{r_1}{\ell})\dfrac{1}{r_1}$ (III.26)

From eqt. III.26 the influence line Fig. III.39b can be drawn, yielding a value for the change of slope of the sphere

                        = m x area under influence line

                        = m x 11.18 x 10^{-4}
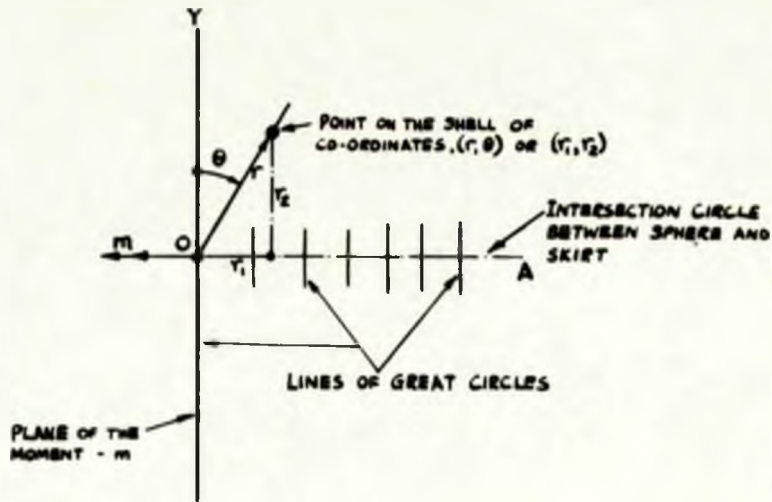
Fig III.39a   VIEW ON THE LOADING PATH OA
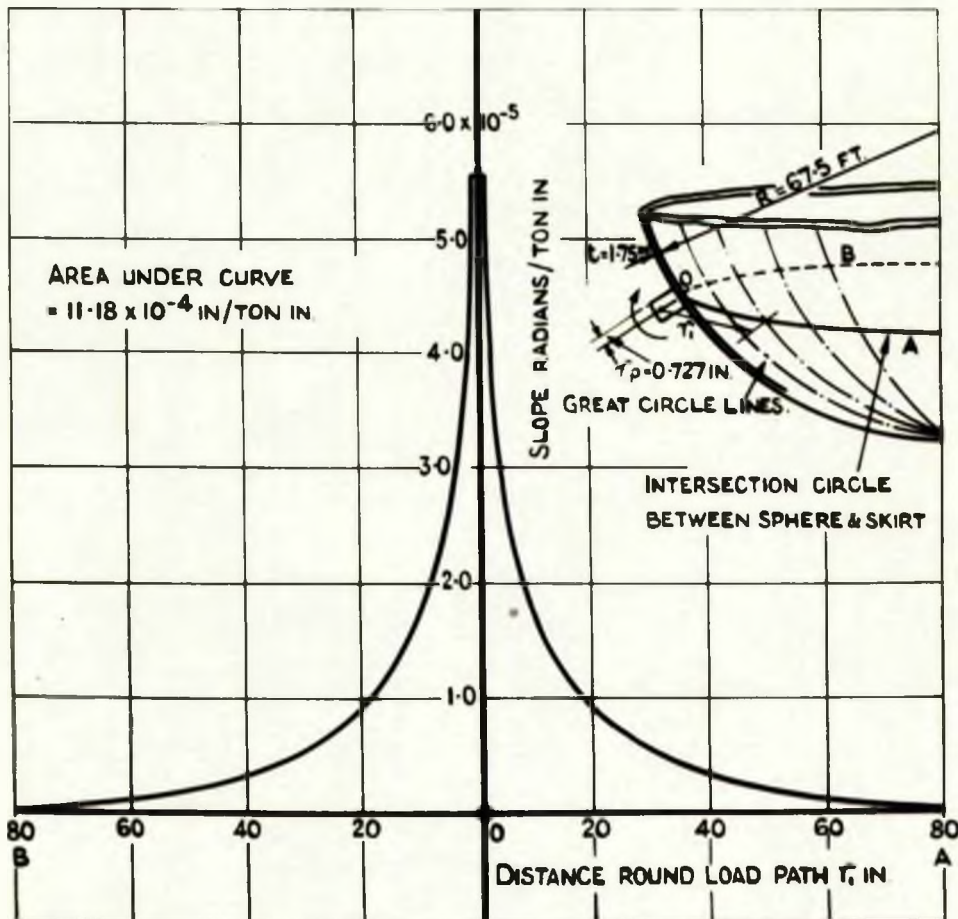
FIG. III.39b   INFLUENCE LINE FOR CHANGE OF SLOPE AT O

FIG. III.39   CONSIDERATION OF CHANGE OF SLOPE OF THE SPHERE AT O

The change of slope of the cylinderical skirt due to q and m

$$= \frac{1}{2\beta^2 D} (2\beta m + q) , \quad \beta \text{ and } D \text{ being as before}$$

$$= 0.00596m + 0.0497q$$

Equating changes of slope for the sphere and skirt:-

$$-11.18 \times 10^{-4} \ m = 0.00596m + 0.0497q \qquad (III.27)$$

From eqts. III.25 and 27 $q = 7.42 \ p$

$$m = -52.09 p$$

The author, in ref. (58), has obtained these redundant actions using the analysis suggested by <u>HICKS</u>[58] for the particular example put forward in this section.   The following results were obtained:-

$q = 7.39p$, $m = -51.90p$, which are seen to be very close to those obtained by the Influence Line Method.

It may, therefore, be concluded that the method put forward in this chapter is an entirely valid method of approach.   Where alternative analyses were used to compare the results obtained by the Influence Line Method, the agreement is seen to be excellent.

The Influence Line Method was further substantiated by experimental investigation; these are discussed in Chapter IV.

CHAPTER IV.   EXPERIMENTAL INVESTIGATIONS

The experimental investigations presented in the thesis were designed to evaluate the basic actions of radial and tangential loading, bending and twisting moment presented in Chapter II.

The experimental scheme was further directed to examine the extent to which the shallow shell concept may be applied, to assess the range of applicability of the principle of super-position and to verify the Influence Line Method by an experimental examination of certain of the specific cases discussed in Chapter III.

The work was carried out on shallow shell segments of 60 in radius and of $\frac{1}{4}$ in, $\frac{1}{2}$ in and 1 in thicknesses, and on a complete sphere, of 13 ft. 6 in diameter, built-up from plates of various thicknesses, thus permitting the degree of approximation introduced by the 'shallowness concept' to be evaluated by direct experiment.

CHAPTER IV.   EXPERIMENTAL INVESTIGATIONS

IV.1   BASIC ACTIONS

    IV.1.1   RADIAL LOAD

        (a)   Uniformly Distributed over a circular area

        (b)   Applied via a rigid stud

    IV.1.2   'BENDING' MOMENT

    IV.1.3   'TWISTING' MOMENT

    IV.1.4   TANGENTIAL LOAD

IV.2   THE SHALLOW CAP CONCEPT

    IV.2.1   BOUNDARY EFFECTS

    IV.2.2   STRESSES AND DEFLECTIONS

    IV.2.3   SUPERPOSITION OF SHALLOW CAPS

IV.3   EXAMINATION OF SELECTED COMPOSITE ACTIONS

    IV.3.1   RADIAL RING LOADS

        (a)   Transmitted by a Freely supported ring

        (b)   Transmitted by a rigidly fixed ring

    IV.3.2   RING 'BENDING' MOMENT

    IV.3.3   RING 'TWISTING' MOMENT

P

DIAL
GAUGES

STEEL SHOT, OR WATER FILLED
RUBBER MEMBRANE

$\frac{1}{4}$ IN.

SHELL UNDER TEST

60 IN. R

EXTENDED TABLE
SUPPORT

LOWER PLATEN
OF TESTING MACHINE

3 FT. 3 IN.
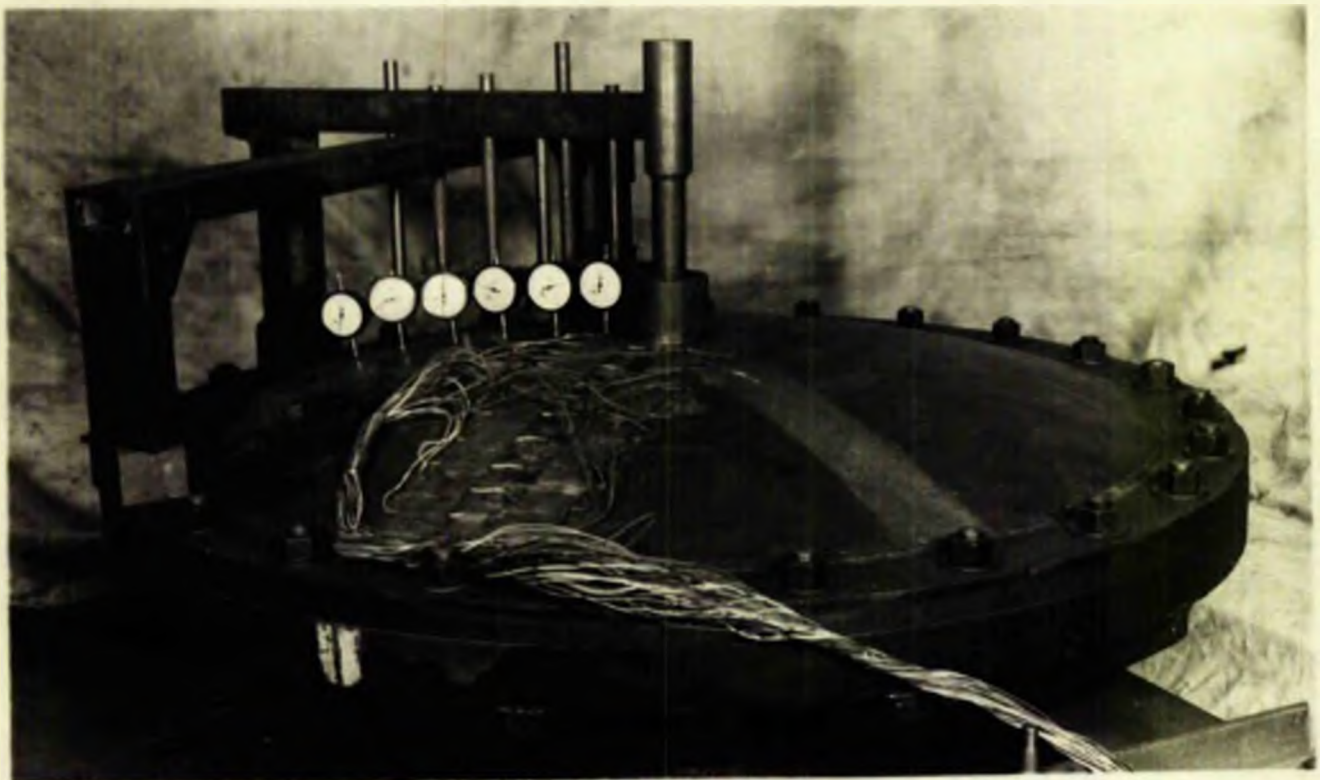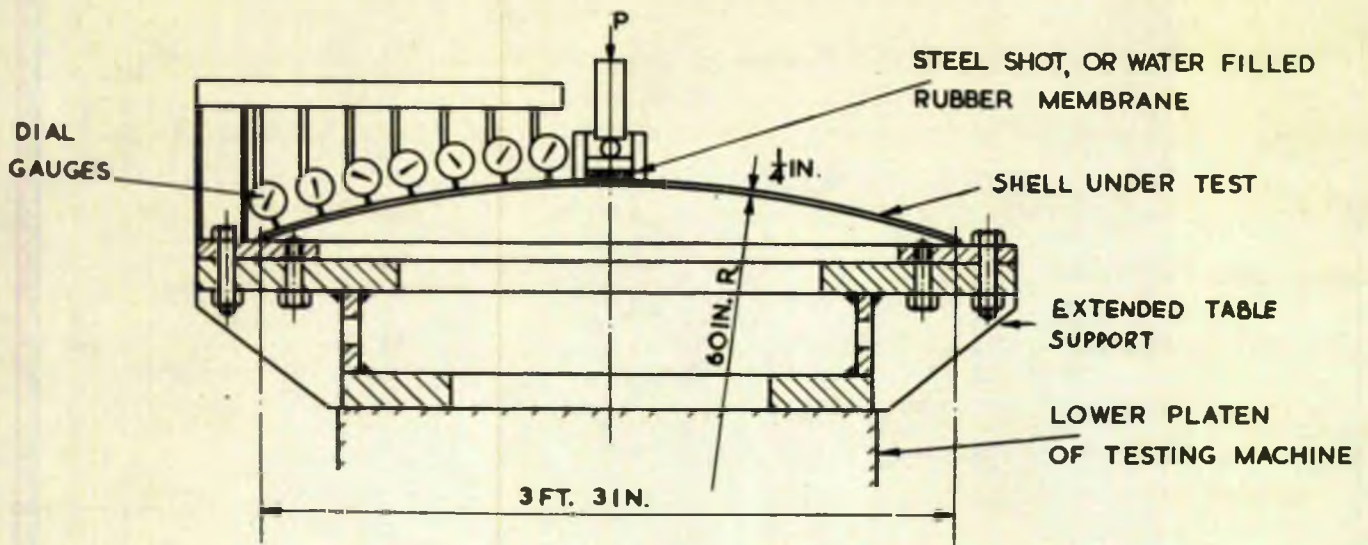
Fig. IV.1   Arrangement of Shallow Spherical Shell under Radial
Loads Uniformly Distributed Over a Circular Area.

IV.1 BASIC ACTIONS

IV.1.1 RADIALLY APPLIED LOADS

The radial loads were applied to the shallow shell segments in two ways. In the first place, uniformly distributed over a circular area, and in the second place by means of a stud welded to the shell, this being considered equivalent to a rigid insert. In the case of the complete sphere it was only possible to investigate the rigid insert case of radial loading.

(a) Uniformly Distributed Over a Circular Area

Experimental Model:- The investigations for this type of loading have been carried out on shallow spherical shells of 1 in and $\frac{1}{4}$ in thickness and of 60 in internal radius.   At the boundary (3ft.$3\frac{1}{4}$in and 3 ft. 3 in chord diameters, for 1 in and $\frac{1}{4}$ in respectively) the shells were welded to heavy flange rings $1\frac{1}{8}$ in thick, 3ft.10in outside diameter and 2 ft. $8\frac{1}{2}$ in inside diameter.   These flange rings were then bolted, using fitted bolts, to a heavy base in the form of an extended table.   A typical assembly is shown in Fig. IV.1.

Loading Technique:-   The shallow spherical shells were subjected to a radial load uniformly distributed over areas of various diameters. On the $\frac{1}{4}$ in thick shell these areas were of $\frac{1}{4}$, $1\frac{1}{4}$, $2\frac{1}{2}$, 5, $7\frac{1}{2}$, 10 and 12 in diameters.   In the experiments on the 1 in thick shell the $\frac{1}{4}$ in diameter was omitted.

The technique of applying a uniformly distributed load was varied to suit the magnitudes of the loads required to produce measurable strains.   In the case of the 1 in thick shell, the loading device consisted of a piston acting on steel shot of

approximately 1 in depth contained in a cylinder, the shot (of
approximately $\frac{1}{32}$ in diameter), being the loading medium between
the piston and the shell (Fig. IV.1).   Tests of the loading
set up on aluminium plate, indicated that the shot produced a
uniform distribution of shot marks over the whole of the loaded
area.   It was, therefore, considered that under such an arran
ment the shell would undergo uniformly distributed loading. Fo
this type of loading, the measurement of strains was restricted
to the region outside the loaded area as attempts to obtain
reliable readings from strain gauges under the load and in con-
tact with the shot were unsuccessful.

In loading the $\frac{1}{4}$ in thick shell an alternative loading
technique was adopted permitting the measurement of strains bot
inside and outside the loaded area because of the considerably
lower loads required to produce measurable strains.   The shot
in this case was replaced by water contained in a thin rubber
membrane and the strain gauges under the rubber membrane were
found to perform satisfactorily.   Tests were carried out to
estimate the effect of the normal pressure on the characteristi
of the strain gauges, and it was found that under the pressure
applied during testing, these effects were small and could be
neglected.   In order to contain the rubber membrane within t
cylinder, carpenter's putty was used to provide a small fillet
between the cylinder and the shell.   This material was found
to be ideal since it hardened under pressure.

In both types of loading the piston was designed to allow
the radial load to be applied through a steel ball bearing of

$1\frac{1}{4}$ in diameter situated as close to the surface of the shell as possible, thus reducing the possibility of any applied moment.

These tests were carried out in the compression side of a Universal Testing Machine. The loads were applied to the shell either by the loading ram of the machine itself or by a dynamometer, in this case a proving ring, placed between the fixed head and the load point on the shell. These alternatives were used as required appropriate to the magnitude of the load applied.

Measurement of Strain and Deflection. Circumferential and meridional strains were measured on the outer (loaded) and inner surfaces of the shells using, in the first place, Maihak strain gauges positioned in the above directions, on several great circles passing through the crown. These results established the rotational symmetry of the crown loaded system, and in later tests of this series only one great circle passing through the crown was strain gauged. In certain cases additional gauges were fixed in the vicinity of the load on another great circle near to that which was fully gauged.

Electrical resistance strain gauges of both the bonded wire and foil types were employed in this and in all further tests reported in the thesis. Strain gauge details which are common to all loadings will be discussed in this section.

Calibration:- In order to obtain a gauge factor for the strain gauges a selection from each batch of gauges was fixed to a standard calibration set-up, using exactly the same fixing techniques as those employed by gauges fixed to the actual shells

Layout:-   The layout of the strain gauges on the various shell; was such that in the region of high stress gradient the gauges were closely grouped together, while in other areas they were relatively more widely spaced.   For the loads dealt with, the region of high stress gradient is in the immediate vicinity of the load.

Zero Drift:-   During the tests routine checks for zero drift were incorporated.   It was found that accurately repeatable results were obtained when readings of the gauges were taken in batches of fifteen, the loading being repeated for each batch.

Loading:-   The loads were applied in a number of increments, usually four, up to the maximum value, readings of strain being recorded throughout.   Each test was repeated three or more times to ensure that repeatability was obtained.   Values of strain per unit load were thus obtained for each gauge.

Derivation of Stress values:-   From the experimental values of the strain per unit load (in the meridional and circumferen; directions), values of the bending and direct stresses per uni; load in both the meridional and circumferential directions wer; determined using the following standard relationships:-

$$\sigma_T^{\,o} = \frac{E}{1-v^2}(\varepsilon_r^o + v\,\varepsilon_\theta^o) \quad ; \quad \sigma_T^{\,i} = \frac{E}{1-v^2}(\varepsilon_r^i + v\,\varepsilon_\theta^i)$$

$$\text{and} \quad \sigma_\theta^{\,o} = \frac{E}{1-v^2}(\varepsilon_\theta^o + v\,\varepsilon_r^o) \quad ; \quad \sigma_\theta^{\,i} = \frac{E}{1-v^2}(\varepsilon_\theta^i + v\,\varepsilon_r^i) \tag{IV.1}$$

where $\sigma_T^{\,o}$, $\sigma_r^{\,i}$, $\sigma_\theta^{\,o}$ and $\sigma_\theta^{\,i}$ are the total meridional and circumferential stresses on the outer and inner surfaces res-pectively, and ε_r^o, ε_r^i, ε_θ^o and ε_θ^i the experimental strain; in the meridional and circumferential directions on the outer
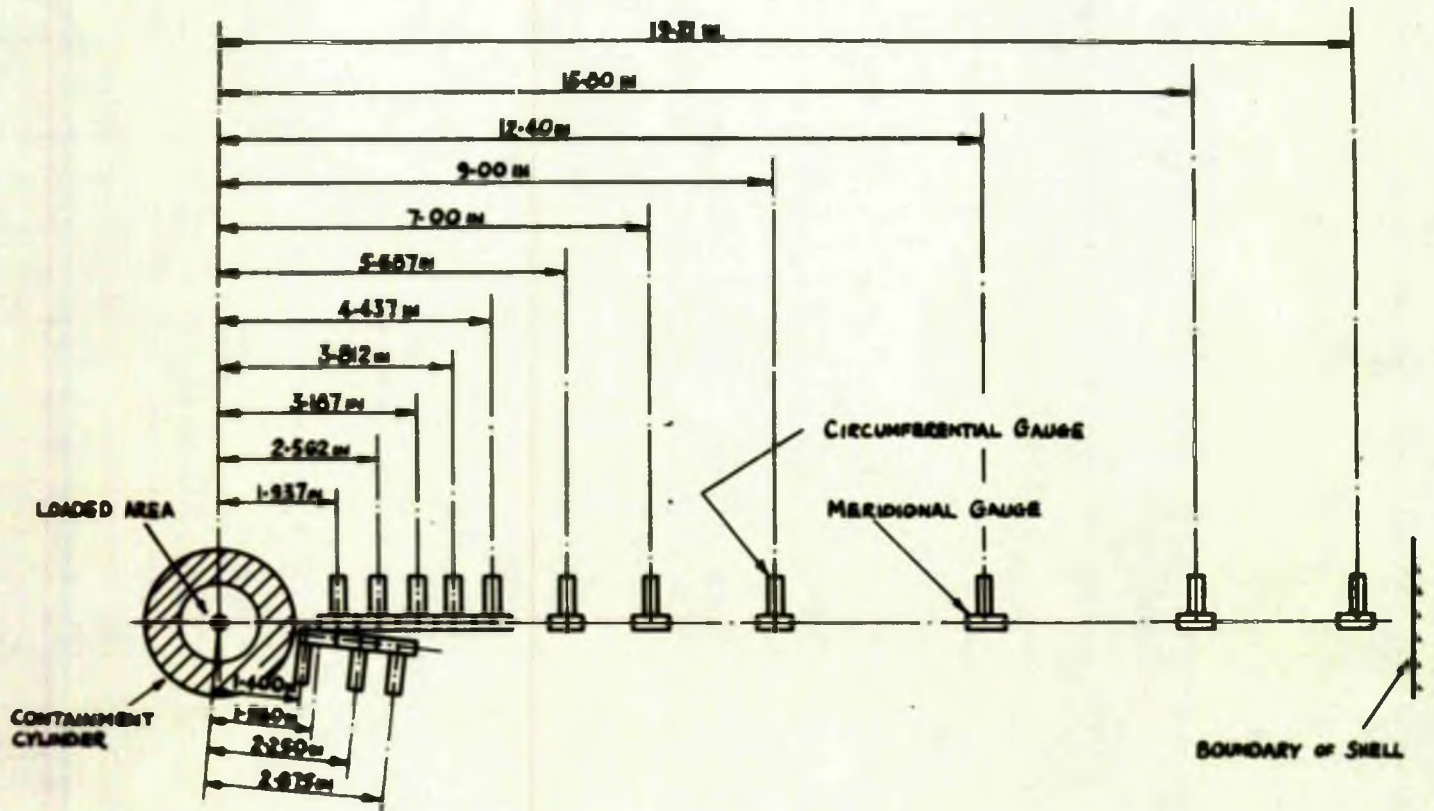
FIG. IV.2   A TYPICAL STRAIN GAUGE LAYOUT FOR INNER AND OUTER SURFACES FOR
UNIFORMLY DISTRIBUTED LOAD TESTS

and inner surfaces.   From these total stresses the bending

and direct stress values are obtained as:-

$$\sigma_{r,B} = \frac{\sigma_r^o - \sigma_r^i}{2} \quad ; \qquad \sigma_{r,D} = \frac{\sigma_r^i + \sigma_r^o}{2}$$

$$\sigma_{\theta,B} = \frac{\sigma_\theta^o - \sigma_\theta^i}{2} \qquad\qquad \sigma_{\theta,D} = \frac{\sigma_\theta^i + \sigma_\theta^o}{2} \qquad\qquad (IV.2)$$

Finally, the experimental values were plotted in non-

dimensional form.

For the present case - radially applied loads uniformly

distributed over a circular area - nichrome wire bonded

electrical resistance strain gauges, of 200ohm and $\frac{1}{2}$in length,

were used.   A typical layout of these gauges is shown in

Fig. IV.2.

The percentage change in resistance in the strain gauges

due to straining of the shell was measured, in this case, using

a 50-way Static Strain Recorder.

Using the procedure outlined above (pp 173-174) the stress

variations were obtained in non-dimensional form for all loading

areas on both thicknesses of shells ($\frac{1}{4}$in and 1in).   A typical

set of results for both thicknesses is shown in Fig. IV.3.   All

results are shown in Appendix VIII.7 where they are compared with

the theoretical values.

The radial deflections of the shell were measured along a

great circle using 0.0001in dial gauges.   The arrangement for

support, adjustment and alignment of the dial gauges is shown in

Fig. IV.1.   The same standard of repeatability was observed in

the deflection measurements as in the measurement of the strains.

In order to obtain the radial deflection at close intervals of

horizontal radius, r, along the great circle, several positions
of the dial gauges were selected, the loading procedure being
repeated for each series.

The results from two such tests, one for each thickness,
are shown graphically, plotted in a non-dimensional manner in
Fig. IV.3.   The complete results are shown in Appendix VIII.7
where they are compared with the theoretical values.

(b) Radial Loads applied by means of a rigid stud welded to
     the shell.

A series of stud-attachments on both a shallow shell and
a complete sphere have been examined under the application of a
radial load.   Discussion of these is grouped in two sections,
the one dealing with the shallow shell, the other with the
complete sphere.

Shallow Shell -

Experimental Model:-

A shallow shell of $\frac{1}{4}$in thickness and 60in radius was welded
at its outer boundary - a 3 ft. 3in chord diameter - to a heavy
flange ring, and mounted as in the previous case on a heavy base
in the form of an extended table.   At the crown of the shell a
radial cylindrical insert (0.978in dia., i.e. $\mu = 0.23$) penetrated
the shell, being welded to the shell on both outer and inner sur
faces by continuous fillet welds.   On the outer surface the
weld was machined to retain the cylindrical form of the insert
Fig. IV.4.

Loading Technique.   The radial loading was applied to the she
by means of a loading frame, thrust washer, 600lb. proving ring
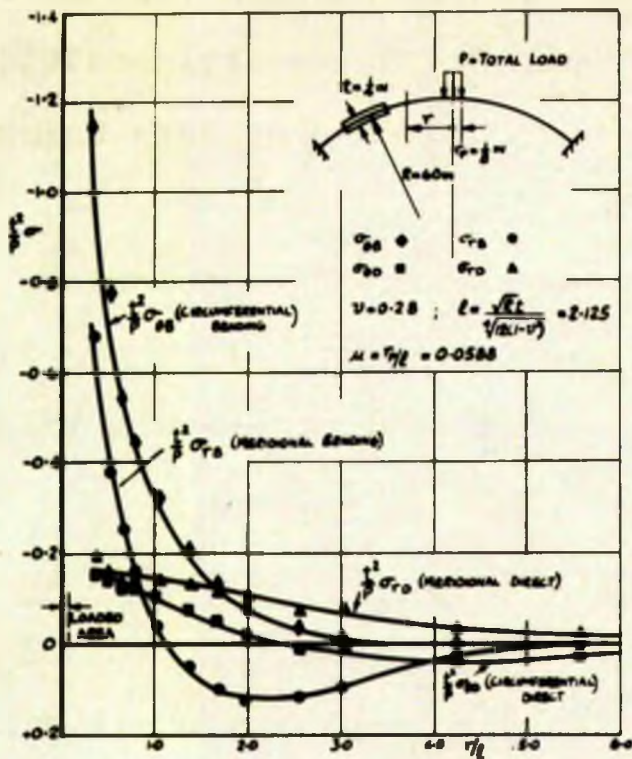
Fig. IV.3a Direct Stress and Bending Stress on the outer surface due to a u.d. load P on a ½in Thick Shell
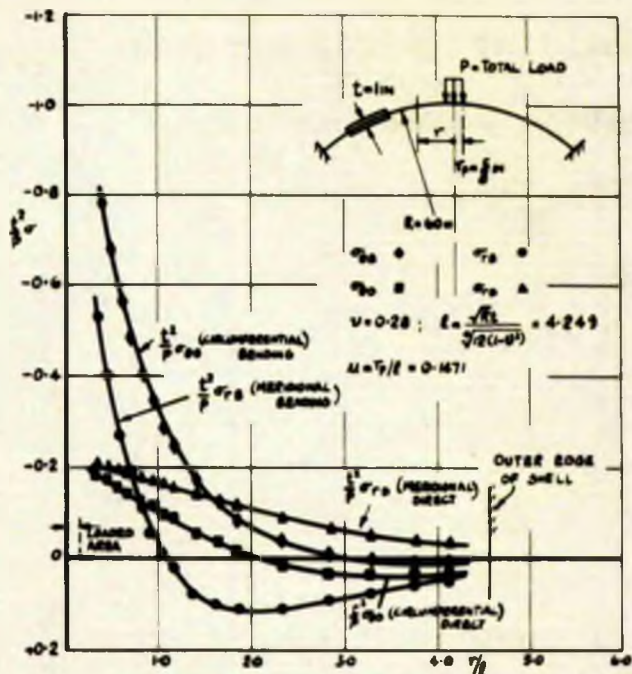
Fig IV.3b Direct Stress and Bending Stress on the outer surface due to a u.d load on a 1in Thick Shell
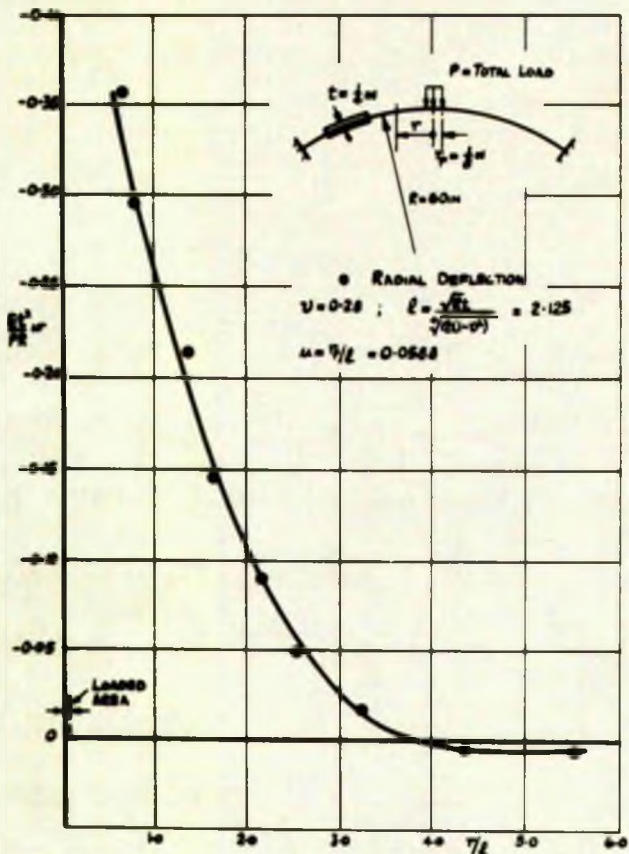
Fig. IV.3c Radial Deflection due to a u.d. load P on a ½in Thick Shell
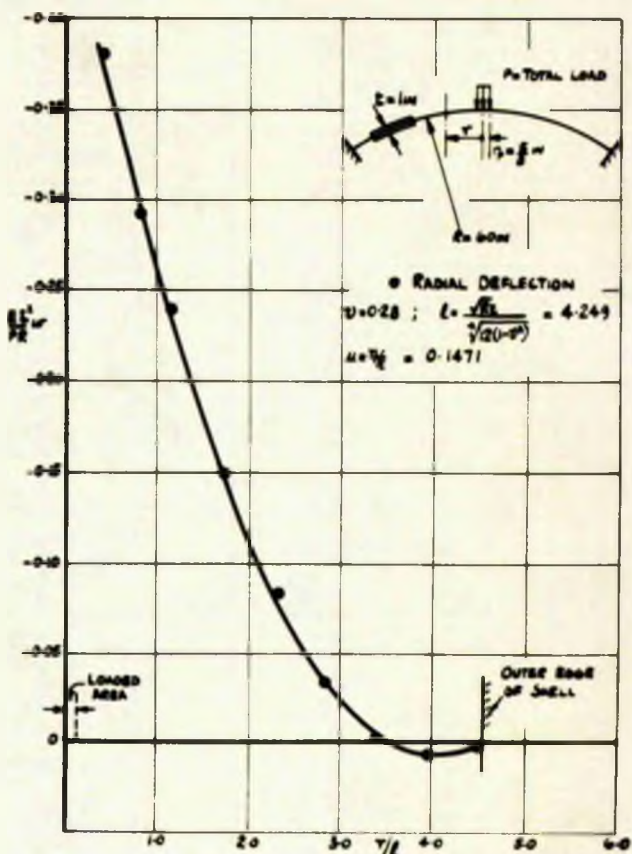
Fig. IV.3d Radial Deflection due to a u.d load P on a 1in Thick Shell

Fig. IV.3 Experimentally obtained Direct Stress, Bending Stress on the outer surface and Radial Deflections of a shallow spherical Shell due to a Radial load P, uniformly Distributed over a circular area – Typical Results for ½in and 1in thicknesses
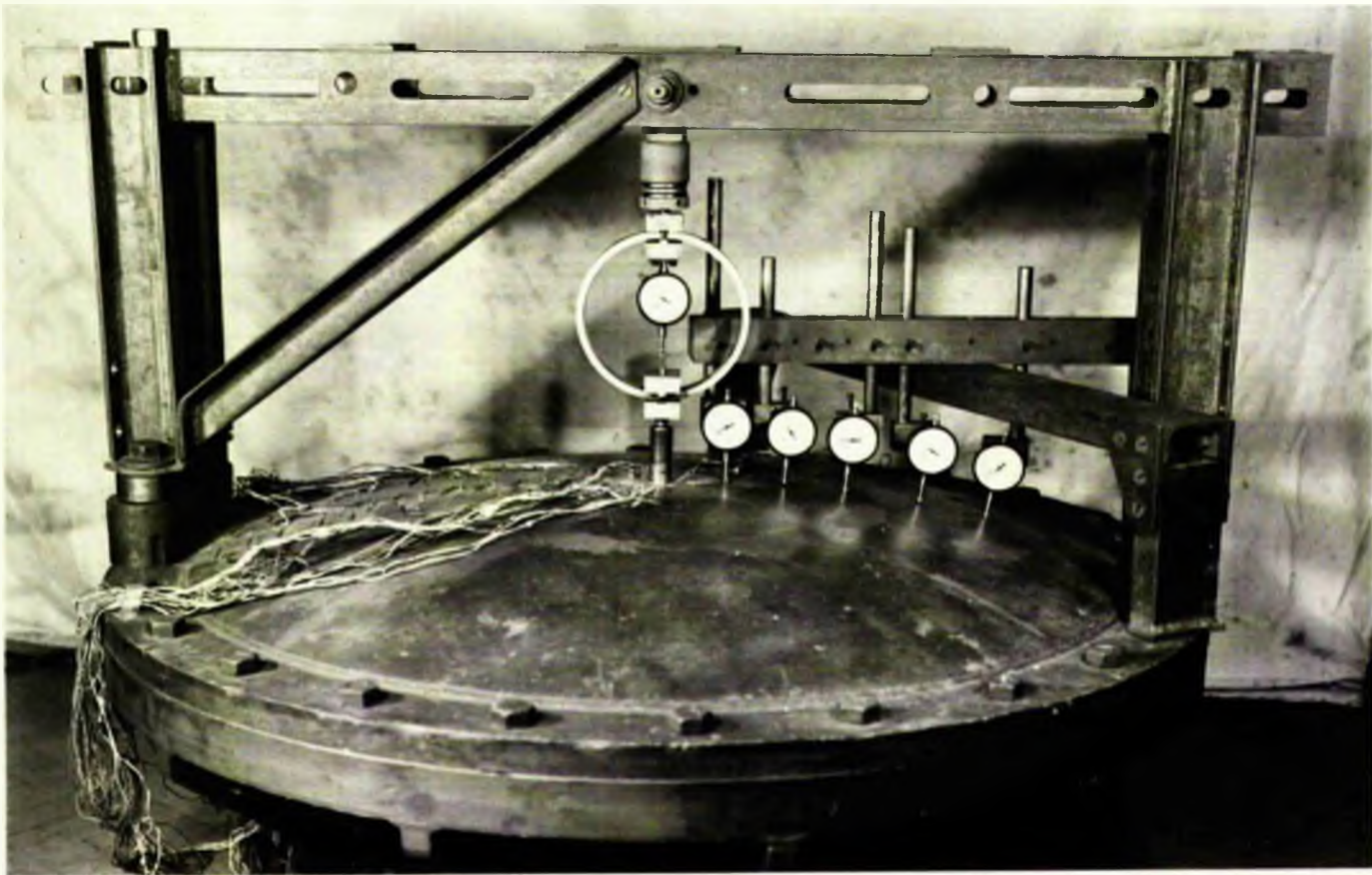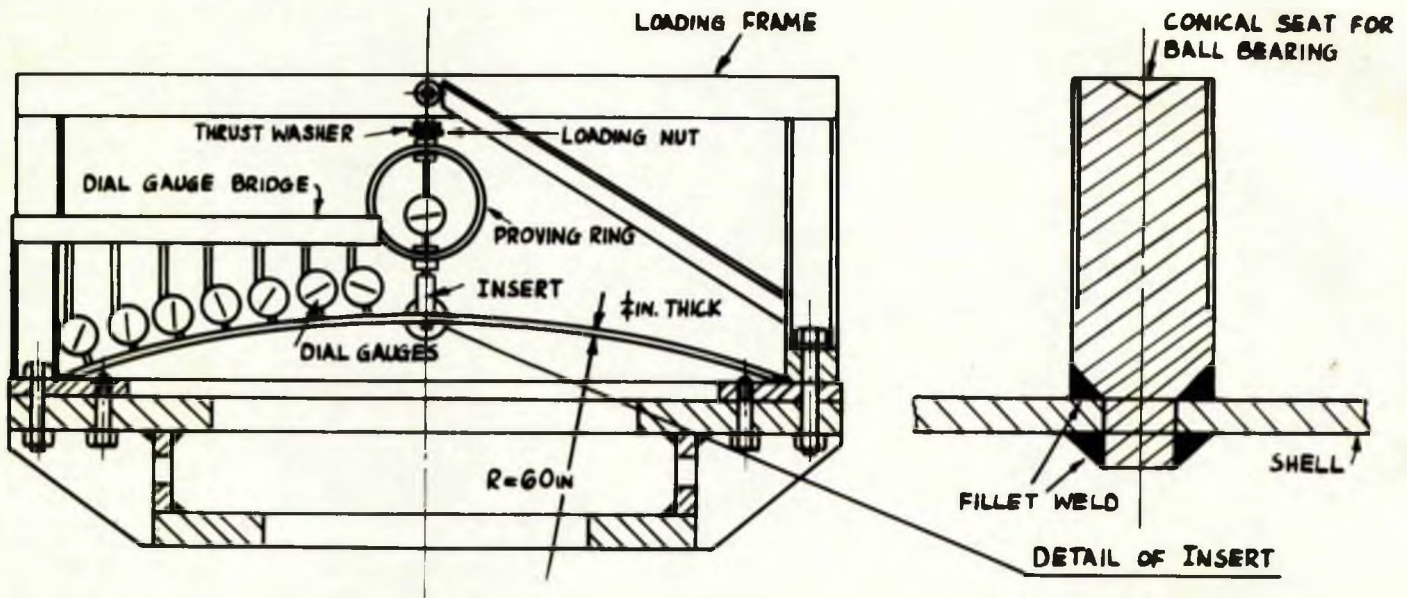
Fig.IV.4 Arrangement of Shallow Spherical Shell under Radial
Loads Applied Through a Rigid Insert.
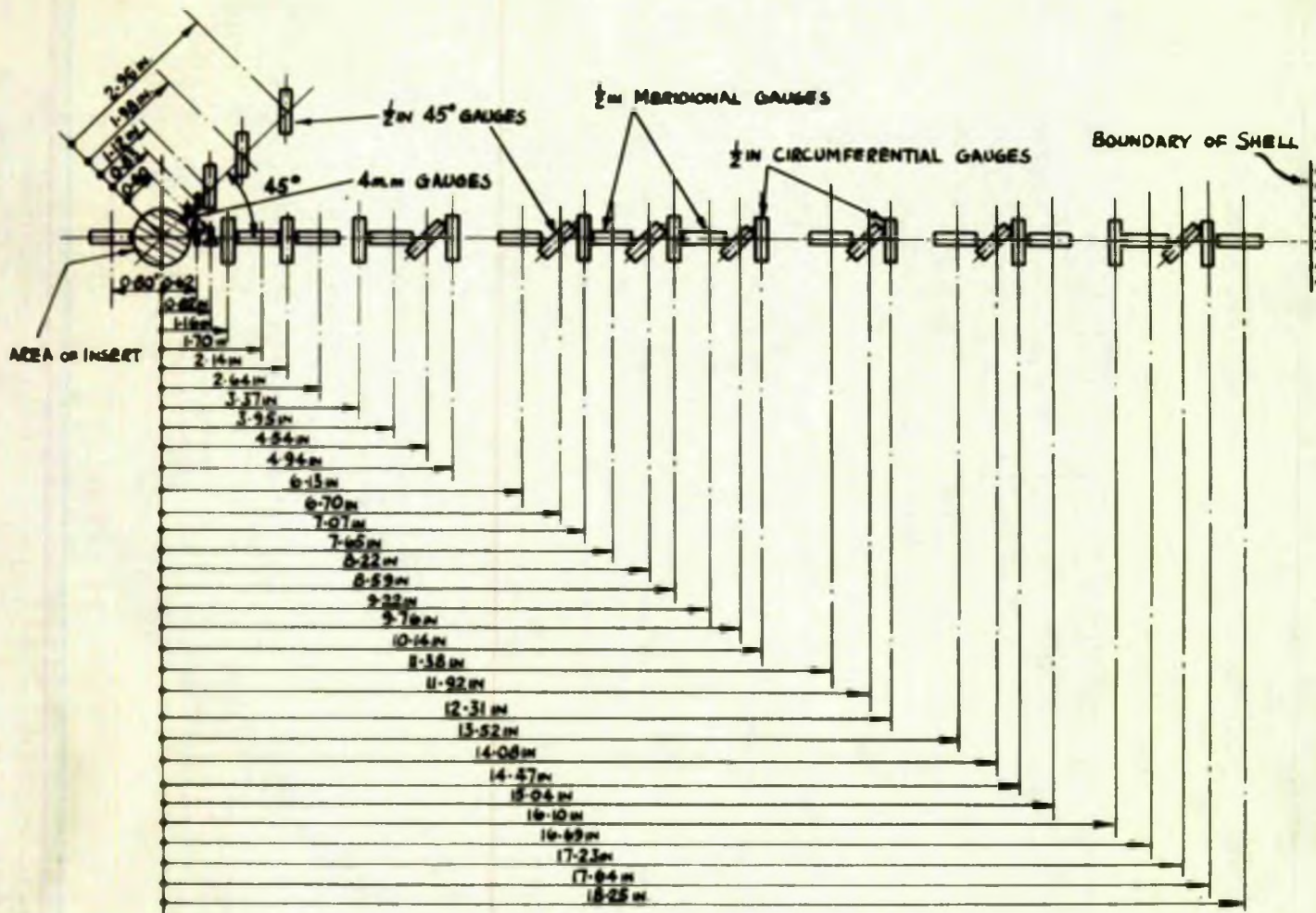
Fig. IV.5 A Typical Strain Gauge Layout for Inner and Outer Surfaces for Rigid Insert Tests

which was previously calibrated, and a ball bearing, as shown
in Fig. IV.4.   The proving ring was used both as a load applying
and load measuring device.

Measurement of Strain and Deflection.   In this series, two types
of electrical resistance strain gauges were employed to measure
the strain in the circumferential and meridional directions on
the outer and inner surfaces.   In the near vicinity of the
load, Phillips foil gauges of 4m.m. length and 120 ohms resis-
tance were used, and elsewhere, Saunders Roe, Ferry foil printed
circuit gauges, with epoxy-ethylene backing, of $\frac{1}{2}$in length and
45-50 ohms.

Owing to the symmetrical nature of the loading, only one
great circle was strain gauged.   A typical layout, which is the
same on both the outer and inner surfaces is shown in Fig.IV.5.
It is noted that in the immediate vicinity of the insert the
4 m.m. gauges,enabled strains to be recorded at stations much
closer to the insert than the $\frac{1}{2}$in length type.   As a check on
the meridional strain close to the insert a $\frac{1}{2}$in strain gauge
was fixed on a great circle 180° to the gauged great circle, an d
as near as possible to the insert.

It will be further noted, that apart from the two stations
near the insert, occupied by the 4 m.m. gauges, all the other
gauges are placed on the great circle.   This alternative lay-
out was considered to be of greater accuracy for those load
cases that were not axi-symmetric and which were imposed later
on this particular model.   Using this type of layout the
strains at any given position are determined, by interpolation,

from the plots of strain (or strain per unit load) against radii

The strain gauges mounted at 45° to the gauged great circl
and those 45° gauges on the other great circle (shown in Fig.IV.
were not used in the present test, but were used in the torsion
test, reported later.

The 50-way strain recorder was again employed in this seri
all other details being as outlined on p.p. 173-175

Utilizing eqts. IV.1 and 2, the values of the correspondin
bending and direct stresses in both the meridional and circum-
ferential directions were obtained.   The results are plotted
non-dimensionally and shown in Fig. IV.6.

The radial deflections of the shell were measured along a
great circle using 0.0001in Dial Gauges as outlined on p. 175
The arrangement for support, adjustment and alignment of the
dial gauges, is that previously described, and shown in Fig.IV.
The results for the $\mu = 0.23$ insert are plotted non-dimensionall
on Fig. IV.6.

Complete Sphere

Experimental Model:-   The overall dimensions of the model sphe
which is 13ft. 6in diam., are one tenth of the Dounraey Contair
ment Building, with access doors in the side and top of the
vessel.   The sphere plate thickness for the upper tiers is $\frac{1}{4}$i
and for the lower tiers, 5/16, $\frac{3}{8}$, $\frac{1}{2}$ and $\frac{1}{4}$in, the thickest secti
being placed at the supporting skirt.   The model has twin sk
support inside and outside, together with an anchor ring. A
general view of the model is shown in Fig. IV.7 and a section
Fig. IV.8.
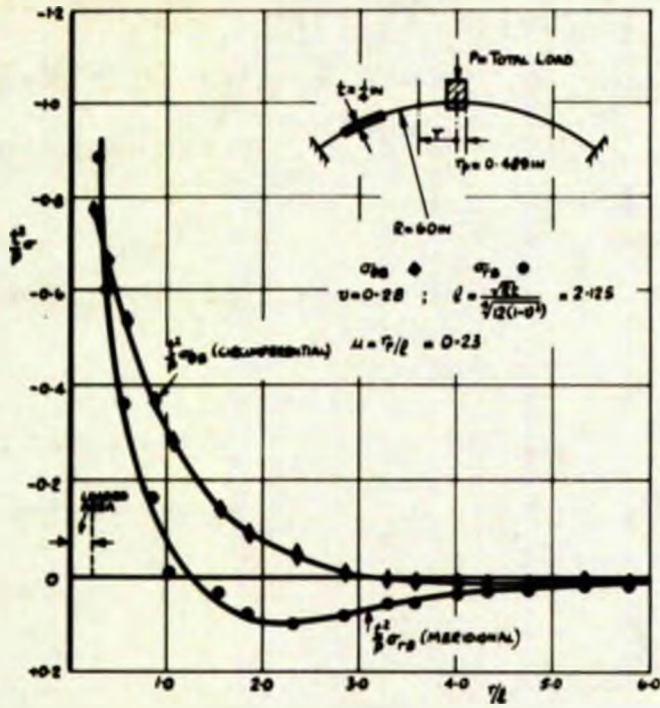
Fig. IV.6a BENDING STRESS ON THE OUTER SURFACE DUE TO A RIGID INSERT RADIAL LOAD P
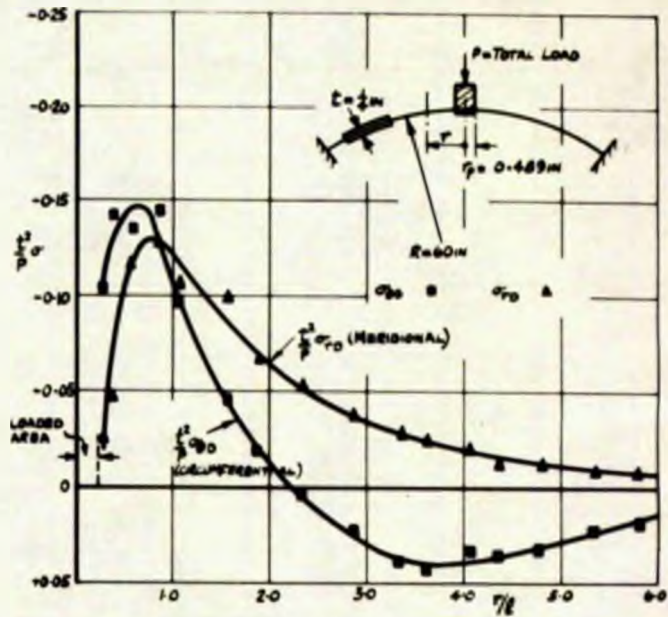
Fig.IV.6b DIRECT STRESS DUE TO A RIGID INSERT RADIAL LOAD P
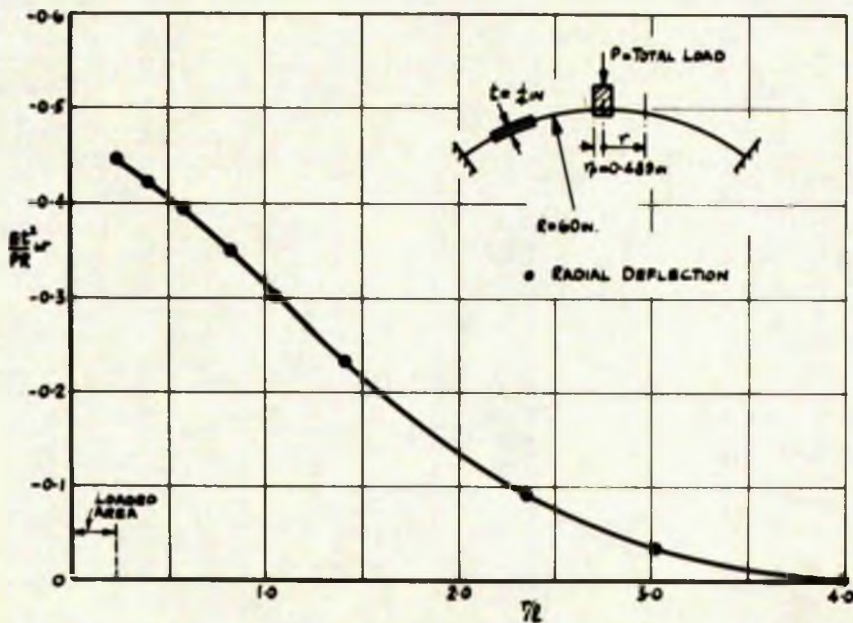
FIG.IV.6c RADIAL DEFLECTION DUE TO A RIGID INSERT RADIAL LOAD P

FIG IV.6 EXPERIMENTALLY OBTAINED DIRECT STRESS, BENDING STRESS ON THE OUTER SURFACE AND RADIAL DEFLECTION OF A SHALLOW SPHERICAL SHELL DUE TO A RADIAL LOAD P APPLIED TO THE SHELL BY MEANS OF A RIGID INSERT (μ=0.23)

Fig.IV.7 General View of 13ft-6in Diameter Model Sphere.

A continuous programme of research on the vessel is in
progress.   Details are given in ref. (108) a copy of which
is appended to the thesis.

The tests on the model which are of direct relevance to
the work presented in the thesis are those relating to a rigid
insert, or stud attachment, under a variety of load actions and
those of certain pipe attachments under radial load.   In this
section the rigid insert case under a radial load is discussed.

In the first instance two different diameter studs were
considered in the investigation.Prior to welding the studs on
to the inside surface of the vessel,the radii of curvature were
measured over the region selected for stud-attachment.   On the
basis of these measurements the position of the attachment was
established.   It was found necessary in all cases to avoid
areas in the immediate vicinity of a weld or other discontinuity,
such as an access door.   The stud-attachment positions were
thus arranged diametrically opposite on the same great circle.
Marking of the Vessel:-   Great circles were marked on the outer
surface of the vessel at $0°$, $90°$, $180°$ and $270°$ together with
the equator line.   In order to transfer these lines and other
positions relevant to the strain-gauging from the outer surface
to the inner surface of the vessel, a series of circles of 1in
diameter was scribed at 6in intervals along the line on the
outer surface.   A thin layer of 'Tempilstik', a chalk with a
given melting point (in this case $250°F$) was applied to the
inside surface in the approximate region of the line. A torch
with a small area acetylene flame was concentrated for a

predetermined time on the outer surface in one of the 1 in diam
soribed circles.   As the heat from the flame penetrated the
sphere material a small circle of melted chalk, of from $\frac{1}{2}$ to 1ii
diam. became visible on the inner surface.   As each position
on the outer line was so treated a series of such 'templistik
circles' appeared on the inner surface.   The centres of these
circles were joined to give the required line on the inner surf

Before using the above method several test runs were carri
out using a rectangular plate, marked off at identical points o
each side.   The 'Tempilstik' technique applied to this plate
invariably defined the appropriate circle centres within $\frac{1}{8}$in of
the actual marked positions.   Since, in the case of the spher
a considerable number of 'tempilstik circles' defined the line
the accuracy of loacating the inner line was considered satis-
factory.

On completion of the preliminary marking of the vessel th
studs were welded on to the inside of the vessel using a conti
fillet weld, oare being taken to ensure that they were positio
radially.   Studs of different diameters were fixed to differe
thicknesses of plate as shown in Fig. IV.8.   The correspondin
μ values are 0.092 and 0.195.

Loading Technique:-   A radial load was applied to both stud
one and the same time, using a $\frac{1}{4}$in diam. steel wire stretched
across the sphere connecting the studs.   Suitable shackles we
incorporated to ensure axiality of the load.   A turnbuckle w
used to apply the load and a 1,250lb capacity proving ring to
measure its magnitude as shown in Fig. IV.8.
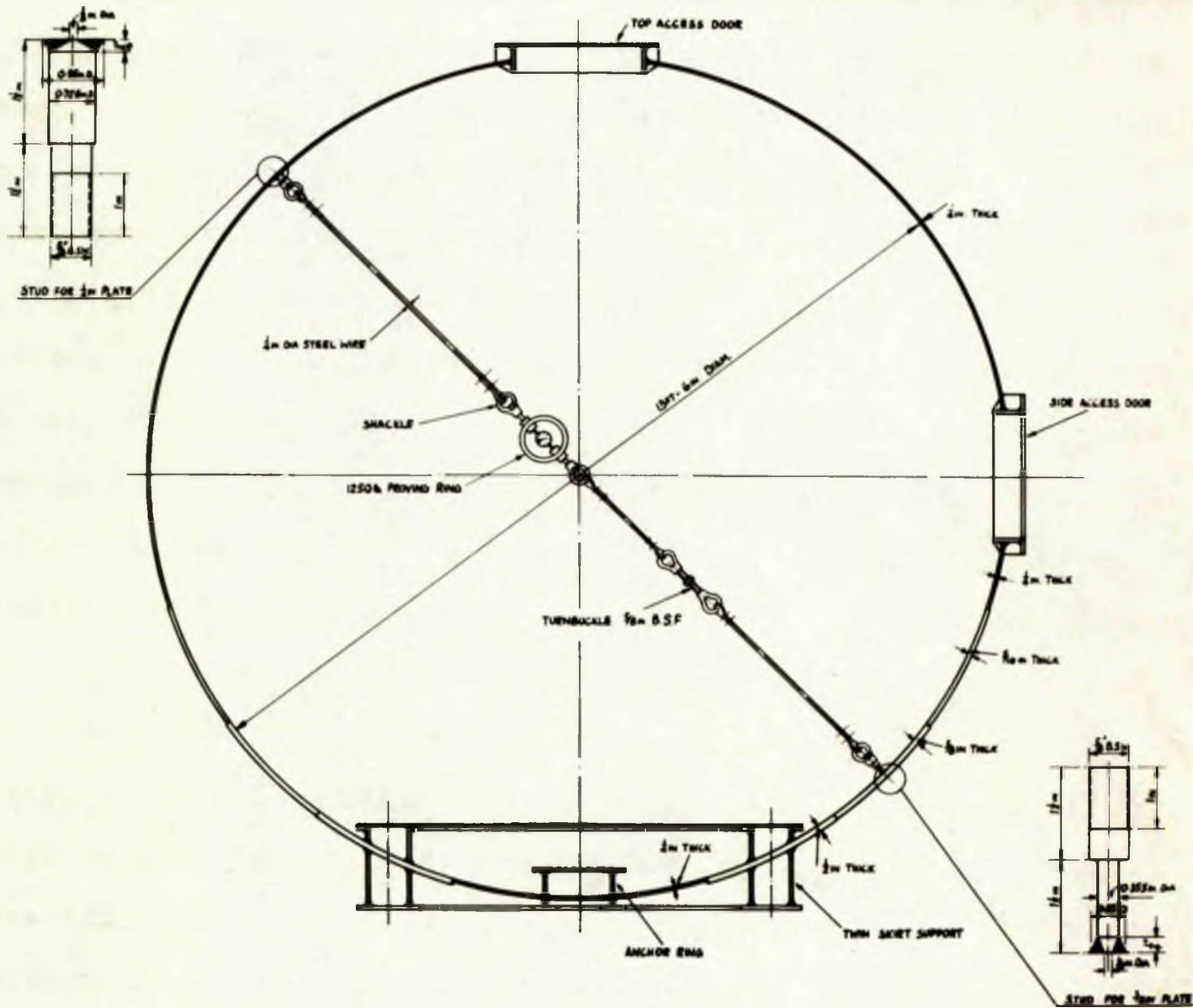
FIG. IV.8 SECTION OF 13FT-6IN DIAM MODEL SPHERE SHOW STUD LOADING DEVICE
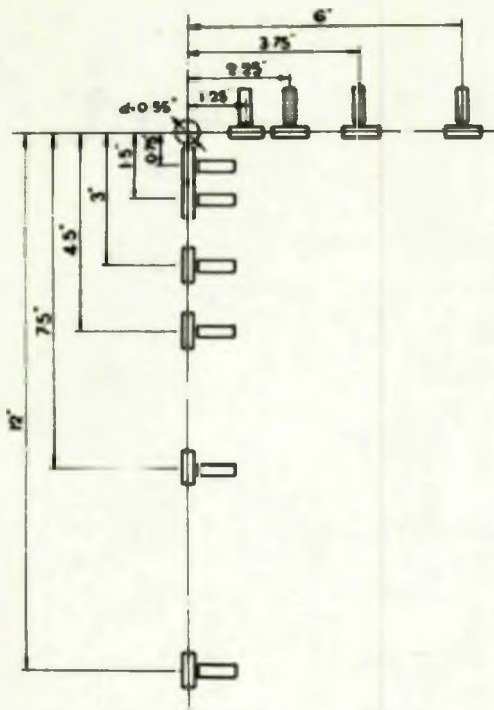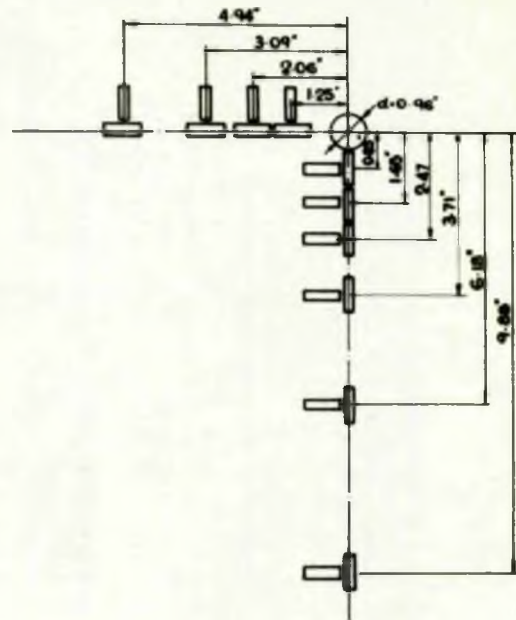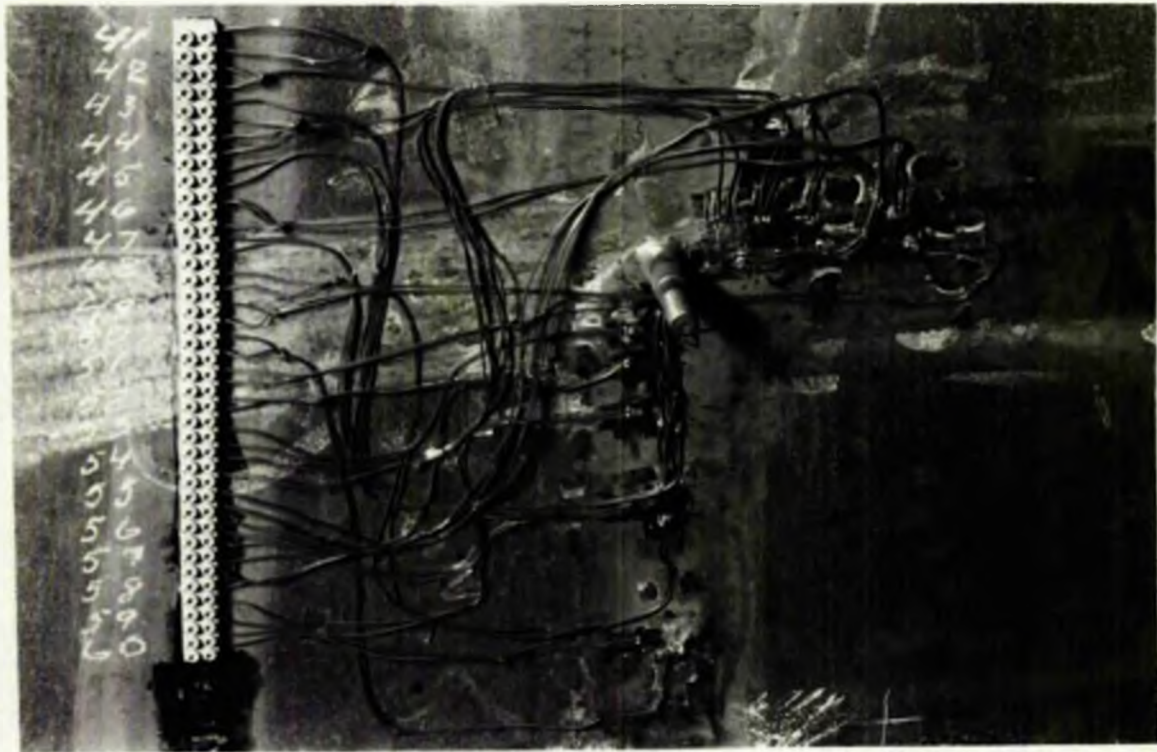
Fig.IV.9   Layout of Strain Gauges for Stud-Attachments
on Model Sphere.
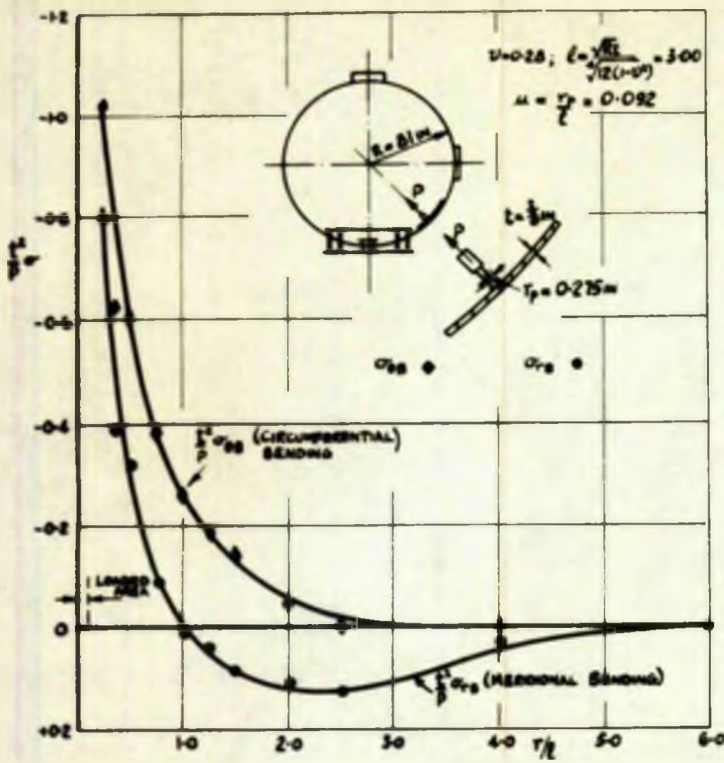
FIG. IV. 10a BENDING STRESS ON THE OUTER SURFACE DUE TO A RADIALLY LOADED STUD

FIG. IV. 10b DIRECT STRESS DUE TO A RADIALLY LOADED STUD
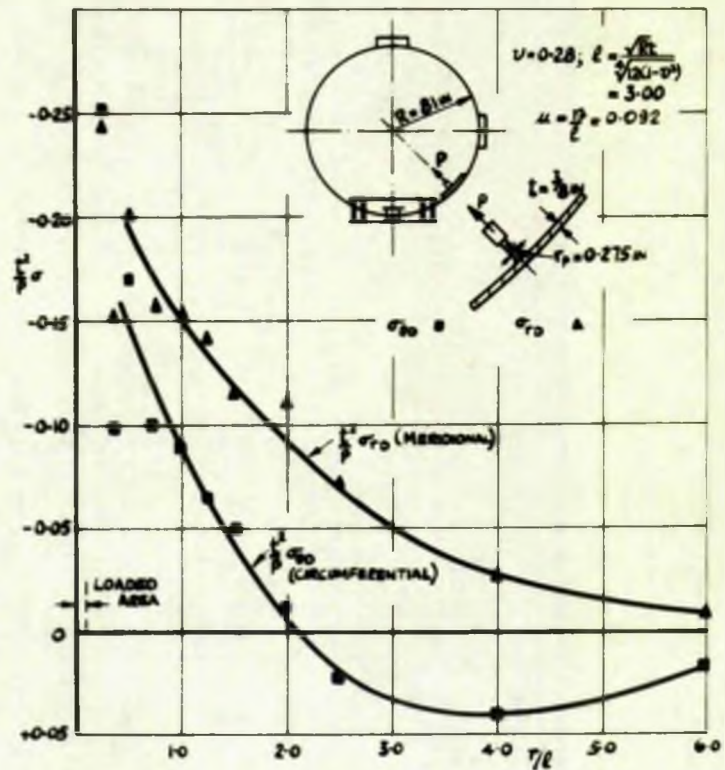
FIG. IV. 10 EXPERIMENTALLY OBTAINED DIRECT STRESS AND BENDING STRESS ON THE OUTER SURFACE OF A COMPLETE SPHERE (13FT-6IN DIAM) DUE TO A RADIAL LOAD P APPLIED TO THE SHELL THROUGH A WELDED STUD — TYPICAL RESULTS FOR STUD ON 7/8 IN PLATE (μ = 0.092)

Measurement of Strain:- Saunders Roe $\frac{1}{8}$in length foil strain
gauges were fixed along two lines 90° apart to measure strains
on the inner and outer surfaces in the circumferential and
meridional directions.

The purpose of gauging the two lines was two fold; in the
first place it would provide information as to the symmetrical
distribution, or otherwise, of the loading, and secondly, since
the gauges on the two lines were positioned at stations of
different radii it would give additional information as to the
strain distribution in the regions of high strain gradient.
The strain gauge layouts for the two studs are shown in Fig.IV.9.
The strain gauge leads for each gauge were connected into a
plastic terminal strip cemented to the surface of the sphere in
the vicinity of the stud-attachment, as shown in Fig.IV.9.
Multicore cables (25 x 7/.0076, 25 core) were then used from the
terminal strip to the strain recorder.

As in the earlier tests the 50-way strain recorder and the
gauge procedure outlined in pp. 173-175, were employed.

Typical experimental results for one of the attachments,
for the bending and direct stresses are plotted non-dimensionally
in Fig. IV.10. It is noted that the results from gauges placed
on both lines lie on one and the same curve, thus indicating the
symmetrical nature of the loading.

A further radial load test was carried out on a $1\frac{1}{2}$in diam.
stud. This stud of $\mu = 0.394$ and described on p.184 and shown
in Fig. IV.13, was used primarily for bending moment and
tangential shear loading; however, facilities were provided to

enable a radial load to be applied by means of two such studs, welded diametrically opposite onto the equator of the sphere, and loaded using the same technique as employed for the other radially loaded studs.   The strain gauge layout for this stud is shown in Fig. IV.15.

Complete experimental results for this series of radial stud loadings is given in Appendix VIII.7.

IV.1.2   'BENDING' MOMENT

The bending moment was applied to the shell through a rigid insert, or stud attachment, welded to the shell.   Two types of experimental models were investigated, namely, the shallow shell and the complete sphere.

Shallow Shell

Experimental Model:-   The shallow shell of $\frac{1}{4}$in thickness and 60 in radius and rigid insert 0.978 in diam. was again used for this investigation.   The insert penetrated the shell, being welded to it on both outer and inner surfaces.   On the outer surface, the weld was machined to retain the cylindrical form of the insert as shown in Fig. IV.4.   The outer boundary, 3ft.3 chord diameter, was welded to a heavy flange ring and mounted onto the extended table.

Loading Technique:-   The bending moment was applied to the insert by means of a 3" x 1$\frac{1}{2}$" channel of 4 ft. 6 in length rigidly secured at its centre to the insert. Equal and opposite vertical forces were applied to the ends of the channel at 50 i
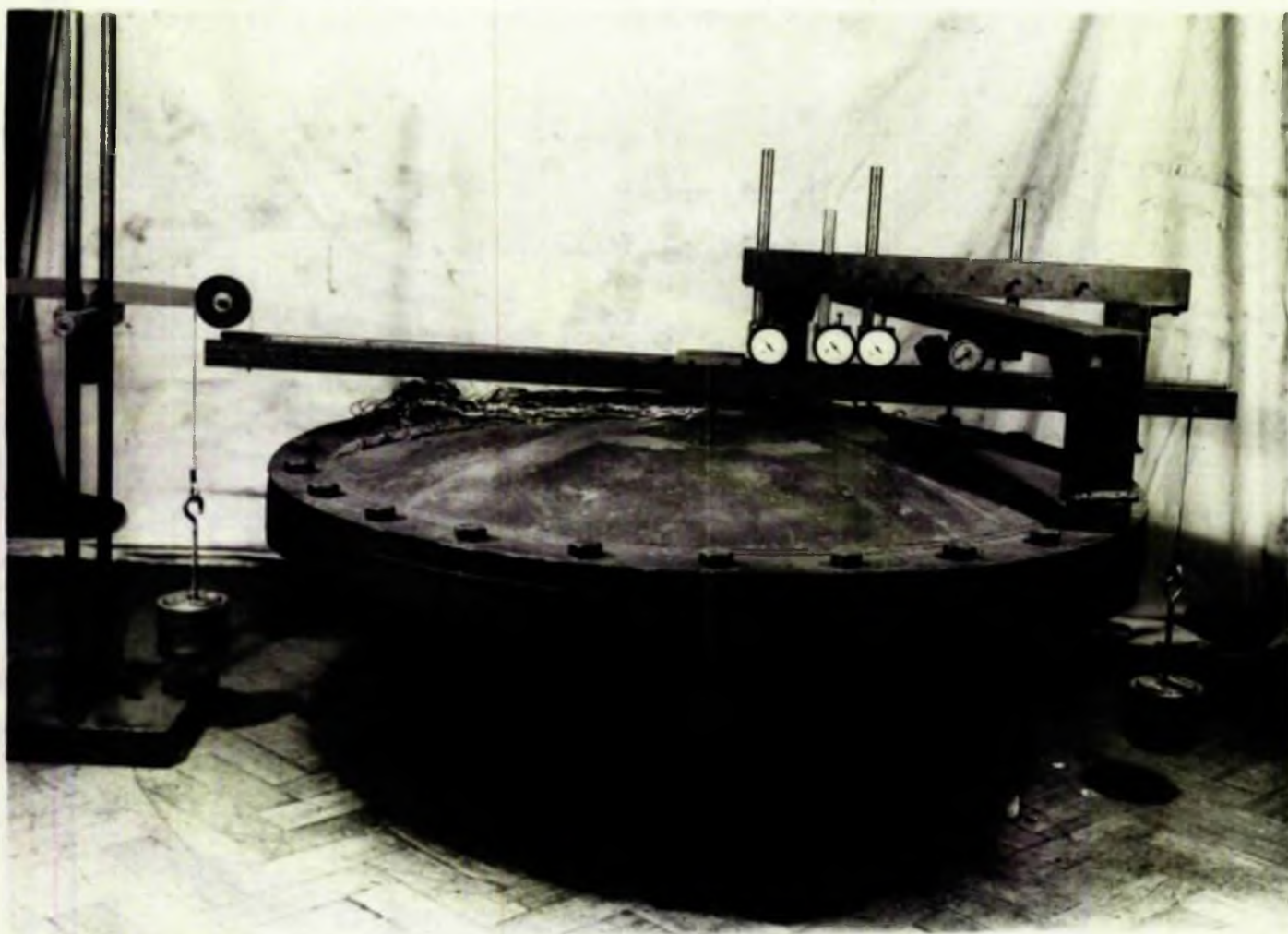
Fig.IV.11   A Bending Moment Applied to a Shallow Shell
              Through a Rigid Insert.

centres, in such a manner that a pure bending moment was applied - as shown in Fig. IV.11.

Measurement of Strain and Deflection:-   The electrical resistance strain gauges used in the earlier tests (the layout of which is shown in Fig. IV.5) were again employed in the present investigation.   The comments made in the previous section (IV.1.1b; p.176, 177 , 178) regarding gauge layout and strain recording being again relevant.   The plane of the applied moment was arranged to coincide with the gauged great circle.   The measured strains were thus those corresponding to the line $\theta = 0°$.

The loading was applied by means of dead weights, as shown in Fig. IV.11 and, as previously, was applied in increments up to the maximum load, readings of strain being recorded throughout.   The procedure for strain recording and stress analysis outlined earlier on p.173-175 was followed and experimental results for bending and direct stresses obtained.   These are plotted in Fig. IV.12.

The radial deflections of the shell were again measured using 0.0001 in dial gauges, the arrangement for support adjustment and alignment previously mentioned being utilized. In order to facilitate these measurements in the plane of the moment, holes were drilled and slots milled along the channel centre line. Extended spindles were then fitted to the dial gauges as shown in Fig. IV.11.   A series of loadings with different dial gauge positions were carried out, to enable the deflections to be obtained at close intervals of the horizontal radius r.   The same standard of repeatability was observed in the deflection

measurements as in the strain measurements.

The results of these tests plotted in a non-dimensional manner are shown in Fig. IV.12.

Complete Sphere

<u>Experimental Model</u>:-   The 13 ft. 6in diam. model sphere shown earlier in Fig. IV.7 and discussed on p.178 was again used for the present investigation.

To enable a bending moment and also a tangential shear load (reported later) to be applied to the shell, the attachments were positioned on the equator of the shell which, in fact, coincided with a welded seam in the vessel.   The radii of curvature over the selected region were measured and on the basis of these measurements the position of the attachment was duly established. The vessel was marked on the inner and outer surfaces in such locations as to enable the attachment position and that of the strain gauges to be determined on both surfaces.   The technique used for marking the inner surface of the vessel from the outer surface was by using the 'Tempilstik' and acetylene flame, described in detail on p.179.

<u>Loading Technique</u>:-   The load was transmitted to the shell by means of 1½in diam. stud attachments each welded with a continuous fillet weld to the surface of the sphere.   These studs were located diametrically opposite on the equator, and on the inner and outer surfaces on the same radial axes.   Every effort was made to retain the cylindrical form of the studs after welding, although unavoidably a small radius did exist at the sphere to stud connection.   This, however, was nowhere greater than 0.1in
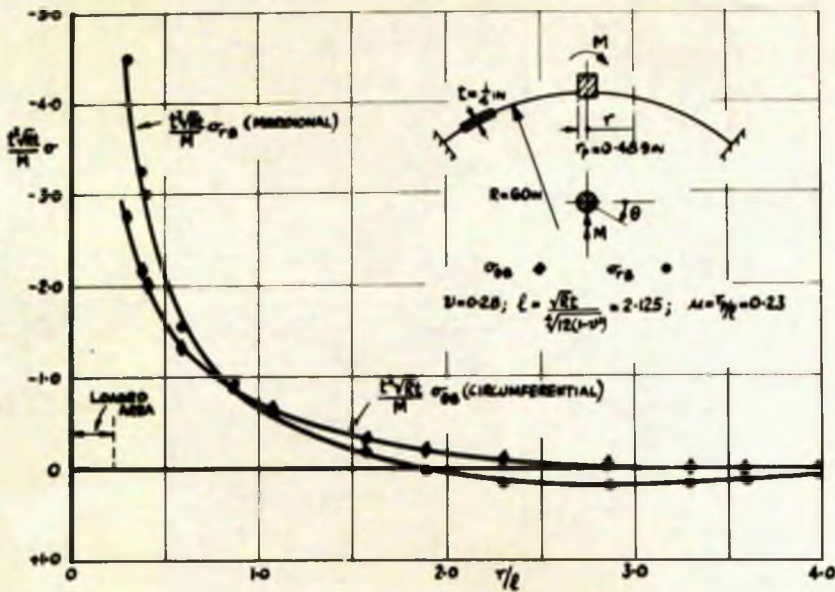
FIG.IV.12a BENDING STRESS ON THE OUTER SURFACE DUE TO A BENDING MOMENT M

FIG.IV.12b DIRECT STRESS DUE TO A BENDING MOMENT M
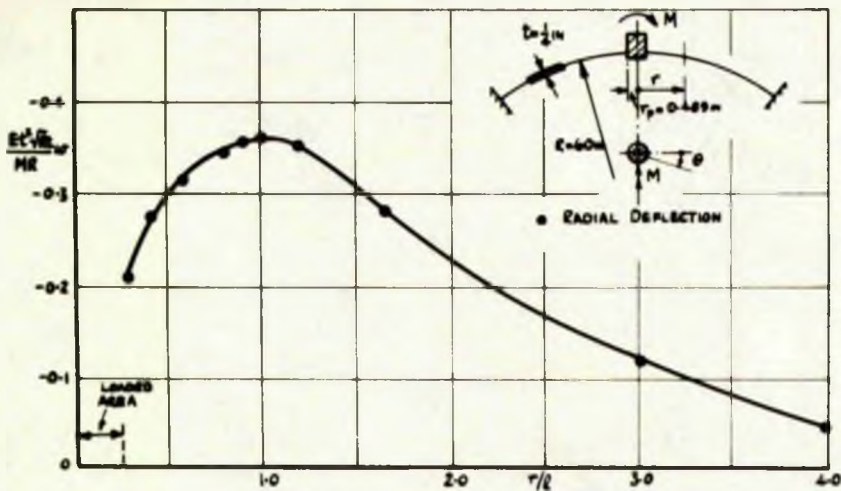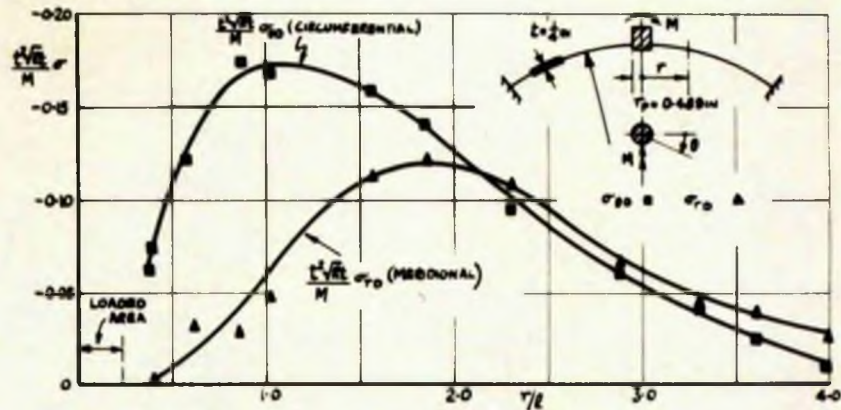
FIG.IV.12c RADIAL DEFLECTION DUE TO A BENDING MOMENT M

FIG. IV.12 EXPERIMENTALLY OBTAINED DIRECT STRESS, BENDING STRESS ON THE OUTER SURFACE AND RADIAL DEFLECTION IN THE GREAT CIRCLE, θ=0°, OF A SHALLOW SPHERICAL SHELL DUE TO A BENDING MOMENT M APPLIED TO THE SHELL BY MEANS OF A RIGID INSERT (μ = 0.23)
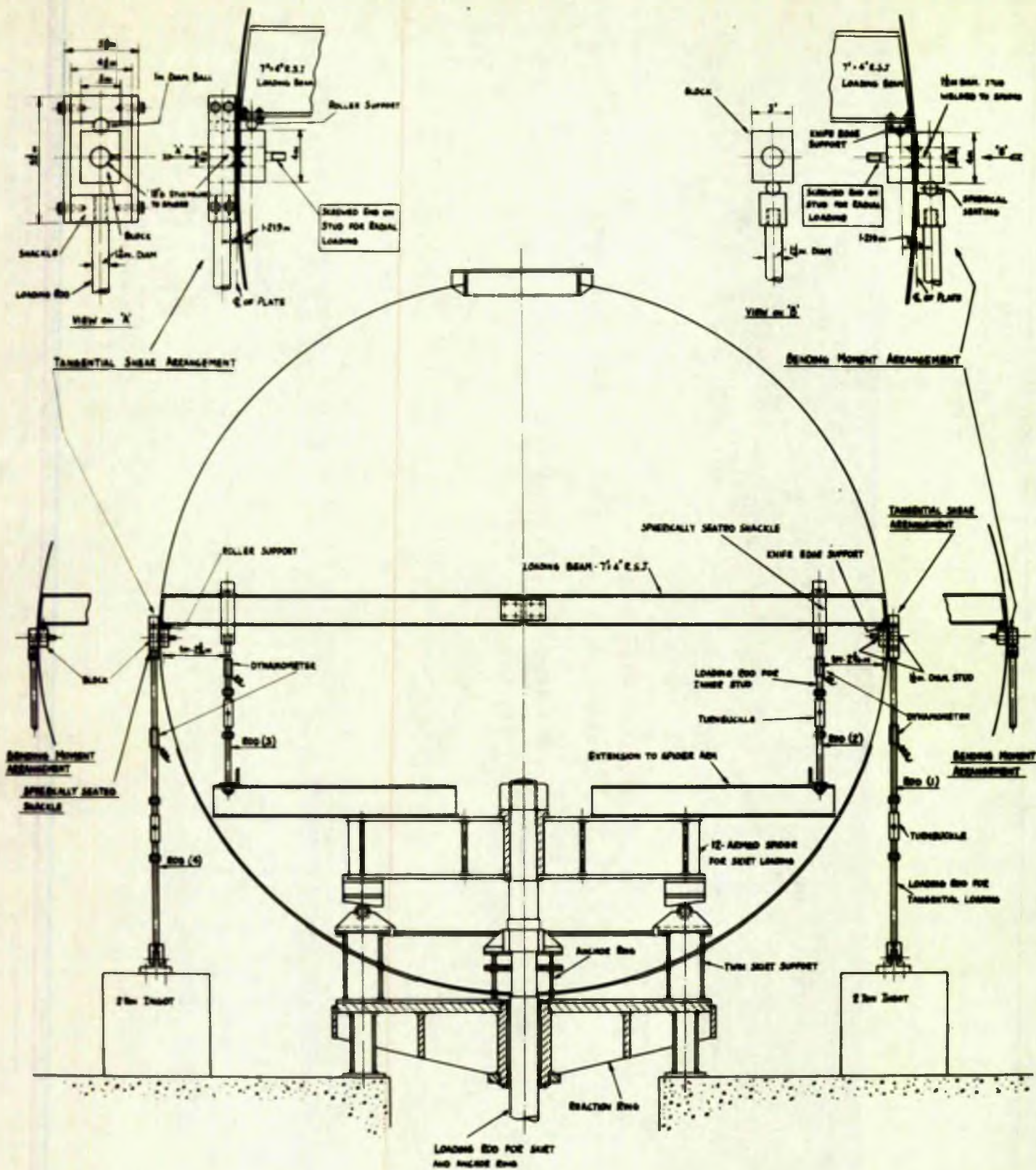
Fig. IV.13 GENERAL SECTION OF 13ft-6in DIAM SPHERE SHOWING THE BENDING MOMENT AND TANGENTIAL SHEAR LOADING OF A STUD

A maximum value of the weld diameter of 1.70in was therefore recorded.

The studs on the inside of the vessel were loaded by forces acting vertically down, while those on the outside surface could be loaded in either direction depending on the force action under investigation (i.e. bending moment or tangential load).

The inside studs were loaded as follows. Over each stud, a closely fitted block was secured by means of a small grubscrew. The block on one stud was suitably machined to enable a hardened, $\frac{1}{2}$in side, knife edge to be located on its upper surface thus providing a knife edge support. The other inside block, diametrically opposite, was machined and suitably ground to provide a roller support on its upper surface, as shown in Fig. IV.13.

Spanning the inside of the vessel and resting on the blocks at either end was a 7 x 4in R.S.J. Loading Beam, cut at the centre and joined by fish plates to provide suitable adjustment. Hardened steel plates were fixed at the extreme ends of the beam, on its underside. At one end the plate was machined to locate the knife edge and at the other, ground for the roller support, (Fig. IV.13).

At distances of $14\frac{3}{16}$ in from the point of the knife edge and the roller support, two identical vertical loading rods were situated. At the upper end of each loading rod a shackle was mounted such as to straddle the Loading Beam and locate a 1in diam. steel ball, which was suitably seated in a hardened plate on the beam. A dynamometer and turnbuckle arrangement, screwed into the lower end of the shackle, was secured at the other end to

an extension of the 12-armed spider.   The spider arrangement
used for loading the twin skirt support was not in use at this
juncture, and provided a rigid fixture for the loading rod.
Details of this are shown in Figs. IV.13 and IV.14.

In order to load the two inside studs, equal forces were
applied, by means of the loading rods, to the loading beam and
thus were transferred to the studs, the magnitude of the force at
the stud being the same as that in the loading rod.   As indicated
on Fig. IV.13 the vertical force thus applied was situated some
distance from the centre of the shell plate, producing a bending
moment and a direct force in the vessel.

For the investigation of pure bending moment applied to the
shell, it was therefore necessary to apply to the vessel on outs
force equal in magnitude and opposite in direction to that alrea
applied to the inside stud, that is, vertically upwards.   Such
action was applied through the stud on the outer surface.   In t
case the loading technique was as follows: Over each of the ou
studs, a closely fitted block was secured by means of a small gr
screw.   The lower surface of these blocks were machined to give
a spherical seating located at exactly the same distance from th
outer sphere surface, as the knife edge and roller support were
located from the inner surface.   A 1in diam. steel ball was
placed between this seating and a corresponding seating screwed
to the dynamometer, turnbuckle and loading rod arrangement.   A
forked end was screwed onto the lower end of this loading rod
providing a 1in diam. pin support.   The above arrangement was
repeated on the other outside stud as indicated in Fig. IV.13.
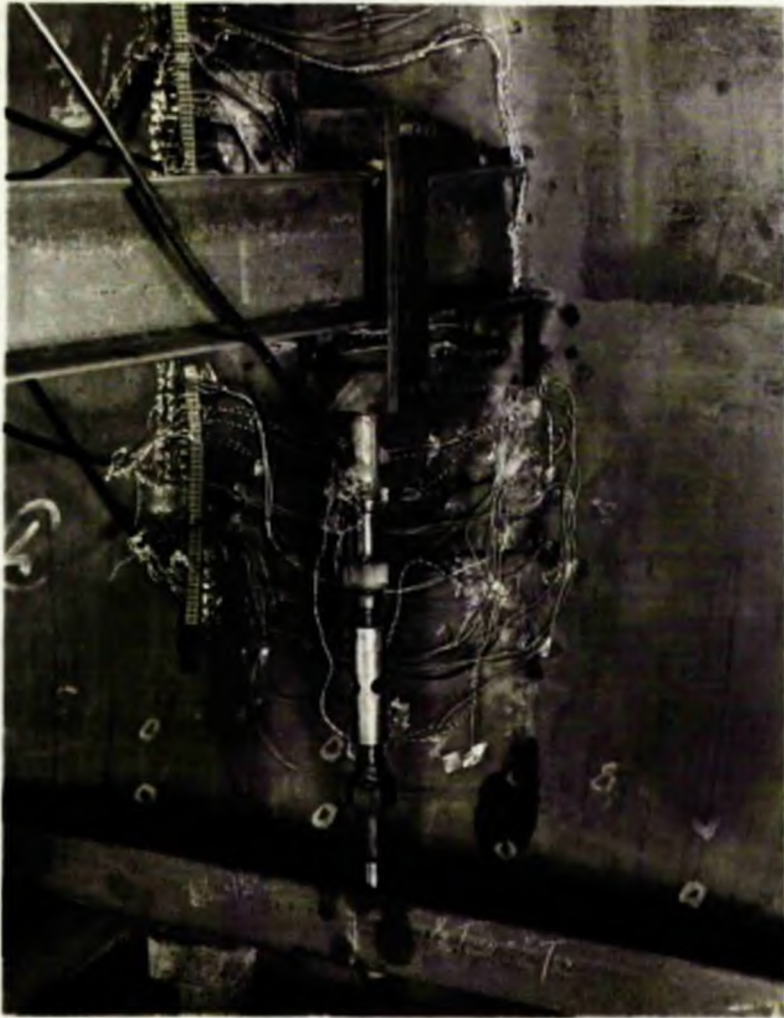
The Loading of the Stud
Attachment - Inside the
Sphere.
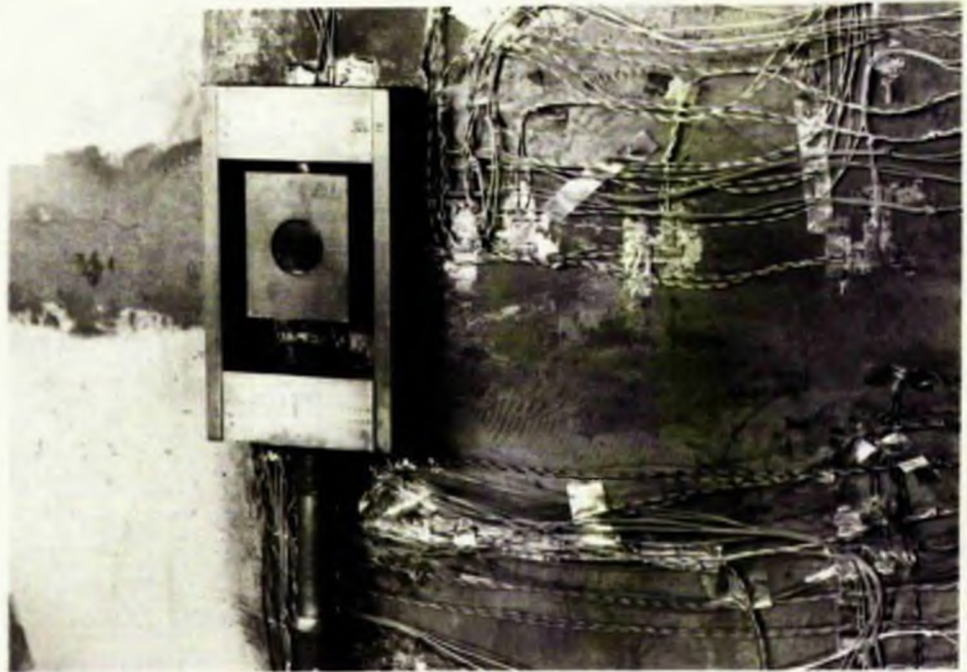
The Loading of the
Stud Attachment -
Outside the Sphere.

Fig.IV.14   Inside and Outside Loading for Bending Moment and
            Tangential Load on the Complete Sphere.

In order to check the results from this type of loading and also to perform the tangential shear loading test, the direction of the load was reversed to act vertically down. The block was therefore turned through 180° to allow the spherical seating to be on the upper surface. A shackle, of similar design to those used within the vessel, was then fitted over the block locating the 1in diam. steel ball (Fig. IV.14). The same turnbuckle and dynamometer arrangement was used as in the previous case, except that in this instance the loading rod was in tension. A 2 ton ingot was used to provide a reaction for the load in the rod. The ingot, which rested on the floor of the building, was connected to the rod by means of a bracket, 1in diam. pin and a forked end on the loading rod. Preliminary lining-up of the rod was done by raising the 2 ton ingot from the floor by using the turnbuckle, and allowing the stud to carry the full weight of the ingot.

The magnitude of the load in each of the four loading rods, was measured by means of a dynamometer which was made up of four electrical resistance strain gauges fixed to a machined section of the rod. The gauges were placed diametrically opposite on the 0°, 90°, 180° and 270° lines, in the longitudinal direction and connected in series, thus avoiding the recording of any strains arising from bending stresses in the rod. As a protective measure the gauges were given a coating of 'Evostik' and covered with 'Prestik'. Suitably matched compensating gauges were employed and protected in the same manner as the active gauges.

Each rod was calibrated up to 5 ton in the laboratory prior to installation on the model sphere. The calibration was carried

out in a testing machine using the spherical shackles incorporate

in the actual set up.   The readings of strain were noted in $\frac{1}{2}$ton

intervals up to the maximum of 5 ton. Several tests were made on

each rod to ensure that repeatability obtained. From the plots

of load against dynamometer strain reading, the calibration for

each loading rod was obtained.   For rods 1 → 4 (see Fig. IV.13),

these were respectively as follows:-   79.2, 80.6, 81.6 and 83.4

microinches/in per ton of load.

Preliminary testing of the loading mechanism established

that the following loading procedure should be adopted.   In the

first instance, the inside studs were loaded, using the loading

beam and the inner rods 2 and 3, applying equal forces to both

rods and thus to both studs.   Four increments of load were

applied as in earlier tests and strains suitably recorded. Next

the outside studs were loaded using rods 1 and 4. Application o

this loading was carried out in both directions, that is, vertic

upward and downward, in order to provide a check on the readings

strain.   Four increments of load, similar to those applied to t

inner studs were used and strains recorded as before.

In order to obtain the results relevant to the bending

moment, the results from the inside loading and from the outside

loading, when the load was vertically upward, were superposed.

A further final test was undertaken in which all four rod

were used, equal loads being applied to all stud attachments.

this means the strain readings for bending moment were obtained

directly.   Although this latter procedure appeared somewhat mo

direct than that previously outlined, the interdependence of th
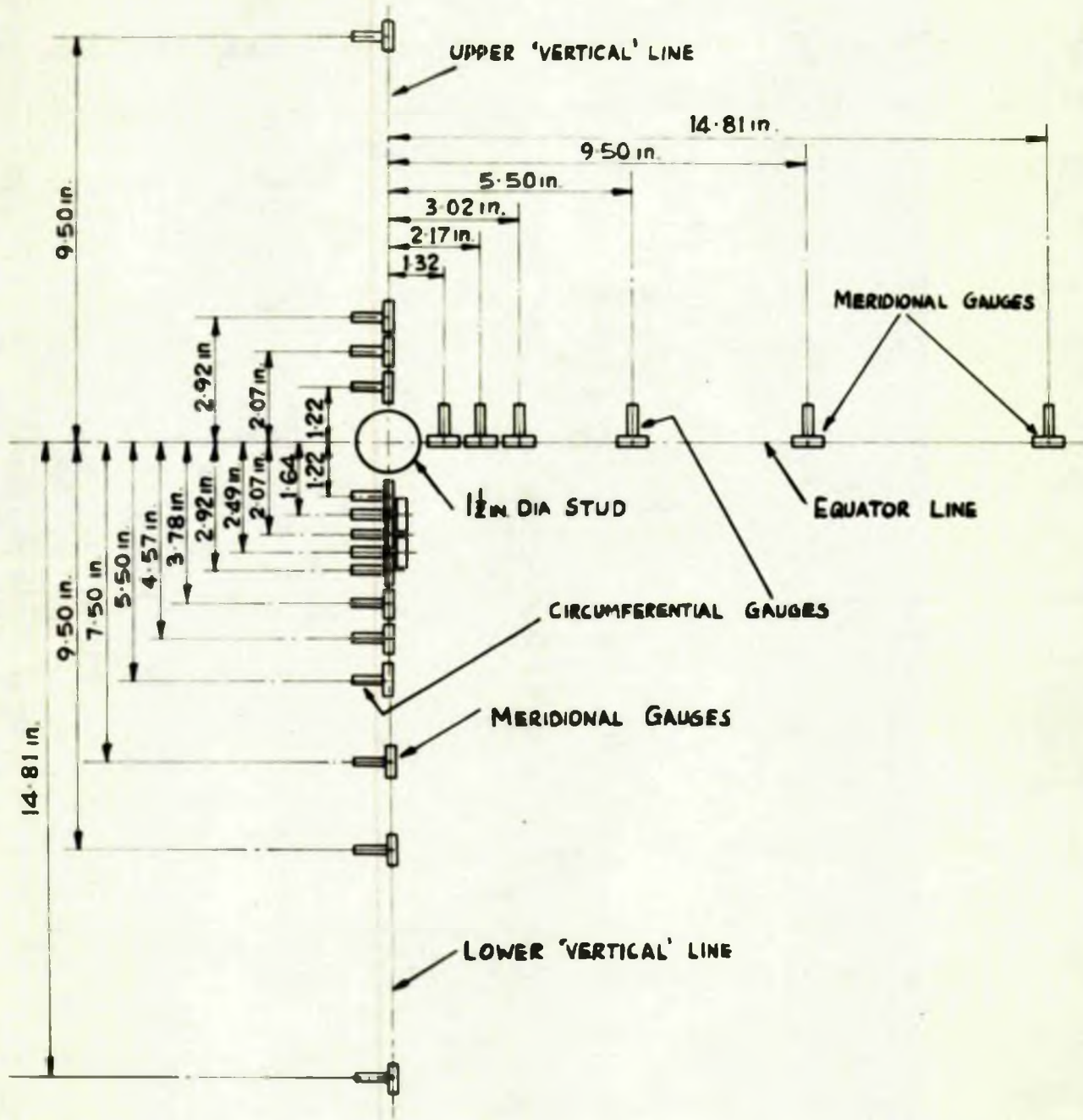
Fig. IV. 15 STRAIN GAUGE LAYOUT FOR INNER AND OUTER SURFACES FOR BENDING MOMENT, TANGENTIAL SHEAR AND RADIAL LOADING OF THE 1½IN. DIAM. STUD ON THE MODEL SPHERE

stud loads gave rise to difficulties in obtaining identically equal loads in the rods. It was therefore more difficult to achieve the same standard of repeatability as that obtained in earlier tests. For this reason the results presented are those obtained, by applying the inner and outer loads separately.

Measurement of Strain:- Electrical resistance foil strain gauges (Saunders Roe $\frac{1}{2}$in length) were again employed in these tests for the measurement of strain on the inner and outer surfaces in the circumferential and meridional directions in the vicinity of one set of studs.

Two 'vertical' lines, that is, in the plane of the moment, and one line on the equator at 90° to the plane of the moment, were strain gauged as shown in Fig. IV.15. The gauges on the upper line were installed to provide a comparison of strain with that obtained on the more completely gauged lower line. These additional gauges together with those on the equator provided a means of assessing the asymmetry of the loading.

As in the radial load tests on the sphere, the strain gauge leads for each gauge were connected into a plastic terminal strip cemented to the surface of the sphere in the vicinity of the stud attachment as shown in Fig. IV.14. Twenty five core cable was then used from the terminal strip to the strain recorder.

In this series of tests a Baldwin-Lima-Hamilton Portable Strain Recorder was employed, together with five of the 20-channel switching units. Using these switching units it was possible to economise in the use of compensating gauges, by using one compensator for a number of strain gauges situated closely together.

Since in these investigations the active strain gauges were closely grouped in the vicinity of the stud, it was arranged that one compensator gauge served 20 active gauges. Compensating gauges were therefore located at central points in the gauge layout on both the inner and outer surfaces.

A comparison of strains on the upper and lower 'vertical' lines, showed that good agreement between the two was obtained, the only exception being the circumferential strain on the inner surface (ε_θ^i) in the immediate vicinity of the load. This divergence was attributed to a slight local imperfection of the sphere in the vicinity of the stud in the circumferential directi

From the strain results on the 'vertical' line ($\theta = 0°$ and $\theta = 180°$), the corresponding bending and direct stresses were obtained, in the manner outlined on pp. 174 and 175, and are plotted in non-dimensional form in Fig. IV.16.

IV.1.3   TWISTING MOMENT

As in the earlier load actions, the twisting moment was applied to the shell through a rigid insert, or stud attachment welded to the shallow shell.

Experimental Model:-   The shallow shell of $\frac{1}{4}$in thickness, 60 in radius and rigid insert 0.978in diam. was again used for this investigation. The insert penetrated the shell, being welded to the shell on both the outer and inner surfaces.   On the outer surface the weld was machined to retain the cylindrical form of the insert as shown previously in Fig. IV.4. The outer
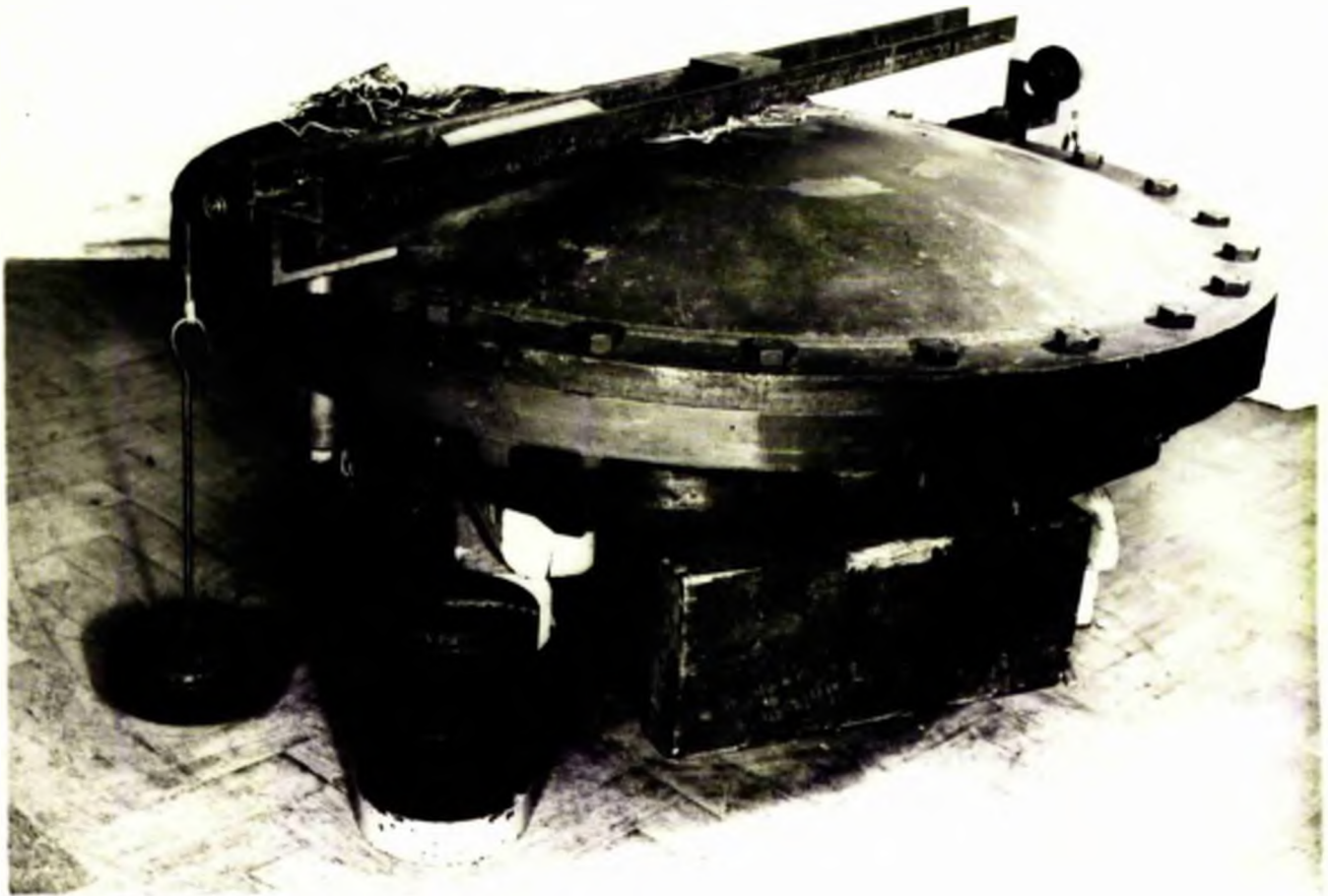
Fig.IV.17   A 'Twisting' Moment Applied to a Shallow Shell
             Through a Rigid Insert.
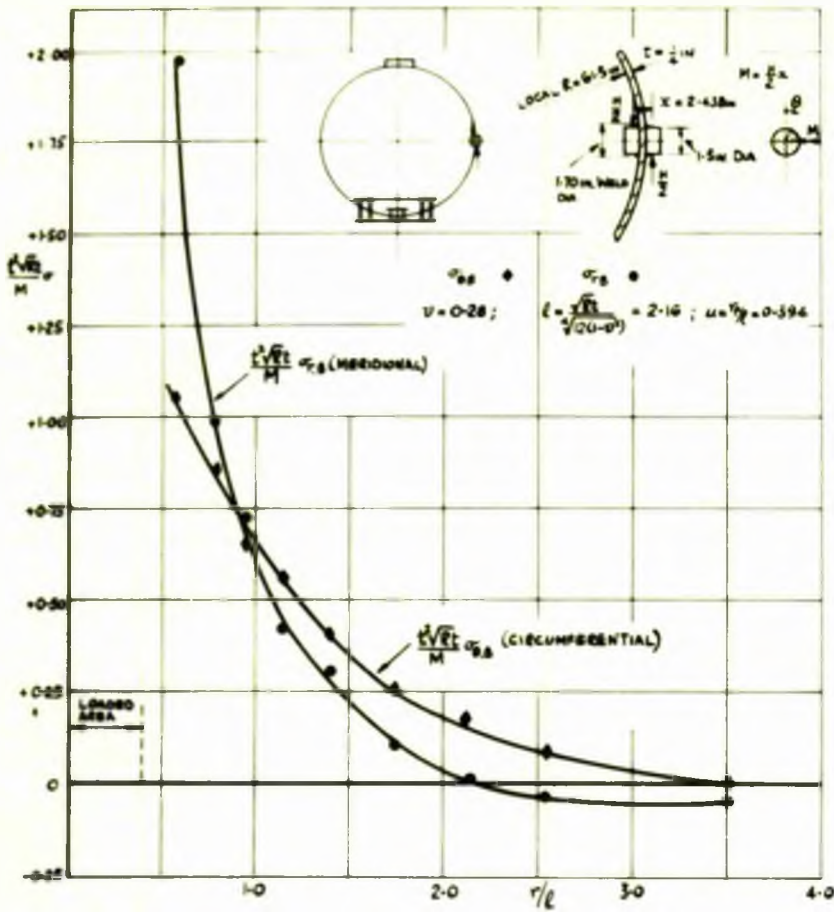
Fig. IV-16a Bending Stress on the outer
Surface due to a Bending Moment M
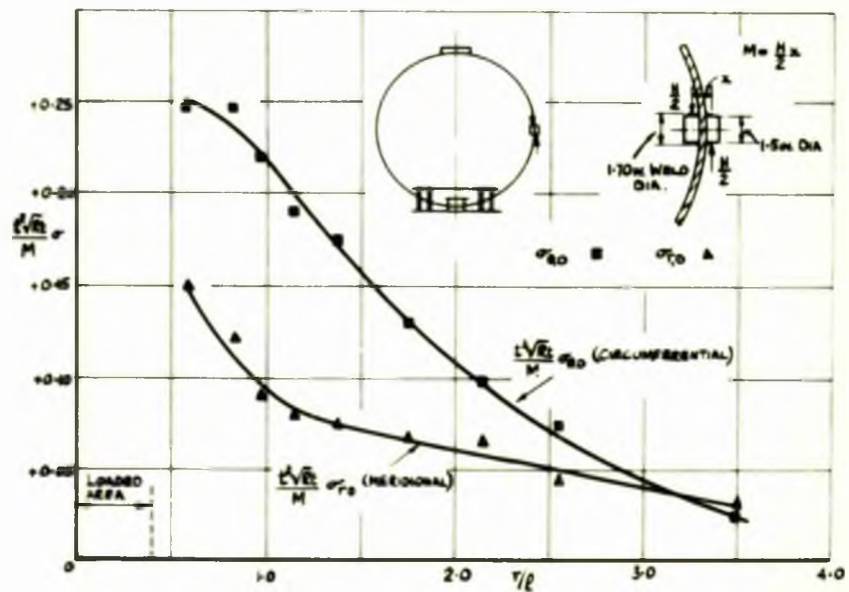
Fig. IV-16b Direct Stress due to a Bending
Moment M

Fig. IV-16 Experimentally obtained Direct Stress and Bending Stress on the outer surface, in a great circle line $\theta=180°$
of a Complete Sphere (13ft-6in Dia.) due to a Bending Moment M applied to the shell by means of welded pads
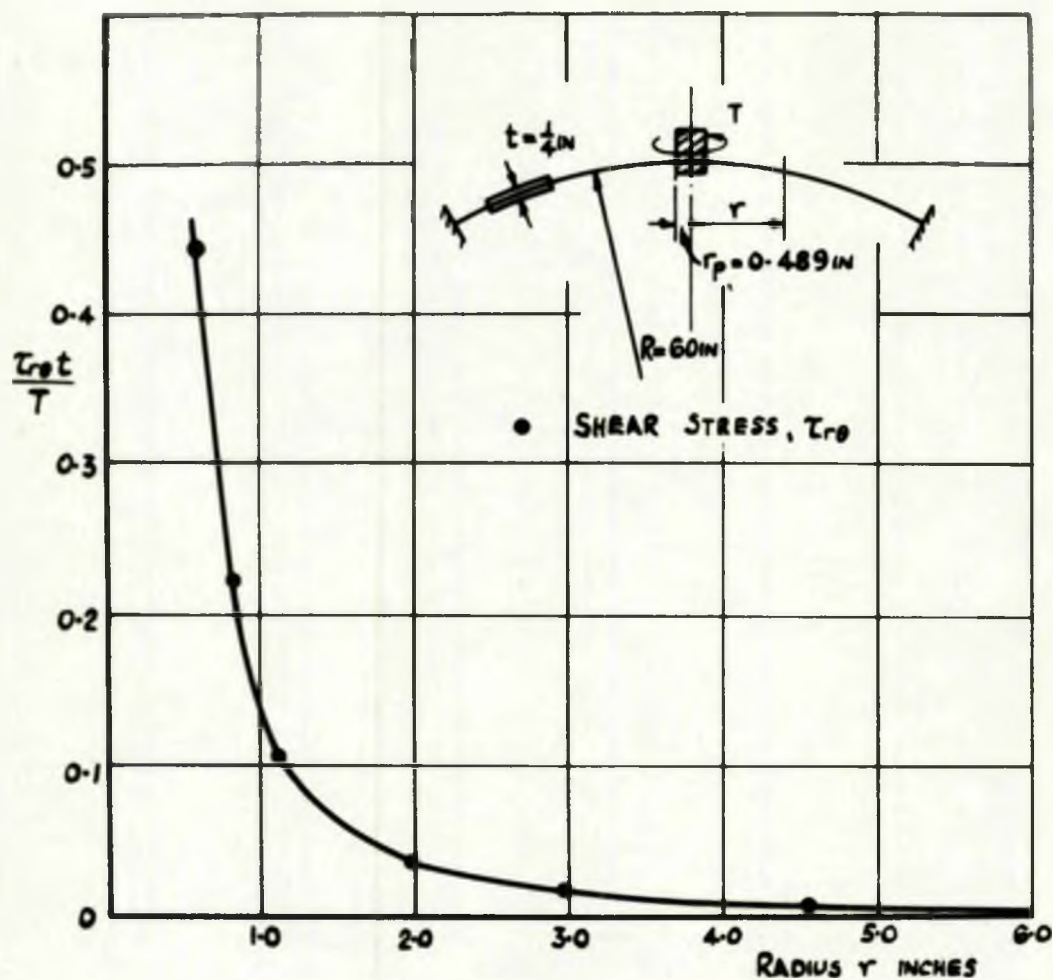
FIG. IV.18 EXPERIMENTALLY OBTAINED MAXIMUM 'MID-SURFACE' SHEAR STRESS IN A SHALLOW SHELL DUE TO A TWISTING MOMENT T, APPLIED TO THE SHELL BY MEANS OF A RIGID INSERT.

boundary, - 3ft. 3in chord diam., - was welded to a heavy flange ring and mounted in the horizontal plane, on the extended table.

Loading Technique:-   The twisting moment was applied to the insert by means of a 3" x 1½" channel of 4 ft. 6in length, rigidly secured at its centre to the insert.   Equal horizontal forces, acting in opposite directions, were applied to the ends of the channel at 50in centres using suitable pulley arrangements and dead weights as shown in Fig. IV.17.

Measurement of Strain and Displacement:-   The electrical resistance strain gauges discussed earlier, the layout of which is shown on Fig. IV.5, were used in this investigation.   The remarks made in the previous section, (IV.1.1b, pp.177-178) regarding gauge layout and strain recording are again relevant.   In this case, however, the gauges positioned at 45° to the great circles were also used.

For this type of loading it was noted that the 45° strain gauges were the only gauges to show any significant strain reading and also that the values of the strain on the inner and outer surfaces were substantially the same, apart from in the immediate vicinity of the stud where small differences occurred.

The application of the twisting moment, therefore, only produced 'mid-surface' shear stresses in the shell, the bending stresses and direct stresses being insignificant.   From the recorded strains $\varepsilon_{45°}$ the maximum shear stress was determined at the various stations using the relationship $\tau_{r\theta} = G\gamma_{r\theta} = 2G\varepsilon_{45°}$ (IV.3) these are plotted in Fig. IV.18.

IV.1.4   TANGENTIAL LOADING

Tangential loading was applied to the shell through a rigid insert, or stud attachment, welded to the vessel. Experiments were carried out on both the shallow shell and the complete sphere, and discussion of this load action is considered under these two sections.

Shallow Shell

Experimental Model:-   The shallow shell, previously described in connection with the radial loading and bending and twisting moments, was used for the present investigations.   The shell was $\frac{1}{4}$in thick, 60in radius, with a rigid insert of 0.978in diam. as shown in Fig. IV.19.   The outer boundary, 3 ft. 3in chord diam., was welded to a heavy flange ring and mounted, in the horizontal plane, on the extended table.

Loading Technique:-   The tangential shear load was applied at the surface of the shell by a force $(H + \delta H)$ and at some distan from the surface by a smaller force (δH) as indicated in Fig.IV. The magnitude of δH and the distance from the mid-surface was su that the resultant moment action at the attachment and on the mid-surface, was zero.

The lower loading arm, placed as near to the surface of th shell as possible, consisted of:-   a 2" x $\frac{5}{16}$" loading plate, wh was a push fit over the insert;   a loading rod of $1\frac{1}{4}$in diam;   a thrust washer and loading nut.   The load was applied to the plate and rod by screwing up the loading nut.   To prevent the torque, which was applied to the nut during loading, from reach the insert, a torque reaction block was fixed to the loading ro
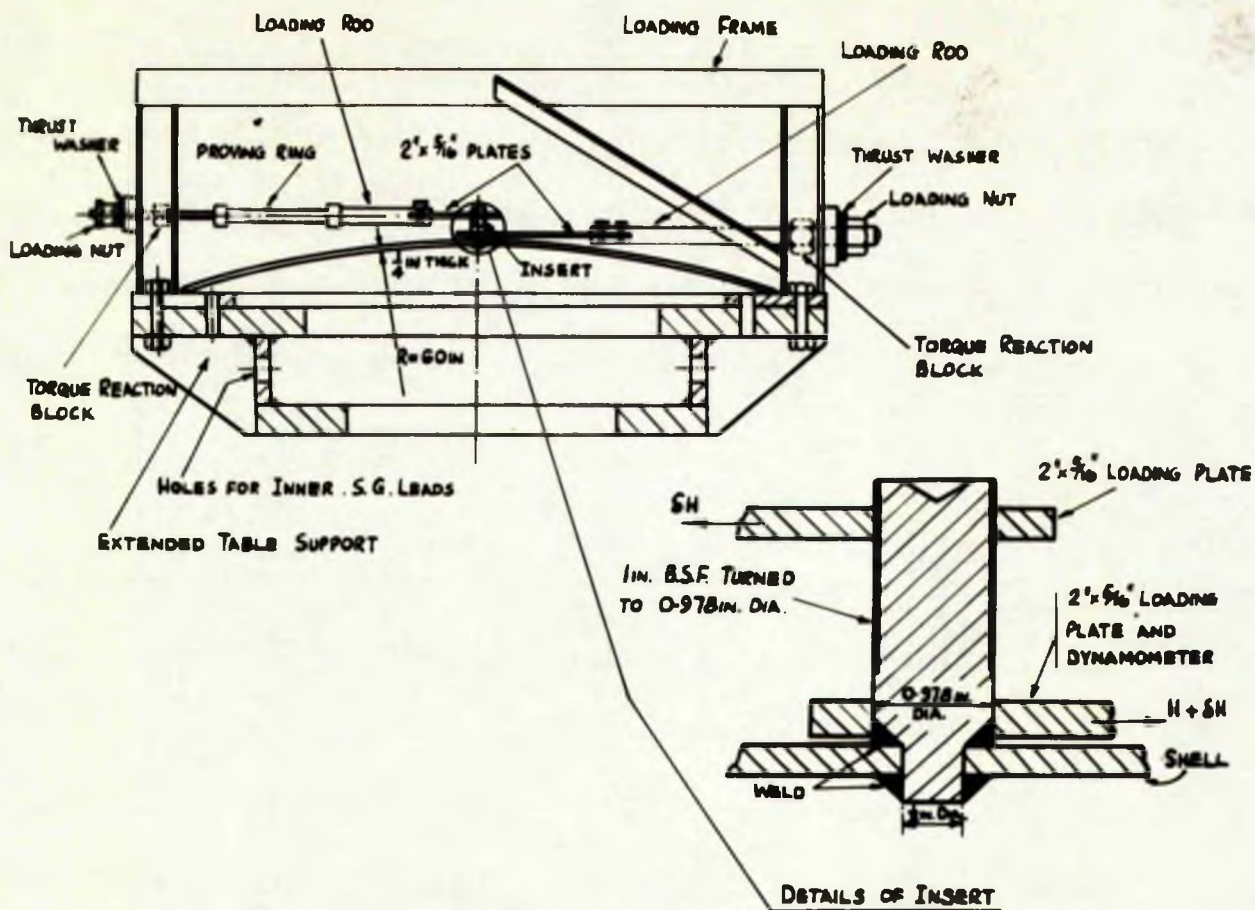
Fig.IV.19   Arrangement of the Shallow Shell under Tangential Loading Applied Through a Rigid Insert.

This reaction was transferred from the block to the loading frame and thus to the extended table.

The horizontal reaction from the loading arm was also carried by the loading frame and transmitted thereby to the extended table support.

The magnitude of the load in the arm was measured by means of a strain gauge dynamometer. Two $\frac{1}{2}$in long electrical resistance foil gauges, connected in series, were fixed to the upper and lower faces of the 2in wide loading plate, thus eliminating the measurement of strains due to bending. The loading arm was calibrated up to 3.0tons in a testing machine.

The upper loading arm was of similar construction to that of the lower arm. In this case, however, the force (δH) was measured by a 1250lb. proving ring which had been previously calibrated in a testing machine. The horizontal and torque reactions were again transferred to the loading frame.

In order to determine the magnitude of the force (δH) in the upper loading arm, corresponding to the force (H + δH) in the lower arm, such that the resultant moment at the attachment and in the mid-surface was zero, the following procedure was adopted.

The distance of the lower arm from the surface of the shell was first determined. Using this information the distance of the upper arm was fixed and the probable values of the force (δH) or values of (H + δH) were determined. On this basis the insert was loaded up to the first increment.

The force (δH) was further adjusted so that the inner and outer strains, in any one direction, in the station nearest the

insert, were identical.   That is, all bending stresses were
eliminated from the shell at the insert.   When such a condition
was established, the values of the strain at all stations were
recorded.

This procedure was repeated for each increment of load.

Measurement of Strain:-   The electrical resistance strain gauges
used in the earlier tests, the layout of which is shown in Fig.IV.
were employed in this investigation, the comments made earlier
regarding gauge layout and strain recording being again relevant,
pp.177-178.

The load was arranged to be applied in the plane containing
the strain gauged line $\theta = 0°$ and also in the plane $\theta = 90°$.   This
enabled both the normal and shear strains to be obtained on both
these lines.

It was found that in the line $\theta = 0°$, only normal strains
were of significance, whereas in the line $\theta = 90°$ the significant
gauges were those at $45°$.

From these values of strain, the stresses in the meridiona
and circumferential directions on the $\theta = 0°$ line and the shear
stresses on the $\theta = 90°$ line were computed, using eqts. IV.1, IV.
and IV.3.   The direct stresses, thus calculated, are shown in
Fig. IV.20.   The bending stresses were found to be wholly
negligible in comparison with the direct stresses.

Complete Sphere

Experimental Model:-   The 13 ft. 6in diam. model sphere shown i
Figs. IV.7 and IV.13 and discussed on pp.178, 184, 185, was agai
used for the present investigation.
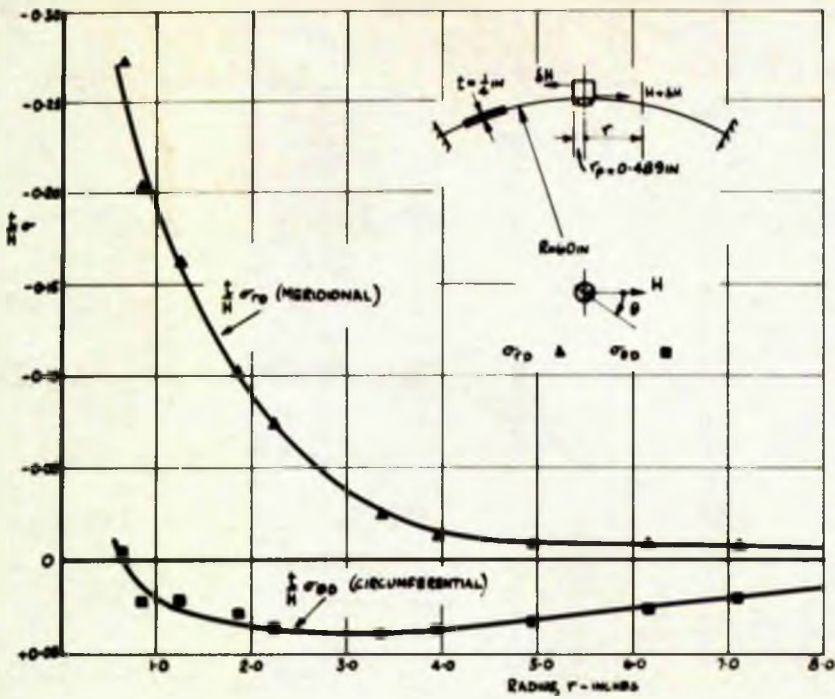
Fig. IV·20a   DIRECT NORMAL STRESS on θ=0° LINE due TO A TANGENTIAL LOAD H
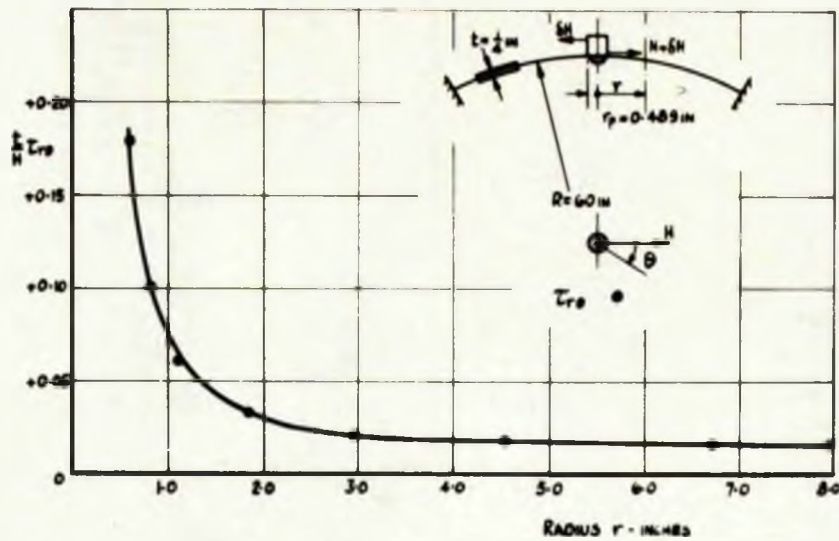
Fig. IV·20b   'MID SURFACE' SHEAR STRESS on θ=90° LINE

Fig. IV·20   EXPERIMENTALLY OBTAINED DIRECT NORMAL STRESSES (on θ=0°LINE) AND 'MID-SURFACE' SHEARING STRESS (on θ=90°LINE) OF A SHALLOW SPHERICAL SHELL DUE TO A TANGENTIAL LOAD H APPLIED THROUGH A RIGID INSERT

<u>Loading Technique</u>:-   The load was transmitted to the shell by means of stud attachments of $1\frac{1}{2}$in diam., welded with continuous fillet welds to the surface of the sphere.   The studs were located diametrically opposite on the equator and on the inner and outer surfaces on the same radial axes.

The studs on the inside of the vessel were loaded by forces acting vertically down, while those on the outside surface could be loaded in either direction - in this case vertically down.

The method of applying these loads is shown in Fig. IV.13 and 14 and discussed in detail on pp.184-188.   The loading procedure adopted in this case was the same as in the bending moment application, and was as follows.   The inside studs were first loaded, using the loading beam and inner rods 2 and 3, the strains being suitably recorded.   Secondly the outside studs were loaded, first in one and then in the other direction, using rods 1 and 4.   It will be noted that these separate results are exactly those of the bending moment application.   In order to determine the strain values for the tangential shear load, the two relevant inner and outer results were superposed.

A further test was undertaken in which all four rods were used, equal loads being applied vertically down to all stud attachments.   As in the case of the bending moment reported earlier, p.188, difficulties were encountered regarding repeatability of results, due to slight differences in the load values at the attachments.   The results presented, therefore, are those obtained by applying the inner and outer loads separately.

<u>Measurement of Strain</u>:-   The electrical resistance strain gauges

used for the bending moment test, on the complete sphere, the
layout of which is shown in Fig. IV.15, were employed in the
present investigations.   The two 'vertically' gauged lines
were in the plane of the tangential force (H) and the gauges
on the equator were at 90° to the plane of (H).

The other comments regarding the gauge layout, wiring and
strain recording given on pp.189 and 190 are again relevant in
this case.

A comparison of strains on the upper and lower 'vertical'
lines, showed that good agreement between the two was obtained.
As in the bending moment case, the only exception to this was
the circumferential strain on the inner surface (ε_{θ}^{i}) in the
immediate vicinity of the load, this divergence being attributed
to local imperfection of the sphere.

From the strain results on the 'vertical' lines ($\theta = 0^{\circ}$
and $\theta = 180^{\circ}$) the corresponding bending and direct stresses were
obtained, using eqts. IV.1 and IV.2.   The direct stresses are
plotted in Fig. IV.21 and as in the earlier test on the shallow
shell the bending stresses were found to be wholly negligible in
comparison with the direct stresses.

The strains on the equator line, $\theta = 90^{\circ}$ were also recorded
and it is noted that these values were very small, yielding
corresponding bending and direct stresses which were negligible
in comparison with those on the $\theta = 0^{\circ}$ line.
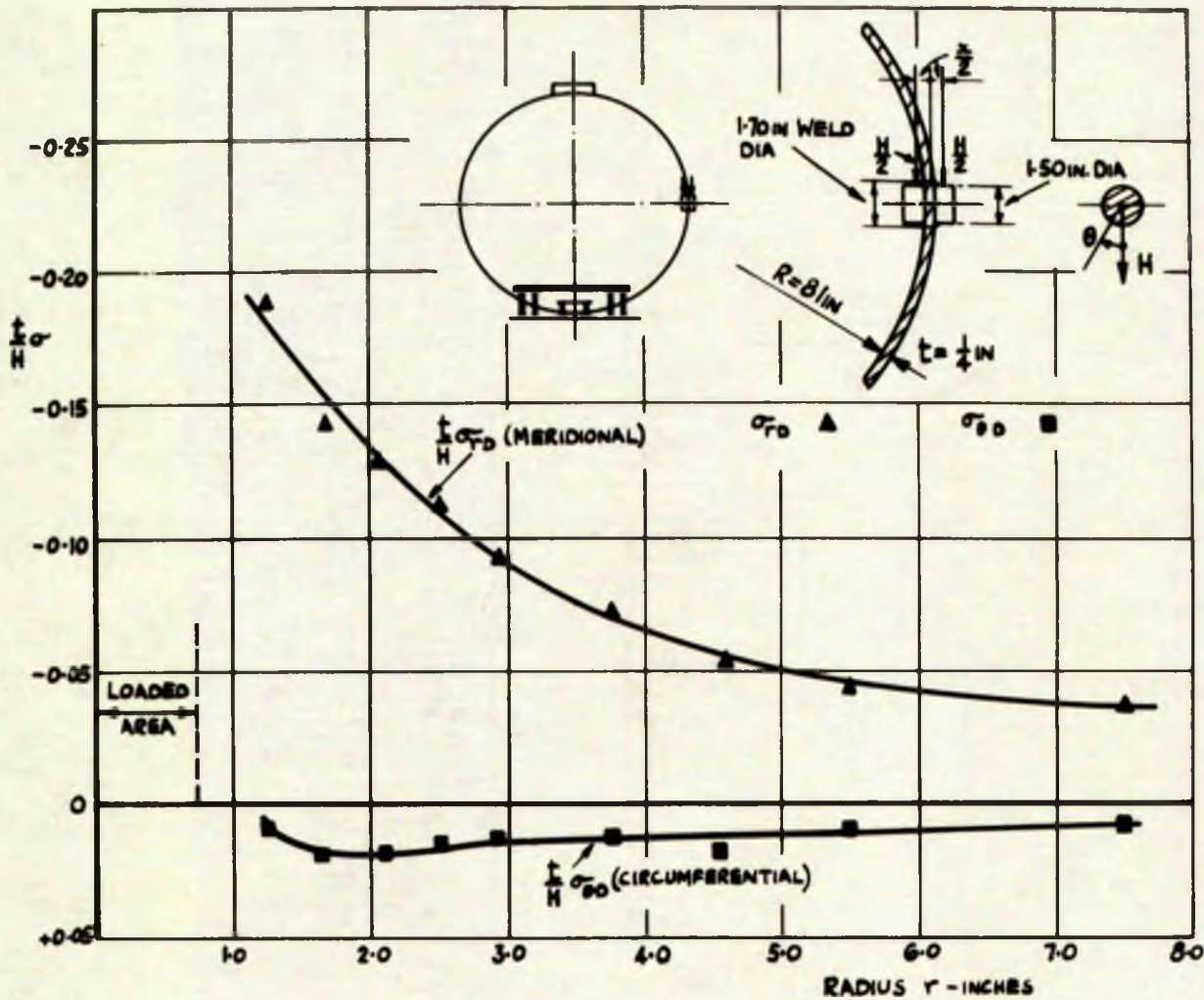
Fig. IV-21 EXPERIMENTALLY OBTAINED DIRECT STRESSES IN A GREAT CIRCLE LINE θ=0° OF A COMPLETE SPHERE (13FT-6IN DIAM) DUE TO A TANGENTIAL LOAD H, APPLIED TO THE SHELL BY MEANS OF WELDED PADS

IV.2   THE SHALLOW CAP CONCEPT

In introducing the Influence Line Method (Chapter II.3) attention has been drawn to the fact that the primary analysis necessary when applying the method is always that of a unit radial or tangential load, moment or torque, concentrated or distributed over a small area. This is the case irrespective of whether the problem is symmetrical or unsymmetrical in nature. These unit actions are always considered to act at the centre, or crown, of a shallow cap, the extent of which corresponds to the 'die-out' distance for the particular action considered.

The second phase of the experimental work was directed towards the examination of this concept in the case of radial loading.   This type of loading was selected owing to its ease f application at any point on the shell surface.

The radial load was applied to the shell in a number of ositions 'off-set' from the geometric centre of the shallow hell.   The point of application of the load became the centre r crown of a shallow cap which is essentially unsymmetrical in elation to the geometric centre of the finite shallow shell. hese experiments investigated:-

(a)   the influence of the welded boundary on the stress distribution in a shallow cap;

(b)   the distribution of stress and radial deflection in several directions around the crown of the shallow cap;

(c)   the effect of superposing two loads centred at the crowns of two different shallow caps.

The experimental model, loading technique and strain

measurement are common to all the above tests and are, therefore, discussed at this point.

Experimental Model:-   This series of experiments was carried out on a $\frac{1}{4}$in thick, 60in radius shallow shell.   As in earlier work the outer boundary - 3 ft. 3in chord diam. - was welded to a heavy flange ring and mounted, in the horizontal plane, on the extended table.

Loading Technique:-   The radial loadings were applied to the shell by means of a loading frame, loading shackles, thrust washers and proving rings of 1250lb capacity which had been previously calibrated.   The frame, which was fabricated from 3" x 1$\frac{1}{2}$" channel and 2" x 1$\frac{1}{2}$" angle, was capable of housing the loading shackles in a variety of 'off-set' positions and always normal to the shell surface - as shown in Fig. IV.22.

The applied load was distributed over a circular area of $\frac{1}{4}$in diam. corresponding to a μ value of 0.0588.   To ensure that the load was uniformly distributed a renewable lead insert was placed between the $\frac{1}{4}$in diam. anvil on the proving ring and the shell, thus allowing for any surface irregularities.

Measurement of Strain and Deflection:-   Saunders Roe $\frac{1}{2}$in length foil gauges were again employed to measure the strain on the outer and inner surfaces, using the same fixing techniques and calibration procedure as described earlier.   The gauges were fixed in three directions, corresponding to the meridional, circumferential and 45° lines of the shell, and placed along one great circle. The layout is shown in Fig. IV.23. As discus on p.177, this type of layout was considered more accurate for
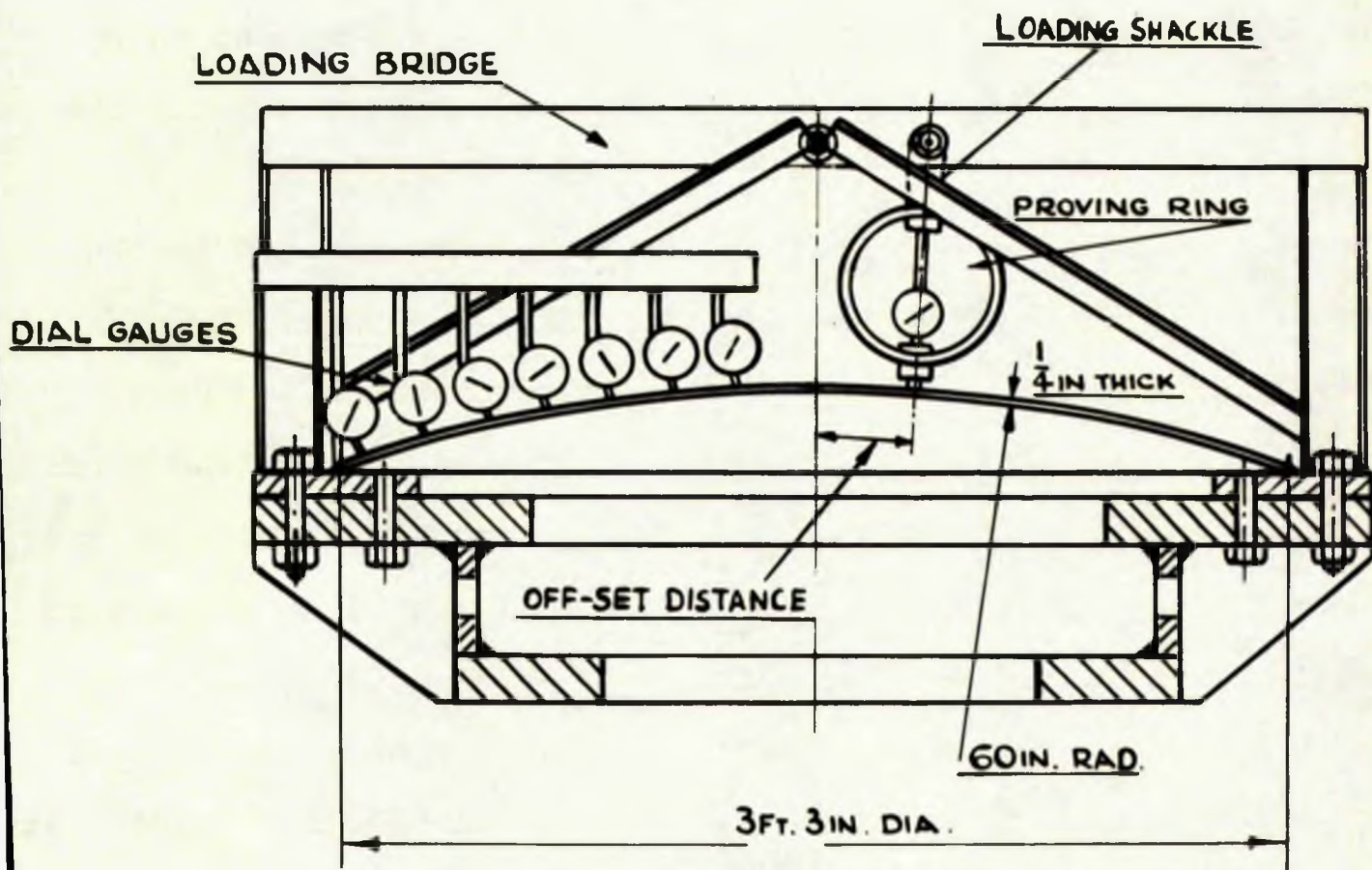
Fig.IV.22 Arrangement of the Shallow Spherical Shell under
Radial Loads 'Off-Set' from the Geometric Centre.
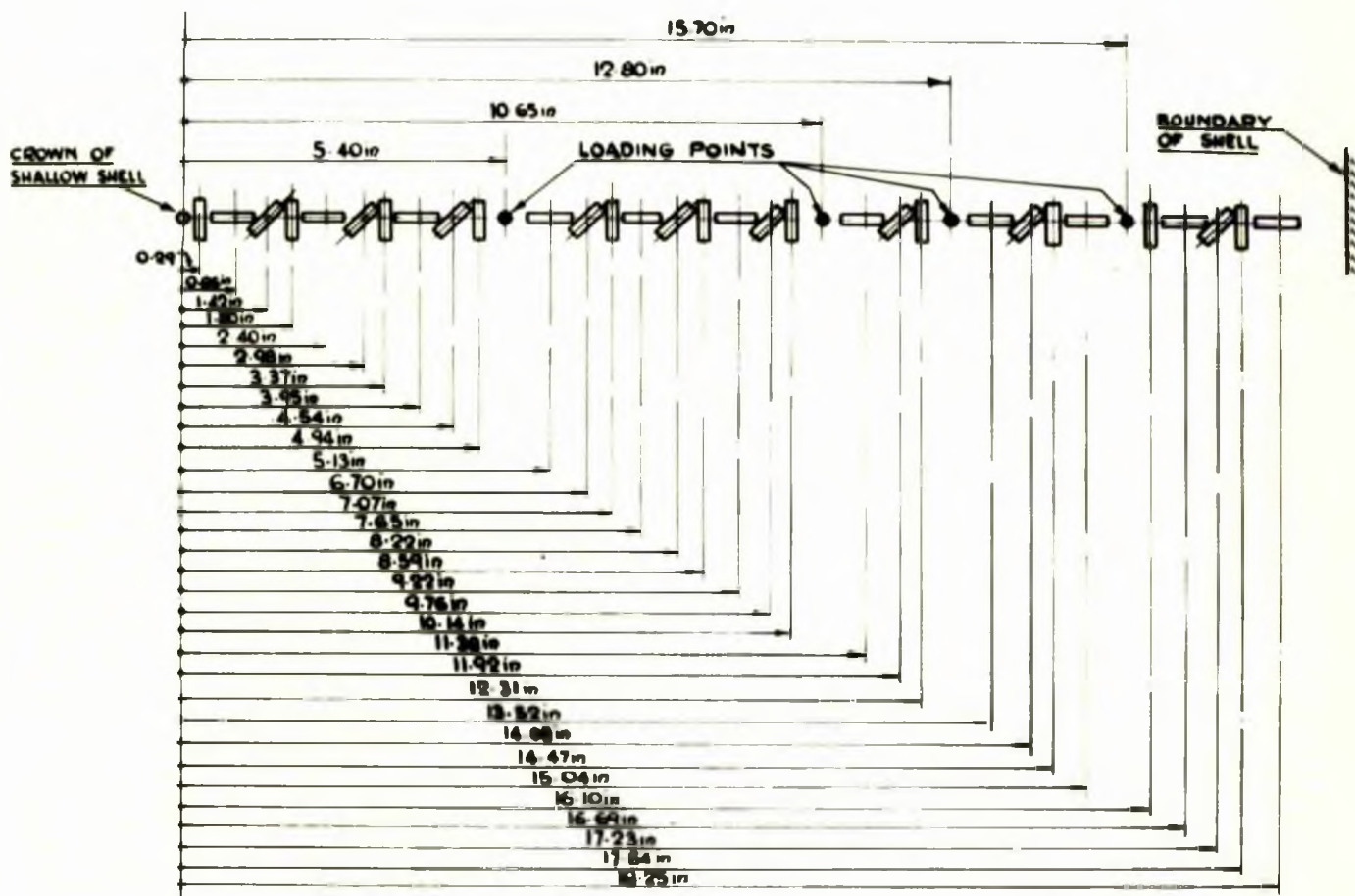
FIG. IV-23 STRAIN GAUGE LAYOUT FOR INNER AND OUTER SURFACES FOR 'SHALLOW CAP' TESTS
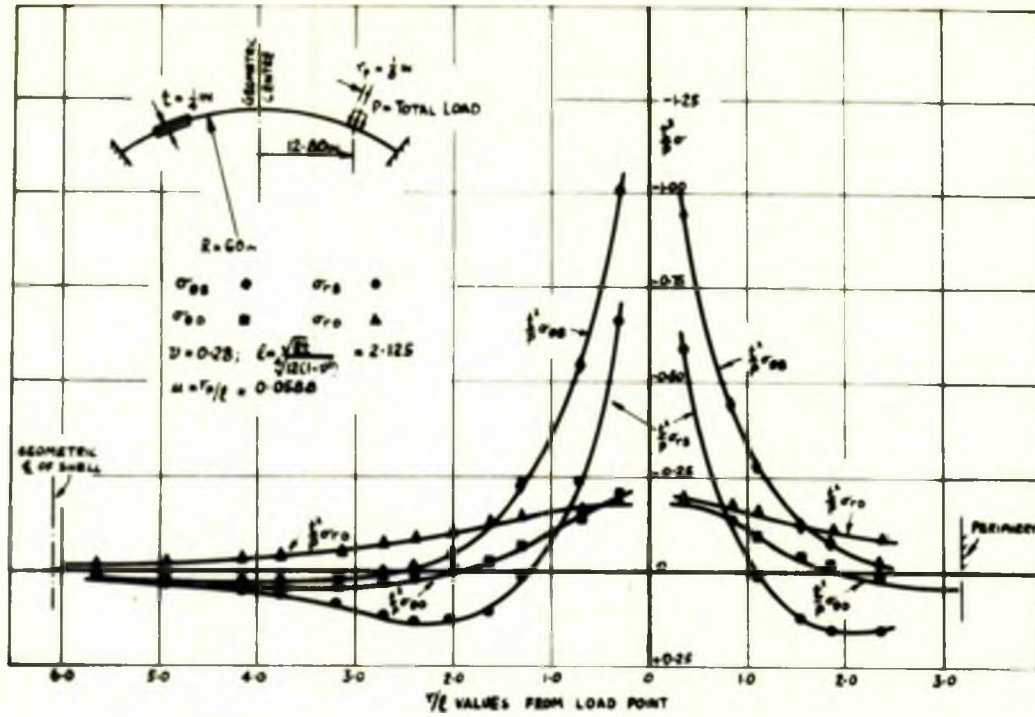
FIG. IV·24a THE DISTRIBUTION OF BENDING AND DIRECT STRESSES DUE TO A RADIAL LOAD AT A POSITION 12·80IN FROM THE GEOMETRIC CENTRE
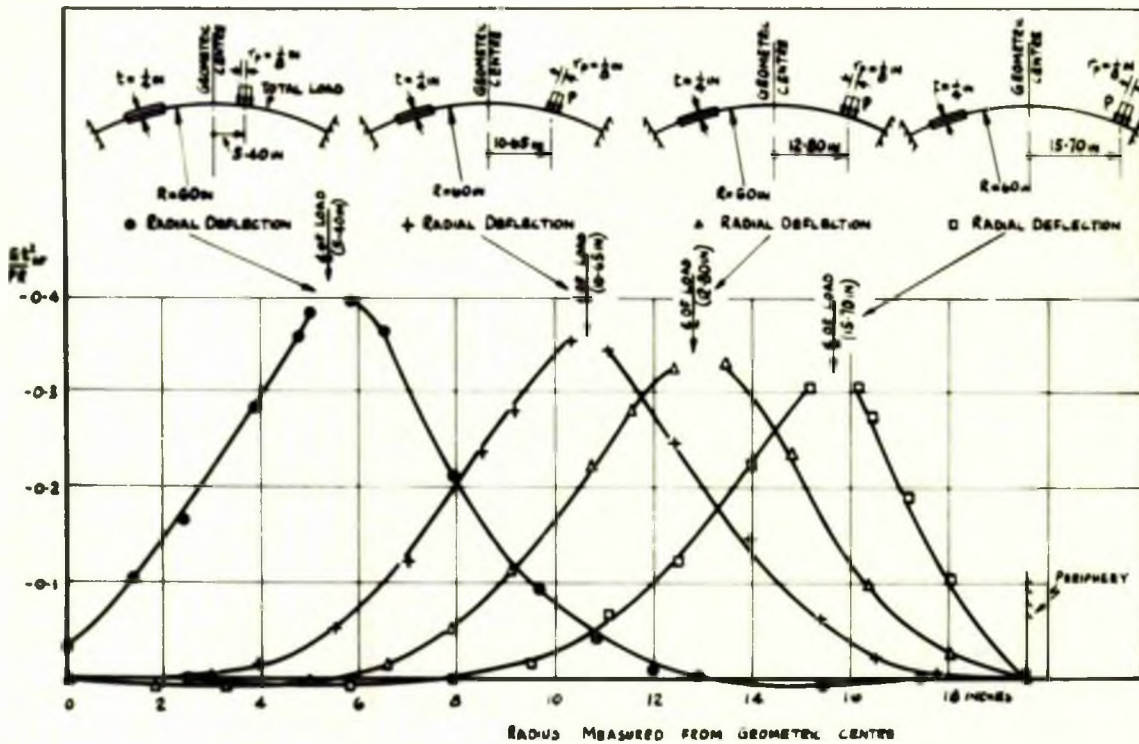
FIG. IV·24b THE DISTRIBUTION OF RADIAL DEFLECTION DUE TO RADIAL LOADS AT 5·40, 10·65, 12·80 AND 15·70IN FROM THE GEOMETRIC CENTRE

FIG. IV·24 THE INFLUENCE OF THE WELDED BOUNDARY ON STRESSES AND DEFLECTIONS IN A SHALLOW SPHERICAL SHELL OF THICKNESS ½IN AND RADIUS 60IN UNDER A RADIAL LOAD P

non-axisymmetric loading, though interpolation from the plots of
strain (or strain per unit load) against radius was required to
determine the three strains at any one point.

The 50-way strain recorder was employed in these tests and
the procedure for measurement and repeatability of readings (i.e.
zero drift of gauges, etc.) was as described in connection with
earlier tests pp.173-175.

The radial deflections of the shell were measured using
.0001in dial gauges.   The arrangement for support, adjustment
and alignment of the dial gauges is shown in Fig. IV.22.   The
dial gauge rig could be so arranged that radial deflections could
be measured at any point on the shell surface.

IV.2.1   THE INFLUENCE OF THE WELDED BOUNDARY

The radial load was applied at four different positions at
8.40, 10.65, 12.80 and 15.70in radius, measured in plan from the
crown of the shallow shell.   These positions were located on the
strain gauged great circle and are shown in Fig. IV.23.   The
strains in both the meridional and circumferential directions
along this great circle were measured for each position of the
load.   Using eqts. IV.1 and IV.2 the values of the direct and
bending stresses corresponding to the experimental strains were
computed.

The results from one such position (12.80in) are plotted
non-dimensionally in Fig. IV.24a.   The complete series are shown
later in Chapter V where they are compared with the theoretical
values.

In order to measure the radial deflection on a great circle

for the various load positions, the shell was loaded along a
line 180° to the gauged line – thus avoiding the strain gauges.
The results for the four load positions are shown in Fig. IV.24b.

IV.2.2 DISTRIBUTION OF DEFLECTION AND STRESS AROUND THE CROWN OF THE SHALLOW CAP

The investigation of the previous section was extended to
consider the distribution of both deflection and stress around
each load point.   That is, to examine the behaviour of several
shallow caps, whose crowns were situated off-set from the
geometric centre of the shell.

Firstly, radial deflections were measured along 0°, 45°,
90°, and 180° shallow cap great circles.   Typical results for
one such cap, the 5.40in, are shown in Fig. IV.25, and are seen
to lie on a common curve.

Secondly, in order to examine the behaviour of the stresse
in the shallow caps, the strain gauges on the great circle passi
through the crown, or geometric centre, of the shallow shell wer
used.   In this case the load itself was successively applied
around the circumference of a circle of radius equal to that of
the loading point position (or shallow cap crowns) and the strai
recorded on the gauged great circle for each load position.   O
average, eight such positions were considered for each of the o
set distances.

Each gauge point, such as C shown in Fig. IV.26, on the
gauged great circle was thus looked upon as a point on a series
of shallow spherical caps with the appropriate load points (for
example B) as their crowns.   The procedure adopted will be
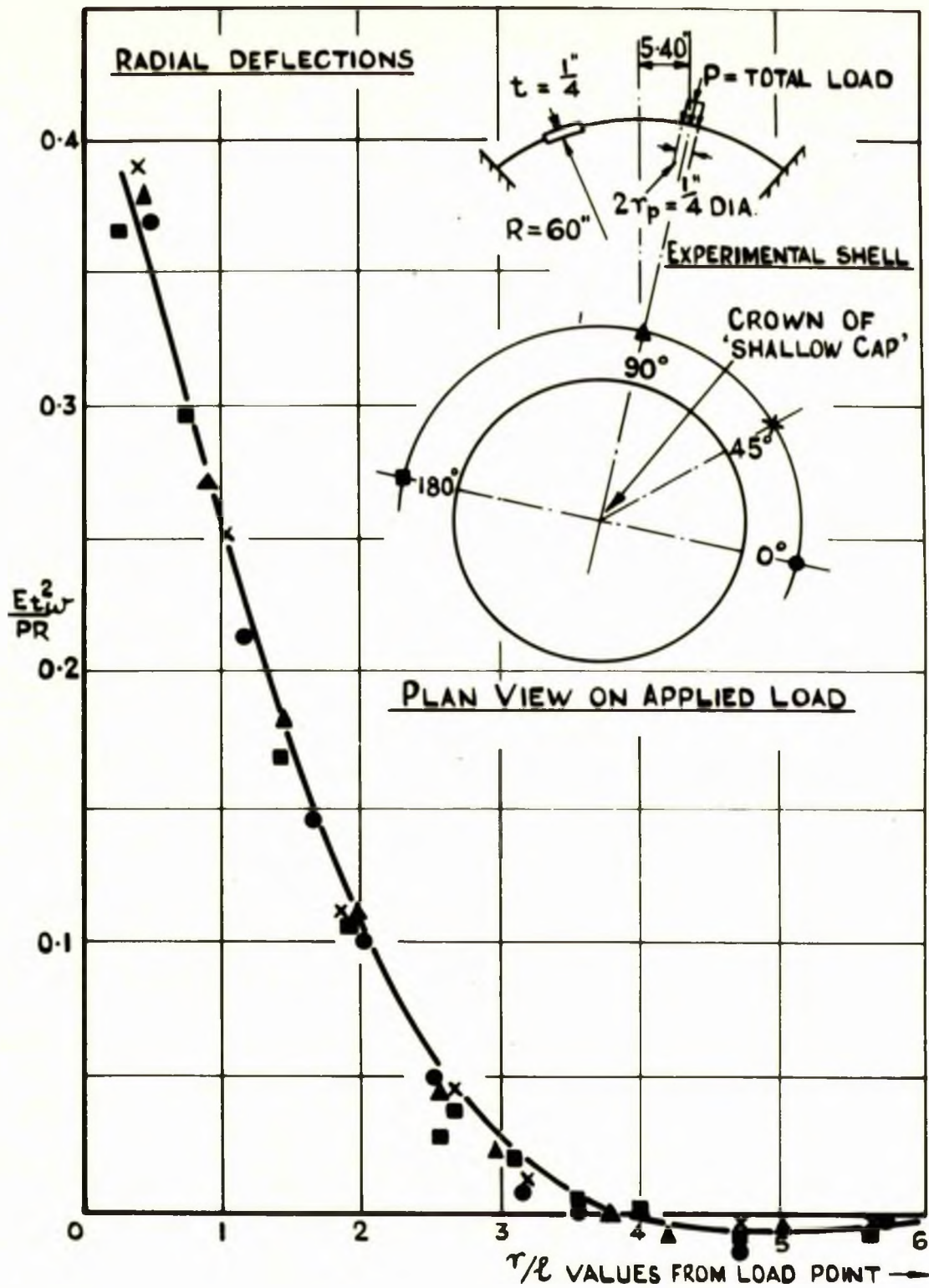
FIG. IV·25 THE DISTRIBUTION OF RADIAL DEFLECTION AROUND THE CROWN OF A SHALLOW CAP 5·40 IN FROM THE GEOMETRIC CENTRE.

POLE POINT

REFERENCE PLANE

-ve   +ve

45°

$E^\circ_{45} = 0.250$
$E^\circ_1 = 0.082$

-0.220   -0.17   -0.100

LOAD POINT B

0°

-22½°

180°

GEOMETRIC CENTRE
OF SHELL

D   0.220   0.100   E   A   F   G

0.117

1.10 IN

1½ IN

GAUGED GREAT CIRCLE

45°

4.38 IN

157½°

GAUGED POINT
C

5.4 IN
LOAD POINT RADIUS

135°

112½°

90°

67½°
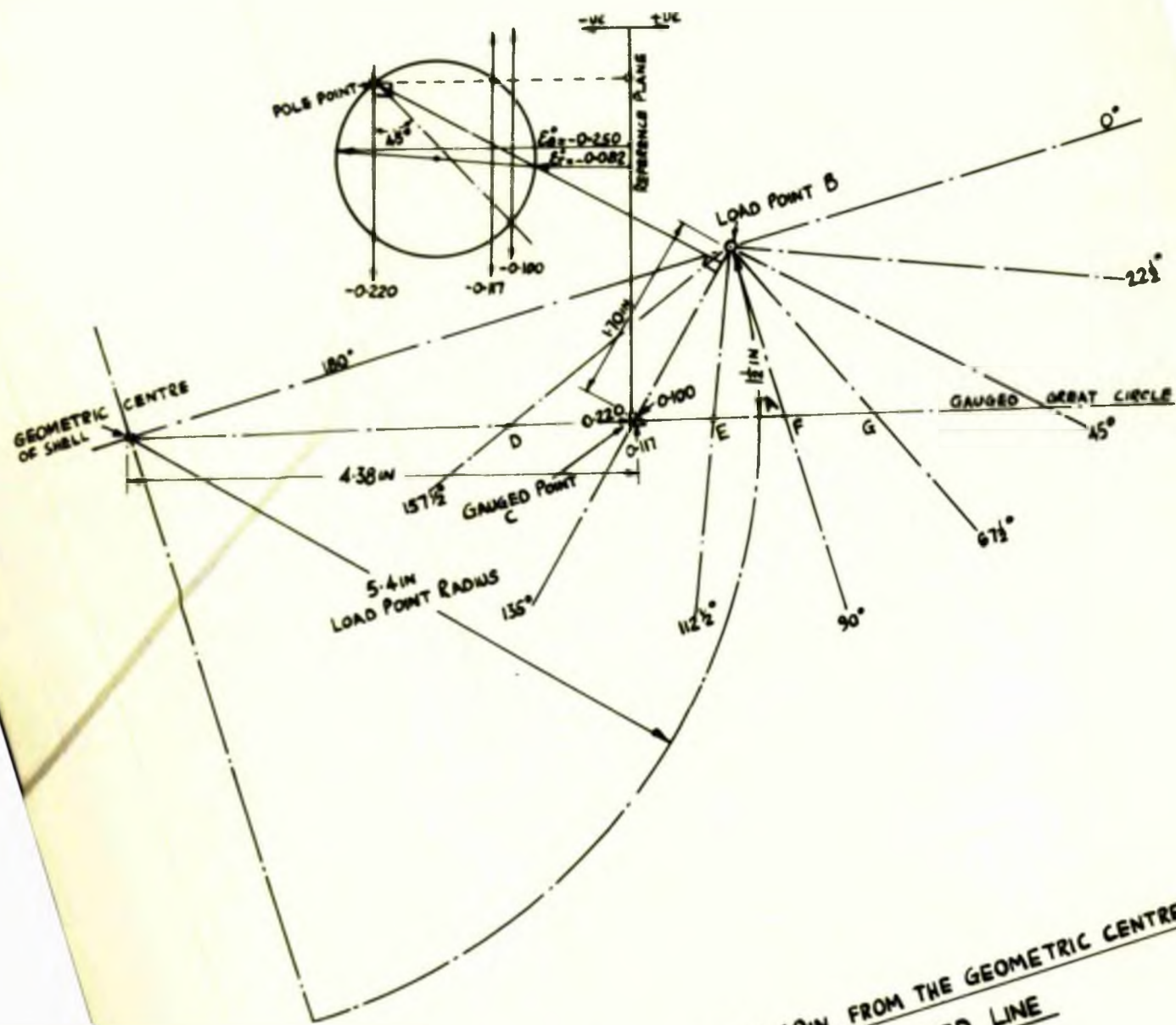
FIG. IV·26   A LOAD POINT 'B' SITUATED 5·40IN FROM THE GEOMETRIC CENTRE AND AN ARC

DISTANCE OF 1½IN FROM 'A' ON THE GAUGED LINE

described with reference to the 5.40in off-set position, and
with the load point in position B, 1½in from the gauged line as
shown in Fig. IV.26.

The inner and outer strains on the gauged line were recorded
due to the application of the radial load at point B and, using
the procedures outlined earlier, their variations were plotted.
From these graphs the magnitudes of the three strains at any
point C on the gauged line were determined.   In this case the
magnitudes of the three outer strains at C in directions $0°$, $45°$,
$90°$ to the gauged line were -0.220, -0.100 and -0.117 respectively.

These strains were then resolved, using the Mohr's circle
of strain, to give strains in planes corresponding to the meridional
and circumferential directions of the shallow cap at B (i.e. in the
line BC and perpendicular to BC).   Thus $\varepsilon_\theta^o = -0.250$ and $\varepsilon_r^o = -0.082$.
It will be noted, from the strain circle in Fig. IV.26, that the
two strains ε_θ^o and ε_r^o are not exactly principal strains.   Their
deviation, however, is exceptionally small, representative of
experimental error, and in consequence it is permissible to con-
clude that the meridional and circumferential directions of the
shallow cap are, in fact, principal directions on the outer surface
at B.

In a similar manner the strains on the inner surface at B
are computed and using the eqts. IV.1 and IV.2 the direct and
bending stresses determined.

Similar values of stress were determined for the points D,
F, G and H (Fig. IV.26) which lie on $157\frac{1}{2}°$, $112\frac{1}{2}°$, $90°$, $67\frac{1}{2}°$,
$5°$ lines, respectively, and at various distances from the load
point.

This procedure was repeated for loads situated at distances other than 1½in from A and again stresses were obtained at points rotationally displaced around the load points.

The stresses obtained from all these tests were then transposed, using the condition of reciprocal symmetry, on a shallow cap whose crown was the point A and situated 5.40in from the geometric centre of the shallow shell.   The complete results for the 5.40in off-set are shown in Fig. IV.27.   It should be noted in this figure that the ordinate of the direct stresses is five times that of the bending stresses.

It is seen that, within the limit of experimental error, the stress values define a single curve, thus substantiating the rotationally symmetrical nature of the shallow cap, and also the concept of reciprocal symmetry inherent in the derivation of Fig. IV.27.

The results for the other off-set positions are similar to those of Fig. IV.27, and indicate that the boundary influences the experimental stresses and deflections around each load point in the manner shown by the results in Fig. IV.24 and Figs.V.9 & 1

IV.2.3   THE EFFECT OF SUPERPOSING TWO LOADS BOTH 'OFF-SET' FRC
                          THE GEOMETRIC CENTRE

To investigate the applicability of the Principle of Super position, two equal radial loads, 'off-set' from the geometric centre of the shallow shell, were applied simultaneously. Two series of tests were conducted; firstly, the two loads were situated in the 5.40in and 12.80in positions, that is 7.40in apart (Fig. IV.28) and secondly in the 10.65 and 12.80in positi
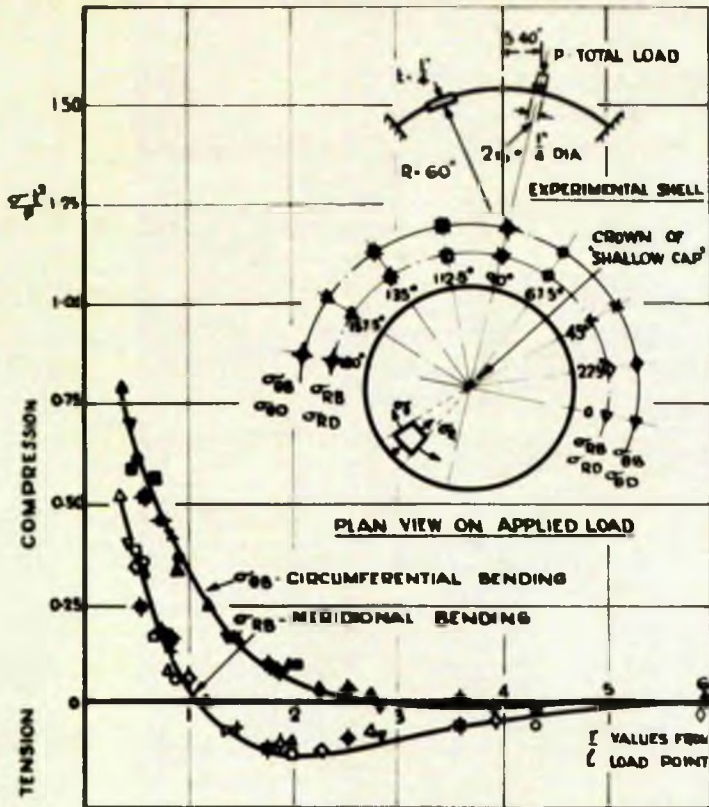
FIG IV 27a THE DISTRIBUTION OF BENDING STRESSES

FIG IV 27b THE DISTRIBUTION OF DIRECT STRESSES
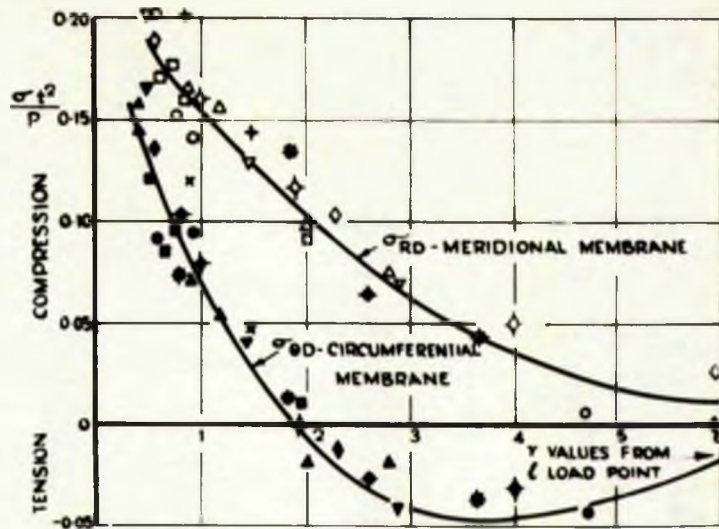
FIG. IV 27 THE DISTRIBUTION OF BENDING AND DIRECT STRESS AROUND THE CROWN OF A SHALLOW CAP

Fig.IV.28   The Arrangement of Two Radial Loads Both 'Off-Set'
                    from the Geometric Centre.
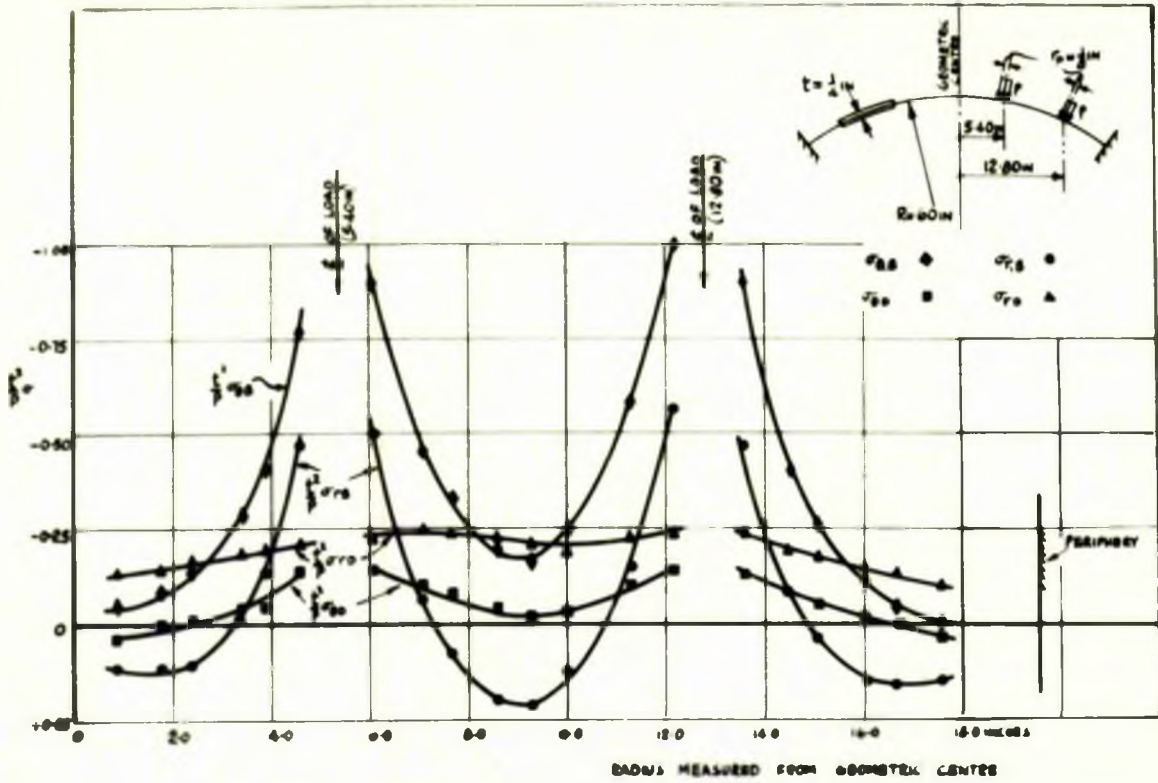
Fig. IV. 29a. THE DISTRIBUTION OF BENDING AND DIRECT STRESS DUE TO TWO SIMULTANEOUSLY APPLIED RADIAL LOADS AT 5·40in AND 12·80in FROM THE GEOMETRIC CENTRE
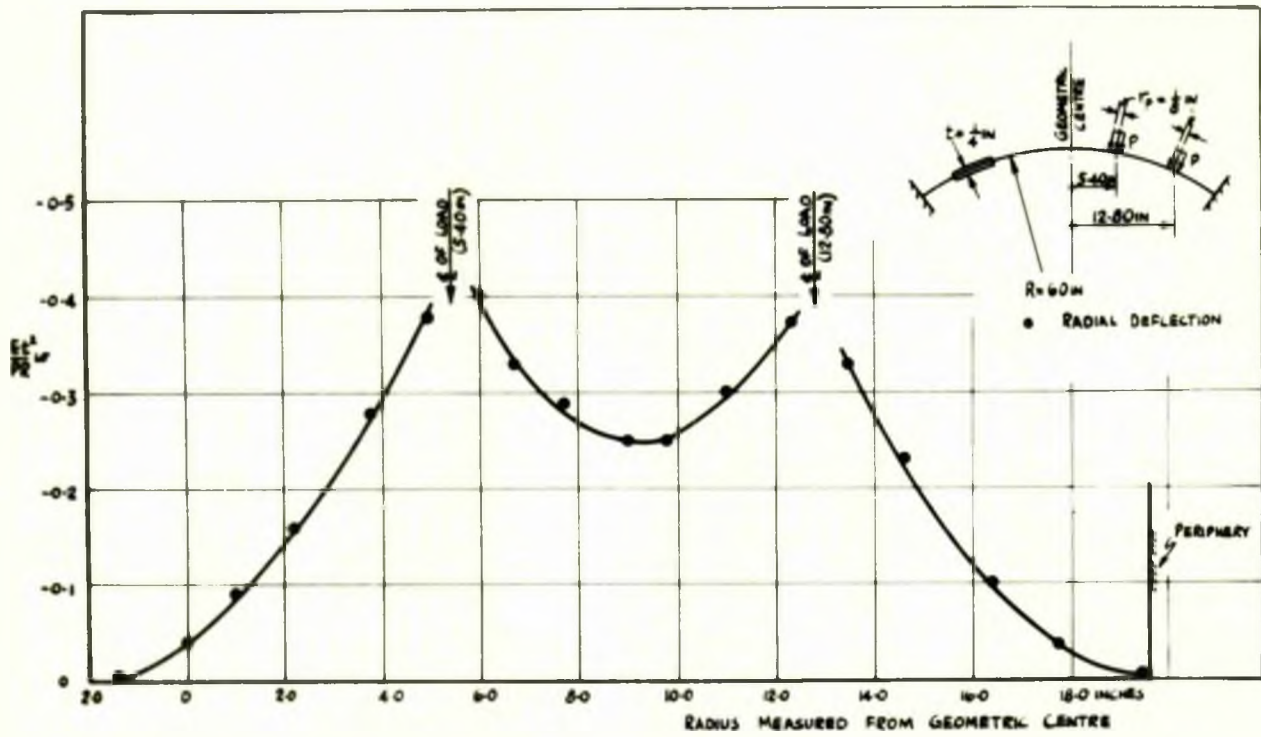
Fig IV. 29b THE DISTRIBUTION OF RADIAL DEFLECTION DUE TO TWO SIMULTANEOUSLY APPLIED RADIAL LOADS AT 5·40in AND 12·80in FROM THE GEOMETRIC CENTRE

Fig. IV. 29 THE EFFECT OF SUPERPOSING TWO RADIALLY APPLIED LOADS BOTH 'OFF-SET' FROM THE GEOMETRIC CENTRE OF THE SHELL

that is 2.15 in apart.

For recording the strains, the loads were positioned on the
gauged great circle, and for measuring the deflections, on the
line 180° to the gauged line.   The two loads were increased
at the same rate and with the usual four increments.   The
strain and deflection were recorded in the manner discussed
earlier.   Results for one such test are presented in Fig.
IV.29.

IV.3   EXAMINATION OF SELECTED COMPOSITE ACTIONS

In this section, experimental work designed to test the
Influence Line Method is presented.   Selected load cases
inclusive of radial loads and moments were experimentally
investigated.   These load cases were amenable to analysis by
the Influence Line Method thus permitting direct comparison of
predicted with experimental values.   These comparisons are
presented in a later chapter, the present text containing the
description of experimental techniques and typical results.
Investigations were carried out on shallow shell segments and a
complete sphere.

IV.3.1   RADIAL RING LOAD

The radial loading was applied in two ways.   Firstly, with
no restriction on the change of slope of the shell across and
along the load path, and secondly with complete fixity of the
shell across and along the load path, preventing any change of
slope in the loaded region.   Discussion of the radial load will
be considered under these two sections.

(a)   Radial Loading Transmitted by a Freely Supported Ring

Experimental Model:-   These investigations were carried out on
a shallow shell of the type previously described, $\frac{1}{4}$in thick and
60in radius.   The outer boundary, 3 ft. 3in chord diam., being
welded to a heavy flange ring and mounted, in the horizontal
plane, on the extended table - shown in Fig. IV.30.

Loading Technique:-   The shell was loaded by means of rotational
symmetrical ring load systems.   Because of the rotational
symmetry it was unnecessary to develop an articulated load, and

UPPER PLATEN OF
TESTING MACHINE

RING LOAD ASSEMBLY

DIAL GAUGE SUPPORT
IN TWO POSITIONS

SHELL UNDER TEST

$\frac{1}{4}$ IN THICK

$R = 60$ IN

EXTENDED TABLE
SUPPORT

LOWER PLATEN OF
TESTING MACHINE

GENERAL ARRANGEMENT

P

LOADING ROD

DIAL GAUGE SUPPORT

SPHERICAL SEATING

DIAL GAUGE ADJUSTMENT
AND ALIGNMENT RIG

LOADING FLANGE FOR
VARIOUS SIZES OF RING

LOADING RING

EXTENDED LEG ON
DIAL GAUGE

PRESTIK PAD

8 IN DIAM.

$\frac{1}{4}$ IN WIDE
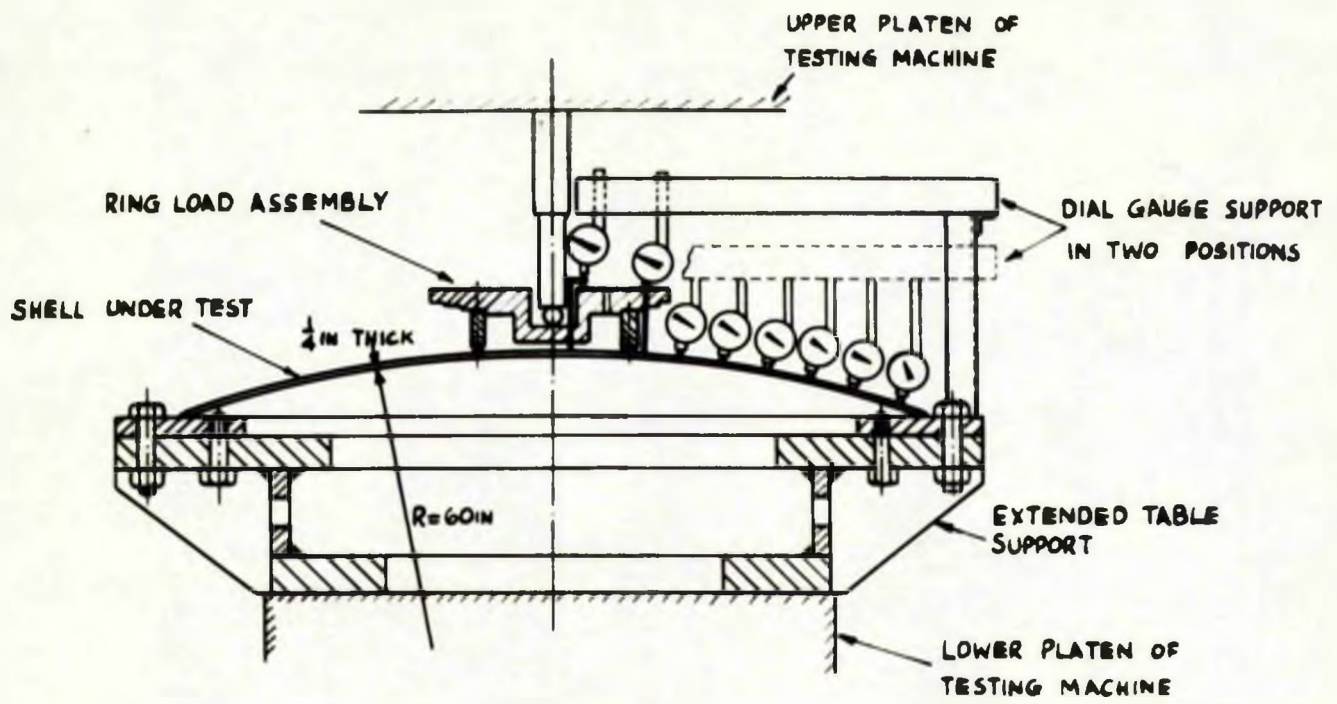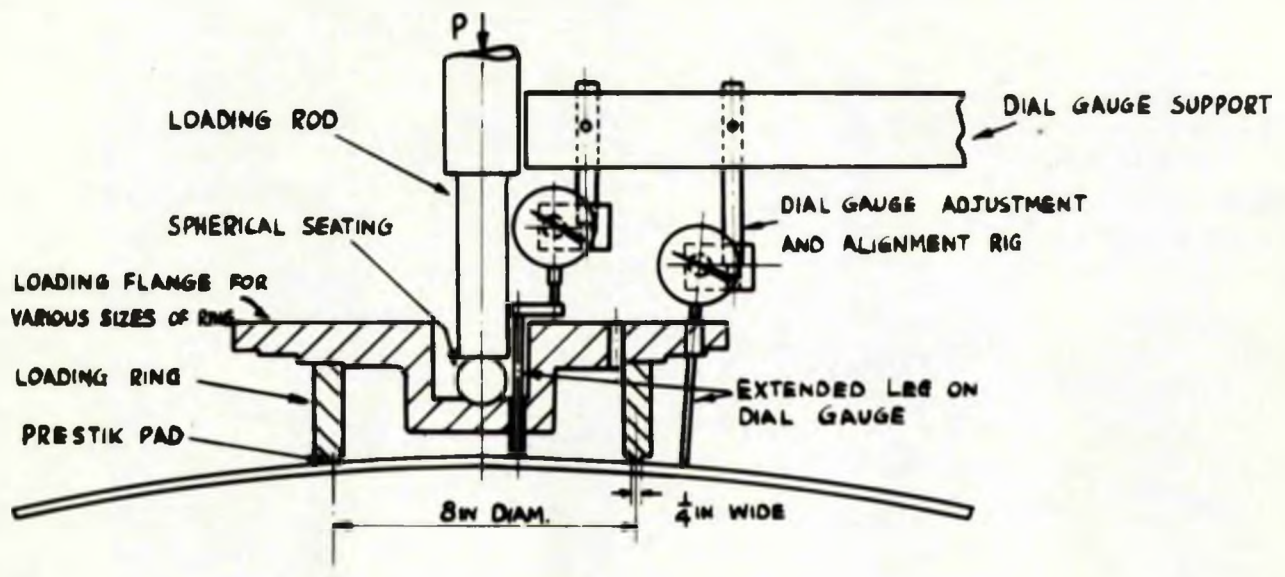
DETAIL OF RING LOADING DEVICE

FIG. IV 30 RADIAL RING LOADING WITHOUT SHELL RESTRAINT AT THE LOAD

a rigid ring or tube, faced to provide a loaded width of $\frac{1}{4}$in,
was used as the load transmitting device.   In order to ensure
that any local irregularities in the shell surface under the
load path did not unduly influence the uniform distribution of
radial pressure around the ring, the load was transmitted to the
shell through a pad of 'Prestik', as shown in Fig. IV.30.

The shell and extended table support were placed on the
lower platen of the compression side of a universal testing
machine.   The load was applied to the ring through the loading
rod, spherical seating ($1\frac{1}{4}$in diam. ball) and loading flange.   As
in the case of uniformly distributed loading, p.173, the spherical
seating was situated as close to the surface of the shell as pos-
sible, thus reducing the possibility of any applied moment.

Five different diameter rings were used in the investi-
gation, having mean diameters as follows:- $2\frac{3}{4}$, $5\frac{1}{2}$, 8, $10\frac{1}{2}$ and
$2\frac{1}{2}$in.   The loading flange shown in Fig. IV.30 was used for the
three larger rings.   A similar flange was designed and used for
the $2\frac{3}{4}$ and $5\frac{1}{2}$in diam. rings.

Measurement of Strain and Deflection:-   Since the crown of the
shell was not under load it was possible to measure both the
strains (by means of electrical resistance strain gauges) and
deflections (by means of 0.0001in dial gauges) within the.
loaded ring.

The strain gauges employed in this series, were nichrome
wire, paper backed, flattened helical grid type, of 200 ohm and
in length.   As in earlier work, a batch of these were cali-
brated using the standard calibration procedure.   Owing to the

symmetrical nature of the loading, essentially only one great circle was strain gauged.   The layout of gauges was that used in the earlier tests for the uniformly distributed loading of the $\frac{1}{4}$in shell.   This is shown in Fig. IV.31 together with the positions of the ring loads.   As the radial pressure at the loaded ring was relatively low, it was possible to make use of the strain gauges situated under the ring itself.   Thus reading of strain were obtained on both surfaces close to the ring.

As in earlier tests on the shallow shells the 50-way strain recorder was used to measure the strains in the meridional and circumferential directions on both the inner and outer surfaces. The loading was applied as before in four increments up to the maximum load.   The procedure for measurement and repeatability of readings (i.e. zero drift of gauges, etc.) was as in the earli tests pp.173-175.

From the strain per unit load values the bending and direc stresses were obtained using eqts. IV.1 and IV.2.   The results one of these tests are plotted non-dimensionally in Fig. IV.32a,

The radial deflection of the shell was measured using the 0.0001in dial gauges, supported, adjusted and aligned in the man shown in Fig. IV.30. In order to measure the radial deflection of the shell within the ring a series of holes was drilled in th loading flange.   Three such holes are shown in Fig. IV.30, and a further two were located on another flange diametral line. Extended legs were fitted to the dial gauges to enable these deflections to be measured.

The results for one of these tests are plotted non-dimensio
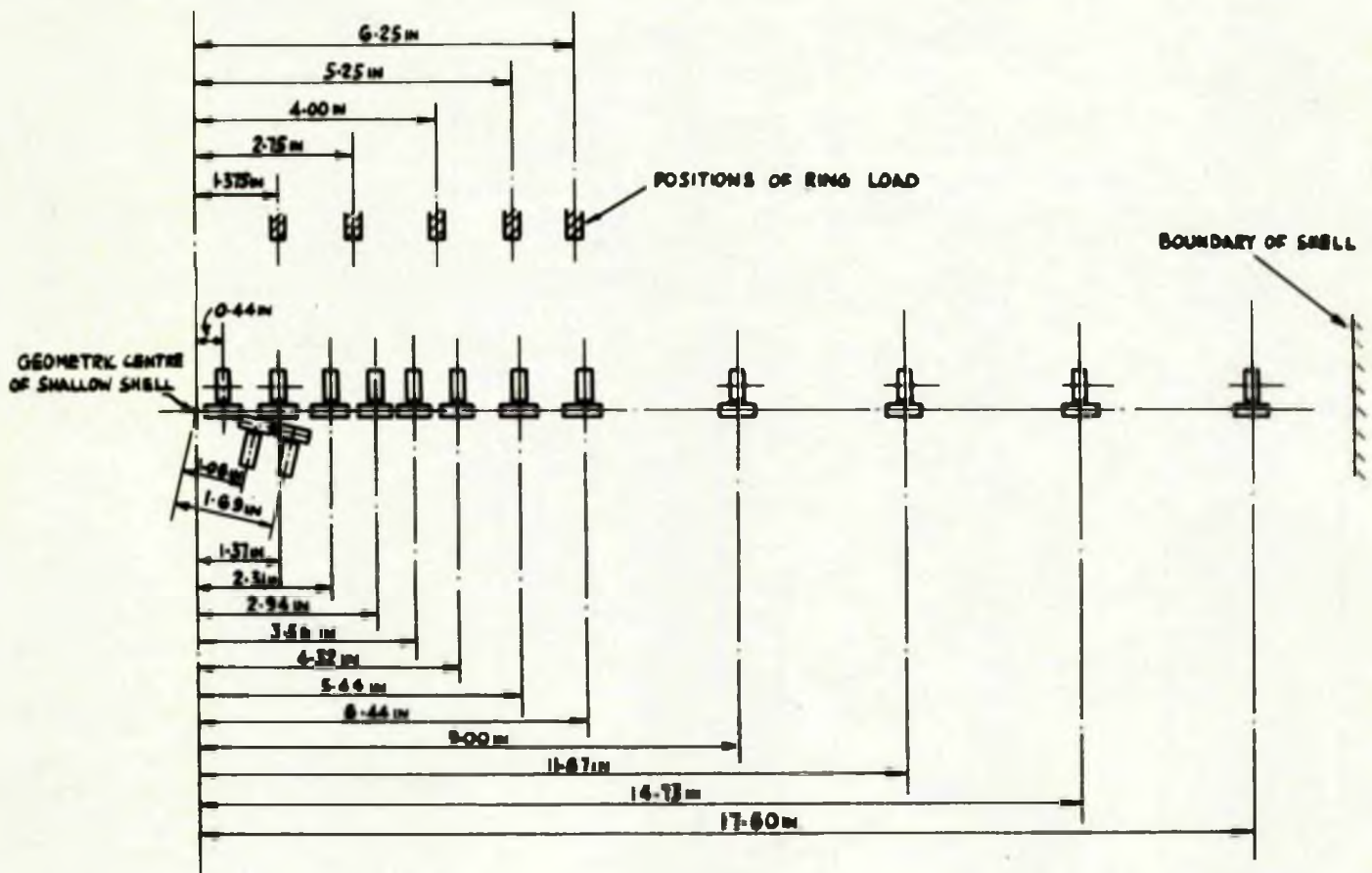
FIG. IV.31   STRAIN GAUGE LAYOUT FOR INNER AND OUTER SURFACES FOR A RADIAL RING LOAD
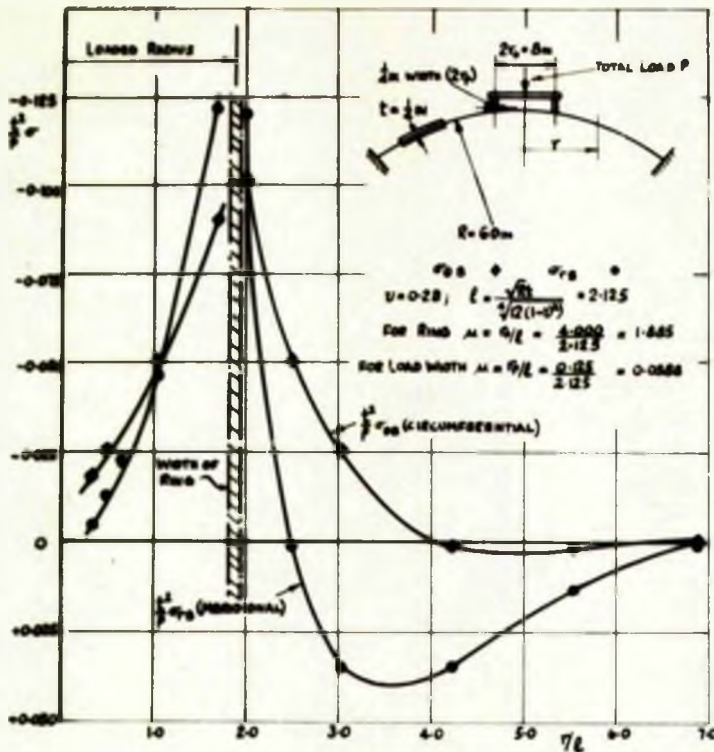
Fig. IV.32a BENDING STRESSES ON THE OUTER SURFACE DUE TO A RADIAL RING LOAD

Fig. IV.32b DIRECT STRESSES DUE TO A RADIAL RING LOAD
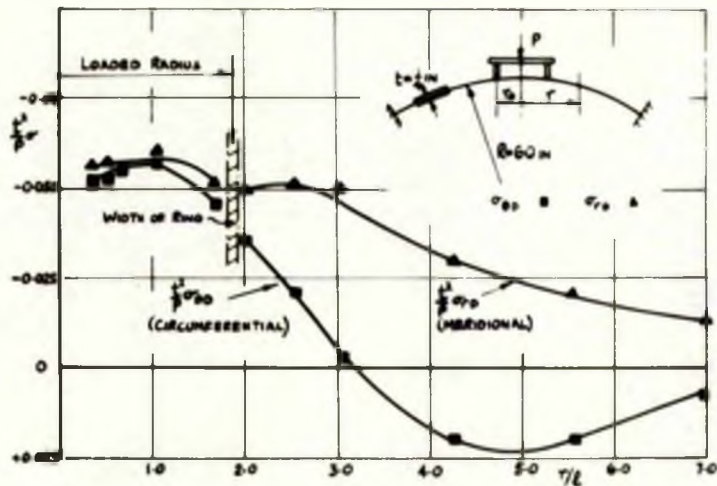
Fig. IV.32c RADIAL DEFLECTION DUE TO A RADIAL RING LOAD
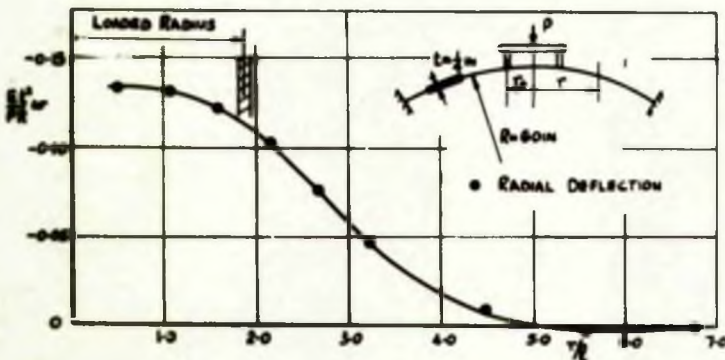
FIG. IV.32 TYPICAL EXPERIMENTALLY OBTAINED DIRECT STRESS, BENDING STRESS ON THE OUTER SURFACE AND RADIAL DEFLECTION OF A SHALLOW SPHERICAL SHELL DUE TO A RADIAL LOAD P TRANSMITTED BY A FREELY SUPPORTED RING – RESULTS FOR THE 8IN MEAN DIAM. RING

in Fig. IV.32c.   The complete results for both stresses and deflections are presented in Chapter V where they are compared with the theoretical values.

(b)   Radial Loading Transmitted by a Rigidly Fixed Ring

Experimental Model :-   The complete sphere, shown in Fig.IV.7 and discussed on p.178, was used to investigate the behaviour of a shell under the action of a radial load applied by means of two different diameter welded pipes.   As in the earlier cases the radii of curvature were measured over the regions selected for pipe attachment.   On the basis of these measurements the positions of the attachments were fixed, avoiding areas in the immediate vicinity of a weld or other discontinuities and positioned on the same great circle diametrically opposite each other.

The vessel was marked on the inner and outer surfaces in such locations as to enable the attachment positions and those of the strain gauges to be fixed on both surfaces.   The technique used for marking the inner surface of the vessel from the outer surface was the 'Tempilstik' and acetylene flame method, described in detail on p.179.

Two pipe attachments of mean diameters 7.72 and 9.32in were welded to the inside surface of the continuous vessel by means of continuous fillet welds on both the inside and outside diameters of the pipe.   The widths of the welds were measured and found to be 0.66 and 0.92in respectively.   The 7.72in mean diam. pipe was welded to the $\frac{3}{8}$in thick plate and the 9.32in mean diam. to the $\frac{1}{4}$in plate, the two pipes being diametrically opposite, as shown in Fig. IV.33.   The corresponding μ values

for the pipes were 1.48 and 2.20, and for the load widths
0.125 and 0.216 respectively.

Loading Technique:-   Owing to the higher loads envisaged in
this case, compared with the stud attachments, it was found more
convenient to use a solid loading rod spanning the sphere between
the two attachments.   In order to maintain axiality of loading,
shackles were mounted at either end of the loading rod. The
shackles were of similar design to those described earlier and
incorporated a spherical seating and $1\frac{1}{4}$in diam. steel ball.

        The load was transferred from the shackle to the actual
pipe by means of a short rod screwed into the shackle and fixed
to a blank flange.   This in turn was bolted to a further flange
welded onto the pipe.   The bolts used had the same pitch circle
diameter as the mean diameter of the pipe. Using this double
flange system the surface of the sphere within the enclosed pipe
area was accessible.   Details of the above arrangement are shown
in Fig. IV.33.

        Radial loads were applied to both attachments simultaneous
by means of a turnbuckle which was of similar design to that use
for the bending moment and tangential load tests on the sphere.
The load was measured by means of four Maihak strain gauges, as
shown in Fig. IV.33b, mounted on a machined section of the rod,
and placed diametrically opposite on the $0°$, $90°$, $180°$ and $270°$
lines in the longitudinal direction.   The four gauges were eac
read separately and the mean value determined.   The loading rod
with its Maihak strain gauge dynamometer was calibrated up to
4 ton in the Laboratory prior to installation in the model spher
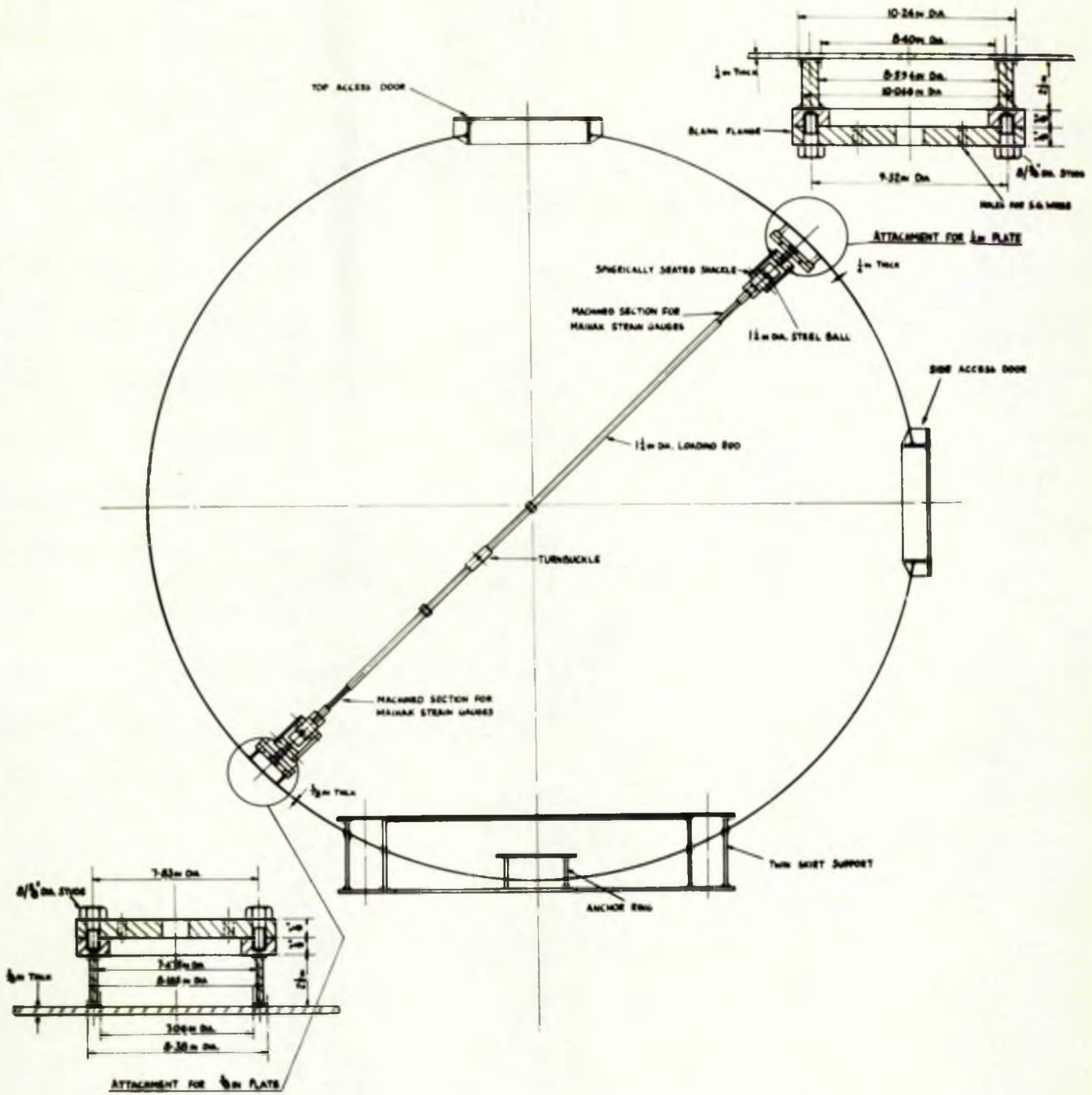
FIG. IV.33a SECTION OF 13FT-6IN DIAM MODEL SPHERE SHOWING PIPE ATTACHMENTS
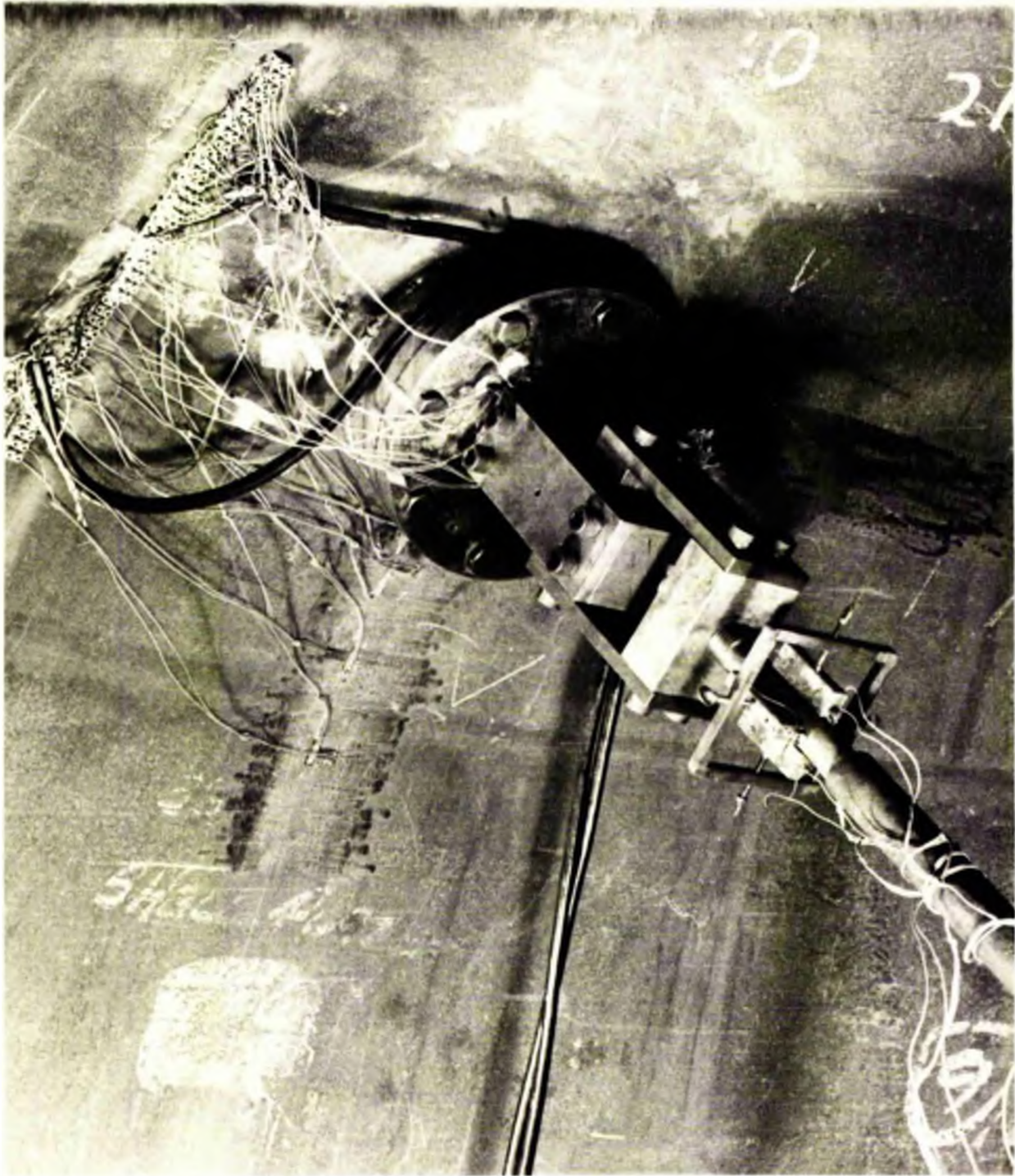
Fig.IV.33b   Arrangement of Radial Loading of Pipe Attachments
             on the 13ft-6in Diam. Model Sphere, showing the
             Maihak Strain Gauges.
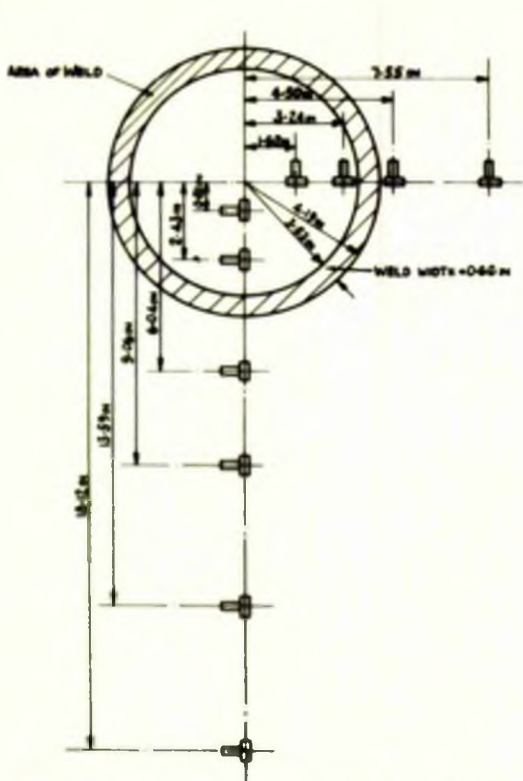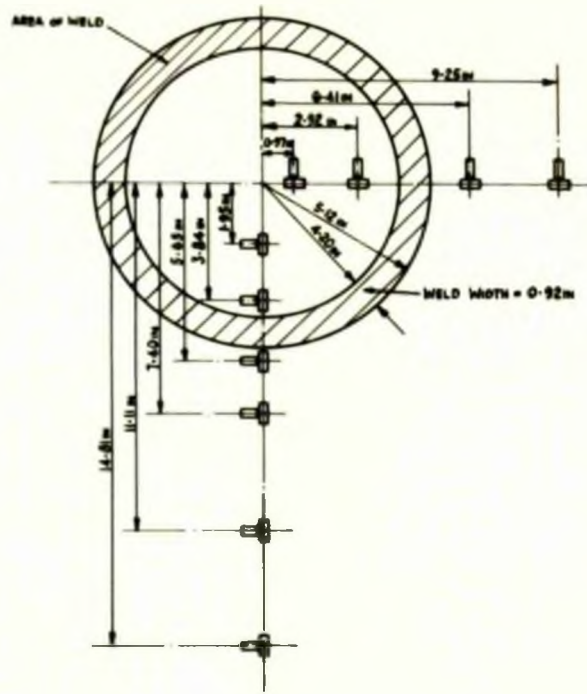
Fig.IV.34   Layout of Strain Gauges for Pipe Attachments
on the Model Sphere.

The shackles used in the actual set up and shown in Fig. IV.33
were employed in the calibration arrangement. Several cali-
bration tests were performed to ensure that repeatability obtained.

Measurement of Strain:- As in the other cases, electrical
resistance strain gauges were employed in these tests for the
measurement of strain on the inner and outer surfaces in the
circumferential and meridional directions. Saunders Roe $\frac{1}{2}$in
length foil gauges were used throughout, a selection of them
being calibrated in the manner previously indicated.

As in the case of the stud loading on the sphere, two lines
$90°$ apart were strain gauged using the above gauges. The purpose
of gauging the two lines was, as in the previous case, to obtain
information as to the symmetrical distribution, or otherwise, of
the loading. The strain gauge layouts for the two attachments
are shown in Fig. IV.34. The strain gauge leads for each gauge
were connected into a plastic terminal strip cemented to the
surface of the sphere in the vicinity of the attachment. Twenty
five core cable was then used from the terminal strip to the
strain recorder. In this series the 50-way strain recorder was
employed and the procedure for measurement and repeatability of
readings (i.e. zero drift of gauges) was as in the uniformly
distributed radial load tests, pp.173-175.

The loads were applied to the attachments in four incre-
ments up to the maximum value, readings of strain being recorded
throughout. The procedure for obtaining the corresponding
bending and direct stresses was the same as that of the earlier
tests and outlined on pp.174 and 175.

Typical experimental results for one of the attachments for the bending and direct stresses are plotted non-dimensionally in Fig. IV.35.   It is noted that the results from gauges placed on both lines lie on one and the same curve, indicating the symmetrical nature of the loading.   The other results are given in Chapter V.

IV.3.2   RING BENDING MOMENT

Experimental Model:-   A bending moment was applied to a continuous shallow shell through a pipe attachment.   The shallow shell, of $\frac{1}{2}$in thickness and 60in radius, was welded at its outer boundary, 3 ft. $2\frac{3}{4}$in chord diam., to a heavy flange ring and mounted, in the horizontal plane, on the extended table.   The extended table was bolted to a heavy base which consisted of two 9" x 7" R.S.J's - as shown in Fig. IV.36.

A pipe attachment of 5in mean diam. and $\frac{1}{2}$in thickness was welded to the shallow shell using continuous fillet welds on the inside and outside diameters of the pipe, giving a weld width of 1in at the shell.   The centre line of the attachment coincided with the crown of the shell.   A flange was welded to the pipe and after welding was machined parallel to the base of the shell. The value of μ for the ring was 0.832 and for the load width:- 0.1

Loading Technique:-   The bending moment was applied to the pipe attachment by means of a 5" x $2\frac{1}{2}$" channel of 4 ft. 6in length to which was welded, at its centre, a 10in diam. blank flange.   This flange was bolted to the pipe flange as shown in Fig. IV.36.   At the ends of the channel section, two proving rings were position
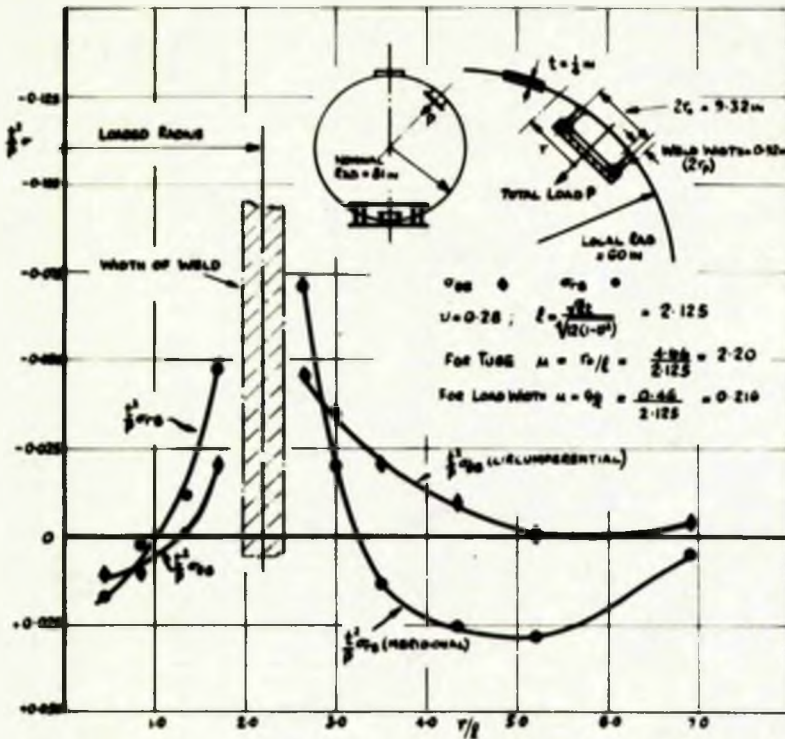
FIG IV.35a BENDING STRESSES ON THE OUTER SURFACE
DUE TO A RADIAL FIXED RING LOADING
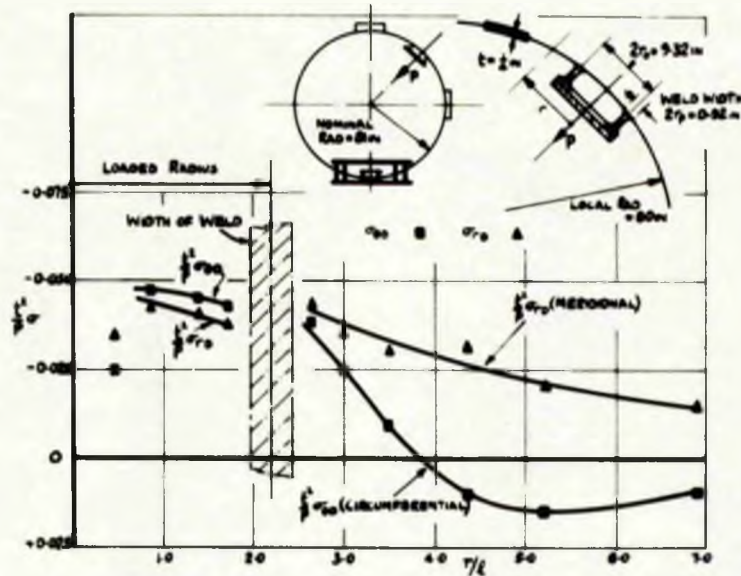
FIG IV.35b DIRECT STRESSES DUE TO A RADIAL
FIXED RING LOADING

FIG. IV.35 TYPICAL EXPERIMENTALLY OBTAINED DIRECT STRESS AND BENDING STRESS ON THE OUTER SURFACE OF A
COMPLETE SPHERE (15FT 6IN DIAM) DUE TO A RADIAL LOAD P TRANSMITTED BY A RIGIDLY FIXED RING
- RESULTS FOR A 9·32IN MEAN DIAM. TUBE ON $\frac{1}{2}$IN PLATE
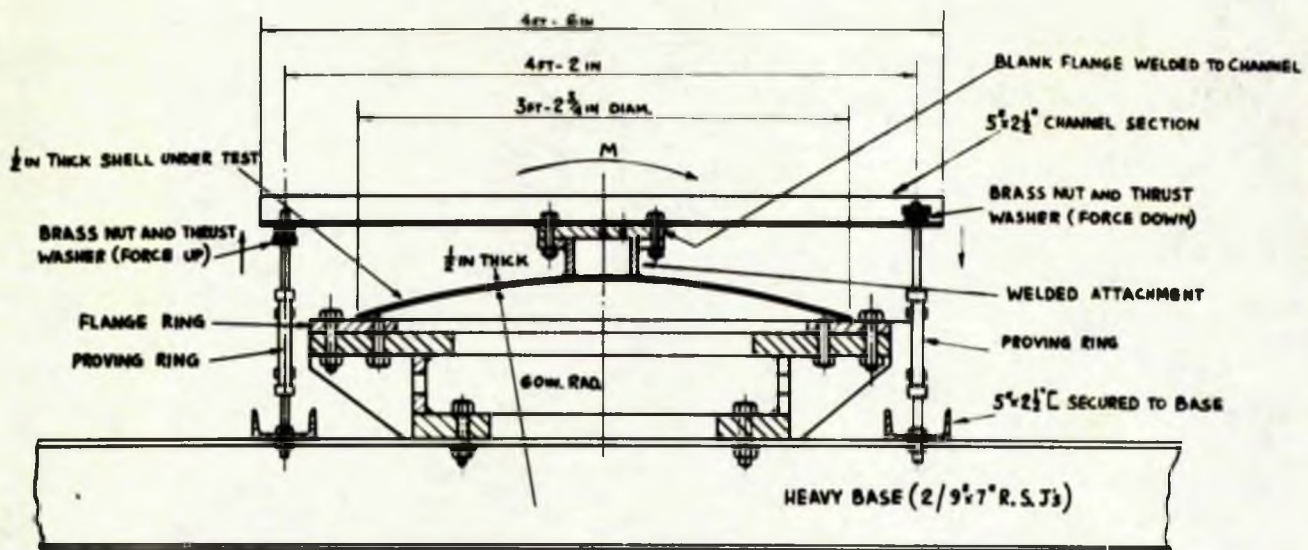
GENERAL ARRANGEMENT OF LOADING RIG
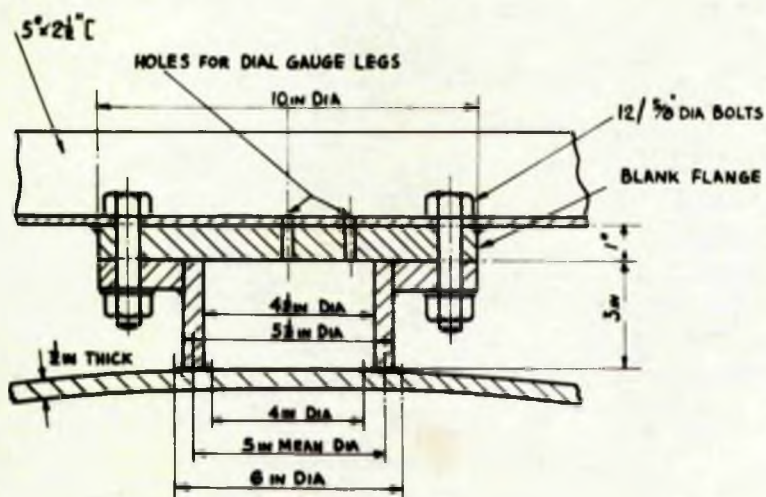
DETAIL OF ATTACHMENT
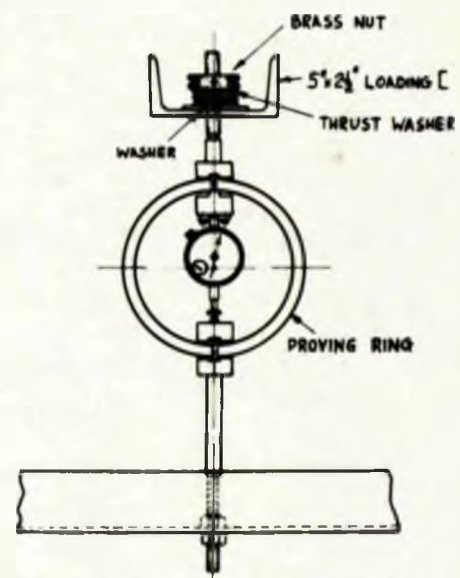
VIEW OF PROVING RING LOADING

Fig.IV.36a   The Arrangement of the Shallow Spherical Shell
Subject to a 'Bending' Moment.
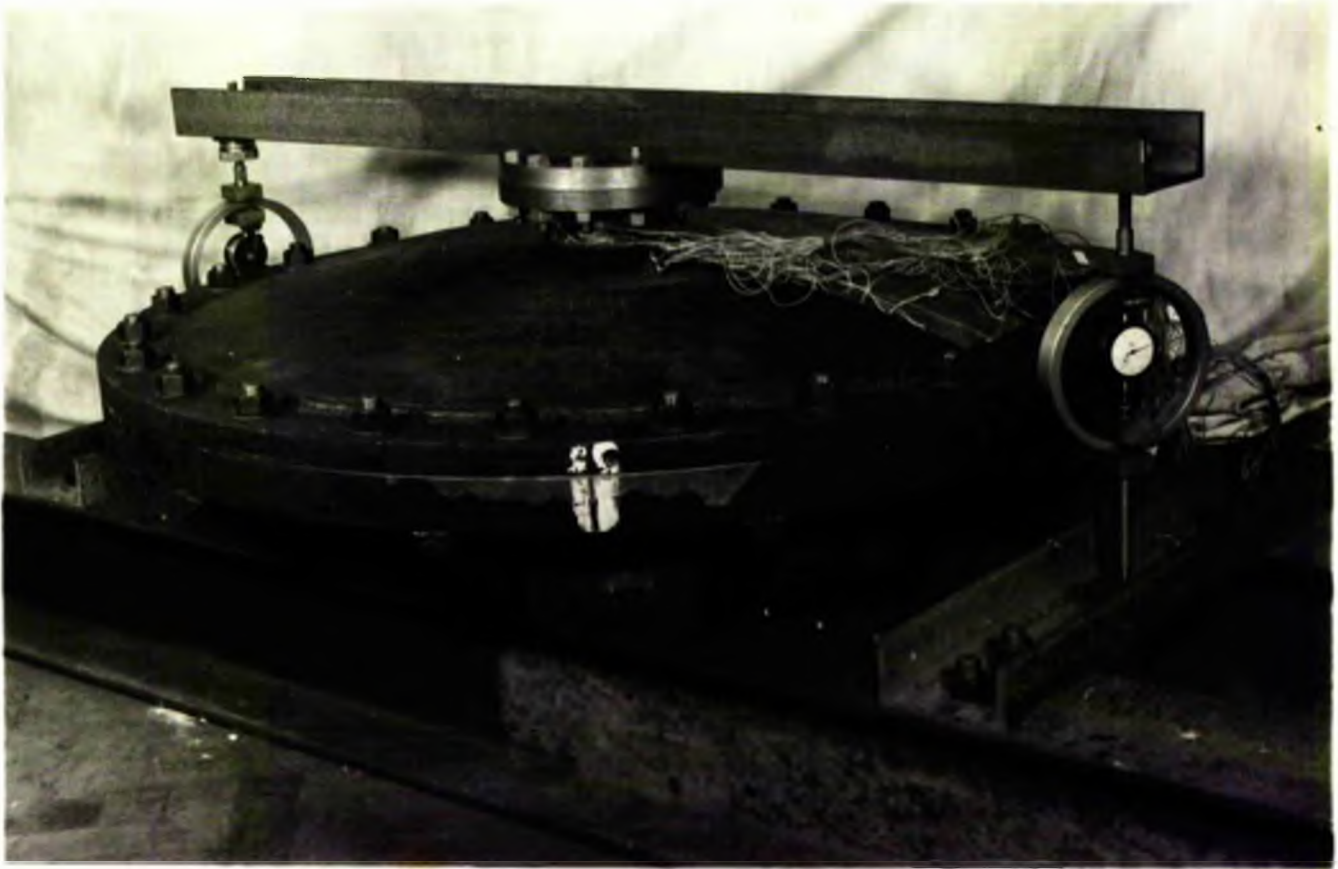
Fig.IV.36b   The Shallow Shell Subject to a 'Bending' Moment.
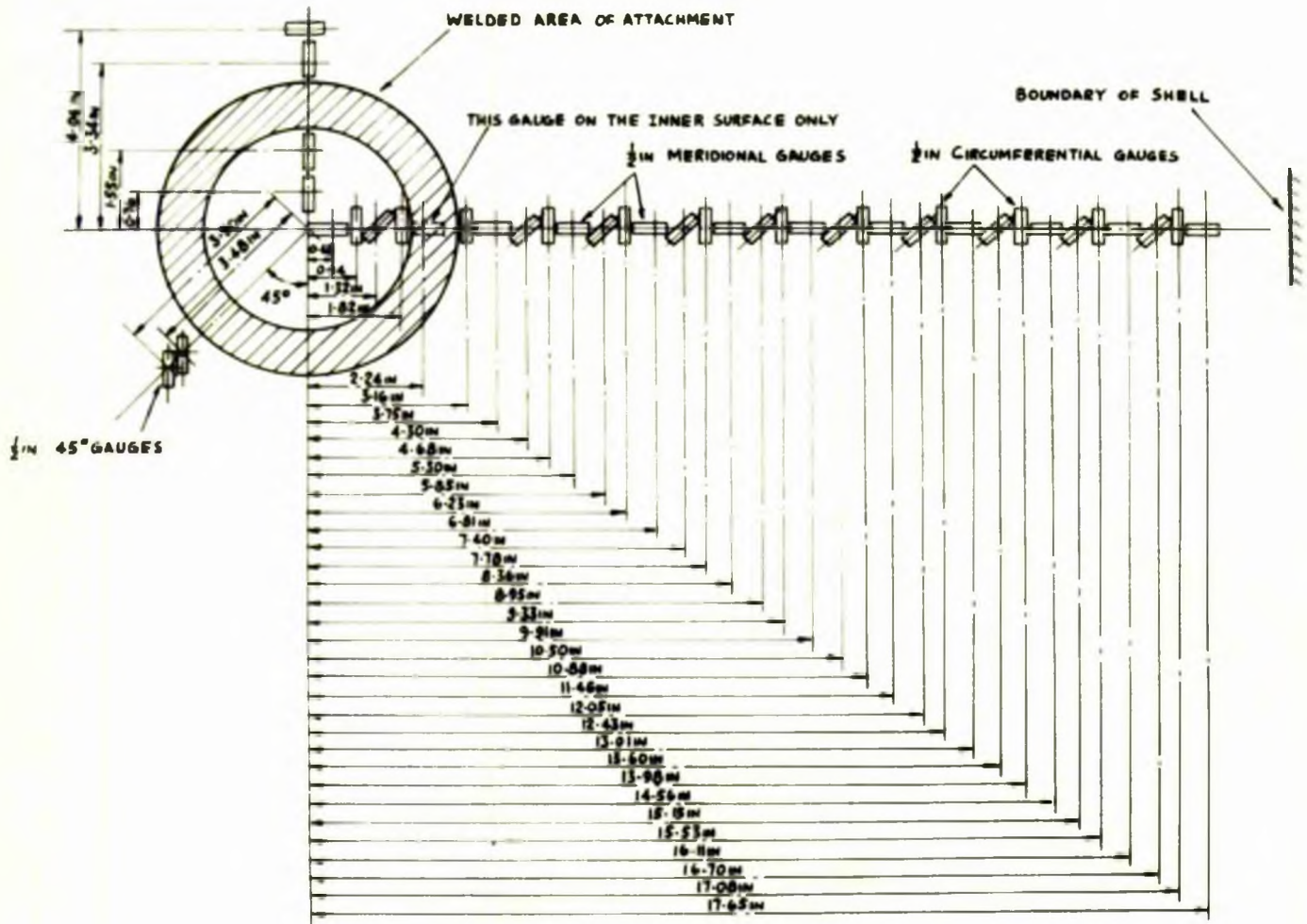
FIG IV·37 STRAIN GAUGE LAYOUT FOR INNER AND OUTER SURFACES FOR 'BENDING' AND 'TWISTING' MOMENTS APPLIED TO A PIPE ATTACHMENT

equally disposed about the centre of the shell and a distance
50in apart.   The proving rings were secured to the base beams
by means of 5" x 2½" channels, as shown in Fig. IV.36.   To
facilitate the load application, thrust bearings were employed
between the loading channel and the loading nut. As in a previous
test, the proving rings were used both as a load applying and
measuring device.   In order to apply a moment to the set-up
the two rings were arranged to act in opposite directions. A
reversal of these directions enabled the direction of the moment
to be reversed and this provided, in each of the tests, a check
on its method of application.

Measurement of Strain and Deflection:-   Ferry foil electrical
resistance strain gauges of ½in length were again employed in
these tests. Calibration of the gauges was as previously
indicated.   The majority of the strain gauges were mounted on
one great circle and were fixed on the inner and outer surfaces
in three directions corresponding to the meridional, circum-
ferential and 45° lines of the shell.   Two additional groups of
gauges were fixed to record strains in the vicinity of the welded
ring.   The layout is shown in Fig. IV.37.

As discussed on p.177, this type of layout was considered
more accurate for the non-axisymmetric loading, though inter-
polation from the plots of strain (or strain per unit load)
against radius was required to determine the three strains at
any one point.   The additional strain gauges mounted close to
the weld were of particular value in this connection.

The 50-way strain recorder was employed in these tests and

the procedure for measurement and repeatability of reading (i.e. zero drift of gauges, etc.) was as in earlier tests, pp.173-175.

By suitably positioning the shell on the base beams it was possible to apply the bending moment in a series of planes having great circles rotationally displaced to those great circles containing the gauges. Four such positions were considered, these being $\theta = 0°$, $30°$, $60°$, and $90°$. In all cases the bending moment was applied to the shell in four increments, readings of strain being recorded throughout. Repeat loadings were carried out by applying the moment in the opposite directic

From the strain per unit load values at the various static the bending and direct stresses in the meridional and circumferential directions (relative to the particular great circle under consideration) were obtained using eqts. IV.1 and IV.2. The values of the bending (outer-fibre) shear stress and the direct (mid-surface) shear stress for the same great circle were obtained from the derived values of the shear strain on planes containing the particular great circle. These values of shear strain were obtained using the Mohr's circle of strain construc from the experimental strains in the three directions. From th values the magnitudes of the shear stresses on the inner and ou surfaces were computed using the following equations:-

$$\tau_{r\theta}^o = G\,\gamma_{r\theta}^o \qquad \text{and} \qquad \tau_{r\theta}^i = G\,\gamma_{r\theta}^i$$

From these values the bending (outer-fibre) and direct (mid-surface) shear stresses were found from the following:-

$$\tau_{r\theta,\theta} = \frac{\tau_{r\theta}^o - \tau_{r\theta}^i}{2} \qquad \text{and} \qquad \tau_{r\theta,\rho} = \frac{\tau_{r\theta}^o + \tau_{r\theta}^i}{2} \qquad \text{(IV.}$$
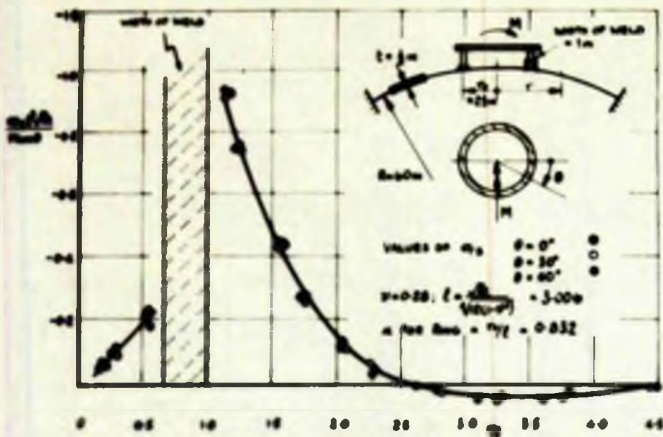
FIG. IV-38a MERIDIONAL BENDING STRESS ON THE OUTER SURFACE DUE TO A BENDING MOMENT
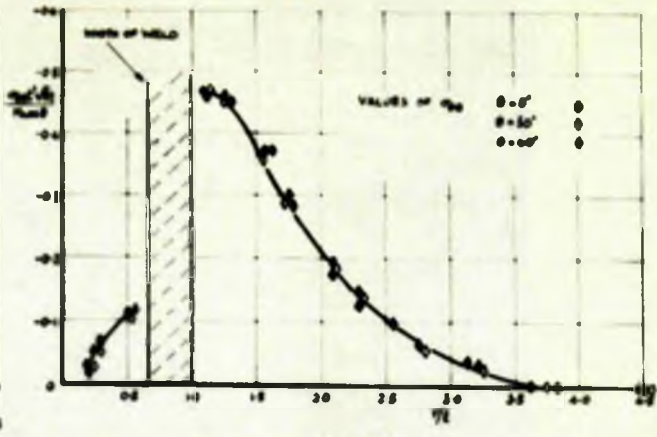
FIG. IV-38b CIRCUMFERENTIAL BENDING STRESS ON THE OUTER SURFACE DUE TO A BENDING MOMENT
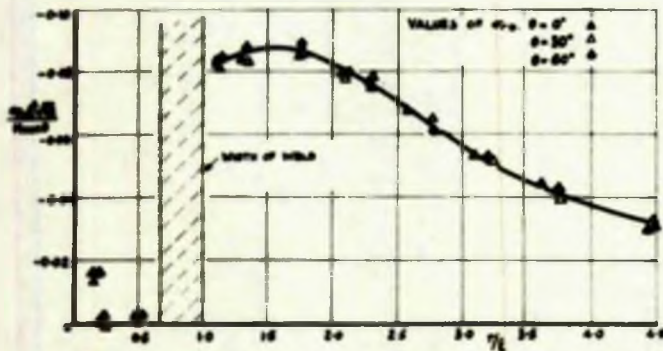
FIG. IV-38c MERIDIONAL DIRECT STRESS DUE TO A BENDING MOMENT
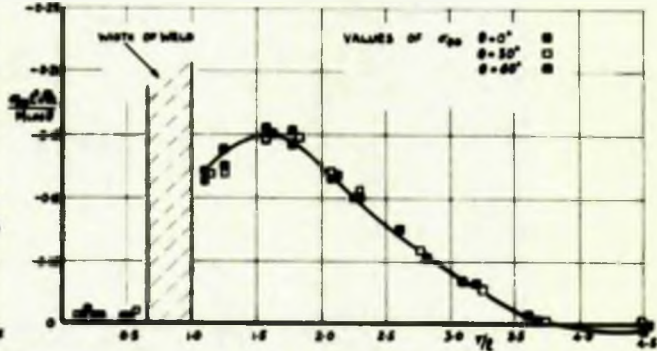
FIG. IV-38d CIRCUMFERENTIAL DIRECT STRESS DUE TO A BENDING MOMENT
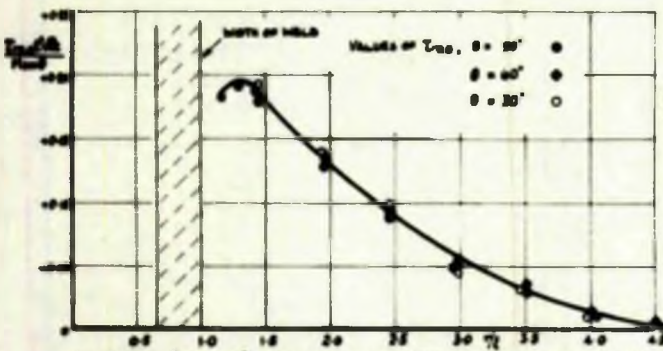
FIG. IV-38e 'BENDING' SHEAR STRESS ON THE OUTER SURFACE DUE TO A BENDING MOMENT
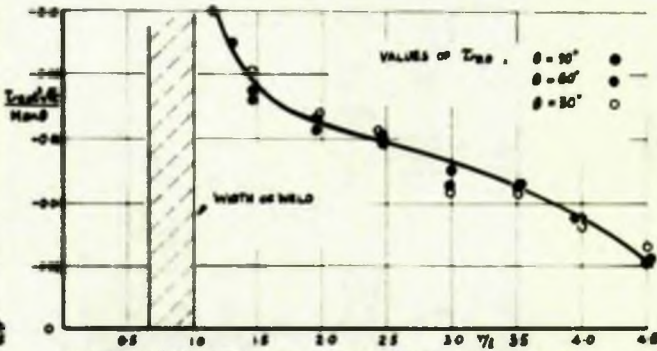
FIG. IV-38f SHEAR STRESS ON THE MID-SURFACE DUE TO A BENDING MOMENT
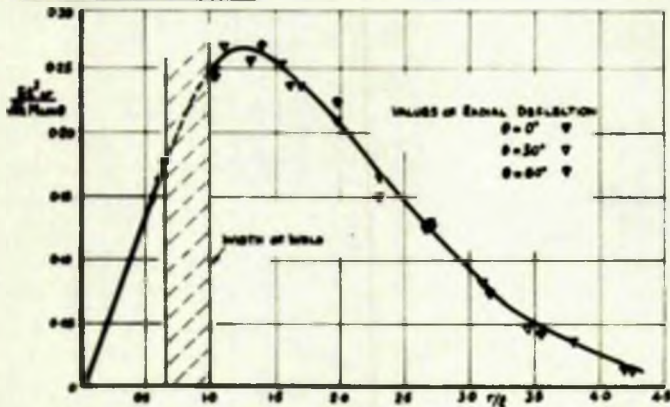
FIG. IV-38g RADIAL DEFLECTION DUE TO A BENDING MOMENT

FIG. IV-38 EXPERIMENTALLY OBTAINED DIRECT STRESS, BENDING STRESS ON THE OUTER SURFACE, 'BENDING' AND 'MID-SURFACE' SHEAR STRESS AND RADIAL DEFLECTIONS ON A SHALLOW SPHERICAL SHELL DUE TO A BENDING MOMENT M APPLIED TO THE SHELL THROUGH A 5IN MEAN DIAM. PIPE ATTACHMENT AND IN FOUR PLANES, $\theta = 0°, 30°, 60°$ AND $90°$

The results obtained from the above indicated that when the moment was applied in the line of the great circle containing the strain gauges ($\theta = 0°$) the principal stresses were in the direction of the meridional and circumferential gauges, there being no shear stress on the great circle. When the moment was applied at $90°$ ($\theta = 90°$) to the gauged great circles, only the $45°$ gauges recorded a strain reading - indicating a condition of pure shear on this line. Considering the above results, together with those obtained from the other two cases ($\theta = 30°$ and $\theta = 60°$), it was concluded:-

> (i)   that the meridional and circumferential stress distribution in great circles rotationally displaced by an angle θ from the applied moment varied as the cosine of the angle θ;

> (ii) that the shear stress distribution in the above planes varied as the sine of the angle θ.

Typical results are plotted non-dimensionally in Fig. IV.38a-f.

The radial deflections of the shell were measured as before using the standard 0.0001in dial gauges. The dial gauge supporting rig was positioned, in the first instance, to enable deflections to be measured along the $\theta = 0°$ line.

In order to facilitate these measurements in the plane of the moment, holes were drilled and slots milled along the loading channel centre line. Extended spindles were then fitted, where necessary, to the dial gauges. As an extension of these tests deflections were also measured along the $\theta = 30°$, $60°$ and $90°$ lines. In order to measure the deflections of the shell within

the loaded ring, holes were drilled in the channel and its blank
flange along the four lines θ - 0°, 30°, 60° and 90°.

As in earlier tests, the bending moment was increased in
four increments, readings of deflection being recorded throughout.
It was later reversed in direction as a check on the readings.

From the results it was concluded that the distribution of
radial deflection along great circles rotationally displaced by
an angle θ from the applied moment varied as the cosine of the
angle θ.   Results are shown in Fig. IV.38g.

At a later stage the portion of shell inside the pipe attach
ment was removed leaving what was virtually a nozzle attachment.
In a similar manner to that outlined above a bending moment was
applied to the nozzle, the strains and deflections being recorded
as before.   It was found in this case that the resulting stress
and deflections were almost identical to those obtained for the
earlier case of the continuous shell.

IV.3.3   RING 'TWISTING' MOMENT

Experimental Model :-   A twisting moment was applied to a continu
shallow shell through a pipe attachment at the crown.   The shell
used was that previously described on p.210 of ½in thickness and
60in radius, and welded at its outer boundary (3 ft. 2¾in chord
diam.) to a heavy flange ring.   The pipe attachment of 5in mean
diam. and 1in thickness was welded to the shell using continuous
fillet welds on the inside and outside of the pipe. As mentioned
earlier, the flange welded to the attachment was machined paralle
to the base of the shell.

HEAVY FLANGE RING

KEYWAY PLATE ATTACHED TO
STRAINING HEAD BY 4/C.SK BOLTS
ON 7⅛ IN P.C.D (OFF-CENTRE) AND
BY THE KEYWAY

8/FITTED BOLTS ⅞"DIA. 8¼"P.C.D

½ IN DIA HOLE FOR S.G. LEADS

12/FITTED BOLTS ¹¹⁄₁₆"DIA. 9½"P.C.D

3FT-10IN DIAM.

3FT-2⅝IN DIAM.

12IN DIAM.

6IN DIAM.

4IN DIAM.

10IN DIA.

2·75 IN
3·45 IN D.

5IN DIA.

2IN

1IN

R=60IN

½IN THICK

3IN

1IN½IN

2⅛IN

STRAINING HEAD OF
TORSION MACHINE

1½IN DIA HOLE FOR INNER
STRAIN GAUGE LEADS

24/FITTED BOLTS ⅞IN DIA. 3FT-7IN P.C.D

FLATS ON SHAFT FOR GRIPPING
IN WEIGHING HEAD

WEIGHING HEAD OF
TORSION MACHINE

FIG.IV-39IN SECTION OF SHALLOW SHELL MOUNTED IN TORSION MACHINE

<u>Loading Technique</u>:- The shell was suitably mounted in a
180,000 in.lb capacity torsion machine.   The heavy flange ring
base of the shell was bolted, using fitted bolts, to a large 1in
thick disc attached by means of a 2in thick keyway plate to the
straining side of the torsion machine.   The keyway plate was
bolted to the torsion machine and to the 1in thick disc by means
of specially designed fitted bolts.   The welded pipe attachment
was bolted, using fitted bolts, to a suitable flange and shaft
arrangement which could be gripped in the weighing head of the
machine.   The set-up is shown in Fig. IV.39.

<u>Measurement of Strain and Displacement</u>:-   The electrical
resistance strain gauges used in the earlier tests in connection
with the application of the bending moment, and shown in Fig.IV.37
were again employed in the present investigation.   The comments
made in the previous section pp.211 and 212 regarding this layout
and strain recording are again relevant here.

A total torque of 160,000 in.lb was applied to the shell
in four increments, the readings of strain being recorded through-
out.   It was noted that only the gauges along the 45° lines
recorded a strain reading, and that the values of strain on the
inner and outer surfaces were identical.   The system was thus
in pure shear, and using eqt. IV.3 the 'mid-surface' shear stress
was obtained.   These results are shown in Fig. IV.40.

The tangential displacements of a great circle of the shell
were determined at six radial positions by means of 0.0001in dial
gauges.   Each dial gauge was mounted so that the measuring leg
was at right angles to the great circle under investigation, and

in a plane parallel to that containing the tangents at the
particular point in that circle.   At six different radial
positions down the relevant great circle small brass cleats
($\frac{5}{8}$" x $\frac{1}{4}$") were cemented to the shell, the longer side of the
cleat being in a plane containing the great circle and the normal
of the shell. The dial gauges were then suitably adjusted so
that the measuring leg of a gauge was positioned at the centre
of one of the cleats, and at right angles to the section.

Owing to the shallow nature of the shell it was necessary
to fit a special measuring leg to the dial gauges which enabled
the displacement to be measured in a line parallel to the centre
line of the dial gauge and close to the surface of the shell.

The twisting moment was increased in this case, in eight
increments, readings of displacement being recorded throughout.
Several tests were carried out for each radial position to ensure
that repeatability was achieved.   The results are plotted in
Fig. IV.40.
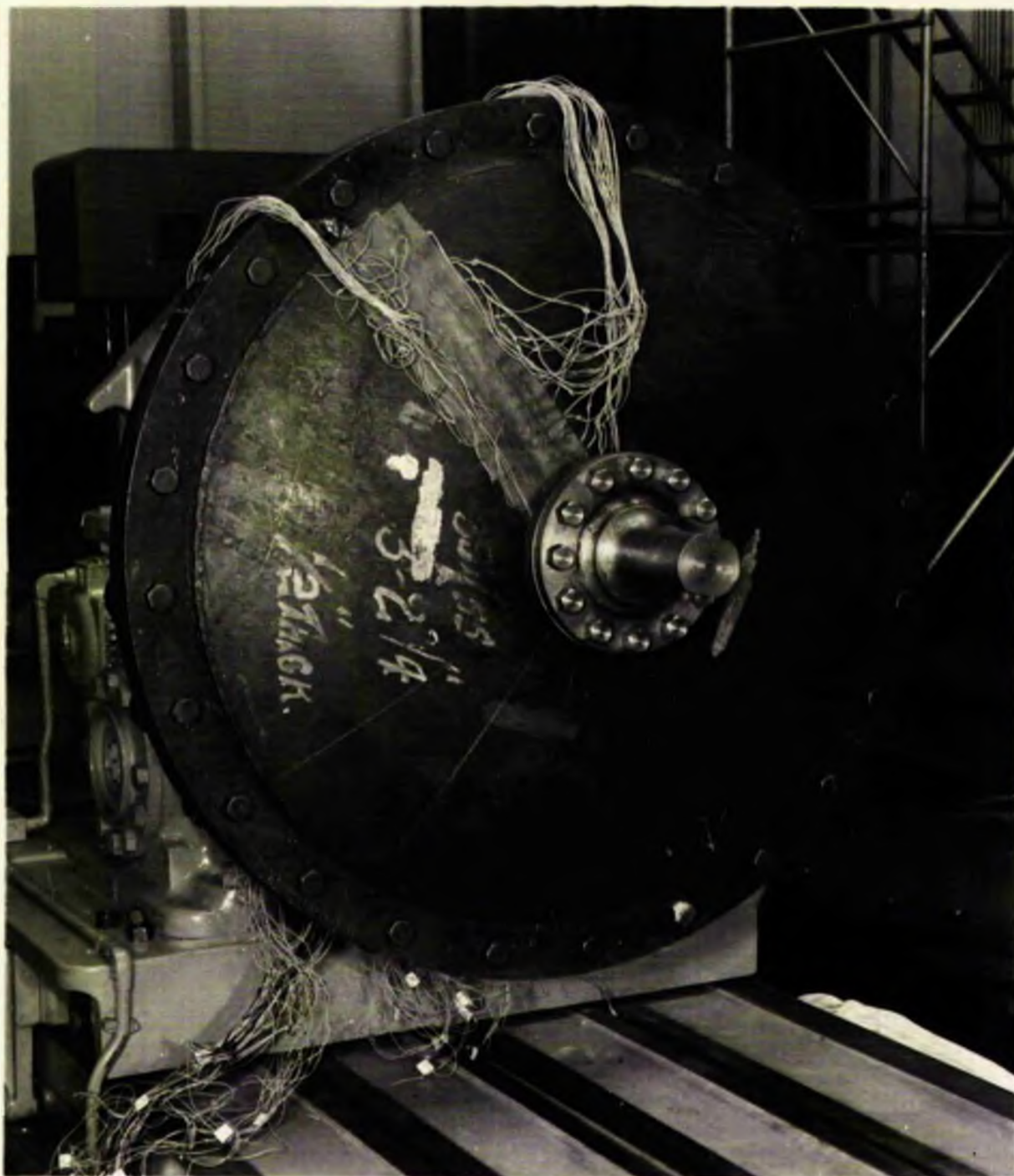
Fig.IV.39b   Arrangement of a Shallow Spherical Shell
            Subject to a 'Twisting' Moment.
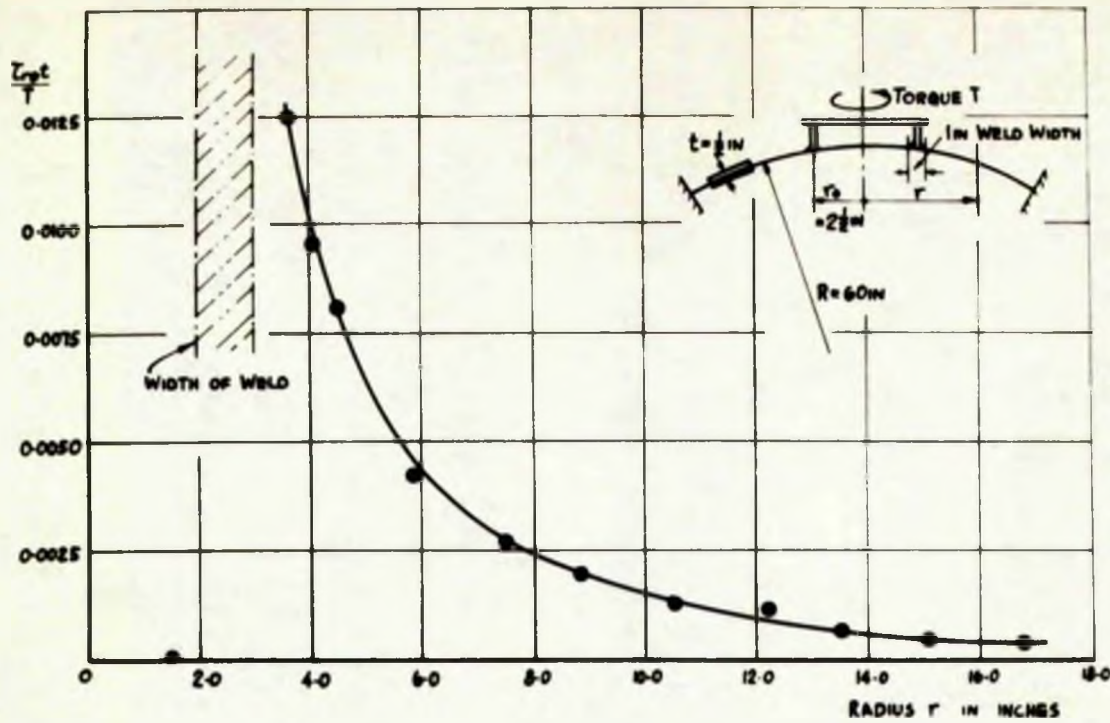
Fig. IV. 40a The Distribution of 'Mid-Surface' Shear Stress due to a 'Twisting' Moment T
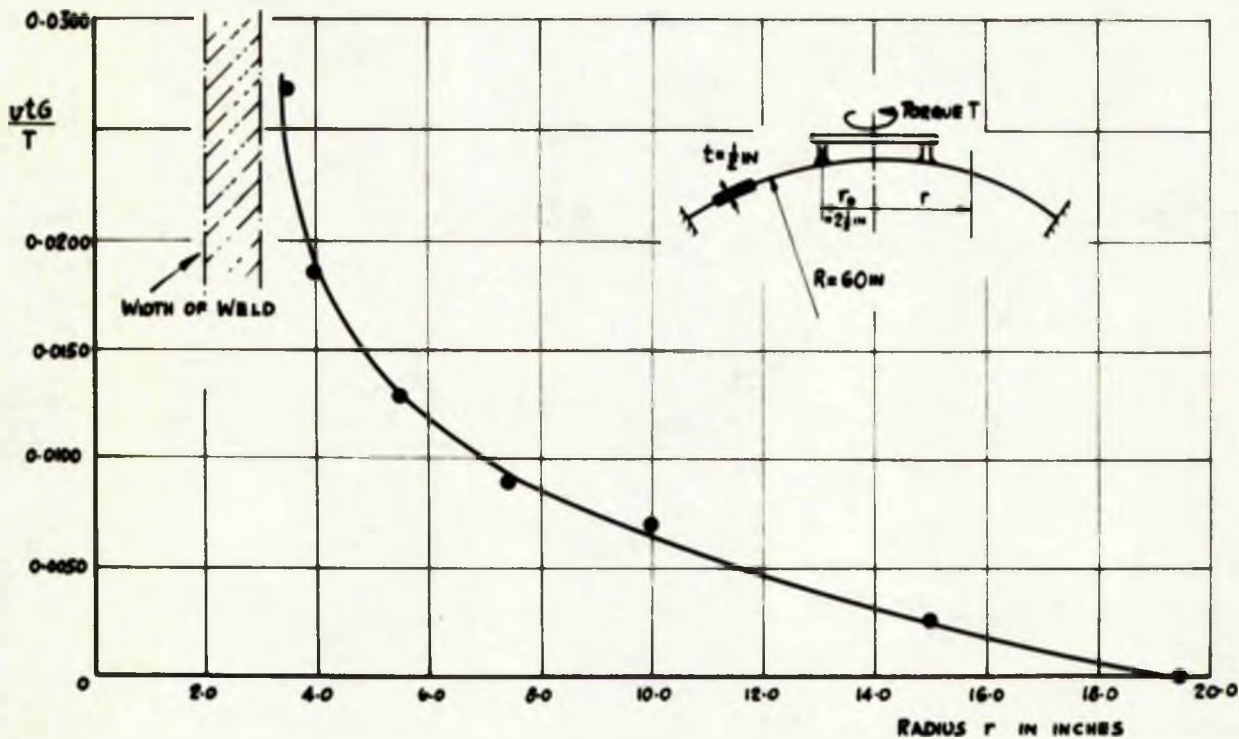
Fig. IV. 40b The Distribution of Tangential Displacement v, due to a 'Twisting' Moment T.

Fig. IV. 40 Experimentally obtained 'Mid-surface' Shear Stress and Tangential Displacement on a Shallow Spherical Shell due to a 'Twisting' Moment T. Applied to the Shell Through a 5in Mean Diam. Pipe Attachment

CHAPTER V.

COMPARISON OF THEORETICAL AND EXPERIMENTAL RESULTS

In Chapters II and III of the thesis the theoretical
analyses for a spherical shell under a variety of load cases
are presented.   These load cases are examined experimentally
in Chapter IV.   The present chapter compares the theoretical
analyses of Chapters II and III and the experimental work of
Chapter IV;   examining in turn the basic actions, the shallow
shell concept and selected composite actions.

CHAPTER V.   COMPARISON OF THEORETICAL AND EXPERIMENTAL
                                  RESULTS

V.1   BASIC ACTIONS

           V.1.1   RADIAL LOADS

                    (a)   Uniformly Distributed over a circular area

                    (b)   Applied via a rigid stud or insert

           V.1.2   'BENDING' MOMENT

           V.1.3   'TWISTING' MOMENT

           V.1.4   TANGENTIAL LOAD

V.2.   THE SHALLOW CAP CONCEPT

           V.2.1   INFLUENCE OF SHELL BOUNDARY

           V.2.2   STRESSES AND DEFLECTIONS

           V.2.3   SUPERPOSITION OF SHALLOW CAPS

V.3   EXAMINATION OF SELECTED COMPOSITE ACTIONS

           V.3.1   RADIAL RING LOADS

                    (a)   Transmitted by a freely supported ring

                    (b)   Transmitted by a rigidly fixed ring

           V.3.2   RING 'BENDING' MOMENT

           V.3.3.   RING 'TWISTING' MOMENT
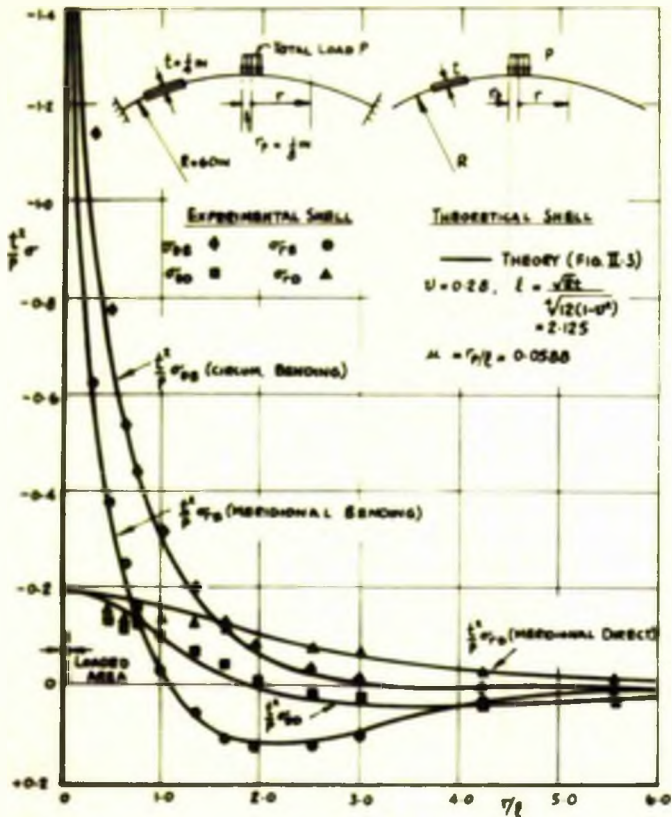
FIG. V.1a DIRECT AND BENDING STRESS. $t=\frac{1}{4}$ in, $r_p=\frac{1}{4}$ in, $\mu=0.0588$
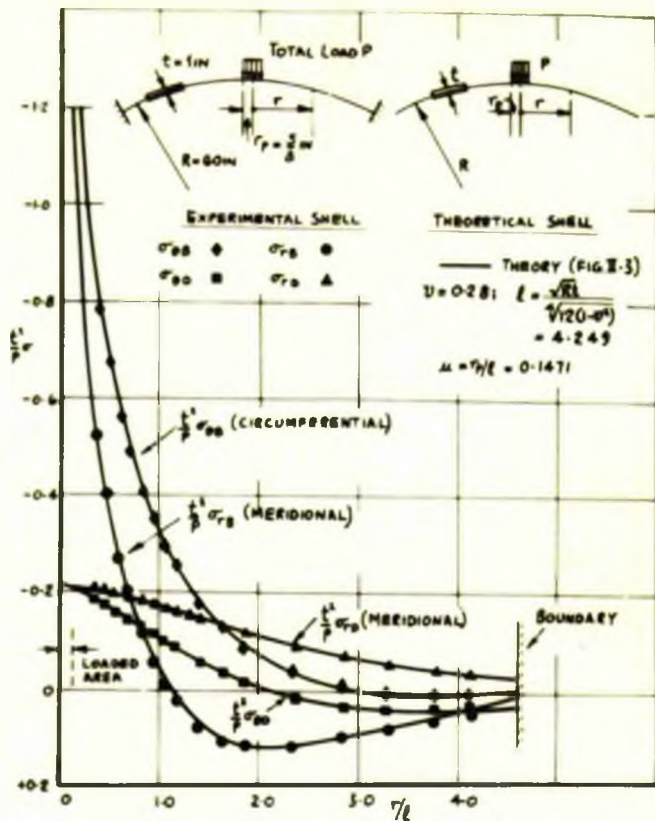
FIG. V.1b DIRECT AND BENDING STRESSES, $t=1$ in, $r_p=\frac{5}{8}$ in, $\mu=0.1471$
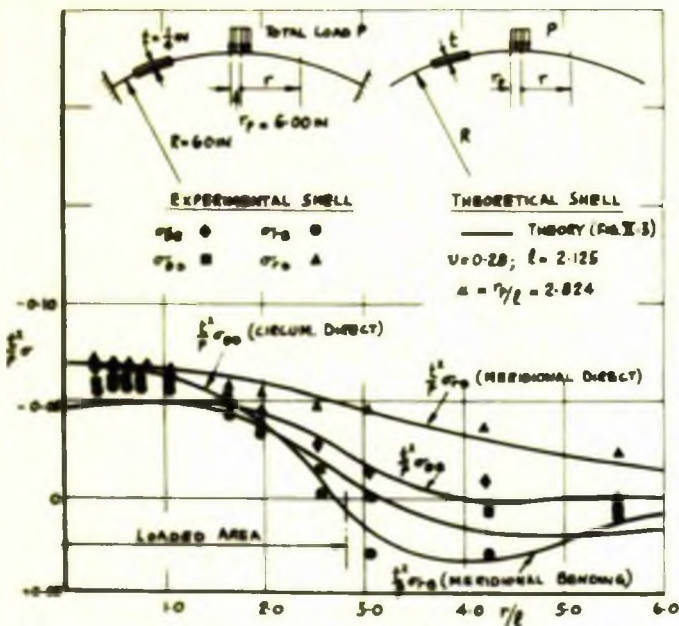
FIG. V.1c DIRECT AND BENDING STRESSES, $t=\frac{1}{4}$ in, $r_p=6.00$ in, $\mu=2.824$
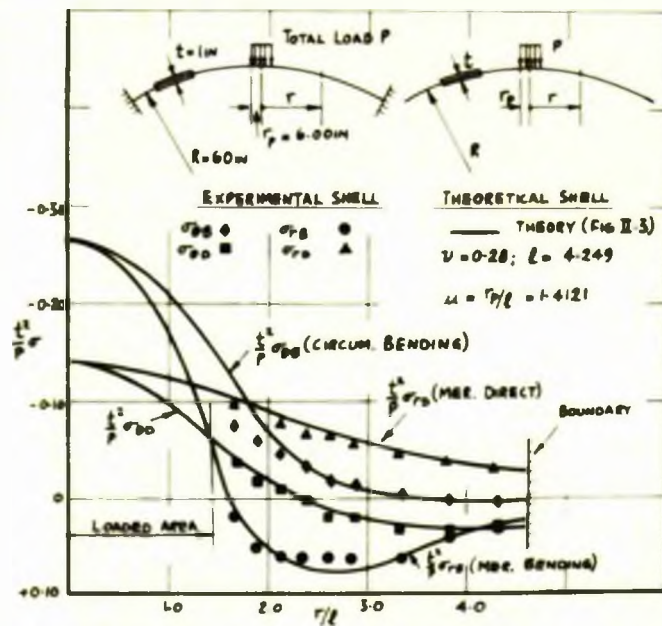
FIG. V.1d DIRECT AND BENDING STRESSES, $t=1$ in, $r_p=6.00$ in, $\mu=1.4121$

FIG. V.1 TYPICAL RESULTS OF DIRECT STRESS AND BENDING STRESS ON THE OUTER SURFACE OF A SHALLOW SPHERICAL SHELL DUE TO A UNIFORMLY DISTRIBUTED RADIAL LOAD — A COMPARISON BETWEEN THEORY AND EXPERIMENT.

V.1   BASIC ACTIONS

V.1.1   RADIAL LOADS

The radial loading was investigated theoretically and experimentally in two forms;   firstly, uniformly distributed over a circular area of the continuous shell and secondly, applied in the same manner to a rigid insert.

(a)   Uniformly Distributed over a Circular Area - Shallow Shell Models (Figs. V.1,2)

The comparison between the theoretical values and typical experimental stress results are illustrated by considering the two extreme μ values for each shell, i.e. 0.0588 and 2.824 for the $\frac{1}{4}$in thick shell and 0.147 and 1.412 for the 1in thick shell. These are presented in Fig. V.1.   The complete set of comparisons for both the $\frac{1}{4}$in and 1in shells is presented in Appendix VIII.7 Figs. VIII.4 and 5.

These results show significantly good agreement between theory and experiment.   It is of interest to note that the agreement is particuarly good for the smaller area loads.   This is ascribed to uniformity of load distribution being more closely approached in these cases.   Generally any deviations present are insignificant and it is considered that the theory is wholly substantiated by the experimental results.

In a similar manner the experimentally obtained radial deflections are compared with the corresponding theoretical curves, again for the $\frac{1}{4}$in and 1in shells.   Typical results for these cases are shown in Fig. V.2.   In Figs. V.2a and 2b the results for the smaller area loads for shells of $\frac{1}{4}$in and 1in are shown.   In these cases it was possible to measure the deflection

at a large number of points and so define precisely the
deflected form of the shell as a whole.   This permits criti-
cally searching comparison with theory and indicate good agree-
ment.

It is relevant to mention that there appears to be slight
divergence in the results obtained for the larger area loads in
the 1in shell, as shown in Fig. V.2d. This is considered to be
due to a ring load action originated possibly by friction of
the steel shot on the retaining ring in the arrangement described
on p.172.   The reason for ascribing this effect to the steel
shot loading device is that the deviation was not present in the
water filled membrane loading arrangement used for the $\frac{1}{4}$in shell,
the results of which are shown in Fig. V.2c.

On this basis it is considered that the deflection variatio
also substantiate the theory in a satisfactory manner.

The complete series of results for both shells is presented
in Appendix VIII.7, Figs. VIII. 6,7.

(b)   Radial Loads Applied by means of a Rigid Insert - Shallow
      Shell (Fig. 3a,b)   Complete Sphere (Fig.3c)

The shallow shell stress and deflection results (for $\mu = 0.23$
are shown in Figs. V.3a,b and those of the complete sphere for
the case $\mu = 0.092$ in Fig.V.3c. (The other complete sphere result
for $\mu = 0.195$ and 0.394 are shown in Appendix VIII.7, Fig.VIII.8

The deviations that occur between the theory and the exper:
mental results are seen to obtain in the immediate vicinity of
the insert.   It would appear, therefore, that the boundary con-
dition at the insert of $\varepsilon_\theta = 0$, assumed in the theory, is not
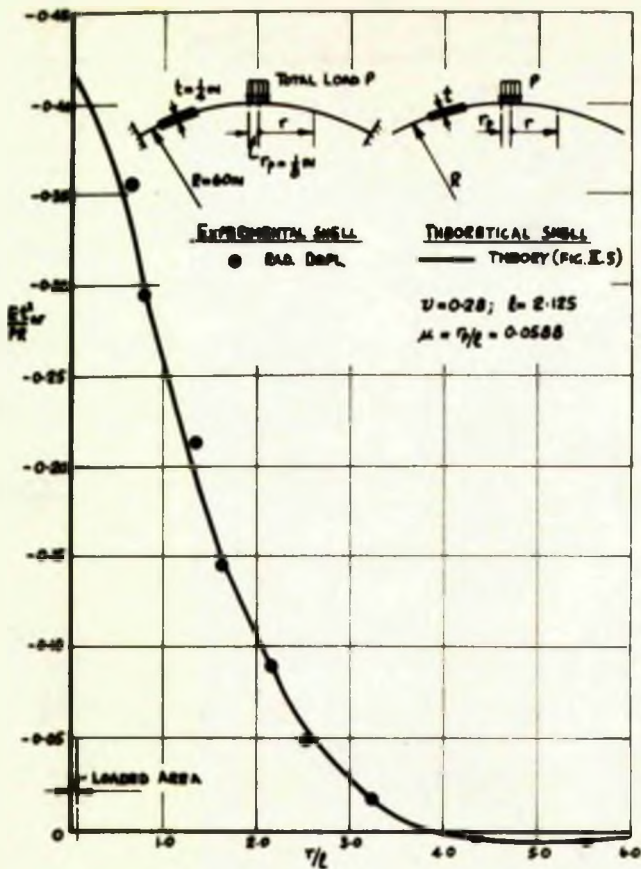
Fig. V.2a Radial Deflections, $t = \frac{1}{2}$ in, $r_p = \frac{1}{8}$ in, $\mu = 0.0588$
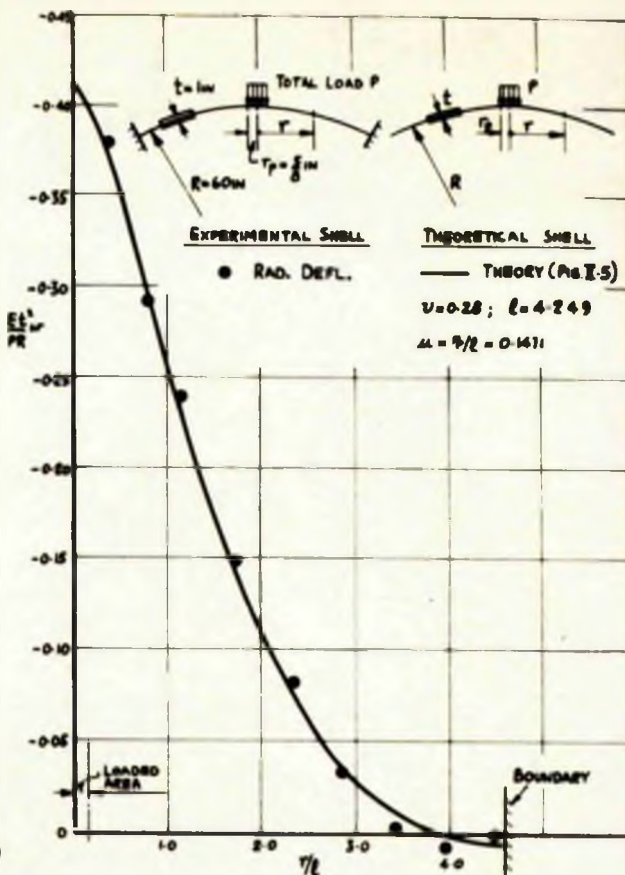
Fig. V.2b. Radial Deflections, $t = 1$ in, $r_p = \frac{5}{8}$ in, $\mu = 0.1471$
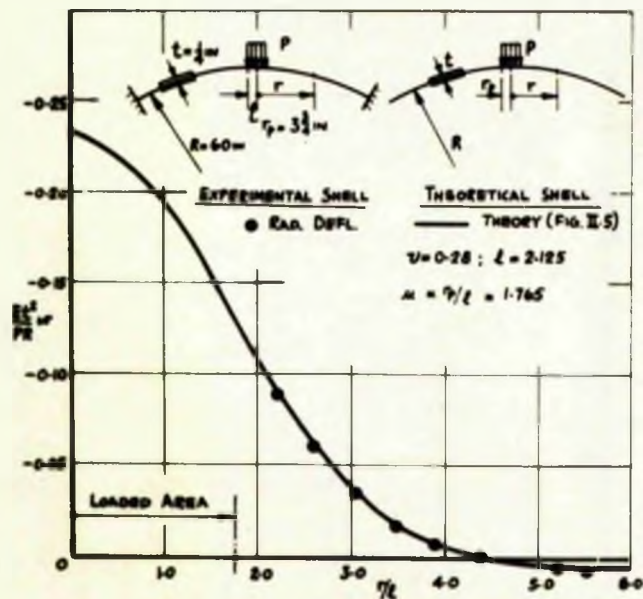
Fig. V.2c Radial Deflections, $t = \frac{1}{2}$ in, $r_p = 3.75$ in, $\mu = 1.765$
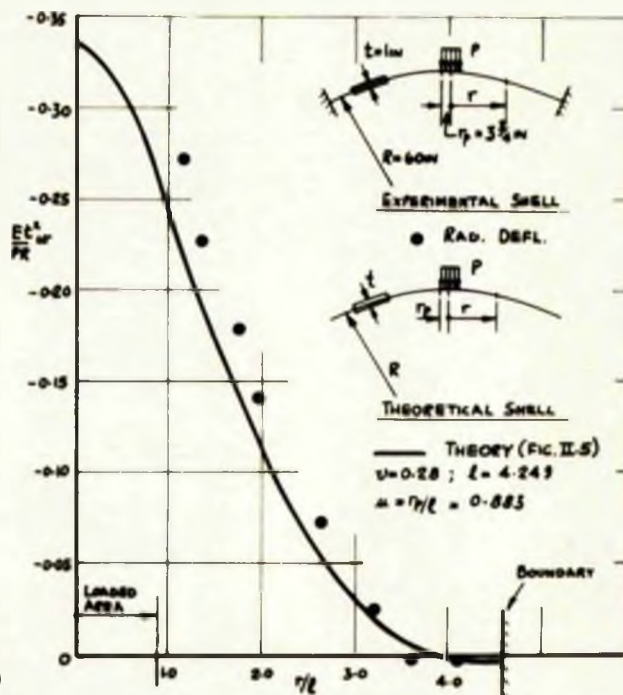
Fig. V.2d Radial Deflections, $t = 1$ in, $r_p = 3.75$ in, $\mu = 0.883$

Fig. V.2 TYPICAL RESULTS OF RADIAL DEFLECTIONS OF A SHALLOW SPHERICAL SHELL DUE TO A UNIFORMLY DISTRIBUTED RADIAL LOAD — A COMPARISON BETWEEN THEORY AND EXPERIMENT
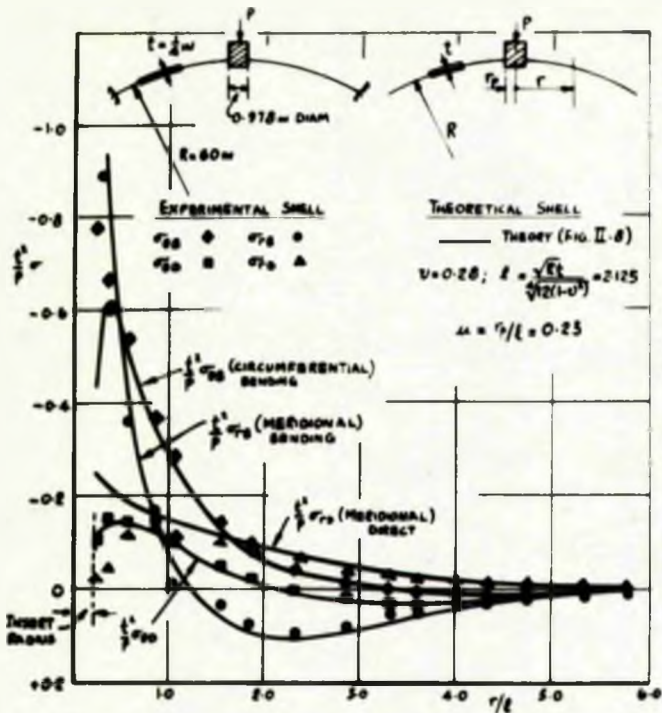
Fig. V.3a DIRECT STRESS AND BENDING STRESS ON THE OUTER SURFACE ON A SHALLOW SHELL, μ=0.23
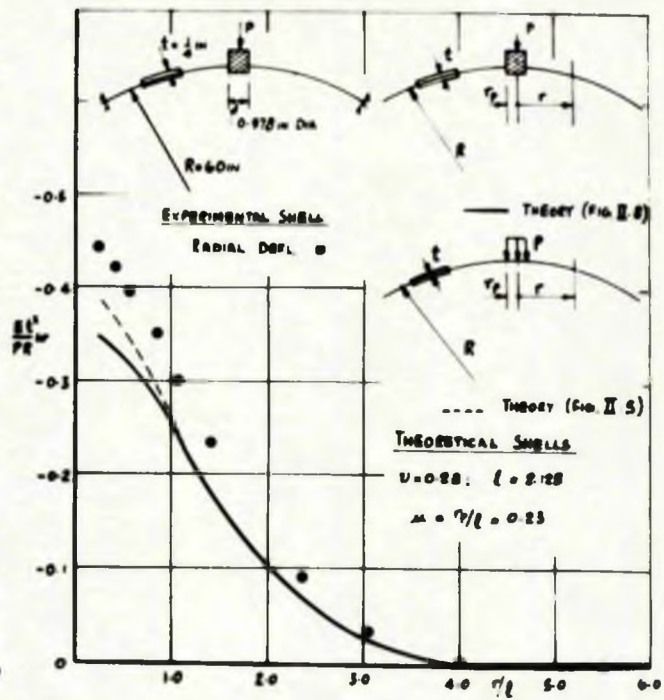
Fig. V 3b RADIAL DEFLECTION ON A SHALLOW SHELL, μ=0.23
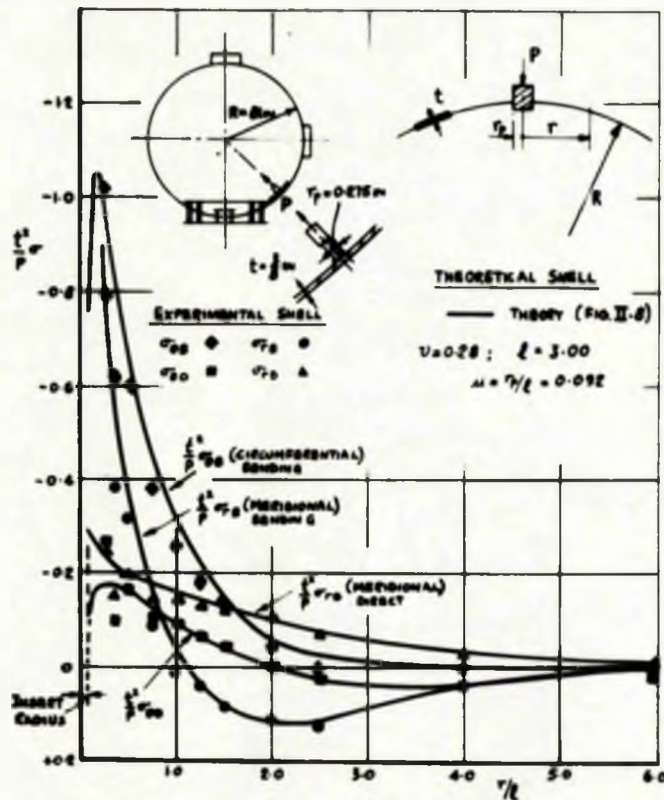
Fig. V 3c DIRECT STRESS AND BENDING STRESS ON THE OUTER SURFACE ON A COMPLETE SPHERE. μ=0.092

FIG. V.3 TYPICAL RESULTS OF DIRECT STRESS, BENDING STRESS ON THE OUTER SURFACE AND RADIAL DEFLECTION, OF A SHALLOW SHELL AND COMPLETE SPHERE (15 FT. 6 IN DIAM.) DUE TO A RADIALLY LOADED RIGID INSERT — A COMPARISON BETWEEN THEORY AND EXPERIMENT
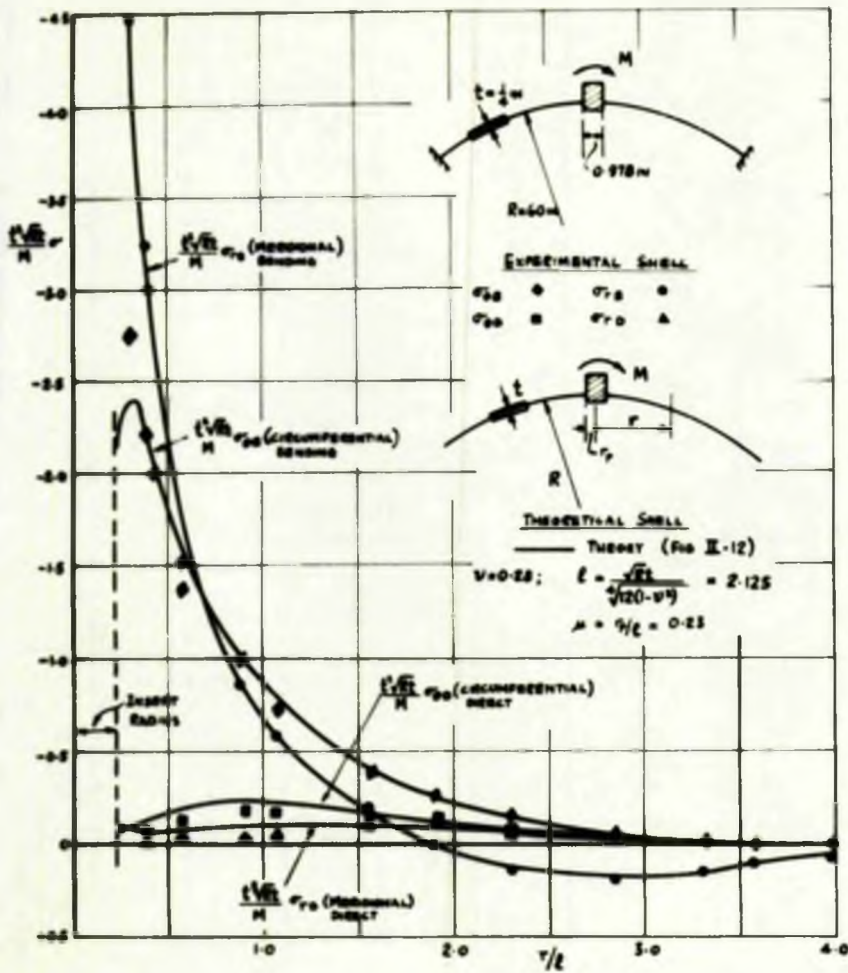
Fig. V. 4a DIRECT STRESS AND BENDING STRESS ON THE OUTER SURFACE ON A SHALLOW SHELL, $\mu = 0.23$

Fig. V. 4b RADIAL DEFLECTION ON A SHALLOW SHELL, $\mu = 0.23$
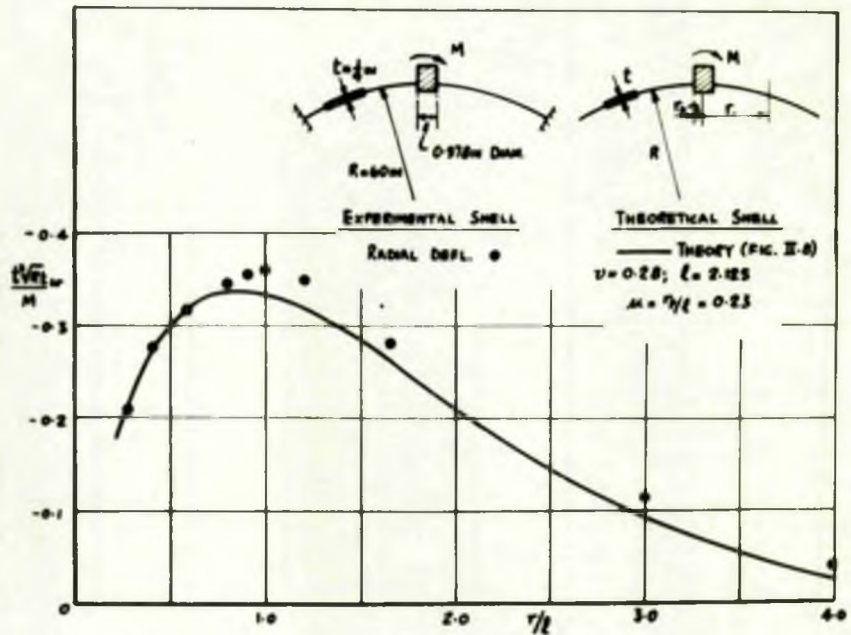
Fig. V. 4 DIRECT STRESS, BENDING STRESS ON THE OUTER SURFACE AND RADIAL DEFLECTION OF A SHALLOW SHELL (IN THE GREAT CIRCLE, $\theta = 0°$) DUE TO A BENDING MOMENT M APPLIED THROUGH A RIGID INSERT ($\mu = 0.23$) — A COMPARISON BETWEEN THEORY AND EXPERIMENT

realised in practice, despite the precautions taken during the
welding of the inserts.   It is further noted that the stresses
would be equally well predicted by the theory of the uniformly
distributed radial load applied to the continuous shell as given
by eqts. II.49-51 and Figs. II.3,5.

The experimental results for the deflections of the shallow
shell are seen to be somewhat higher than both the rigid insert
and the uniformly distributed load theories.   This is considered
to be due to the method of construction of the models, which con-
sisted of drilling a hole in the shell and welding a solid insert
of appropriate size to fill the hole.   It seems fairly clear that
complete integrity of the shell was not obtained leading to a
degree of 'weakness' which resulted in increased experimentally
recorded deflections in comparison with the theoretically pre-
dicted values.

V.1.2   BENDING MOMENT - Shallow Shell (Fig.V.4) and Complete
         Sphere (Fig. V.5)

The theoretical predictions are fully confirmed by the
experimental results for all actions except the circumferential
stress in the immediate vicinity of the insert.   This again is
attributed to the lack of integral continuity between insert
and shell.

V.1.3   TWISTING MOMENT - Shallow Shell (Fig. V.6)

All that need be noted here is that the agreement obtained
between theory and experiment is excellent.

V.1.4   TANGENTIAL LOADING - Shallow Shell (Fig.V.7) and Complete
         Sphere (Fig.V.8)

It is seen that the shallow shell results for both the

circumferential direct stress and mid-surface shear stress
(Fig.V.7) show good agreement between the theoretical and
experimental results.   The same measure of agreement, however,
was not found in the case of the meridional direct stress for
the shallow shell, where the experimental curve has a more rapid
'die out' than that predicted by the theory.   It is of signifi-
cance that in the case of the complete sphere generally good
agreement was obtained particularly in the case of this same
meridional stress (Fig.V.8)

     This conflicting evidence for the meridional stress for
the shallow shell and complete sphere is explicable in terms of
the method of tangential load transfer to the shell.

     In the tests carried out on the complete sphere the load wa
applied through pads welded to the surface of the sphere, in the
form of a 'tractive' force of total value H. In this case the
experimental and theoretical results show good agreement.

     In the shallow shell tests the insert penetrated the shell,
being welded on both the upper and lower surfaces.   These doubl
welds were intended as a practical precaution to ensure that the
tangential load would in fact be applied as a tractive force.
It now seems clear, however, that this did not materialize, and
load transmission is presumed to have been partly tractive and
partly in the form of a bearing action applied over the contact
area between insert and shell wall.   Such a condition would
naturally affect the meridional stress results to a greater exter
than those of the circumferential and shearing stresses and would
produce just this more rapid 'die-out' effect manifested by the
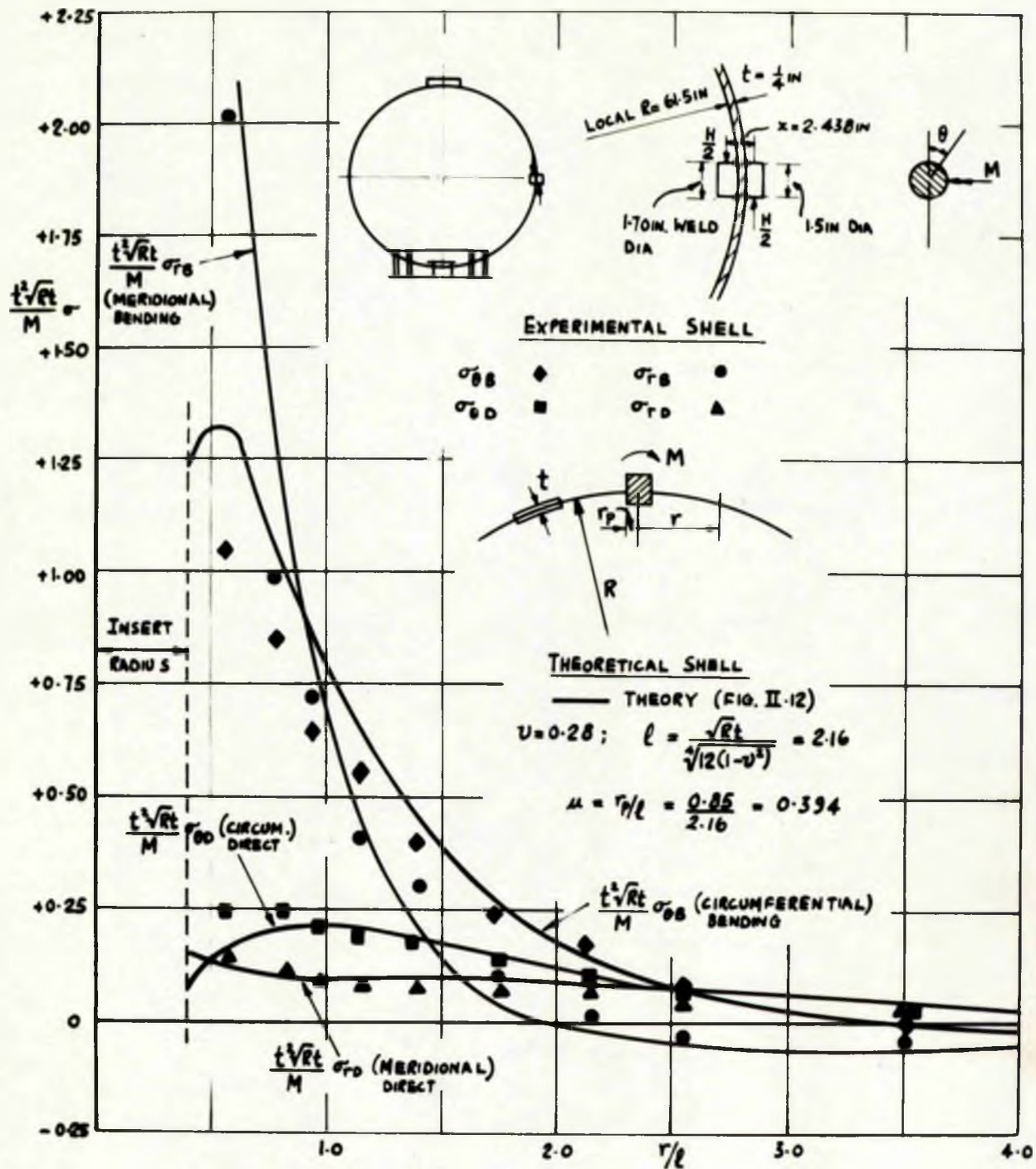
FIG.V.5 DIRECT STRESS AND BENDING STRESS ON THE OUTER SURFACE OF A COMPLETE SPHERE (IN THE GREAT CIRCLE, θ = 180°) DUE TO A BENDING MOMENT M, APPLIED THROUGH A RIGID INSERT (μ = 0.394) – A COMPARISON BETWEEN THEORY AND EXPERIMENT
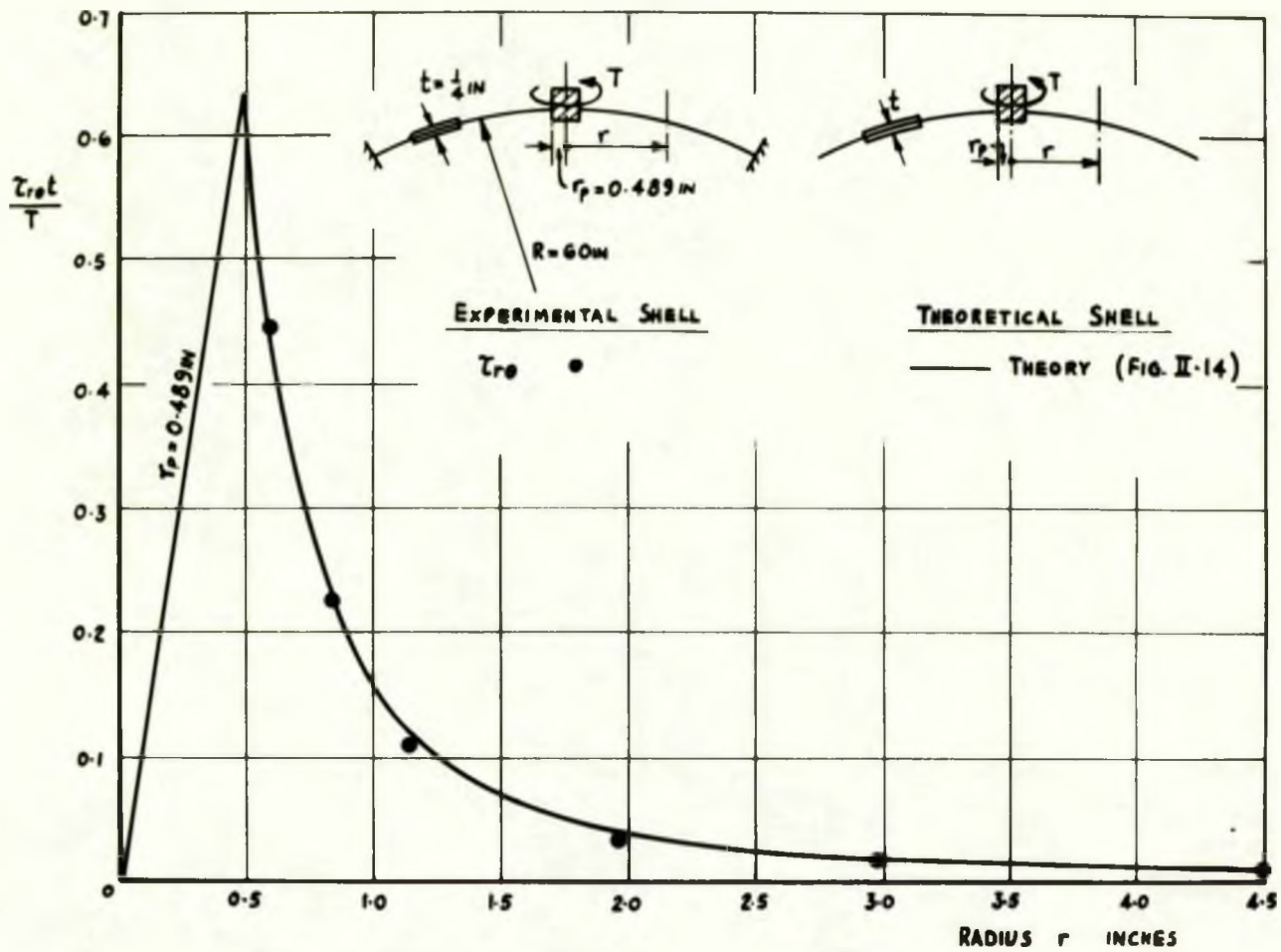
FIG. V.6 'MID-SURFACE' SHEAR STRESS IN A SHALLOW SHELL DUE TO A 'TWISTING' MOMENT T, APPLIED THROUGH A RIGID INSERT(r_p = 0.489 IN) - A COMPARISON BETWEEN THEORY AND EXPERIMENT
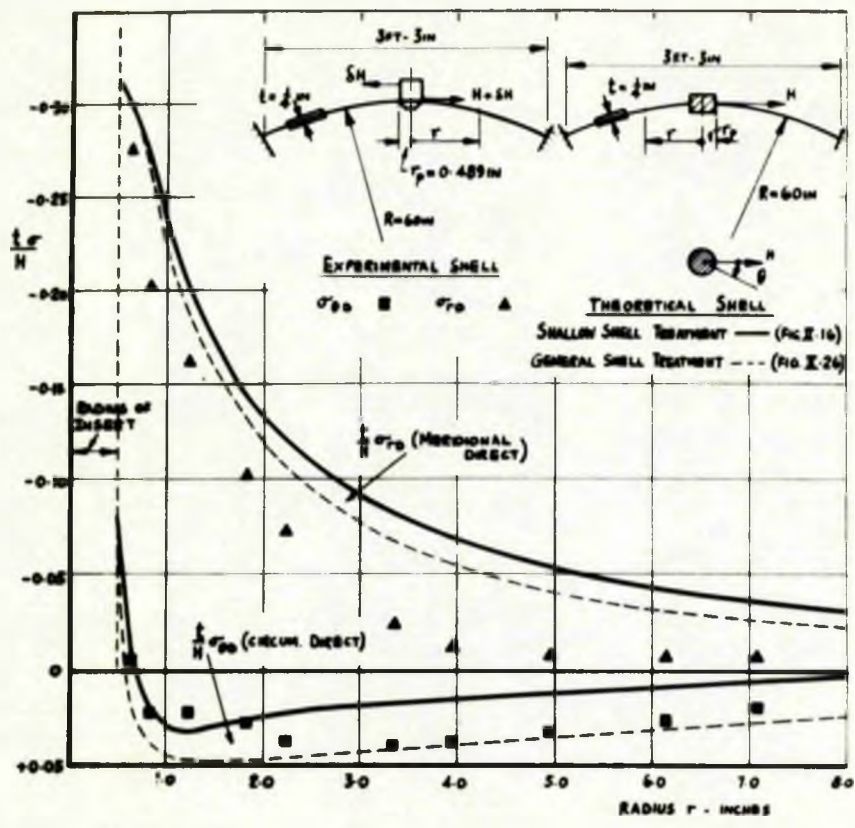
FIG. V. 7a DIRECT STRESS ON θ=0° LINE DUE TO A TANGENTIAL LOAD H ON A SHALLOW SHELL
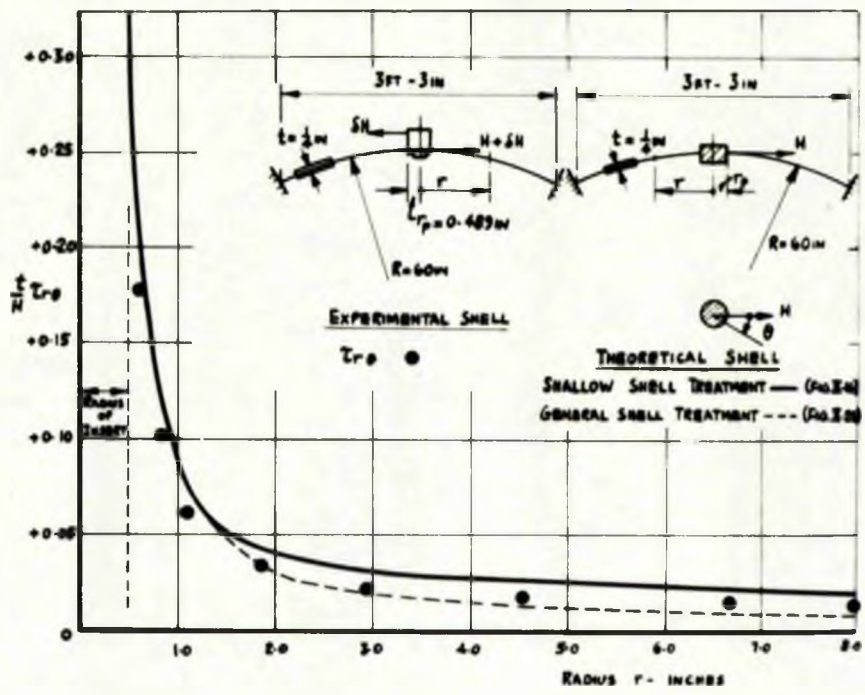
FIG. V. 7b 'MID-SURFACE' SHEAR STRESS ON θ=90° LINE

FIG.V.7 DIRECT STRESS (ON θ=0°LINE) AND 'MID-SURFACE' SHEAR STRESS (ON θ=90°LINE) OF A SHALLOW SHELL DUE TO A TANGENTIAL LOAD H APPLIED THROUGH A RIGID INSERT (r_p=0.489IN) - A COMPARISON BETWEEN THEORY AND EXPERIMENT
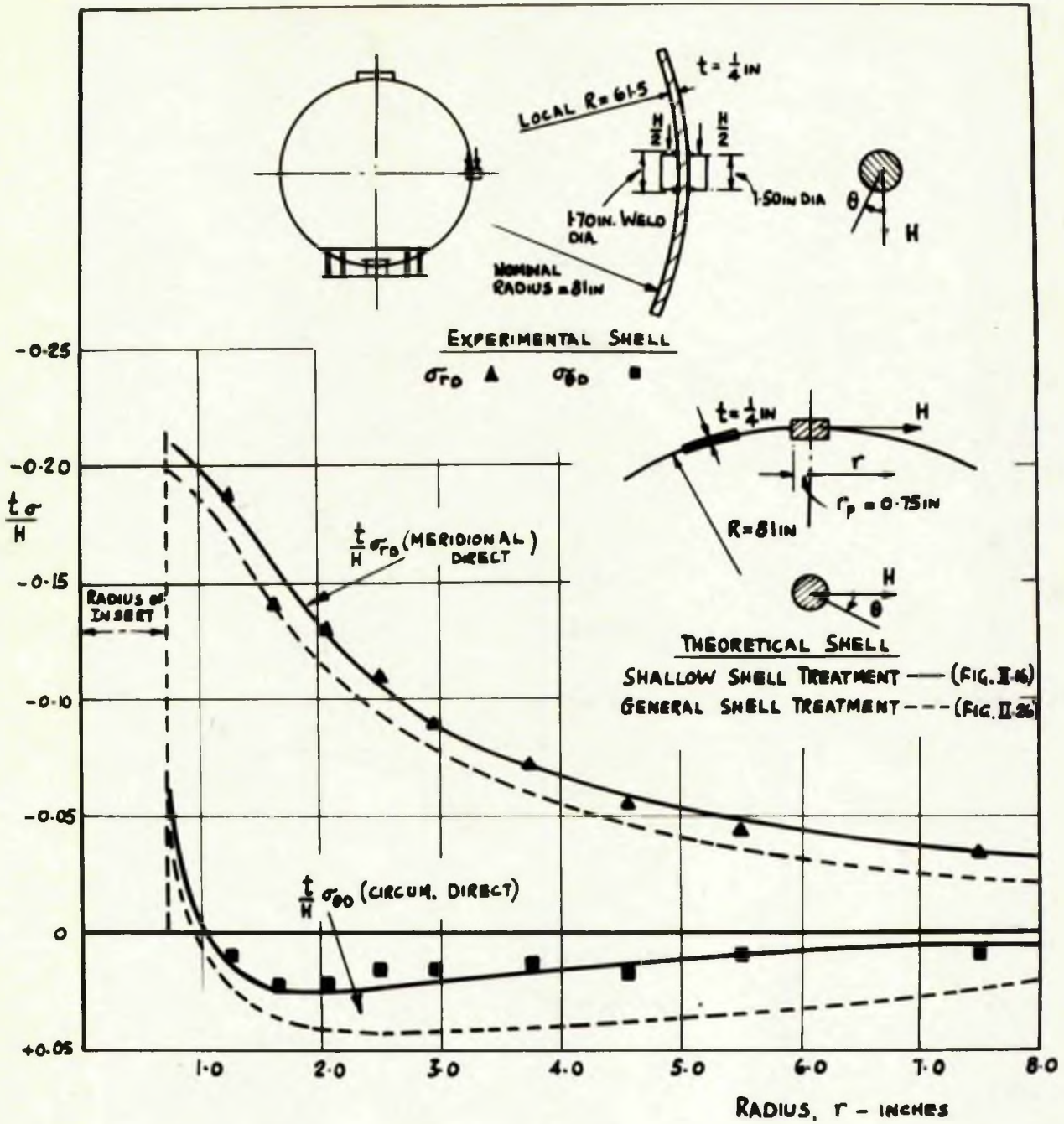
FIG. V. 8 DIRECT STRESSES IN A GREAT CIRCLE ($\theta = 0°$) OF A COMPLETE SPHERE (13FT - 6IN DIAM.) DUE TO A TANGENTIAL LOAD H, APPLIED THROUGH A RIGID INSERT— A COMPARISON BETWEEN THEORY AND EXPERIMENT

appropriate experimental results.

Further experimental confirmation of this effect was specifically provided through a subsidiary series of tests. In this, the insert was removed and a hole, of the same diameter, was drilled in the shell wall. A closely fitting bar was then passed through this hole and was used to apply a tangential load to the shell wall practically wholly by bearing action. This had the effect of increasing the peak value of meridional stress above that corresponding to the rigid insert and was accompanied by a much more rapid 'die-out' than that shown by the theoretical and by the other experimental results.

These effects emphasise the care necessary in ascertaining the actual load transmission mechanism of the particular loading attachment used.

V.2   THE SHALLOW CAP CONCEPT

The experimental work, as already indicated, has been directed in certain instances to the substantiation of aspects which may be used as the basis for design methods.   These concern the significance of the 'die-out' distance for both stresses and deflections and are discussed in the following.

V.2.1   INFLUENCE OF SHELL BOUNDARY - Shallow Shell (Figs.V.9,10)

Figs. V.9 and V.10 compare the experimental and rotationally symmetrical theoretical distributions for a series of 'off-centre' radial loads. It can be seen from the stress values presented in Fig. V.9:-

(i)   That the theory for the rotationally symmetrical case (applied at the load point) is in complete agreement with the experimental stress results for an 'off-centr load, provided the boundary of the shell is out with t 'die-out' distance.

(ii)   that the experimental results have the intriguing feature that even when the boundary is within this 'die-out' distance the stress distributions tend to follow the variation predicted by the theory, being in a sense 'cut-off' at the boundary.

The radial deflections, shown in Fig.V.10, for the same ser of loads indicate, as expected, greater divergence from the rotat ally symmetrical theory since they are forced to conform to the physical condition of zero radial deflection at the boundary. In the 10.65in and 12.80in centre distance loading the deviation of the radial deflection is only of significant magnitude in the
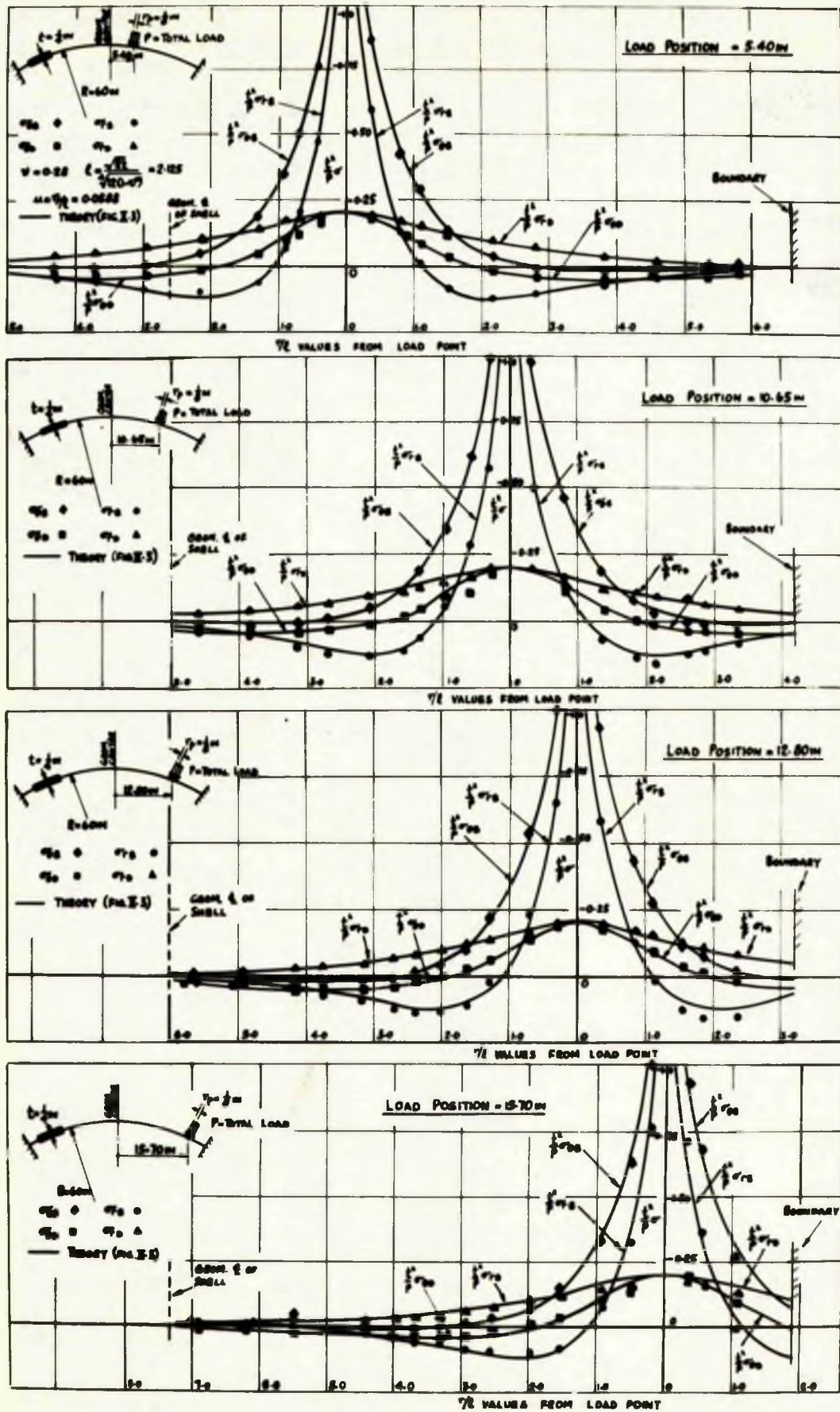
FIG. V. 9 THE INFLUENCE OF THE WELDED BOUNDARY ON BENDING AND DIRECT STRESSES IN A SHALLOW
SHELL ($t = \frac{1}{2}$ IN, R = 60 IN) UNDER A RADIAL LOAD P. APPLIED AT FOUR DIFFERENT POSITIONS —
A COMPARISON BETWEEN THEORY AND EXPERIMENT
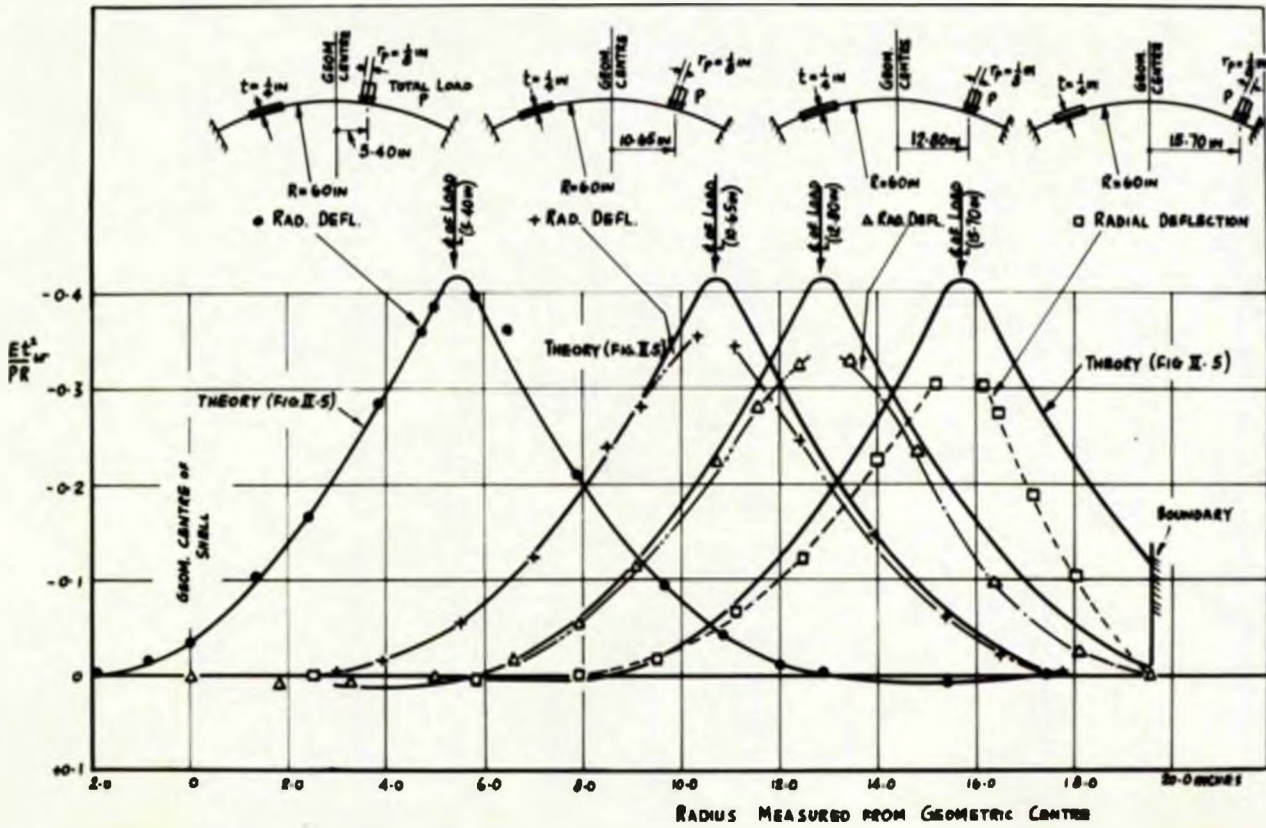
FIG. V. 10 THE INFLUENCE OF THE WELDED BOUNDARY ON RADIAL DEFLECTION IN A SHALLOW SHELL (t= ½ in, R= 60 in) UNDER A RADIAL LOAD P APPLIED AT FOUR DIFFERENT POSITIONS - A COMPARISON BETWEEN THEORY AND EXPERIMENT
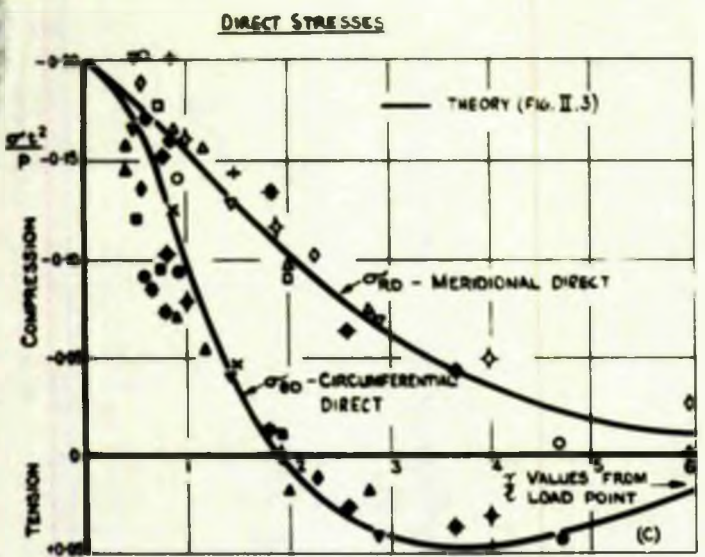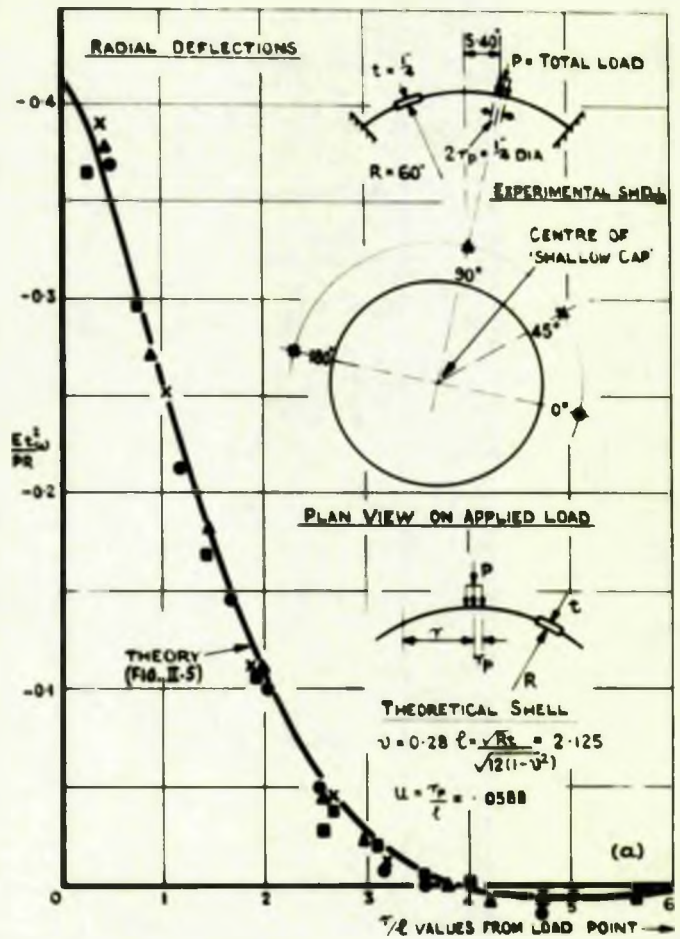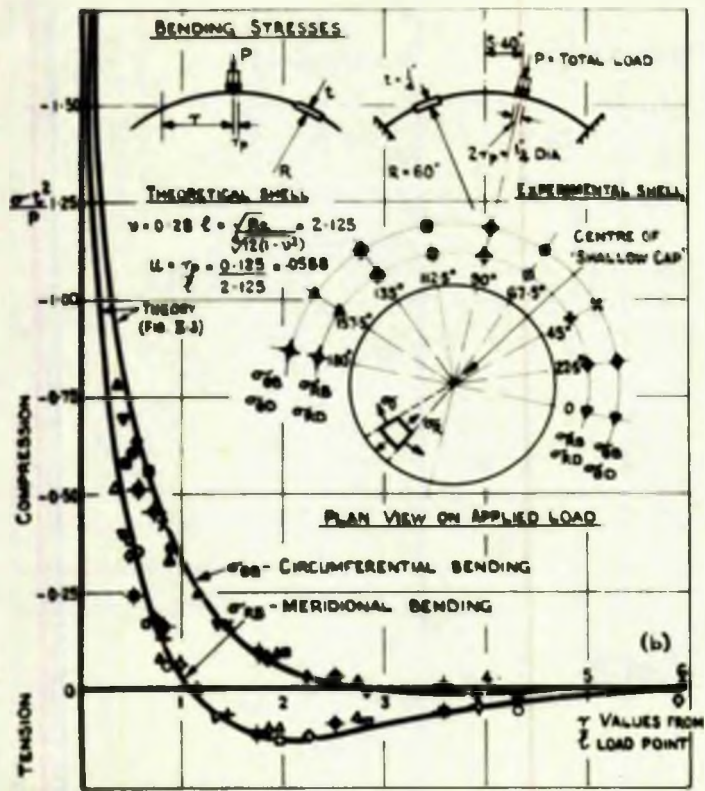
FIG V.II   BENDING AND DIRECT STRESSES AND RADIAL DEFLECTIONS ON A SHALLOW SPHERICAL
SHELL DUE TO A RADIAL LOAD 'OFF-SET' FROM THE CROWN OF THE SHELL

vicinity of the load point, and in these cases it would not be
unreasonable to predict the radial deflection on the basis of
this theory.

V.2.2   DISTRIBUTION OF DEFLECTION AND STRESS AROUND THE CROWN
         OF THE SHALLOW CAP - Shallow Shell (Fig . V.11).

The behaviour of several shallow caps whose crowns were
situated off-set from the geometric centre of the shell were
investigated experimentally. Typical results for such a cap, for
which the load position defining its crown is 5.40 in from the
geometric centre of the shell, are presented in Fig.V.11. In
this figure the experimental stress and deflection results and
the corresponding rotationally symmetrical theoretical values
are given.

It is seen that not only do the stresses and deflections
define respective single curves but these curves are the appro-
priate theoretical curves for the case of a shell loaded in a
rotationally symmetrical manner.   Thus the evidence is again
indicative of the applicability of the rotationally symmetrical
theory.

V.2.3   THE EFFECT OF SUPERPOSING TWO LOADS BOTH 'OFF-SET' FROM
         THE GEOMETRIC CENTRE - Shallow Shell (Fig.V.12)

Fig. V.12 presents the stress results of experiments des-
igned as a direct demonstration of the Principle of Superposition.
The theoretical values with which these experimental results are
compared have been obtained by superposing two rotationally
symmetrical systems situated with their crown at the corresponding
load positions.   There is good agreement between the experimental
and theoretical values.

The radial deflections for the two series of tests are also shown in Fig.V.12. These experimental points are compared, in the first place, with the superposed experimental values for the relevant single load cases (Fig.IV.24). In this case it is seen there is good agreement between the two. Secondly, they are compared with the superposed theoretical values for the rotationally symmetrical case, where, as expected from the single load results (Fig.V.10), there are deviations between the experimental and theoretical results in the region of the load nearest the boundary.

It may, therefore, be concluded that within the limits of experimental error it is possible to superpose the effects of two shallow caps placed in close proximity to each other, and that the rotationally symmetrical theory may be used in those cases where the single load results are predicted by the rotationally symmetrical theory.
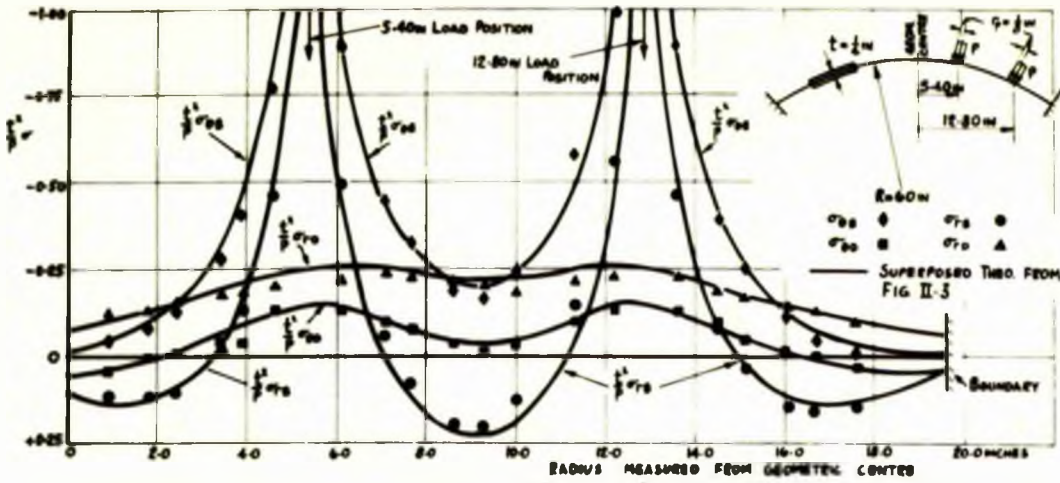
FIG. V.12a DIRECT & BENDING STRESS DUE TO RADIAL LOADS AT 5·40IN AND 12·80IN
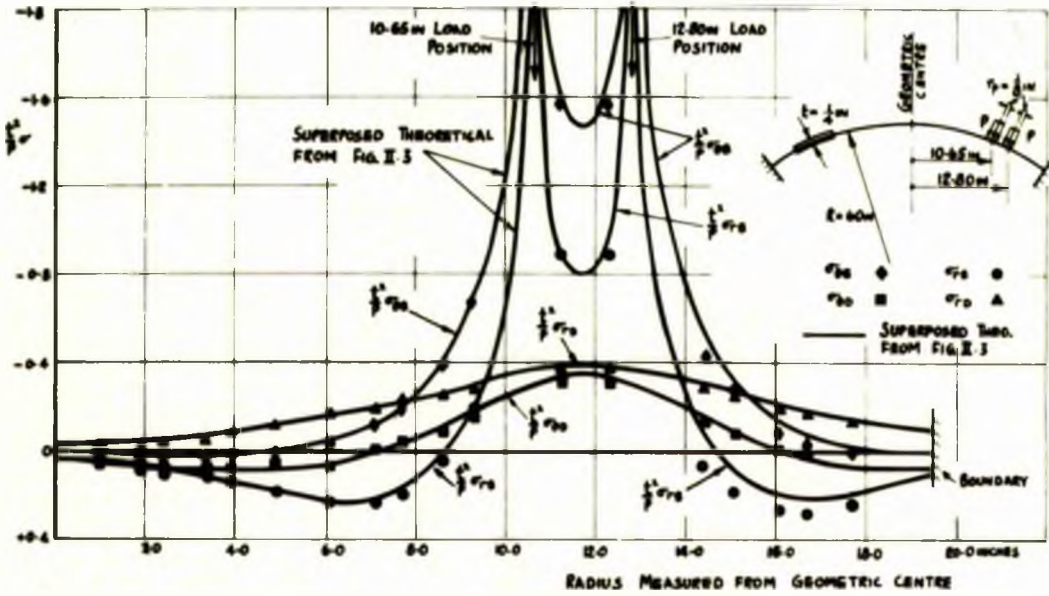
FIG. V.12b DIRECT & BENDING STRESS DUE TO RADIAL LOADS AT 10·65IN AND 12·80IN
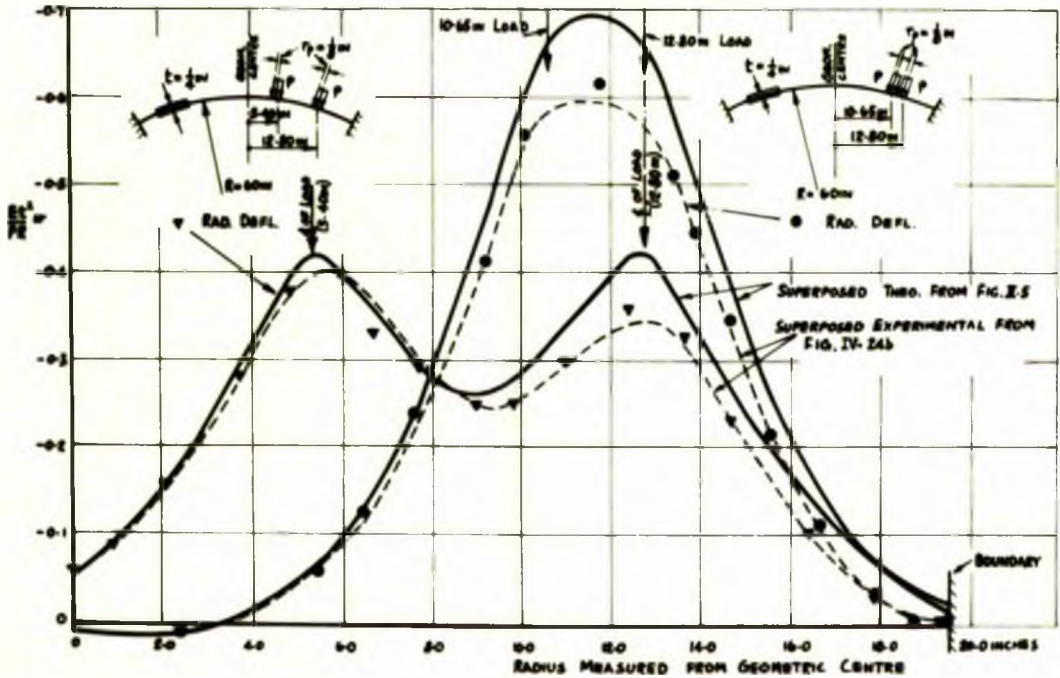
FIG. V.12c DEFLECTIONS DUE TO TWO SETS OF RADIAL LOADS — 5·40 & 12·80IN, 10·65 & 12·80IN

FIG. V.12 THE EFFECT OF SUPERPOSING TWO RADIALLY APPLIED LOAD SYSTEMS BOTH 'OFF-SET' FROM THE GEOMETRIC CENTRE — A COMPARISON BETWEEN THEORY AND EXPERIMENT
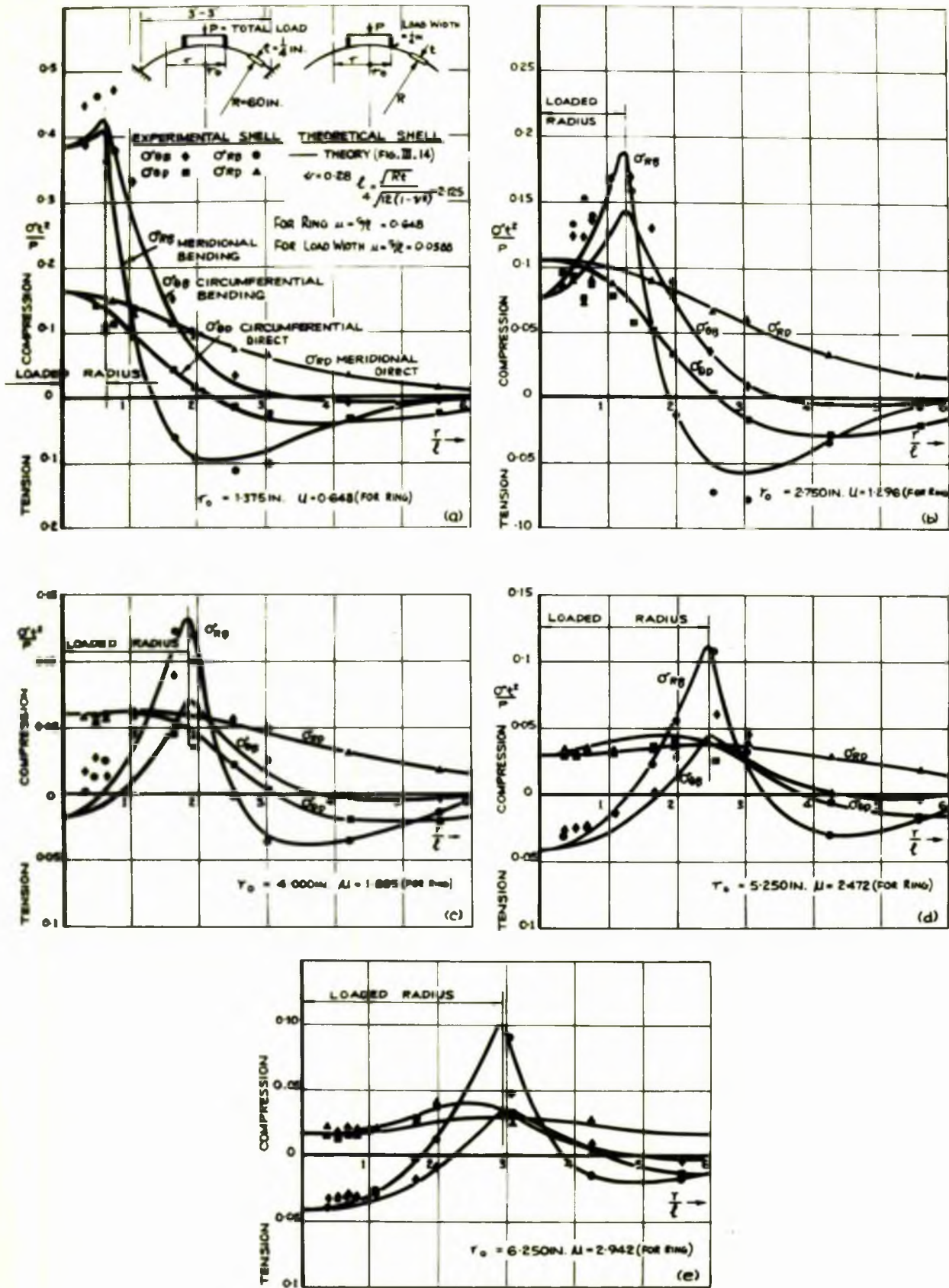
FIG. V. 13 DIRECT STRESS AND BENDING STRESS ON THE OUTER SURFACE OF A SHALLOW SPHERICAL SHELL DUE TO A RADIAL LOAD P TRANSMITTED BY A FREELY SUPPORTED RING - A COMPARISON BETWEEN THE INFLUENCE LINE METHOD AND EXPERIMENT

V.3   EXAMINATION OF SELECTED COMPOSITE ACTIONS

As indicated in Chapter IV (section IV.3) selected load cases inclusive of radial loads and moments were investigated experimentally.   These load cases were amenable to analysis by the Influence Line Method (Chapter III) thus permitting direct comparison with predicted and experimental values.   These comparisons are presented in this section.

V.3.1   RADIAL RING LOADS

These were applied to the shell firstly, by a freely supported ring and secondly, by a rigidly fixed ring.

(a)   Radial Loading Transmitted by a Freely Supported Ring - Shallow Shell (Figs. V.13 and 14)

The comparison between the theoretical values, obtained by the Influence Line Method, and the experimental values from the shallow shell for stresses and radial deflections are shown in Figs. V.13 and V.14, respectively.

It is seen from these results that the agreement between the theory and the experimental results is quite satisfactory and would appear to be within the experimental accuracy of the set-up.   The experimental difficulties in these tests were in ensuring that the load was distributed uniformly round the ring, and that there was complete freedom of constraint at the load point.   It will be noticed that the results of the smaller rings of $2\frac{3}{4}$ and $5\frac{1}{2}$in diam. show some divergence from the theoretical values in the region of the ring.   This is undoubtedly due to these difficulties, which despite improvements in the experimental technique were still present.   The larger rings do not show this divergence in the region of the ring because of the fact that in these cases the

load per unit length was smaller and the above difficulties corres
pondingly reduced.

(b)   Radial Loading Transmitted by a Rigidly Fixed Ring - Complete
      Sphere (Fig.V.15)

The comparison between the predictions of the Influence
Line Method and the experimental results are shown in Fig.V.15
and it is noted that there is good agreement between the two.
Some divergence, however, is noted in the case of the smaller
ring ($\mu = 1.48$) in the region of the shell contained within the
ring.   These are thought to be due to local irregularities in
the vessel surface in this region, a defect not present in the
shell surface associated with the larger ring.

V.3.2   RING BENDING MOMENT - Shallow Shell (Figs. V.16, 17)

In the experimental set-up discussed in Chapter IV, the
moment transmission to the shell almost certainly took place by
a combination of radial and tangential loads and moment actions,
the magnitude of these depending upon the relative stiffness of
the ring (or tube) and shell.   To illustrate this effect a
selection of the experimental results shown in Fig.IV.38, namely
radial deflections and meridional stresses, are compared with the
theoretical values derived on the basis of moment transmission by
varying radial load (Fig. III.18).   These are shown in Fig.V.16a,b

It will be seen that the deflections vary in a similar way
to that of the theory though lower in magnitude, this being par-
ticularly noticeable in the region of the loaded ring.   At point
outside and some distance from the region of the ring the agree-
ment with the theory is not unreasonable. The meridional bending
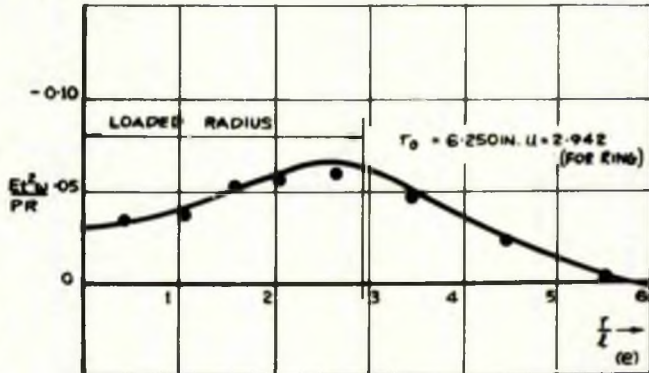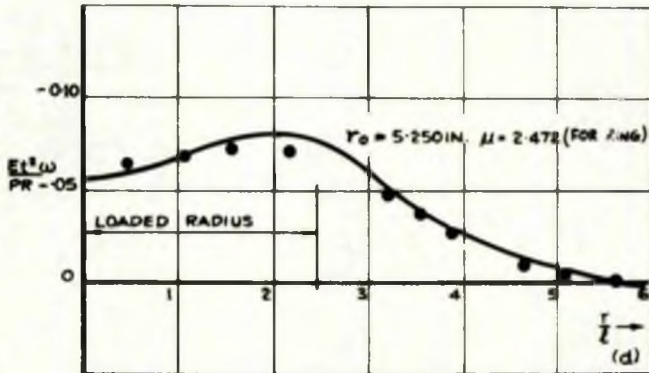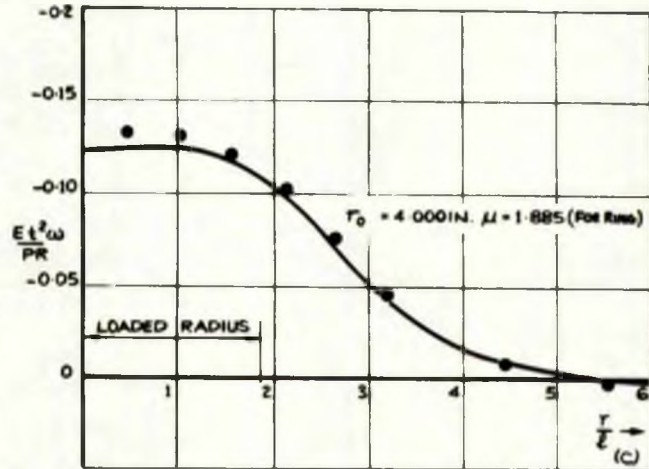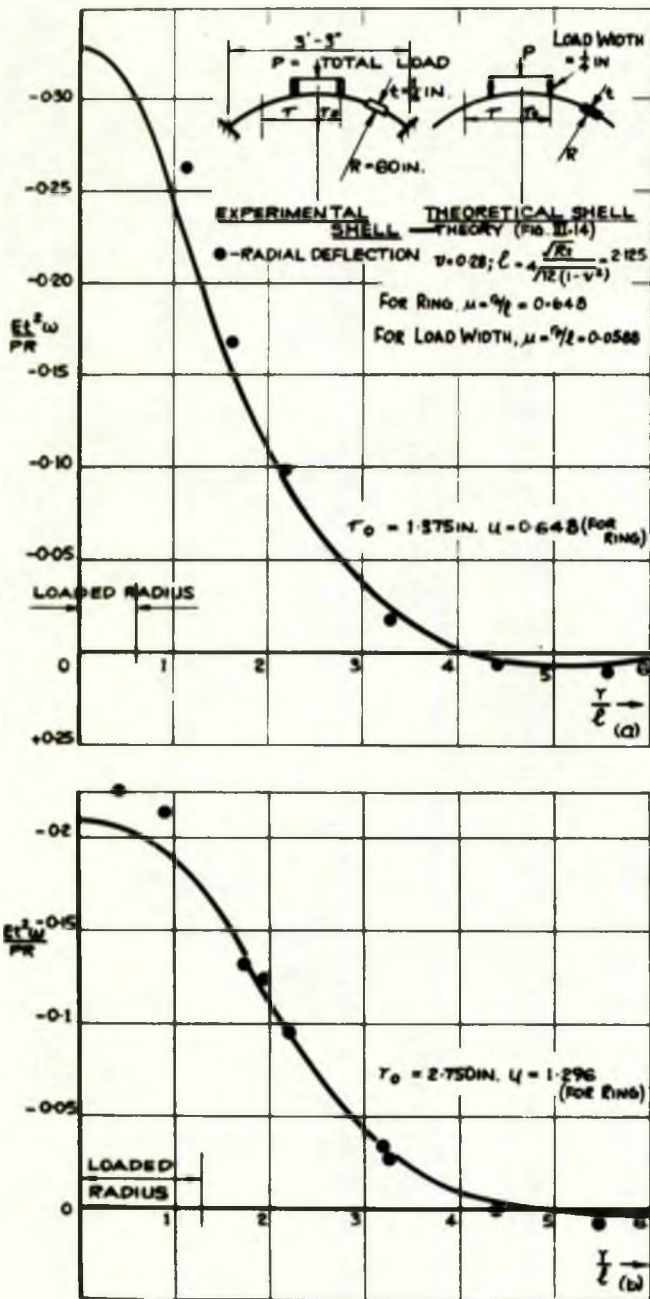
FIG. V.14 RADIAL DEFLECTION OF A SHALLOW SPHERICAL SHELL DUE TO A RADIAL LOAD P TRANSMITTED BY A FREELY SUPPORTED RING - A COMPARISON BETWEEN THE INFLUENCE LINE METHOD AND EXPERIMENT
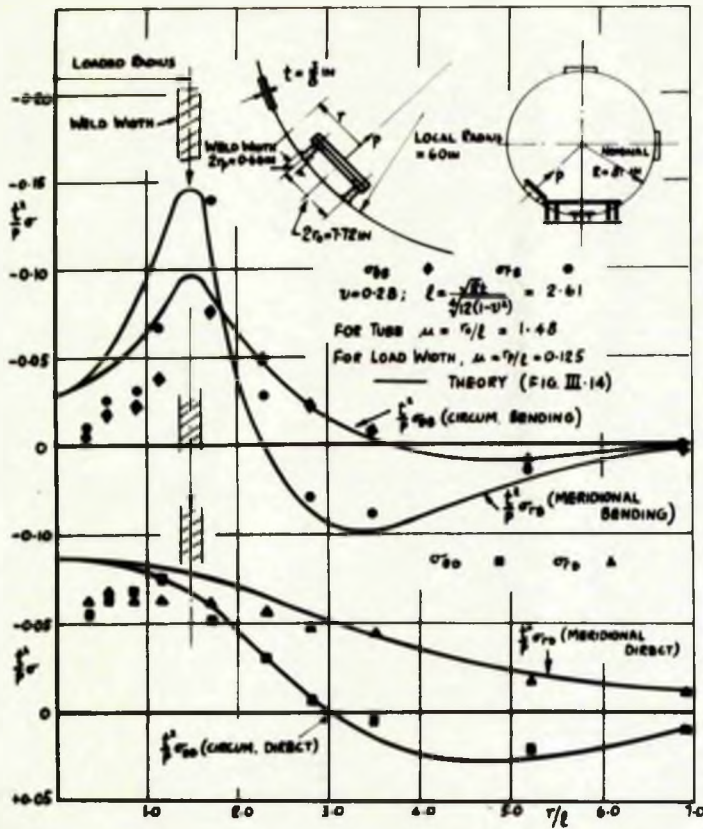
FIG.V.15a DIRECT STRESS AND BENDING STRESS ON THE OUTER SURFACE OF A COMPLETE SPHERE $\mu = 1.48$

FIG.V.15b DIRECT STRESS AND BENDING STRESS ON THE OUTER SURFACE OF A COMPLETE SPHERE, $\mu = 2.20$
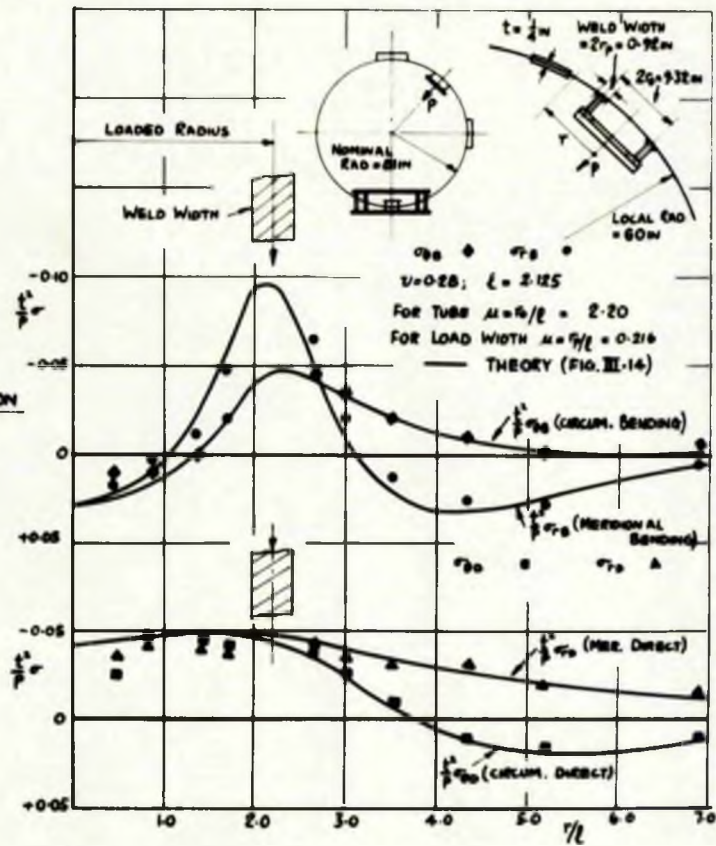
FIG.V.15 DIRECT STRESS AND BENDING STRESS ON THE OUTER SURFACE OF A COMPLETE SPHERE DUE TO A RADIAL LOAD P TRANSMITTED BY A RIGIDLY FIXED RING ($\mu = 1.48$ AND 2.20) - A COMPARISON BETWEEN THE INFLUENCE LINE METHOD AND EXPERIMENT
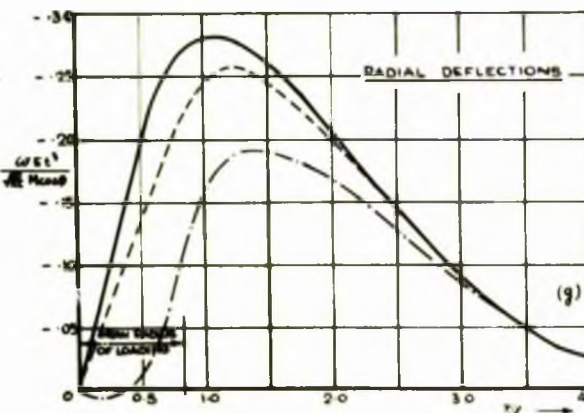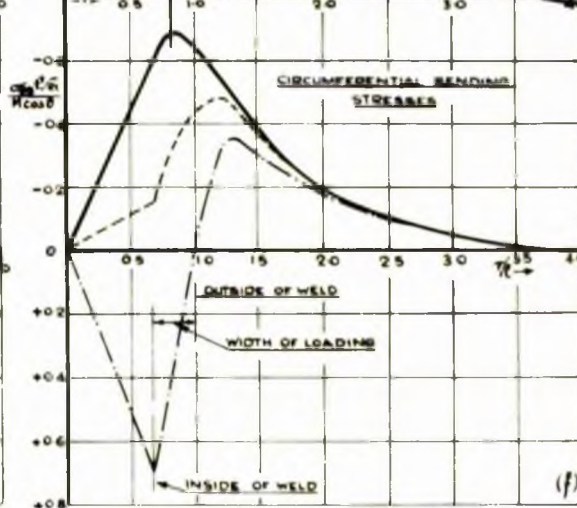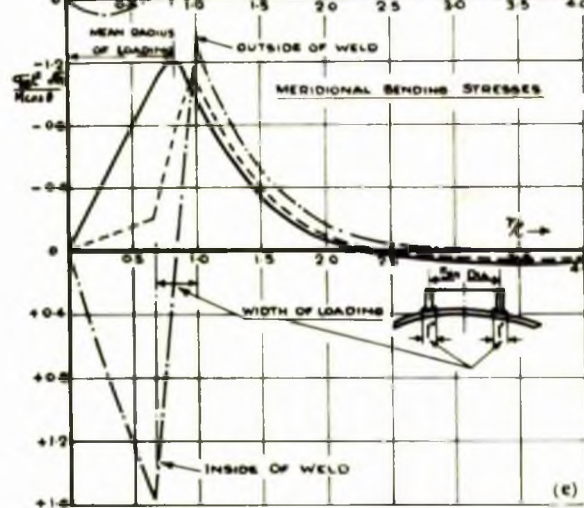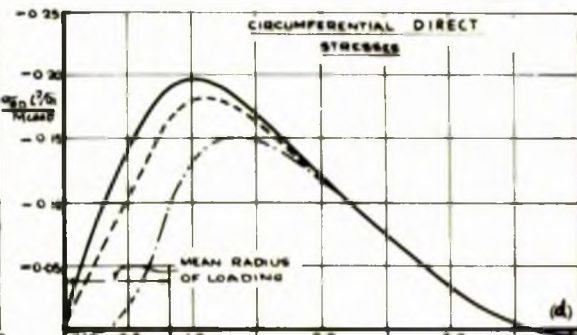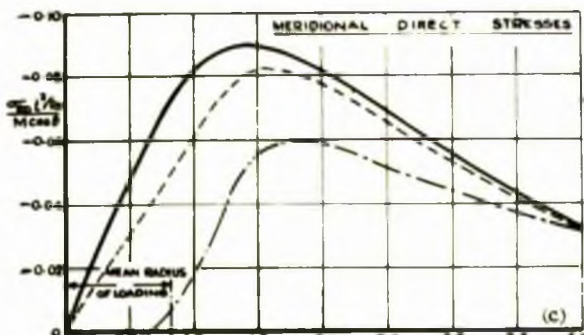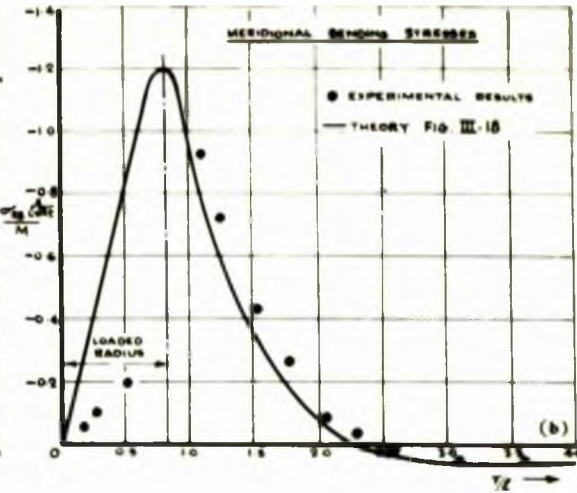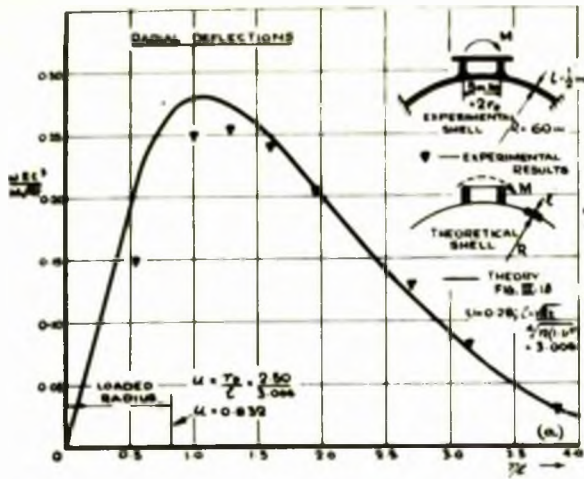
FIG. V.16 THE APPLICATION OF A BENDING MOMENT TO A SHALLOW SPHERICAL SHELL VIA A WELDED RING OF μ=0.832 AND LOAD PATH WIDTH μ=0.17. A THEORY COMBINING RADIAL LOAD AND RADIAL MOMENT TRANSMISSION OF THE BENDING MOMENT
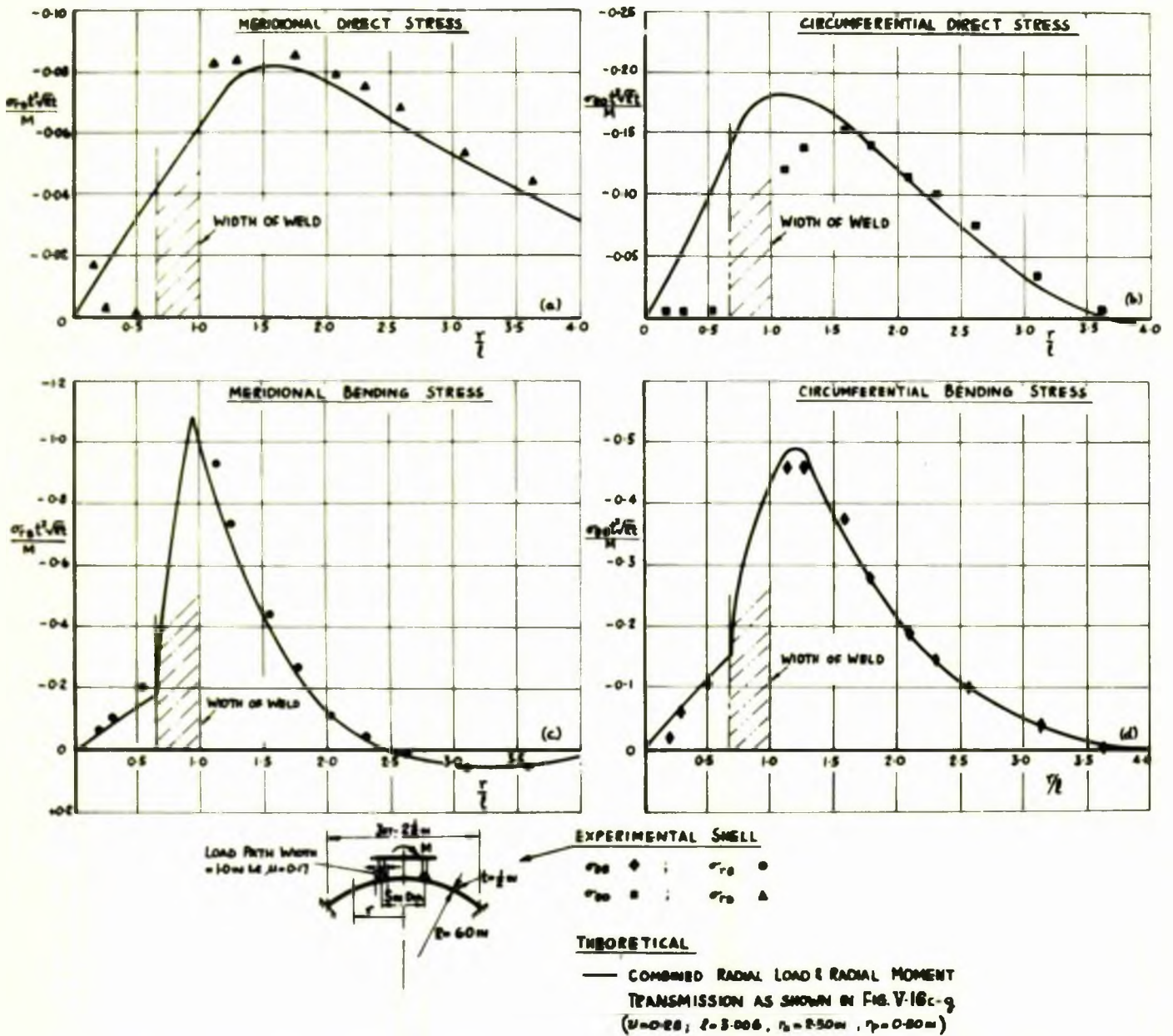
FIG. V.17 DIRECT STRESS AND BENDING STRESS ON THE OUTER SURFACE OF A SHALLOW SPHERICAL SHELL DUE TO A BENDING MOMENT APPLIED VIA A WELDED RING OF $\mu = 0.832$ AND LOAD PATH WIDTH $\mu = 0.17$ — A COMPARISON BETWEEN THE INFLUENCE LINE METHOD AND EXPERIMENT

stresses shown in Fig.V.16b exhibit similar characteristics,
the deviation from the values predicted by the theory being
clearly defined.

It was, therefore, proposed to superpose the effects of
the moment transmission by radial load and by radial moment.
The effects of the tangential load at the ring/shell junction
are neglected since they are considered of small magnitude.
The individual actions are those analysed by the Influence Line
Method and presented in Chapter III.   That of the moment trans-
mission by a varying radial load is given in section III.2 and
presented graphically for the particular ring/sphere under test
in Fig. III.18, while that of the varying radial moment is given
in section III.3 and Fig.III.22.   These curves are also shown in
Fig. V.16c-g.

The actions were then combined, using a semi-empirical
analysis, in proportion appropriate to the experimentally measured
radial deflection distribution.   The combined curves so derived
for the bending and direct stresses are shown in Fig.V.16c-g.
They are then compared with the experimental results and shown in
Fig.V.17.

It is noted that the experimental bending stresses show good
agreement with the derived curves though the direct stresses show
a certain amount of scatter in the region of the load ring. This
is probably due to the lack of consideration given to the tangential
load, which if of significant value would influence the direct
actions to a greater extent than the bending actions.

V.3.3   RING TWISTING MOMENT - Shallow Shell (Fig.V.18)

The theoretical solutions of this case by the Influence
Line Method are presented in Chapter III, sections III.4 and
III.5, where these have been obtained by two different methods
of load transference.   Fig.V.18 presents the results where the
theoretical line is drawn through the individual theoretical
points.   The experimental points for this case are also shown
in Fig.V.18 where the agreement with the theory is seen to be
excellent.

FIG. V. 18a SHEAR STRESS DUE TO A 'TWISTING' MOMENT (INCH UNITS)

FIG.V.18b TANGENTIAL DISPLACEMENT DUE TO A 'TWISTING' MOMENT (INCH UNITS)

FIG.V.18 SHEAR STRESS AND TANGENTIAL DISPLACEMENT OF A SHALLOW SPHERICAL
SHELL DUE TO A 'TWISTING' MOMENT APPLIED VIA A WELDED RING – A COMPARISON
BETWEEN THE INFLUENCE LINE METHOD AND EXPERIMENT

CHAPTER VI.   SUMMARY AND CONCLUSIONS

CHAPTER VI.   SUMMARY AND CONCLUSIONS

VI.1   BASIC ACTIONS - Comparison of Theoretical Analyses

VI.2   BASIC ACTIONS - Comparison of Experimental and
                         Theoretical Results

VI.3   DESIGN APPLICATION - Influence Line Method

VI.1   BASIC ACTIONS - Comparison of Theoretical Analyses

The theoretical analyses of the 'basic' load actions of
radial and tangential load, bending and twisting moments on
a spherical shell are presented in the thesis. These are
obtained firstly, by using the governing shallow shell equations,
which incorporate the membrane stress function F, and secondly,
by a general shell approach. The stress and displacement
results, for the basic actions, obtained by these two analyses
are compared.

It is concluded for the range of shells considered that:-

(1) Radial loading applied via a rigid insert

The 'shallow' shell theory predicts results in agreement
with the 'general' shell approach for all values of μ.

(2) Radial loading concentrated at the crown

Neglecting second order terms in R and ℓ the stress and
radial deflection equations obtained by the 'general' shell
theory reduce to those obtained by the 'shallow' shell theory.
This is permissible for all values of r, excepting those values
extremely close to the crown.

At the crown the 'general' shell approach and also the
'shallow' shell theory, developed for the rigid insert case,
predict infinite values for the direct stress terms $\sigma_{r,o}$ and $\sigma_{\theta,o}$.
Against this, the 'shallow' shell theory applied to the case
of a continuous shell results in finite values of $\sigma_{r,o}$ and $\sigma_{\theta,o}$
due to the imposed boundary conditions at r =   0.

From a practical point of view the finite values of $\sigma_{r,o}$
and $\sigma_{\theta,o}$ are the ones considered acceptable.

It is of interest to note that FLÜGGE[5] avoids this infinity condition, for these stresses, in the 'general' shell approach by putting $\nu = 0$.

(3) Bending moment applied via a rigid insert

The direct stresses obtained from the 'shallow' shell and the 'general' shell analyses are in agreement for all values of μ.   The bending stresses also agree, apart from their values in the immediate vicinity of the insert.

This divergence in the bending stress values given by the two analyses is of significance for the smaller R/t ratio shells in cases where the μ value is also small.   For example when R/t = 60 and μ = 0.1, the value of the maximum meridional moment, M_{rr} , (which occurs at the insert) as predicted by the 'general' shell theory is 1.43 times that given by the 'shallow' shell, thereas when R/t = 240 and μ = 0.2 the corresponding ratio is only 1.04.   In this respect the 'shallow' shell theory oversimplifies the problem by neglecting consideration of moment terms arising from the mid-surface displacements and, in con- sequence, underestimates bending stress values in this region.

(4) Twisting moment applied via a rigid insert

Both theories produce identical results for this case.

(5) Tangential load applied via a rigid insert.

The results obtained for the 'general' and 'shallow' shell treatments are similar in form.   Good agreement of stress values obtain in the regions near the crown where the stresses are of significant magnitude.

Deviations are shown in the stress values given by the two

theories at points far from the crown.   These, however, are
not considered significant from a practical point of view
since the stress magnitudes in these regions are in themselves
small, of the order of 10% of the maximum stress value.

In the foregoing it is clearly seen that the 'shallow'
shell theory provides a rational and acceptable method of
analysis for evaluating the effects of basic actions, with the
exception stated in (3).

VI.2   BASIC ACTIONS - Comparison of Experimental and Theoretical Results

The comparison between theory and the range of experiments
performed for all the four basic actions (radial and tangential
load, bending and twisting moments) indicate significantly good
agreement and substantiate in every respect the analytical
results derived on the basis of the 'shallow' shell theory.

Small deviations which obtained in a few cases were due
to difference between the theoretical and experimental models.
These were the difficulty of obtaining the boundary condition
$\varepsilon_\theta = 0$ at the periphery of the rigid insert and the unavoidable
transmission by a combination of bearing and tractive forces of
the tangential load when applied to the shallow shell by a welded
stud insert.

It is of interest to note that the existance of a finite
boundary in the experimental shallow shell models did not intro-
duce any detectable deviation from the theoretically predicted
values.

VI.3   DESIGN APPLICATION – Influence Line Method

An application of the theoretically derived and experimentally substantiated basic actions is presented in the form of an Influence Line Concept capable of yielding solutions to a wide variety of complex load cases including those not otherwise amenable to analysis.

To provide a form of theoretical substantiation of the Influence Line Method a number of cases capable of solution by conventional analytical means and involving all the types of load actions considered, were selected for examination.

In every case the Influence Line and conventional analytical solutions show excellent agreement.

In a similar manner experimental substantiation was obtained through performing tests on the variety of load cases presented in the thesis.   These confirmed (1) that for the purposes of design analysis, the 'die-out' distance may be considered as defining the significant shallow cap, and (2) all basic actions for this shallow cap may be superposed to yield results for the many unsymmetrical load cases characteristic of practical shell analysis.

CHAPTER VII   BIBLIOGRAPHY AND AUTHOR INDEX

BIBLIOGRAPHY

1. ARON, H. 'Das Gleichgewicht und die Bewegung einer
      unendlich dünnen beliebig gekrümmten elasticshen
      Schale.' Jn für die reine und angewandte Math
      (Crelle). Vol. 78, 1874.

2. LOVE, A. E. H. 'The Small Free Vibrations and
      Deformation of a Thin Elastic Shell.' Phil. Trans.
      Roy. Soc. Lond(A). 491-546, 1888.

3. LOVE, A. E. H. 'The Mathematical Theory of Elasticity.'
      4th Edition, Cambridge, 1952. Chapter 24.

4. NOVOZHILOV, V. V. 'The Theory of Thin Shells.'
      P. Noordhoff Ltd., Groningen 1959.

5. FLÜGGE, W. 'Stresses in Shells'. Springer-Verlag.
      Berlin 1960.

6. HAVERS, A. 'Asymptotische Biegetheorie der unbelasteten
      Kugelschale.' Ingenieur - Archiv Vol. 6, 1935
      pp. 282-312.

7. BIEZENO, B. & GRAMMEL, R. 'Engineering Dynamics' Vol. II -
      'Elastic Problems of Single Machine Elements', trans-
      lated by M. L. MEYER. Blackie & Son, Ltd., 1956.
      Part III p. 322.

8. BYRNE, R. 'Theory of Small Deformation of a Thin Elastic
      Shell.' Seminar Reports in Mathematics (Los Angeles),
      University of California, Pub. in Math., N.S. Vol. 2,
      no. 1, 1944. pp. 103-152.

9. BASSET, A. B. 'On the Extension and Flexure of Cylind-
      rical and Spherical Thin Elastic Shells.' Phil. Trans.
      Roy. Soc. Lond(A), Vol. 181, 1890. pp. 433-480.

10. HILDEBRAND, F. B., REISSNER, E. & THOMAS, G. B. 'Notes on
      the Foundation of the Theory of Small Displacements of
      Orthotropic Shells.' N.A.C.A. T.N. 1833, March 1949.

11. KENNARD, E. H. 'The New Approach to Shell Theory: Circular
      Cylinders.' Jn. App. Mech. Vol. 20, 1953. pp. 33-40.

12. KENNARD, E. H. 'Cylindrical Shells: Energy, Equilibrium,
      Addenda and Erratum.' Jn. App. Mech. Vol. 22, 1955
      pp. 111-116.

13. EPSTEIN, P. S. 'On the Theory of Elastic Vibrations in
      Plates and Shells.' Jn. Math. & Phys. Vol. 21, 1942
      p. 198.

14. VLASOV, V. S. 'Basic Differential Equations in General
     Theory of Elastic Shells.' Translated from Russian,
     N.A.C.A. Tech. Mem. 1241. Feb. 1951.

15. GALERKIN, B. G. 'Equilibrium of Elastic Cylindrical Shells.'
     Lenin Inst. Sooruzhenii, Trudy 1935, and also 'Stability
     of Cylindrical Shells.' Prikl. Mat. Mek., Vol. 7 No.2
     1943. pp.49-56.

16. REISSNER, E. 'Stress-Strain Relations in the Theory of
     Thin Elastic Shells.' Jn. Math. Phys. Vol. 31 1952.
     pp. 109-119.

17. REISSNER, E. 'On a Variational Theorem in Elasticity.'
     Jn. Math. Phys. Vol. 29,1950. pp. 90-95.

18. NAGHDI, P. M. 'On the Theory of Thin Elastic Shells.'
     Quat. App. Math. Vol. 14, 1956. pp. 369-380.

19. KOITER, W. T. 'A Consistent First Approximation in the
     General Theory of Thin Elastic Shells.' Proc. Sym.
     on 'The Theory of Thin Elastic Shells.' I.U.T.A.M.
     Delft, August 1959.

20. REISSNER, H. 'Spannungen in Kugelschalen' (Kuppeln).
     Festschrift Mueller-Breslau, 1912. pp. 181-193.

21. MEISSNER, E. 'Das Elastizitätsgesetz für dünne Schalen
     von Ring flächen, Kugel-und Kegelform.' Physik.
     Zeitschr., Vol. 14, 1913. English Trans. 238
     D.T.M.B. 1951.

22. MEISSNER, E. 'Über Elastizität und Festigkeit dünner
     Schalen.' Vierteljahrsschrift der Naturforschenden
     Gesellschaft in Zürich. Vol. 60, 1915. pp. 23-47.

23. BOLLE, L. 'Festigkeitsberechnung van Kugelschalen.'
     Schweizerische Bauzeitung. Vol. 66 No. 9, 1915
     pp. 105-108 and Vol. 66 No. 10, 1915, pp. 111-113.

24. TIMOSHENKO, S. & WOINOWSKY-KRIEGER, S. 'Theory of Plates
     and Shells.' McGraw-Hill, 1959.

25. EKSTRÖM, J. E. 'Studien über dünne Schalen von rotations-
     symmetrischer Form und Belastung mit konstanter oder
     veränderlicher Wand stärke.' Ing. Vetenskaps. Akad.,
     Pamphlet No. 121, 1933.

26. BLUMENTHAL, O. 'Über Asymptotische Integration von
     Differential-Gleichungen mit Anwendung auf die Berech-
     nung von Spannungen in Kugelschalen.' 5th Inter. Congr
     Math. 1912. Proc. Vol. 2, pp. 319-327.

27. GECKELER, J. W.   'Über die Festigkeit Achsensymmetrischer
         Schalen.' Forschungsarbeiten. Ing. Wes. Vol. 276,
         1926. pp. 1-52.

28. HETÉNYI, M. 'Spherical Shells subjected to Axial Symmetrical
         Bending.'   International Ass. for Bridge and Structural
         Engineering, Publication 5, Zürich, 1938. pp. 173-185.

29. HETÉNYI, M. 'Beams on Elastic Foundations.' University of
         Michigan Studies. Vol. 16.

30. GECKELER, J. W. 'Zur Theorie der Elastizität flacher
         rotationsymmetrischer Schalen.' Ing. Arch. Vol. 1,
         1930. pp. 255-270.

31. SCHLEICHER, F. 'Kreisplatten auf elastischer Unterlage.'
         Berlin 1926.

32. ESSLINGER, M. 'Statische Berechnung von Kesselböden'.
         Springer, Berlin. 1952. English Translation by Oak
         Ridge Nat. Lab. 56-12-37.

33. PENNY, R. K. 'Stress Concentrations at the Junction of a
         Spherical Pressure Vessel and Cylindrical Duct caused
         by certain Axisymmetric Loadings.' Nucl. Reactor Cont.
         Bldg. & Press. Vessels Symp. 1960. Butterworths,
         London. pp. 347-368.

34. LECKIE, F. A. 'Asymptotic Solutions for the Spherical
         Shell subjected to axially symmetrical Loading.'
         Nucl. Reactor Cont. Bldg. & Press. Vessels Symp. 1960
         Butterworths, London. pp. 286-297.

35. HILDEBRAND, F. B. 'An Asymptotic Integration in Shell
         Theory.'   Proc. of Symposia in App. Maths. Vol. 3,
         1950, pp. 53-66.

36. LANGER, R. E. 'On the Asymptotic Solutions of Ordinary
         Differential Equations with reference to the Stokes'
         Phenomenon about a Singular Point.'   Trans. Amer.
         Math. Soc., Vol. 37, 1935. pp. 397-416.

37. GALLETLY, G. D. 'Ring Loads on Spherical Shells.' - to
         be published.

38. McLACHLAN, N. W. 'Bessel Functions for Engineers.' 2nd
         Edition, Oxford. 1955.

39. LECKIE, F. A. 'Localized Loads Applied to Spherical Shells.'
         Jn. Mech. Eng. Science Vol. 3 No. 2, 1961. pp. 111-118.

40. GALLETLY, G. D. 'Torispherical Shells - A Caution to Designers'. A.S.M.E. Jn. Eng. for Industry, Vol. 81 series B No.1. Feb. 1959, pp. 51-62.

41. GALLETLY, G. D. & RADOK, J. R. M. 'On the Accuracy of Some Shell Solutions'. Paper No. 59-APM-30, Trans. A.S.M.E., Series E, Jn. Appl. Mech., Vol. 81, 1959. pp. 577-583.

42. SCHWERIN, E. 'Über Spannungen in Symmetrisch und unsymmetrisch belasteten Kugelschalen (Kuppeln).' Armierter Beton, Vol. 12, 1919. pp. 25-37, 54-63, 81-88.

43. REISSNER, E. 'Stresses and Small Displacements of Shallow Spherical Shells.' Amer. Jn. Math. Phys. Vol. 25, 1946, pp. 80-85 and 279-300.

44. NAGHDI, P. M. & De SILVA, C. N. 'Deformation of Elastic Ellipsoidal Shells of Revolution.' Proc. 2nd U.S. National Congress Appl. Mech. A.S.M.E. 1955. pp. 333-343.

45. VAN DER NEUT, H. 'De Elastische Stabiliteit van den Dunwandigen Bol.' Diss. Delft 1932.

46. FLÜGGE, W. & LECKIE, F. A. 'Bending Theory for Shells of Revolution subjected to Non-symmetric Edge Loads.' Tech. Report No. 113, Div. of Eng. Mech., Stanford Univ. Nov. 1957.

47. LECKIE, F. A. & PENNY, R. K. 'A Critical Study of the Solution for the Asymmetric Bending of Spherical Shells, submitted for presentation at the World Conference on Shell Structures. California, U.S.A. 1962.

48. AAS JAKOBSEN, A. 'Beitrag zur Theorie der Kugelschale auf Einzelstutzen.' Ingen.-Archiv, Vol. 8, 1937. pp. 275-300.

49. PASTERNAK, P. 'Die praktische Berechnung biegefester Kugelschalen, Kreisrunder Fundamentplatten auf elastischer Bettung und Kreiszylindrischer Wandungen in gegenseitiger monolither Verbindung.' Zeit. für Angewandte Math. und Mech. Vol. 6, 1926. pp. 1-28.

50. PENNY, R. K. 'Symmetric Bending of the General Shell of Revolution by Finite Difference Methods.' Jn. Mech. Eng. Science Vol. 3 No. 4, 1961. pp. 369-377.

51. GALLETLY, G. D. 'Edge Influence Coefficients for Toroidal Shells of Negative or Positive Gaussian Curvature.' 59-PAT-3, 59-PAT-2. Trans. A.S.M.E. Vol. 82, Series B No. 1, Feb. 1960, pp. 60-68, 69-75.

52.   LE COCQ, J. R.   Discussion Contribution to Sym.   Nuc.
        Rea. Cont. Bldg., and Press. Vessels, 1960.   Butterworths
        London.   pp. 327-334.

53.   BERMAN, F. R.   'Analysis of Shallow Spherical Domes.'
        D. Sc. Thesis Massachusetts Institute of Technology,
        1946.

54.   BIJLAARD, P. P.   'On the Stresses from Local Loads in
        Spherical Pressure Vessels or Pressure Vessel Heads.'
        Bulletin No. 34.   Welding Research Council July 1956.

55.   VLASOV, V. S.   'General Theory of Shells.'   Chapter 9.
        1949, translated by M. D. Friedman.

56.   CHINN, J.   'Influence Charts for Deflections and Stresses
        in Spherical Shells.'   Ph. D. Thesis Cornell Univ.
        1958.

57.   REISSNER, E.   'On the Determination of Stresses and Dis-
        placements for Unsymmetrical Deformation of Shallow
        Spherical Shells.'   Jn. Maths. & Physics, Vol. 38,
        No. 1, April 1959. pp. 16-35.

58.   HICKS, R.   'Theoretical Analysis of the Stress induced in
        a Spherical Vessel due to the Constraining Effect of
        a Cylindrical Skirt.'   Proc. Inst. Mech. Engrs.
        Vol. 172, No. 21, 1958.   Contribution to the discus-
        sion by R. M. KENEDI and A. S. TOOTH.   pp. 721-723.

59.   TOOTH, A. S., KENEDI, R. M. & HOSSACK, J. D. W.   'The use
        of Semi-graphical Methods in the Stress Deformation
        Analysis of Shell Forms.'   Struct. Engr. Vol. 38,
        No. 4, 1960.   pp. 129-137.

60.   KENEDI, R. M.   'The Influence Line Method of Shell Analysis.'
        Sym. on Nuc. Rea. Cont. Bldg. and Press. Vessels.
        Butterworths, London, 1960.   pp. 164-173.

61.   TOOTH, A. S., & KENEDI, R. M.   'The Influence Line Tech-
        nique of Shell Analysis.'   Inter. Coll. on Simplified
        Calculation Methods (organised by I.A.S.S. and A.B.E.M.
        Brussels), Sept. 1961.

62.   BAILEY, R. W. & HICKS, R.   'Stress Analysis Problems
        Associated with the Design of Reactor Pressure Vessels.'
        Sym. on Nuc. Rea. Cont. Bldgs. and Press. Vessels.
        Butterworths, London, 1960.   pp. 134-149.

63.   BACH, C.   'Untersuchung über die Formanderungen und die
        Anstrengung flacher umgekrempter Kesselböden.' Zeit
        V.D.I. Vol. 4, 1897.   p. 1157.

64. BACH, C. 'Anstrengung gewölbter Böden.' Zeit. V.D.I.
         Vol. 43, 1899. pp. 1585-1594.

65. DIEGEL, B. 'Beanspruchung des Materials geschweisster
         Zylindrischer Druckgesässe für Gase und Flüssigkeiten
         mit nach aussen gewölbten Böden durch inneren Druck.'
         Zeit. des Vereines deutscher Ingenieure Vol. 64 No. 7,
         1920. pp. 157-161.

66. SIEBEL, E. & KÖRBER, F. 'Versuche über die Anstrengung und
         die Formänderungen gewölbter Kesselböden mit und ohne
         Mannloch bei der Beanspruchung durch inneren Druck.'
         Mitteilungen aus dem Kaiser-Wilhelm Institut für
         Eisenforschung Düsseldorf. Vol. 7 No. 10, 1925.
         pp. 113-177 & Vol.8 No. 1. pp. 1-51.

67. KORBER, F. & SIEBEL, E. 'Modellversuche an Kesselböden
         mit Böhrungen und Mannlöchern.' Mitt. aus dem Kaiser-
         Wilhelm Institut für Eisenforschung, Vol. 9 No. 2, 1927.
         pp. 13-32.

68. HÖHN, E. 'Der Spannungszustand gewölbter Böden.' Zeit. des
         Vereines deutscher Ingenieure, Vol. 69 No. 6, 1925.
         pp. 155-158.

69. HÖHN, E. 'The Strength of Dished Ends.' Engineering
         Vol. 128, July 1929. Editorial comment pp. 1-4, and
         Engineering Vol. 129, Feb. 1930, pp. 190-191.

70. GECKELER, J. 'Über die Festigkeit Achsensymmetrischer
         Schalen.' Forschungsarbeiten auf dem Gebiete des
         Ingenieur-wesens, Vol. 276, 1926. pp. 1-52.

71. TAYLOR, J. H. & WATERS, E. O. 'Effect of Openings in
         Pressure Vessels.' Trans. A.S.M.E. Vol. 56, No. 3
         1934. pp. 119-140.

72. SIEBEL, E. & SCHWAIGERER, S. 'Neuere Untersuchungen an
         Dampf-kesselteilen und Behaltern.' Ver. Deutsch Ing.-
         Forschungsheft Vol. 400, 1940. pp. 1-18.

73. ROARK, R. J. 'The Strength and Stiffness of Cylindrical
         Shells under Concentrated Loading.' Trans. A.S.M.E.
         Vol. 57, 1935, Jn. App. Mech. pp. A147-152.

74. COOPER, G. K. & SMITH, L.W. 'Purdue University Project
         Design Devision, Pressure Vessel Research Committee.'
         Final Report Aug. 1952.

75. CARLSON, W. B. & McKEAN, J. D. 'Cylindrical Pressure
         Vessels: Stress Systems in Plain Cylindrical Shells
         and in plain and pierced drumheads.' Trans. Inst. Mech.
         Eng. Vol. 169, 1955. pp. 269-293.

76.   LANE, P. H. R. & WELLS, A. A.   'The Strength of Manholes in
         Welded Storage Tanks.'   British Welding Jn. Sept. 1956.
         pp. 414-425.

77.   B.W.R.A.   'Experimental and Analytical Determinations of the
         Stress Systems in a welded Pressure Vessel.' - report
         carried out during 1946-47 by Messrs. Babcock and Wilcox,
         Ltd. for the British Welding Research Ass. - pub. 1952.

78.   WELLS, A. A., LANE, P. H. R. & ROSE, R. T.   'Stress Analysis
         of Nozzles in Cylindrical Pressure Vessels.'   Symp. on
         Pressure Vessel Research towards Better Design.   Inst.
         of Mech. Eng. Paper No. 2, Jan. 1961.   pp. 21-44.

79.   ROSE, R. T. & OTHERS.   'Stresses at Oblique Nozzles in
         Spherical Pressure Vessels, Part I-V.'   Symp. on
         Pressure Vessel Research towards Better Design.   Inst.
         of Mech. Eng. Paper No. 3, Jan. 1961.   pp. 45-70.

80.   CORNISH, G. H.   Discussion Contribution to CRANCH and
         DALLY's paper ref. 85 in Sym. on Nuc. Rea. Cont. Bldgs.
         and Press. Vessels.   Butterworths, London, May 1960.
         pp. 317-320.

81.   HARDENBERGH, D.E.   'Stresses at Nozzle Connections of
         Pressure Vessels.'   Proc. S.E.S.A. Vol. 18 No. 1, 1961.
         pp. 152-158.

82.   TAYLOR, C. E. & SCHWEIKER, J. W.   'A Three-Dimensional
         Photoelastic Investigation of the Stresses near a rein-
         forced Opening in a Reactor Pressure Vessel.'   Proc.
         S.E.S.A. Vol. 17 No. 1, 1959, pp. 25-36.

83.   SCHOESSOW, G. J. & KOOISTRA, L. F.   'Stresses in a Cylin-
         drical Shell due to Nozzle or Pipe Connections.'   Trans.
         A.S.M.E. 1945.   Jn. of App. Mech. Vol. 12 No. 2.
         pp. A107-112.

84.   MEHRINGER, F. J. & COOPER, W. E.   'Experimental Determination
         of Stresses in the Vicinity of Pipe Appendages to a
         Cylindrical Shell.'   Proc. S.E.S.A. Vol. 14 No. 2, 1957.
         pp. 159-174.

85.   CRANCH, E. T. & DALLY, J. W.   'An Experimental Study of
         Attachments to Cylindrical and Shallow Spherical Shells.'
         Sym. on Nuc. Rea. Cont. Bldgs. and Press. Vessels.
         Butterworths, London, 1960.   pp. 221-256.

86.   CRANCH, E. T.   'An Experimental Investigation of Stresses
         in the Neighbourhood of Attachments to a Cylindrical
         Head.'   Welding Research Coun. Bulletin No. 60. 1960.

87. LEVEN, M. M. & SAMPSON, R. C.   'Photoelastic Stress and Deformation Analysis of Nuclear Reactor Components.' Proc. S.E.S.A. Vol. 17 No. 1. 1959. pp. 161-180.

88. LAWTON, C. W. 'Strain Gauge Test on Model Vessels for Nuclear Power Plant Design.'   Proc. S.E.S.A. Vol. 17 No. 1, 1959. pp. 149-160.

89. DURELLI, A. J., DALLY, J. W. & MORSE, S.   'Experimental Study of Large Diameter Thin-Walled Pressure Vessels.' Proc. S.E.S.A. Vol. 18 No. 1, 1961. pp. 33-42.

90. DALLY, J. W. & DURELLI, A. J.   'Stress Analysis of a Reactor Head Closure.'   Proc. S.E.S.A. Vol. 17 No. 2, 1960. pp. 71-86.

91. ZICK, L. P. & CARLSON, C.E.   'Vacuum Test of Sphere to Failure.'   Water Tower Vol. 34 No. 11, 1947. pp. 6-7.

92. ZICK, L. P. & CARLSON, C. E. 'Stress Analysis of a Horton-sphere - Strain Gauge Survey around the Supports of a 48 foot Diameter Hortonsphere.'   Welding Jn. Research Suppl. Vol. 14 No. 5, 1949. pp. 205-214.

93. ZICK, L. P. 'Stresses in Large Horizontal Cylindrical Pressure Vessels on Two Saddle Supports.' Welding Jn. Research Suppl. Vol. 16 No. 9, 1951. pp. 435-445.

94. MARIN, J., DUTTON, V. L. & FAUPEL, J. H.   'Tests on Spherical Shells in the Plastic Range.'   Jn. Am. Welding Soc. (later called Welding Jn), Welding Research Suppl. Vol. 27 No. 12. 1948. pp. 593-607.

95. BREWER, G. 'Electric Strain Gauge Analysis of a 50 ft. Hortonsphere.' Proc. S.E.S.A. Vol. 5, No. 2. 1948. pp. 88-94.

96. WILSON, W. M. & MARIN, J. 'Tests of Thin Hemispherical Shells subjected to Internal Hydro-static Pressure.' University of Illinois Bulletin No. 295. Vol. 34, No. 75. 1937.

97. DUNCAN, J. P. & MURRAY, N. W. 'Lobed Pressure Vessels.' Sym. on Pressure Vessel Research towards Better Design. Inst. Mech. Eng. Paper No. 6, 1961. pp. 107-114.

98. HOUGHTON, D. S. 'Discontinuity Problems in Shell Structures Sym. Nuc. Rea. Cont. Bldgs. & Press. Vessels. Butterworths, London, 1960. pp. 191-220.

99. CARR, J. H. 'Stress Distribution in Hemispherical Shells.' Note 135. U.S. Naval Ordnance Test Station, Navard Report 1018, 1948.

(VII.1)

100. VOSS, W. C., PEABODY, D., STALEY, H. R. & DIETZ, A. G. H.
'Thin-Shelled Domes Loaded Eccentrically.' Proc.
A.S.C.E. Vol. 73, 1947. pp. 1173-1195.

101. TOOTH, A. S. 'An Experimental Investigation of the
Behaviour of Shallow Spherical Domes.' Sym. on Nuc.
Rea. Cont. Bldgs. & Press. Vessels, Butterworths,
London, 1960. pp. 298-315.

102. TOOTH, A. S. Communication to Symposium on Pressure
Vessel Research towards Better Design. Inst. Mech.
Eng. 1961 - p.p. 148-150.

103. TOOTH, A.S. Communication in Jn. of Mech. Engin. Science
Vol. 4 No. 1, 1962. pp. 99-101, relating to
F. A. LECKIE's paper, ref. 39.

104. TIMOSHENKO, S., & GOODIER, J. N. 'Theory of Elasticity.'
McGraw-Hill, New York. 2nd Edition, 1951.

105. BRITISH ASSOCIATION FOR THE ADVANCEMENT OF SCIENCE.
'The Calculation of Methematical Tables'.
1916. pp.59-126.

106. TÖLKE, F. 'Besselsche und Hankelsche, Zylinder-
funktionen nulter bis dritter Ordnung vom Argument
$r\sqrt{i}$'. Stuttgart Wittwer 1936.

107. DWIGHT, H.B. 'A Precise Method of Calculation of Skin
Effect in Isolated Tubes'. Jn. Amer. Inst. Elect.
Engs. vol. 42 No.1, 1923. pp.827-831. (p.830 gives
the Kelvin Functions).

108. TOOTH, A. S. Discussion Contribution to the Symposium
on Nuclear Reactor Cont. Bldgs. and Press. Vessels.
R.C.S.T., Glasgow. Butterworth, 1960. pp.340-343.

VII.2   AUTHOR INDEX

Name		Reference No.	Page No.
AAS JAKOBSEN,	A.	48	50
ARON,	H.	1	3, 5
BRITISH ASSOCIATION		105	259
BACH,	C.	63, 64	63
BAILEY,	R.W.	62	61
BASSET,	A.B.	9	19
BERMAN,	F.R.	53	58, 81
BEWER,	G.	95	65
BIEZEND,	B.	7	18
BIJLAARD,	P.P.	54	58, 59, 76
BLUMENTHAL,	O.	26	30, 34, 38, 46
BOLLE,	L.	23	33
B.W.R.A.		77	64
BYRNE,	R.	8	18, 20, 22
CARLSON,	C.E.	91, 92	65
CARLSON,	W.B.	75	64
CARR,	J.H.	99	65
CHINN,	J.	56	60, 61, 145, 148, 151, 152, 154
COOPER,	G.K.	74	64
COOPER,	W.E.	84	64
CORNISH,	G.H.	80	64
CRANCH,	E.T.	85, 86	64
DALLY,	J.W.	85, 89, 90	64, 65
DE SILVA,	C.N.	44	43

Name		Reference No.	Page No.
KENNARD,	E.H.	11, 12	20
KOITER,	W.T.	19	24
KOOISTRA,	L.F.	83	64
KÖRBER,	F.	66, 67	63
LANE,	P.H.R.	76, 78	64
LANGER,	R.E.	36	38
LAWTON,	C.W.	88	65
LECKIE,	F.A.	34, 39, 46, 47.	38, 41, 46, 48 50, 61, 73, 76, 113, 124
LE COCQ,	J.R.	52	52
LEVEN,	M.M.	87	65
LOVE,	A.E.H.	2, 3	3, 5, 11, 15, 18, 22, 25, 26, 72
MARIN,	J.	94, 95	65
McKEAN,	J.D.	75	64
McLACHLAN,	N.W.	38	41, 91, 142
MEHRINGER,	F.J.	84	64
MEISSNER,	E.	21, 22	30, 31, 32, 42
MORSE,	S.	89	65
MURRAY,	N.W.	97	65
NAGHDI,	P.M.	18, 44	23, 25, 43
NOVOZHILOV,	V.V.	4	14, 15, 33, 41, 43
PASTERNAK,	P.	49	51
PEABODY,	D.	100	66, 69
PENNY,	R.K.	33, 47, 50	38, 43, 49, 51, 61, 73

Name		Reference No.	Page No.
WELLS,	A.A.	76, 78	64
WILSON,	W.M.	96	65
WOINOWSKY-KRIEGER,	S.	24	33, 38
ZICK,	L.P.	91, 92, 93	65

Name		Reference No.	Page No.
WELLS,	A.A.	76, 78	64

CHAPTER VIII   APPENDICES

CHAPTER VIII   APPENDICES

A VERIFICATION OF THE FORM OF SOLUTION OF EQT.II.11

$$\left[\nabla^2 \nabla^2 \omega_h + \omega_h/\rho^4 = 0 \qquad (II\cdot11) \right]$$

To assist the manipulation of the Bessel and Kelvin functions the relations shown in eqt.VIII.2a-d are obtained by substituting:-

$$\omega_n = C_{1\alpha} j^{-n}[ber_n \, r/\rho + j\,bei_n \, r/\rho] + C_{2\alpha} j^n[ker_n \, r/\rho + j\,kei_n \, r/\rho] \qquad (II.17)$$

into $$\qquad \left[\nabla^2 - \left(j/\rho^2 + n^2/r^2 \right) \right] \omega_n(r) = 0 \qquad (II.13b)$$

These are as follows:-

$$C_{1\alpha} j^{-n} \left[\nabla^2 ber_n \, r/\rho - \frac{n^2}{r^2} ber_n \, r/\rho + \frac{1}{\rho^2} bei_n \, r/\rho \right]$$

$$+ C_{1\alpha} j^{-n+1} \left[\nabla^2 bei_n \, r/\rho - \frac{n^2}{r^2} bei_n \, r/\rho - \frac{1}{\rho^2} ber_n \, r/\rho \right]$$

$$+ C_{2\alpha} j^n \left[\nabla^2 ker_n \, r/\rho - \frac{n^2}{r^2} ker_n \, r/\rho + \frac{1}{\rho^2} kei_n \, r/\rho \right]$$

$$+ C_{2\alpha} j^{n+1} \left[\nabla^2 kei_n \, r/\rho - \frac{n^2}{r^2} kei_n \, r/\rho - \frac{1}{\rho^2} ker_n \, r/\rho \right] = 0 \qquad (VIII.1)$$

Thus:-
$$\nabla^2 ber_n \, r/\rho - n^2/r^2 \, ber_n \, r/\rho + 1/\rho^2 \, bei_n \, r/\rho = 0$$

$$\nabla^2 bei_n \, r/\rho - n^2/r^2 \, bei_n \, r/\rho - 1/\rho^2 \, ber_n \, r/\rho = 0$$

$$\nabla^2 ker_n \, r/\rho - n^2/r^2 \, ker_n \, r/\rho + 1/\rho^2 \, kei_n \, r/\rho = 0$$

$$\nabla^2 kei_n \, r/\rho - n^2/r^2 \, kei_n \, r/\rho - 1/\rho^2 \, ker_n \, r/\rho = 0 \qquad (VIII.2a\text{-}d)$$

Eqts.VIII.2a-d will be used in the proceeding analysis.

The solution of eqt.II.11 has been expressed in eqt.II.18 as:-

$$\omega_h = (C_{1n} ber_n \, r/\rho + C_{2n} bei_n \, r/\rho + C_{3n} ker_n \, r/\rho + C_{4n} kei_n \, r/\rho) \cos n\theta \qquad (II\cdot18)$$

Considering only the first term:- $\omega_h = C_{1n} ber_n \, r/\rho \cdot \cos n\theta$ (VIII.3)

expressions for $\nabla^2 \omega_h$ and $\nabla^2 \nabla^2 \omega_h$ can be written as follows:-

$$\nabla^2 \omega_h = C_{1n} \left(\nabla^2 ber_n \, r/\rho - n^2/r^2 \, ber_n \, r/\rho \right) \cos n\theta$$

and $$\quad \nabla^2 \nabla^2 \omega_h = C_{1n} \left[\nabla^2 \nabla^2 ber_n \, r/\rho - n^2/r^2 \, \nabla^2 ber_n \, r/\rho - \nabla^2 \left(\frac{n^2}{r^2} ber_n \, r/\rho \right) + \frac{n^4}{r^4} ber_n \, r/\rho \right] \cos n\theta$$

$$(VIII.4a,b)$$

The right hand side of eqt.VIII.4a,b can be simplified using the relationship of eqts.VIII.2

Operating on eqt.VIII.2a with ∇^2 :-

$$\nabla^2 \nabla^2 ber_n \, r/\rho - \nabla^2 \left(\frac{n^2}{r^2} ber_n \, r/\rho \right) + \frac{\nabla^2}{\rho^2} bei_n \, r/\rho = 0 \qquad (VIII.5)$$

Then substituting for $\nabla^2 bei_n \frac{r}{\ell}$ from eqt.VIII.2b and for $bei_n\frac{r}{\ell}$ from eqt.VIII.2a, eqt.VIII.5 can be written:-

$$\nabla^2\nabla^2 ber_n\tfrac{r}{\ell} - \nabla^2\left(\tfrac{n^2}{r^2} ber_n\tfrac{r}{\ell}\right) - \tfrac{n^2}{r^2}\nabla^2 ber_n\tfrac{r}{\ell} + \tfrac{n^4}{r^4} ber_n\tfrac{r}{\ell} + \tfrac{1}{\ell^4} ber_n\tfrac{r}{\ell} = 0 \qquad \text{(VIII.6}$$

Substituting eqt.VIII.6 into eqt.VIII.4a,b:-

$$\nabla^2\nabla^2 w_h = C_{1n}\left(-\tfrac{1}{\ell^4} ber_n\tfrac{r}{\ell}\right)\cos n\theta \qquad \text{(VIII.7)}$$

Substituting eqt.VIII.7 into eqt.II.11:-

$$C_{1n}\left(-\tfrac{1}{\ell^4} ber_n\tfrac{r}{\ell}\right)\cos n\theta + \tfrac{w_h}{\ell^4} = 0 \qquad \text{(VIII.8)}$$

Eqt.VIII.8 is satisfied when $w_h = C_{1n} ber_n\tfrac{r}{\ell}\cos n\theta$

Thus $w_h = C_{1n} ber_n\tfrac{r}{\ell}\cos n\theta$ is a solution of eqt.II.11.

In a similar way the terms involving bei, ker and kei maybe verified.

THE DERIVATION OF THE CHARACTERISTIC CONSTANTS

In the expressions for w and F a number of constants are introduced. These are determined by considering the boundary conditions for the various loadings.

VIII.2.1.   UNIFORMLY DISTRIBUTED RADIAL AREA LOAD ON A SHALLOW SHELL   (p.82)

(a)   Derivation of C_3, C_4, and b_o (p.84)

The two governing equations for inside the loaded area are:-

$$w_i = C_1 ber\,^r/_\ell + C_2 bei\,^r/_\ell + C_3 ker\,^r/_\ell + C_4 kei\,^r/_\ell - A_o - \frac{p_o R^2}{E t^2}$$

$$F_i = \frac{\ell^2 t E}{R}\left[-C_2 ber\,^r/_\ell + C_1 bei\,^r/_\ell - C_4 ker\,^r/_\ell + C_3 kei\,^r/_\ell\right] + b_o \ell n\,^r/_\ell - \frac{p_o R r^2}{4} \qquad (VIII.9a,b)$$

At $r = 0$
$\begin{cases} w \text{ is to be finite} \\ \int\limits_{im}^{o} (2\pi r\, Q_r) \to 0 \\ N_{rr} \text{ is to be finite} \end{cases}$ (VIII.10a-c)

At $r = 0$, $ker\,^r/_\ell \to \infty$. Thus applying eqt.VIII.10a to eqt.VIII.9a, $C_3 = 0$.   From eqt.II.5a $Q_r = -D \frac{\partial}{\partial r}\nabla^2 w$, using eqt.VIII.9a

$$2\pi r Q_r = -2\pi \frac{D}{\ell^3}(-C_1 r bei'\,^r/_\ell + C_2 r ber'\,^r/_\ell + C_4 r ker'\,^r/_\ell) \qquad (VIII.11)$$

Since at $r = 0$. $C_4 r ker'\,^r/_\ell \to -C_4$ and $bei'\,^r/_\ell$ and $ber'\,^r/_\ell = 0$, the R.H.S. of eqt.VIII.11 $\to \frac{2\pi D}{\ell^3} C_4$. Applying eqt.VIII.10b, $C_4 = 0$

The expression for N_{rr} of eqt.II.4a for this case can be written

$N_{rr} = \frac{1}{r}\frac{dF}{dr}$.   Thus from eqt.VIII.9b,   putting $C_3 = C_4 = 0$

$$N_{rr} = \left[\frac{\ell t E}{R}\left(-C_2 \frac{ber'\,^r/_\ell}{r} + C_1 \frac{bei'\,^r/_\ell}{r}\right) + b_o \frac{\ell}{r^2} - \frac{p_o R}{2}\right]$$

Applying eqt.VIII.10c , $b_o = 0$

Thus $C_3 = C_4 = b_o = 0$ (II.37a-c)

(b)   Derivation of C_6, C_7 and A_1 (p.85)

The governing equation for w, outside the loaded area is:-

$$w_o = C_6 ber\,^r/_\ell + C_7 bei\,^r/_\ell + C_8 ker\,^r/_\ell + C_9 kei\,^r/_\ell - A_1 \qquad (VIII.12)$$

At $r \to \infty$
$$\begin{cases} M_{\theta\theta} \to 0 \\ M_{rr} \to 0 \\ w \to 0 \end{cases}$$ (VIII.13a-c)

The expression for $M_{\theta\theta}$ and M_{rr} from eqts.II.4d,e are:-

$$M_{\theta\theta} = - D\left[\frac{1}{r}\frac{\partial w}{\partial r} + \upsilon\frac{\partial^2 w}{\partial r^2}\right] \quad , \quad M_{rr} = - D\left[\frac{\partial^2 w}{\partial r^2} + \frac{\upsilon}{r}\frac{\partial w}{\partial r}\right]$$

Thus from eqt.VIII.12,

$$M_{\theta\theta} = - D\left[\frac{(1-\upsilon)}{r\ell}(C_6 \, ber'\,r/\ell + C_7 \, bei'\,r/\ell + C_8 \, ker'\,r/\ell + C_9 \, kei'\,r/\ell)\right.$$

$$\left. + \frac{\upsilon}{\ell^2}(-C_6 \, bei\,r/\ell + C_7 \, ber\,r/\ell + C_9 \, ker\,r/\ell - C_8 \, kei\,r/\ell)\right]$$ (VIII.14)

$$M_{rr} = - D\left[\frac{1}{\ell^2}(-C_6 \, bei\,r/\ell + C_7 \, ber\,r/\ell + C_9 \, ker\,r/\ell - C_8 \, kei\,r/\ell)\right.$$

$$\left. - \frac{(1-\upsilon)}{r\ell}(C_6 \, ber'\,r/\ell + C_7 \, bei'\,r/\ell + C_8 \, ker'\,r/\ell + C_9 \, kei'\,r/\ell)\right]$$ (VIII.15)

For large values of r/ℓ, $ker\,r/\ell$, $kei\,r/\ell$, $ker'\,r/\ell$ and $kei'\,r/\ell \to 0$

Thus:- $$M_{\theta\theta} = -D\left[\frac{(1-\upsilon)}{r\ell}(C_6 \, ber'\,r/\ell + C_7 \, bei'\,r/\ell) + \frac{\upsilon}{\ell^2}(-C_6 \, bei\,r/\ell + C_7 \, ber\,r/\ell)\right]$$

$$M_{rr} = -D\left[-\frac{(1-\upsilon)}{r\ell}(C_6 \, ber'\,r/\ell + C_7 \, bei'\,r/\ell) + \frac{1}{\ell^2}(-C_6 \, bei\,r/\ell + C_7 \, ber\,r/\ell)\right]$$

Applying eqts.VIII.13a,b it is seen that for $r \to \infty$:-

$C_6 + C_7 = 0$ and $-C_6 + C_7 = 0$.   Thus $C_6 = C_7 = 0$

Applying eqt.VIII.13c, and putting $C_6 = C_7 = 0$, it is found that

$A_1 = 0$.   Thus $C_6 = C_7 = A_1 = 0$ (II.43a-c)

(c) **Derivation of c_1, c_2, c_5, c_8, and c_9 (p.85)**

The governing equations for w and F are eqts.II.46a-d

$$w_i = \frac{PR\sqrt{12(1-\upsilon^2)}}{Et^2 \pi \mu^2}\left[c_1 \, ber\,r/\ell + c_2 \, bei\,r/\ell + c_5\right]$$

$$w_o = \frac{PR\sqrt{12(1-\upsilon^2)}}{Et^2 \pi \mu^2}\left[c_8 \, ker\,r/\ell + c_9 \, kei\,r/\ell\right]$$

$$F_i = \frac{PR}{\pi\mu^2}\left[c_1 \, bei\,r/\ell - c_2 \, ber\,r/\ell - \frac{1}{4}\left(\frac{r}{\ell}\right)^2\right]$$

$$F_o = \frac{PR}{\pi\mu^2}\left[c_8 \, kei\,r/\ell - c_9 \, ker\,r/\ell - \frac{\mu^2}{2}\ell n\frac{r}{\ell}\right]$$ (II.46a-d)

At $r = r_p$

$r/\ell = \mu$

$$\begin{cases} w_i = w_o \\ \dfrac{dw_i}{dr} = \dfrac{dw_o}{dr} \\ \nabla^2 w_i = \nabla^2 w_o \\ \dfrac{dF_i}{dr} = \dfrac{dF_o}{dr} \\ \nabla^2 F_i = \nabla^2 F_o \end{cases}$$

(VIII.16)

Using eqts.II.46a-d and conditions eqt.VIII.16 it is possible
to set up five simultaneous linear equations:-

$w_i = w_o$:- $c_1\,\text{ber}\mu + c_2\,\text{bei}\,\mu - c_8\,\text{ker}\,\mu - c_9\,\text{kei}\,\mu = -c_5$

$\dfrac{dw_i}{dr} = \dfrac{dw_o}{dr}$:- $c_1\,\text{ber}'\mu + c_2\,\text{bei}'\,\mu - c_8\,\text{ker}'\,\mu - c_9\,\text{kei}'\mu = 0$

$\nabla^2 w_i = \nabla^2 w_o$:- $-c_1\,\text{bei}\,\mu + c_2\,\text{ber}\,\mu + c_8\,\text{kei}\,\mu - c_9\,\text{ker}\,\mu = 0$

$\dfrac{dF_i}{dr} = \dfrac{dF_o}{dr}$:- $c_1\,\text{bei}'\mu - c_2\,\text{ber}'\,\mu - c_8\,\text{kei}'\,\mu + c_9\,\text{ker}'\mu = 0$

$\nabla^2 F_i = \nabla^2 F_o$:- $c_1\,\text{ber}\,\mu + c_2\,\text{bei}\,\mu - c_8\,\text{ker}\,\mu - c_9\,\text{kei}\,u = 1$ (VIII.17a-e)

From inspection of eqts.VIII.17a and e, $c_5 = -1$

By multipying eqt.(b) by bei μ and eqt.(c) by ber$'\mu$ and adding,
c_1 is eliminated.   Similarly multiplying eqt.(d) by ber μ and
eqt.(e) by bei$'\mu$, and adding, c_1 is eliminated.   Subtracting the
two resulting equations the following equation in c_8 and c_9 is
obtained:- $c_8(\text{kei}\mu\,\text{ber}'\mu - \text{ker}'\mu\,\text{bei}\mu - \text{kei}'\mu\,\text{ber}\mu + \text{ker}\mu\,\text{bei}'\mu)$

$-c_9(\text{ker}\mu\,\text{ber}'\mu + \text{kei}'\mu\,\text{bei}\mu - \text{ker}'\mu\,\text{ber}\mu - \text{kei}\mu\,\text{bei}'\mu) = -\text{bei}'\mu$ (VIII.18)

Similarly by multiplying eqt(b) by ber μ and eqt.(e) by ber$'\mu$
and adding, and eqt.(c) by bei$'\mu$ and eqt.(d) by bei μ, and adding
the resulting equations after subtraction yield:-

$c_8(\text{ker}'\mu\,\text{ber}\mu - \text{ker}\mu\,\text{ber}'\mu + \text{kei}\mu\,\text{bei}'\mu - \text{kei}'\mu\,\text{bei}\mu)$

$+ c_9(\text{kei}'\mu\,\text{ber}\mu - \text{kei}\mu\,\text{ber}'\mu - \text{ker}\mu\,\text{bei}'\mu + \text{ker}'\mu\,\text{bei}\mu) = \text{ber}'\mu$ (VIII.19)

From ref.(105) it is noted that:-

$\text{ber}\mu\,\text{ker}'\mu + \text{bei}'\mu\,\text{kei}\mu - \text{ber}'\mu\,\text{ker}\mu - \text{bei}\mu\,\text{kei}'\mu = -1/\mu$

and $\text{ber}\mu\,\text{kei}'\mu + \text{bei}\mu\,\text{ker}'\mu - \text{ber}'\mu\,\text{kei}\mu - \text{bei}'\mu\,\text{ker}\mu = 0$ (VIII.20a,b)

Thus from eqts.VIII.18 and 19, $c_q = \mu \, bei' \mu$ and $c_8 = -\mu \, ber' \mu$

Similarly it is shown that:- $c_1 = \mu \, ker' \mu$ and $c_2 = \mu \, kei' \mu$ (II.47)

VIII.2.2 RADIAL LOADING OF A RIGID INSERT ON A SHALLOW SHELL (p.89)

(a) Derivation of C_8 and C_9 (p.89)

The two governing equations are:-

$$w = \frac{PR\sqrt{12(1-\upsilon^2)}}{Et^2 \pi \mu^2} \left[C_8 \, ker \, {}^r\!/_\ell + C_9 \, kei \, {}^r\!/_\ell \right]$$

$$F = \frac{PR}{\pi \mu^2} \left[C_8 \, kei \, {}^r\!/_\ell - C_9 \, ker \, {}^r\!/_\ell - \frac{\mu^2}{2} \ell n \, {}^r\!/_\ell \right] \qquad \text{(VIII.21a,b)}$$

At $r = r_P$, ${}^r\!/_\ell = \mu$
$$\begin{cases} \dfrac{dw}{dr} = 0 \\[2mm] \mathcal{E}_\theta = (N_{\theta\theta} - \upsilon N_{rr})/Et = 0 \end{cases} \qquad \text{(VIII.22a,b)}$$

From eqt.VIII.21a $\qquad \dfrac{dw}{dr} = \dfrac{PR\sqrt{12(1-\upsilon^2)}}{Et^2 \pi \mu^2} \dfrac{1}{\ell} \left[C_8 \, ker' \, {}^r\!/_\ell + C_q \, kei' \, {}^r\!/_\ell \right]$

Thus from eqt.VIII.22a $\qquad C_q = -C_8 \, ker' \mu / kei' \mu \qquad \text{(II.57a)}$

Using eqts.II.4a.b $\qquad N_{rr} = \dfrac{1}{r}\dfrac{dF}{dr}$ and $\qquad N_{\theta\theta} = \dfrac{d^2 F}{dr^2}$

From eqt.VIII.21b at $r = r_P$, $\dfrac{r}{\ell} = \mu$:-

$$N_{rr} = \frac{1}{r_P} \left[\frac{PR}{\pi \mu^2} \left(\frac{C_8}{\ell} kei' \mu - \frac{C_q}{\ell} ker' \mu - \frac{\mu^2}{2r_P} \right) \right]$$

$$N_{\theta\theta} = \frac{PR}{\pi \mu^2} \left[\frac{C_8}{\ell^2} \left(ker\mu - \frac{kei' \mu}{\mu} \right) - \frac{C_q}{\ell^2} \left(-kei\mu - \frac{ker' \mu}{\mu} \right) + \frac{\mu^2}{2r_P^2} \right] \quad \text{(VIII.23a,b)}$$

Substituting the values of N_{rr} and $N_{\theta\theta}$ of eqt.VIII.23a,b into eqt.VIII.22b:-

$$\frac{C_8}{\ell^2} \left(ker\mu - \frac{kei' \mu}{\mu} \right) - \frac{C_q}{\ell^2} \left(-kei\mu - \frac{ker' \mu}{\mu} \right) + \frac{\mu^2}{2r_P^2} = \frac{\upsilon}{r_P} \left(C_8 \frac{kei' \mu}{\ell} - C_q \frac{ker' \mu}{\ell} - \frac{\mu^2}{2r_P} \right) \quad \text{(VIII.24)}$$

From eqts.II.57a and VIII.24, $\quad C_8 = -\dfrac{(1+\upsilon)\mu \, kei' \mu}{2\,[V]} \qquad \text{(II.57b)}$

where $[V] = \mu(kei' \mu \, ker\mu - ker' \mu \, kei\mu) - (1+\upsilon)(kei'^2 \mu + ker'^2 \mu)$

VIII.2.3 'BENDING' MOMENT ON A SHALLOW SHELL (p.91)

(a) Derivation of constants a_1 and A (p.92)

The governing equation for F, eqt.II.60b is as follows:-

$$F = \left\{ \frac{\ell^2 tE}{R} \left[-C_2 \, ber' \, {}^r\!/_\ell + C_1 bei' \, {}^r\!/_\ell - C_4 ker' \, {}^r\!/_\ell + C_3 kei' \, {}^r\!/_\ell \right] + (a_1 + A)\frac{r}{\ell} + (b_1 + B)\frac{\ell}{r} \right\} \cos\theta \quad \text{(VIII.25)}$$

From eqt.II.4a, $\qquad N_{rr} = \dfrac{1}{r}\dfrac{\partial F}{\partial r} + \dfrac{1}{r^2}\dfrac{\partial^2 F}{\partial \theta^2}$

Thus from eqt. VIII.25,

$$N_{rr} = \left\{ \frac{\ell t E}{R}\left[-\frac{c_2}{r} \text{ber}'\frac{r}{\ell} + \frac{c_1}{r}\text{bei}''\frac{r}{\ell} - \frac{c_4}{r}\text{ker}''\frac{r}{\ell} + \frac{c_3}{r}\text{kei}''\frac{r}{\ell} \right] + \frac{(a_1+A)}{r\ell} - (b_1+B)\frac{\ell}{r^3} \right.$$

$$\left. - \frac{\ell^2 t E}{R}\left[-c_2\text{ber}'\frac{r}{\ell} + c_1\text{bei}'\frac{r}{\ell} - c_4\text{ker}'\frac{r}{\ell} + c_3\text{kei}'\frac{r}{\ell} \right] - \frac{(a_1+A)}{r\ell} - \frac{(b_1+B)\ell}{r^3} \right\}\cos\theta$$

Thus $(a_1 + A)$ is immaterial. The same conclusion is reached
when considering $N_{\theta\theta}$ and $N_{r\theta}$

(b)   <u>Derivation of the constant B₁</u>   (p.92)

The meridional and circumferential strains are defined
as follows from eqts. I.81a,b:- $\varepsilon_r = \frac{\partial v}{\partial r} + \frac{w}{R} = \frac{1}{tE}[N_{rr} - \upsilon N_{\theta\theta}]$

$$\varepsilon_\theta = \frac{1}{r}\frac{\partial u}{\partial \theta} + \frac{v}{r} + \frac{w}{R} = \frac{1}{tE}[N_{\theta\theta} - \upsilon N_{rr}] \quad\quad (VIII.26a,b)$$

Substituting for w from eqt. II.6 and for N_{rr} and $N_{\theta\theta}$ from
eqts. II.4a,b, eqts. VIII.26a,b can be written after simplification :

$$\frac{\partial v}{\partial r} - \frac{w_{\phi}}{R} = -\frac{(1+\upsilon)}{tE}\frac{\partial^2 F}{\partial r^2}$$

$$\frac{1}{r}\frac{\partial u}{\partial \theta} + \frac{v}{r} - \frac{w_{\phi}}{R} = -\frac{(1+\upsilon)}{tE}\left(\frac{1}{r}\frac{\partial F}{\partial r} + \frac{1}{r^2}\frac{\partial^2 F}{\partial \theta^2}\right) \quad\quad (VIII.27a,b)$$

From eqt. VIII.27a $v = -\frac{(1+\upsilon)}{tE}\frac{\partial F}{\partial r} + \int\frac{w_\phi}{R} + f(\theta)$

where $f(\theta)$ is a function of θ only.

Thus eqt. VIII.27b :-

$$\frac{\partial u}{\partial \theta} = \frac{r}{R}w_\phi - \frac{(1+\upsilon)}{tE}\frac{\partial F}{\partial r} - \frac{(1+\upsilon)}{rtE}\frac{\partial^2 F}{\partial \theta^2} + \frac{(1+\upsilon)\partial F}{tE \partial r} - \int\frac{w_\phi}{R} - f(\theta) \quad\quad (VIII.28)$$

After simplification and differentiation w.r.t. r eqt. VIII.28
becomes:- $\frac{\partial}{\partial r}\left(\frac{\partial u}{\partial \theta}\right) = -\frac{(1+\upsilon)}{tE}\left[\frac{\partial}{\partial r}\left(\frac{\partial^2 F}{\partial \theta^2}\right)\right]$ (VIII.29)

Multiplying eqt. VIII.27b by r and differentiating w.r.t. r:-

$$\frac{\partial}{\partial r}\left(\frac{\partial u}{\partial \theta}\right) + \frac{\partial v}{\partial r} - \frac{\partial}{\partial r}\left(\frac{w_\phi}{R}\right) = -\frac{(1+\upsilon)}{tE}\left[\frac{\partial^2 F}{\partial r^2} + \frac{\partial}{\partial r}\left(\frac{1}{r}\frac{\partial^2 F}{\partial \theta^2}\right)\right] \quad (VIII.30)$$

Subtracting eqt. VIII.30 from VIII.27a and substituting for

$\frac{\partial}{\partial r}\left(\frac{\partial u}{\partial \theta}\right)$ from eqt. VIII.29:- $\frac{\partial}{\partial r}\left(w_\phi\frac{r}{R}\right) - \frac{w_\phi}{R} = 0$ (VIII.31)

From eqt. II.7, $w_\phi = (A_1 r + B_1/r)\cos\theta$ (VIII.32)

Since A_1 is shown to be zero from the conditions at $r \to \infty$,

eqt. VIII.31 can be written:- $\frac{\partial}{\partial r}\left(\frac{B_1}{R}\cos\theta\right) - \frac{B_1}{rR}\cos\theta = 0$, ie $B_1 = 0$.

(c)   Derivation of C_1, C_2 and A_1 (p.92 and p.98)

The governing equation for w is:-

$$\omega = \left(C_1 ber'\tfrac{r}{l} + C_2 bei'\tfrac{r}{l} + C_3 ker'\tfrac{r}{l} + C_4 kei'\tfrac{r}{l} - A_1 \tfrac{r}{l}\right)\cos\theta \qquad (VIII.33)$$

Thus $\frac{\partial\omega}{\partial r} = \Big\{ \frac{1}{l}\Big[C_1\left(-bei\tfrac{r}{l} - \frac{ber'\tfrac{r}{l}}{r/l}\right) + C_2\left(ber\tfrac{r}{l} - \frac{bei'\tfrac{r}{l}}{r/l}\right) + C_3\left(-kei\tfrac{r}{l} - \frac{ker'\tfrac{r}{l}}{r/l}\right) +$

$\qquad\qquad + C_4\left(ker\tfrac{r}{l} - \frac{kei'\tfrac{r}{l}}{r/l}\right)\Big] - \frac{A_1}{l}\Big\}\cos\theta$

$\frac{\partial^2\omega}{\partial r^2} = \Big\{ \frac{\cos\theta}{l^2}\Big[C_1\left(-bei'\tfrac{r}{l} + \frac{bei\tfrac{r}{l}}{r/l} + \frac{2ber'\tfrac{r}{l}}{(r/l)^2}\right) + C_2\left(ber'\tfrac{r}{l} - \frac{ber\tfrac{r}{l}}{r/l} + \frac{2bei'\tfrac{r}{l}}{(r/l)^2}\right) +$

$\qquad\qquad + C_3\left(-kei'\tfrac{r}{l} + \frac{kei\tfrac{r}{l}}{(r/l)} + \frac{2ker'\tfrac{r}{l}}{(r/l)^2}\right) + C_4\left(ker'\tfrac{r}{l} - \frac{ker\tfrac{r}{l}}{(r/l)} + \frac{2kei'\tfrac{r}{l}}{(r/l)^2}\right)\Big]\Big\} \quad (VIII.34a,b)$

As $r \to \infty$ $\quad\begin{cases} M_{rr} \to & 0 \\ M_{\theta\theta} \to & 0 \\ w \to & 0 \end{cases}$

$\qquad\qquad\qquad\qquad\qquad\qquad\qquad\qquad\qquad\qquad (VIII.35a-c)$

From eqts. II.4d,e $\quad M_{rr} = -D\Big[\frac{\partial^2\omega}{\partial r^2} + \upsilon\left(\frac{1}{r}\frac{\partial\omega}{\partial r} + \frac{1}{r^2}\frac{\partial^2\omega}{\partial\theta^2}\right)\Big]$

$\qquad\qquad\qquad M_{\theta\theta} = -D\Big[\frac{1}{r}\frac{\partial\omega}{\partial r} + \frac{1}{r^2}\frac{\partial^2\omega}{\partial\theta^2} + \upsilon\frac{\partial^2\omega}{\partial r^2}\Big]$

Thus using eqts. VIII.34a,b, noting that for large $\frac{r}{l}$, $ker\tfrac{r}{l}$, $kei\tfrac{r}{l}$, $ker'\tfrac{r}{l}$, $kei'\tfrac{r}{l} \to 0$

$\qquad M_{rr} = -\frac{D}{l^2}\Big[\left(-C_1 bei'\tfrac{r}{l} + C_2 ber'\tfrac{r}{l}\right) + \frac{(1-\upsilon)(C_1 bei\tfrac{r}{l} - C_2 ber\tfrac{r}{l})}{r/l}$

$\qquad\qquad\qquad + \frac{2(1-\upsilon)(C_1 ber'\tfrac{r}{l} + C_2 bei'\tfrac{r}{l})}{(r/l)^2}\Big]\cos\theta$

$\qquad M_{\theta\theta} = -\frac{D}{l^2}\Big[\upsilon\left(-C_1 bei'\tfrac{r}{l} + C_2 ber'\tfrac{r}{l}\right) + \frac{(1-\upsilon)(-C_1 bei\tfrac{r}{l} + C_2 ber\tfrac{r}{l})}{r/l}$

$\qquad\qquad\qquad + \frac{2(1-\upsilon)(-C_1 ber'\tfrac{r}{l} - C_2 bei'\tfrac{r}{l})}{(r/l)^2}\Big]\cos\theta \qquad (VIII.36a,b)$

Applying conditions, eqts. VIII.35a,b to eqts. VIII.36a,b

$\qquad\qquad -C_1 + C_2 = 0$ $\qquad$ and $\quad C_1 + C_2 = 0$ $\qquad$ Thus $C_1 = C_2 = 0$

Applying condition, eqt. VIII.35c to eqt. VIII.33 and putting

$C_1 = C_2 = 0$, it is found that $A_1 = 0$. Thus $C_1 = C_2 = A_1 = 0$

$\qquad\qquad\qquad\qquad\qquad\qquad\qquad\qquad\qquad\qquad\qquad (II.62a-c)$

(d) <u>Derivation of C_3 and C_4</u> (p.93)

The two governing equations for w and F reduce to the following:- $w = (C_3 \ker'{}^r/_\ell + C_4 \kei'{}^r/_\ell) \cos\theta$

$$F = \frac{Et^2}{\sqrt{12(1-v^2)}} \left[C_3 \kei'{}^r/_\ell - C_4 \ker'{}^r/_\ell + C_5 \left(\tfrac{r}{\ell}\right)^{-1} \right] \cos\theta \qquad \text{(II.63a,b)}$$

At $r = r_P$, $\frac{r}{\ell} = \mu$
$$\begin{cases} \dfrac{dw}{dr} = \dfrac{w}{r} \\[2mm] \varepsilon_\theta = (N_{\theta\theta} - v N_{rr})/Et = 0 \end{cases} \qquad \text{(VIII.37a,b)}$$

From eqt. II.63a, eqt. VIII.37a becomes:-

$$\frac{1}{\ell}(C_3 \ker''\mu + C_4 \kei''\mu)\cos\theta = \frac{1}{r_P}(C_3 \ker'\mu + C_4 \kei'\mu)\cos\theta$$

Using the expressions for $\ker''\mu$ and $\kei''\mu$ given in Appendix VIII.8:-

$$C_4 = -C_3 \frac{(2\ker'\mu + \mu\kei\mu)}{2\kei'\mu - \mu\ker\mu} \qquad \text{(II.67a)}$$

From eqt. II.4a,b : $N_{rr} = \frac{1}{r}\frac{\partial F}{\partial r} + \frac{1}{r^2}\frac{\partial^2 F}{\partial\theta^2}$ and $N_{\theta\theta} = \frac{\partial^2 F}{\partial r^2}$

Using eqt. II.63b for F

$$N_{rr} = \frac{Et}{R(r/\ell)}\left[C_3\left(\ker{}^r/_\ell - \frac{2\kei'{}^r/_\ell}{r/\ell}\right) + C_4\left(\kei{}^r/_\ell + \frac{2\ker'{}^r/_\ell}{r/\ell}\right) - 2C_5\left(\tfrac{r}{\ell}\right)^{-2} \right]\cos\theta$$

$$N_{\theta\theta} = \frac{Et}{R}\left[C_3\left(\ker'{}^r/_\ell - \frac{\ker{}^r/_\ell}{r/\ell} + \frac{2\kei'{}^r/_\ell}{(r/\ell)^2}\right) + C_4\left(\kei'{}^r/_\ell - \frac{\kei{}^r/_\ell}{r/\ell} - \frac{2\ker'{}^r/_\ell}{(r/\ell)^2}\right) + 2C_5\left(\tfrac{r}{\ell}\right)^{-3} \right]\cos\theta$$
$$\text{(VIII.38a,b)}$$

Using the condition of eqt. VIII.37b in conjunction with eqts. VIII.38a,b:-

$$C_3\left[\ker'\mu - (1+v)\frac{\ker\mu}{\mu} + 2\frac{(1+v)\kei'\mu}{\mu^2} \right] +$$
$$+ C_4\left[\kei'\mu - (1+v)\frac{\kei\mu}{\mu} - 2\frac{(1+v)\ker'\mu}{\mu^2} \right] + \frac{2(1+v)}{\mu^3} C_5 = 0 \qquad \text{(VIII.39)}$$

From eqt. II.67a, and the relationship given for C_5 in eqt.II.66, eqt. VIII.39 yields the following value for C_3 :-

$$C_3 = -\frac{(1+v)\sqrt{12(1-v^2)}}{\pi\mu\,[X]}(2\kei'\mu - \mu\ker\mu)\cdot\frac{MR}{Et^2\ell} \qquad \text{(II.67b)}$$

where $[X] = (1+v)\left[\mu^2(\ker^2\mu + \kei^2\mu) + 4(\kei'^2\mu + \ker'^2\mu) + 4\mu(\ker'\mu\kei\mu - \ker\mu\kei'\mu) \right] - \mu^3(\ker'\mu\ker\mu + \kei'\mu\kei\mu)$

VIII.2.4 <u>'TWISTING' MOMENT ON A SHALLOW SHELL</u> (p.95)

(a) <u>Derivation of C_3 and C_4</u> (p.96)

From eqts. II.69a,b, II.70, 71 and 74

$$w = C_3 \ker{}^r/_\ell + C_4 \kei{}^r/_\ell$$

$$F = \frac{\ell^2 t E}{R}(-C_4 \ker {}^r/_\ell + C_3 \kei {}^r/_\ell) + C_5 \theta \qquad \text{(VIII.40a,b)}$$

At $r = r_p$, $\frac{r}{\ell} = \mu$

$$\begin{cases} \frac{dw}{dr} = 0 \\[2mm] \varepsilon_\theta = (N_{\theta\theta} - \upsilon N_{rr})/Et = 0 \end{cases} \qquad \text{(VIII.41a,b)}$$

From eqt. VIII.40a and eqt. VIII.41a $C_3 = -C_4 \dfrac{\kei'\mu}{\ker'\mu}$ $\quad$ (VIII.42)

Using eqts. II.4a,b, $N_{rr} = \dfrac{1}{r}\dfrac{\partial F}{\partial r} + \dfrac{1}{r^2}\dfrac{\partial^2 F}{\partial \theta^2}$ $\quad$ and $\quad$ $N_{\theta\theta} = \dfrac{\partial^2 F}{\partial r^2}$

and eqt. VIII.40b.

$$N_{rr} = \frac{tE}{R}\left(-C_4 \frac{\ker'{}^r/_\ell}{{}^r/_\ell} + C_3 \frac{\kei'{}^r/_\ell}{{}^r/_\ell}\right)$$

$$N_{\theta\theta} = \frac{tE}{R}\left(-C_4 \ker''{}^r/_\ell + C_3 \kei''{}^r/_\ell\right)$$

Thus using eqt. VIII.41b:-

$$C_3\left(\ker\mu - (1+\upsilon)\frac{\kei'\mu}{\mu}\right) + C_4\left(\kei\mu + (1+\upsilon)\frac{\ker'\mu}{\mu}\right) = 0 \qquad \text{(VIII.43)}$$

Equation VIII.42 and 43 are only satisfied when $C_3 = C_4 = 0$
$$\text{(II.75)}$$

VIII.2.5 $\quad$ TANGENTIAL LOAD ON THE SHALLOW SHELL $\quad$ (p.98)

(a) $\quad$ Derivation of C_3 and C_4 $\quad$ (p.99)

The relevant equation for w, eqt. II.89a, is:-

$$w = (C_3 \ker'{}^r/_\ell + C_4 \kei'{}^r/_\ell)\cos\theta \qquad \text{(II.89a)}$$

At $r = r_p$, ${}^r/_\ell = \mu$

$$\begin{cases} \frac{\partial w}{\partial r} = 0 \\[2mm] Q_r = -D \frac{\partial(\nabla^2 w)}{\partial r} = 0 \end{cases} \qquad \text{(VIII.44a,b)}$$

From eqt. II.89a. $\quad \dfrac{\partial w}{\partial r} = \dfrac{1}{\ell}(C_3 \ker''{}^r/_\ell + C_4 \kei''{}^r/_\ell)\cos\theta$

From eqt. VIII.44a, $\quad C_3 = -C_4 \dfrac{\kei'{}^r/_\ell}{\ker''{}^r/_\ell}$ $\qquad$ (VIII.45)

Since $\quad \nabla^2 w = \dfrac{\partial^2 w}{\partial r^2} + \dfrac{1}{r}\dfrac{\partial w}{\partial r} + \dfrac{1}{r^2}\dfrac{\partial^2 w}{\partial \theta^2}$ $\quad$ using eqt. II.89a,

$$\nabla^2 w = \frac{1}{\ell^2}(-C_3 \kei'{}^r/_\ell + C_4 \ker'{}^r/_\ell)\cos\theta$$

Thus $\quad Q_r = -\dfrac{D}{\ell^3}(-C_3 \kei''{}^r/_\ell + C_4 \ker''{}^r/_\ell)\cos\theta$

From eqt. VIII.44b, $\quad C_4 \ker''{}^r/_\ell - C_3 \kei''{}^r/_\ell = 0$ $\qquad$ (VIII.46)

Equations VIII.45 and 46 can only be satisfied when

$$C_3 = C_4 = 0 \qquad \text{(II.93)}$$

VIII.2.6 THE RADIAL LOADING OF A RIGID INSERT - GENERAL SHELL THEORY (p.108)

(a) Derivation of B_1 and B_2 (p.109)

The boundary conditions at the insert $r = r_P$, $r/\ell = \mu$ are

$$\frac{dw_0}{dr} = 0, \qquad \varepsilon_\theta = (N_{\theta\theta} - \nu N_{rr})/Et = 0 \qquad \text{(II.126a,b)}$$

Using eqts. II.124a,b, the values of N_{rr_0} and $N_{\theta\theta_0}$ at the insert are:-

$$N_{rr_0} = \frac{-Et}{(1-\nu^2)r_P}(B_1 \ker'\mu + B_2 \kei'\mu) - \frac{PR}{2\pi r_P^2}$$

$$N_{\theta\theta_0} = -\frac{Et}{(1-\nu^2)\ell}\left[-B_1\left(\kei\mu + \frac{\ker'\mu}{\mu}\right) + B_2\left(\ker\mu - \frac{\kei'\mu}{\mu}\right)\right] + \frac{PR}{2\pi r_P^2}$$

Using condition, eqt. II.126b:-

$$B_1\left[\frac{\kei\mu}{\ell} + \frac{(1+\nu)\ker'\mu}{r_P}\right] + B_2\left[-\frac{\ker\mu}{\ell} + \frac{(1+\nu)\kei'\mu}{r_P}\right] = -\frac{PR(1+\nu)(1-\nu^2)}{2\pi r_P^2 Et} \qquad \text{(VIII.47)}$$

The value of $\frac{dw_0}{dr}$ at the insert is obtained from eqt. II.125:-

$$\frac{dw_0}{dr} = \frac{1}{R(1-\nu^2)}\left[B_1\left(\ker'\mu + \frac{R^2}{\ell^2}\kei'\mu\right) + B_2\left(\kei'\mu - \frac{R^2}{\ell^2}\ker'\mu\right)\right] + \frac{P(1+\nu)}{2Et\pi r_P} \qquad \text{(VIII.48)}$$

Using condition eqt. II.126a, eqt. VIII.48 can be re-arranged to give:-

$$B_1 = \left[-\frac{P(1+\nu)(1-\nu^2)R}{2\pi Et r_P} - B_2\left(\kei'\mu - \frac{R^2}{\ell^2}\ker'\mu\right)\right]\frac{1}{\ker'\mu + \frac{R^2}{\ell^2}\kei'\mu} \qquad \text{(VIII.49)}$$

From eqts. VIII.47 and 49

$$B_1 = -\frac{PR(1+\nu)(1-\nu^2)}{2\pi r_P Et\left(\ker'\mu + \frac{R^2}{\ell^2}\kei'\mu\right)}\left\{1 + \frac{(\kei'\mu - \frac{R^2}{\ell^2}\ker'\mu)(-\ker'\mu - \frac{R^2}{\ell^2}\kei'\mu + \mu\kei\mu - (1+\nu)\ker'\mu)}{\left[\frac{R^2}{\ell^2}\{\mu\kei\mu\ker'\mu + (1+\nu)\ker'^2\mu - \mu\kei'\mu\ker\mu + (1+\nu)\kei'^2\mu\} - \mu\kei'\mu\kei\mu - \mu\ker\mu\ker'\mu\right]}\right\}$$

$$B_2 = \frac{PR(1+\nu)(1-\nu^2)}{2\pi r_P Et}\left\{\frac{-\ker'\mu - \frac{R^2}{\ell^2}\kei'\mu + \mu\kei\mu + (1+\nu)\ker'\mu}{\left[\frac{R^2}{\ell^2}\{\mu\kei\mu\ker'\mu + (1+\nu)\ker'^2\mu - \mu\kei'\mu\ker\mu + (1+\nu)\kei'^2\mu\} - \mu\kei'\mu\kei\mu - \mu\ker\mu\ker'\mu\right]}\right\}$$

$$\text{(II.127a,b)}$$

VIII.2.7 A 'BENDING' MOMENT ON A SHELL - GENERAL THEORY (p.115)

(a) Derivation of B_1 and B_2 (p.119)

The boundary conditions at the insert $r = r_P$, $r/\ell = \mu$ are

$$\frac{dw}{dr} = \frac{w}{r} \qquad \text{and} \qquad \varepsilon_\theta = (N_{\theta\theta} - \nu N_{rr})/Et = 0 \qquad \text{(II.146a,b)}$$

From eqt. II.145g, $\dfrac{d\omega_1}{dr} = \dfrac{1}{(1-v^2)\ell}\left\{ B_1\left[kei\,{}^r/_\ell - \dfrac{ker'{}^r/_\ell}{{}^r/_\ell} + \dfrac{R^2}{\ell^2}(ker\,{}^r/_\ell - \dfrac{kei'{}^r/_\ell}{{}^r/_\ell}) \right] + \right.$

$\left. + B_2\left[ker\,{}^r/_\ell - \dfrac{kei'{}^r/_\ell}{{}^r/_\ell} + \dfrac{R^2}{\ell^2}(kei\,{}^r/_\ell + \dfrac{ker'{}^r/_\ell}{{}^r/_\ell}) \right] \right\}$ (VIII.50)

Using the condition of eqt. II.146a in conjunction with eqt.
II.145g and eqt. VIII.50, the following relationship is obtained:-

$B_1\left[ker'\mu + \dfrac{R^2}{\ell^2}kei'\mu + \mu kei\mu + ker'\mu - \dfrac{R^2}{\ell^2}(\mu ker\mu - kei'\mu) \right] +$

$+ B_2\left[kei'\mu - \dfrac{R^2}{\ell^2}ker'\mu - \mu ker\mu + kei'\mu - \dfrac{R^2}{\ell^2}(\mu kei\mu + ker'\mu) \right] = 0$ (VIII.51)

From the condition of eqt. II.146b, using eqts. II.145a,b:-

$B_1\left[\mu^2 kei'\mu - (1+v)\mu kei\mu - 2(1+v)ker'\mu \right] -$

$- B_2\left[\mu^2 ker'\mu - (1+v)\mu ker\mu + 2(1+v)kei'\mu \right] = -\dfrac{M(1+v)(1-v^2)}{\pi Et\, r_P}$ (VIII.52)

From eqts. VIII.51 and 52,

$B_1 = -\dfrac{M(1+v)(1-v^2)}{\pi Et\,\mu\ell}\left\{ \dfrac{\mu ker\mu - 2kei'\mu + {}^{R^2}/_{\rho^2}(2ker'\mu + \mu kei\mu)}{\begin{array}{l}\dfrac{R^2}{\ell^2}\left[\mu^3(kei'\mu kei\mu + ker'\mu ker\mu) - (1+v)\left\{ \mu^2(kei^2\mu + ker^2\mu) + \right.\right.\\ \left.\left. +4(kei'^2\mu + ker'^2\mu) + 4\mu(ker'\mu kei\mu - kei'\mu ker\mu) \right\}\right] + \\ +\mu^3\left[kei'\mu ker\mu - ker'\mu kei\mu \right] - 2\mu^2\left[kei'^2\mu + ker'^2\mu \right]\end{array}} \right\}$

$B_2 = -\dfrac{M(1+v)(1-v^2)}{\pi Et\,\mu\ell}\left\{ \dfrac{\mu kei\mu + 2ker'\mu + {}^{R^2}/_{\rho^2}(2kei'\mu - \mu ker\mu)}{\begin{array}{l}\dfrac{R^2}{\ell^2}\left[\mu^3(kei'\mu kei\mu + ker'\mu ker\mu) - (1+v)\left\{ \mu^2(kei^2\mu + ker^2\mu) + \right.\right.\\ \left.\left. +4(kei'^2\mu + ker'^2\mu) + 4\mu(ker'\mu kei\mu - kei'\mu ker\mu) \right\}\right] + \\ +\mu^3\left[kei'\mu ker\mu - ker'\mu kei\mu \right] - 2\mu^2\left[kei'^2\mu + ker'^2\mu \right]\end{array}} \right\}$

(II.147a,b)

VIII.2.8   A TANGENTIAL LOAD ON A SHELL - GENERAL THEORY   (p.126)

(a)   Derivation of constants C_1 , C_2 , D_1 and D_2 (p.129)

At the outer edge of the shell, $u_1 = v_1 = w_1 = X_1 = 0$
(II.172a-d)

These relationships give rise to four simultaneous linear
equations, obtained by combining the membrane (eqts. II.166),
inextensional (eqts. II.168) and oscillatory (eqts. II.171),
displacements:-

For u_1 :- $-1.2467 \times 10^{-4}H + D_1 - D_2 \times 0.9457 - 0.00397\bar{C}_1 + 0.00207\bar{C}_2 = 0$

For v_1 :- $+1.2467 \times 10^{-4}H + D_2 - D_1 \times 0.9457 + 0.0389\bar{C}_1 + 0.0125\bar{C}_2 = 0$

For w_1 :- $+2.1616 \times 10^{-4} H - D_1 x .3250 \quad -0.4080\bar{C}_1 - 0.7846\bar{C}_2 = 0$

For RX_1 :- $-60 \times 0.1108 \times 10^{-4} H - D_2 \quad + 8.1030\bar{C}_1 - 22.5720\bar{C}_2 = 0$

(VIII.53a-d)

Solving equations VIII.53 yields:-

$$\bar{C}_1 = +3.684 \times 10^{-4} H \quad ; \quad \bar{C}_2 = +1.118 \times 10^{-4} H$$

Using eqts. II.170a,b, $C_1 = \dfrac{\bar{C}_1}{e^{\chi \phi}} = +0.500 \times 10^{-6} H$, $C_2 = \dfrac{\bar{C}_2}{e^{\chi \phi}} = +0.151 \times 10^{-6} H$

and $D_1 = -0.671 \times 10^{-4} H$, $D_2 = -2.05 \times 10^{-4} H$ (II.173a-d)

(b) Derivation of constants B_1 and B_2 (p.130)

The boundary conditions at the insert $r = r_p = 0.5 in$,

$\phi = 0.0083$ radians are $\dfrac{dw}{d\phi} = 0$ and $\varepsilon_\theta = (N_{\theta\theta} - \upsilon N_{rr})/Et = 0$ (II.175a,b)

The expression for $\dfrac{dw}{d\phi}$ is the combined one involving membrane,

inextensional and oscillatory values. The three values are

set out below:-

Membrane Slope

Differentiating eqt. II.162b, the following equation for $\dfrac{dw_1}{d\phi}$

results:- $\dfrac{dw_1}{d\phi} = -\dfrac{H(1+\upsilon)}{4\pi Et}\left[\cos\phi \ \ln\dfrac{1-\cos\phi}{1+\cos\phi} + 2 + \dfrac{2}{\sin^2\phi}\right]$

which in this case leads to:- $\dfrac{dw_1}{d\phi} = -0.8954 H$ (VIII.54)

Inextensional Slope

From eqt. II.163b:- $\dfrac{dw_1}{d\phi} = -D_1 \cos\phi$

substituting the value of $D_1 = -0.671 \times 10^{-4} H$ from eqt. II.173c,

$$\dfrac{dw_1}{d\phi} = +0.670 \times 10^{-4} H \qquad\qquad (VIII.55)$$

Oscillatory Slope

From eqt. II.144c, taking $\sqrt{\dfrac{\phi}{\sin\phi}} = 1$:-

$\dfrac{dw_1}{d\phi} = \dfrac{\sqrt{2}\,\chi\,B_1}{(1-\upsilon^2)}\left[\ker''\sqrt{2}\,\chi\phi + 2\chi^2 \ker''\sqrt{2}\,\chi\phi\right] + \dfrac{\sqrt{2}\,\chi\,B_2}{(1-\upsilon^2)}\left[\kei''\sqrt{2}\,\chi\phi - 2\chi^2 \ker''\sqrt{2}\,\chi\phi\right]$

leading to:- $\dfrac{dw_1}{d\phi} = 1.443 \times 10^4 B_1 - 46.65 \times 10^4 B_2$ (VIII.56)

The combined slope is obtained by adding the results of eqts.

VIII.54, 55 and 56 which from condition, eqt. II.175a becomes:-

$$\frac{dw_1}{d\phi} = -0.8953H + 1.443 \times 10^4 B_1 - 46.65 \times 10^4 B_2 = 0 \qquad (VIII.57)$$

The expressions for $N_{\theta\theta_1}$ and $N_{\phi\phi_1}$ are obtained from eqts. II.164a,b and II.144d,e, and considering only the terms associated with B_1 and B_2 result in the following expressions at the insert:-

$$N_{\theta\theta_1} = 7.766 \times 10^6 B_1 + 1.110 \times 10^5 B_2 + 0.325 H$$

$$N_{\phi\phi_1} = -7.752 \times 10^6 B_1 + 9.640 \times 10^4 B_2 - 0.325 H \qquad (VIII.58)$$

Using the condition, eqt. II.175b :-

$$10.092 \times 10^6 B_1 + 8.210 \times 10^4 B_2 + 0.422H = 0 \qquad (VIII.59)$$

From equations VIII.57 and 59:-

$$B_1 = -2.622 \times 10^{-8} H \quad \text{and} \quad B_2 = -1.920 \times 10^{-6} H \qquad (II.176a,b)$$

A 'TWISTING' MOMENT APPLIED TO A FLAT PLATE

A plate of outside radius r_2 is subjected to a 'twisting' moment T acting in its plane. The moment is applied to the plate through a cylindrical insert of radius r_p - Fig.VIII.1.
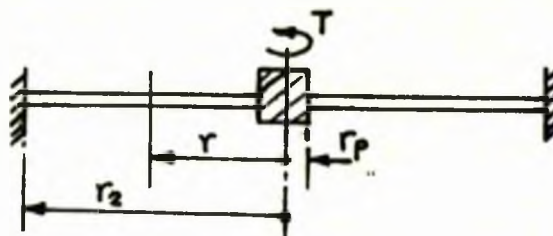
Fig. VIII.1

Owing to the rotational symmetry of the problem, the stress function selected must be independent of terms which involve $\sin\theta$ or $\cos\theta$. A suitable form is thus:-

$$F = a_0 \ln r + b_0 r^2 + c_0 r^2 \ln r + d_0 r^2 \theta + e_0 \theta \qquad (VIII.60)$$

where r and θ are polar co-ordinates referred to the plate centre. Using eqts. II.4a-c with $\Omega = 0$.

$$N_{rr} = \frac{a_0}{r^2} + 2c_0 \ln r + 2b_0 + c_0 + 2d_0\theta$$

$$N_{\theta\theta} = -\frac{a_0}{r^2} + 2b_0 + 3c_0 + 2c_0 \ln r + 2d_0\theta$$

$$N_{r\theta} = \frac{e_0}{r^2} - d_0 \qquad (VIII.61a\text{-}c)$$

The strains are defined as follows:-

$$\varepsilon_r = \frac{\partial v}{\partial r} = \frac{1}{tE}(N_{rr} - \upsilon N_{\theta\theta})$$

$$\varepsilon_\theta = \frac{v}{r} + \frac{1}{r}\frac{\partial u}{\partial \theta} = \frac{1}{tE}(N_{\theta\theta} - \upsilon N_{rr})$$

$$\gamma_{r\theta} = \frac{\partial v}{r\partial\theta} + \frac{\partial u}{\partial r} - \frac{u}{r} = \frac{N_{r\theta}}{tG} \qquad (VIII.62a\text{-}c)$$

Substituting eqts. VIII.61a,b into eqt. VIII.62a and integrating:-

$$v = \frac{1}{tE}\left[-\frac{a_0(1+\upsilon)}{r} + 2c_0 r(1-\upsilon)(\ln r - 1) + 2b_0 r(1-\upsilon) + c_0 r(1-3\upsilon) + 2d_0 r\theta(1-\upsilon)\right] + f(\theta) \qquad (VIII.63)$$

where $f(\theta)$ is a function of θ.

Substituting eqts. VIII.61a,b into eqt. VIII.62b and using eqt. VIII.63

$$u = \frac{4c_0 r\theta}{Et} - \int f(\theta) + F(r) \qquad (VIII.64)$$

where $F(r)$ is a function of r.

Substituting eqts. VIII.61c into eqt. VIII.62c using eqts.VIII.

63 and 64:- $\dfrac{1}{tG}\left[\dfrac{e_0}{r} - d_0 r\right] = f'(\theta) + r F'(r) + \int f(\theta)d\theta - F(r)$ (VIII.65)

Equating the θ's, $f'(\theta) + \int f(\theta) = K$

i.e. $f(\theta) = A\sin\theta + B\cos\theta$ (VIII.66)

and r's $\dfrac{1}{tG}\left[\dfrac{e_0}{r} - d_0 r\right] - K = r F'(r) - F(r)$ (VIII.67)

Eqt. VIII.67 is a linear differential equation of the first order with a solution, $F(r) = -\dfrac{e_0}{2Gtr} - \dfrac{d_0}{Gt} r\, \ell u r + Cr + K$ (VIII.68)

Substituting eqts. VIII.66 and 68 into the eqts. VIII.63 and 64 for v and u:-

$$v = \frac{1}{tE}\left[-\frac{a_0(1+v)}{r} + 2c_0 r(1-v)(\ell n r - 1) + 2b_0 r(1-v) + c_0 r(1-3v)\right.$$
$$\left. + 2d_0 r\theta(1-v)\right] + A\sin\theta + B\cos\theta$$

$$u = \frac{4c_0 r\theta}{Et} - \frac{e_0}{2Gtr} - \frac{d_0 r}{Gt}\,\ell u r + Cr - A\cos\theta + B\sin\theta \qquad \text{(VIII.69a,b)}$$

Equations VIII.61 and 69 give the values of N_{rr}, $N_{\theta\theta}$, $N_{r\theta}$, v and u and contain EIGHT constants.

Derivation of Constants

Since N_{rr}, $N_{\theta\theta}$, $N_{r\theta}$, v and u must be independent of θ

$d_0 = c_0 = A = B = 0$ (VIII.70a-d)

At $r = r_2$, $v = u = 0$ and $r = r_p$, $\varepsilon_\theta = \dfrac{1}{Et}(N_{\theta\theta} - v N_{rr}) = 0$

At any radius r, $N_{r\theta} = T/2\pi r^2$ (VIII.71a-d)

(VIII.72a-d)

Using the conditions eqt. VIII.71, $a_0 = b_0 = 0$, $e_0 = \dfrac{T}{2\pi}$, $C = \dfrac{T}{4\pi tG r_2^2}$

Substituting eqts. VIII.70 and 72 into eqts. VIII.61 and 69

$N_{rr} = N_{\theta\theta} = v = 0$; $N_{r\theta} = \dfrac{T}{2\pi r^2}$, $u = \dfrac{T}{4\pi tG}\left[\dfrac{r}{r_2^2} - \dfrac{1}{r}\right]$ (VIII.73a-e)

When $r_2 \to \infty$, then u becomes $u = -\dfrac{T}{4\pi tG}\cdot\dfrac{1}{r}$ (VIII.74)

VIII.4   A 'TWISTING' MOMENT APPLIED TO A SPHERE

A sphere is subjected to a 'twisting' moment T, acting in its plane and applied at the crown.

The following method consists of simplifying the general equations of equilibrium by omitting the membrane normal stress and the bending stress resultants, as second order terms. Such results in a shear stress resultant $N_{\phi\theta}$ at colatitude angle (ϕ) and angle θ of

$$N_{\phi\theta} = T/2\pi r^2 \qquad\qquad\qquad (VIII.75)$$

This equation is the same as that for a flat plate under the same load action.

From eqt. I.29c the shear strain may be defined as follows:-

$$\gamma_{\phi\theta} = \frac{\partial u}{\partial \phi}\frac{1}{R} - \frac{u}{r}\cos\phi + \frac{1}{r}\frac{\partial v}{\partial \theta} \qquad\qquad (VIII.76)$$

For this case the displacements are independent of θ , thus eqt. VIII.76 can be written:-

$$\gamma_{\phi\theta} = \frac{du}{d\phi}\frac{1}{R} - \frac{u}{r}\cos\phi$$

$$\gamma_{\phi\theta} = \frac{du}{Rd\phi} - \frac{u}{Rr}\cdot\frac{dr}{d\phi} \qquad \text{since } r = R\sin\phi .$$

Thus, $\gamma_{\phi\theta} = \left[\frac{d}{d\phi}\left(\frac{u}{r}\right)\right]\frac{r}{R} = \frac{N_{\phi\theta}}{Gt} = \frac{T}{2\pi r^2 Gt}$ \qquad from eqt. VIII.75

$$\therefore \frac{d}{d\phi}\left(\frac{u}{r}\right) = \frac{T}{2\pi R^2 \sin^3\phi . Gt}$$

Thus \qquad $\frac{u}{r} = \frac{T}{2\pi R^2 Gt}\left[\int\frac{d\phi}{\sin^3\phi}\right]$

$$\frac{u}{r} = \frac{T}{2\pi R^2 Gt}\left[-\frac{1}{2}\text{cosec}\,\phi\cot\phi + \frac{1}{2}\ln.\tan\frac{\phi}{2}\right] + C$$

in terms of r and R, \quad $\frac{u}{r} = \frac{T}{4\pi R^2 Gt}\left[-\frac{R}{r^2}\sqrt{R^2-r^2} + \ln\left(\frac{r}{R+\sqrt{R^2-r^2}}\right)\right] + C$

At the outer boundary $r = r_2$ and u = 0, thus C can be found, giving:-

$$u = \frac{T}{4\pi t G}\left[\frac{\sqrt{R^2-r_2^2}}{Rr_2^2} - \frac{\sqrt{R^2-r^2}}{Rr^2} + \frac{1}{R^2}\ln\left(\frac{r}{r_2}\right)\left(\frac{R+\sqrt{R^2-r_2^2}}{R+\sqrt{R^2-r^2}}\right)\right]r \qquad (VIII.77)$$

VIII.5 AN EXAMINATION OF MEMBRANE DISPLACEMENTS AS EXACT SOLUTIONS OF THE GENERAL EQUATION FOR THE EDGE LOADED SHELL

As stated in Chapter I p.47, the complete solution to the problem of the edge loaded spherical shell is the sum of the following three effects:-

(1) Membrane Displacement:- giving rise to membrane resultant forces, and to small 'membrane moments'.

(2) Inextensional Deformation

(3) Oscillatory Solutions

It is proposed to examine section (1) in this Appendix, discussing in some detail the case of $n = 1$.

The governing equation is eqt. I.73:-

$$\frac{d^2 w_n}{d\phi^2} + \frac{d w_n}{d\phi} \cot\phi + w_n\left(2 - \frac{n^2}{\sin^2\phi}\right) = 0 \qquad (I.73)$$

Axi-Symmetrical Case, $n = 0$

In this case eqt. I.73 becomes:- $\frac{d^2 w_0}{d\phi^2} + \frac{d w_0}{d\phi}\cot\phi + w_0\left(2 - \frac{n^2}{\sin^2\phi}\right) = 0$

Substituting $\quad w_0 = \left(\int q \cdot dq + C\right)\cos\phi \qquad (VIII.79)$

into eqt. VIII.78, the equation is then reduced to a first order differential equation in q:- $\frac{dq}{d\phi} + q\left(\cot\phi - 2\tan\phi\right) = 0$

with a solution $q = B_0/\cos^2\phi.\sin\phi$. Thus from eqt. VIII.79,

$$w_0 = \frac{B_0}{2}\left[\cos\phi \ln\frac{1-\cos\phi}{1+\cos\phi} + 2\right] + C\cos\phi \qquad (VIII.80).$$

Comparing this equation with eqt. II.117 it is seen that the membrane displacement is $\frac{B_0}{2}\left[\cos\phi \ln\frac{1-\cos\phi}{1+\cos\phi} + 2\right]$ where $\frac{B_0}{2} = \frac{P(1+v)}{\pi E t}$

The term $C\cos\phi$ is the inextensional deformation.

It is thus concluded that the membrane displacement given by eqt. II.117 is an exact solution of the eqt. I.73.

First Harmonic $\quad n = 1.$ $\qquad$ In this case eqt. I.73 becomes:-

$$\frac{d^2 w_1}{d\phi^2} + \frac{d w_1}{d\phi}\cot\phi + w_1\left(2 - \frac{1}{\sin^2\phi}\right) = 0 \qquad (VIII.81)$$

By the substitution $\quad w_1 = \left(\int q \cdot d\phi - D_1\right)\sin\phi \qquad (VIII.82)$

eqt. VIII.81 is reduced to a second order differential equation

in q:- $\frac{dq}{d\phi}\sin\phi + 3q\cos\phi = 0$ with a solution $q = \frac{4B_4}{\sin^3\phi}$

Thus from eqt. VIII.82:- $w_1 = B_4\left[-2\cot\phi + \sin\phi \ln\frac{1-\cos\phi}{1+\cos\phi}\right] - D_1\sin\phi$ (VIII.83)

where B_4 and D_1 are constants.

Similar relations can be obtained for u_1 and v_1 in the follow-

ing manner.

Determination of u_1 Since $T = 0$, for these solutions (Chapter

I p.45) eqt. I.68c may be written:- $\Gamma = \omega - \frac{1}{2}\frac{\partial\omega}{\partial\phi}\sin\phi$ (VIII.84)

Since from eqt. I.66a $u = \partial\Gamma/\partial\theta\sin\phi$, eqt. VIII.84 may be

written:- $u = \frac{\partial\omega}{\partial\theta\sin\phi} - \frac{1}{2}\frac{\partial^2\omega}{\partial\theta\partial\phi}$ (VIII.85)

Putting $u = u_n \sin n\theta$, $w = w_n \cos n\theta$, $\omega = \omega_n \cos n\theta$ into eqt. VIII.85:-

$u_n \sin n\theta = -\frac{n\omega_n \sin n\theta}{\sin\phi} + \frac{1}{2}n\sin n\theta\frac{\partial\omega_n}{\partial\phi}$ which for $n = 1$

becomes:- $u_1 = -\frac{\omega_1}{\sin\phi} + \frac{1}{2}\frac{\partial\omega_1}{\partial\phi}$ (VIII.86)

The value of w_1 is given by eqt. VIII.83, and since $H(\omega) = 0$ from

eqt. I.68a, the form of ω_1 is similar to w_1 , thus:-

$\omega_1 = -(2B_3 + 2B_4)\left[-2\cot\phi + \sin\phi \ln\frac{1-\cos\phi}{1+\cos\phi}\right] - 2D_2\sin\phi$ (VIII.87)

where B_3 and B_4 are constants relating to possible types of

loading and D_2 to a body rotation.

Thus from eqts. VIII.83 and 87:- $u_1 = -B_4\left[\frac{2(1-\cos\phi)}{\sin^2\phi} + 2 + (1+\cos\phi)\ln\frac{1-\cos\phi}{1+\cos\phi}\right] -$

$-B_3\left[\frac{2}{\sin^2\phi} + 2 + \cos\phi \ln\frac{1-\cos\phi}{1+\cos\phi}\right] + D_1 - D_2\cos\phi$ (VIII.88)

Determination of v_1 From eqts. I.66b and I.67b,c,

$v = \frac{\partial\Theta}{\partial\phi} = \frac{\partial\Gamma}{\partial\phi} - \omega\sin\phi$ (VIII.89)

From eqt. VIII.84 using the relation $H(\omega) = 0$

$v = \frac{\partial\omega}{\partial\phi} + \frac{\partial^2\omega}{\partial\theta^2}\frac{1}{2\sin\phi}$ (VIII.90)

Putting $w = w_n \cos n\theta$, $\omega = \omega_n \cos n\theta$ and $v = v_n \cos n\theta$ into eqt. VIII.90

yields:- $v_n = \frac{\partial\omega_n}{\partial\phi} - \frac{n^2}{2\sin\phi}\omega_n$

Thus for $n = 1$, $v_1 = \frac{\partial\omega_1}{\partial\phi} - \frac{\omega_1}{2\sin\phi}$ (VIII.91)

Using eqts. VIII.83 and VIII.87, eqt. VIII.91 becomes:-

$$v_1 = B_4\left[2\frac{(1-\cos\phi)}{\sin^2\phi} + 2 + (1+\cos\phi)\ln\frac{(1-\cos\phi)}{(1+\cos\phi)}\right]$$

$$+ B_3\left[\ln\frac{1-\cos\phi}{1+\cos\phi} - 2\frac{\cos\phi}{\sin^2\phi}\right] + D_2 - D_1\cos\phi \qquad (VIII.92)$$

The equations VIII.83, 88 and 92 give values of w, u and v which satisfy the general equations I.68a,b, and which are in fact the membrane and inextensional displacement relations. For the membrane displacements the constants B_3 and B_4 have particular values relating to the appropriate applied loading - in this case moment and tangential loading of the shell, and are determined by considering the membrane state. These displacements give rise to both resultant forces and moments, and these will also be determined since they are used in Chapter II of the thesis.

Membrane Analysis

(1) Membrane Forces. From the equilibrium equations relevant to the membrane case and for the first harmonic, it is possible to express $N_{\phi\phi}$, $N_{\theta\theta}$ and $N_{\phi\theta}$ in terms of two integration constants (FLÜGGE[5]) such that:- $N_{\phi\phi_1} = -N_{\theta\theta_1} = \frac{1}{2\sin^2\phi}\left(C_1\cot\frac{\phi}{2} + C_2\tan\frac{\phi}{2}\right)$

$$N_{\phi\theta_1} = \frac{1}{2\sin^2\phi}\left(C_1\cot\frac{\phi}{2} - C_2\tan\frac{\phi}{2}\right) \qquad (VIII.93a,b)$$

where $N_{\phi\phi} = N_{\phi\phi_1}\cos\theta$, $N_{\theta\theta} = N_{\theta\theta_1}\cos\theta$, $N_{\phi\theta} = N_{\phi\theta_1}\sin\theta$.

It is noted that at the poles $\phi = 0$ and $\phi = \pi$ these values become infinite. In order to examine the singularity at the pole a spherical cap of radius R, and chord radius $R\sin\phi$ is considered. The forces acting on the cap are the resultant forces $N_{\phi\phi}$ and $N_{\phi\theta}$ and the external forces at the pole as yet undetermined - Fig. VIII.2. Summing the resultant forces:-

$$\int_0^{2\pi} N_{\phi\phi}\cos\phi.\cos\theta.R\sin\phi.d\theta - \int_0^{2\pi} N_{\phi\theta}\sin\theta.R\sin\phi.d\theta \qquad (VIII.94)$$

and the resultant moment with respect to the diameter $\theta = \frac{\pi}{2}$:-

$$\int_0^{2\pi} N_{\phi\phi}\sin\phi . R\sin\phi \cos\theta . R\sin\phi . d\theta \qquad \text{(VIII.95)}$$

Using $N_{\phi\phi} = N_{\phi\phi_1}\cos\theta$ and $N_{\phi\theta} = N_{\phi\theta_1}\sin\theta$, the integrals may be evaluated. Considering the limiting values of the resulting actions, eqts. VIII.94 and 95, at $\phi = 0$, it is seen that external actions must
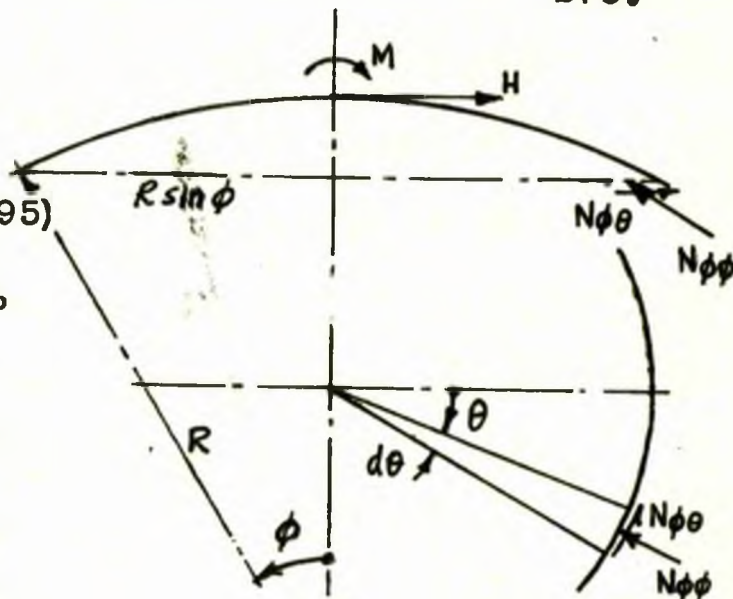
Fig. VIII.2

be applied at the pole to maintain equilibrium. These are:-

A tangential force $H = -\pi R \lim_{\phi \to 0}(N_{\phi\phi_1}\cos\phi\sin\phi - N_{\phi\theta_1}\sin\phi)$ (VIII.96)

and an external moment $M = -\pi R^2 \lim_{\phi \to 0}(N_{\phi\phi_1}\sin^3\phi)$ (VIII.97)

Introducing eqts. VIII.93 into eqt. VIII.96 leads to :-

$$H = \frac{\pi R}{2}(C_1 - C_2) \qquad \text{(VIII.98)}$$

and introducing eqts. VIII.93 into eqt. VIII.97, $M = -\pi R^2 C_1$ (VIII.99)

From eqts. VIII.98 and 99, $C_1 = -\dfrac{M}{\pi R^2}$, and $C_2 = -\dfrac{2H}{\pi R} - \dfrac{M}{\pi R^2}$ (VIII.100a,b)

Substituting these values for C_1 and C_2 into eqts. VIII.93a,b

$$N_{\theta\theta_1} = -N_{\phi\phi_1} = \frac{M}{\pi R^2 \sin^3\phi} + \frac{H(1-\cos\phi)}{\pi R \sin^3\phi}$$

$$N_{\phi\theta_1} = -\frac{M\cos\phi}{\pi R^2 \sin^3\phi} + \frac{H(1-\cos\phi)}{\pi R \sin^3\phi} \qquad \text{(VIII.101a,b)}$$

(2) <u>Displacements.</u> The general equations for strain and deformation are given in Chapter I, (eqts. I.29a-c). They can be written as follows:-

$$\frac{\partial u}{\partial\theta} + v\cos\phi + w\sin\phi = R\varepsilon_\theta \sin\phi$$

$$\frac{\partial v}{\partial\phi} + w = R\varepsilon_\phi$$

$$\frac{\partial u}{\partial\phi}\sin\phi - u\cos\phi + \frac{\partial v}{\partial\theta} = R\gamma_{\phi\theta}\sin\phi \qquad \text{(VIII.102a-c)}$$

These can be reduced to a set of ordinary differential equations for the first harmonic by the substitution:-

$u = u_1\sin\theta$, $v = v_1\cos\theta$, $w = w_1\cos\theta$, $\varepsilon_\phi = \varepsilon_{\phi_1}\cos\theta$, $\varepsilon_\theta = \varepsilon_{\theta_1}\cos\theta$, $\gamma_{\phi\theta} = \gamma_{\phi\theta_1}\sin\theta$.

$$u_1 + v_1 \cos\phi + w_1 \sin\phi \quad = R\varepsilon_{\theta_1} \sin\phi$$

$$\frac{dv_1}{d\phi} + w_1 \quad = R\varepsilon_{\phi_1}$$

$$\frac{du_1}{d\phi} \sin\phi - u_1 \cos\phi - v_1 \quad = R\gamma_{\phi\theta_1} \sin\phi \qquad \text{(VIII.103a-c)}$$

Eliminating u_1 and w_1 from eqt. VIII.103a-c

$$\frac{d^2v_1}{d\phi^2} \sin^2\phi - \frac{dv_1}{d\phi} \sin\phi\cos\phi = R\gamma_{\phi\theta_1}\sin\phi + R\sin^2\phi\left[\frac{d\varepsilon_{\phi_1}}{d\phi} - \frac{d\varepsilon_{\theta_1}}{d\phi}\right] \qquad \text{(VIII.104)}$$

The R.H.S. of eqt. VIII.104 contains $\gamma_{\phi\theta_1}$, $\dfrac{d\varepsilon_{\phi_1}}{d\phi}$ and $\dfrac{d\varepsilon_{\theta_1}}{d\phi}$

Rearranging eqts. I.32:-

$$\varepsilon_{\phi_1} = \frac{1}{Et}(N_{\phi\phi_1} - vN_{\theta\theta_1}), \quad \varepsilon_{\theta_1} = \frac{1}{Et}(N_{\theta\theta_1} - vN_{\phi\phi_1}), \quad \gamma_{\phi\theta_1} = \frac{2(1+v)}{Et}N_{\phi\theta_1}$$

From eqts. VIII.101a,b,

$$\varepsilon_{\phi_1} = -\frac{(1+v)}{Et\,\pi R\sin^3\phi}\left[\frac{M}{R} + H(1-\cos\phi)\right]$$

$$\varepsilon_{\theta_1} = +\frac{(1+v)}{Et\,\pi R\sin^3\phi}\left[\frac{M}{R} + H(1-\cos\phi)\right]$$

$$\gamma_{\phi\theta_1} = \frac{-2(1+v)}{Et\,\pi R\sin^3\phi}\left[\frac{M}{R}\cos\phi - H(1-\cos\phi)\right] \qquad \text{(VIII.105)}$$

Thus from eqt. VIII.105,

$$\frac{d\varepsilon_{\phi_1}}{d\phi} = -\frac{(1+v)}{Et\pi R\sin^3\phi}\left\{-\frac{3\cos\phi}{\sin\phi}\left[\frac{M}{R} + H(1-\cos\phi)\right] + H\sin\phi\right\}$$

$$\frac{d\varepsilon_{\theta_1}}{d\phi} = +\frac{(1+v)}{Et\pi R\sin^3\phi}\left\{-\frac{3\cos\phi}{\sin\phi}\left[\frac{M}{R} + H(1-\cos\phi)\right] + H\sin\phi\right\} \quad \text{(VIII.106)}$$

Substituting eqts. VIII.105 and 106 into eqt. VIII.104 yields:-

$$\frac{d^2v_1}{d\phi^2}\sin^2\phi - \frac{dv_1}{d\phi}\sin\phi\cos\phi = +\frac{4(1+v)\cos\phi}{Et\pi\sin^2\phi}\left[\frac{M}{R} + H(1-\cos\phi)\right] \qquad \text{(VIII.107)}$$

Using the substitution $x = 1-\cos\phi$ in eqt. VIII.107, it reduces to:-

$$\frac{d^2v_1}{dx^2} = +\frac{4(1+v)(1-x)}{Et\,\pi x^3(2-x)^3}\left[\frac{M}{R} + Hx\right] \qquad \text{(VIII.108)}$$

The R.H.S. of eqt. VIII.108 can be separated using partial

fractions and by this means a particular solution can be obtained.

To this must be added the complementary function, $v_1 = D_2 - D_1\cos\phi$.

The complete result is:- $v_1 = -\dfrac{M(1+v)}{4\pi REt}\left[\ln\dfrac{1-\cos\phi}{1+\cos\phi} - \dfrac{2\cos\phi}{\sin^2\phi}\right] -$

$$- \frac{H(1+v)}{4\pi Et}\left[\frac{2(1-\cos\phi)}{\sin^2\phi} + 2 + (1+\cos\phi)\ln\frac{1-\cos\phi}{1+\cos\phi}\right] + D_2 - D_1\cos\phi \quad \text{(VIII.109)}$$

From eqt. VIII.103b $w_1 = R\varepsilon_{\phi_1} - \dfrac{dv_1}{d\phi}$. Thus using eqts. VIII.105 & 109

$$w_1 = -\frac{H(1+v)}{4\pi Et}\left[\sin\phi\ln\frac{1-\cos\phi}{1+\cos\phi} - \frac{2\cos\phi}{\sin\phi}\right] - D_1\sin\phi \qquad \text{(VIII.110)}$$

Substituting eqts. VIII.109 and 110 into eqt. VIII.103a gives:-

$$u_1 = +\frac{M(1+\upsilon)}{4\pi Et R}\left[\frac{2}{\sin^2\phi} + 2 + \cos\phi\, \ell u \frac{1-\cos\phi}{1+\cos\phi}\right] +$$

$$+ \frac{H(1+\upsilon)}{4\pi Et}\left[\frac{2(1-\cos\phi)}{\sin^2\phi} + 2 + (1+\cos\phi)\ell u \frac{1-\cos\phi}{1+\cos\phi}\right] + D_1 - D_2\cos\phi \quad \text{(VIII.111)}$$

Comparing eqts. VIII.109, 110 and 111 for v_1, w_1 and u_1 with

eqts. VIII.92, 83 and 88 obtained earlier, it is noted that

the constants B_3 and B_4 are as follows:- $B_3 = -\frac{M(1+\upsilon)}{4\pi REt}$ & $B_4 = -\frac{H(1+\upsilon)}{4\pi Et}$

(3) Resulting Moment Actions. The displacements v_1, w_1

and u_1 are the displacements of the middle surface of the shell,

and in the general case will produce membrane rotation with

corresponding 'membrane moments'. These are generally of small

magnitude depending on the R/t ratio and the value of ϕ. Their

values may be obtained from the resultant moment - displacement

relationships:-

$$M_{\theta\theta} = \frac{Et^3}{12(1-\upsilon^2)R^2}\left[-\frac{\partial u}{\partial\theta\sin\phi} - \upsilon\cot\phi + \frac{\partial w}{\partial\phi}\cot\phi + \frac{\partial^2 w}{\partial\theta^2\sin^2\phi} - \upsilon\frac{\partial v}{\partial\phi} + \upsilon\frac{\partial^2 w}{\partial\phi^2}\right]$$

$$M_{\phi\phi} = \frac{Et^3}{12(1-\upsilon^2)R^2}\left[-\frac{\partial v}{\partial\phi} + \frac{\partial^2 w}{\partial\phi^2} - \upsilon\frac{\partial u}{\partial\theta\sin\phi} - \upsilon\upsilon\cot\phi + \upsilon\frac{\partial w}{\partial\phi}\cot\phi + \frac{\upsilon}{\sin^2\phi}\frac{\partial^2 w}{\partial\theta^2}\right]$$

$$M_{\theta\phi} = M_{\phi\theta} = \frac{Et^3(1-\upsilon)}{24(1-\upsilon^2)R^2}\left[u\cot\phi - \frac{\partial u}{\partial\phi} - \frac{\partial v}{\partial\theta\sin\phi} - 2\frac{\partial w}{\partial\theta}\frac{\cos\phi}{\sin^2\phi} + 2\frac{\partial^2 w}{\partial\theta\partial\phi\sin\phi}\right] \quad \text{(VIII.112a-c)}$$

Using the relationships, $u = u_1\sin\theta$, $v = v_1\cos\theta$, $w = w_1\cos\theta$,

$$M_{\theta\theta} = M_{\theta\theta_1}\cos\theta, \quad M_{\phi\phi} = M_{\phi\phi_1}\cos\theta, \quad M_{\phi\theta} = M_{\phi\theta_1}\sin\theta$$

eqts. VIII.112a-c can be reduced to a set of ordinary differential

equations:- $M_{\theta\theta_1} = \frac{Et^3}{12(1-\upsilon^2)R^2}\left[-\frac{u_1}{\sin\phi} - \upsilon_1\cot\phi + \frac{dw_1}{d\phi}\cot\phi - \frac{w_1}{\sin^2\phi} - \upsilon\frac{dv_1}{d\phi} + \upsilon\frac{d^2w_1}{d\phi^2}\right]$

$$M_{\phi\phi_1} = \frac{Et^3}{12(1-\upsilon^2)R^2}\left[-\frac{dv_1}{d\phi} + \frac{d^2w_1}{d\phi^2} - \frac{\upsilon u_1}{\sin\phi} - \upsilon\upsilon_1\cot\phi + \upsilon\frac{dw_1}{d\phi}\cot\phi - \frac{\upsilon w_1}{\sin^2\phi}\right]$$

$$M_{\theta\phi_1} = M_{\phi\theta_1} = \frac{Et^3(1-\upsilon)}{24(1-\upsilon^2)R^2}\left[u_1\cot\phi - \frac{du_1}{d\phi} + \frac{v_1}{\sin\phi} + \frac{2w_1\cos\theta}{\sin^2\phi} - \frac{2dw_1}{d\phi\sin\phi}\right] \quad \text{(VIII.113a-c)}$$

By substituting values for v_1, w_1 and u_1 from eqts. VIII.109, 110,

111 together with their differentials into eqts. VIII.113a-c:-

$$M_{\theta\theta_1} = -\frac{Mk}{\pi R\sin^3\phi} - \frac{Hk}{\pi\sin^3\phi}, \qquad M_{\phi\phi_1} = +\frac{Mk}{\pi R\sin^3\phi} + \frac{Hk}{\pi\sin^3\phi}$$

$$M_{\phi\theta_1} = +\frac{Mk\cos\phi}{\pi R\sin^3\phi} + \frac{Hk\cos\phi}{\pi\sin^3\phi} \qquad \text{(VIII.114a-c) where } k = \frac{t^2}{12R^2}$$

VIII.6   A 'TWISTING' MOMENT APPLIED TO A SHALLOW SPHERICAL SHELL BY MEANS OF A CIRCULAR RING

The spherical shell is loaded
by a moment T, transmitted to the
shell round the circumference of a
ring radius r_o - Fig. VIII.3.   The
solution of this problem is con-
sidered in two parts.
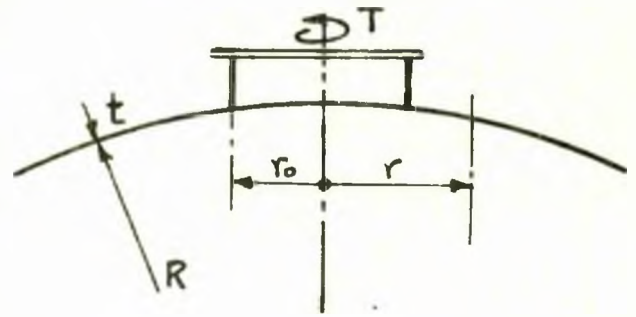
Fig. VIII.3

(1)   The part of the shell inside the loaded ring.

(2)   The part of the shell outside the loaded ring.

(1)   Inside the Loaded Ring. $0 \leqslant r \leqslant r_o$

Using the relevant equations obtained from the basic actions
for the shallow shell, eqts. II.69, 70, 71 and 74:-

$$w_i = C_1 \, ber \, r/\ell + C_2 \, bei \, r/\ell + C_3 \, ker \, r/\ell + C_4 \, kei \, r/\ell - A_o$$

$$F_i = \frac{\ell^2 t E}{R} \left(-C_2 \, ber \, r/\ell + C_1 \, bei \, r/\ell - C_4 \, ker \, r/\ell + C_3 \, kei \, r/\ell \right) + C_5 \theta \qquad \text{(VIII.115a-b)}$$

Derivation of Constants C_3 , C_4 , C_5

At $r = 0$ $\begin{cases} w & \text{are to be finite} \\ N_{rr} & " \\ N_{\theta\theta} & " \end{cases}$ yielding $\begin{cases} C_3 = 0 \\ C_4 = 0 \\ C_5 = 0 \end{cases}$

(VIII.116a-c)

Verification of eqts. VIII.116a-c is as follows:-

(a)   At $r = 0$, $ker \, r/\ell \to \infty$.   Thus for w_i to be finite, $C_3 = 0$.

(b) $N_{rr} = \frac{\ell t E}{R} \left[-C_2 \frac{ber' \, r/\ell}{r} + C_1 \frac{bei' \, r/\ell}{r} - C_4 \frac{ker' \, r/\ell}{r} \right]$

At $r \to 0$, $\frac{ber' \, r/\ell}{r} \to 0$, $\frac{bei' \, r/\ell}{r} \to 0$ and $\frac{ker' \, r/\ell}{r} \to \infty$

Therefore for Nrr to be finite at $r = 0$, $C_4 = 0$.

(c) $N_{r\theta} = -\frac{\partial}{\partial r} \left(\frac{1}{r} \frac{\partial F}{\partial \theta} \right) = +\frac{C_5}{r^2}$ At $r = 0$, $N_{r\theta}$ must be finite, i.e. $C_5 = 0$

Therefore :- $w_i = C_1 \, ber \, r/\ell + C_2 \, bei \, r/\ell - A_o$

$$F_i = \frac{\ell^2 t E}{R} \left(C_1 \, bei \, r/\ell - C_2 \, ber \, r/\ell \right) \qquad \text{(VIII.117a,b)}$$

(2)   Outside the Loaded Ring. i.e. $r_0 \leqslant r \leqslant \infty$

$$w_0 = C_6 \, ber \, ^r\!/_\ell + C_7 \, bei \, ^r\!/_\ell + C_8 \, ker \, ^r\!/_\ell + C_9 \, kei \, ^r\!/_\ell - A_1$$

$$F_0 = \frac{\ell^2 t E}{R}\left(C_6 \, bei \, ^r\!/_\ell - C_7 \, ber \, ^r\!/_\ell - C_9 \, ker \, ^r\!/_\ell + C_8 \, kei \, ^r\!/_\ell\right) + C_{10}\theta \quad \text{(VIII.118a,b)}$$

Derivation of constants - C_6, C_7, A_1

At $r \to \infty$ $\begin{cases} M_{rr} \to 0 \\ M_{\theta\theta} \to 0 \\ w \to 0 \end{cases}$ yielding $\begin{cases} C_6 = C_7 = 0 \\ \\ A_1 = 0 \end{cases}$

The complete derivation of these constants is the same as that

given in Appendix VIII.2.1(b)

Thus:- $w_0 = C_8 \, ker \, ^r\!/_\ell + C_9 \, kei \, ^r\!/_\ell$

$$F_0 = \frac{\ell^2 t E}{R}\left(-C_9 \, ker \, ^r\!/_\ell + C_8 \, kei \, ^r\!/_\ell\right) + C_{10}\theta \quad \text{(VIII.119a,b)}$$

Derivation of Constants C_1, C_2, A_0, C_8 and C_9

These five constants are determined from the conditions at

the loaded ring radius, $r = r_0$, namely:-

$\begin{cases} w_i = w_0 \\ Q_{r_i} = Q_{r_0} \\ \mathcal{E}_{\theta_i} = \mathcal{E}_{\theta_0} \\ v_i = v_0 \\ \dfrac{dw_i}{dr} = \dfrac{dw_0}{dr} \end{cases}$ yielding after solving 5 simultaneous linear equations $\Big\} \; C_1 = C_2 = A_0 = C_8 = C_9 = 0$

$$\text{(VIII.120a-e)}$$

The details of the above are given below:-

From eqts. VIII.117 and 118

$w_i = w_0$:- $C_1 \, ber \, ^{r_0}\!/_\ell + C_2 \, bei \, ^{r_0}\!/_\ell - C_8 \, ker \, ^{r_0}\!/_\ell - C_9 \, kei \, ^{r_0}\!/_\ell = A_0$

$Q_{r_i} = Q_{r_0}$:- $C_1 \, bei' \, ^{r_0}\!/_\ell - C_2 \, ber' \, ^{r_0}\!/_\ell - C_8 \, kei' \, ^{r_0}\!/_\ell + C_9 \, ker' \, ^{r_0}\!/_\ell = 0$

$\mathcal{E}_{\theta_i} = \mathcal{E}_{\theta_0}$:- $C_1\left[ber \, ^{r_0}\!/_\ell - (1+v)\dfrac{\ell}{r_0} \, bei' \, ^{r_0}\!/_\ell\right] + C_2\left[bei \, ^{r_0}\!/_\ell + (1+v)\dfrac{\ell}{r_0} \, ber' \, \dfrac{r_0}{\ell}\right]$

$\qquad - C_8\left[ker \, ^{r_0}\!/_\ell - (1+v)\dfrac{\ell}{r_0} \, kei' \, ^{r_0}\!/_\ell\right] - C_9\left[kei \, ^{r_0}\!/_\ell + (1+v)\dfrac{\ell}{r_0} \, ker' \, \dfrac{r_0}{\ell}\right] = 0$

$v_i = v_0$:- $-C_1 \, bei' \, ^{r_0}\!/_\ell + C_2 \, ber' \, ^{r_0}\!/_\ell - C_8 \, kei' \, ^{r_0}\!/_\ell + C_9 \, ker' \, ^{r_0}\!/_\ell = -\dfrac{A_0 r_0}{(1+v)\ell}$

$\dfrac{dw_i}{dr} = \dfrac{dw_0}{dr}$:- $C_1 \, ber' \, ^{r_0}\!/_\ell + C_2 \, bei' \, ^{r_0}\!/_\ell - C_8 \, ker' \, ^{r_0}\!/_\ell - C_9 \, kei' \, ^{r_0}\!/_\ell = 0$ (VIII.121a-e)

Multiplying eqt. VIII.121b by $(1+v)\,^\ell\!/_{r_0}$ and adding to eqt.VIII.121c

gives:- $C_1 \, ber \, ^{r_0}\!/_\ell + C_2 \, bei \, ^{r_0}\!/_\ell - C_8 \, ker \, ^{r_0}\!/_\ell - C_9 \, kei \, ^{r_0}\!/_\ell = 0$ (VIII.122)

Comparison of eqt. VIII.121a with eqt. VIII.122 shows that $A_o = 0$.
The resulting four equations are:-

$$C_1 \, \text{ber}\, {}^{r_o}\!/_\ell + C_2 \, \text{bei}\, {}^{r_o}\!/_\ell - C_8 \, \text{ker}\, {}^{r_o}\!/_\ell - C_9 \, \text{kei}\, {}^{r_o}\!/_\ell = 0$$

$$C_1 \, \text{bei}'\, {}^{r_o}\!/_\ell - C_2 \, \text{ber}'\, {}^{r_o}\!/_\ell - C_8 \, \text{kei}'\, {}^{r_o}\!/_\ell + C_9 \, \text{ker}'\, {}^{r_o}\!/_\ell = 0$$

$$C_1 \, \text{ber}'\, {}^{r_o}\!/_\ell + C_2 \, \text{bei}'\, {}^{r_o}\!/_\ell - C_8 \, \text{ker}'\, {}^{r_o}\!/_\ell - C_9 \, \text{kei}'\, {}^{r_o}\!/_\ell = 0$$

$$- C_1 \, \text{bei}'\, {}^{r_o}\!/_\ell + C_2 \, \text{ber}'\, {}^{r_o}\!/_\ell - C_8 \, \text{kei}'\, {}^{r_o}\!/_\ell + C_9 \, \text{ker}'\, {}^{r_o}\!/_\ell = 0 \qquad \text{(VIII.123)}$$

Using simple Determinant Theory:- $C_1 = C_2 = C_8 = C_9 = 0$

Derivation of Constant C_{10}

From rotational equilibrium it is assumed that:-

$$N_{r\theta} \cdot 2\pi r^2 = T \qquad \text{(VIII.124)}$$

Also from eqt. II.4c and eqt. VIII.119b; $\quad N_{r\theta} = C_{10}/r^2 \qquad \text{(VIII.125)}$

From eqts. VIII.124 and 125, $\qquad C_{10} = T/2\pi \qquad \text{(VIII.126)}$

The Tangential Displacement u

From eqt. II.81 $\qquad \gamma_{r\theta} = \dfrac{\partial v}{r\,\partial\theta} + \dfrac{\partial u}{\partial r} - \dfrac{u}{r} = \dfrac{N_{r\theta}}{tG}$

since $\dfrac{\partial v}{\partial \theta} = 0$; $\quad \gamma_{r\theta} = r\dfrac{\partial}{\partial r}\left(\dfrac{u}{r}\right) = \dfrac{N_{r\theta}}{tG} \qquad \text{(VIII.127)}$

Outside the Loaded Ring; From eqt. VIII.124; $N_{r\theta} = \dfrac{T}{2\pi r^2}$ and

thus in eqt. VIII.127 $\quad \gamma_{r\theta} = r\dfrac{\partial}{\partial r}\left(\dfrac{u}{r}\right) = \dfrac{T}{2\pi r^2 tG}$

$$\therefore \quad \dfrac{u_o}{r} = -\dfrac{T}{4\pi tG r^2} + \bar{K}$$

$$u_o = -\dfrac{T}{4\pi tG r} + \bar{K}r$$

when $r \to \infty$, $u \to 0$ $\therefore \bar{K} = 0$ and $u_o = -\dfrac{T}{4\pi tG r} \qquad \text{(VIII.128)}$

Inside the Loaded Ring, since $C_1 = C_2 = 0$, it follows in eqt.
VIII.18b that $F_i = 0$ and further that $N_{r\theta} = 0$. Therefore, in
eqt. VIII.127 $\quad \gamma_{r\theta} = r\dfrac{\partial}{\partial r}\left(\dfrac{u}{r}\right) = 0 \qquad \therefore \quad u_i = \bar{\bar{K}}r$

From eqt. VIII.128 the value of u at $r = r_o$ is:- $u_o = -\dfrac{T}{4\pi tG r_o}$

Since $u_i = u_o$ at $r = r_o$, $\qquad \bar{\bar{K}} = -\dfrac{T}{4\pi tG r_o^2}$

and $\therefore u_i = \dfrac{T}{4\pi tG}\left(\dfrac{r}{r_o^2}\right) \qquad \text{(VIII.129)}$

Meridional Displacement, v

Following out the same procedure as in section II.1.4, relating to the application of a twisting moment at the crown, it is seen that $v = 0$.

The results may be summarized as follows:-

Inside the Ring

$$w_i = F_i = 0$$

$$w = N_{rr} = N_{\theta\theta} = N_{r\theta} = M_{rr} = M_{\theta\theta} = M_{r\theta} = v = 0$$

$$u = -\frac{T}{4\pi Gt}\left(\frac{r}{r_o^2}\right) \qquad\qquad (VIII.130a-i)$$

Outside the Ring

$$w_o = 0, \qquad F_o = \frac{T}{2\pi}\theta$$

$$w = N_{rr} = N_{\theta\theta} = M_{rr} = M_{\theta\theta} = M_{r\theta} = v = 0$$

$$u = -\frac{T}{4\pi Gt}\left(\frac{1}{r}\right), \quad \tau_{r\theta} = \frac{N_{r\theta}}{t} = \frac{T}{2\pi r^2 t} \qquad (VIII.131a-i)$$

It is noted that these equations are similar to those of a flat plate subject to the same loading.

VIII.7 PRESENTATION OF COMPLETE RESULTS FOR THE RADIAL LOADING OF A SHALLOW SHELL AND COMPLETE SPHERE - A Comparison between theory and experiment

In Chapter V typical graphs were presented comparing the experimental and theoretical results for:-

(1) The uniformly distributed radial loading for a shallow shell,

(2) The radial loading of a rigid insert in a complete sphere.

In this section the complete results are given for both these cases.

Figs. VIII.4 and 5 show the direct and bending stresses for the $\frac{1}{4}$in and 1in thick shallow shells, respectively, under the action of a uniformly distributed radial load and Figs. VIII.6 and 7 show radial deflections under the same radial loading, again for both shallow shells.

Fig. VIII.8 presents the direct and bending stresses on a complete sphere due to the radial loading applied to several rigid inserts.
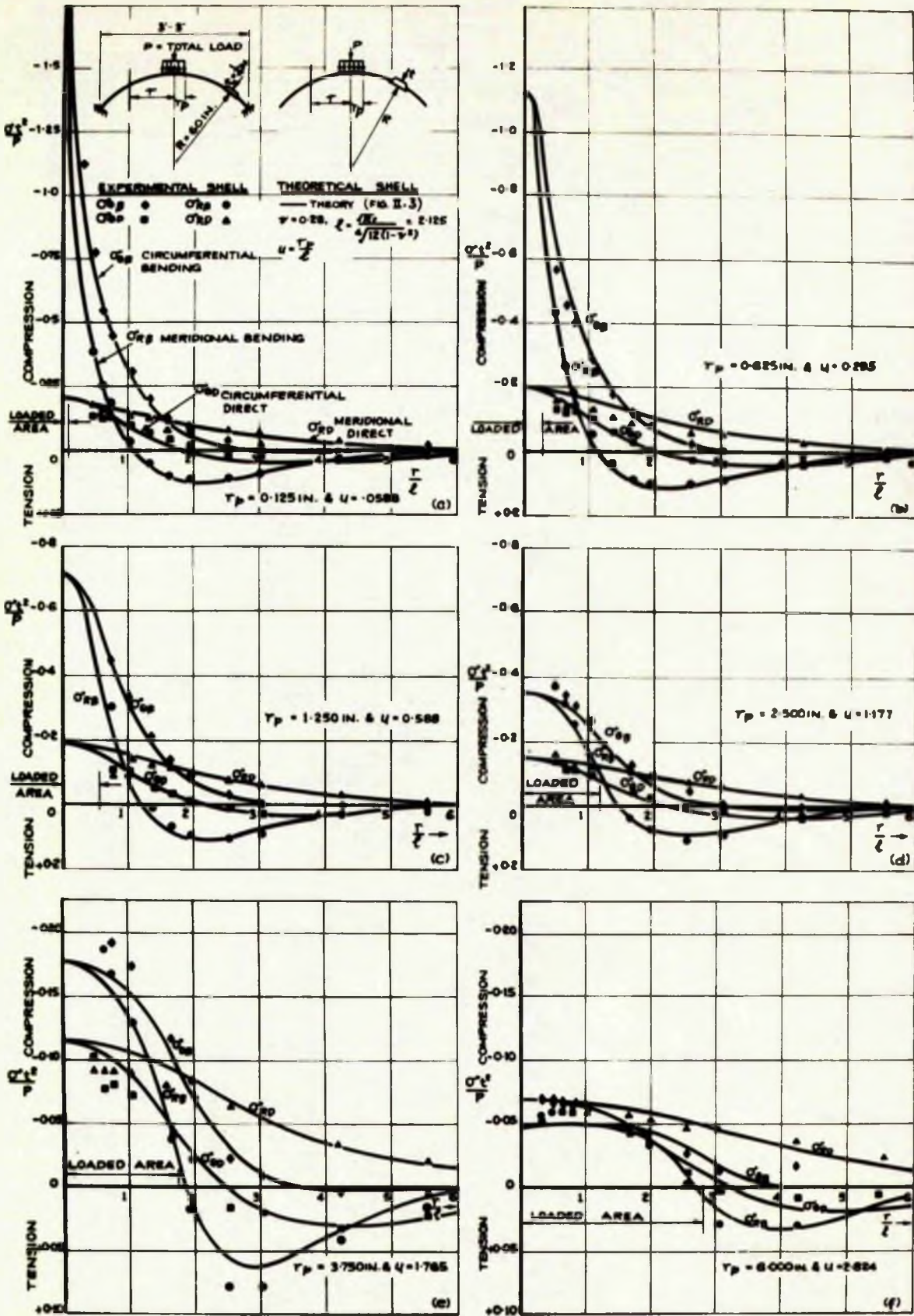
FIG. VII.4   DIRECT AND BENDING STRESSES IN THE MERIDIONAL AND CIRCUMFERENTIAL DIRECTIONS
DUE TO UNIFORMLY DISTRIBUTED AREA LOADS RADIALLY APPLIED AT THE CROWN OF
A ½ IN THICK SHALLOW SPHERICAL SHELL – A COMPARISON OF THEORY AND EXPERIMENT
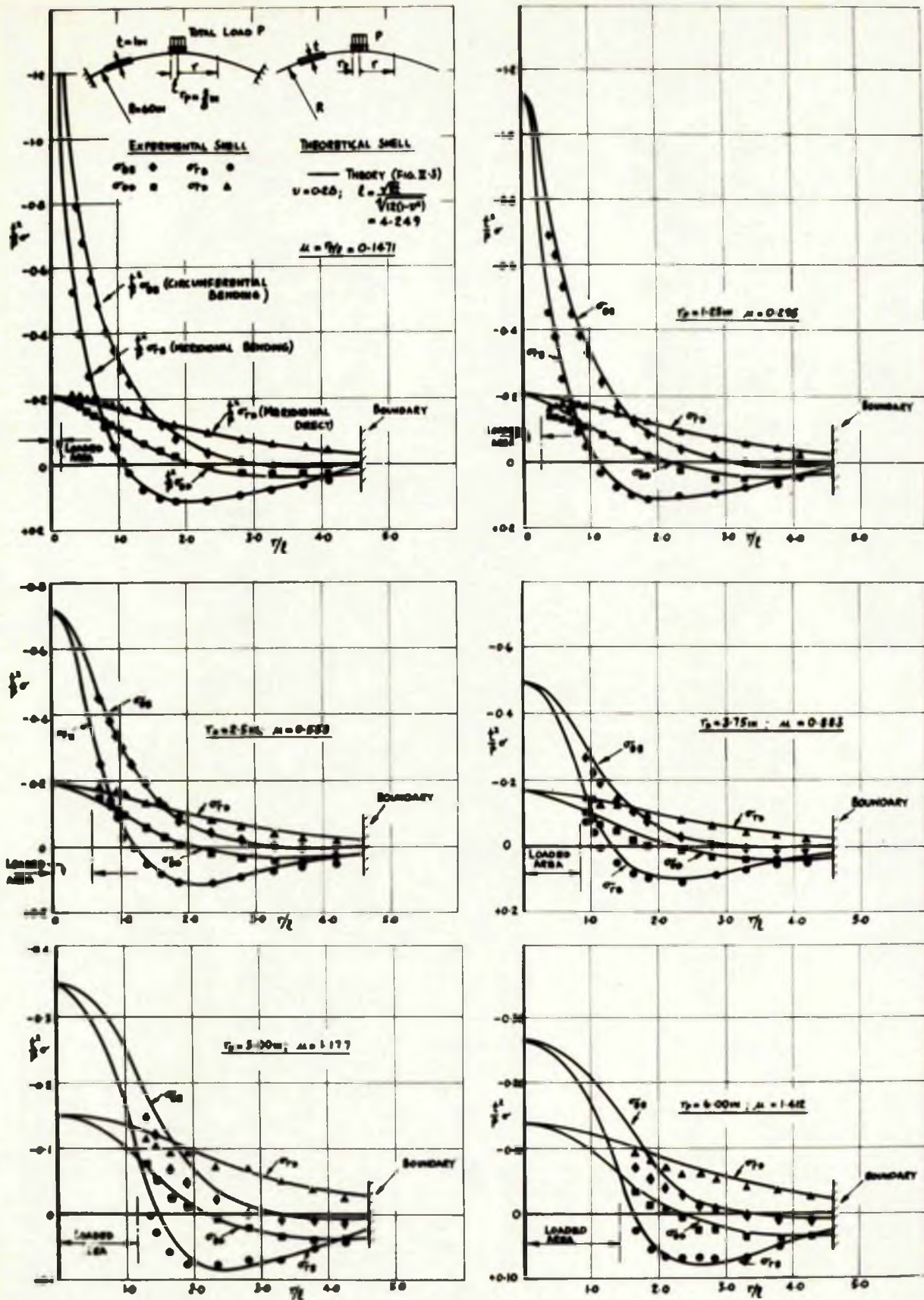
FIG. VIII.5 DIRECT AND BENDING STRESSES IN THE MERIDIONAL AND CIRCUMFERENTIAL DIRECTIONS DUE TO A UNIFORMLY DISTRIBUTED AREA LOADS RADIALLY APPLIED AT THE CROWN OF A 1 IN THICK SHALLOW SHELL - A COMPARISON OF THEORY AND EXPERIMENT
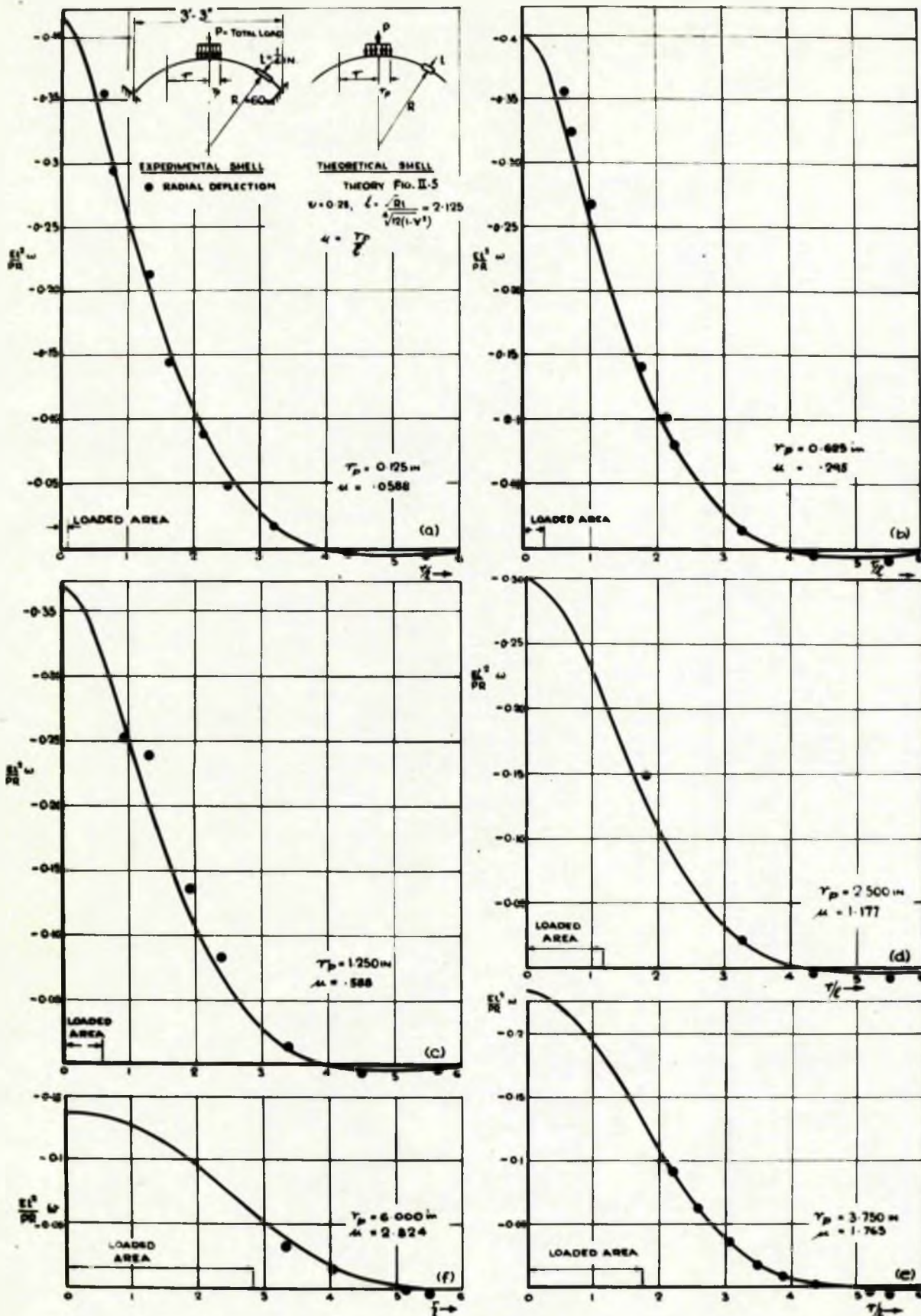
Fig. VIII.6 Radial Deflections due to Uniformly Distributed area loads, radially applied at the crown of a ½ in thick shallow spherical shell – A comparison of Theory and Experiment
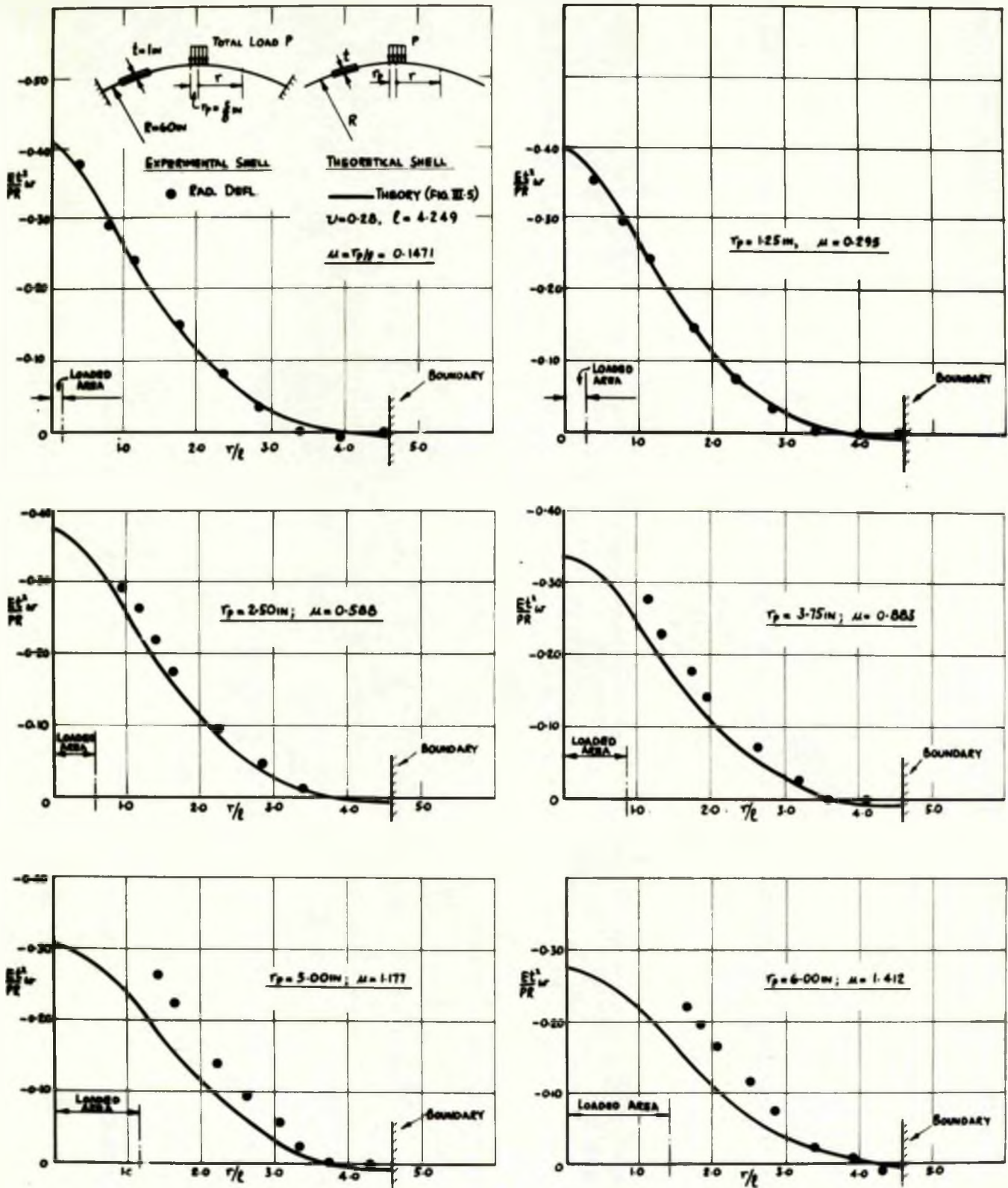
FIG. VIII.7 RADIAL DEFLECTIONS DUE TO UNIFORMLY DISTRIBUTED AREA LOADS RADIALLY APPLIED AT THE CROWN OF A 1IN THICK SHALLOW SPHERICAL SHELL – A COMPARISON OF THEORY AND EXPERIMENT
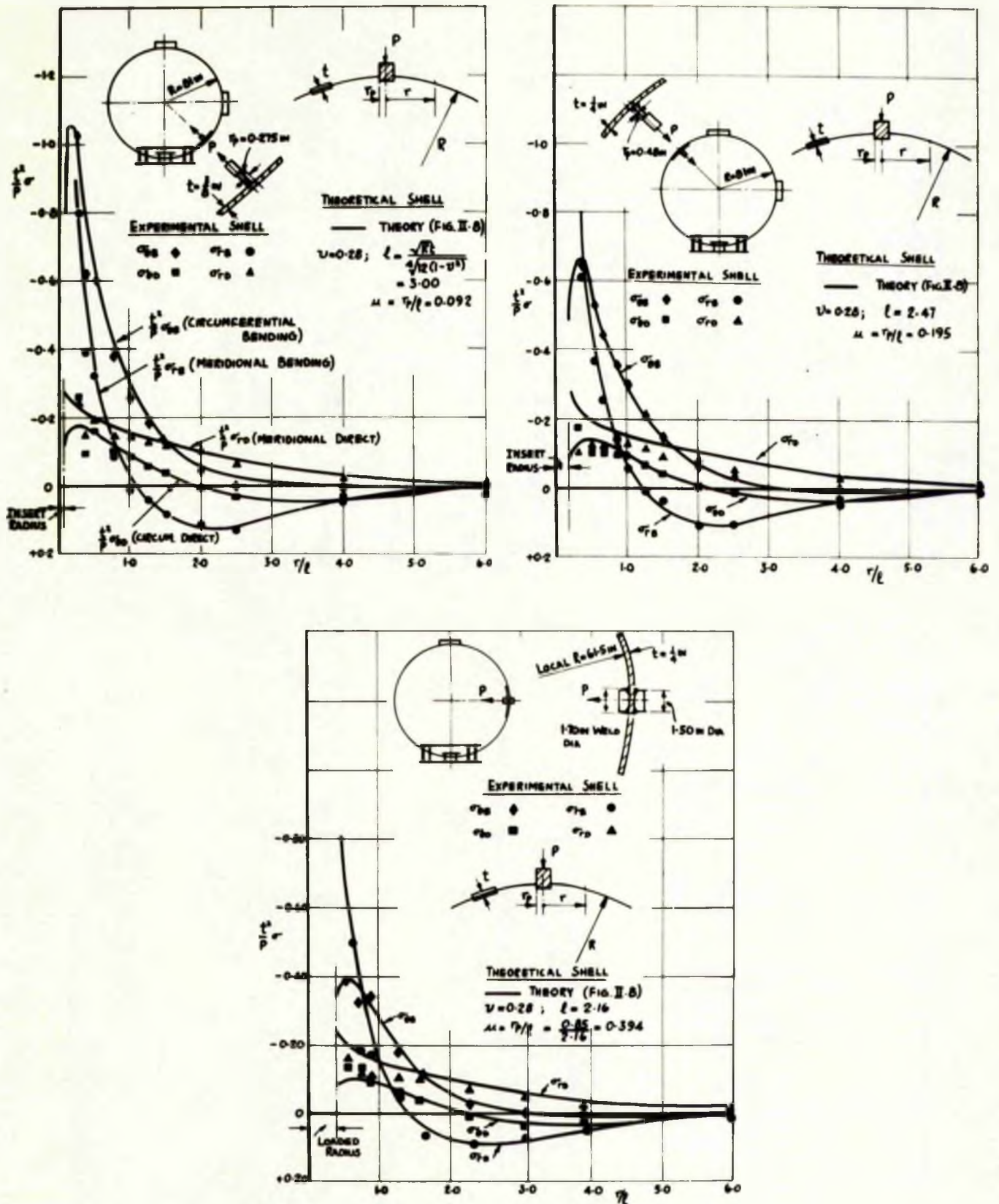
FIG. VIII. 8 DIRECT AND BENDING STRESSES IN THE MERIDIONAL AND CIRCUMFERENTIAL DIRECTIONS DUE TO A RADIALLY LOADED RIGID INSERT ON A COMPLETE SPHERE (μ VALUES 0.092, 0.195 AND 0.394) – A COMPARISON OF THEORY AND EXPERIMENT

VIII.8 NOMENCLATURE

α, β, z	Orthogonal curvilinear co-ordinates. Fig.I.1
x, y, z	Rectangular co-ordinates Fig. I.1
ϕ, θ, R	Spherical Polar co-ordinates Fig. I.2
r, θ	Polar Co-ordinates, - two dimensional Fig. I.6
δs	A distance on the middle surface.
A, B	Lamé Parameters, which define the shell form.
N_{xx}, N_{yy}	Normal forces per unit length acting on sections perpendicular to the x and y directions respectively Fig. I.1a.
N_{xy}, N_{yx}	Shearing forces per unit length in the direction of the y and x axes respectively Fig. I.1a
Q_{xz}, Q_{yz}	Transverse shearing forces per unit length in the direction of the z axis - Fig. I.1a
M_{xx}, M_{yy}	Bending moments per unit length acting on sections perpendicular to the x and y axes respectively Fig. I.1b
M_{xy}, M_{yx}	Twisting moments per unit length.
X, Y, Z	Components of the intensity of the external load (estimated per unit area of the middle surface), parallel to x, y and z axes respectively Fig.I.1a
L, M	Components of the intensity of the external moment. Fig. I.1b
$N_{\theta\theta}, N_{\phi\phi}, N_{rr}$	Normal forces per unit length acting on sections perpendicular to the θ, ϕ and r directions, respectively Figs. I.2 and 6.
$N_{\theta\phi}, N_{\phi\theta}, N_{\theta r}, N_{r\theta}$	Shearing forces per unit length in the direction of the θ, ϕ and r, θ axes respectively, Figs.I.2 & 6.
$Q_{\theta}, Q_{\phi}, Q_{r}$	Transverse shearing forces per unit length in sections θ, ϕ and r = constant. Figs. I.2 and I.6
$M_{\theta\theta}, M_{\phi\phi}, M_{rr}$	Bending moments per unit length acting on sections perpendicular to the θ, ϕ and r axes respectively.
$M_{\theta\phi}, M_{\phi\theta}, M_{\theta r}, M_{r\theta}$	Twisting moments per unit length on sections θ, ϕ and r = constant. Figs. I.2 and I.6.
p_{θ}, p_{r}, p	Components of the intensity of external load, parallel to θ, ϕ and z axes, Fig. I.2.

$p_1', q_1', r_1', p_2',$ q_2', r_2'	Parameters arising from the elastic deformations of the middle surface.
$\varepsilon_1, \varepsilon_2$	Extensional strains of the middle surface in the x, y directions - eqts. I.4a,b.
γ_{12}	Shear strain of the middle surface, eqt. I.4c.
K_1, K_2	Curvature changes of the middle surface in the x, y directions - eqts. I.4d,e.
K_3	Change of twist of the middle surface, eqt. I.4f.
$\varepsilon_x, \varepsilon_y, \varepsilon_z$	Components of strain in the x, y and z directions, situated a distance z from the middle surface, eqts. I.5a,b,d.
$\gamma_{xy}, \gamma_{zx}, \gamma_{yz}$	Components of shear strain situated a distance z from the middle surface, eqts. I.5c,e,f.
$\varepsilon_\theta, \varepsilon_\phi, \varepsilon_r$	Components of strain in the circumferential and meridional directions, eqts. I.29a,b, I.31 & I.81a,b.
$\gamma_{\theta\phi}, \gamma_{\theta r}$	Shear Strain in the θ, ϕ and θ, r planes, eqts. I.29c, I.31 and I.81c.
K_θ, K_ϕ, K_r	Curvature changes in the circumferential and meridional directions - eqts. I.31 and I.81d,e.
$K_{\phi\theta}, K_{r\theta}$	Change of twist in the ϕ, θ and r, θ planes, eqt. I.81f.
u, v, w	Components of displacement of any point on the unstrained middle surface in the x, y and z directions - Fig. I.1c.
X_o, X_1	Tangent rotation for n = 0 and n = 1 respectively.
R_1, R_2	The principal radii of curvature of the middle surface.
R_1', R_2'	The radii of curvature of the normal of the strained middle surface.
R	The radius of a spherical vessel.
R_{min}	Minimum radius of curvature.
ξ, η, ζ	Displacements in the x, y, z directions, defined on p9
$\sigma_x, \sigma_Y, \sigma_z$	Normal components of stress parallel to the x, y, z axes.
$\tau_{xy}, \tau_{xz}, \tau_{yz}$	Shearing stress components in rectangular co-ordinates.

$\sigma_{\bar{r},D}$, $\sigma_{\theta,D}$ Direct stresses in the meridional and circumferential directions.

$\sigma_{\bar{r},B}$, $\sigma_{\theta,B}$ Bending stresses in the meridional and circumferential directions.

$\tau_{r\theta,D}$, $\tau_{r\theta,B}$ Direct (mid-surface) and Bending (outer fibre) Shear Stresses in the r,θ plane.

$\overset{+}{q}$, $\overset{-}{q}$ Values of σ_z at $z = \pm \frac{t}{2}$

u_0, w_0, X_0 --- Displacement, Resultant force and moment relating
$N_{\phi\phi_0}, N_{\theta\theta_0}$ --- to n = 0 in e.g. $N_{\phi\phi} = \sum N_{\phi\phi_n} \cos n\theta$ etc.
$M_{\phi\phi_0}, M_{\theta\theta_0}$ ---

v_1, w_1, X_1 --- Displacement, Resultant force and moment relating
$N_{\phi\phi_1}, N_{\theta\theta_1}$ --- to n = 1 in e.g. $N_{\phi\phi} = \sum N_{\phi\phi_n} \cos n\theta$ etc.
$M_{\phi\phi_1}, M_{\theta\theta_1}$ --

$\sigma_{\bar{r}}^o, \sigma_r^i, \sigma_\theta^o, \sigma_\theta^i$ Total meridional, circumferential and shear stresses
$\tau_{r\theta}^o, \tau_{r\theta}^i$ on the outer and inner surfaces.

$\varepsilon_r^o, \varepsilon_r^i, \varepsilon_\theta^o, \varepsilon_\theta^i$ Meridional, circumferential and shear strains on
$\gamma_{r\theta}^o, \gamma_{r\theta}^i$ the outer and inner surfaces.

E   Young's modulus of elasticity in tension and compression.

G   Modulus of elasticity in shear.

υ Poisson's ratio.

E_z, G_z, υ_z Tension and Shear modulii and Poisson's ratio in the z direction for the anisotropic case.

t   Thickness of shell.

D   Flexural rigidity of the shell, $D = E t^3 / 12(1-\upsilon^2)$

C   Extensional rigidity of the shell, $C = E t / (1-\upsilon^2)$

P   Total radial load $= p_o \pi r_P^2$ where $p_o = -p$ (Fig.II.1)

M   'Bending' Moment, Fig. II.15

T   'Twisting' Moment, Fig. II.20

H   Tangential Load, Fig. II.23

r_P Radius of uniformly distributed load and radius of Rigid Insert.

r_0 Radius of loaded ring.

ℓ	Parameter $\ell = \sqrt{Rt}/\sqrt[4]{12(1-v^2)}$
μ	Parameter $\mu = r_p/\ell$ for U.D. Area or Load Width $2r_p$ and $\mu = r_o/\ell$ for loaded ring.
Ω	Load potential eqts. I.84a,b.
F	Membrane Stress function.
w_p, F_p	Particular Integrals in the deflection and stress function equations, respectively.
k	Foundation modulus, eqt. I.97.
$L(...)$	Linear homogeneous differential operator:- For the 'general' shell $= \frac{1}{\sin\phi}\frac{d}{d\phi}\left[\frac{R_2\sin\phi}{R_1}\frac{d(...)}{d\phi}\right] - \frac{R_1}{R_2}\cot^2\phi\,(...)$ For the spherical shell $= \frac{d^2(...)}{d\phi^2} + \frac{d(...)}{d\phi}\cot\phi - (...)\cot^2\phi$
$H(...)$	Differential operator $= \frac{\partial^2(...)}{\partial\phi^2} + \frac{\partial(...)}{\partial\phi}\cot\phi + 2(...) + \frac{\partial^2(...)}{\partial\theta^2\sin^2\phi}$
$\nabla^2(...)$ ∇^4	Laplacian Operator $\nabla^2(...) = \frac{\partial^2(...)}{\partial r^2} + \frac{1}{r}\frac{\partial}{\partial r}(...) + \frac{1}{r^2}\frac{\partial^2(...)}{\partial\theta^2}$ $= \nabla^2\nabla^2$
$\chi, b, \rho, \lambda, \Lambda$	Parameters given by:- $\chi^4 = 3(1-v^2)\frac{R^2}{t^2} - \frac{v^2}{4}$; $b^4 = (1-v^2)\left[1 + 12\frac{R^2}{t^2}\right]$ $\rho^4 = \frac{1}{4}(1-v^2)\left[1 + 12\frac{R^2}{t^2}\right]$; $\lambda^4 = 3(1-v^2)\frac{R^2}{t^2}$; $\Lambda^4 = 12(1-v^2)\frac{R^2}{t^2}$
$C_1 \rightarrow C_{14}, A_o \rightarrow A_n$ $B_o \rightarrow B_n, D_1, D_2$ $b_o, b_1, a_o, c_o d_o e_o$	Characteristic Constants.
$\ell u\,(...)$	Natural logarithm
k	$= t^2/12R^2$
n	nth term of the Fourier series.
j	$\sqrt{-1}$
$\psi_1, \psi_2, \psi_3, \psi_4$	Schleicher functions
J_n	Bessel function of the first kind - nth order.
Y_n	Bessel function of the second kind - nth order.
I_n	Modified Bessel function of the first kind - nth order. eqt. II.16a.

K_n Modified Bessel function of the second kind -
                  nth order. eqt. II.16b.

$ber_n z, bei_n z$ Kelvin functions, real and imaginary parts of
                  $j^n I_n(z\sqrt{j}) = J_n(z j^{1/2})$

$ker_n z, kei_n z$ Kelvin functions, real and imaginary parts of
                  $j^{-n} K_n(z j^{1/2})$

$$ber''z = -bei\,z - \frac{ber'z}{z}$$
$$bei''z = \ ber\,z - \frac{bei'z}{z}$$
$$ker''z = -kei\,z - \frac{ker'z}{z}$$
$$kei''z = \ ker\,z - \frac{kei'z}{z}$$

From eqts. VIII.2a-d

For small arguments:-

$$berz = 1 - \frac{z^4}{2^2.4^2}$$

$$beiz = \frac{z^2}{2^2} - \frac{z^6}{2^2.4^2.6^2}$$

$$kerz = -\ln z + 0.1159 + \frac{\pi z^2}{16} +$$

$$keiz = -\left(\frac{z^2}{4}\right)\ln z - \frac{\pi}{4} + 1.1159\frac{z^2}{4}$$

$$\frac{ber'z}{z} = -\frac{z^2}{16}$$

$$\frac{bei'z}{z} = \frac{1}{2} - \frac{z^4}{2^2.4^2.6^2}$$

$$\frac{ker'z}{z} = -\frac{1}{z^2} + \frac{\pi}{8} + \frac{z^2}{16}\ln z$$

$$\frac{kei'z}{z} = -\frac{1}{2}\ln z - \frac{1}{4} + 0.5580$$

$$ber'z = \frac{d}{dz}(berz) \quad \text{and} \quad ber''z = \frac{d^2}{dz^2}(berz)$$

<u>A C K N O W L E D G M E N T S</u>